

Reconstructing paleodiets: Challenges and advances

Edited by

Eduardo Jiménez-Hidalgo, Ferran Estebaranz-Sánchez,
Larisa R. G. DeSantis, Maciej Tomasz Krajcarz and Carlo Meloro

Published in

Frontiers in Ecology and Evolution



FRONTIERS EBOOK COPYRIGHT STATEMENT

The copyright in the text of individual articles in this ebook is the property of their respective authors or their respective institutions or funders. The copyright in graphics and images within each article may be subject to copyright of other parties. In both cases this is subject to a license granted to Frontiers.

The compilation of articles constituting this ebook is the property of Frontiers.

Each article within this ebook, and the ebook itself, are published under the most recent version of the Creative Commons CC-BY licence. The version current at the date of publication of this ebook is CC-BY 4.0. If the CC-BY licence is updated, the licence granted by Frontiers is automatically updated to the new version.

When exercising any right under the CC-BY licence, Frontiers must be attributed as the original publisher of the article or ebook, as applicable.

Authors have the responsibility of ensuring that any graphics or other materials which are the property of others may be included in the CC-BY licence, but this should be checked before relying on the CC-BY licence to reproduce those materials. Any copyright notices relating to those materials must be complied with.

Copyright and source acknowledgement notices may not be removed and must be displayed in any copy, derivative work or partial copy which includes the elements in question.

All copyright, and all rights therein, are protected by national and international copyright laws. The above represents a summary only. For further information please read Frontiers' Conditions for Website Use and Copyright Statement, and the applicable CC-BY licence.

ISSN 1664-8714
ISBN 978-2-8325-3386-4
DOI 10.3389/978-2-8325-3386-4

About Frontiers

Frontiers is more than just an open access publisher of scholarly articles: it is a pioneering approach to the world of academia, radically improving the way scholarly research is managed. The grand vision of Frontiers is a world where all people have an equal opportunity to seek, share and generate knowledge. Frontiers provides immediate and permanent online open access to all its publications, but this alone is not enough to realize our grand goals.

Frontiers journal series

The Frontiers journal series is a multi-tier and interdisciplinary set of open-access, online journals, promising a paradigm shift from the current review, selection and dissemination processes in academic publishing. All Frontiers journals are driven by researchers for researchers; therefore, they constitute a service to the scholarly community. At the same time, the *Frontiers journal series* operates on a revolutionary invention, the tiered publishing system, initially addressing specific communities of scholars, and gradually climbing up to broader public understanding, thus serving the interests of the lay society, too.

Dedication to quality

Each Frontiers article is a landmark of the highest quality, thanks to genuinely collaborative interactions between authors and review editors, who include some of the world's best academicians. Research must be certified by peers before entering a stream of knowledge that may eventually reach the public - and shape society; therefore, Frontiers only applies the most rigorous and unbiased reviews. Frontiers revolutionizes research publishing by freely delivering the most outstanding research, evaluated with no bias from both the academic and social point of view. By applying the most advanced information technologies, Frontiers is catapulting scholarly publishing into a new generation.

What are Frontiers Research Topics?

Frontiers Research Topics are very popular trademarks of the *Frontiers journals series*: they are collections of at least ten articles, all centered on a particular subject. With their unique mix of varied contributions from Original Research to Review Articles, Frontiers Research Topics unify the most influential researchers, the latest key findings and historical advances in a hot research area.

Find out more on how to host your own Frontiers Research Topic or contribute to one as an author by contacting the Frontiers editorial office: frontiersin.org/about/contact

Reconstructing paleodiets: Challenges and advances

Topic editors

Eduardo Jiménez-Hidalgo — University of the Sea, Mexico

Ferran Estebanz-Sánchez — Milà y Fontanals Institution for Research in Humanities, Spanish National Research Council (CSIC), Spain

Larisa R. G. DeSantis — Vanderbilt University, United States

Maciej Tomasz Krajcarz — Institute of Geological Sciences, Polish Academy of Sciences, Poland

Carlo Meloro — Liverpool John Moores University, United Kingdom

Citation

Jiménez-Hidalgo, E., Estebanz-Sánchez, F., DeSantis, L. R. G., Krajcarz, M. T., Meloro, C., eds. (2023). *Reconstructing paleodiets: Challenges and advances*. Lausanne: Frontiers Media SA. doi: 10.3389/978-2-8325-3386-4

Table of contents

05	Editorial: Reconstructing paleodiets: challenges and advances Eduardo Jiménez-Hidalgo, Ferran Estebanz-Sánchez, Maciej T. Krajcarz, Carlo Meloro and Larisa DeSantis
08	Dental microwear texture analysis correlations in guinea pigs (<i>Cavia porcellus</i>) and sheep (<i>Ovis aries</i>) suggest that dental microwear texture signal consistency is species-specific Louise Françoise Martin, Daniela Eileen Winkler, Nicole Lauren Ackermans, Jaqueline Müller, Thomas Tütken, Thomas Kaiser, Daryl Codron, Ellen Schulz-Kornas, Jean-Michel Hatt and Marcus Clauss
20	Microwear textures associated with experimental near-natural diets suggest that seeds and hard insect body parts cause high enamel surface complexity in small mammals Daniela E. Winkler, Marcus Clauss, Mugino O. Kubo, Ellen Schulz-Kornas, Thomas M. Kaiser, Anja Tschudin, Annelies De Cuyper, Tai Kubo and Thomas Tütken
36	Reconstructing diets of hunted sika deer from Torihama Shell Midden site (ca. 6,000 years ago) by dental microwear texture analysis Koyo Sato, Takao Sato and Mugino O. Kubo
48	Carbon-isotope composition of artiodactyl tooth enamel and its implications for paleodiets Bian Wang and Catherine Badgley
68	Accuracy of dental microwear impressions by physical properties of silicone materials Ryohei Sawaura, Yuri Kimura and Mugino O. Kubo
80	Controlled feeding experiments with juvenile alligators reveal microscopic dental wear texture patterns associated with hard-object feeding Daniela E. Winkler, Masaya Iijima, Richard W. Blob, Tai Kubo and Mugino O. Kubo
92	The dental microwear texture of wild boars from Japan reflects inter- and intra-populational feeding preferences Kohga Miyamoto, Mugino O. Kubo and Yasushi Yokohata
108	Dental topography and dietary specialization in Papionini primates Yasmina Avià, Alejandro Romero, Ferran Estebanz-Sánchez, Alejandro Pérez-Pérez, Elisabeth Cuesta-Torralvo and Laura Mónica Martínez

- 125 **Interpreting spatially explicit variation in dietary proxies through species distribution modeling reveals foraging preferences of mammoth (*Mammuthus*) and American mastodon (*Mammut americanum*)**
Melissa I. Pardi and Larisa R. G. DeSantis
- 139 **On the relationship between collagen- and carbonate-derived carbon isotopes with implications for the inference of carnivore dietary behavior**
Larisa R. G. DeSantis, Robert S. Feranec, John Southon, Thure E. Cerling, John Harris, Wendy J. Binder, Joshua E. Cohen, Aisling B. Farrell, Emily L. Lindsey, Julie Meachen, Frank Robin O'Keefe and Gary T. Takeuchi
- 155 **Behavioral strategies of prehistoric and historic children from dental microwear texture analysis**
Almudena Estalrich and Kristin L. Krueger
- 163 **Neanderthal subsistence at Chez-Pinaud Jonzac (Charente-Maritime, France): A kill site dominated by reindeer remains, but with a horse-laden diet?**
William Rendu, Sylvain Renou, Anastasiia Koliashnikova, Malvina Baumann, Hugues Plisson, Emmanuel Discamps, Marie-Cécile Soulier, Arthur Gicqueau, Mathilde Augoyard, Manon Bocquel, Guillaume Guerin, Svetlana Shnaider and Kseniya Kolobova
- 181 **Multiproxy approach to reconstruct fossil primate feeding behavior: Case study for macaque from the Plio-Pleistocene site Guefaït-4.2 (eastern Morocco)**
Iván Ramírez-Pedraza, Laura M. Martínez, Hassan Aouraghe, Florent Rivals, Carlos Tornero, Hamid Haddoumi, Ferran Estebanaranz-Sánchez, Antonio Rodríguez-Hidalgo, Jan van der Made, Aïcha Oujaa, Juan José Ibáñez, Hicham Mhamdi, Mohamed Souhir, Al Mahdi Aissa, M. Gema Chacón and Robert Sala-Ramos
- 197 **Sharpening the mesowear tool: geometric morphometric analysis of cusp shape and diet in ruminants**
Matthew C. Mhlbachler, Christina I. Barrón-Ortiz, Brian D. Rankin and Jessica M. Theodor



OPEN ACCESS

EDITED AND REVIEWED BY
Laura Parducci,
Sapienza University of Rome, Italy

*CORRESPONDENCE

Eduardo Jiménez-Hidalgo
✉ eduardojhi@gmail.com
Ferran Estebaranz-Sánchez
✉ estebaranz@protonmail.com
Maciej T. Krajcarz
✉ mkrajcarz@twarda.pan.pl
Carlo Meloro
✉ c.meloro@lmu.ac.uk
Larisa DeSantis
✉ la.risa.desantis@vanderbilt.edu

RECEIVED 25 July 2023

ACCEPTED 03 August 2023

PUBLISHED 16 August 2023

CITATION

Jiménez-Hidalgo E, Estebaranz-Sánchez F, Krajcarz MT, Meloro C and DeSantis L (2023) Editorial: Reconstructing paleodiets: challenges and advances. *Front. Ecol. Evol.* 11:1267012. doi: 10.3389/fevo.2023.1267012

COPYRIGHT

© 2023 Jiménez-Hidalgo, Estebaranz-Sánchez, Krajcarz, Meloro and DeSantis. This is an open-access article distributed under the terms of the [Creative Commons Attribution License \(CC BY\)](#). The use, distribution or reproduction in other forums is permitted, provided the original author(s) and the copyright owner(s) are credited and that the original publication in this journal is cited, in accordance with accepted academic practice. No use, distribution or reproduction is permitted which does not comply with these terms.

Editorial: Reconstructing paleodiets: challenges and advances

Eduardo Jiménez-Hidalgo^{1*}, Ferran Estebaranz-Sánchez^{2*}, Maciej T. Krajcarz^{3*}, Carlo Meloro^{4*} and Larisa DeSantis^{5,6*}

¹Laboratorio de Paleobiología, Instituto de Recursos, Campus Puerto Escondido, Universidad del Mar, Puerto Escondido, Oaxaca, Mexico, ²Archaeology of Social Dynamics (2021 SGR501), Institut Milà i Fontanals de Recerca en Humanitats (IMF-CSIC), Barcelona, Spain, ³Institute of Geological Sciences, Polish Academy of Sciences, Warszawa, Poland, ⁴Research Centre in Evolutionary Anthropology and Palaeoecology, School of Biological and Environmental Sciences, Liverpool John Moores University, Liverpool, United Kingdom, ⁵Department of Biological Sciences, Vanderbilt University, Nashville, TN, United States, ⁶Department of Earth and Environmental Sciences, Vanderbilt University, Nashville, TN, United States

KEYWORDS

niche partitioning, feeding habits, mesowear analysis, stable isotopes, dental microwear texture analysis (DMTA), low magnification microwear, habitat

Editorial on the Research Topic

Reconstructing paleodiets: challenges and advances

Reconstruction of past diets allows tracking numerous ecological and behavioral aspects through time and across diverse geographic areas, such as the trophic position of species, niche sharing and niche partitioning; it also provides information about the structure of past vegetation and its change, migration patterns, ontogenetic and individual food preferences, and adaptations to environmental changes (Clementz, 2012; Pineda-Munoz et al., 2017). These insights are also key to reconstructing and understanding past ecosystems' structure, composition, and function, and extracting lessons learned of direct relevance to modern conservation.

One of the most widely used techniques to reconstruct diets of fossil mammals is dental microwear texture analysis (DMTA, Kaiser and Brinkmann, 2006) and in this Research Topic, Sato et al. provide an interesting case study on the dietary habits of a 6,000 years ago population of sika deer (*Cervus nippon*) from Torihama Shell Midden, Japan. Their results showed that fossil sika deer had a mixed diet based on herbaceous vegetation, which may reflect its flexible ecological adaptations. By elucidating the diet of this ancient herbivore population, their study also informed on prehistoric human communities' hunting practices and their dietary habits. Miyamoto et al. equally applied DMT to the study of wild boars (*Sus scrofa*) from Toyama Prefecture, Japan. Results indicated that tooth surfaces of boarlets were rougher than those of juvenile or adult animals. A comparison of boars from different habitats showed that mainland boars inhabiting deciduous broad-leaved forests had flatter and less rough tooth surfaces than those in the subtropical evergreen broad-leaved forest. This study gives important information about microwear texture data of an underrepresented ungulate group such as suids.

Standardised *in vitro* experiments with controlled diets to associate specific microtexture patterns with the ingestion of specific food types or their mechanical properties is another methodological aspect that has recently gained importance. Martin

et al. analysed the effect of DMT on adding or not adding various extrinsic abrasives to pelleted diets compared to natural diets in guinea pigs (*Cavia porcellus*). Specimens fed a natural diet had a lower range of DMT values. The normalised DMT data range of guinea pigs and sheep (*Ovis aries*) fed identical diets were also compared: while the DMT data range was higher in sheep, the absolute Spearman's correlation coefficient between the different variables was lower in sheep than in pigs. This suggests that DMT is species specific and its variation between species must be interpreted with caution.

Winkler et al. conducted a pilot feeding experiment with five juvenile *Alligator mississippiensis*. Each individual received a diet of different hardness: crocodylian pellets (control), sardines, quails, rats, or crawfish. DMT showed similar dental microwear texture patterns before they were switched to their designated experimental diet, but from the first feeding bout on, dental microwear textures differed across the diets. The crawfish-feeder showed consistently higher surface complexity, followed by the rat-feeder. Quail- and fish-feeding resulted in similar wear signatures, with low complexity. Such patterns can support the identification of hard-object feeding in the Crocodylia fossil record.

Winkler et al. investigated which objects or food items can produce high-complexity DMT patterns (in the absence of external abrasives). A feeding trial on a sample of 36 laboratory rats separated into six distinct groups, each receiving a different diet indicated that seeds are the main cause of complex microwear textures, but that hard insect parts may also be a major factor causing high complexity in the enamel surface of small mammals.

The increase in the number of published microtexture studies is associated with the use of different commercial resins by different researchers. Sawaura et al. analysed the accuracy of using different types of commercial silicone resins on dental microtexture variables to improve the reproducibility of studies and ensure comparability of data between different studies. Results showed that silicones with rapid completion and showing steep viscoelastic curves and those that had a delayed change in shrinkage show better reproducibility and accuracy of microwear features with less blurring and air bubble contamination.

Avià et al. explored the relationship between wear-related dental functional morphology and dietary ecological constraints within Papionini primates. Their results indicate that hard-object feeders and grass eaters papionines exhibit a pattern of occlusal complexity, surface curvature, relief, and morphological wear resistance that is significantly different from the omnivores and folivore-frugivore species despite the overall homogeneity of the bilophodont dentition. In another multiproxy analysis of papionini, Ramírez-Pedraza et al. inferred the feeding habits of *Macaca cf. sylvanus* from the Plio-Pleistocene site Guefât-4.2 (eastern Morocco). The occlusal microwear results showed that *M. cf. sylvanus* had a pattern similar to the extant *Cercocebus atys* and *Lophocebus albigena*, African forest-dwelling species characterized by a durophagous diet. Buccal microtexture results also supported the consumption of some grasses and the exploitation of more open habitats. At the same time, stable isotopes of *M. cf. sylvanus* indicated a C3-based diet without the presence of C4 plants.

Stable isotopes provide valuable information on animal physiology and dietary adaptations (Ehleringer et al., 1986). By

collating data from over 24 studies with an additional sample of 80 teeth specimens, Wang and Badgley provided in this Research Topic an extensive overview of carbon isotopic variation ($\delta^{13}\text{C}$ diet) within living terrestrial artiodactyls. Because most species of this clade are primary consumers, the interpretation of carbon data is linked to their consumption of C3 or C4 plants. Variation in C3 within and between artiodactyl species exhibits similar shifts following plant distribution across different continents.

DeSantis et al. equally offered an interesting application of stable isotope to clarify diet of carnivorous mammals, by analyzing bone collagen (carbon and nitrogen) and enamel carbonate (carbon) of extinct and extant North American felids and canids, supplementing it with data from African wild dog (*Lycaon pictus*) and African lion (*Panthera leo*). Their results revealed that $\Delta_{\text{ca-co}}$ values are positively related to enamel carbonate values in secondary consumers and are less predictive of trophic level. Foraging habitat and diet of prey affect $\Delta_{\text{ca-co}}$ in carnivores, like in herbivore species. Average $\Delta_{\text{ca-co}}$ values in Pleistocene canids ($8.7 \pm 1\%$) and felids ($7.0 \pm 0.7\%$) overlap with previously documented extant herbivore $\Delta_{\text{ca-co}}$ values, suggesting that trophic level estimates may be relative to herbivore $\Delta_{\text{ca-co}}$ values in each ecosystem and not directly comparable between disparate ecosystems.

In another paper, Pardi and DeSantis presented an approach in which species distribution modeling allows interpreting variation in stable isotope and dental microwear texture data. They investigated the resource use over space and time from the last glacial maximum to the end of the Pleistocene in North American mastodon (*Mammuthus americanum*) and mammoths of the genus *Mammuthus*. Mammoth dietary behavior varied by context across north american geographic range while dietary preferences of mastodon are less resolved and isotopic data does not allow to identify significant geographical changes in its diet.

Ecomorphological variation of terrestrial herbivores is further explored in the work of Mühbachler et al. that present an interesting application of the geometric morphometric techniques (GMM, Adams et al., 2013) to 2D images of the second upper molar from 91 ruminant species. Two landmarks and twenty semi-landmarks that slide along the cusp curvy surface were used. A substantial degree of covariation between cusp shape data generated with GMM and more traditional mesowear scoring was validated by Mühbachler et al. and supported its further biological interpretation for dietary reconstruction. Discriminant Function Analysis applied to cusp shape data improved dietary classification from 56.1% of the traditional mesowear method to 67.2%, showing the potential of GMM to accomplish a more comprehensive understanding of tooth-wearing biological processes.

Regarding studies involving hominins, Estalrich and Krueger analyzed prehistoric and historic children through DMTA of deciduous anterior teeth. Their results showed that DMTA successfully differentiated the samples by all texture variables examined. The Neanderthal and Point Hope children had similar mean values across all the texture variables, and both groups were significantly different from the Amarna, Egyptian children. These results suggest diversity in abrasive load exposure and participation in non-dietary anterior tooth-use behaviors. They also showed that

some prehistoric and historic children took part in similar behaviors as their adult counterparts.

Rendú et al. reported new zooarchaeological data analyses on the site of Chez-Pinaud, Jonzac (France). Previous recognition of the Quina Mousterian techno-complex supported adaptations to reindeer (*Rangifer tarandus*) hunting in Neanderthals from Jonzac. However, Rendú et al. new data indicate that the contribution of the horse and bison to Neanderthal economy was higher than expected by previous interpretations and that the reindeer was overestimated in the faunal spectrum. Horses and bovids were significant sources of protein for the Quina Neanderthals population.

The studies presented in this Research Topic are either aimed at improving our understanding of how dietary behavior is recorded in extant taxa or clarifying how we can reconstruct dietary behavior in ancient ecosystems. By applying different methodologies, this topic demonstrates the myriad of ways in which we can improve accuracy and precision in palaeodietary reconstruction, a discipline that is progressing rapidly with novel technological applications.

Author contributions

EJ-H: Writing – original draft, Writing – review & editing. FE-S: Writing – original draft, Writing – review & editing. MK: Writing –

original draft, Writing – review & editing. CM: Writing – original draft, Writing – review & editing. LD: Writing – original draft, Writing – review & editing.

Conflict of interest

The authors declare that the research was conducted in the absence of any commercial or financial relationships that could be construed as a potential conflict of interest.

The authors declared that they were an editorial board member of Frontiers, at the time of submission. This had no impact on the peer review process and the final decision.

Publisher's note

All claims expressed in this article are solely those of the authors and do not necessarily represent those of their affiliated organizations, or those of the publisher, the editors and the reviewers. Any product that may be evaluated in this article, or claim that may be made by its manufacturer, is not guaranteed or endorsed by the publisher.

References

- Adams, D. C., Rohlf, F. J., and Slice, D. E. (2013). A field comes of age: geometric morphometrics in the 21st century. *Hystrix It. J. Mamm.* 24 (1), 7–14. doi: 10.4404/hystrix-24.1-6283
- Clementz, M. T. (2012). New insight from old bones: stable isotope analysis of fossil mammals. *J. Mammalogy* 93 (2), 368–380. doi: 10.1644/11-MAMM-S-179.1
- Ehleringer, J. R., Rundel, P. W., and Nagy, K. A. (1986). Stable isotopes in physiological ecology and food web research. *Trends Ecol. Evol.* 1 (2), 42–45. doi: 10.1016/0169-5347(86)90072-8
- Kaiser, T. M., and Brinkmann, G. (2006). Measuring dental wear equilibriums—the use of industrial surface texture parameters to infer the diets of fossil mammals. *Palaeogeography Palaeoclimatology Palaeoecol.* 239 (3–4), 221–240. doi: 10.1016/j.palaeo.2006.01.013
- Pineda-Munoz, S., Lazagabaster, I. A., Alroy, J., and Evans, A. R. (2017). Inferring diet from dental morphology in terrestrial mammals. *Methods Ecol. Evol.* 8, 481–491. doi: 10.1111/2041-210X.12691



OPEN ACCESS

EDITED BY

Ferran Estebanaranz-Sánchez,
Milá y Fontanals Institution
for Research in Humanities (CSIC),
Spain

REVIEWED BY

Miriam Belmaker,
University of Tulsa, United States
Céline Robinet,
Universidad Nacional de La Plata,
Argentina

*CORRESPONDENCE

Louise Françoise Martin
lfmartin@vetclinics.uzh.ch

SPECIALTY SECTION

This article was submitted to
Paleoecology,
a section of the journal
Frontiers in Ecology and Evolution

RECEIVED 31 May 2022

ACCEPTED 29 July 2022

PUBLISHED 25 August 2022

CITATION

Martin LF, Winkler DE, Ackermans NL,
Müller J, Tütken T, Kaiser T, Codron D,
Schulz-Kornas E, Hatt J-M and
Clauss M (2022) Dental microwear
texture analysis correlations in guinea
pigs (*Cavia porcellus*) and sheep (*Ovis
aries*) suggest that dental microwear
texture signal consistency is
species-specific.
Front. Ecol. Evol. 10:958576.
doi: 10.3389/fevo.2022.958576

COPYRIGHT

© 2022 Martin, Winkler, Ackermans,
Müller, Tütken, Kaiser, Codron,
Schulz-Kornas, Hatt and Clauss. This is
an open-access article distributed
under the terms of the [Creative
Commons Attribution License \(CC BY\)](#).
The use, distribution or reproduction in
other forums is permitted, provided
the original author(s) and the copyright
owner(s) are credited and that the
original publication in this journal is
cited, in accordance with accepted
academic practice. No use, distribution
or reproduction is permitted which
does not comply with these terms.

Dental microwear texture analysis correlations in guinea pigs (*Cavia porcellus*) and sheep (*Ovis aries*) suggest that dental microwear texture signal consistency is species-specific

Louise Françoise Martin ^{1*}, Daniela Eileen Winkler ^{2,3,4},
Nicole Lauren Ackermans ^{1,5}, Jacqueline Müller¹,
Thomas Tütken², Thomas Kaiser ⁴, Daryl Codron ⁶,
Ellen Schulz-Kornas ^{4,7}, Jean-Michel Hatt ¹ and
Marcus Clauss ¹

¹Clinic for Zoo Animals, Exotic Pets and Wildlife, Vetsuisse Faculty, University of Zurich, Zurich, Switzerland, ²Applied and Analytical Paleontology, Institute of Geosciences, Johannes Gutenberg University, Mainz, Germany, ³Department of Natural Environmental Studies, Graduate School of Frontier Sciences, The University of Tokyo, Chiba, Japan, ⁴Center of Natural History, University of Hamburg, Hamburg, Germany, ⁵Nash Family Department of Neuroscience, Friedman Brain Institute, Center for Anatomy and Functional Morphology, Icahn School of Medicine at Mount Sinai, New York, NY, United States, ⁶Department of Zoology and Entomology, University of the Free State, Bloemfontein, South Africa, ⁷Department of Cariology, Endodontology and Periodontology, University of Leipzig, Leipzig, Germany

Dental microwear texture (DMT) analysis is used to differentiate abrasive dental wear patterns in many species fed different diets. Because DMT parameters all describe the same surface, they are expected to correlate with each other distinctively. Here, we explore the data range of, and correlations between, DMT parameters to increase the understanding of how this group of proxies records wear within and across species. The analysis was based on subsets of previously published DMT analyses in guinea pigs, sheep, and rabbits fed either a natural whole plant diet (lucerne, grass, bamboo) or pelleted diets with or without added quartz abrasives (guinea pigs and rabbits: up to 45 days, sheep: 17 months). The normalized DMT parameter range (P4: 0.69 ± 0.25 ; M2: 0.83 ± 0.16) and correlation coefficients (P4: 0.50 ± 0.31 ; M2: 0.63 ± 0.31) increased along the tooth row in guinea pigs, suggesting that strong correlations may be partially explained by data range. A comparison between sheep and guinea pigs revealed a higher DMT data range in sheep (0.93 ± 0.16 ; guinea pigs: 0.47 ± 0.29), but this did not translate into more substantial correlation coefficients (sheep: 0.35 ± 0.28 ; guinea pigs: 0.55 ± 0.32). Adding rabbits to an interspecies comparison of low abrasive dental wear (pelleted lucerne diet), the softer enamel of the hypselodont species showed a smaller data range for DMT parameters (guinea pigs 0.49 ± 0.32 , rabbit 0.19 ± 0.18 , sheep 0.78 ± 0.22) but again slightly higher correlations coefficients compared to the hypsodont teeth (guinea pigs

0.55 ± 0.31 , rabbits 0.56 ± 0.30 , sheep 0.42 ± 0.27). The findings suggest that the softer enamel of fast-replaced ever-growing hypselodont cheek teeth shows a greater inherent wear trace consistency, whereas the harder enamel of permanent and non-replaced enamel of hypsodont ruminant teeth records less coherent wear patterns. Because consistent diets were used across taxa, this effect cannot be ascribed to the random overwriting of individual wear traces on the more durable hypsodont teeth. This matches literature reports on reduced DMT pattern consistency on harder materials; possibly, individual wear events become more random in nature on harder material. Given the species-specific differences in enamel characteristics, the findings suggest a certain species-specificity of DMT patterns.

KEYWORDS

dental microwear texture analysis, rodent, ruminant, phytolith, quartz abrasive, feeding experiment

Introduction

Standardized experiments have recently been used to explore the mechanics of abrasive dental wear and the various proxies to record it (Schulz et al., 2013; Merceron et al., 2016; Winkler et al., 2019; Ackermans et al., 2020; Louail et al., 2021; Martin et al., 2022). The principal aim of those studies is to supply information for the understanding of evolutionary adaptations and to increase the precision of paleodietary reconstructions. *In vitro* experiments on a single tooth or enamel sample use a standardized approach to model dental wear dependent on diet. Many diet samples can be run in a short period, or one diet can be “chewed on” by speeding up the chewing apparatus to simulate more extended periods (Hua et al., 2015; Karme et al., 2016; Rodriguez-Rojas et al., 2020; Fischer et al., 2022). This standardization, however, oversimplifies a process that is dependent on the physical properties of the dental tissues, tooth geometry [i.e., arrangement of enamel, dentine, and cementum (Winkler and Kaiser, 2015)], tooth position along the tooth row and the corresponding jaw (Taylor et al., 2016; Ramdarshan et al., 2017), physical properties, and concentration of the abrasive elements in the diet and biomechanical properties of the diet matrix (Kaiser et al., 2016). Therefore, *in vivo* experiments better represent the complex nature of abrasive tooth wear but are time and labor intensive and must be ethically justified.

Whether the assay is *in vitro* or *in vivo*, the amount of tissue lost to wear is inherently difficult to quantify. By contrast, changes to the remaining tissue are comparatively easier to record and are commonly assessed using macroscopic or microscopic parameters serving as proxies for dental wear. Dental microwear texture (DMT) analysis characterizes tooth wear on a micrometer scale. It has been widely employed

in the study of dental wear in wild animals (Winkler et al., 2016; Yamada et al., 2018; Schulz-Kornas et al., 2019; Robinet et al., 2020) or fossil species (Donohue et al., 2013; Desantis, 2016) as well as in experimental settings (Schulz et al., 2013; Merceron et al., 2016; Teaford et al., 2017; Winkler et al., 2019, 2020a; Ackermans et al., 2020; Louail et al., 2021) and has sometime shown a high intra- and interspecies variability (Robinet et al., 2022). For DMT analysis (DMTA), a selected enamel surface is scanned and described using up to 46 areal surface texture parameters. Some of the parameters follow international standards, e.g., the ISO 25178 and the ISO 12871. In contrast, other parameters home in on specific geometric elements such as particular lines, points, or specific scale-dependent features (such as motif, furrow, isotropy parameters, and SSFA parameters). Following the ISO 25178 and MountainsMap® Software reference guide, the areal surface texture parameter can be grouped by their main characterizing features (area, complexity, density, direction, height, peak sharpness, plateau size, slope and volume; e.g., Winkler et al. (2021) for further description) to ease the understanding and facilitate the presentation of results. While all 46 DMT parameters describe at least parts of the same surface and should therefore correlate with each other (Ackermans et al., 2021), the relationship between DMT parameters within and between functional groups needs to be analyzed, to increase the understanding how abrasive tooth wear is dependent on species, tooth position, and abrasive elements, among many other factors (Scott et al., 2006). Preliminary explorations of the relationship between the DMT parameters in goats and sheep (Schulz-Kornas et al., 2020; Ackermans et al., 2021) and in rabbits (Martin et al., 2020) have led us to hypothesize that the putatively softer enamel of hypselodont teeth—as seen in Fischer et al. (2022) for rodent incisors and in

Shakila et al. (2015) with a preliminary test in cheek teeth in rabbits—should make the detection of interrelationships between different wear proxies easier; a hypothesis also supported by the observation that on soft material like cartilage, more significant correlations between DMTA parameters were evident (Tian et al., 2012; Wang et al., 2013) than on a hard material like steel (Korzynski et al., 2018).

We used the skulls of three groups of guinea pigs (*Cavia porcellus*) from feeding experiments focusing on the effect of natural diets (lucerne, grass and bamboo) and different external abrasives added to a pelleted diet on DMT analysis for this study. The DMT data was reported previously (Winkler et al., 2019, 2020b) for the effect of plant internal silica, the impact of different shapes, sizes and quantities of external abrasives, and a difference between tooth positions along the tooth row. Because several identical pelleted diets had been used for a feeding experiment in sheep (*Ovis aries*) (Ackermans et al., 2021) and rabbits (*Oryctolagus cuniculus*) (Martin et al., 2020), a direct comparison of the interrelationships among DMT measures within each species was feasible. Using specific data subsets, we hypothesize more DMT parameters correlations, or, in other words, a more consistent tooth wear pattern, if (a) the tooth position causes more intensive masticatory forces and if (b) the substrate (enamel) is more malleable (“softer”) (i.e., rodent vs. ruminant). Because one of the many reasons for the emergence of correlations lies in the range of the data submitted to correlation analysis, we do not only consider correlation coefficients but also the (normalized) range of the DMT measurements.

Materials and methods

The dental microwear texture (DMT) analysis datasets were accumulated from feeding experiments approved by the Cantonal Veterinary Office of Zurich (guinea pigs: license no. ZH135/2016; sheep ZH10/2016; rabbits: ZH80/2012). The guinea pigs were fed either a natural whole plant diet (lucerne, grass or bamboo) or a pelleted formulation based on lucerne meal with or without the addition of different external abrasive agents (i.e., quartz in different amounts and grain sizes; see Table 1 and Supplementary Table 1 for diet composition, feeding time and body mass). In guinea pigs, each diet had been fed for a period of three to 6 weeks, and for rabbits for 2 weeks; due to the fast turnover of the chewing surface of these species' hypselodont cheek teeth (Schulz et al., 2013), this time is sufficient to ensure only traces of the respective diet are recorded. The identical pelleted diets were used in sheep for a feeding time of 17 months with the addition of lucerne hay at a rate of 200 g as fed per animal and day. Additional data were available from six rabbits that had also received a pelleted lucerne diet for 2 weeks. Detailed experimental conditions, including husbandry, feed management and descriptions, are available in the corresponding original publications [guinea

pigs: Winkler et al. (2019), Winkler et al. (2020b); sheep: Ackermans et al. (2020); rabbits: Müller et al. (2014)].

The above publications offer a detailed description of the dental microwear texture analysis following the published routine for DMT data in MountainsMap v.9.0.9878 (Schulz et al., 2010, 2013) with adjustment for guinea pigs (Winkler et al., 2019, 2020a, 2021). In short, the surface texture of a predefined molar enamel area (guinea pigs 60 μm^2 , sheep 120 μm^2 , rabbits 40 μm^2) is scanned using a high-resolution confocal disk-scanning measurement system (μsurf custom, NanoFocus AG, Oberhausen, Germany) at the LIB Hamburg (former Center of Natural History (CeNak) of the University of Hamburg). From the mean of 4 non-overlapping scans, forty-six surface texture parameters (Supplementary Table 2) are quantified using the ISO 25178 (roughness), motif, furrow, isotropy, ISO 12871 (flatness), and Scale-sensitive fractal analysis (SSFA). Only scans from maxillary cheek teeth were included in the respective datasets, and subsets are based on criteria for the respective analysis.

Analysis

One reason for more significant non-parametric correlations in a dataset might simply be a more extensive range of parameter values. To account for this, we normalized all DMT measurements in a dataset in which comparisons were made (all guinea pig tooth positions within a diet category; guinea pigs and sheep within the common diet category) to a scale from 0–1 and expressed the range within each subset (a tooth position; a species) as the difference between the normalized maximum and minimum for each parameter. Subsequently, each subset was characterized by the average (\pm standard deviation SD) normalized range of all parameters.

Because many parameter measures were not normally distributed, all correlations were assessed using non-parametric correlation matrices (Supplementary Figure 1 for an example plot); to further visualize these results, we show histograms representing the distribution of the Spearman's correlation coefficients (from -1 to 1), and a boxplot of all absolute Spearman's correlation coefficients. Descriptive and test statistics were conducted in R Studio (Version 1.3.1093) using the packages tidyverse (Wickham et al., 2019), corrplot (Wei and Simko, 2021) and ggplot (Wickham, 2016).

Datasets

The example plots that outline our approach were built using all scans available for the guinea pigs (dataset A, Table 1). To account for DMT differences between tooth positions (Winkler et al., 2021), only guinea pigs for which scans of each tooth position (P4 to M3) were available were included in the actual analysis, and DMT parameter correlations

TABLE 1 Overview of diet groups for which DMTA data was included in the correlation analyses.

Species	Diet		Time on diet	n	Dataset
Guinea pigs	No abrasives	P	28–35 days	6	A B C D E
	4% fine silt	P	28–35 days	6	A B D
	Kaolin	P	28–35 days	6	A B
	Loess	P	28–35 days	6	A B
	4% coarse silt	P	28–35 days	6	A B D
	4% fine sand	P	28–35 days	6	A B D
	8% fine silt	P	45 days	6	A B D
	Mixed abrasives	P	45 days	6	A B
	Fine sand	P	45 days	6	A B
	Volcanic ash small	P	45 days	6	A B
	Volcanic ash large	P	45 days	6	A B
	Fresh lucerne	N	21 days	6	A B
	Dry lucerne	N	21 days	6	A B C
	Fresh grass	N	21 days	6	A B
	Dry grass	N	21 days	6	A B
	Fresh bamboo	N	21 days	6	A B
	Dry bamboo	N	21 days	6	A B
Sheep*	No abrasives	P	17 months	7	D E
	4% fine silt	P	17 months	4	D
	4% coarse silt	P	17 months	5	D
	4% fine sand	P	17 months	7	D
	8% fine sand	P	17 months	5	D
Rabbits	No abrasives	P	14 days	3	E

P, pelleted lucerne based diet; N, natural whole leave diet.

*Additional 200 g of lucerne hay per animal per day. The different datasets were compiled for all guinea pigs (A), guinea pigs for which all 4 tooth positions could be measured (B), guinea pigs on natural or pelleted lucerne diet (C), sheep and guinea pigs on pelleted diets with external abrasives (D) and sheep, guinea pigs and rabbits fed pelleted lucerne (E).

and ranges were compared between P4 and M2 (dataset B, [Table 1](#)). Two groups of guinea pigs (6 animals per group) had received low-abrasive lucerne diets but in a different formulation (dried whole plant diet or dried and pelleted) which allowed for a direct comparison of parameter ranges and correlations (dataset C, [Table 1](#)). Some guinea pigs and sheep received the same pelleted diet formulations with the addition of external quartz abrasives [control (quartz free), 4% fine silt, 4% coarse silt, 4% fine sand, 8% fine silt], facilitating an inter-species comparison (dataset D, [Table 1](#)). Moreover, the rabbit DMT data was added from a pilot on DMT correlations ([Martin et al., 2020](#)) to expand the interspecies comparison of animals fed only a lucerne pellet diet (dataset E, [Table 1](#)).

Results

In guinea pigs (dataset A), DMT parameters generally correlated well with each other. For area, height, plateau size, slope, peak sharpness, and volume, most parameters

correlated positively (or, in fewer cases, negatively) with each other. The direction, density, and complexity parameters show fewer significant correlations with other measures, evident in the “lighter areas” of the triangular diagram ([Supplementary Figure 1](#) and [Supplementary Table 3](#)). The mean absolute Spearman’s correlation coefficient was 0.53 ± 0.31 .

Tooth positions (dataset B)

The normalized DMT data range based on all teeth was lower for P4 (0.69 ± 0.25) than for M2 (0.83 ± 0.16 ; [Figure 1A](#)), indicating more variance in DMT measures on the M2. For all teeth, the mean absolute Spearman’s correlation coefficient was 0.56 ± 0.31 ([Figure 1B](#)). Here again, the mean for P4 (0.50 ± 0.31) was lower than for the M2 (0.63 ± 0.31 ; [Figure 1B](#)), which is also visible in the distribution of the Spearman’s correlation coefficients ([Figures 1D–F](#)), indicating more significant correlations in the tooth position with the larger measurement range.

Diet consistency (dataset C)

Comparing two diet groups with six guinea pigs each, fed either natural whole plant lucerne hay or pelleted lucerne, the normalized DMT data range was smaller for the animals receiving the natural diet (0.44 ± 0.32) than for those receiving the pelleted diets (0.91 ± 0.13 ; [Figure 2A](#)). The mean absolute Spearman’s correlation coefficient was 0.38 ± 0.27 for the natural diets compared to 0.55 ± 0.31 for the pelleted diets ([Figure 2B](#)), again indicating more significant correlations in the diet consistency with the larger measurement range.

Species comparison of external abrasive diets (dataset D)

When comparing two data subsets of animals fed identical pelleted diets with added abrasives (i.e., quartz) across all tooth positions, the measurement range for DMT in sheep was higher (0.93 ± 0.16) than in guinea pigs (0.47 ± 0.29 ; [Figure 3A](#)). But this did not translate into a more robust correlation pattern, with a mean absolute Spearman’s correlation coefficient of 0.35 ± 0.28 for sheep compared to 0.55 ± 0.32 for the guinea pigs ([Figures 3B–F](#)).

Species comparison lucerne diets (dataset E)

The normalized data range for rabbits fed a lucerne based pelleted diet was small compared to the guinea pigs and the

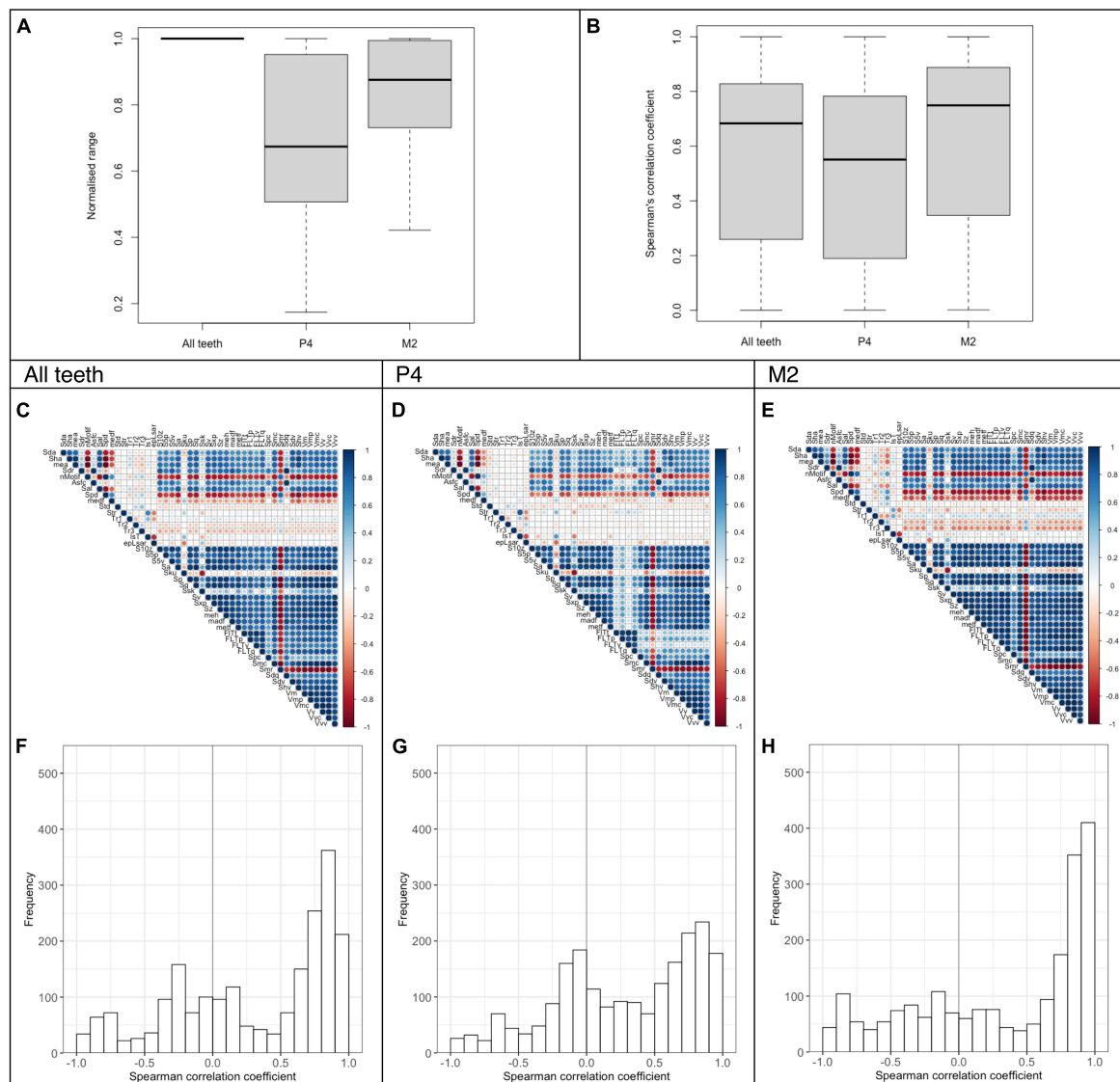


FIGURE 1

Analysis of DMT parameters for guinea pigs fed different natural (lucerne, grass, bamboo) and pelleted diets with additional external abrasives (dataset B). The data is presented as a summary for all teeth (P4-M3, 228 scans) and separately for P4 (57 scans) and M2 (57 scans). The normalized data range and the Spearman's correlations coefficients are given as boxplots (A,B). The Spearman's correlation of the DMT parameters is also shown as a correlation matrix (C–E) and a histogram (F–H).

sheep that had received the same diet (rabbit 0.19 ± 0.18 , guinea pigs 0.49 ± 0.32 , sheep 0.78 ± 0.22 , Figure 4A). However, the correlation pattern was still more robust in the rabbits and guinea pigs (rabbits 0.56 ± 0.30 , guinea pigs 0.55 ± 0.31) than in the sheep (sheep 0.42 ± 0.27 , Figures 4B–H).

Discussion

The present study confirms the well-known fact that DMT parameters correlate among each other (Martin et al., 2020; Ackermans et al., 2021). Due to the nature of DMT

parameters, which are applied on the same surface and are partially calculated from, or complementary to, each other, this finding in itself is not surprising (International Organization For Standardization, 2012). Therefore, correlations between DMT parameters are rarely reported and re-examined. Due to these interdependencies and the implied redundancy of information when reporting all parameters, some studies only report “key” parameters. These are selected based on various criteria, e.g., by robust but complex statistical approaches (Calandra et al., 2012), often justified and defined as reporting the parameters which have the most significant and stable relations to the anticipated functionalities (Tian et al., 2012). Other studies

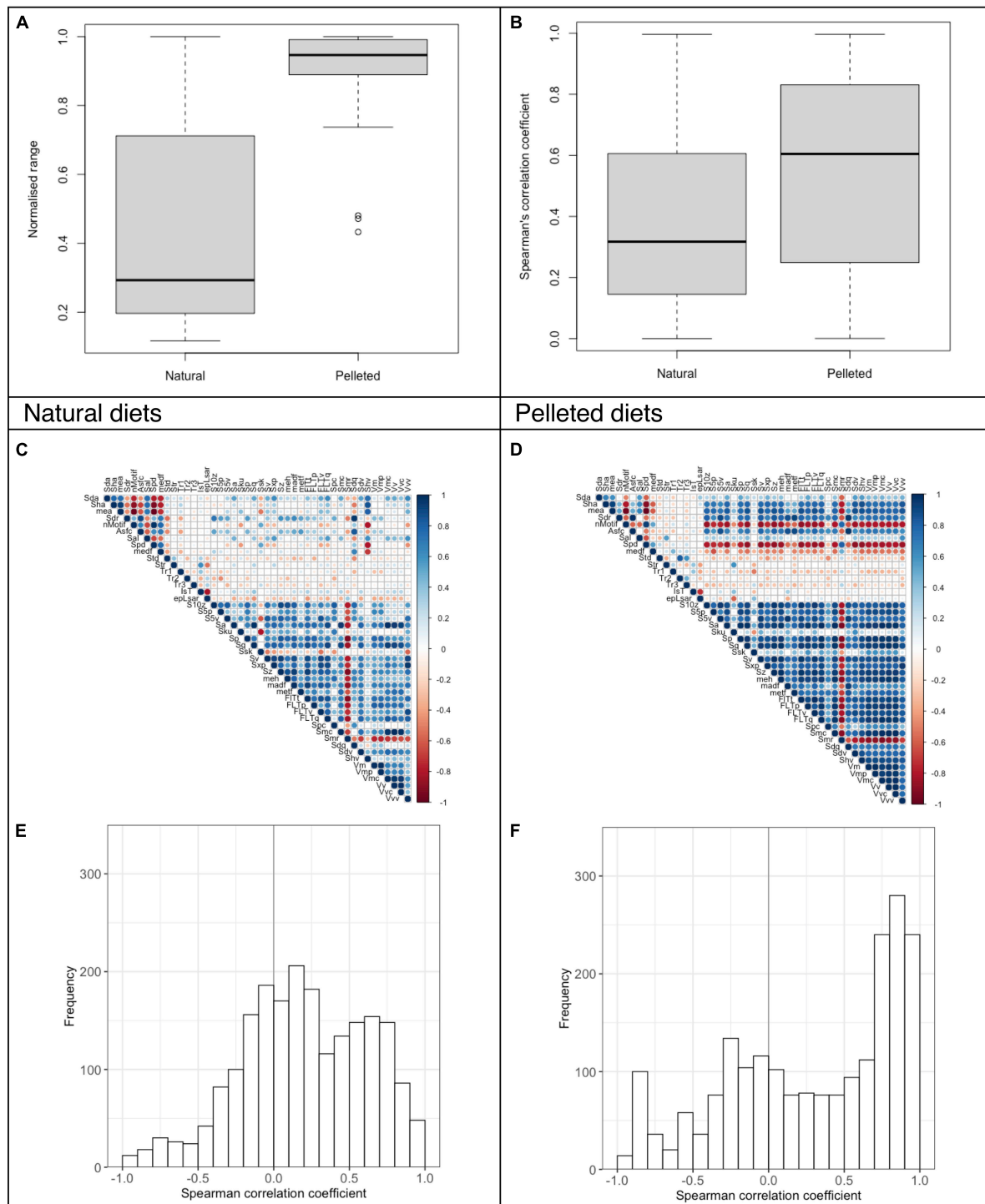


FIGURE 2

Analysis of DMT parameters for guinea pigs fed a lucerne diet either as whole plant hay or as a pelleted diet for P4 to M3 (dataset C). The data is presented as a summary for all teeth (24 scans for natural diet, 22 scans for pelleted diet). For two animals on the pelleted diet M3 could not be measured). The normalized data range and the Spearman's correlation coefficients are given as boxplots (A,B). The Spearman's correlation of the DMT parameters is also shown as a correlation matrix (C,D) and a histogram (E,F).

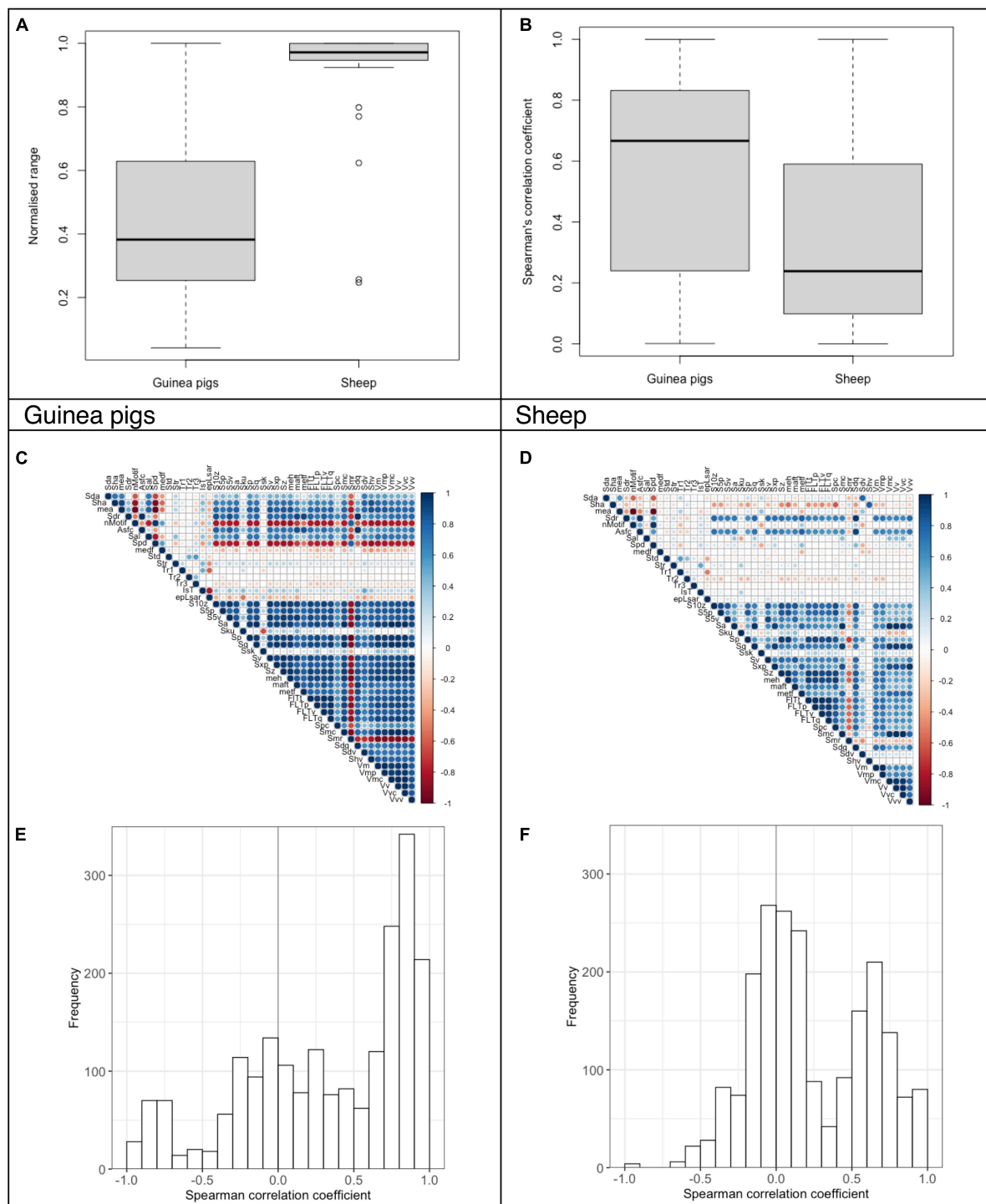


FIGURE 3

Analysis of DMT parameters for guinea pigs (96 scans) and sheep (78 scans) fed a lucerne based pelleted diet with or without external quartz abrasives (diet groups: control, 4% fine silt, 4% coarse silt, 4% fine sand, 8% fine silt; dataset D). The normalized data range and the Spearman's correlation coefficients are given as boxplots (A,B). The Spearman's correlation of the DMT parameters is also shown as a correlation matrix (C,D) and a histogram (E,F).

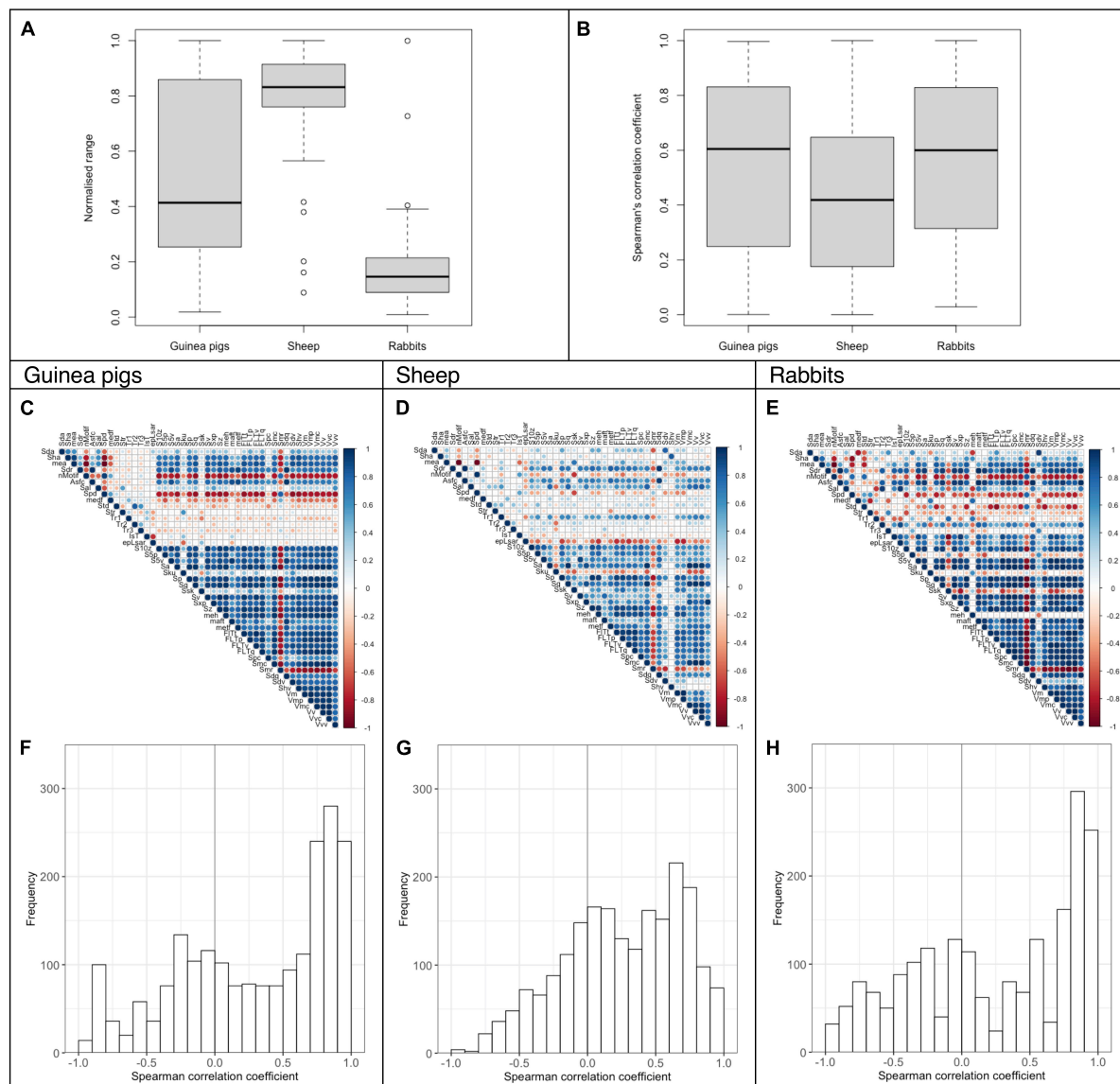


FIGURE 4

Analysis of DMT parameters for guinea pigs (22 scans), sheep (19 scans) and rabbits (6 scans) fed a lucerne based pelleted diet (without any abrasive added; dataset E). The normalized data range and the Spearman's correlation coefficients are given as boxplots (A,B). The Spearman's correlation of the DMT parameters is also shown as a correlation matrix (C–E) and a histogram (F–H).

considered most representative and independent parameters (Martisius et al., 2018), or applied factor analysis to reduce the large number of parameters to put them in a common score (Stuhlträger et al., 2019) or did a review on how commonly they have previously been reported in the DMT literature (Winkler et al., 2020b). Louail et al. (2021) combined 25 DMT parameters into a principal component as an approach to summarize DMT for a comparison between two chewing phase surfaces. Another way to summarize DMT results, “key” parameters could be defined as those that render other parameters superfluous due to consistent correlations—ideally,

regardless of tooth position, diet, or species. However, the present study suggest that all these factors influence how well DMT parameters correlate with each other, or, in other words, how inherently consistent the DMT description of a surface is.

Methodological constraints

Constraints of our study were mainly the size differences between the DMT scan windows, and that the sheep received

additional lucerne hay (200 g per animal per day) to fulfill their physiological diet requirements which might have had a polishing effect on otherwise more consistent DMT patterns (Ackermans et al., 2020). At present, we cannot rule out that the observed differences between the small mammals and the sheep were due to the larger scan windows investigated in the latter. If there was no random component that makes DMT wear patterns inherently inconsistent, then the size of the window should play no role. It should also play no role if a random component made a scale-independent, constant contribution to DMT patterns because a larger window would, in that scenario, just mean a larger number of both inherently consistent and inherently inconsistent wear elements. On the contrary, if we assume that a larger scan window increases the chance of detecting a more extensive range of DMT signals (Ramdarshan et al., 2017), we might expect more significant correlations among the DMT parameters due to these larger scan windows, not less. Future studies in guinea pigs and rabbits could further investigate the effect of different scan windows on DMT patterns.

The assumption that larger measurement ranges are more likely to yield significant parameter correlations seemed to hold within the guinea pig results. In the tooth position comparison (Figure 1) and the diet comparison (Figure 2), the group with the larger mean measurement range also had the higher mean correlation coefficient. This makes the inter-specific comparisons even more remarkable, where the species with the largest measurement range, the sheep, had less significant correlations between parameters (Figure 3). By carefully selecting teeth of animal groups that differed mainly in only one specific factor, such as tooth position (in the same set of animals), diet type across similar-sized groups of animals, or species across individuals that received similar diets, our analysis provides evidence that these factors do influence the inherent consistency of the wear pattern.

Dental microwear texture data range across the diet groups

Based on macroscopic measurements, it is well known that tooth wear affects individual tooth positions differently (Clauss et al., 2007; Laws, 2008; Müller et al., 2014, 2015; Martin et al., 2020, 2022), either due to the way the abrasives elements are distributed during chewing, the occlusal force along the jaw, the morphology of the occlusal surface, or the ontogenetic difference in the time the teeth are subjected to wear due to their eruption sequence. The same has been explored for microscopic wear along the tooth row: no gradient could be shown in ruminating species such as sheep (Ramdarshan et al., 2017; Ackermans et al., 2020) and blue wildebeest (Schulz et al., 2010), most likely due to the bidirectional chewing process while ruminating. By contrast, a microwear gradient

could be identified using DMTA in several crocodilians and varanid species (Bestwick et al., 2021) as well as in Grevy's zebras [*Equus grevyi*, (Schulz et al., 2010), rabbits (Martin et al., 2020) and guinea pigs (Winkler et al., 2021)]. The biomechanical properties of all the diets used in Winkler et al. (2021) and this study were undoubtedly very different: some animals received natural whole plant diets containing different amounts of phytoliths (up to 3.25% of acid detergent insoluble ash, a proxy for silica, in dry matter of bamboo); other lucerne based pellets with different size quartz abrasives (up to 8% fine silt for 8sS). After feeding on a pelleted diet, several DMT parameters in guinea pigs showed an increasing abrasive signal along the maxillary tooth row. Here, we show that the DMT data range across the diet groups is also higher on M2 compared to P4 and the concomitant correlation pattern is more robust with a higher mean correlation. The abrasive gradient seems to be represented not only in a few selected parameters and visual overview as seen in Winkler et al. (2021) but also in the overall DMT signal summarized as a mean correlation coefficient. Correlation patterns could be more efficient to recognize tooth wear gradients and mechanical changes in the chewing process than looking at each DMT parameter individually. The explanation for the more pronounced patterns in M2 compared to P4 may lie in the higher chewing forces that apply closer to the mandibular joint (Watson et al., 2014; Taylor et al., 2016). The M2 has a broader measurement range (Figure 1), implying that the higher chewing forces do not only lead to more distinct wear features but also a higher number of very mild wear traces, possibly caused by diet components that would not leave any trace at lower chewing forces.

We did not have enough data points to compare the gradient of the correlation pattern for individual diet groups. Still, we found a marked difference in correlation patterns between the natural and the pelleted diets when comparing the DMT across all teeth. Although consisting of the same material (dried lucerne), the pelleted diets most likely have a harder consistency than the whole dried plants. Additionally, whole plant processing most likely depends more on gnawing particle size reduction by the incisors prior to grinding by the cheek teeth, giving the material that reaches the cheek teeth a certain homogeneity that likely does not lead to particularly distinct wear traces. By contrast, pellets are crushed on the cheek teeth (Weijts and Dantuma, 1981), resulting in a large variety of wear traces, with larger DMT measurement ranges and more DMT correlations.

Dental microwear texture parameter correlations between and within different species

Comparing the correlation of DMT measured in sheep after a 17-month feeding experiment with the results in guinea

pigs fed the identical pelleted diets for 28–45 days, we show a clear difference between these species. DMT data in sheep was distributed over a more extensive data range, but DMT parameters correlate stronger and more consistently in the guinea pigs. The original sheep study reported solid correlations within the functional groups for height and volume parameters (Ackermans et al., 2021). Yet these correlations seem small compared to the intra- and intergroup correlations seen in guinea pigs (see [Supplementary Tables 3, 4](#)). This difference cannot be attributed to the feeding time difference, as microwear is thought to be an effect of a few tooth diet interactions (Teaford and Oyen, 1989) with a turnover rate of around 2 weeks in rats (*Rattus norvegicus*), for example (Winkler et al., 2020a). To further elucidate interspecies differences and avoid bias by looking only at highly abrasive diets, we compared sheep, guinea pigs, and rabbits fed a low-abrasive diet consisting of pelleted lucerne only. The normalized data range was again greater in sheep than in guinea pigs, while the small sample size can explain the narrow range in rabbits. Nevertheless, the correlations were again better in the hypselodont species.

In ruminant teeth, the chewing surface is not replaced anywhere near as expeditiously as in animals with hypselodont cheek teeth. Under natural feeding conditions in free-ranging animals, we expect the ruminant chewing surface to still display wear traces of diet items ingested a long time ago (Solounias et al., 1994; Damuth and Janis, 2014), which have not been overwritten entirely yet. However, in the present study, this effect was excluded due to the prolonged time the sheep received a consistent diet. Hence, another factor than the slow replacement of the chewing surface must be evoked to explain our findings. We hypothesize that the main driver for the more stable DMT correlations in guinea pigs is the supposedly softer enamel of species with hypselodont dentition (Shakila et al., 2015; Fischer et al., 2022). For the harder ruminant enamel, we hypothesize that wear trace formation is subject to a greater degree of randomness at the microscopic level due to the many factors involved in forming DMT wear traces. These factors include the volume of diet material between the teeth during a chewing stroke, the exact position of the abrasive components in the diet matrix, or the forces during a particular chewing stroke (Kaiser et al., 2016). The less malleable the trace-bearing surface, the more inconsistency in the recorded wear patterns of a specific diet is the apparent consequence. Again, this finding warns against considering tooth wear a taxon-free signal (Fischer et al., 2022), and suggests that understanding the formation of a single wear trace will remain a particular challenge (Van Casteren et al., 2020).

Conclusion

In guinea pigs, we demonstrate a stable correlation pattern of DMT parameters dependent on biomechanical properties

of the diet and tooth position. Interspecies comparisons show that regardless of abrasive source, DMT in hypselodont species shows a narrower data range and more robust correlation patterns. We propose that the correlation pattern is stronger when the abrasive wear increases on a particular tooth position or because of a higher abrasive diet, and when the tooth wear is measured in softer enamel. Based on the correlations pattern shown here, key DMT parameters can be identified in DMT datasets but require at least a diet consistency and diet abrasiveness, and a species or taxon-specific approach taking into consideration different chewing mechanisms and dental anatomy.

Data availability statement

The original contributions presented in this study are included in the article/[Supplementary material](#), further inquiries can be directed to the corresponding author.

Ethics statement

This animal study was reviewed and approved by Cantonal Veterinary Office of Zurich, Switzerland.

Author contributions

DW, TT, TK, DC, ES-K, J-MH, and MC designed the study. LM, DW, NA, JM, and MC performed the animal experiment. TK and ES-K provided analytical tools. LM and MC analyzed the data. LM and MC wrote the first draft of the manuscript, which received input from all co-authors. All authors contributed to the article and approved the submitted version.

Funding

The work of LM was funded in part by the Candoc Forschungskredit of the University of Zurich (FK-16-052) and a SNF grant (Schweizerischer Nationalfonds zur Förderung der Wissenschaftlichen Forschung, 31003A_163300/1) to J-MH, which also funded the sheep experiment. The guinea pig feeding experiment was funded by the European Research Council (ERC) under the European Union's Horizon 2020 Research and Innovation Program (ERC CoG grant agreement No. 681450) to TT. DW was granted a Postdoctoral fellowship from the Japan Society for the Promotion of Science (KAKENHI Grant No. 20F20325).

Acknowledgments

We thank Sandra Heldstab, Kathrin Zbinden (both University of Zurich), and Annelies De Cuyper (Ghent University) for their support in animal husbandry and Lisa Krause (University of Hamburg) for her initial DMTA work in the rabbits.

Conflict of interest

The authors declare that the research was conducted in the absence of any commercial or financial relationships that could be construed as a potential conflict of interest.

References

- Ackermans, N. L., Winkler, D. E., Martin, L. F., Kaiser, T. M., Clauss, M., and Hatt, J.-M. (2020). Dust and grit matter: Abrasives of different size lead to opposing dental microwear textures in experimentally fed sheep (*Ovis aries*). *J. Exp. Biol.* 223:jeb220442. doi: 10.1242/jeb.220442
- Ackermans, N. L., Winkler, D. E., Schulz-Kornas, E., Kaiser, T. M., Martin, L. F., Hatt, J. M., et al. (2021). Dental wear proxy correlation in a long-term feeding experiment on sheep (*Ovis aries*). *J. R. Soc. Interface* 18:20210139. doi: 10.1098/rsif.2021.0139
- Bestwick, J., Unwin, D. M., Henderson, D. M., and Purnell, M. A. (2021). Dental microwear texture analysis along reptile tooth rows: Complex variation with non-dietary variables. *R. Soc. Open Sci.* 8:201754. doi: 10.1098/rsos.201754
- Calandra, I., Schulz, E., Pinnow, M., Krohn, S., and Kaiser, T. M. (2012). Teasing apart the contributions of hard dietary items on 3D dental microtextures in primates. *J. Hum. Evol.* 63, 85–98. doi: 10.1016/j.jhevol.2012.05.001
- Clauss, M., Franz-Odenaál, T. A., Brasch, J., Castell, J. C., and Kaiser, T. (2007). Tooth wear in captive giraffes (*Giraffa camelopardalis*): Mesowear analysis classifies free-ranging specimens as browsers but captive ones as grazers. *J. Zoo Wildl. Med.* 38, 433–445. doi: 10.1638/06-032.1
- Damuth, J., and Janis, C. M. (2014). A comparison of observed molar wear rates in extant herbivorous mammals. *Ann. Zool. Fennici* 51, 188–200. doi: 10.5735/086.051.0219
- Desantis, L. R. G. (2016). Dental microwear textures: Reconstructing diets of fossil mammals. *Surf. Topogr.* 4:23002. doi: 10.1088/2051-672X/4/2/023002
- Donohue, S. L., Desantis, L. R. G., Schubert, B. W., and Ungar, P. S. (2013). Was the giant short-faced bear a hyper-scavenger? A new approach to the dietary study of ursids using dental microwear textures. *PLoS One* 8:e77531. doi: 10.1371/journal.pone.0077531
- Fischer, V. L., Winkler, D., Głogowski, R., Attin, T., Hatt, J.-M., Clauss, M., et al. (2022). Species-specific enamel differences in hardness and abrasion resistance between the permanent incisors of cattle (*Bos primigenius taurus*) and the ever-growing incisors of nutria (*Myocastor coypus*). *PLoS One* 17:e0265237. doi: 10.1371/journal.pone.0265237
- Hua, L. C., Brandt, E. T., Meullenet, J. F., Zhou, Z. R., and Ungar, P. S. (2015). Technical note: An in vitro study of dental microwear formation using the Bite Master II chewing machine. *Am. J. Phys. Anthropol.* 158, 769–775. doi: 10.1002/ajpa.22823
- International Organization For Standardization (2012). *ISO 25178-2, geometrical product specifications (Gps)—surface texture: Areal—Part 2: Terms, definitions and surface texture parameters*. Geneva: ISO.
- Kaiser, T. M., Clauss, M., and Schulz-Kornas, E. (2016). A set of hypotheses on tribology of mammalian herbivore teeth. *Surf. Topogr.* 4:014003. doi: 10.1088/2051-672X/4/1/014003
- Karme, A., Rannikko, J., Kallonen, A., Clauss, M., and Fortelius, M. (2016). Mechanical modelling of tooth wear. *J. R. Soc. Interface* 13:20160399. doi: 10.1098/rsif.2016.0399
- Korzynski, M., Dudek, K., Palczak, A., Kruczek, B., and Kocurek, P. (2018). Experimental models and correlations between surface parameters after slide diamond burnishing. *Meas. Sci. Rev.* 18, 123–129. doi: 10.1515/msr-2018-0018
- Laws, R. (2008). Dentition and ageing of the hippo. *Afr. J. Ecol.* 6, 19–52. doi: 10.1111/j.1365-2028.1968.tb00899.x
- Louail, M., Ferchaud, S., Souron, A., Walker, A. E. C., and Merceron, G. (2021). Dental microwear textures differ in pigs with overall similar diets but fed with different seeds. *Palaeogeogr. Palaeoclimatol. Palaeoecol.* 572:110415. doi: 10.1016/j.palaeo.2021.110415
- Martin, L. F., Ackermans, N. L., Tollefson, T. N., Kircher, P. R., Richter, H., Hummel, J., et al. (2022). Tooth wear, growth and height in rabbits (*Oryctolagus cuniculus*) fed pelleted or extruded diets with or without added abrasives. *J. Anim. Physiol. Anim. Nutr.* 106, 630–641. doi: 10.1111/jpn.13565
- Martin, L. F., Krause, L., Ulbricht, A., Winkler, D. E., Codron, D., Kaiser, T. M., et al. (2020). Dental wear at macro- and microscopic scale in rabbits fed diets of different abrasiveness: A pilot investigation. *Palaeogeogr. Palaeoclimatol. Palaeoecol.* 556:109886. doi: 10.1016/j.palaeo.2020.109886
- Martius, N. L., Sidéra, I., Grote, M. N., Steele, T. E., Mcpherron, S. P., and Schulz-Kornas, E. (2018). Time wears on: Assessing how bone wears using 3D surface texture analysis. *PLoS One* 13:e0206078. doi: 10.1371/journal.pone.0206078
- Merceron, G., Ramdarshan, A., Blondel, C., Boisserie, J.-R., Brunetiere, N., Francisco, A., et al. (2016). Untangling the environmental from the dietary: Dust does not matter. *Proc. R. Soc. B Biol. Sci.* 283:20161032. doi: 10.1098/rspb.2016.1032
- Müller, J., Clauss, M., Codron, D., Schulz, E., Hummel, J., Fortelius, M., et al. (2014). Growth and wear of incisor and cheek teeth in domestic rabbits (*Oryctolagus cuniculus*) fed diets of different abrasiveness. *J. Exp. Zool.* 321, 283–298. doi: 10.1002/jez.1864
- Müller, J., Clauss, M., Codron, D., Schulz, E., Hummel, J., Kircher, P., et al. (2015). Tooth length and incisal wear and growth in guinea pigs (*Cavia porcellus*) fed diets of different abrasiveness. *J. Anim. Physiol. Anim. Nutr.* 99, 591–604. doi: 10.1111/jpn.12226
- Ramdarshan, A., Blondel, C., Gautier, D., Surault, J., and Merceron, G. (2017). Overcoming sampling issues in dental tribology: Insights from an experimentation on sheep. *Palaeontol. Electron.* 20, 1–19. doi: 10.26879/762
- Robinet, C., Merceron, G., Candela, A. M., and Marivaux, L. (2020). Dental microwear texture analysis and diet in caviomorphs (Rodentia) from the Serra do Mar Atlantic forest (Brazil). *J. Mammal.* 101, 386–402. doi: 10.1093/jmammal/gyz194

Publisher's note

All claims expressed in this article are solely those of the authors and do not necessarily represent those of their affiliated organizations, or those of the publisher, the editors and the reviewers. Any product that may be evaluated in this article, or claim that may be made by its manufacturer, is not guaranteed or endorsed by the publisher.

Supplementary material

The Supplementary Material for this article can be found online at: <https://www.frontiersin.org/articles/10.3389/fevo.2022.958576/full#supplementary-material>

- Robinet, C., Merceron, G., Catzeflis, F., Candela, A. M., and Marivaux, L. (2022). About inter- and intra-specific variability of dental microwear texture in rodents: Study of two sympatric *Proechimys* (Echimyidae) species from the Cacao locality, French Guiana. *Palaeogeogr. Palaeoclimatol. Palaeoecol.* 591:110880. doi: 10.1016/j.palaeo.2022.110880
- Rodriguez-Rojas, F., Borrero-Lopez, O., Constantino, P. J., Henry, A. G., and Lawn, B. R. (2020). Phytoliths can cause tooth wear. *J. R. Soc. Interface* 17:20200613. doi: 10.1098/rsif.2020.0613
- Schulz, E., Calandra, I., and Kaiser, T. (2010). Applying tribology to teeth of hoofed mammals. *Scanning* 32, 162–182. doi: 10.1002/sca.20181
- Schulz, E., Piotrowski, V., Clauss, M., Mau, M., Merceron, G., and Kaiser, T. M. (2013). Dietary abrasiveness is associated with variability of microwear and dental surface texture in rabbits. *PLoS One* 8:e56167. doi: 10.1371/journal.pone.0056167
- Schulz-Kornas, E., Stuhltrager, J., Clauss, M., Wittig, R. M., and Kupczik, K. (2019). Dust affects chewing efficiency and tooth wear in forest dwelling Western chimpanzees (*Pan troglodytes verus*). *Am. J. Phys. Anthropol.* 169, 66–77. doi: 10.1002/ajpa.23808
- Schulz-Kornas, E., Winkler, D. E., Clauss, M., Carlsson, J., Ackermans, N. L., Martin, L. F., et al. (2020). Everything matters: Molar microwear texture in goats (*Capra aegagrus hircus*) fed diets of different abrasiveness. *Palaeogeogr. Palaeoclimatol. Palaeoecol.* 552:109783. doi: 10.1016/j.palaeo.2020.109783
- Scott, R. S., Ungar, P. S., Bergstrom, T. S., Brown, C. A., Childs, B. E., Teaford, M. F., et al. (2006). Dental microwear texture analysis: Technical considerations. *J. Hum. Evol.* 51, 339–349. doi: 10.1016/j.jhevol.2006.04.006
- Shakila, N., Ali, A., and Zaidi, S. (2015). Micro hardness of dental tissues influenced by administration of aspirin during pregnancy. *Int. J. Morphol.* 33, 586–593. doi: 10.4067/S0717-95022015000200028
- Solounias, N., Fortelius, M., and Freeman, P. (1994). Wear rates in ruminants. *Ann. Zool. Fennici* 31, 219–227.
- Stuhlträger, J., Schulz-Kornas, E., Wittig, R. M., and Kupczik, K. (2019). Ontogenetic dietary shifts and microscopic tooth wear in western chimpanzees. *Front. Ecol. Evol.* 7:298. doi: 10.3389/fevo.2019.00298
- Taylor, L. A., Müller, D. W. H., Schwitzer, C., Kaiser, T. M., Castell, J. C., Clauss, M., et al. (2016). Comparative analyses of tooth wear in free-ranging and captive wild equids. *Equine Vet. J.* 48, 240–245. doi: 10.1111/evj.12408
- Teaford, M. F., and Oyen, O. J. (1989). In vivo and in vitro turnover in dental microwear. *Am. J. Phys. Anthropol.* 80, 447–460. doi: 10.1002/ajpa.1330800405
- Teaford, M. F., Ungar, P. S., Taylor, A. B., Ross, C. F., and Vinyard, C. J. (2017). In vivo rates of dental microwear formation in laboratory primates fed different food items. *Biosurf. Biotribol.* 3, 166–173. doi: 10.1016/j.bsbt.2017.11.005
- Tian, Y., Wang, J., Peng, Z., and Jiang, X. (2012). A new approach to numerical characterisation of wear particle surfaces in three-dimensions for wear study. *Wear* 282, 59–68. doi: 10.1016/j.wear.2012.02.002
- Van Casteren, A., Strait, D. S., Swain, M. V., Michael, S., Thai, L. A., Philip, S. M., et al. (2020). Hard plant tissues do not contribute meaningfully to dental microwear: Evolutionary implications. *Sci. Rep.* 10:582. doi: 10.1038/s41598-019-57403-w
- Wang, M., Peng, Z., Wang, J., and Jiang, X. (2013). Wear characterisation of articular cartilage surfaces at a nano-scale using atomic force microscopy. *Tribol. Int.* 63, 235–242. doi: 10.1016/j.triboint.2012.11.001
- Watson, P. J., Gröning, F., Curtis, N., Fitton, L. C., Herrel, A., McCormack, S. W., et al. (2014). Masticatory biomechanics in the rabbit: A multi-body dynamics analysis. *J. R. Soc. Interface* 11:20140564. doi: 10.1098/rsif.2014.0564
- Wei, T., and Simko, V. (2021). R package 'corrplot': Visualization of a correlation matrix. *^cy, pub.*
- Weijs, W. A., and Dantuma, R. (1981). Functional anatomy of the masticatory apparatus in the rabbit (*Oryctolagus cuniculus*). *Neth. J. Zool.* 31, 99–147. doi: 10.1163/002829680X00212
- Wickham, H. (2016). *ggplot2: Elegant graphics for data analysis*. New York, NY: Springer-Verlag. doi: 10.1007/978-3-319-24277-4
- Wickham, H., Averick, M., Bryan, J., Chang, W., McGowan, L., François, R., et al. (2019). Welcome to the tidyverse. *J. Open Source Softw.* 4:1686. doi: 10.21105/joss.01686
- Winkler, D. E., Andrianasolo, T. H., Andriamandimbiasoa, L., Ganzhorn, J. U., Rakotondranary, S. J., Kaiser, T. M., et al. (2016). Tooth wear patterns in black rats (*Rattus rattus*) of Madagascar differ more in relation to human impact than to differences in natural habitats. *Ecol. Evol.* 6, 2205–2215. doi: 10.1002/ece3.2048
- Winkler, D. E., Clauss, M., Rölle, M., Schulz-Kornas, E., Codron, D., Kaiser, T. M., et al. (2021). Dental microwear texture gradients in guinea pigs reveal that material properties of the diet affect chewing behaviour. *J. Exp. Biol.* 224:jeb.242446. doi: 10.1242/jeb.242446
- Winkler, D. E., and Kaiser, T. (2015). Uneven distribution of enamel in the tooth crown of a Plains Zebra (*Equus quagga*). *PeerJ.* 3:e1002. doi: 10.7717/peerj.1002
- Winkler, D. E., Schulz-Kornas, E., Kaiser, T. M., Codron, D., Leichter, J., Hummel, J., et al. (2020a). The turnover of dental microwear texture: Testing the "last supper" effect in small mammals in a controlled feeding experiment. *Palaeogeogr. Palaeoclimatol. Palaeoecol.* 557:109930. doi: 10.1016/j.palaeo.2020.109930
- Winkler, D. E., Schulz-Kornas, E., Kaiser, T. M., De Cuyper, A., Clauss, M., and Tütken, T. (2019). Forage silica and water content control dental surface texture in guinea pigs and provide implications for dietary reconstruction. *Proc. Natl. Acad. Sci. U.S.A.* 116, 1325–1330. doi: 10.1073/pnas.1814081116
- Winkler, D. E., Tütken, T., Schulz-Kornas, E., Kaiser, T. M., Müller, J., Leichter, J., et al. (2020b). Shape, size, and quantity of ingested external abrasives influence dental microwear texture formation in guinea pigs. *Proc. Natl. Acad. Sci. U.S.A.* 117:22264. doi: 10.1073/pnas.2008149117
- Yamada, E., Kubo, M. O., Kubo, T., and Kohno, N. (2018). Three-dimensional tooth surface texture analysis on stall-fed and wild boars (*Sus scrofa*). *PLoS One* 13:e0204719. doi: 10.1371/journal.pone.0204719



OPEN ACCESS

EDITED BY

Ferran Estebanaranz-Sánchez,
Milá y Fontanals Institution
for Research in Humanities (CSIC),
Spain

REVIEWED BY

Mark Purnell,
University of Leicester,
United Kingdom
Gina Marie Semperebon,
Bay Path University, United States
Mark Teaford,
Touro University California,
United States

*CORRESPONDENCE

Thomas Tütken
tuetken@uni-mainz.de

SPECIALTY SECTION

This article was submitted to
Paleoecology,
a section of the journal
Frontiers in Ecology and Evolution

RECEIVED 31 May 2022

ACCEPTED 01 September 2022

PUBLISHED 27 September 2022

CITATION

Winkler DE, Clauss M, Kubo MO,
Schulz-Kornas E, Kaiser TM,
Tschudin A, De Cuyper A, Kubo T and
Tütken T (2022) Microwear textures
associated with experimental
near-natural diets suggest that seeds
and hard insect body parts cause high
enamel surface complexity in small
mammals.
Front. Ecol. Evol. 10:957427.
doi: 10.3389/fevo.2022.957427

COPYRIGHT

© 2022 Winkler, Clauss, Kubo,
Schulz-Kornas, Kaiser, Tschudin, De
Cuyper, Kubo and Tütken. This is an
open-access article distributed under
the terms of the [Creative Commons
Attribution License \(CC BY\)](#). The use,
distribution or reproduction in other
forums is permitted, provided the
original author(s) and the copyright
owner(s) are credited and that the
original publication in this journal is
cited, in accordance with accepted
academic practice. No use, distribution
or reproduction is permitted which
does not comply with these terms.

Microwear textures associated with experimental near-natural diets suggest that seeds and hard insect body parts cause high enamel surface complexity in small mammals

Daniela E. Winkler ^{1,2,3}, Marcus Clauss ⁴,
Mugino O. Kubo ², Ellen Schulz-Kornas ^{3,5},
Thomas M. Kaiser ³, Anja Tschudin ⁶,
Annelies De Cuyper ⁷, Tai Kubo ^{2,8} and
Thomas Tütken ^{1*}

¹Applied and Analytical Palaeontology, Institute of Geosciences, Johannes Gutenberg University, Mainz, Germany, ²Department of Natural Environmental Studies, Graduate School of Frontier Sciences, The University of Tokyo, Kashiwa, Chiba, Japan, ³Leibniz Institute for the Analysis of Biodiversity Change, Zoological Museum, Hamburg, Germany, ⁴Clinic for Zoo Animals, Exotic Pets and Wildlife, Vetsuisse Faculty, University of Zurich, Zurich, Switzerland, ⁵Department of Cariology, Endodontology and Periodontology, University of Leipzig, Leipzig, Germany, ⁶Granovit Zoofeed, Granovit AG, Kaiseraugst, Switzerland, ⁷Department of Veterinary and Biosciences, Faculty of Veterinary Medicine, Ghent University, Merelbeke, Belgium, ⁸The University Museum, The University of Tokyo, Tokyo, Japan

In mammals, complex dental microwear textures (DMT) representing differently sized and shaped enamel lesions overlaying each other have traditionally been associated with the seeds and kernels in frugivorous diets, as well as with sclerotized insect cuticles. Recently, this notion has been challenged by field observations as well as *in vitro* experimental data. It remains unclear to what extent each food item contributes to the complexity level and is reflected by the surface texture of the respective tooth position along the molar tooth row. To clarify the potential of seeds and other abrasive dietary items to cause complex microwear textures, we conducted a controlled feeding experiment with rats. Six individual rats each received either a vegetable mix, a fruit mix, a seed mix, whole crickets, whole black soldier fly larvae, or whole day-old-chicks. These diets were subjected to material testing to obtain mechanical properties, such as Young's modulus, yield strength, and food hardness (as indicated by texture profile analysis [TPA] tests). Seeds and crickets caused the highest surface complexity. The fruit mix, seed mix, and crickets caused the deepest wear features. Moreover, several diets resulted in an increasing wear gradient from the first to the second molar, suggesting that increasing bite force along the tooth row affects dental wear in rats on these diets. Mechanical properties of the diets showed different

correlations with DMT obtained for the first and second molars. The first molar wear was mostly correlated with maximum TPA hardness, while the second molar wear was strongly correlated with maximum yield stress, mean TPA hardness, and maximum TPA hardness. This indicates a complex relationship between chewing mechanics, food mechanical properties, and observed DMT. Our results show that, in rats, seeds are the main cause of complex microwear textures but that hard insect body parts can also cause high complexity. However, the similarity in parameter values of surface textures resulting from seed and cricket consumption did not allow differentiation between these two diets in our experimental approach.

KEYWORDS

hard-object feeding, mechanical properties, dental wear, material properties, microwear

Introduction

The reconstruction of paleodiets is a central aspect of paleoecology. Diet provides insights not only to an animal's ecology but also, indirectly, to aspects of its habitat and predominant climatic conditions (e.g., closed vs. open, arid vs. humid) (e.g., Merceron et al., 2007a,b; Rivals et al., 2008) and on how these are linked to the evolution of different taxa (e.g., Teaford and Ungar, 2000). Thus, methods for paleodietary inference have always been of interest to the scientific community, but even more so when they allowed inferences about our ancestors and human evolution (e.g., Walker, 1981). However, when hominids are involved, not only is the interest but also the potential for debate high, as new results may challenge long-standing paradigms (Lee-Thorp, 2011). One important question is whether seeds played a prominent role as a key dietary component responsible for distinct morphological adaptations like thick enamel, enlarged, bunodont teeth, and complex microwear patterns. It applies to primates in general and hominids in particular.

Extant primates (Kay, 1981; Dumont, 1995; Shellis et al., 1998; Martin et al., 2003) and bats (Dumont, 1995) that incorporate a large proportion of so-called hard objects into their diet possess thick enamel. Hence, the presence of thick enamel has also been interpreted as an adaptation toward hard-object feeding in fossil species (e.g., Alba et al., 2010), including hominids (e.g., Martin et al., 2003). The relationship is, however, not straightforward, as thinner enamel may also be suitable for processing hard objects, as seen, for instance, in sea otters (Constantino et al., 2011). It seems that tooth crown morphology, enamel distribution, and enamel microstructure also need to be considered to predict the resistance of teeth during hard-object feeding (Constantino et al., 2011; Ungar, 2011; Schwartz et al., 2020).

Microwear and dental microwear texture (DMT) are often-applied “proxies” that are analyzed to infer the mechanical properties of the foods consumed (Calandra and Merceron, 2016). By directly observing the two-dimensional (pits and scratches) (Rivals et al., 2007; Semprebon and Rivals, 2007) or three-dimensional (roughness, complexity, anisotropy) patterns on enamel wear facets in extant species, inferences can be drawn about the dietary habits of extinct species (e.g., Scott et al., 2005; Ungar et al., 2008, 2010; DeSantis et al., 2012). One long-standing paradigm regarding specifically primate and hominid diets has been that hard object feeding (i.e., seeds and nuts) results in pitted enamel surfaces (Grine and Kay, 1988) with high complexity (Scott et al., 2005, 2012; Daegling et al., 2011).

However, there are cases when dental morphology and observed microwear features seem to be incongruent. The genus *Paranthropus* is an excellent example of how similar morphologies may have been used in different dietary specializations (Ungar et al., 2008; Sponheimer et al., 2022). There is an ongoing debate whether their enlarged molars with thick enamel caps were an adaptation for processing bulk low-quality forage (e.g., grasses). The similarity of the enlarged molars to extant hard object-feeders (e.g., otters, peccary) suggests that fracture resistance while processing nuts and seeds was the driving force behind the evolution of this particular tooth morphology [see Sponheimer et al. (2022) for a comprehensive review].

Both eastern (*Paranthropus boisei*) and southern (*Paranthropus robustus*) members of the genus *Paranthropus* possessed enlarged, bunodont molars with thick enamel caps, yet their reconstructed diet differs drastically. Dental microwear texture analysis (DMTA) (Ungar et al., 2008; Ungar, 2012) and isotope evidence (van der Merwe et al., 2008) suggest that *P. boisei* was primarily feeding on C₄/CAM plants (and/or meat of animals that consumed C₄ grasses), which is considered

tough but not hard food—an interpretation not easily reconciled with their thick enamel cusps (Sponheimer et al., 2022). By contrast, *P. robustus* is reconstructed as a hard-object feeder (Constantino et al., 2018), based on microwear and DMTA that reveal high complexity but low anisotropy values, both typically associated with hard-object feeding (Scott et al., 2005; Ungar et al., 2008; Ungar and Berger, 2018). Until recently, the diet of *P. robustus* was less subject to debate, as most studies (microwear, DMTA, tooth macrowear) suggested hard objects as an important dietary component. When talking about hard objects in an herbivorous diet, we usually imply seeds and nuts (Daegling et al., 2011; Ungar and Sponheimer, 2011).

Recently, this notion has been challenged by an experimental *in vitro* study by van Casteren et al. (2020). *In vitro*, they brought endocarps into contact with isolated human teeth and found that the endocarp *per se* was not able to cause deep lesions but only rubbing (plastic deformation) of the enamel. Thus, they concluded that seeds could not be the source of the high complexity in surface textures that were conventionally associated with hard-object feeding. Moreover, they suggested that this would bring seeds back on the table as a possible diet for *Paranthropus boisei*, as the lack of complexity in microwear textures would no longer be indicative of an absence of seeds in the diet. This is not the first debate that has arisen in the dental wear community. Similarly, the discussion of whether phytoliths (amorphous silica bodies inside the plant tissue) or external grit and mineral dust are more responsible for abrasive wear has been a long one as controlled feeding experiments provided abundant evidence for the importance of both as dietary abrasives (Merceron et al., 2016; Winkler et al., 2019a, 2020a; Schulz-Kornas et al., 2020a). Similarly, controlled feeding experiments demonstrated that hard-object (nut) feeding results in new dental microwear features after only one feeding bout in capuchin monkeys (Teaford et al., 2020), and the inclusion of seeds or nuts into otherwise identical diets results in distinct DMT in pigs (Louail et al., 2021), but without resolving whether high complexity is linked to seed consumption.

In the present study, we conducted a feeding experiment with rats to better determine which naturally ingested animal and plant diets can produce high complexity (in absence of external abrasives). We chose rats because they are omnivorous and can deal with various diets. Rat molar teeth have served as models for human molars in numerous studies, although evident differences in masticatory behavior and dental morphology are acknowledged (Ohba, 1974; Nishijima et al., 2007, 2009; Dammaschke, 2010). Rats cannot serve as a model organism for replication of the *Paranthropus* masticatory behavior. What rats can do, however, is to show what kind of diets do result in more complex microwear textures that are traditionally associated with herbivorous hard-object feeding.

Diets of omnivores are naturally diverse and complex in composition and are thus likely diverse in mechanical

properties, and we did not aim at mimicking the natural diet of either rats or primates. Rather, we aimed to design experimental diets that resemble a specialized feeding type. Thus, we used several herbivore and faunivore diets with different components that remain constant over the duration of the experiment: a vegetable mix, a fruit mix (whole fruits with seeds), a seed mix (legume, C₃ and C₄ grass, and sunflower seeds), whole house crickets (hereafter: crickets), whole black soldier fly larvae (hereafter: BSFL) and whole day-old chicks (hereafter: daychicks). We subjected these diets to tests of mechanical properties that can be obtained through compression tests to relate them to the observed DMT. The mechanical properties we focused on were as follows: Young's modulus (*E*), yield stress, and texture profile analysis (TPA) hardness, because they are well-represented in biomechanical anthropological studies (Young's modulus, yield stress) (e.g., Lucas et al., 2009; Thompson et al., 2014; Berthaume, 2016) or food texture studies (TPA hardness) (e.g., Nishinari et al., 2019). In addition, they can be obtained with a relatively simple analytical setup. We note that this approach is simplified and does not cover other commonly used measures of mechanical properties (e.g., obtained through wedge or scissor tests) or potential cuticle hardness in insects (Evans and Sanson, 2005) and have discussed the benefits and limitations.

In a previous study on guinea pigs, we found that, for hard and brittle, pelleted diets, a DMTA gradient indicating increasing wear from front to rear along the molar tooth row could be observed (Winkler et al., 2021), while natural plant diets displayed no such gradient or even showed an opposite trend of decreasing wear from the fourth premolar toward the third molar. As the rats in the present study were subjected to diets of very different mechanical properties, we were interested to see if they would also show tooth position-specific differences that reflected specific mastication behavior on different diets. We thus compared DMTA not only between diet groups but also between the first and second upper molars within each diet group.

Materials and methods

The feeding experiment was approved by the Swiss Cantonal Animal Care and Use Committee Zurich (animal experiment license No. ZH135/16) and was conducted during February/March 2018 at the Vetsuisse Faculty, University of Zurich. All animals in this experiment were female adult WISTAR (RjHan:WI) rats (*Rattus norvegicus* forma domestica; *n* = 36; initial body mass = 216.5 ± 16.5 g; initial age 12–14 weeks). Rats were kept in groups of 3 in indoor stables (0.58 m² each), each equipped with one or two large food dishes containing their assigned experimental diet and two nipple drinkers of tap water. Stables were enriched with dust-free softwood granulate, a shelter, a climbing frame, two tubes,

and a running plate (Frei et al., 2021). Two groups (i.e., 6 animals in total) received the same diet for 37 consecutive days. Initially, the breeder diet was provided in addition to the experimental diet and phased out until the 5th day of the experiment. Following the conclusion of the experiment, animals were euthanized with carbon dioxide and enzymatic maceration of the skulls was conducted at LIB Hamburg [former Center of Natural History (CeNak) of the University of Hamburg]. For the vegetable and fruit groups, one specimen each lost its label during maceration and could not be assigned without uncertainty to the correct diet group. Thus, the groups of vegetable and fruit eaters are only comprised of five individuals each.

Experimental diets

The six experimental diets consisted of a vegetable mix, a fruit mix, a seed mix, crickets, black soldier fly larvae, and day-old chicks. Weight percentages of each main dietary component are given in [Table 1](#). Diets were designed to be isocaloric and to contain all nutrients to sustain healthy growth in a 250 g rat. Rats received their designated diets one time per day in the morning. Each diet was supplemented by a specifically balanced supplement powder that was admixed to a quark (a type of dairy product, also known as curd or curd cheese) or a quark and sunflower oil base ([Table 1](#)), which were chosen as additional protein and fat supply that could not be chewed but had to be lapped up by the animals. The composition of each supplement powder is given in the [Supplementary Table 1](#).

Mechanical properties testing and limitations

Several diets included a mixture of food items, with likely different mechanical properties. Thus, rats could theoretically choose foods that they preferred over foods they disliked. Such behavior was observed in the group receiving a vegetable mix, where several rats would avoid eating root celery (pers. observation DEW). The groups receiving crickets and black soldier fly larvae had no such choice, except for avoiding eating body parts of the crickets (e.g., legs). Similarly, the daychick group could selectively feed on certain parts of the whole daychicks, but only left the beak and parts of the integument with feathers (pers. observation DEW). In the groups receiving fruit mixture and seed mixture, no preferences were observed, as food was consumed completely. However, we cannot rule out that individual rats had specific preferences and avoided specific items, while other rats consumed them. Therefore, we expect more variability of DMT parameters in groups that received a mixture of food items (vegetables, fruits, and seeds) as compared to more homogenous diets (crickets, BSFL, and daychicks).

Although the behavior and individual preferences of the rats could likely affect the items they consumed (and thus the tooth wear they developed), we conducted compression tests to derive quantitative mechanical properties of the items. Through the compression tests, we obtained stress-strain curves from which representative mechanical properties, i.e., Young's modulus, yield stress, and TPA hardness, were calculated. Due to limitations in the preparation of analyzed samples, these three mechanical properties could not be obtained simultaneously for all items but had to be derived from linear regressions with other highly correlated mechanical properties (see Statistics section).

For obtaining Young's modulus and yield stress, samples of fruit and vegetables were cut into rectangular, circular, or cubic pieces; seeds were tested as whole grains and insects as whole specimens. In crickets, we additionally tested the head capsule and the gizzard separately. For both, an approximately circular shape was assumed. The surface area of whole insects and grains was approximated from a rectangular shape. For daychicks, it was not possible to obtain circular or rectangular pieces, thus we only subjected them to TPA hardness tests (see below). The vegetable diet included two leafy greens (parsley, spinach) which are not suitable for compression tests. We did not assess the mechanical properties of these two items. Similarly, for the fruit mix, we restricted testing of figs to the isolated fig seeds, as the available figs were too soft to be cut into circular or rectangular pieces. Fig seeds are expected to be the hardest component of the fruit mix diet and, consequently, to contribute more to the observed wear differences than the soft parts of the figs.

Testing was conducted over several days of one week, in the same laboratory environment, to reduce variations in humidity and temperature. Each sample was placed on a circular platform of 60 mm diameter under a force gauge and compressed in a cutoff setup until breaking or until the force gauge registered an overload (due to contact with the platform). We used circular solid testers of different diameters (60 mm, 15 mm, 3 mm) but ensured that the tester was larger than the sample for obtaining Young's modulus and yield stress so that compression would be evenly exerted over the complete surface area of the sample. The movement speed of the circular solid tester was set to 600 mm/min and the test speed (from contact point on) to 120 mm/min. We used two different force gauges, HF-100 and HF-10 (JISC, Japan Instrumental Systems Inc., Nara, Japan), attached to an automated servo stand (JSV-H1000, JISC, Japan Instrumental Systems Inc., Nara, Japan). The HF-100 has a maximum load capacity of 1000 N and a resolution of 0.1 N, while the HF-10 has a maximum load capacity of 100 N and a resolution of 0.01 N. Thus, for soft, easily deformable samples, the force gauge HF-10 with a higher precision was employed. For fruit and vegetables that were fed including the skin, we conducted multiple compression tests both from the skin side or from the side without skin. A representative stress-strain diagram and the results of mechanical properties testing are shown in [Figure 1](#). Detailed results of mechanical properties

(Young's modulus, yield stress, false yield stress, TPA hardness) are illustrated in [Supplementary Tables 2–4](#). We note that values obtained for Young's modulus are negative, because we used a compression setup. However, the sign is usually omitted in the literature, thus when we are referring to larger Young's modulus, we would refer to a more negative value. To avoid confusion, we presented all values as positive numbers.

Additionally, the food texture tester TEX-100 (JISC, Japan Instrumental Systems Inc., Nara, Japan) was used to obtain the standardized parameter TPA hardness. In food science, TPA hardness is measured by compressing a sample two times for the same compression depth or ratio, with the peak force occurring during the first compression divided by the tester area being the hardness (Bourne, 2002; Nishinari et al., 2019). An example curve is represented in [Supplementary Figure 1](#). All raw measurement results are given in [Supplementary Table 4](#). We used a 3-mm circular solid tester (area = 7.069 mm²), at a test movement speed of 120 mm/min, and an indentation depth of 2 mm. We chose this small 3-mm tester following the advice from Nishinari et al. (2019) that the tester should be less than one-third of the diameter of the sample. The hold time between the first and second indentations was set to 3 s. This hardness measure is different from (micro) indentation hardness measures such as Vickers or Knoop hardness. As TPA hardness should only be measured on food items with a certain elasticity so that repeated compression would be possible, we did not test individual items from the seed mix, the cricket head capsules, and the cricket gizzards using this procedure, as they fractured during the first indentation.

Dental microwear texture measurements

Measurements were conducted at the LIB Hamburg [former Center of Natural History (CeNak) of the University of Hamburg], Germany, on a μ surf Custom (NanoFocus AG, Oberhausen, Germany) confocal disc-scanning microscope, equipped with a blue LED (470 nm) and high-speed progressive-scan digital camera (984 × 984 pixel), a 100x long working-distance objective (resolution in $x, y = 0.16 \mu\text{m}$, step size in $z = 0.06 \mu\text{m}$), following the published routine for DMT data (Schulz et al., 2010, 2013) with adjustment for rats (Winkler et al., 2016) and guinea pigs (Winkler et al., 2019a, 2020a, 2021). Measurements were performed on original tooth surfaces of the first and second upper molars on central anterior enamel bands. Depending on wear stage and preservation, up to four (minimum 2) non-overlapping scans were taken from each specimen. Forty-four DMT parameters were calculated after filtering surfaces [leveling, spatial filtering (denoising median 5 × 5 filter size and Gaussian 3 × 3 filter size

with default cut-offs), filling of non-measured points, noise-reduction by thresholding (upper and lower 0.5%), removal of outliers (maximum slope of 85%), 2nd order form removal] and cropping them to 60 × 60 μm in MountainsMap v.9.0.9878. From the two to four scans per specimen, median values were calculated for each parameter to adequately represent the surface texture of the enamel and avoid bias by picking particularly worn or unworn locations. Parameter results for each specimen are given in [Supplementary Table 5](#).

Statistics

Descriptive and test statistics were computed in JMP Pro v. 16.0. A non-parametric, heteroscedastic pairwise comparison test (Wilcoxon test) was performed for DMTA of all dietary pairs. The application of multiple comparison tests increases the probability of Type I error; however, conservative corrections for multiple testing would inflate the probability of Type II error in small samples such as ours. We hence applied the Benjamini-Hochberg procedure with an accepted false discovery rate (FDR) of 0.25. We therefore note that the results of diet group comparisons presented here were prone to include false positives but accepted this on the basis of it being an exploratory study and including both raw p -values and critical p -values using an FDR of 0.25 into the supplements ([Supplementary Table 10](#)).

Mechanical properties parameters (Young's modulus, yield stress, TPA hardness) were repeatedly measured for multiple individual samples (4–20 repetitions) and then averaged for each dietary item. Individual measurements are given in [Supplementary Tables 2–4](#). Some diets were composed of several different items (vegetable mix, fruit mix, seed mix), while others were composed of one item only (BSFL, crickets, and daychicks). To generate representative mechanical properties from each diet, we calculated two values for each mechanical properties parameter: a weighted mean using relative proportions of diet items and a maximum using the largest value obtained for an individual diet component. For crickets, we tested whole specimens, head capsules, and gizzards and calculated a weighted mean based on weight percentages ([Supplementary Tables 6, 7](#)). For the diets BSFL and daychicks, the weighted mean and maximum value were identical.

As we could not obtain either Young's modulus and yield stress for daychicks or TPA hardness for the seed mix, cricket heads, and cricket gizzards, we used linear regressions to establish the nature of the relationships between measurable mechanical properties and used these regressions to infer the parameter values that we were unable to measure.

A fourth parameter, false yield strength, was employed to estimate yield stress for daychicks. We calculated false yield strength during compression of irregularly shaped objects as maximum force recorded divided by the area of the circular

TABLE 1 Composition of experimental diets (weight %) and supplementation in % fresh weight.

Diet name	Composition						Supplementation		
Vegetable mix	Celery root (32.2%)	Carrot (27.1%)	Stalk celery (10.9%)	Kohlrabi (10.7%)	Parsley (10.1%)	Spinach (9.00%)	Quark (7.3%)	Sunflower oil (1.2%)	Suppl. powder (0.8%)
Fruit mix		Figs (37.20%)	Banana (22.0%)	Papaya (17.0%)	Apple (12.7%)	Mango (11.2%)	Quark (20.1%)	Sunflower oil (1.1%)	Suppl. powder (1.1%)
Seed mix	Wheat (25%)	Barley (20%)	Dried peas (20%)	Oats (15%)	Corn (10%)	Sunflower kernels (10%)	Quark (22.2%)	Suppl. powder (7.7%)	
Crickets	Whole frozen crickets						Quark (9.8%)	Suppl. powder (3.4%)	
Black soldier fly larva	Whole frozen black soldier fly larvae						Quark (12.1%)	Suppl. powder (4.3%)	
Daychicks	Whole frozen day-old chicks						Quark (8.3%)	Suppl. powder (3.0%)	

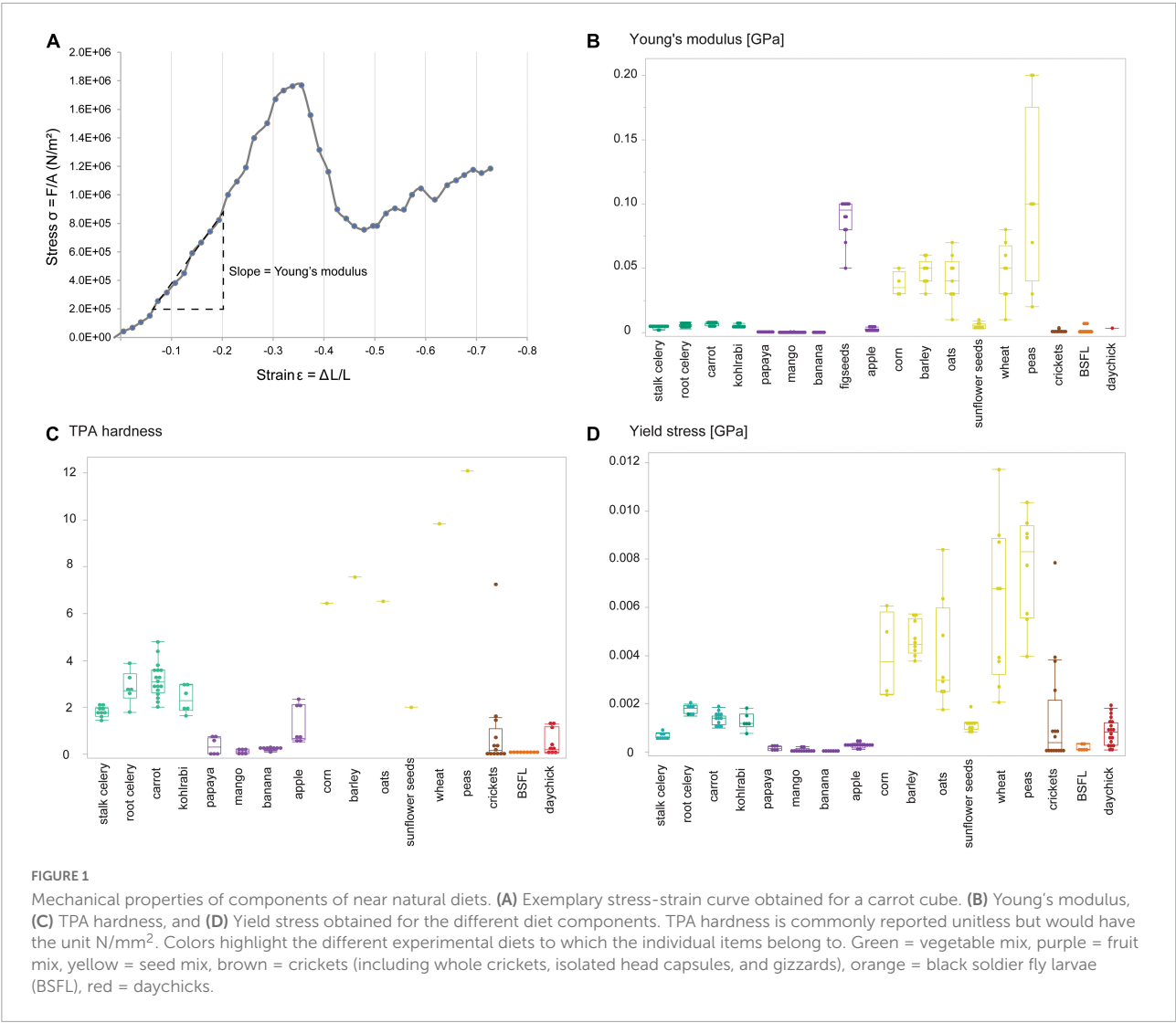


FIGURE 1 Mechanical properties of components of near natural diets. (A) Exemplary stress-strain curve obtained for a carrot cube. (B) Young's modulus, (C) TPA hardness, and (D) Yield stress obtained for the different diet components. TPA hardness is commonly reported unitless but would have the unit N/mm². Colors highlight the different experimental diets to which the individual items belong to. Green = vegetable mix, purple = fruit mix, yellow = seed mix, brown = crickets (including whole crickets, isolated head capsules, and gizzards), orange = black soldier fly larvae (BSFL), red = daychicks.

solid tester (maxF/testerArea). The false yield was found to be significantly correlated with yield stress ($R^2 = 0.986$, $p < 0.0001$) for the dietary items in which we could obtain both. Yield stress for daychicks was inferred from the regression equation:

$$\text{Yield} = 0.000314 + 5.26 \times \text{falseYield} \quad (n = 18, r^2 = 0.683)$$

Young's modulus was also found to be significantly correlated with yield stress ($R^2 = 0.967$, $p < 0.0001$). Young's modulus for daychicks was obtained from the regression equation:

$$\text{Young's modulus} = 0.004499 - 10.22 \times \text{Yield} \quad (n = 18, r^2 = 0.774)$$

TPA hardness was significantly correlated with yield stress ($R^2 = 0.966$, $p < 0.0001$), and TPA hardness values for seeds, cricket heads, and cricket gizzards were obtained from the equation:

$$\text{TPA hardness} = 0.1966 + 1565.00 \times \text{Yield} \quad (n = 11, r^2 = 0.729)$$

It is important to note that, in the case of seeds and cricket gizzards, the extrapolated values were mostly outside of the range of the other measurements used to generate the regression equation and hence were particularly susceptible to error. Therefore, the following evaluation of these data was done using non-parametric tests only.

As mechanical properties parameters could not be normalized by common transformations, and DMTA parameters are also not normally distributed, we subsequently conducted Spearman correlations between all DMTA and mechanical properties parameters (Supplementary Tables 8, 9).

Results

Dietary differences

The vegetable mix, BSFL, and daychick diets caused visibly lower surface roughness and smaller wear features on the M1 (Figure 2). The groups receiving daychicks and BSFL were best distinguished from the other diet groups when the M1 is considered (Table 2 and Figure 3; Supplementary Figure 2). For the M2, the daychick diet was less distinct from the other diet groups. Seeds and crickets were not significantly different from each other for any parameter on both M1 and M2. Seeds and crickets showed the highest complexity values, but these were not significantly larger compared to the other diet groups due to the large variance observed. A detailed description of

DMTA parameter results for each diet group is given in the supplementary text in the [Supplementary material](#). There was no trend of an increased variability in DMTA parameters for the more heterogenous diets.

Tooth position-specific differences

For all diet groups, except fruit and BSFL, more than one DMTA parameter was significantly different between M1 and M2 within the same diet (Table 2). The differences were mostly due to height and volume parameters, with parameter values consistently increasing from M1 to M2.

Diet mechanical properties

Young's modulus was largest for dried peas and fig seeds (Figure 1B). Overall, the items from the seed mix had larger Young's modulus than other diets, resulting in the largest mean per diet. Insects (crickets and BSFL) and fruit mix showed the lowest mean Young's modulus, followed by vegetables and daychicks.

Using regression equations, it was inferred that TPA hardness was largest in all items from the seed mix except sunflower seeds and cricket gizzards (Figure 1C; Supplementary Table 4). The largest measured TPA hardness values were found for several vegetables (root celery, carrot, kohlrabi), followed by stalk celery and apple. Some individual samples of daychick body parts had higher values that were obtained from whole specimens, while on average, fruits, insects, and daychicks showed the lowest TPA hardness values.

The highest yield stress was found for items of the seed mix, with dried peas exceeding all other seeds, and cricket gizzards (Figure 1D; Supplementary Table 3). Sunflower seeds had much lower yield stress values, comparable to vegetables and daychicks. Fruit and whole insects (crickets and BSFL) had the lowest yield stress, while intermediate values were inferred for daychicks.

Correlations of mechanical properties and dental microwear textures analysis

For the M1, no significant correlation was found between any DMTA and mean mechanical properties parameter (Supplementary Table 8). When considering maximum values for each mechanical property, several significant correlations were found with DMTA parameters. Maximum Young's modulus was significantly correlated with the volume parameters V_v (void volume) and V_{vc} (void volume of the core) (Figure 4; Supplementary Table 8). Maximum TPA hardness was significantly correlated with 16 DMTA parameters

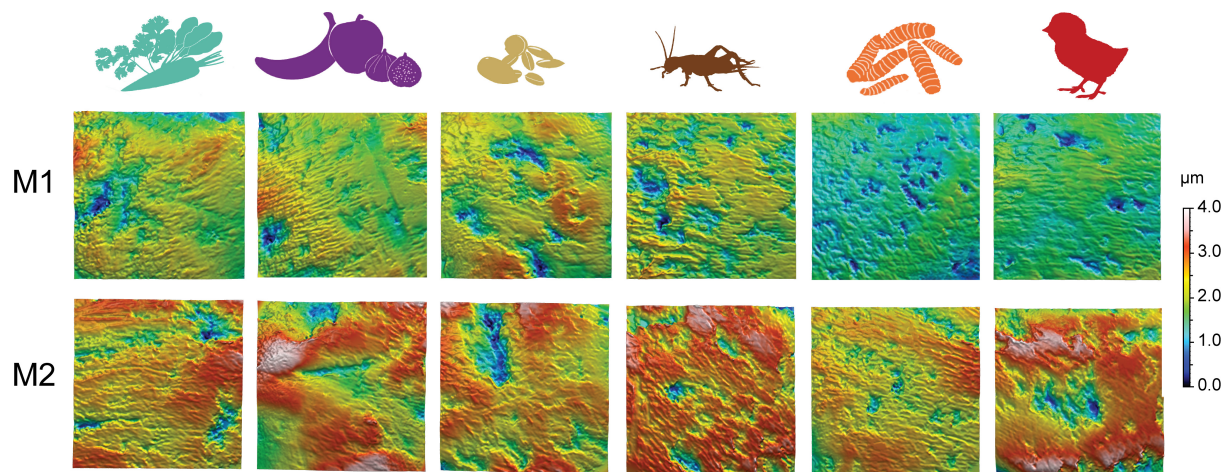


FIGURE 2

Exemplary 3D photosimulations of representative enamel surface scans for each diet group (from left to right: vegetable mix, fruit mix, seed mix, crickets, BSFL, black soldier fly larvae, and daychicks). Scans of the first (M1) and second upper molars (M2) belong to the same individual and are displayed on the same scale. Each surface scan is $60 \times 60 \mu\text{m}$.

TABLE 2 DMTA parameters displaying significant differences after the application of the Benjamini–Hochberg procedure between diet groups for the same tooth position (white cells) and between tooth positions within the same diet group (gray shaded cells).

		M2					
		Vegetable mix	Fruit mix	Seed mix	Crickets	BSFL	Daychicks
M1	Vegetable mix	matf, metf, S5p, S5v, S10z, Sa, Sdq, Sdr, Sk, Smc, Sp, Spc, Sq, Sz, Vmc, Vvc	metf, Sa, Vmc	matf, Sku, Ssk	matf, metf, S5v, Sku, Smc	metf, S5p, S5v, S10z, Sa, Sdq, Sdr, Sk, Sku, Sp, Sq, Spc, Ssk, Vmc, Vvc	Sk, Sku, Smc, Vmc, Vvc
	Fruit mix	matf, metf, Sa, Sdq, Sdr		matf, metf, S5v, Sdq	IsT, matf, new_epLsar, Sdq, Sdr, Spc		IsT, S5v, Spc
	Seed mix	matf, S5v, Sdq, Sdr, Ssk	Ssk	matf, S5v, Sa, Sk, Smc, Spc, Sq, Vmc, Vvc		matf, metf, S5v, S10z, Sa, Sdq, Sdr, Sp, Spc, Sq, Vmc	matf, Sku
	Crickets	matf			matf, metf, new_epLsar, S5p, S5v, S10z, Sa, Sdc, Sdq, Sdr, Sk, Smc, Sp, Spc, Sq, Vmc, Vvc	metf, S5p, S5v, S10z, Sa, Sdc, Sdq, Sdr, Sp, Spc	matf
	BSFL	Sku, Ssk	matf, S5p, S5v, S10z, Sa, Sk, Smc, Sp, Sq, Ssk, Vmc, Vvc	matf, S5v, S10z, Sa, Sdc, Smc, Sq, Vmc	Vmc		matf, Spc
	Daychicks	Sku, Smc, Ssk, Vmc, Vvc	matf, metf, S5p, S10z, Sa, Sdc, Sdq, Sdr, Sk, Sku, Smc, Sq, Ssk, Vmc, Vvc	matf, metf, S5v, S10z, Sa, Sdc, Sk, Smc, Sq, Vmc, Vvc	matf, Sa, Sdc, Sdq, Sk, Sq, Vmc, Vvc		matf, metf, S5p, S5v, S10z, Sa, Sdc, Sdq, Sdr, Sk, Smc, Sp, Spc, Sq, Vmc, Vvc

Due to using an FDR of 0.25, several p -values > 0.05 were judged significant. Significance levels of raw p -values were as follows: > 0.05 = gray, 0.05 = regular, 0.01 = *italics*, 0.001 = **bold**.

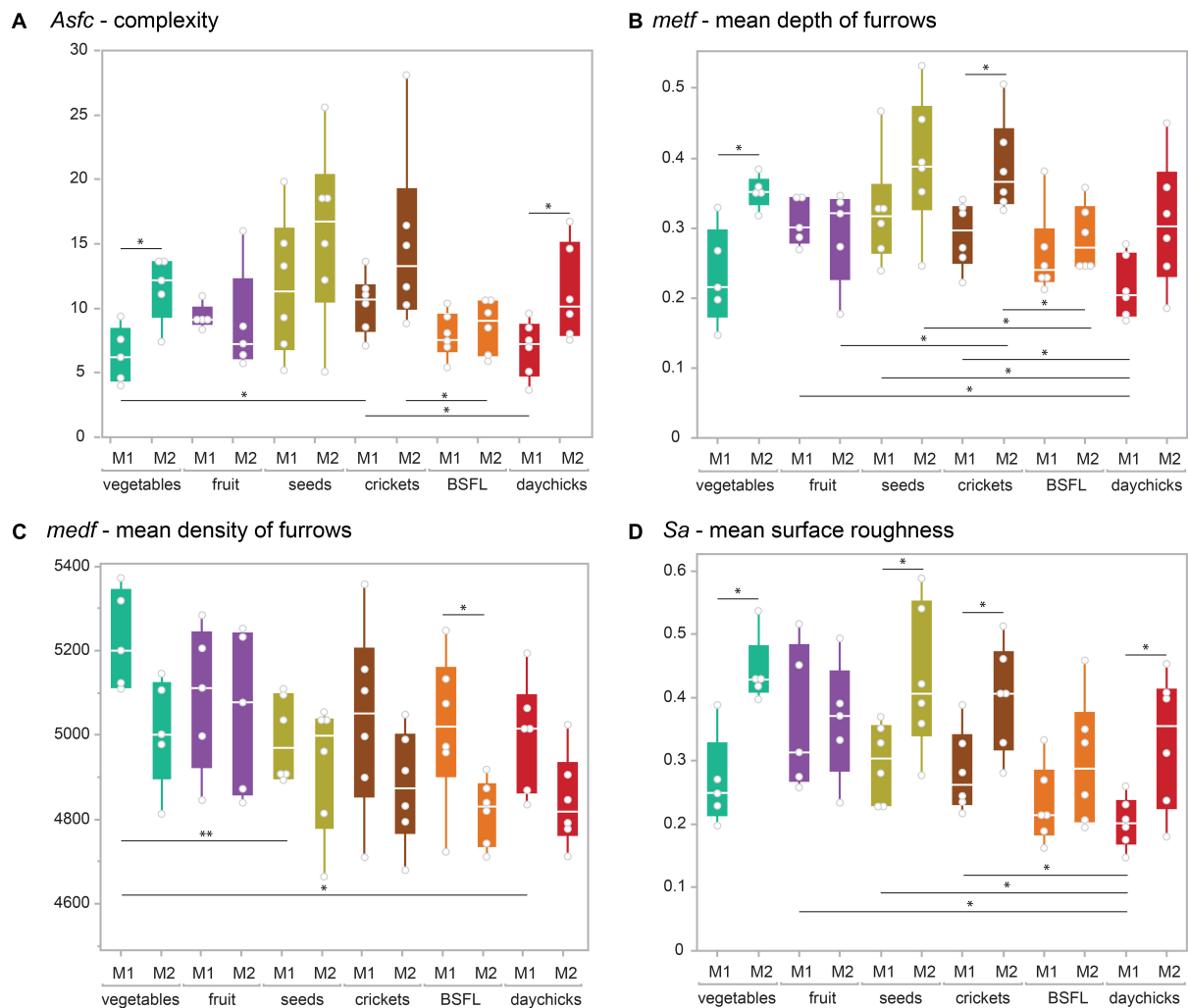


FIGURE 3

Boxplots depicting representative (A) complexity (*Asfc*), (B) density (*medf*), (C) and height (*metf*), (D) (*Sa*) parameters for the first (M1) and second upper molars (M2) of all dietary groups. Significant differences between tooth positions within one dietary group are displayed above, while differences between dietary groups for the same tooth position are displayed below the boxplots. Significance levels: *0.05, **0.01, from the Wilcoxon test for multiple comparisons without correction. BSFL, black soldier fly larvae.

representing height, complexity, volume, and area parameters (Figure 4; Supplementary Table 8). There were no significant correlations between any DMTA parameter for M1 and yield stress.

For the M2, mean TPA hardness and maximum TPA hardness showed multiple significant correlations (17 and 20, respectively) with several height, volume, slope, and complexity parameters (Figure 5; Supplementary Table 9). Mean yield stress showed no significant correlations, while for maximum yield stress, 21 DMTA parameters showed significant correlations (Figure 5; Supplementary Table 9). There were no significant correlations of DMTA parameters with mean Young's modulus, and only one parameter (*IsT* — texture isotropy) was significantly correlated with maximum Young's modulus (Supplementary Table 8).

Discussion

Limitations of the experimental setup

We have to note that several circumstances of the experimental setup likely introduced a source of variability and uncertainty. Therefore, all results obtained have to be interpreted with caution.

Firstly, rats received diets while housed in groups of 3 in bulk one time per day. Hence, for the mixed diets (vegetable mix, fruit mix, seed mix), individual rats were free to choose among the diet items offered. We could not control if each individual consumed equal amounts of each dietary component, as either dietary preferences or dominance of other individuals may have affected food choice. This is likely a source of the

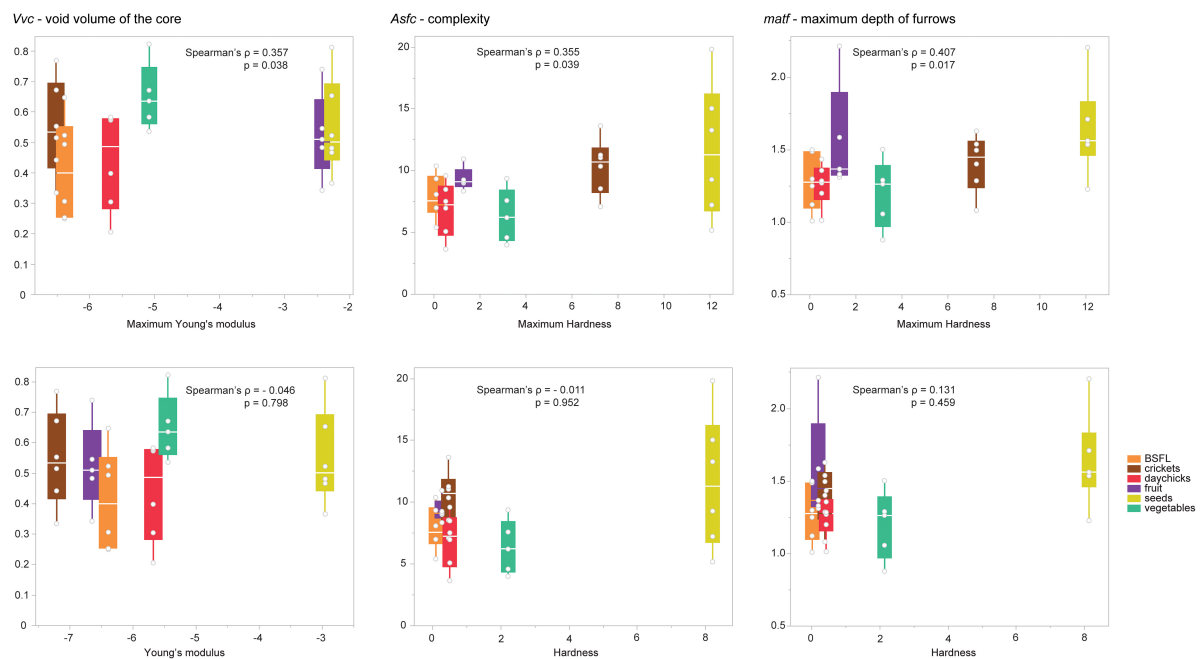


FIGURE 4

Correlations of selected DMTA parameters were obtained from the first upper molar (M1) of all rat diet groups with Young's modulus and TPA hardness. The upper row shows a correlation with the maximum Young's modulus and maximum TPA hardness per diet, and the lower row shows a correlation with the mean Young's modulus and the mean TPA Hardness per diet. Note that correlations are stronger and significant for maximum mechanical properties (upper row) only. Young's modulus is shown log-transformed for better visualization. BSFL, black soldier fly larvae.

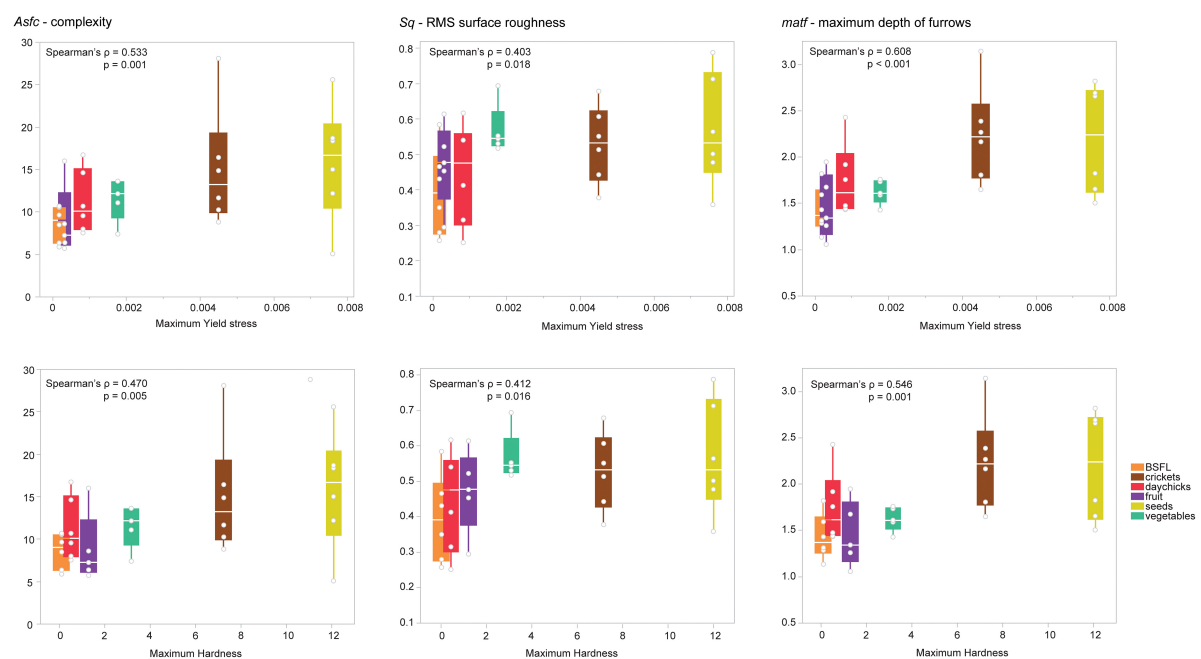


FIGURE 5

Correlations of selected DMTA parameters were obtained from the second upper molar (M2) of all rat diet groups for maximum yield stress and maximum TPA hardness. The upper row shows a correlation with maximum yield stress per diet, and the lower row shows a correlation with maximum TPA hardness per diet. BSFL, black soldier fly larvae.

observed variability in the DMTA data and may have influenced clearer separation between diet groups. We thus suggest that future feeding experiments should focus on one food item, or more homogenous food mixes, instead of trying to create a more natural diet mix.

Second, the components of the vegetable and fruit mix were purchased on a day-to-day basis, over the course of 37 days, to provide fresh food every day. The source of vegetables and fruits may have differed, as well as their degree of ripeness, water content, or other parameters, which might have added variability to the mechanical properties of these diets and could have influenced dental wear. The measurement of mechanical properties took place after the feeding experiment, hence—except for the seed mix—not on the same batches of food that the rats received. The seed mix was stored in a cool, dry place after the experiment and used for mechanical properties testing. Still, the storage time could potentially have altered the water content of the kernels to some degree (even though it was initially low). We purchased the same dietary items the rats received and treated them the same way (buying frozen crickets, black soldier fly larvae, and daychicks and defrosting them before testing). Still, the mechanical properties obtained may slightly differ from the mechanical properties of the original experimental diets but should nevertheless provide a good approximation of these food items.

Third, we excluded parsley and spinach from the mechanical properties testing, because their geometric shape does not allow for compression tests. Additionally, for daychicks and the seed mix, not all mechanical property parameters could be obtained but had to be inferred from linear regression equations.

Finally, choosing parameters for mechanical properties testing is similar to opening Pandora's box, as numerous methods for items with different structural properties (homogenous vs. inhomogeneous, brittle, tough, elastic, etc.) and an equally large number of opinions on which are the best practices exist [see Berthaume (2016) for a review]. The selection of testing methods and parameters presented in our study followed two principles: simplicity and feasibility. By only conducting compression tests, we limited our obtained parameters to Young's modulus and yield stress, hereby omitting other often measured parameters like energy release rate or toughness (e.g., Strait and Vincent, 1998). Our setup required only a force gauge, stiff testers, and measurement of the sample area and can hence be easily repeated. Regarding hardness testing, several methods are available but require sophisticated equipment such as diamond indenters and thin sections of the material (Vickers and Knoop hardness). Still, it has been questioned whether the observed hardness is an intrinsic mechanical property of the material or a product of the local testing environment, as argued by Berthaume (2016). We did not wish to engage in this discussion but did hope to simply find a hardness measure that was obtainable with our setup. Therefore, we chose TPA hardness. Parameters

from food texture studies (TPA) have been subjected to criticism because calculations of these parameters are often not consistently applied by researchers or details of the testing setup are insufficiently reported (e.g., size of the tester, test speed). However, TPA hardness has been evaluated as “probably the most reliable TPA parameter” by Nishinari et al. (2019). The general pitfall is that TPA intends to mimic human masticatory behavior using an instrument and compress (indenting) a food sample two times and that this measure only works for elastic foods. For hard and brittle items, such as the seeds in our experiment, TPA hardness thus had to be inferred, which introduced further uncertainty. This setup is an oversimplification of the actual masticatory process. In the case of our study, we did not intend to mimic masticatory behavior of the rats but to gain quantitative results related to the diet's intrinsic physical properties. The interaction between tooth morphology, bite force, mastication behavior (movement), lubrication of the food through saliva, and many more aspects cannot be accounted for in our approach but will all affect the observed tooth (micro)wear (Schulz-Kornas et al., 2020b). Therefore, our characterization of diet mechanical properties is not extensive but can still highlight several correlations between observed DMTs and diet mechanical properties.

Tooth position-specific dental microwear texture

The controlled rat feeding experiment of various near-natural diets revealed several systematic dental wear patterns. Comparable to guinea pigs feeding on pelleted diets (Winkler et al., 2021), overall surface roughness, including depth of wear features, increased from M1 to M2 in rats (Figure 3; Supplementary Figure 2). The only exception is the fruit diet, which showed similar roughness values on M1 and M2. The most pronounced increase was seen for vegetables, seeds, crickets, and daychicks. Due to the variable magnitude of increase in surface roughness from M1 to M2, differences observed between the diet groups were more pronounced when only considering the M1 and weaker when considering only the M2. Overall, the number of significantly different DMTA parameters between tooth positions on the same diet is even larger than between diet groups for the same tooth position (Table 2). This finding highlights that DMTA is likely tooth-position-specific—an observation made before for ungulates (Schulz et al., 2010) and macropods (Arman et al., 2019)—and cautions against lumping tooth positions together to increase sample sizes (for example in fossil samples). It might be that, in small mammals, DMTA conducted on anterior cheek tooth positions better reflects dietary differences than when using posterior teeth. This observation is in agreement with Winkler et al. (2021), who found that the fourth premolar showed the best dietary discrimination

in guinea pigs receiving natural plant diets of different abrasiveness.

When focusing on the M1, the six experimental diets can be roughly separated into three groups according to their resulting DMT patterns. However, differentiation between diets within these groups is difficult. Group one includes fruit mix, seed mix, and crickets, which are showing the highest surface complexity (*Sdr*, *Asfc*) and largest height differences (e.g., depth of furrows, peak height, mean surface roughness). These are the groups containing diet components that are often considered hard objects. Group two is composed of BSFL and daychicks, which had the lowest complexity, height, and volume parameter values. Black soldier fly larvae can be considered, in contrast to crickets, as soft-bodied insects, as they are not covered by a hard, sclerotized cuticle (Chapman, 2013a). Strait and Vincent (1998) tested the toughness of insects through scissor tests. They found beetles to be tough and brittle, while caterpillars were soft and compliant. We would suggest that crickets might be more comparable to beetles, while BSFL bear more resemblance to caterpillars (Evans and Sanson, 2005).

Finally, the vegetable mix diet would fall into group three, which is characterized by intermediate height and volume parameter values, but has distinctly higher anisotropy (*new epLsar*, *Sfrax epLsar*) and mean density of furrows. In herbivorous ungulates, high anisotropy values are characteristic of grazing species (Ungar et al., 2007), while in guinea pigs, the differences between browse and grass diets were less pronounced (Winkler et al., 2021). For rats, it seems that mastication of the vegetables required a different mastication mode as compared to the other diets. We believe that the more fibrous vegetables may require more frequent shearing motions, while diets such as fruit, seeds, and insects may require crushing movements. The stronger alignment (anisotropy) and higher density of wear features would hence result from such a repeated shearing motion.

What causes high complexity?

Patterns of complex surfaces have been associated with hard-object feeding not only in primates (Scott et al., 2005, 2012; Ungar et al., 2008, 2010; Ungar and Berger, 2018) and carnivorous mammals (DeSantis et al., 2012), but also in lepidosaurs (Winkler et al., 2019b), archosaurs (Bestwick et al., 2019), and fish (Purnell and Darras, 2015). Rats are no exception, as they also display the highest surface complexity (both by *Asfc* and *Sdr*) on the hardest diet (seeds) after feeding on their designated diet for 37 consecutive days. Yet, how complexity develops over longer feeding periods cannot be predicted. van Casteren et al. (2020) argued that “occasional contacts between seeds and irregular spicules of enamel could result in the latter being fractured, but over time this process should result in a decrease, rather than increase, in texture

complexity.” We cannot rule out that our experimental animals would have displayed a change in complexity values over time. However, from the current viewpoint of DMTA, it is likely that texture turnover in (small) mammals is fast (Winkler et al., 2020b) and continuously feeding on the same diet will produce similar DMTA over and over again, thus resulting in a short-term dietary proxy that reflects the last few weeks of an individual’s diet. We therefore conclude that the connection between high surface complexity and hard-object feeding is independent of body size, chewing mode, and taxonomic affinity [a similar conclusion was reached by Purnell and Darras (2015) for fishes], and thus a universal wear pattern following the oral processing of stress-limited foodstuffs.

However, we note that our hardness measure yielded low values for crickets, which resulted in the second highest surface complexity observed in this experiment. Overall, the mechanical properties of the two insect diets (crickets, BSFL) were found to be similar when testing whole insects, while the DMT pattern diverged completely. Cricket feeding resulted in high complexity, surface roughness, and deep and voluminous wear features, while BSFL feeding resulted in the lowest complexity, surface roughness, and lowest depth of wear features observed among all diet groups. For insectivorous bats, Purnell et al. (2013) found that species consuming “harder” prey (e.g., coleoptera) showed larger volume parameter values than species consuming “softer” prey, which is consistent with the disparity in our results observed between supposedly harder crickets and softer BSFL. It is therefore evident that our approach toward measuring mechanical properties of foodstuffs is not sufficient to describe the essential differences between these two insect diets. When testing individual cricket body parts, the head capsule displayed much higher TPA hardness than the abdomen, and a part of the digestive system (the gizzard) showed mechanical properties comparable to seeds (see raw data, Supplementary Tables 2–4). The gizzard is lined with strong cuticular plates or “teeth” in house crickets and other Orthoptera (Kirby et al., 1982 and references within, Elzinga, 1996; Chapman, 2013b). When considering maximum yield stress and maximum TPA hardness values for crickets (that were derived from regression equations for the gizzards), we found strong correlations with a variety of DMTA parameters. Although the hardness data were inferred from the regression equation, and the extrapolated values were mostly outside of the range of the other measurements (see Statistics section), these results suggest that crickets are much more heterogeneous as compared to BSFL, and likely, their sclerotized body parts greatly exceed less sclerotized body parts (like the abdomen) in hardness. Also, Young’s modulus of individual body parts has been found to differ greatly in locusts (over seven orders of magnitude, Li et al., 2020). Such subtle differences were not well-captured by our experimental approach but are likely responsible for the pronounced differences in DMT observed between crickets and BSFL.

Dental microwear texture and mechanical properties

Maximum values of mechanical properties have a stronger impact on the DMTA of M1. We found maximum Young's modulus to be significantly correlated with 2 DMTA parameters, while mean Young's modulus was not significantly correlated with any DMTA parameter (**Supplementary Table 8**). For maximum TPA hardness, M1 showed 16 significant correlations, while mean TPA hardness was not significantly correlated with DMTA parameters at all (**Supplementary Table 8**). M2 showed more significant correlations between material properties parameters and DMTA than M1. Here, maximum yield stress and maximum TPA hardness showed abundant strong correlations with DMTA parameters, and mean TPA hardness was significantly correlated with 17 DMTA parameters (**Supplementary Table 9**). In conclusion, differences in (maximum and mean) Young's modulus between diet items did not explain differences observed in DMTA, while maximum TPA hardness was strongly correlated with DMTA on both M1 and M2. For the M2, also maximum yield stress and mean TPA hardness were equally well-correlated with DMTA parameters, which may result from different chewing behavior when processing harder items. If harder items would be primarily processed using the M2, the observed wear might be more correlated with yield stress, which determines the fracture point of the diet item and overall hardness. Although our methodology has several limitations, this general trend highlights that mechanical properties and tooth position-specific wear are interrelated.

Parameters associated with increased abrasion such as height, volume, and complexity parameters increased from M1 to M2 on most diets. The stronger correlation of maximum mechanical properties indicates that M1 dental microwear may be more sensitive toward detecting inhomogeneous diets, more singular feeding events, and thus potentially fallback feeding events (Lambert et al., 2004). The M2, on the other hand, is strongly affected by overall TPA hardness and maximum TPA hardness of the diet. This may indicate that stiff, resistant food items (commonly termed hard objects) are more frequently and thoroughly processed using the M2 (and hence in the rear of the dentition). This is in accordance with observations from guinea pigs (Winkler et al., 2021), for which it was suggested that increased bite force toward the rear of the dentition results in increased abrasive wear when feeding on hard pellets. Under the previously discussed limitations, our results here need to be treated with caution, but in the context of the increased wear on posterior teeth in guinea pigs, it is plausible that rats also exert stronger bite forces toward the rear of the dentition and utilize the posterior teeth to break harder foodstuff.

Outlook and conclusion

Different foodstuffs can likely cause high complexity of DMT; however, in our controlled feeding experiment seeds, fruit (with seeds) and harder insect body parts resulted in the highest recorded complexity. The findings of this study emphasize that DMT formation in small mammals (i.e., rodents) seems to be strongly connected to mastication behavior and mechanics (likely bite force) and is hence significantly different for different tooth positions. These results call for a more thorough investigation of DMT gradients along the tooth row in other taxa, including large mammals.

We attempted to associate quantitative food mechanical properties with quantitative DMT. We considered this approach relevant to better understand the interrelation between ingesta and observed dental (micro)wear, beyond the detection of differences between diet categories. As noted, the masticatory system is highly complex, and accounting for all possible factors that affect DMT formation is impossible in an experimental setup. However, we can approach this complex system by controlling isolated factors and quantifying them. Future research may further elucidate how food mechanical properties affect dental (micro)wear, but also manage to take into account different occlusal morphologies and chewing mechanics, including movement, speed, bite force, fluid dynamics on the occlusal surface, and many more. At the moment, we are still only scratching the surface of understanding dental wear.

Data availability statement

The dataset presented in this study is permanently stored in the following online repository: ZFDM online repository of the University of Hamburg, doi.org/10.25592/uhhfdm.10235.

Ethics statement

The animal study was reviewed and approved by Swiss Cantonal Animal Care and Use Committee Zurich animal experiment license No. ZH135/16.

Author contributions

DEW, MC, MOK, ES-K, and TT: conceptualization. DEW, MC, MOK, and ADC: methodology. DEW: formal analysis and visualization. MOK, TMK, and AT: resources. DEW, MC, and MOK: writing—original draft. TT, DEW, and TK: funding acquisition. All authors: writing—review and editing and approve the submitted version.

Funding

This project received funding from the European Research Council (ERC) under the European Union's Horizon 2020 Research and Innovation Programme (Grant Agreement 681450) (ERC Consolidator Grant Agreement to TT) and from the Japan Society for the Promotion of Science (JSPS) under Postdoctoral fellowship awarded to DEW (KAKENHI Grant No. 20F20325) and TK (KAKENHI Grant No. 19J40003).

Acknowledgments

We thank Louise Martin, Nicole Schmid, Sandra Heldstab, and Kathrin Zbinden (from the University of Zurich) for support with animal husbandry, and three reviewers for their helpful comments on the manuscript. We further thank Professor Shinji Nagata (University of Tokyo) for the helpful discussion about potentially mechanically challenging body parts of crickets, including the gizzard.

Conflict of interest

Author AT was employed by Granovit Zoofeed, Granovit AG.

References

- Alba, D. M., Fortuny, J., and Moyà-Solà, S. (2010). Enamel thickness in the Middle Miocene great apes *Anoiapithecus*, *Pierolapithecus* and *Dryopithecus*. *Proc. R. Soc. B Biol. Sci.* 277, 2237–2245. doi: 10.1098/rspb.2010.0218
- Arman, S. D., Prowse, T. A. A., Couzens, A. M. C., Ungar, P. S., and Prideaux, G. J. (2019). Incorporating intraspecific variation into dental microwear texture analysis. *J. R. Soc. Interface* 16:20180957. doi: 10.1098/rsif.2018.0957
- Berthaume, M. A. (2016). Food mechanical properties and dietary ecology. *Am. J. Phys. Anthropol.* 159, 79–104. doi: 10.1002/ajpa.22903
- Bestwick, J., Unwin, D. M., and Purnell, M. A. (2019). Dietary differences in archosaur and lepidosaur reptiles revealed by dental microwear textural analysis. *Sci. Rep.* 9:11691. doi: 10.1038/s41598-019-48154-9
- Bourne, M. C. (2002). *Food texture and viscosity: Concept and measurement*, 2nd Edn. San Diego, CA: Academic Press, 182–186.
- Calandra, I., and Merceron, G. (2016). Dental microwear texture analysis in mammalian ecology. *Mammal Rev.* 46, 215–228. doi: 10.1111/mam.12063
- Chapman, R. F. (2013a). "The integument, gas exchange and homeostasis," in *The insects: Structure and function*, 5th Edn, eds S. J. Simpson and A. E. Douglas (Cambridge: Cambridge University Press), 463–498.
- Chapman, R. F. (2013b). "Alimentary canal, digestion and absorption," in *The insects: Structure and function*, 5th Edn, eds S. J. Simpson and A. E. Douglas (Cambridge: Cambridge University Press), 46–80. doi: 10.1017/CBO9781139035460.006
- Constantino, P. J., Borrero-Lopez, O., and Lawn, B. R. (2018). Mechanisms of tooth damage and *Paranthropus* dietary reconstruction. *Biosurf. Biotribol.* 4, 73–78. doi: 10.1049/bsbt.2018.0017
- Constantino, P. J., Lee, J. J. W., Morris, D., Lucas, P. W., Hartstone-Rose, A., Lee, W. K., et al. (2011). Adaptation to hard-object feeding in sea otters and hominins. *J. Hum. Evol.* 61, 89–96. doi: 10.1016/j.jhevol.2011.02.009
- Daegling, D. J., McGraw, W. S., Ungar, P. S., Pampush, J. D., Vick, A. E., and Bitty, E. A. (2011). Hard-object feeding in sooty mangabeys (*Cercocebus atys*) and interpretation of early hominin feeding ecology. *PLoS One* 6:e23095. doi: 10.1371/journal.pone.0023095
- Dammaschke, T. (2010). Rat molar teeth as a study model for direct pulp capping research in dentistry. *Lab. Anim.* 44, 1–6. doi: 10.1258/la.2009.008120
- DeSantis, L. R., Schubert, B. W., Scott, J. R., and Ungar, P. S. (2012). Implications of diet for the extinction of saber-toothed cats and American lions. *PLoS One* 7:e52453. doi: 10.1371/journal.pone.0052453
- Dumont, E. R. (1995). Enamel thickness and dietary adaptation among extant primates and chiropterans. *J. Mammal.* 76, 1127–1136. doi: 10.2307/1382604
- Elzinga, R. J. (1996). A comparative study of microspines in the alimentary canal of five families of Orthoptera (Saltatoria). *Int. J. Insect Morphol. Embryol.* 25, 249–260. doi: 10.1016/0020-7322(96)00007-4
- Evans, A. R., and Sanson, G. D. (2005). Biomechanical properties of insects in relation to insectivory: Cuticle thickness as an indicator of insect 'hardness' and 'intractability'. *Aust. J. Zool.* 53, 9–19. doi: 10.1071/ZO04018
- Frei, J., Clauss, M., Winkler, D. E., Tütken, T., and Martin, L. F. (2021). Use of running plates by floor housed rats: A pilot study. *Lab. Anim.* 55, 521–530. doi: 10.1177/00236772211036572
- Grine, F. E., and Kay, R. F. (1988). Early hominid diets from quantitative image analysis of dental microwear. *Nature* 333, 765–768. doi: 10.1038/333765a0
- Kay, R. F. (1981). The nut-crackers—a new theory of the adaptations of the Ramapithecinae. *Am. J. Phys. Anthropol.* 55, 141–151. doi: 10.1002/ajpa.1330550202

The remaining authors declare that the research was conducted in the absence of any commercial or financial relationships that could be construed as a potential conflict of interest.

Publisher's note

All claims expressed in this article are solely those of the authors and do not necessarily represent those of their affiliated organizations, or those of the publisher, the editors and the reviewers. Any product that may be evaluated in this article, or claim that may be made by its manufacturer, is not guaranteed or endorsed by the publisher.

Supplementary material

The Supplementary Material for this article can be found online at: <https://www.frontiersin.org/articles/10.3389/fevo.2022.957427/full#supplementary-material>

- Kirby, P., Beck, R., and Clarke, K. U. (1982). Undescribed anatomical features of the gut of the house cricket, *Acheta domestica* L. (Insecta, Orthoptera). *J. Nat. Hist.* 16, 707–714. doi: 10.1080/00222938200770541
- Lambert, J. E., Chapman, C. A., Wrangham, R. W., and Conklin-Brittain, N. L. (2004). Hardness of cercopithecine foods: Implications for the critical function of enamel thickness in exploiting fallback foods. *Am. J. Phys. Anthropol.* 125, 363–368. doi: 10.1002/ajpa.10403
- Lee-Thorp, J. (2011). The demise of “Nutcracker Man”. *Proc. Natl. Acad. Sci. U.S.A.* 108, 9319–9320. doi: 10.1073/pnas.1105808108
- Li, C., Gorb, S. N., and Rajabi, H. (2020). Cuticle sclerotization determines the difference between the elastic moduli of locust tibiae. *Acta Biomater.* 103, 189–195. doi: 10.1016/j.actbio.2019.12.013
- Louail, M., Ferchaud, S., Souron, A., Walker, A. E., and Merceron, G. (2021). Dental microwear textures differ in pigs with overall similar diets but fed with different seeds. *Palaeogeogr. Palaeoclimatol. Palaeoecol.* 572:110415. doi: 10.1016/j.palaeo.2021.110415
- Lucas, P. W., Constantino, P. J., Chalk, J., Zisocovic, C., Wright, B. W., Fragaszy, D. M., et al. (2009). Indentation as a technique to assess the mechanical properties of fallback foods. *Am. J. Phys. Anthropol.* 140, 643–652. doi: 10.1002/ajpa.21026
- Martin, L. B., Olejniczak, A. J., and Maas, M. C. (2003). Enamel thickness and microstructure in pitheciin primates, with comments on dietary adaptations of the middle Miocene hominoid *Kenyanthropus*. *J. Hum. Evol.* 45, 351–367. doi: 10.1016/j.jhevol.2003.08.005
- Merceron, G., Ramdarshan, A., Blondel, C., Boissier, J. R., Brunetiere, N., Francisco, A., et al. (2016). Untangling the environmental from the dietary: Dust does not matter. *Proc. R. Soc. B Biol. Sci.* 283:20161032. doi: 10.1098/rspb.2016.1032
- Merceron, G., Blondel, C., Viriot, L., Koufos, G. D., and de Bonis, L. (2007a). Dental microwear analysis of bovids from the Vallesian (late Miocene) of Axios Valley in Greece: Reconstruction of the habitat of *Ouranopithecus macedoniensis* (Primates, Hominoidea). *Geodiversitas* 29, 421–433.
- Merceron, G., Schulz, E., Kordos, L., and Kaiser, T. M. (2007b). Paleoenvironment of *Dryopithecus brancoi* at Rudabánya, Hungary: Evidence from dental meso- and micro-wear analyses of large vegetarian mammals. *J. Hum. Evol.* 53, 331–349. doi: 10.1016/j.jhevol.2007.04.008
- Nishijima, K., Kuwahara, S., Ohno, T., Miyaishi, O., Ito, Y., Sumi, Y., et al. (2007). Occlusal tooth wear in female F344/N rats with aging. *Arch. Oral Biol.* 52, 844–849. doi: 10.1016/j.archoralbio.2007.03.001
- Nishijima, K., Kuwahara, S., Ohno, T., Miyaishi, O., Ito, Y., Sumi, Y., et al. (2009). Occlusal tooth wear in male F344/N rats with aging. *Arch. Gerontol. Geriatr.* 48, 178–181. doi: 10.1016/j.archger.2008.01.006
- Nishinari, K., Fang, Y., and Rosenthal, A. (2019). Human oral processing and texture profile analysis parameters: Bridging the gap between the sensory evaluation and the instrumental measurements. *J. Texture Stud.* 50, 369–380. doi: 10.1111/jtxs.12404
- Ohba, Y. (1974). Form of the molar crown with especial reference to tooth wear, and occlusion in rats. *Aichi Gakuin Daigaku Shigakkai Shi* 12, 171–192.
- Purnell, M. A., Crumpton, N., Gill, P. G., Jones, G., and Rayfield, E. J. (2013). Within-guild dietary discrimination from 3-D textural analysis of tooth microwear in insectivorous mammals. *J. Zool.* 291, 249–257. doi: 10.1111/jzo.12068
- Purnell, M. A., and Darras, L. P. (2015). 3D tooth microwear texture analysis in fishes as a test of dietary hypotheses of durophagy. *Surf. Topogr.* 4:014006. doi: 10.1088/2051-672X/4/1/014006
- Rivals, F., Schulz, E., and Kaiser, T. M. (2008). Climate-related dietary diversity of the ungulate faunas from the middle Pleistocene succession (OIS 14–12) at the Caune de l’Arago (France). *Paleobiology* 34, 117–127. doi: 10.1666/07023.1
- Rivals, F., Solounias, N., and Muhlbacher, M. C. (2007). Evidence for geographic variation in the diets of late Pleistocene and early Holocene Bison in North America, and differences from the diets of recent Bison. *Quat. Res.* 68, 338–346. doi: 10.1016/j.yqres.2007.07.012
- Schulz, E., Calandra, I., and Kaiser, T. M. (2010). Applying tribology to teeth of hoofed mammals. *Scanning* 32, 162–182. doi: 10.1002/sca.20181
- Schulz, E., Calandra, I., and Kaiser, T. M. (2013). Feeding ecology and chewing mechanics in hoofed mammals: 3D tribology of enamel wear. *Wear* 300, 169–179. doi: 10.1016/j.wear.2013.01.115
- Schulz-Kornas, E., Winkler, D. E., Clauss, M., Carlsson, J., Ackermans, N. L., Martin, L. F., et al. (2020a). Everything matters: Molar microwear texture in goats (*Capra aegagrus hircus*) fed diets of different abrasiveness. *Palaeogeogr. Palaeoclimatol. Palaeoecol.* 552:109783. doi: 10.1016/j.palaeo.2020.109783
- Schulz-Kornas, E., Kaiser, T. M., Calandra, I., and Winkler, D. E. (2020b). “A brief history of quantitative wear analyses with an appeal for a holistic view on dental wear processes,” in *Mammalian teeth – form and function*, eds T. Martin and W. von Koenigswald (Munich: Verlag Dr. Friedrich Pfeil), 44–53.
- Schwartz, G. T., McGrosky, A., and Strait, D. S. (2020). Fracture mechanics, enamel thickness and the evolution of molar form in hominins. *Biol. Lett.* 16:20190671. doi: 10.1098/rsbl.2019.0671
- Scott, R., Ungar, P., Bergstrom, T. S., Brown, C. A., Grine, F. E., Teaford, M. F., et al. (2005). Dental microwear texture analysis shows within-species diet variability in fossil hominins. *Nature* 436, 693–695. doi: 10.1038/nature03822
- Scott, R. S., Teaford, M. F., and Ungar, P. S. (2012). Dental microwear texture and anthropoid diets. *Am. J. Phys. Anthropol.* 147, 551–579. doi: 10.1002/ajpa.22007
- Semperebon, G. M., and Rivals, F. (2007). Was grass more prevalent in the pronghorn past? An assessment of the dietary adaptations of Miocene to recent Antilocapridae (Mammalia: Artiodactyla). *Palaeogeogr. Palaeoclimatol. Palaeoecol.* 253, 332–347. doi: 10.1016/j.palaeo.2007.06.006
- Shellis, R. P., Beynon, A. D., Reid, D. J., and Hiemae, K. M. (1998). Variations in molar enamel thickness among primates. *J. Hum. Evol.* 35, 507–522. doi: 10.1006/jhev.1998.0238
- Sponheimer, M., Daegling, D. J., Ungar, P. S., Bobe, R., and Paine, O. C. (2022). Problems with *Paranthropus*. *Quat. Int.* doi: 10.1016/j.quaint.2022.03.024 [Epub ahead of print].
- Strait, S. G., and Vincent, J. F. V. (1998). Primate faunivores: Physical properties of prey items. *Int. J. Primatol.* 19, 867–878. doi: 10.1023/A:1020397430482
- Teaford, M. F., and Ungar, P. S. (2000). Diet and the evolution of the earliest human ancestors. *Proc. Natl. Acad. Sci. U.S.A.* 97, 13506–13511. doi: 10.1073/pnas.260368897
- Teaford, M. F., Ungar, P. S., Taylor, A. B., Ross, C. F., and Vinyard, C. J. (2020). The dental microwear of hard-object feeding in laboratory *Sapajus apella* and its implications for dental microwear formation. *Am. J. Phys. Anthropol.* 171, 439–455. doi: 10.1002/ajpa.24000
- Thompson, C. L., Valença-Montenegro, M. M., Melo, L. D. O., Valle, Y. M., Oliveira, M. D., Lucas, P. W., et al. (2014). Accessing foods can exert multiple distinct, and potentially competing, selective pressures on feeding in common marmoset monkeys. *J. Zool.* 294, 161–169. doi: 10.1111/jzo.12164
- Ungar, P. S. (2011). Dental evidence for the diets of Plio-Pleistocene hominins. *Am. J. Phys. Anthropol.* 146, 47–62. doi: 10.1002/ajpa.21610
- Ungar, P. S. (2012). Dental evidence for the reconstruction of diet in African early *Homo*. *Curr. Anthropol.* 53, 318–329. doi: 10.1086/666700
- Ungar, P. S., and Berger, L. R. (2018). Brief communication: Dental microwear and diet of *Homo naledi*. *Am. J. Phys. Anthropol.* 166, 228–235. doi: 10.1002/ajpa.23418
- Ungar, P. S., Grine, F. E., and Teaford, M. F. (2008). Dental microwear and diet of the Plio-Pleistocene hominin *Paranthropus boisei*. *PLoS One* 3:e2044. doi: 10.1371/journal.pone.0002044
- Ungar, P. S., Merceron, G., and Scott, R. S. (2007). Dental microwear texture analysis of Varswater bovids and early Pliocene paleoenvironments of Langebaanweg, Western Cape Province, South Africa. *J. Mamm. Evol.* 14, 163–181. doi: 10.1007/s10914-007-9050-x
- Ungar, P. S., Scott, R. S., Grine, F. E., and Teaford, M. F. (2010). Molar microwear textures and the diets of *Australopithecus anamensis* and *Australopithecus afarensis*. *Philos. Trans. R. Soc. B Biol. Sci.* 365, 3345–3354. doi: 10.1098/rstb.2010.0033
- Ungar, P. S., and Sponheimer, M. (2011). The diets of early hominins. *Science* 334, 190–193. doi: 10.1126/science.1207701
- van Casteren, A., Strait, D. S., Swain, M. V., Michael, S., Thai, L. A., Philip, S. M., et al. (2020). Hard plant tissues do not contribute meaningfully to dental microwear: Evolutionary implications. *Sci. Rep.* 10:582. doi: 10.1038/s41598-019-57403-w
- van der Merwe, N. J., Masao, F. T., and Bamford, M. K. (2008). Isotopic evidence for contrasting diets of early hominins *Homo habilis* and *Australopithecus boisei* of Tanzania. *S. Afr. J. Sci.* 104, 153–155.
- Walker, A. (1981). Diet and teeth. Dietary hypotheses and human evolution. *Philos. Trans. R. Soc. Lond. B Biol. Sci.* 292, 57–64. doi: 10.1098/rstb.1981.0013
- Winkler, D. E., Andrianasolo, T. H., Andriamandimbarisoa, L., Ganzhorn, J. U., Rakotonandrarany, S. J., Kaiser, T. M., et al. (2016). Tooth wear patterns in black rats (*Rattus rattus*) of Madagascar differ more in relation to human impact than to differences in natural habitats. *Ecol. Evol.* 6, 2205–2215. doi: 10.1002/ece3.2048
- Winkler, D. E., Clauss, M., Rölle, M., Schulz-Kornas, E., Codron, D., Kaiser, T. M., et al. (2021). Dental microwear texture gradients in guinea pigs reveal that material properties of the diet affect chewing behaviour. *J. Exp. Biol.* 224:jeb242446. doi: 10.1242/jeb.242446

Winkler, D. E., Schulz-Kornas, E., Kaiser, T. M., De Cuyper, A., Clauss, M., and Tütken, T. (2019a). Forage silica and water content control dental surface texture in guinea pigs and provide implications for dietary reconstruction. *Proc. Natl. Acad. Sci. U.S.A.* 116, 1325–1330. doi: 10.1073/pnas.1814081116

Winkler, D. E., Schulz-Kornas, E., Kaiser, T. M., and Tütken, T. (2019b). Dental microwear texture reflects dietary tendencies in extant Lepidosauria despite their limited use of oral food processing. *Proc. R. Soc. B* 286:20190544. doi: 10.1098/rspb.2019.0544

Winkler, D. E., Tütken, T., Schulz-Kornas, E., Kaiser, T. M., Müller, J., Leichliter, J., et al. (2020a). Shape, size, and quantity of ingested external abrasives influence dental microwear texture formation in guinea pigs. *Proc. Natl. Acad. Sci. U.S.A.* 117, 22264–22273. doi: 10.1073/pnas.2008149117

Winkler, D. E., Schulz-Kornas, E., Kaiser, T. M., Codron, D., Leichliter, J., Hummel, J., et al. (2020b). The turnover of dental microwear texture: Testing the “last supper” effect in small mammals in a controlled feeding experiment. *Palaeogeogr. Palaeoclimatol. Palaeoecol.* 557:109930. doi: 10.1016/j.palaeo.2020.109930



OPEN ACCESS

EDITED BY

Ferran Estebanaranz-Sánchez,
Milá y Fontanals Institution for
Research in Humanities (CSIC), Spain

REVIEWED BY

Florent Rivals,
Catalan Institution for Research
and Advanced Studies (ICREA), Spain
Lua Valenzuela-Suau,
Universitat de les Illes Balears, Spain

*CORRESPONDENCE

Koyo Sato
koyo.sato@keio.jp

SPECIALTY SECTION

This article was submitted to
Paleoecology,
a section of the journal
Frontiers in Ecology and Evolution

RECEIVED 30 May 2022

ACCEPTED 16 September 2022

PUBLISHED 10 October 2022

CITATION

Sato K, Sato T and Kubo MO (2022)
Reconstructing diets of hunted sika
deer from Torihama Shell Midden site
(ca. 6,000 years ago) by dental
microwear texture analysis.
Front. Ecol. Evol. 10:957038.
doi: 10.3389/fevo.2022.957038

COPYRIGHT

© 2022 Sato, Sato and Kubo. This is an
open-access article distributed under
the terms of the [Creative Commons
Attribution License \(CC BY\)](#). The use,
distribution or reproduction in other
forums is permitted, provided the
original author(s) and the copyright
owner(s) are credited and that the
original publication in this journal is
cited, in accordance with accepted
academic practice. No use, distribution
or reproduction is permitted which
does not comply with these terms.

Reconstructing diets of hunted sika deer from Torihama Shell Midden site (ca. 6,000 years ago) by dental microwear texture analysis

Koyo Sato^{1,2*}, Takao Sato² and Mugino O. Kubo³

¹Shiga Prefectural Association for Cultural Heritage, Otsu, Shiga, Japan, ²Department of Archaeology and Ethnology, Faculty of Letters, Keio University, Minato-ku, Tokyo, Japan,

³Department of Natural Environmental Studies, Graduate School of Frontier Sciences, The University of Tokyo, Kashiwa, Chiba, Japan

Sika deer (*Cervus nippon*) is the most abundant ruminant in the Japanese archipelago and has been the primary hunting target, including during the prehistoric ages. Abundant skeletal remains of sika deer have been excavated from archeological sites of the Jomon periods (ca. 15,000–2,400 BP). We reconstructed the feeding habits of sika deer from the Torihama Shell Midden site in Fukui Prefecture, western Japan. The Torihama site is one of the most well-preserved archeological sites of the Jomon period, and we investigated materials from the layers of the Early Jomon period (ca. 6,000 BP). In this study, we obtained three-dimensional tooth surface texture from the lower molars of excavated deer and measured microwear texture using international surface roughness parameters (ISO 25178-2) to infer their habitat use. Next, we estimated the percentage of grasses in the diet by using the reference dataset for extant sika deer with known diets. The results show that the Torihama deer overlapped with mixed feeding and grazing sika deer populations. Moreover, the proportion of grasses in the diet was estimated to be 50.7% on average but showed a wide range among the Torihama deer. This result implied that Torihama deer were mixed feeders of dicot leaves and grasses and had a flexible diet adapted to the vegetation of its habitat. Our results support the paleoenvironmental estimation that the Torihama Shell Midden site contained mixed vegetation of evergreen, deciduous, and coniferous trees around the Mikata Five Lakes in the Early Jomon period. These findings provide insights into the highly plastic diets of the extant sika deer in the Japanese archipelago.

KEYWORDS

Archaeology, Jomon period, Torihama Shell Midden site, Sika deer, Microwear, ISO 25178

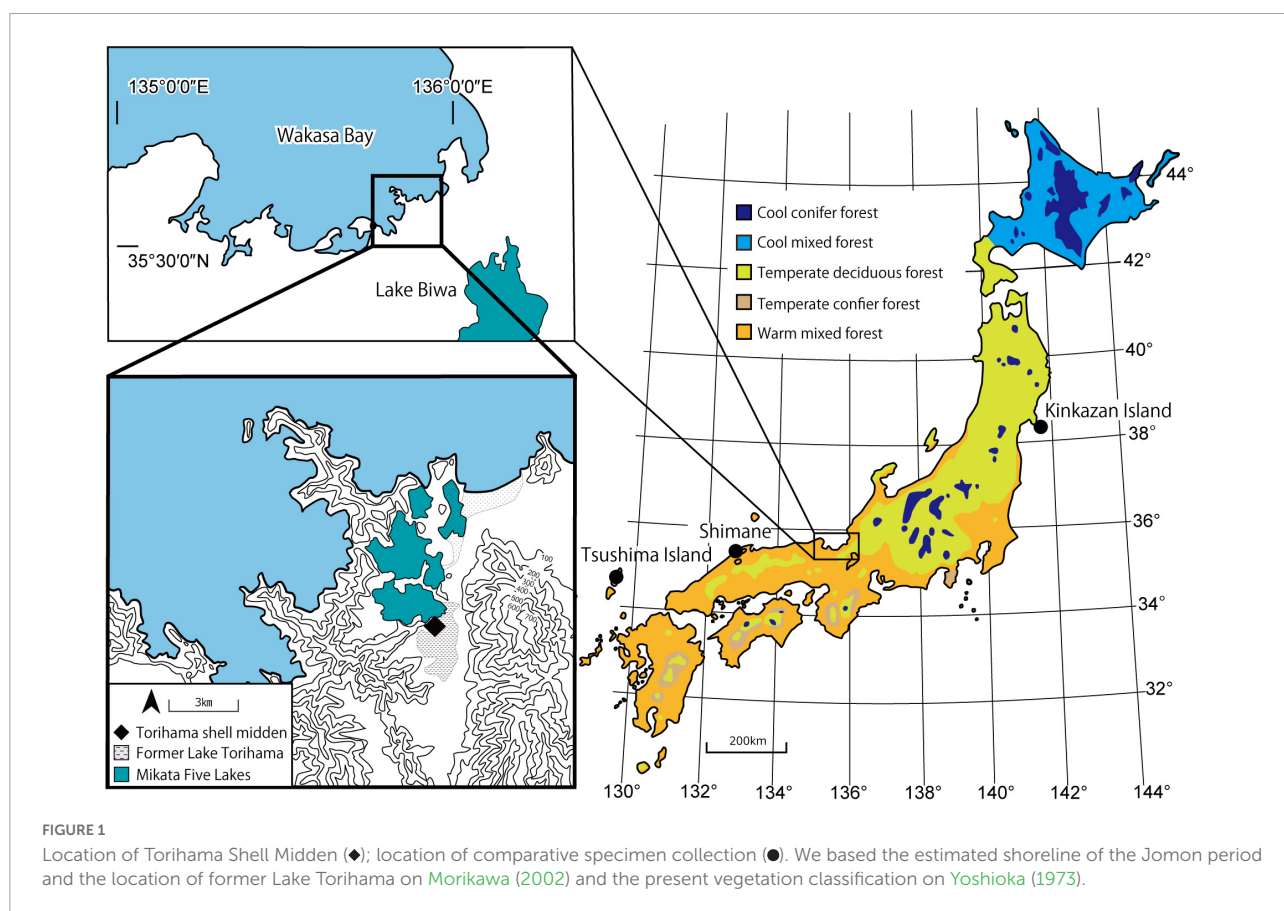
Introduction

Sika deer (*Cervus nippon*), a medium-sized species of deer that inhabit a wide area of East Asia, from Amurland in the north to Vietnam in the south, are distributed in the Japanese archipelago from Hokkaido to the Kerama Islands, where there are five subspecies (Ohtaishi, 1986; Miura, 2008). Sika deer are thought to have migrated from the Asian continent to the Japanese archipelago during MIS12 (approximately 430,000 years ago) (Kawamura, 2009). Although the acidic soil in Japan is not conducive to the preservation of organic remains, animal skeletal remains have been found, along with artifacts in prehistoric shell middens, caves, and low wetland sites. Skeletal remains of sika deer and wild boar (*Sus scrofa*) have often been excavated from those archeological sites, and these animals are thought to be among the major animals hunted during the Jomon period (ca. 15,000–2,400 BP) (Nishimoto, 1991).

From Torihama shell midden, abundant skeletal remains of sika deer have been excavated (Figure 1). This site was occupied by Paleolithic people from the Incipient to Early Jomon period. Because of the environmental condition of wetlands, this site has yielded various artifacts, for example, Jomon pottery and stone and bone tools; botanical artifacts, namely, fibers and wooden tools, represented by a well-preserved

comb coated with red lacquer (Torihama Shell Midden Study Group, 1987); and many plant and animal remains. Therefore, Torihama Shell Midden has been one of the most intensively studied archeological sites in Japan. This research has been conducted by an interdisciplinary research team of archeologists and natural science researchers motivated by this slogan, “the reconstruction of the Jomon lifestyle focusing on their subsistence” (Kojima, 2015). Analyses of abundant sika deer and wild boar remains have been conducted based on various objectives and methodologies, for example, species identification and the quantitative analysis of each skeletal element (Morikawa, 1963; Nishida, 1979; Inami, 1983; Shigehara et al., 1991; Uchiyama, 2000; Anezaki et al., 2005; Sato, 2021a), the estimation of hunting seasons (Nishida, 1980; Ohtaishi, 1980; Uchiyama, 2005; Sato, 2021b), the examination of cut marks (Hongo, 1991), and the manufacturing of bone tools (Yamakawa, 1992a,b).

Studies have also been conducted to reconstruct the paleoenvironment and the use of plant resources by analyzing pollen (Yasuda, 1979), seed (Kasahara, 1983, 1984), phytolith (Sasaki, 1983), natural wood (Noshiro and Suzuki, 1990), and wood tools (Noshiro et al., 1996; Kudo et al., 2016a) in the sediments of the site. In addition, pollen analysis of lakes and lowland sediments has provided insights into long-term climatic



changes around the site (Yasuda, 1982; Takahara and Takeoka, 1992; Nakagawa et al., 2002, 2005; Kitagawa et al., 2018).

The vegetation around the site in the Early Jomon period was estimated to be evergreen broadleaved forests, consisting of evergreen oak (*Quercus* subgen *Cyclobalanopsis*), chinquapin (*Catanopsis sieboldii*), and camellia (*Camellia japonica* Linn.) on the top of the hill; Japanese cedar (*Cryptomeria japonica*) on the hillsides; and deciduous broadleaved forests consisting of willow (*Salix*) and alder (*Alnus* sect. *Gymnothyrsus*) and Japanese ash (*Fraxinus*) in the waterside low areas (Noshiro and Suzuki, 1990). Subsequently, Yoshikawa et al. (2016) analyzed excavated pollen and seeds; their results suggest that the flora around the site was mixed vegetation: evergreen trees, broadleaved trees, and coniferous trees.

Therefore, clarifying the diets of sika deer in such a vegetation environment would help uncover the habitat use of the deer in the ecosystem and humans' hunting activities. To estimate the diets of the excavated deer, we applied dental microwear texture analysis (DMTA) for the first time in the Jomon archeological sites. The DMTA measured the surface roughness of microscopic tooth enamel surfaces in three dimensions, obtained by optical profilometers such as confocal microscopes. The application of DMTA has been expanded to various types of vertebrates for dietary estimation (DeSantis, 2016) and has been most intensively applied to herbivores (e.g., Merceron et al., 2010; Berlioz et al., 2017), including extant, extinct, and excavated animals (Kubo and Fujita, 2021).

Because tooth surfaces retain dietary signals for a shorter period (days to weeks) than stable carbon and nitrogen isotopes of soft tissues and bones (Matsubayashi and Tayasu, 2019; Winkler et al., 2020), seasonal differences in a population can be detected, providing insights into hunting seasons and sites occupied by humans (Rivals et al., 2009, 2015). These results reveal human activity but are based on observations at low magnification; thus, they are not applicable to the method used in this study to quantitatively observe the three-dimensional (3D) shape of microwear. Kubo et al. (2017) and Kubo and Fujita (2021) have provided the reference dataset of extant sika deer sampled from various environments with quantitative dietary information; thus, the dental microwear texture (DMT) of the excavated deer can be compared with theirs.

In this study, we estimate the foraging behavior of the hunted sika deer from the Torihama Shell Midden site (hereafter "Torihama deer") by using DMTA to infer the habitat use of the deer that lived during the Early Jomon period (ca. 6,000 BP).

Materials and methods

Materials

We used mandibles of the Torihama deer ($n = 56$) housed in the Wakasa History Museum and analyzed lower second

molars (M2), which were not separated from the mandibles (Figure 2 and Supplementary Data 1). According to the correspondence between age in months and eruption of the molars (Niimi, 1997), the mandibles were 29 months old or older. Therefore, we observed the second molars, which had begun to wear down and had relatively few defects. They might have been derived from the same individual because the hemi-mandibles had been excavated in isolated conditions from the archeological site. However, in order to obtain the maximum number of samples, we included the left and right sides in the analysis. They were excavated during the ninth survey in 1984 (Torihama Shell Midden Study Group, 1985) and obtained from sediment layers yielding potteries of the Early Jomon period (Kitashirakawa Kaso II types). The layers, organic soils or shell deposits consisting primarily of freshwater mollusks, were dated to ca. 5,900–5,655 cal BP by radiocarbon dating (Kudo et al., 2016b). The deer remains showed evidence of human use, namely, scars from removal and dismantling and traces of extracting bone marrow and brain (Inami, 1983; Hongo, 1991; Yamakawa, 1992a; Uchiyama, 2000; Sato, 2021a). Additionally, many stone arrowheads, thought to have been used for hunting, were excavated (Torihama Shell Midden Study Group, 1987). These suggested that the bones probably originated from hunted individuals and were disposed of in the lowlands after being used as resources for food and tools. We expected those materials to include dead individuals from all seasons. The Torihama Shell Midden site yielded the evidence of hunting activity throughout the year, though it seemed to be intensively used from fall to winter based on the death-season of sika deer remains which were estimated from observations of antlers, the cementum layer, and mandibular tooth eruption (Nishida, 1980; Ohtaishi, 1980; Sato, 2021b).

We compared the data from the archeological remains with the published DMT data of extant sika deer. Among the 15 sika deer populations in Japan that Kubo and Fujita (2021) analyzed, we selected three populations (Figure 1 and Table 1): typical

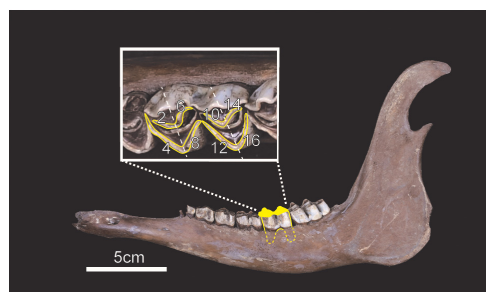


FIGURE 2
Example of analyzed materials and position of scanned enamel facets. We investigated the occlusal surface of lower second molars enclosed in yellow (i.e., facet No. 2, 4, 6, 8, 10, 12, 14, and 16).

TABLE 1 Habitat environment and food habits related to the materials in this study.

Region of the materials	Specimen no.	Scan no.	Annual mean temperature (°C)	Annual precipitation (mm)	Major vegetation	% Grass in diet ^{*1}
Kinkazan Island	32	123	11.9	1,150	Deciduous broad-leaves forest with some open grasslands	65.8
Shimane	27	100	14.6	1,685	Evergreen broad-leaves forest	38.1
Tsushima Island	28	129	15.8	2,235	Evergreen broad-leaves forest	3.4
Torihamma shell midden	M2:56 (L:31, R:25)	205	15 ^{*2}	2,000 ^{*2}	Evergreen broad-leaves forest with Japanese cedar and Deciduous broad-leaves	

^{*1} We referenced Kubo and Yamada (2014) and Kubo and Fujita (2021) which contained the quantitative dietary data showing the consumption rate of graminoids obtained from stomach content analysis and fecal analysis. ^{*2} Temperature and precipitation around the site are estimated from 5,900 to 5,600 cal.bp based on the results of Kitagawa et al. (2018).

grazing (Kinkazan Island), browsing (Tsushima Island), and mixed-feeding (Shimane) populations. The Shimane population was selected because of its habitat's geological proximity and environmental similarity to the Torihamma Shell Midden location. We selected the Kinkazan and Tsushima populations because of their contrasting north–south diets in the Japanese archipelago, and many samples have been analyzed. Sika deer on Kinkazan Island inhabit a small island near the Oshika Peninsula in Miyagi Prefecture, facing the Pacific Ocean. The main vegetation is deciduous broadleaved forest with some open grasslands. Kinkazan deer feed mainly on grasses such as silver grass (*Miscanthus sinensis*) and lawn grass (*Zoysia japonica*) (Takatsuki, 1980). The Tsushima deer inhabited an evergreen broadleaved forest. Stomach content analysis revealed that they fed mainly on woody plants, followed by herbaceous plants, seeds, and fruits; graminoids were a minor component of their diet (Suda, 1997). Deer from the Shimane population inhabited the Misen Mountains of Shimane Prefecture, in the San-in region, at the same latitude as the Torihamma site. Evergreen broadleaved forests are the primary vegetation in the area. Stomach content analysis of Shimane deer showed that they consumed both graminoids and leaves of broadleaved trees and forbs year-round, although there was seasonal variation (Shimane Prefectural Government, 2002). The dietary differences among the three populations were represented in the percentage of grasses in the diets: 65.8% in Kinkazan (grazers), 38.1% in Shimane (mixed feeders), and 3.4% in Tsushima (browsers) (Kubo and Yamada, 2014; Kubo and Fujita, 2021).

Methods: Dental microwear texture analysis

Molding of tooth enamel surfaces of Torihamma deer

We used the methodology of Kubo et al. (2017) and made molds of the M2. To remove dirt adhered during the sedimentation, we cleaned the molar occlusal surfaces with

cotton swabs soaked with acetone. Next, the surface was molded using high-resolution A-silicone dental impression material (Dr. Silicon regular type, BSA Sakurai, Japan). We selected the occlusal enamel band as our target for scanning (Figure 2) because we expected it to be less affected than other parts by factors other than diet (Schulz et al., 2010).

Obtaining dental microwear texture (DMT) data and calculating DMT parameters

We scanned the dental impressions by using a confocal laser microscope (VK-9700, Keyence, Osaka, Japan) equipped with a 100× long-distance lens (N.A. = 0.95). Three-dimensional data was obtained with a lateral (x, y) sampling interval of 0.138 μm and a vertical resolution (z) of 0.001 μm. Occlusal enamel facets were scanned on areas of 140 × 105 μm, and grayscale images of the tooth surfaces were acquired for graphical comparison. The 3D surface data were processed by applying the methods in Yamada et al. (2018), Aiba et al. (2019), and Kubo and Fujita (2021), using MountainsMap Imaging Topography (7.4.8872, Digital Surf, Besançon, France). The methods provide an objective evaluation of quantitative data and scratch depth by measuring microwear three-dimensionally. First, we scanned and trimmed the 135 × 100 μm area of the microwear impressions, avoiding dust and large scratches. Because the scanned images were mirror images of real tooth surfaces, the coordinates were mirrored in the x- and z-axes. Second, through the least square plane by subtraction, the surfaces were leveled to remove the inclination of the molds. Next, we applied a robust Gaussian filter with a cutoff value of 0.8 μm to remove measurement noise (S-filter as defined in ISO25178) and the form removal function (polynomial of increasing power = 2) to remove the large-scale curvature of the enamel bands (F-operation in ISO25178). We used the automated outlier removal function of MountainsMap, which removes features with a slope > 80°, and a threshold to remove the upper and lower 0.1% of the data. Scans with a non-measured point above 0.5% of

total data points were discarded from the following analyses. The non-measured points were filled by using the smoothing function of MountainsMap. Finally, the values of 31 parameters of ISO 25178-2 were calculated, of which the names and definitions are shown in **Table 2**. These 31 ISO parameters were used in Kubo and Fujita (2021) to investigate the relationship between DMTA parameters and the extant sika deer diet. Because we used the same analytical template of the same software (MountainsMap) that Kubo and Fujita (2021) used, their published parameters are directly comparable to ours.

Statistical analyses

To clarify the feeding habits of the Torihama deer, we compared their DMT parameters with those of the three populations of sika deer (Kinkazan Island, Shimane, and Tsushima Island). We conducted principal component analysis (PCA) followed by a varimax rotation to interpret the 31 parameters and summarize them into a few principal components (PCs). We also conducted the Mann–Whitney *U*-test to determine differences in the parameters and the PC scores between Torihama and the three populations. The

TABLE 2 Names and definitions of 31 DMT parameters.

Category	Parameter	Description	Unit
Height parameters	<i>Sq</i>	Standard deviation of the height distribution	μm
	<i>Ssk</i>	Skewness of the height distribution	no unit
	<i>Sku</i>	Kurtosis of the height distribution	no unit
	<i>Sp</i>	Maximum peak height, height between the highest peak and the mean plane	μm
	<i>Sv</i>	Maximum pit height, depth between the mean plane and the deepest pit	μm
	<i>Sz</i>	Maximum height, sum of the maximum peak height and the maximum pit height ($Sp + Sv$)	μm
	<i>Sa</i>	Arithmetic mean height	μm
Spatial parameters	<i>Sal</i>	Autocorrelation length ($s = 0.2$)	μm
	<i>Str</i>	Texture aspect ratio ($s = 0.2$)	no unit
Hybrid parameters	<i>Sdq</i>	Root mean square gradient	no unit
	<i>Sdr</i>	Developed interfacial area ratio	%
Functional parameters	<i>Smr</i>	Areal material ratio, ratio of the area of the material at a specified height c ($c = 1 \mu\text{m}$ under the highest peak)	%
	<i>Smc</i>	Inverse areal material ratio, height at which a given areal material ratio ($p = 10\%$)	μm
	<i>Sxp</i>	Peak extreme height, difference in height between the p and q material ratio ($p = 50\%$, $q = 97.5\%$)	μm
	<i>Sk</i>	Distance between the highest and lowest level of the core surface	μm
	<i>Spk</i>	Average height of the protruding peaks above the core surface	μm
	<i>Svk</i>	Average height of the protruding dales below the core surface	μm
Functional volume parameters	<i>Vm</i>	Material volume at a given material ratio ($p = 10\%$)	$\mu\text{m}^3/\mu\text{m}^2$
	<i>Vv</i>	Void volume at a given material ratio ($p = 10\%$)	$\mu\text{m}^3/\mu\text{m}^2$
	<i>Vmc</i>	Material volume of the core at a given material ratio ($p = 10\%$, $q = 80\%$)	$\mu\text{m}^3/\mu\text{m}^2$
	<i>Vvc</i>	Void volume of the core ($p = 10\%$, $q = 80\%$)	$\mu\text{m}^3/\mu\text{m}^2$
	<i>Vvv</i>	Void volume of the dale at a given material ratio ($q = 80\%$)	$\mu\text{m}^3/\mu\text{m}^2$
Feature parameters	<i>Spd</i>	Density of peaks	$1/\mu\text{m}^2$
	<i>Spc</i>	Arithmetic mean peak curvature	$1/\mu\text{m}$
	<i>S10z</i>	Ten-point height	μm
	<i>S5p</i>	Five-point peak height	μm
	<i>S5v</i>	Five-point pit height	μm
	<i>Sda</i>	Closed dale area	μm^2
	<i>Sha</i>	Closed hill area	μm^2
	<i>Sdv</i>	Closed dale volume	μm^3
	<i>Shv</i>	Closed hill volume	μm^3

statistical analyses were conducted using SPSS statistics ver.28 (IBM, Chicago, USA).

Estimation of the percentage of grasses (% grass) in the Torihama deer diet

Kubo and Fujita (2021) presented an equation, as follows, to estimate the % grass in diets from an ISO 25178-2 parameter, Sk , which showed the highest correlation with the % grass in the diet in their analysis:

$$\text{Logit (\% grass)} = \frac{(Sk - 0.341)}{0.0299} \quad (1)$$

where logit (% grass) is transformed into the % grass by the equation

$$\% \text{ grass} = \frac{e^{\text{logit (\% grass)}}}{1 + e^{\text{logit (\% grass)}}} \quad (2)$$

We used those two equations to estimate the % grass in the diet of 56 Torihama deer.

Results

Assessment of tooth microwear of Torihama deer by two-dimensional images

Representative microwear images and 3D models of the tooth surfaces are shown in Figure 3. Of the two-dimensional

(2D) images, we excluded those in which the tooth surface was clearly damaged or the non-measured point was above 0.5% of the total data points. As a result, of the 224 scans ($N = 224$), we used data from 205 scans (Supplementary Data 1). Although some materials showed heavily worn surfaces, microwear features were well-preserved in the Torihama deer specimens, and the diagenetic alteration was considered negligible. Small pits were commonly observed among the Torihama deer samples. Some samples had flat surfaces with a visible enamel prism structure (Figure 3A: FTS84-086), and others showed abundant scratches (Figure 3B: FTS084-096 and Figure 3C: FTS84-054). Coarse scratches were observed on the surface of some individuals (Figure 3C).

Comparison between Torihama deer and extant deer from representative populations

The PCA of the 31 DMT parameters showed that the first, second, and third components explained approximately 52.6, 15.9, and 12.8% of the total variance, respectively. Table 3 indicates the factor loadings of the 31 parameters. The first component (PC1) can be interpreted as overall surface roughness because 22 of the 31 parameters had factor loadings higher than the critical threshold value of 0.4, and 20 parameters were larger than 0.8. The height (e.g., Sq , Sz , Sa) and volume (e.g., Vm , Vv , Vmc , Vvc , Vvv) parameters had positive loads; thus, the larger the PC1 value, the larger the surface relief. On the other hand, parameters related to surface segmentation (Sda , Sha , Sdv , Shv , and Spd) contributed significantly to PC2. The

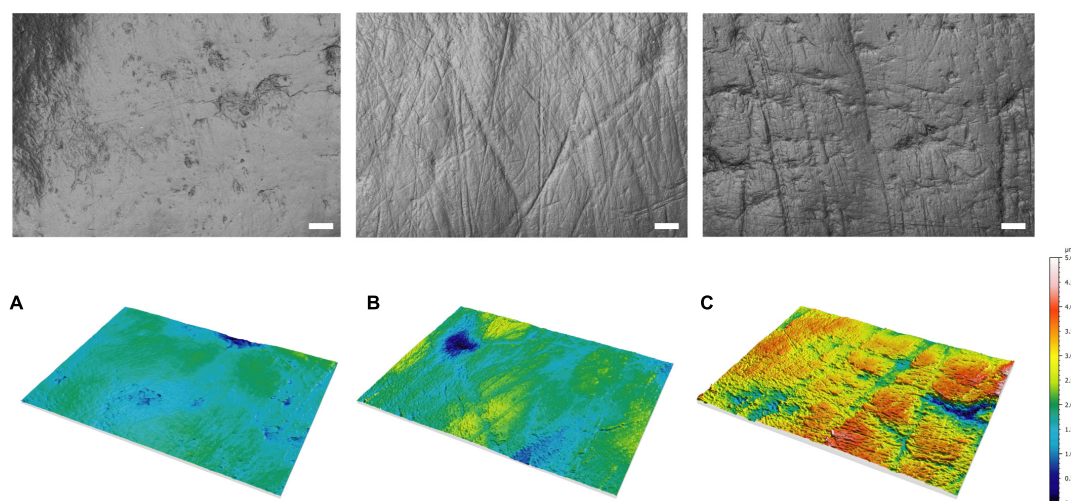


FIGURE 3

Representative microwear 2D images and 3D models of tooth surfaces of Torihama deer [specimen number (A) FTS084-086, (B) FTS084-096, (C) FTS84-054]. Enamel prism structures can be observed in (A). (B,C) Show show scratches. We also plotted the principal component scores of these specimens in Figure 4. White bars in the 2D micrographs are 10 μm .

TABLE 3 Factor loadings obtained from PCA conducted using 31DMT parameters.

	PC1	PC2	PC3
Variance explained (%)	52.659	15.933	12.832
<i>Sq</i>	0.903	0.230	0.329
<i>Ssk</i>	0.080	0.056	0.940
<i>Sku</i>	−0.037	−0.081	−0.894
<i>Sp</i>	0.887	0.109	0.348
<i>Sv</i>	0.910	0.204	−0.191
<i>Sz</i>	0.960	0.170	0.068
<i>Sa</i>	0.875	0.228	0.392
<i>Smr</i>	−0.822	−0.107	−0.321
<i>Smc</i>	0.856	0.213	0.439
<i>Sxp</i>	0.919	0.245	0.131
<i>Sal</i>	0.224	0.289	0.593
<i>Str</i>	−0.006	−0.053	−0.184
<i>Sdq</i>	0.895	−0.393	−0.101
<i>Sdr</i>	0.866	−0.405	−0.076
<i>Vm</i>	0.817	0.179	0.384
<i>Vv</i>	0.858	0.213	0.439
<i>Vmc</i>	0.841	0.226	0.443
<i>Vvc</i>	0.837	0.207	0.476
<i>Vvv</i>	0.912	−0.231	−0.012
<i>Spd</i>	0.026	−0.752	−0.302
<i>Spc</i>	0.506	0.095	−0.007
<i>S10z</i>	0.881	0.081	−0.087
<i>S5p</i>	0.756	−0.109	0.068
<i>S5v</i>	0.824	0.231	−0.206
<i>Sda</i>	0.087	0.931	0.123
<i>Sha</i>	−0.079	0.946	0.030
<i>Sdv</i>	0.338	0.833	0.021
<i>Shv</i>	0.184	0.878	−0.028
<i>Sk</i>	0.892	−0.149	0.224
<i>Spk</i>	0.898	−0.303	−0.092
<i>Svk</i>	0.812	−0.093	−0.413

Parameters with factor loadings higher than the critical threshold of 0.4 are shown in bold.

factor loadings of *Sda*, *Sha*, *Sdv*, and *Shv*, which indicate the areas and volumes of segmented hills and dales on the surface, were positive values, and that of *Spd*, which indicates the density of the peaks, was negative. Therefore, PC2 can be interpreted as the fineness of the microwear features, with the smaller values indicating a surface characterized by abundant fine features.

We found significant differences between the Torihama deer and the three populations of extant deer ($P < 0.05$; Table 4). The comparison with the Kinkazan deer showed statistically significant differences in 23 parameters, except for some hybrid, functional, and feature parameters. Statistically significant differences between the Torihama deer and the Shimane deer were found in 21 parameters, excluding the spatial, functional volume, and feature parameters. The largest

number of statistical differences (28 parameters) was found in the comparison between the Torihama deer and the Tsushima deer, indicating that the difference between the Torihama deer and the Tsushima deer is larger than that between the deer in Kinkazan and Shimane.

The results of the statistical comparison of the PC scores between the Torihama and extant deer populations are also shown in Table 4. A scatter plot of PC1 and PC2 scores are shown in Figure 4 for the populations of Torihama, Shimane, Kinkazan, and Tsushima. Deer on Kinkazan Island, typical grazers, were characterized by higher PC1 scores (i.e., large surface roughness), whereas those deer on Tsushima Island, typical browsers, were located at the lower bottom. The Shimane population, mixed feeders, was located between them. Thus, we found a separation between the grazing, mixed feeding, and browsing populations of the extant deer, although the Shimane and Tsushima populations overlapped. The Torihama deer overlapped with the distribution of the grazing and mixed-feeding sika deer but not with the browsing population.

Estimation of % grass in the diet of Torihama deer and its variation within the assemblage

We applied the estimation equation of Kubo and Fujita (2021) to estimate the % grass in the diet of 56 Torihama deer (Figure 5). The Torihama deer were estimated to have consumed a diet of, on average, 50.7% grass, which supported a general mixed-feeding habit of the Torihama deer. Browsing and grazing individuals occurred with a similar frequency, and there was a wide range in % grass within the Torihama deer population.

Discussion

In this study, we used DMTA to estimate the diets of Torihama deer inhabited approximately 6,000 years ago. Deer mandibles excavated from the site were in satisfactory preservation conditions; thus, observing the antemortem microwear was possible. The results of the comparison with the extant sika deer showed that the Torihama deer overlapped with the populations that had mixed-feeding and grazing-feeding habits and showed a wide range in % grass in the diet.

Reconstruction of the diet of the Torihama deer based on extant sika deer references

The results of PCA on 31 parameters of surface roughness showed that the Torihama deer overlapped with the grazing

TABLE 4 Comparison of DMT parameters and principal component scores between Torihama deer and extant deer.

Parameter	Torihama vs. Kinkazan		Torihama vs. Shimane		Torihama vs. Tsushima	
	<i>z</i>	<i>P</i>	<i>z</i>	<i>P</i>	<i>z</i>	<i>P</i>
<i>Sq</i>	-4.910	<0.001	2.100	0.036	2.647	0.008
<i>Ssk</i>	-4.944	<0.001	-3.723	<0.001	-2.960	0.003
<i>Sku</i>	5.465	<0.001	3.703	<0.001	3.112	0.002
<i>Sp</i>	-3.817	<0.001	2.751	0.006	3.596	<0.001
<i>Sv</i>	-0.998	0.319	4.782	<0.001	4.735	<0.001
<i>Sz</i>	-2.559	0.011	4.219	<0.001	4.678	<0.001
<i>Sa</i>	-5.152	<0.001	1.594	0.111	2.211	0.027
<i>Smr</i>	3.131	0.002	-2.663	0.008	-3.359	<0.001
<i>Smc</i>	-5.152	<0.001	1.303	0.193	1.993	0.046
<i>Sxp</i>	-3.869	<0.001	2.809	0.005	3.255	0.001
<i>Sal</i>	0.295	0.768	-0.778	0.437	0.247	0.805
<i>Str</i>	4.779	<0.001	1.526	0.127	2.752	0.006
<i>Sdq</i>	-2.377	0.017	6.250	<0.001	6.841	<0.001
<i>Sdr</i>	-1.631	0.103	6.610	<0.001	7.003	<0.001
<i>Vm</i>	-4.294	<0.001	1.380	0.168	2.059	0.039
<i>Vv</i>	-5.126	<0.001	1.361	0.174	2.021	0.043
<i>Vmc</i>	-5.447	<0.001	1.098	0.272	1.841	0.066
<i>Vvc</i>	-5.248	<0.001	0.953	0.341	1.784	0.074
<i>Vvv</i>	-3.340	<0.001	3.042	0.002	3.615	<0.001
<i>Spd</i>	3.088	0.002	3.791	<0.001	5.845	<0.001
<i>Spc</i>	-2.897	0.004	2.926	0.003	2.752	0.006
<i>S10z</i>	-0.252	0.801	4.481	<0.001	4.583	<0.001
<i>S5p</i>	0.789	0.430	3.528	<0.001	4.346	<0.001
<i>S5v</i>	-1.102	0.271	4.219	<0.001	3.568	<0.001
<i>Sda</i>	-3.652	<0.001	-3.392	<0.001	-5.238	<0.001
<i>Sha</i>	-2.915	0.004	-3.626	<0.001	-5.987	<0.001
<i>Sdv</i>	-2.628	0.009	0.233	0.816	-2.685	0.007
<i>Shv</i>	-3.478	<0.001	-0.301	0.763	-3.909	<0.001
<i>Sk</i>	-5.456	<0.001	4.335	<0.001	4.479	<0.001
<i>Spk</i>	-1.934	0.053	5.434	<0.001	6.433	<0.001
<i>Svk</i>	-1.015	0.310	5.550	<0.001	4.706	<0.001
PC1	-3.218	0.001	4.831	<0.001	-5.371	<0.001
PC2	-1.717	0.086	-2.654	0.008	5.105	<0.001
PC3	-4.589	<0.001	-4.121	<0.001	2.334	0.020

P-values of Mann–Whitney *U*-tests are shown. Significant ($P < 0.05$) differences are shown in bold.

and mixed-feeding deer. However, they did not overlap with the browsing Tsushima deer. The Tsushima deer did not have well-developed microwear. A reason for this observation is that their diets were less abrasive than those of the Torihama deer. For example, the former ate dicot leaves, which polished tooth surfaces rather than abrading them. The absence of overlap between the Tsushima and the Torihama deer indicates that the diet of the Torihama deer was not primarily dicots. The Torihama deer overlapped with the Kinkazan deer, a typical grazer type that developed microwear by feeding on grass, and with the Shimane deer, a mixed feeder type, which demonstrates the possibility that the Torihama deer were

feeding on both grass plants and the leaves and fruits of dicotyledonous plants.

Furthermore, some Torihama deer developed abundant scratches on their tooth surfaces, which were finer than those of grazing deer on Kinkazan Island (Figure 3B). These individuals did not overlap with the Kinkazan deer in the scatter plot of PC1 and PC2 (Figure 4). These results may indicate that some Torihama deer foraged on grass species, which differ from those foraged by the Kinkazan deer. The Kinkazan deer feed primarily on short-statured lawn grass (*Z. japonica*) (Takatsuki, 1980), which may force them to ingest the soil secondarily when feeding on lawn grass at the ground level (Rivals et al., 2014;

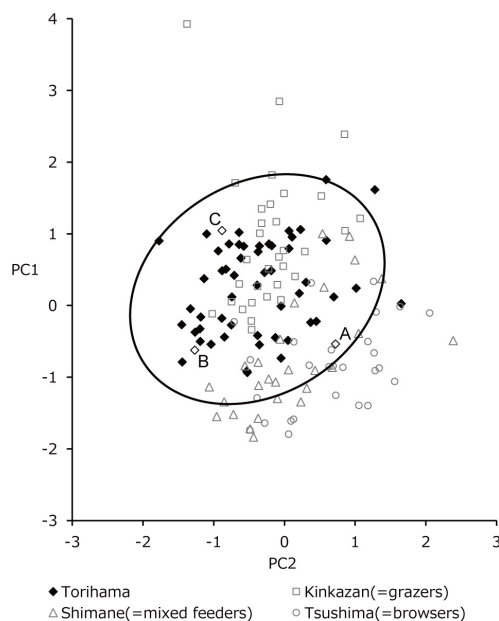


FIGURE 4

Scatter plot of the first (PC1) and second (PC2) principal component scores calculated by PC analysis using 31 parameters of ISO 25178-2. PC1 is interpreted as overall surface roughness because the height and volume parameters had positive loads. PC2 presents the fineness of the microwear features because the parameters related to surface segmentation had positive loads: larger PC2 values indicate that surfaces are segmented into larger hills and dales. The 95% confidence range of Torihama deer is indicated by the bold line. Kinkazan, Shimane, and Tsushima deer are typical grazers, mixed feeders, and browsers, respectively.

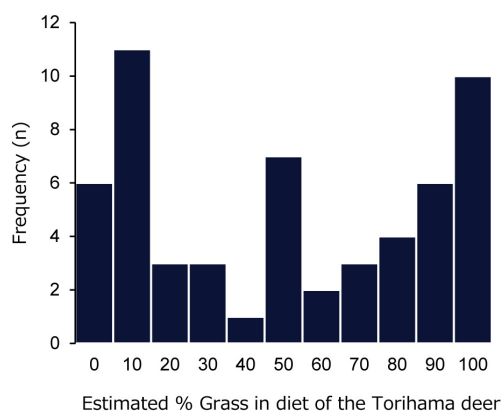


FIGURE 5

Histogram of estimated % grass in the diet of the Torihama deer, using the estimation equation of Kubo and Fujita (2021).

the rumination process to some extent (Ackermans et al., 2020; Schulz et al., 2020). The comparison of 15 populations of sika deer demonstrated that the Kinkazan deer had rougher surfaces than other grazing deer (Kubo and Fujita, 2021). Therefore, the Torihama deer might not have fed on short grasses contaminated by soil. Around the Torihama Shell Midden site grew graminoid (Poaceae and Cyperaceae) plants, indicated by the analyses of pollen and macrobotanical remains (Kasahara, 1983, 1984; Kitagawa et al., 2018). The analysis of phytoliths has also identified grasses such as the reed *Phragmites* and *Bambusoideae* species (Sasaki, 1983). Therefore, the Torihama deer could also have fed on these grasses when they were available.

The flexible diet of Torihama deer

The proportion of grass in the diets of the Torihama deer was estimated to be 50.7% on average, with a wide range of 0 to 100% among these individuals (Figure 5). This estimate indicates that Torihama deer are mixed feeders and may reflect the dietary flexibility of sika deer during the Jomon period. It is also assumed that the Torihama deer would change diets according to seasonal availability. The Torihama deer in this study were over 2 years old, representing the diets of weaned individuals. Furthermore, the average age in the Torihama population was estimated to be 6.96 years (Koike and Ohtaishi, 1985); thus, the tendencies of sexually mature individuals can be observed. We could not estimate the mortality seasons for each material used in this study. However, the literature has suggested that the people who lived at the Torihama Shell Midden site may have hunted sika deer year-round, mainly during fall and winter (Nishida, 1980; Ohtaishi, 1980; Sato, 2021b).

The result of stomach content analysis of the Shimane populations, which we used as the reference in this study, showed a seasonal change in diets of deer with a high consumption rate of grasses in summer, seeds and nuts in fall, and tree leaves in winter (Shimane Prefectural Government, 2002). Such seasonal change in diets was also identified for sika deer populations in Hyogo, the closest area to the archeological site; the consumption of seeds and nuts was high in fall; and that of evergreen leaves was high in winter (Yokoyama, 2009). Therefore, although we did not estimate the mortality seasons, the individuals that died in each season were analyzed by the DMTA. Based on the seasonal changes in the diets of the extant sika deer with geographical proximity and the background information that the Torihama deer may have been hunted year-round, the DMT of the Torihama deer may reflect their seasonal dietary changes. As mentioned in the introduction, the flora around the site was mixed vegetation of evergreen trees, broadleaved trees, and coniferous trees, which allowed the Torihama deer to change their forage plants seasonally.

Rivals and Takatsuki, 2015). Microwear can also be affected by sand and dust attached to foods (Maas, 1994; Gügel et al., 2001; Lucas et al., 2013). However, experimental feeding has clarified that the effects of external abrasives are mediated by

Additionally, the extant sika deer have dietary flexibility and can inhabit a wide range of habitat environments in Japan (Takatsuki, 2009). Takatsuki (2006) suggested that the ecological plasticity of the sika deer is associated with the extinction of large herbivores in the Japanese archipelago around the Pleistocene–Holocene boundary, through the process that vacant ecological niches after those extinctions were occupied by a survived species, sika deer. The argument of Takatsuki (2006) is vague regarding the cause–effect relationship, namely, “sika deer could survive the extinction because they had the ability to adapt to changing environments” or “since there were vacant ecological niches after the extinction, the sika deer became ecologically diverse according to the respective habitats.” To clarify this issue, information on the ecological variability of Pleistocene and Holocene sika deer, as well as other extinct ruminants, is necessary. This study is the first step toward this clarification. Our study indicates that sika deer in the Early Jomon period (approximately 6,000 years ago) had a flexible feeding habit of adapting to the vegetation of their habitats. Further investigation of excavated sika deer from older archeological sites than the site we examined would provide insights into when and how they attained high ecological plasticity.

Conclusion

We investigated the feeding habits of the sika deer in the Early Jomon period by analyzing the DMT of abundant skeletal remains excavated from an archeological site. The Torihama deer were mixed feeders, with a wide range in the estimated percentage of foraged grasses. These results are consistent with the estimate of paleo-vegetation around the Torihama Shell Midden site. Similar to the extant deer populations inhabiting the evergreen broadleaved forest in Honshu, the Torihama deer might have changed their foraging plants seasonally, depending on the growth of plants around their habitat. Their flexible diets are important for understanding how they survived the extinction of large mammals at the end of the Pleistocene and are widely present around the Japanese archipelago today. Most of the Japanese extant samples were collected during the opening of hunting seasons, and in the un hunted population of Kinkazan deer, they were individuals that died of natural causes. Therefore, because the comparative data are mainly from autumn to early spring, further research on seasonal variation in microwear should be conducted by obtaining samples that can be compared among seasons.

For further research, DMTA results will be able to further elucidate the paleoecology of deer by including studies of the mortality season and range of behavior in individuals.

Data availability statement

The datasets presented in this study can be found in online repositories. The names of the repository/repositories and accession number(s) can be found in the article/ **Supplementary material**. The original scan data of all individuals in common 3D surface format (“sur” format) and 3D surface analytical files including raw scans and procedures of analyses in DMTA standard format (“mnt”) were uploaded to an online repository (Zenodo): <https://doi.org/10.5281/zenodo.7058460>.

Ethics statement

Ethical review and approval was not required for the animal study because it is focused on archeological materials.

Author contributions

KS: conceptualization, investigation, formal analysis, data curation, visualization, and writing—original draft preparation. TS: conceptualization, resources, supervision, and writing—review and editing. MOK: resources, supervision, and writing—review and editing. All authors contributed to the article and approved the submitted version.

Funding

This study was partially funded by JSPS KAKENHI (Grant No. 16H03106) to TS and the Keio University Doctorate Student Grant-in-Aid Program from Ushioda Memorial Fund to KS.

Acknowledgments

We thank the following institutions and people for their support. The Wakasa History Museum permitted us to use the collections. Mayumi Ajimoto (Wakasa History Museum) and Hideaki Kojima (Wakasa Town Section of History and Culture) provided us with suggestions and support. In addition, we received valuable comments from professors of the Department of Archaeology and Ethnology, Keio University, and the Mammal Society of Japan. We would like to thank Enago (www.enago.jp) for the English language review. Finally, we appreciate the two reviewers for their constructive comments on the earlier version of this manuscript.

Conflict of interest

The authors declare that the research was conducted in the absence of any commercial or financial relationships that could be construed as a potential conflict of interest.

Publisher's note

All claims expressed in this article are solely those of the authors and do not necessarily represent those of their affiliated

organizations, or those of the publisher, the editors and the reviewers. Any product that may be evaluated in this article, or claim that may be made by its manufacturer, is not guaranteed or endorsed by the publisher.

Supplementary material

The Supplementary Material for this article can be found online at: <https://www.frontiersin.org/articles/10.3389/fevo.2022.957038/full#supplementary-material>

References

- Ackermans, N. L., Winkler, D. E., Martin, L. F., Kaiser, T. M., Clauss, M., and Hatt, J.-M. (2020). Dust and grit matter: Abrasives of different size lead to opposing dental microwear textures in experimentally fed sheep (*Ovis aries*). *J. Exp. Biol.* 223:jeb220442. doi: 10.1242/jeb.220442
- Aiba, K., Miura, S., and Kubo, M. O. (2019). Dental microwear texture analysis in two ruminants, Japanese serow (*Capricornis crispus*) and sika deer (*Cervus nippon*), from central Japan. *Mamm. Study* 44, 183–192. doi: 10.3106/ms2018-0081
- Anezaki, T., Nishimoto, T., and Niimi, M. (2005). Faunal analysis of the Torihama shell midden, materials from the area 1 of the 1985 excavation (In Japanese). *Torihama Shell Midden Pap.* 4–5, 19–30.
- Berlioz, E., Azorit, C., Blondel, C., Ruiz, M. S. T., and Merceron, G. (2017). Deer in an arid habitat: Dental microwear textures track feeding adaptability. *Hystrix* 28, 222–230. doi: 10.4404/hystrix-28.2-12048
- DeSantis, L. (2016). Dental microwear textures: Reconstructing diets of fossil mammals. *Surf. Topogr.* 4:e023002. doi: 10.1088/2051-672X/4/2/023002
- Gügel, I. L., Grupe, G., and Kunzelmann, K. H. (2001). Simulation of dental microwear: Characteristic traces by opal phytoliths give clues to ancient human dietary behavior. *Am. J. Phys. Anthropol.* 114, 124–138. doi: 10.1002/1096-8644(200102)114:2<124::AID-AJPA1012<3.0.CO;2-S
- Hongo, H. (1991). Analysis of cut marks on mammal remains from section 85 of the Torihama shell midden (In Japanese). *Bull. Natl. Mus. Jpn. Hist.* 29, 149–195.
- Inami, M. (1983). "Remains of sika deer and wild boar from the Torihama shell midden," in *The summary report of excavation in 1981 and 1982 and research results of Torihama shell midden – research 3 on archaeological site located in lowland area from the early Jomon period (In Japanese)*, ed. Torihama Shell Midden Study Group (Wakasa Town: Board of Fukui Prefecture and Wakasa Museum of History and Folklore), 65–81.
- Kasahara, Y. (1983). "The detection and identification of plant seeds from Torihama shell midden (the 6th excavation)," in *The summary report of excavation in 1981 and 1982 and research results of Torihama shell midden – research 3 on archaeological site located in lowland area from the early Jomon period (In Japanese)*, ed. Torihama Shell Midden Study Group (Wakasa Town: Board of Fukui Prefecture and Wakasa Museum of History and Folklore), 47–64.
- Kasahara, Y. (1984). "The detection and identification of plant seeds from the Torihama shell midden (7th excavation)," in *The summary report of excavation in 1983 and research results of Torihama shell midden – research 4 on archaeological site located in lowland area from the early Jomon period (In Japanese)*, ed. Torihama Shell Midden Study Group (Wakasa Town: Board of Fukui Prefecture and Wakasa Museum of History and Folklore), 49–90.
- Kawamura, Y. (2009). "Fossil record of sika deer in Japan," in *Sika deer*, eds D. R. McCullough, S. Takatsuki, and K. Kaji (Tokyo: Springer), 11–25. doi: 10.1007/978-4-431-09429-6_2
- Kitagawa, J., Kojima, H., Yoshida, T., and Yasuda, Y. (2018). Adaptations of the early Jomon people in their settlement relocation to climate change around Lake Mikata, Central Japan. *Archaeol. Res. Asia* 16, 66–77. doi: 10.1016/j.ara.2018.03.002
- Koike, H., and Ohtaishi, N. (1985). Prehistoric hunting pressure estimated by the age composition of excavated sika deer (*Cervus nippon*) using the annual layer of tooth cement. *Archaeol. Sci.* 12, 443–456. doi: 10.1016/0305-4403(85)90004-4
- Kojima, H. (2015). The consideration of the excavation and study history of Torihama shell midden and its contribution to the zooarchaeological study (In Japanese with English abstract). *Zooarchaeology* 32, 11–24.
- Kubo, M. O., and Fujita, M. (2021). Diets of Pleistocene insular dwarf deer revealed by dental microwear texture analysis. *Paleogeogr. Palaeoclimatol. Palaeoecol.* 562:e110098. doi: 10.1016/j.palaeo.2020.110098
- Kubo, M. O., and Yamada, E. (2014). The inter-relationship between dietary and environmental properties and tooth wear: Comparisons of mesowear, molar wear rate, and hypsodonty index of extant sika deer populations. *PLoS One* 9:e90745. doi: 10.1371/journal.pone.0090745
- Kubo, M. O., Yamada, E., Kubo, T., and Kohno, N. (2017). Dental microwear texture analysis of extant sika deer with considerations on inter-microscope variability and surface preparation protocols. *Biosurf. Biotribol.* 3, 155–165. doi: 10.1016/j.bsbt.2017.11.006
- Kudo, Y., Suzuki, M., Noshiro, S., Ajimoto, M., and Amitani, K. (2016a). Radiocarbon dating of *Castanea crenata* wood from the incipient and initial Jomon periods excavated from the Torihama shell midden site, Fukui Prefecture, Japan (In Japanese with English abstract). *Jpn. Assoc. Hist. Bot.* 24, 59–68. doi: 10.34596/hisbot.24.2_59
- Kudo, Y., Amitani, K., Yoshikawa, J., Sasaki, Y., Ajimoto, M., and Noshiro, S. (2016b). Radiocarbon dating of plant macrofossils excavated from the Torihama shell midden site, Fukui Prefecture, Japan—a chronological reconsideration of sediment layers and types of pottery from the incipient to early Jomon periods (In Japanese with English abstract). *Jpn. Assoc. Hist. Bot.* 24, 43–58. doi: 10.34596/hisbot.24.2_43
- Lucas, P. W., Omar, R., Al-Fadhalah, K., Almusallam, A. S., Henry, A. G., Michael, S., et al. (2013). Mechanisms and causes of wear in tooth enamel: Implications for hominin diets. *J. R. Soc. Interface* 10:e20120923. doi: 10.1098/rsif.2012.0923
- Maas, M. C. (1994). A scanning electron microscopic study of *in vitro* abrasion of mammalian tooth enamel under compressive loads. *Arch. Oral Biol.* 39, 1–11. doi: 10.1016/0003-9969(94)90028-0
- Matsubayashi, J., and Tayasu, I. (2019). Collagen turnover and isotopic records in cortical bone. *J. Archaeol. Sci.* 106, 37–44. doi: 10.1016/j.jas.2019.03.010
- Merceron, G., Escarguel, G., Angibault, J.-M., and Verheyden-Tixier, H. (2010). Can dental microwear textures record inter-individual dietary variations? *PLoS One* 5:e9542. doi: 10.1371/journal.pone.0009542
- Miura, S. (2008). "Sika deer," in *A guide to the mammals of Japan*, ed. Japan Wildlife Research Center (Tokyo: Tokai university press), 110–111.
- Morikawa, M. (1963). Some problems concerning the Torihama shell midden site in Fukui Prefecture (In Japanese). *Mater. Cult.* 1, 19–34.
- Morikawa, M. (2002). *The Torihama shell midden- time capsule of the Jomon people*. Tokyo: Miraisya.
- Nakagawa, T., Kitagawa, H., Yasuda, Y., Tarasov, P. E., Gotanda, K., and Sawai, Y. (2005). Pollen/event stratigraphy of the varved sediment of Lake Suigetsu, Central Japan from 15,701 to 10,217 SG vyr BP (Suigetsu varve years before present): Description, interpretation, and correlation with other regions. *Quat. Sci. Rev.* 24, 1691–1701. doi: 10.1016/j.quascirev.2004.06.022
- Nakagawa, T., Tarasov, P. E., Nishida, K., Gotanda, K., and Yasuda, Y. (2002). Quantitative pollen-based climate reconstruction in Central Japan: Application to

surface and Late Quaternary spectra. *Quat. Sci. Rev.* 21, 2099–2113. doi: 10.1016/S0277-3791(02)00014-8

Niimi, M. (1997). The preliminary report of the determination of deer hunting seasons by the teeth eruption and wearing (In Japanese with English abstract). *Zooarchaeology* 9, 21–32.

Nishida, M. (1979). “Animal remains,” in *Torihamas shell midden – research 1 on archaeological site located in lowland area from the early Jomon period (In Japanese)*, ed. Torihama Shell Midden Study Group (Wakasa Town: Board of Fukui Prefecture), 164–166.

Nishida, M. (1980). Food resources and subsistence activities in the Jomon period on the organic remains of the Torihama shell midden (In Japanese). *Anthropol. Q.* 11, 3–41.

Nishimoto, T. (1991). Hunted deer and wild boar in the Jomon period (In Japanese). *Kodai* 91, 114–132.

Noshiro, S., and Suzuki, M. (1990). A palaeobotanical study of natural woods from the Torihama shell midden and reconstruction of the forest vegetation (In Japanese with English abstract). *Bull. Jpn. Sea Res. Inst.* 22, 63–152.

Noshiro, S., Suzuki, M., and Amitani, K. (1996). Species of wooden products from the Torihama shell midden (In Japanese). *Torihamas Shell Midden Pap.* 1, 23–79.

Ohtaishi, N. (1980). Estimation of sex, age, and season of death using mandibles of *Cervus nippon* excavated from an archaeological site (In Japanese). *Archaeol. Nat. Sci.* 13, 51–74.

Ohtaishi, N. (1986). Preliminary memorandum of classification, distribution and geographic variation on sika deer (In Japanese). *Honyurui Kagaku* 53, 13–17.

Rivals, F., Schulz, E., and Kaiser, T. M. (2009). A new application of dental wear analyses: Estimation of duration of hominid occupations in archaeological localities. *J. Hum. Evol.* 56, 329–339. doi: 10.1016/j.jhevol.2008.11.005

Rivals, F., Takatsuki, S., Albert, R. M., and Macià, L. (2014). Bamboo feeding and tooth wear of three sika deer (*Cervus nippon*) populations from northern Japan. *J. Mammal.* 95, 1043–1053. doi: 10.1644/14-MAMM-A-097

Rivals, F., and Takatsuki, S. (2015). Within-island local variations in tooth wear of sika deer (*Cervus nippon centralis*) in northern Japan. *Mammal. Biol.* 80, 333–339. doi: 10.1016/j.mambio.2015.02.001

Rivals, F., Prignano, L., Semprebon, G. M., and Lozano, S. (2015). A tool for determining duration of mortality events in archaeological assemblages using extant ungulate microwear. *Sci. Rep.* 5:e17330. doi: 10.1038/srep17330

Sasaki, S. (1983). “Plant opal analysis of soil from Torihama shell midden,” in *The summary report of excavation in 1981 and 1982 and research results of Torihama shell midden – research 3 on archaeological site located in lowland area from the early Jomon period (In Japanese)*, ed. Torihama Shell Midden Study Group (Wakasa Town: Board of Fukui Prefecture and Wakasa Museum of History and Folklore), 37–41.

Sato, K. (2021a). The resource utilization of sika deer from Torihama shell midden (In Japanese). *Annu. Bull. Shiga Prefect. Assoc. Cult. Herit.* 34, 1–12.

Sato, K. (2021b). Death-season of sika deer remains from the Torihama shell midden: Nondestructive analyses on mandibular molariform tooth development (In Japanese with English abstract). *Zooarchaeology* 38, 11–22.

Schulz, E., Calandra, I., and Kaiser, T. M. (2010). Applying tribology to teeth of hoofed mammals. *Scanning* 32, 162–182. doi: 10.1002/sca.20181

Schulz, E., Winkler, D. E., Clauss, M., Carlsson, J., Ackermans, N. L., Martin, L. F., et al. (2020). Everything matters: Molar microwear texture in goats (*Capra aegagrus hircus*) fed diets of different abrasiveness. *Palaeogeogr. Palaeoclimatol. Palaeoecol.* 552:109783. doi: 10.1016/j.palaeo.2020.109783

Shigehara, N., Hongo, H., and Amitani, K. (1991). Mammalian remains from the Torihama shell midden excavation in 1985 (In Japanese). *Bull. Natl. Mus. Jpn. Hist.* 29, 329–341.

Shimane Prefectural Government (2002). *A survey on the sika deer (Cervus nippon) in Misen mountainous region on the Shimane Peninsula, Japan (In Japanese)*. Shimane: Shimane Prefectural Government.

Suda, K. (1997). Rumen contents and food selectivity of sika deer (*Cervus nippon*) on Tsushima Islands (In Japanese with English abstract). *Wildl. Conserv. Jpn.* 2, 125–134.

Takahara, H., and Takeoka, M. (1992). Vegetation history since the last glacial period in the Mikata lowland, the sea of Japan area, western Japan. *Ecol. Res.* 7, 371–386. doi: 10.1007/BF02347104

Takatsuki, S. (1980). Food habits of sika deer on Kinkazan Island. *Sci. Rep. Tohoku Univ. Ser. IV Biol.* 38, 7–31.

Takatsuki, S. (2006). *Ecological history of sika deer*. Tokyo: University of Tokyo Press.

Takatsuki, S. (2009). “Geographical variations in food habits of sika deer: The Northern Grazer vs. the Southern Browser,” in *Sika deer*, eds D. R. McCullough, S. Takatsuki, and K. Kaji (Tokyo: Springer), 231–237. doi: 10.1007/978-4-431-09429-6_17

Torihamas Shell Midden Study Group (1985). *Summary report of excavation in 1984 and research results of Torihama shell midden – research 5 on archaeological site located in lowland area from the early Jomon period (In Japanese)*. Wakasa Town: Board of Fukui Prefecture and Wakasa Museum of History and Folklore.

Torihamas Shell Midden Study Group (1987). *Torihamas shell midden – summary of research from 1980-1985 (In Japanese)*. Wakasa Town: Board of Fukui Prefecture and Wakasa Museum of History and Folklore.

Uchiyama, J. (2000). The problem of deer and wild boar in Torihama shell midden: The function of the site revealed by the remains of sika deer and wild boar excavated in 1984 (In Japanese). *Torihamas Shell Midden Pap.* 2, 1–22.

Uchiyama, J. (2005). Hunting seasonality of sika deer (*Cervus nippon*) and wild boar (*Sus scrofa*) at Torihama shell midden (Early Jomon): A zooarchaeological analysis of the faunal remains of the excavation in 1984 (In Japanese). *Torihamas Shell Midden Pap.* 4-5, 79–113.

Winkler, D. E., Schulz-Kornas, E., Kaiser, T. M., Codron, D., Lechliter, J., Hummel, J., et al. (2020). The turnover of dental microwear texture: Testing the “last supper” effect in small mammals in a controlled feeding experiment. *Palaeogeogr. Palaeoclimatol. Palaeoecol.* 557:e109930. doi: 10.1016/j.palaeo.2020.109930

Yamada, E., Kubo, O. M., Kubo, T., and Kohno, N. (2018). Three-dimensional tooth surface texture analysis on stall-fed and wild boars (*Sus scrofa*). *PLoS One* 13:e0204719. doi: 10.1371/journal.pone.0204719

Yamakawa, F. (1992a). Method of making bone piercing tools in the Jomon: Analysis of animal remains excavated from Torihama shell midden (In Japanese). *J. Archaeol. Soc. Nippon* 78, 61–106.

Yamakawa, F. (1992b). Bone piercing tools from Torihama shell midden (In Japanese). *Bull. Wakasa Mus. Hist. Folk.* 4, 1–42.

Yasuda, Y. (1979). “Pollen analysis,” in *Torihamas shell midden – research 1 on archaeological site located in lowland area from the early Jomon period (In Japanese)*, ed. Torihama Shell Midden Study Group (Wakasa Town: Board of Fukui Prefecture), 176–196.

Yasuda, Y. (1982). Pollen analytical study of the sediment from the Lake Mikata in Fukui Prefecture, Central Japan –especially on the fluctuation of precipitation since the Last Glacial age on the side of Sea of Japan (In Japanese with English abstract). *Q. Res.* 21, 255–271. doi: 10.4116/jaqua.21.255

Yokoyama, M. (2009). “Biology of sika deer in Hyogo: Characteristics of reproduction, food habits, growth, and condition,” in *Sika deer*, eds D. R. McCullough, S. Takatsuki, and K. Kaji (Tokyo: Springer), 193–205. doi: 10.1007/978-4-431-09429-6_14

Yoshikawa, M., Yoshikawa, J., Noshiro, S., Kudo, Y., Sasaki, Y., Suzuki, M., et al. (2016). Vegetation history and use of plant resources from the incipient to early Jomon periods at the Torihama shell midden site, Fukui Prefecture, central Japan (In Japanese with English abstract). *Jpn. Assoc. Hist. Bot.* 24, 69–82. doi: 10.34596/hisbot.24.2_69

Yoshioka, K. (1973). *Plant-geography (In Japanese)*. Tokyo: Kyouritsu-Shuppan.



OPEN ACCESS

EDITED BY

Carlo Meloro,
Liverpool John Moores University,
United Kingdom

REVIEWED BY

Aurora Grandal-d'Anglade,
Universidade da Coruña, Spain
Phil Hopley,
Birkbeck, University of London,
United Kingdom

*CORRESPONDENCE

Bian Wang
bianwang@umich.edu

SPECIALTY SECTION

This article was submitted to
Paleoecology,
a section of the journal
Frontiers in Ecology and Evolution

RECEIVED 01 June 2022

ACCEPTED 05 September 2022

PUBLISHED 12 October 2022

CITATION

Wang B and Badgley C (2022)
Carbon-isotope composition
of artiodactyl tooth enamel and its
implications for paleodiets.
Front. Ecol. Evol. 10:958859.
doi: 10.3389/fevo.2022.958859

COPYRIGHT

© 2022 Wang and Badgley. This is an
open-access article distributed under
the terms of the [Creative Commons
Attribution License \(CC BY\)](#). The use,
distribution or reproduction in other
forums is permitted, provided the
original author(s) and the copyright
owner(s) are credited and that the
original publication in this journal is
cited, in accordance with accepted
academic practice. No use, distribution
or reproduction is permitted which
does not comply with these terms.

Carbon-isotope composition of artiodactyl tooth enamel and its implications for paleodiets

Bian Wang^{1,2,3*} and Catherine Badgley^{2,4}

¹Department of Earth and Environmental Sciences, College of Literature, Science, and the Arts, University of Michigan, Ann Arbor, MI, United States, ²Museum of Paleontology, University of Michigan, Ann Arbor, MI, United States, ³Institute of Vertebrate Paleontology and Paleoanthropology, Chinese Academy of Sciences (CAS), Beijing, China, ⁴Department of Ecology and Evolutionary Biology, College of Literature, Science, and the Arts, University of Michigan, Ann Arbor, MI, United States

The stable carbon-isotope composition of mammalian tooth enamel is a powerful tool for reconstructing paleodiet and paleoenvironment. Its application in the fossil record relies on a thorough understanding of the isotopic composition of mammalian diets in modern ecosystems. We compiled and evaluated a global dataset of the carbon-isotope values of artiodactyl tooth enamel, supplemented by new samples, for 79 extant species. After correcting for differences in atmospheric carbon-isotope composition, body mass, and digestive physiology, we compared the inferred carbon-isotope values of ingested forage ($\delta^{13}\text{C}_{\text{diet}}$) among seven feeding categories. The artiodactyl herbivore dietary spectrum is expressed through a wide range of $\delta^{13}\text{C}_{\text{diet}}$ values, with the most depleted mean value in frugivores and the most enriched in obligate grazers. In general, grazing species have a broader range of isotope values than browsing species, suggesting a wider dietary niche breadth. Notably, variable grazers exhibit a bimodal distribution of $\delta^{13}\text{C}_{\text{diet}}$ values, with North American and Asian taxa consuming C_3 diets and African taxa consuming C_4 diets, reflecting the amount of C_4 vegetation in the environment. Variation in $\delta^{13}\text{C}_{\text{diet}}$ values also occurs among terrestrial ecoregions and artiodactyl clades. Grassland ecoregions differ significantly from forest ecoregions. We detected a low but significant phylogenetic signal in the mean $\delta^{13}\text{C}_{\text{diet}}$ values of extant species, with some of the oldest ruminant lineages having maintained C_3 feeding and pure C_4 diets being restricted to two bovid clades. Determining variation in $\delta^{13}\text{C}_{\text{diet}}$ values in different feeding categories and lineages will help refine paleoecological and paleoenvironmental reconstructions from the rich fossil record of artiodactyls.

KEYWORDS

stable isotope, herbivore, ungulates, tooth enamel, paleodiet

Introduction

Stable isotopes are one of nature's great ecological recorders and have been widely used to study organisms and ecosystems across time and space (West et al., 2006; Clementz, 2012). Among the animal tissues that are commonly sampled for stable isotope analyses of mammals (tooth enamel, dentin, bone collagen, hair, blood), only tooth enamel is resistant to long-term fossilization processes and diagenesis (Wang and Cerling, 1994; Koch et al., 1997; Lee-Thorp, 2002). Therefore, data generated from modern mammal teeth can be readily applied to the interpretation of deep-time records. Isotope data from extant ungulates have contributed substantial insights into our understanding of herbivore dietary ecology and have laid the foundations for a large body of literature inferring paleodiet and paleoenvironment from fossil herbivore teeth (e.g., Koch et al., 1991; Bocherens et al., 1996; Cerling and Harris, 1999; Passey and Cerling, 2002; Cerling et al., 2003, 2010; Sponheimer et al., 2003; Sponheimer and Cerling, 2014). Extant terrestrial ungulates are represented by over 250 species of artiodactyls and 18 species of perissodactyls (Burgin et al., 2018). Artiodactyls are naturally widespread in the ecosystems of Africa, Eurasia, North America, and South America. The taxonomic and ecological diversity of this family renders them good modern analogs for many extinct ungulates.

Carbon isotopes in tooth enamel

The stable isotope composition of carbon ($\delta^{13}\text{C}$) in the enamel of mammalian herbivores provides information about the animals' feeding ecology and vegetation present in the habitat. Plants that use different photosynthetic pathways differ in their fractionation of atmospheric CO_2 during photosynthesis. The resulting $\delta^{13}\text{C}$ values in plant tissues are lowest in plants using the C_3 pathway, intermediate in plants using the crassulacean acid metabolism (CAM) pathway, and highest in plants using the C_4 pathway (O'Leary, 1988; Cerling et al., 1997). When plants are consumed by mammalian herbivores and incorporated into their body tissues, tooth enamel bioapatites are systematically enriched in $\delta^{13}\text{C}$ relative to bulk plant diet with measurable enrichment factors (Lee-Thorp and van der Merwe, 1987; Cerling and Harris, 1999; Passey et al., 2005). Thus, the carbon isotope composition of enamel reliably reflects the values in the ingested plants. Pure C_3 and C_4 consumers have non-overlapping $\delta^{13}\text{C}$ values, while mammals with mixed C_3 - C_4 diets have intermediate $\delta^{13}\text{C}$ values (Cerling et al., 1997, 2015; Koch, 1998). CAM plants commonly grow in xeric habitats (Ehleringer et al., 1991) and are not typically consumed by ungulates. Therefore, they are not usually considered when interpreting the carbon isotopic values of modern or fossil ungulates.

Isotopic variability among C_3 plants is generally greater than that in C_4 plants (e.g., Cerling et al., 1997). In general, higher (more enriched) values of the carbon isotope composition of tooth enamel of herbivorous mammals are representative of open-canopy, drier habitats (such as shrubland and grassland), while low values represent closed-canopy habitats (such as woodlands and forests) (O'Leary et al., 1992; Koch, 1998; Cerling and Harris, 1999; Feranec and MacFadden, 2006; Feranec, 2007; Secord et al., 2008). Resource partitioning in diet and habitat use may be revealed through stable isotope analysis (Feranec and MacFadden, 2006) and has been documented for medium-to large-bodied herbivores in both modern and ancient environments in which a mixture of C_3 and C_4 plants is present (e.g., Wang et al., 1994; MacFadden and Cerling, 1996; Koch, 1998; Feranec and MacFadden, 2006; Kita et al., 2014; Wang and Secord, 2020).

The browser–grazer spectrum

Most artiodactyls are herbivorous, and they are typically classified as browsers, grazers, or mixed feeders. Browsers primarily feed on dicotyledonous material, such as leaves, fruits, and twigs; grazers primarily feed on monocotyledonous material, such as grasses or sedges, which are generally more abrasive than dicotyledonous material; and mixed feeders consume a mixture of dicotyledonous and monocotyledonous materials across space and seasons (Hofmann and Stewart, 1972). Much of the existing literature classifies living and fossil herbivores using these categories. Finer dietary classifications have been used in some studies to capture more details in the foraging behavior of various artiodactyls (e.g., Janis and Ehrhardt, 1988; Spencer, 1995; Sponheimer et al., 1999; Mendoza et al., 2002). These studies show promise for differentiating artiodactyl feeding categories beyond three broad categories, giving consideration to the specialization or generality of species' diets, the canopy-cover of feeding environment, and sometimes the level (height from the ground) that species feed at. Other studies in recent years have used the percentage of grass in species' diets to place species quantitatively along a dietary continuum. This approach overcomes the potential weaknesses of categorical trait data and conceptualizes diet as a spectrum with two end members: browsers and grazers (e.g., Clauss et al., 2003).

Research questions

Recent research has identified gaps in our knowledge of the stable isotope ecology of large mammals and its application in the fossil record, such as what factors influence enrichment processes and how much variability in resource partitioning exists among different faunas (Tejada-Lara et al., 2018;

DeSantis et al., 2020; Tejada et al., 2020). These findings highlight the need for more data from a range of modern ecosystems for better understanding of processes and factors that affect the isotopic signatures in mammal tissues. In addition, stable-isotope ratios of ungulate tooth enamel can be compared to the dental hypsodonty index, dental mesowear (sharpness of tooth cusps), dental microwear (microscopic abrasion patterns on the occlusal surface), ecomorphological analysis of craniomandibular features, as well as stomach- and fecal contents and other types of data that are used to document ungulate dietary ecology. It has been shown that combining results from multiple methods improves accuracy of paleoecological reconstructions (e.g., Rivals and Ziegler, 2018; Sewell et al., 2019). Such cross-method comparisons capture dietary behaviors and adaptations recorded through different processes and over different time scales, thus providing more reliable and detailed dietary information for extant and fossil species (e.g., Sponheimer et al., 2003; Boissarie et al., 2005; Merceron et al., 2006; Louys et al., 2012; Bradham et al., 2018; Uno et al., 2018; Gong et al., 2020).

In this study, we compile and compare the carbon-isotope data published to date from the tooth enamel of extant artiodactyls. To build on existing data and increase the range and distribution of isotopic values across taxa and regions, we additionally sampled and analyzed 80 tooth specimens from 23 species of artiodactyls. Each species was chosen either because it had not been previously analyzed for stable isotopes of enamel

or because existing isotope data for the species included small sample sizes from restricted locations. The resulting dataset includes published and new isotope data for 79 artiodactyl species, covering a range of habitats and dietary ecology. We adopt a more detailed classification scheme of herbivore diets than what is commonly used in the literature. This classification scheme includes seven feeding categories and provides more information about dietary habits than the three broad categories of browsing, grazing, and mixed feeding. Combining the isotope data from artiodactyl enamel, dietary data derived from other studies, and the environmental setting of localities, we address the following research questions: (1) How do species with different dietary habits compare in the mean and range of $\delta^{13}\text{C}$ values of their diet? (2) How do artiodactyl diets in different ecoregions of the world compare in the mean and range of $\delta^{13}\text{C}$ values? (3) How do phylogenetic groups of artiodactyls compare in the mean and range of $\delta^{13}\text{C}$ values?

Materials and methods

We compiled a global dataset of the carbon-isotope values of artiodactyl tooth enamel ($\delta^{13}\text{C}_\text{E}$) from the literature, supplemented by 80 newly analyzed samples to expand the taxonomic and geographic coverage of our data (Figure 1 and Table 1). After correcting for differences in atmospheric carbon-isotope composition ($\delta^{13}\text{C}_\text{atm}$), body mass, and digestive

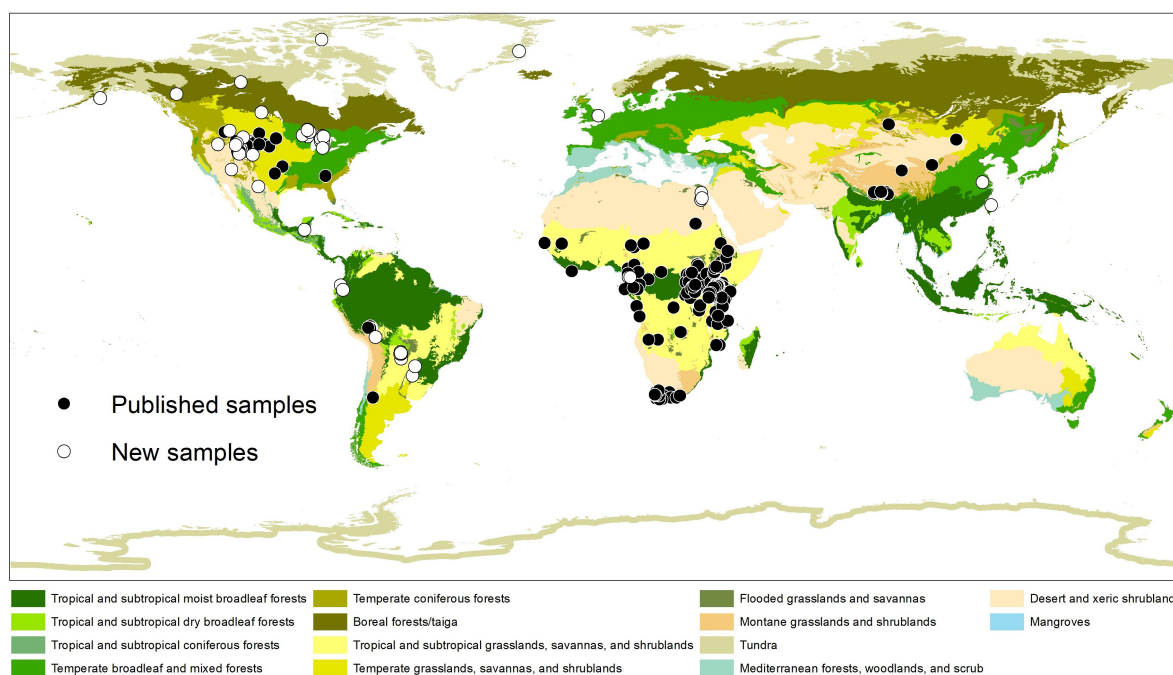


FIGURE 1

Collecting locations of tooth enamel samples used in this study. Ecoregions of the world follow Olson et al. (2001). See Table 1 for sources of published samples. Note that sampling effort is highly uneven among geographic regions and ecoregions of the world.

TABLE 1 Eighty new samples of artiodactyl tooth enamel collected from specimens housed in the University of Michigan Museum of Zoology (UMMZ) and analyzed for carbon-isotope composition ($\delta^{13}\text{C}_\text{E}$).

Species	Collection No.	Tooth	Region	Country	Latitude	Longitude	$\delta^{13}\text{C}_\text{E}$
<i>Alces americanus</i>	UMMZ 60536	Lp4	Michigan	United States	48.10	-88.70	-14.4
<i>Alces americanus</i>	UMMZ 61782	Rm3	Michigan	United States	47.37	-88.11	-14.9
<i>Alces americanus</i>	UMMZ 64975	Lm3	Michigan	United States	48.03	-88.77	-14.3
<i>Antilocapra americana oregona</i>	UMMZ 44370	Lm3	Montana	United States	45.78	-108.50	-10.1
<i>Antilocapra americana oregona</i>	UMMZ 44372	Lm3	Montana	United States	45.78	-108.50	-9.2
<i>Antilocapra americana oregona</i>	UMMZ 65026	Rm3	Michigan	United States	42.46	-84.01	-13.9
<i>Antilocapra americana oregona</i>	UMMZ 65502	Rm3	Michigan	United States	42.46	-84.01	-12.2
<i>Antilocapra americana oregona</i>	UMMZ 67482	Lm3	Michigan	United States	42.46	-84.01	-11.2
<i>Capra nubiana</i>	UMMZ 163513	Lm3	Red Sea	Egypt	26.57	32.20	-6.2
<i>Capra nubiana</i>	UMMZ 164923	Lp4	Red Sea	Egypt	28.70	32.37	-7.9
<i>Cv-apra nubiana</i>	UMMZ 164942	Lm3	Red Sea	Egypt	27.15	32.53	-8.1
<i>Capreolus capreolus</i>	UMMZ 125684	Lm3	England	United Kingdom	52.40	0.70	-11.1
<i>Cephalophus</i> sp.	UMMZ 38376	Lm3	Kribi	Cameroon	2.95	9.92	-12.1
<i>Cervus elaphus canadensis</i>	UMMZ 57713	Lm3	Michigan	United States	42.81	-83.78	-11.8
<i>Cervus elaphus canadensis</i>	UMMZ 57755	Lm3	Michigan	United States	44.85	-83.96	-12.0
<i>Cervus elaphus canadensis</i>	UMMZ 59189	Lm3	Utah	United States	40.85	-109.89	-11.0
<i>Cervus elaphus canadensis</i>	UMMZ 59798	Rm3	Wyoming	United States			-11.2
<i>Cervus elaphus canadensis</i>	UMMZ 59799	Rm3	Wyoming	United States			-10.8
<i>Cervus elaphus canadensis</i>	UMMZ 62121	Lm3	Wyoming	United States	44.00	-110.41	-11.3
<i>Cervus elaphus canadensis</i>	UMMZ 62122	RM3	Wyoming	United States	43.48	-110.76	-10.6
<i>Gazella dorcas</i>	UMMZ 158959	Lm3	Wadi	Egypt			-12.1
<i>Gvazella dorcas</i>	UMMZ 158960	Lm3	Wadi	Egypt			-10.1
<i>Gazella dorcas</i>	UMMZ 158962	Rm3	Wadi	Egypt			-11.0
<i>Gazella dorcas</i>	UMMZ 158966	Lm3	Wadi	Egypt			-8.7
<i>Gazella dorcas</i>	UMMZ 158967	Lm3	Wadi	Egypt			-10.6
<i>Gazella dorcas</i>	UMMZ 158969	Rm3	Wadi	Egypt			-10.1
<i>Gazella dorcas</i>	UMMZ 158970	Lm3	Wadi	Egypt			-10.1
<i>Gazella dorcas</i>	UMMZ 158972	Lp4	Wadi	Egypt			-12.3
<i>Hydropotes inermis inermis</i>	UMMZ 56527	Rm3	Kiang-su	China	32.07	118.78	-14.2
<i>Mazama americana</i>	UMMZ 126128	Rm3	Canindeyu	Paraguay	-24.45	-55.65	-14.8
<i>Mazama americana</i>	UMMZ 126854	Lm3	La Paz	Bolivia	-15.52	-67.82	-14.0
<i>Mazama americana</i>	UMMZ 146493	Rm3	Canindeyu	Paraguay	-24.45	-55.65	-14.5
<i>Mazama americana</i>	UMMZ 146494	RM3	Canindeyu	Paraguay	-24.45	-55.65	-15.0
<i>Mazama americana gualaea</i>	UMMZ 77816	RM3	Imbabura	Ecuador	0.35	-78.53	-14.2
<i>Mazama americana zamora</i>	UMMZ 82862	Rm3	Napo	Ecuador	-0.98	-77.82	-14.1
<i>Mazama gouazoubira</i>	UMMZ 124699	Lm3	Nueva asuncion	Paraguay	-22.10	-59.90	-6.6
<i>Mazama gouazoubira</i>	UMMZ 124700	Lm3	Chaco	Paraguay	-20.63	-60.32	-10.7
<i>Mazama gouazoubira</i>	UMMZ 124701	Lm3	Nueva asuncion	Paraguay	-20.70	-60.00	-9.0
<i>Mazama gouazoubira</i>	UMMZ 125569	Lm3	Chaco	Paraguay	-20.63	-60.32	-10.0
<i>Mazama gouazoubira</i>	UMMZ 125572	Lm3	Chaco	Paraguay	-20.13	-60.15	-9.6
<i>Mazama gouazoubira</i>	UMMZ 125573	Lm3	Chaco	Paraguay	-20.40	-60.10	-11.9
<i>Mazama rufina</i>	UMMZ 126126	Lm3	Itapua	Paraguay	-27.33	-56.42	-15.8
<i>Mazama temama cerasina</i>	UMMZ 63500	Lm3	Peten	Guatemala	17.39	-89.63	-13.6
<i>Mazama temama cerasina</i>	UMMZ 63502	Lm2	Peten	Guatemala	17.39	-89.63	-13.2
<i>Mazama temama cerasina</i>	UMMZ 76637	Rm2	Peten?	Guatemala			-14.4
<i>Muntiacus reevesi roberti</i>	UMMZ 97617	Lm3	Taiwan	China	25.02	121.45	-11.2
<i>Neotragus batesi</i>	UMMZ 39516	Rm3	Kribi	Cameroon	2.78	10.53	-24.6
<i>Neotragus batesi</i>	UMMZ 39517	Rm3	Kribi	Cameroon	2.78	10.53	-19.4
<i>Odocoileus hemionus crooki</i>	UMMZ 46190	Rm3	Texas	United States	30.60	-103.88	-7.5

(Continued)

TABLE 1 (Continued)

Species	Collection No.	Tooth	Region	Country	Latitude	Longitude	$\delta^{13}\text{C}_\text{E}$
<i>Odocoileus hemionus crooki</i>	UMMZ 79419	Lm3	Texas	United States	30.60	−103.89	−10.1
<i>Odocoileus hemionus hemionus</i>	UMMZ 59187	Rm3	Utah	United States	40.64	−109.72	−12.3
<i>Odocoileus hemionus hemionus</i>	UMMZ 59638	Lm3	Arizona	United States	35.92	−112.05	−11.5
<i>Odocoileus hemionus sitkensis</i>	UMMZ 103357	Lm3	Alaska	United States	57.86	−152.41	−14.4
<i>Odocoileus virginianus borealis</i>	UMMZ 5240	Rm3	Michigan	United States			−12.5
<i>Odocoileus virginianus borealis</i>	UMMZ 59029	Rm3	Michigan	United States	44.66	−84.71	−13.4
<i>Odocoileus virginianus borealis</i>	UMMZ 60964	Lm3	Michigan	United States	46.24	−84.18	−13.7
<i>Odocoileus virginianus borealis</i>	UMMZ 61004	Lm3	Michigan	United States	46.09	−88.64	−12.2
<i>Odocoileus virginianus borealis</i>	UMMZ 61038	Lm3	Michigan	United States	45.27	−84.58	−13.8
<i>Odocoileus virginianus borealis</i>	UMMZ 61048	Lm3	Michigan	United States	46.00	−83.85	−14.5
<i>Odocoileus virginianus borealis</i>	UMMZ 61147	Lm3	Michigan	United States	46.46	−90.17	−13.7
<i>Odocoileus virginianus borealis</i>	UMMZ 80213	Lm3	Michigan	United States	42.46	−84.01	−14.1
<i>Odocoileus virginianus thomasi</i>	UMMZ 76630	Rm3	Peten?	Guatemala			−13.2
<i>Odocoileus virginianus thomasi</i>	UMMZ 76631	Rm3	Peten?	Guatemala			−11.9
<i>Odocoileus virginianus thomasi</i>	UMMZ 76632	Rm3	Peten?	Guatemala			−12.4
<i>Odocoileus virginianus thomasi</i>	UMMZ 76634	Rm3	Peten?	Guatemala			−12.7
<i>Odocoileus virginianus thomasi</i>	UMMZ 76638	Rm3	Peten?	Guatemala			−14.1
<i>Odocoileus virginianus thomasi</i>	UMMZ 76641	Rm3	Peten?	Guatemala			−12.5
<i>Odocoileus virginianus thomasi</i>	UMMZ 76648	Rm3	Peten?	Guatemala			−14.1
<i>Odocoileus virginianus thomasi</i>	UMMZ 76654	Rm3	Peten?	Guatemala			−13.2
<i>Oreamnos americanus missoulae</i>	UMMZ 60546	Rm3	Alberta	Canada	53.50	−102.90	−9.8
<i>Oreamnos americanus missoulae</i>	UMMZ 87772	Rm3	Montana	United States	47.77	−112.70	−10.5
<i>Oryx beisa</i>	UMMZ 124068	Rm3					3.2
<i>Ovibos moschatus</i>	UMMZ 112377	Lm3	Greenland	Denmark	72.18	−23.75	−10.1
<i>Ovibos moschatus</i>	UMMZ 116376	Lm3	Northwest Territories	Canada	75.70	−84.40	−2.3
<i>Ovis canadensis canadensis</i>	UMMZ 167428	RM3	Colorado	United States	40.38	−105.52	−2.9
<i>Ovis canadensis canadensis</i>	UMMZ 42316	RM3	Idaho	United States	43.61	−116.20	−10.8
<i>Ovis dalli stonei</i>	UMMZ 53659	Lm3	British Columbia	Canada	59.00	−129.00	−10.2
<i>Philantomba monticola monticola</i>	UMMZ 39515	Lm3	Kribi	Cameroon	2.78	10.53	−14.8
<i>Rangifer tarandus groenlandicus</i>	UMMZ 97462	Rm3	Northwest Territories	Canada	62.71	−109.20	−8.6
<i>Rangifer tarandus osborni</i>	UMMZ 53658	Lm3	British Columbia	Canada	59.00	−129.00	−8.8

L, left; R, right; M, upper molar; m, lower molar; p, lower premolar.

physiology, the inferred carbon-isotope values of the vegetation that artiodactyls fed on ($\delta^{13}\text{C}_{\text{diet}}$) were compared among seven feeding categories, 11 terrestrial ecoregions, and phylogenetic groups.

Published $\delta^{13}\text{C}_\text{E}$ data

We assembled published $\delta^{13}\text{C}_\text{E}$ values of extant artiodactyls from 24 primary sources (Table 2). Data from paleontological or archeological sites or from other body tissues were not included. In most instances, we considered only samples from wild animals. Two exceptions are studies of free-range livestock (Wang et al., 2008; Lazzerini et al., 2021), included to increase the sample size from Asia. Along with published $\delta^{13}\text{C}_\text{E}$ data, we collected the following information from

the literature whenever available: taxonomic identification, sample identification number (field number or museum catalog number), provenance (locality name, geographic coordinates, elevation), year of collection from the field, sampled element (tooth position), method of sampling (serial or bulk), and whether or not samples were pretreated before analysis. If multiple samples were taken from the same tooth or duplicates were run for the same bulk sample, then average values for the tooth were used. If multiple teeth were sampled from an individual animal, then samples taken from teeth that erupted late in the sequence (more posteriorly positioned in the premolar or molar row) were used, as these teeth are among the last ones to develop (Hillson, 2005), thereby avoiding a weaning signal. Some data have appeared in multiple studies or review papers since they were first published, in which case we traced them back to the original publication. Only studies that reported

TABLE 2 Summary statistics for calculated $\delta^{13}\text{C}_{\text{diet}}$ values of 79 species of artiodactyls documented in this study.

Family	Species	Count	Min.	Max.	Mean	Median	S.D.
Antilocapridae	<i>Antilocapra americana</i>	36	-25.6	-21.1	-23.1	-23.2	0.82
Bovidae	<i>Aepyceros melampus</i>	63	-23.5	-8.9	-15.8	-16.3	2.95
Bovidae	<i>Alcelaphus buselaphus</i>	49	-14.0	-8.2	-9.8	-9.5	1.28
Bovidae	<i>Antidorcas marsupialis</i>	7	-22.9	-20.7	-21.6	-21.5	0.80
Bovidae	<i>Beatragus hunteri</i>	2	-11.2	-10.6	-10.9	-10.9	0.38
Bovidae	<i>Bison bison</i>	88	-25.6	-13.4	-20.9	-22.3	3.44
Bovidae	<i>Bos grunniens</i>	7	-24.3	-21.3	-22.9	-22.8	1.29
Bovidae	<i>Capra hircus</i>	17	-23.1	-19.8	-21.4	-21.4	0.74
Bovidae	<i>Capra nubiana</i>	3	-19.3	-17.5	-18.6	-19.1	1.00
Bovidae	<i>Capra walie</i>	1	-23.9	-23.9	-23.9	-23.9	
Bovidae	<i>Cephalophus</i> sp.	9	-27.2	-22.2	-25.5	-26.1	1.68
Bovidae	<i>Cephalophus callipygus</i>	4	-26.5	-17.7	-23.4	-24.6	3.90
Bovidae	<i>Cephalophus dorsalis</i>	4	-26.1	-24.9	-25.5	-25.5	0.71
Bovidae	<i>Cephalophus leucogaster</i>	4	-25.5	-24.1	-24.9	-25.1	0.65
Bovidae	<i>Cephalophus nigrifrons</i>	10	-28.1	-24.6	-26.3	-25.8	1.26
Bovidae	<i>Cephalophus silvicultor</i>	2	-26.9	-24.9	-25.9	-25.9	1.42
Bovidae	<i>Cephalophus weynsi</i>	1	-25.9	-25.9	-25.9	-25.9	
Bovidae	<i>Connochaetes gnou</i>	10	-10.9	-8.9	-9.8	-10.0	0.69
Bovidae	<i>Connochaetes taurinus</i>	40	-12.9	-8.3	-10.2	-9.9	1.24
Bovidae	<i>Damaliscus lunatus</i>	15	-13.4	-8.3	-10.2	-9.8	1.34
Bovidae	<i>Eudorcas thomsonii</i>	16	-18.7	-10.9	-13.7	-13.0	2.49
Bovidae	<i>Gazella dorcas</i>	8	-22.6	-19.1	-21.0	-20.7	1.16
Bovidae	<i>Hippotragus equinus</i>	5	-15.1	-8.3	-11.1	-10.1	2.65
Bovidae	<i>Hippotragus niger</i>	3	-11.4	-9.5	-10.3	-9.9	1.02
Bovidae	<i>Kobus ellipsiprymnus</i>	75	-14.2	-8.8	-11.3	-11.0	1.24
Bovidae	<i>Kobus kob</i>	11	-12.5	-8.8	-10.7	-10.4	1.11
Bovidae	<i>Litocranius walleri</i>	8	-24.2	-21.1	-23.2	-23.4	1.00
Bovidae	<i>Madoqua guentheri</i>	2	-18.8	-18.3	-18.6	-18.6	0.35
Bovidae	<i>Madoqua kirkii</i>	25	-24.3	-17.6	-21.8	-21.9	1.61
Bovidae	<i>Madoqua saltiana</i>	5	-24.2	-19.7	-21.7	-21.7	1.78
Bovidae	<i>Nanger granti</i>	57	-27.9	-13.5	-21.3	-22.1	3.02
Bovidae	<i>Nanger soemmerringii</i>	1	-22.6	-22.6	-22.6	-22.6	
Bovidae	<i>Neotragus batesi</i>	4	-35.0	-29.5	-33.3	-34.4	2.56
Bovidae	<i>Oreamnos americanus</i>	2	-22.5	-21.9	-22.2	-22.2	0.45
Bovidae	<i>Oreotragus oreotragus</i>	3	-24.6	-19.9	-22.5	-23.1	2.37
Bovidae	<i>Oryx beisa</i>	27	-17.0	-9.4	-12.0	-11.9	1.71
Bovidae	<i>Ourebia ourebi</i>	1	-16.3	-16.3	-16.3	-16.3	
Bovidae	<i>Ovibos moschatus</i>	2	-22.8	-15.1	-19.0	-19.0	5.47
Bovidae	<i>Ovis</i> sp.	3	-22.6	-20.7	-21.5	-21.3	0.94
Bovidae	<i>Ovis canadensis</i>	2	-23.1	-15.2	-19.1	-19.1	5.62
Bovidae	<i>Ovis dalli</i>	1	-22.1	-22.1	-22.1	-22.1	
Bovidae	<i>Philantomba monticola</i>	7	-25.4	-21.3	-23.4	-23.3	1.60
Bovidae	<i>Raphicerus campestris</i>	8	-25.0	-18.4	-22.2	-23.2	2.33
Bovidae	<i>Redunca fulvorufula</i>	2	-11.0	-10.3	-10.7	-10.7	0.47
Bovidae	<i>Redunca redunca</i>	13	-17.9	-7.7	-10.5	-9.3	2.76
Bovidae	<i>Sylvicapra grimmia</i>	5	-25.9	-21.4	-23.5	-23.1	1.84
Bovidae	<i>Syncerus caffer</i>	116	-28.5	-9.6	-13.2	-12.1	3.52
Bovidae	<i>Taurotragus oryx</i>	29	-25.2	-18.0	-22.1	-22.4	1.81
Bovidae	<i>Tragelaphus buxtoni</i>	5	-25.7	-23.5	-24.6	-24.3	1.00

(Continued)

TABLE 2 (Continued)

Family	Species	Count	Min.	Max.	Mean	Median	S.D.
Bovidae	<i>Tragelaphus euryceros</i>	2	-27.3	-26.7	-27.0	-27.0	0.40
Bovidae	<i>Tragelaphus imberbis</i>	6	-24.5	-19.5	-22.9	-23.3	1.72
Bovidae	<i>Tragelaphus scriptus</i>	16	-28.1	-21.7	-24.8	-25.2	1.59
Bovidae	<i>Tragelaphus spekii</i>	4	-29.3	-26.5	-27.9	-27.9	1.21
Bovidae	<i>Tragelaphus strepsiceros</i>	13	-27.9	-20.6	-23.6	-23.2	1.94
Camelidae	<i>Llama guanaco</i>	4	-26.7	-25.9	-26.4	-26.5	0.37
Cervidae	<i>Alces americanus</i>	3	-28.0	-27.4	-27.7	-27.6	0.31
Cervidae	<i>Capreolus capreolus</i>	1	-22.2	-22.2	-22.2	-22.2	
Cervidae	<i>Cervus elaphus</i>	32	-28.3	-23.2	-24.6	-24.6	0.96
Cervidae	<i>Hydropotes inermis</i>	1	-25.1	-25.1	-25.1	-25.1	
Cervidae	<i>Mazama americana</i>	10	-26.9	-24.5	-25.4	-25.4	0.66
Cervidae	<i>Mazama gouazoubira</i>	9	-24.5	-17.2	-21.6	-21.3	2.43
Cervidae	<i>Mazama rufina</i>	1	-25.9	-25.9	-25.9	-25.9	
Cervidae	<i>Mazama temama</i>	3	-25.6	-24.4	-24.9	-24.7	0.64
Cervidae	<i>Muntiacus reevesi</i>	1	-21.8	-21.8	-21.8	-21.8	
Cervidae	<i>Odocoileus hemionus</i>	29	-26.4	-19.5	-24.2	-24.4	1.44
Cervidae	<i>Odocoileus virginianus</i>	23	-28.2	-17.0	-25.4	-25.8	2.15
Cervidae	<i>Rangifer tarandus</i>	2	-21.0	-20.7	-20.9	-20.9	0.22
Giraffidae	<i>Giraffa camelopardalis</i>	51	-28.6	-20.6	-25.0	-25.2	1.59
Giraffidae	<i>Okapia johnstoni</i>	2	-32.4	-31.7	-32.0	-32.0	0.54
Hippopotamidae	<i>Choeropsis liberiensis</i>	1	-28.3	-28.3	-28.3	-28.3	
Hippopotamidae	<i>Hippopotamus amphibius</i>	182	-25.5	-10.7	-16.8	-16.2	2.36
Suidae	<i>Hylochoerus meinertzhageni</i>	13	-34.2	-24.6	-28.6	-27.8	2.82
Suidae	<i>Phacochoerus aethiopicus</i>	58	-24.3	-8.9	-12.9	-12.0	2.89
Suidae	<i>Phacochoerus africanus</i>	33	-14.9	-9.8	-12.6	-12.1	1.21
Suidae	<i>Potamochoerus larvatus</i>	14	-26.0	-13.2	-20.7	-20.9	4.62
Suidae	<i>Potamochoerus porcus</i>	23	-28.2	-19.6	-25.6	-26.1	1.96
Tayassuidae	<i>Pecari tajacu</i>	4	-24.8	-23.9	-24.4	-24.4	0.42
Tayassuidae	<i>Tayassu pecari</i>	4	-26.1	-24.6	-25.4	-25.5	0.60
Tragulidae	<i>Hyemoschus aquaticus</i>	3	-25.6	-24.7	-25.2	-25.2	0.45

Data sources: Bocherens et al. (1996), Cerling and Harris (1999), Cerling et al. (1999), Harris and Cerling (2002), Cerling et al. (2003), Cerling et al. (2004), Boissier et al. (2005), Hoppe et al. (2006), Feranec (2007), Cerling et al. (2008), Fenner (2008), Copeland et al. (2008), Levin et al. (2008), Wang et al. (2008), Copeland et al. (2009), Cerling et al. (2011), Kingston (2011), Nelson (2013), van der Merwe (2013), Cerling et al. (2015), Martin et al. (2015), Luyt and Sealy (2018), Rivera-Araya and Birch (2018), Lazzarini et al. (2021), and this study.

original $\delta^{13}\text{C}_\text{E}$ data of extant artiodactyls were cited as primary sources.

New $\delta^{13}\text{C}_\text{E}$ data

Eighty enamel samples from 23 species of extant artiodactyls were gathered from specimens housed in the University of Michigan Museum of Zoology (UMMZ). We chose samples with consideration for their prior taxonomic representation and geographic coverage in the literature, as well as the availability and abundance of specimens in the UMMZ collection.

The general method for sampling and pretreating tooth enamel followed Koch et al. (1997). Bulk samples were gathered by drilling approximately 5 mg of pristine enamel powder on the lateral surface of the tooth parallel to the growth axis.

Sampling was done using a portable dental drill with a 1-mm diamond burr. All samples were taken from third molars or fourth premolars. Samples were treated with 3% reagent grade NaOCl for 24 h to remove organic matter and with 1M buffered acetic acid for 24 h to remove non-structural carbonate. Each treatment was followed by centrifuging and rinsing five times with deionized water. Samples were dried by lyophilization. At the University of Michigan Stable Isotope Laboratory, samples were reacted at $77^\circ \pm 1^\circ\text{C}$ with anhydrous phosphoric acid for 8 min in a Thermo Scientific Kiel IV preparation device coupled directly to the inlet of a Thermo Delta V triple collector isotope ratio mass spectrometer, which measured the resultant CO_2 . Analytical precision was better than $\pm 0.1\text{‰}$ (1 S.D.), based on international standards for carbonate (NBS-18, NBS-19). Isotope values are expressed in standard δ -notation: $\delta^{13}\text{C}_\text{E} = [(R_{\text{sample}}/R_{\text{standard}}) - 1] \times 1000$,

where $R = {}^{13}\text{C}/{}^{12}\text{C}$. The $\delta^{13}\text{C}_\text{E}$ values are reported relative to the Vienna Pee Dee Belemnite (VPDB) standard.

Correcting for the Suess effect and calculating $\delta^{13}\text{C}$ of dietary sources

Sampled tooth specimens in our data compilation were collected from the field as long ago as 1891 to as recently as 2017 (Supplementary Table 1). During this time interval, $\delta^{13}\text{C}_\text{atm}$ has decreased by $\sim 1.8\text{‰}$ due to anthropogenic activities (Suess effect). To account for this effect, all $\delta^{13}\text{C}_\text{E}$ data were corrected to the preindustrial $\delta^{13}\text{C}_\text{atm}$ level of the year 1750 ($\delta^{13}\text{C}_{1750}$, taken to be -6.3‰). Correction values were based on $\delta^{13}\text{C}$ data from Antarctic ice cores, fern samples, and direct measurements of air (Rubino et al., 2013; Keeling et al., 2017). These records show that change in $\delta^{13}\text{C}_\text{atm}$ since 1750 occurred in three stages (Supplementary Table 2). The first 130 years witnessed a slow decrease, bringing $\delta^{13}\text{C}_\text{atm}$ from -6.3 to -6.7‰ by 1880. Another 0.4‰ -decrease took only over 80 years, with a rate of $\sim 0.005\text{‰}$ per year during this interval. From the early 1960s to the early 2010s, $\delta^{13}\text{C}_\text{atm}$ dropped by 1.3‰ , meaning an accelerated annual decrease of 0.025‰ . Based on these observed trends, we corrected the $\delta^{13}\text{C}_\text{E}$ value of each sample with the offset in $\delta^{13}\text{C}_\text{atm}$ between its collection year and 1750. For some samples, the exact year of collection was not reported, so the correction value could not be accurately determined. In these cases, we estimated the correction value based on year of publication or other information provided in the primary study. These samples constitute a small proportion (2.5%) of the dataset and should not affect the overall analytical results.

The $\delta^{13}\text{C}$ values of the ingested vegetation ($\delta^{13}\text{C}_\text{diet}$) were calculated from $\delta^{13}\text{C}_{1750}$ to facilitate cross-species comparison of forage selection. Conventionally, an average enrichment factor between diet and enamel ($\epsilon^*_{\text{diet-bioapatite}}$) of $14.1 \pm 0.5\text{‰}$, derived by Cerling and Harris (1999), have been used in paleodietary reconstructions of large ungulate mammals. Recently, Tejada-Lara et al. (2018) found that fractionation between diet and enamel increases with species' body mass and is also affected by digestive physiology (foregut vs. hindgut fermentation). Because our dataset covers artiodactyls with a range of body sizes, we use equations derived by Tejada-Lara et al. (2018) to determine the $\epsilon^*_{\text{diet-bioapatite}}$ for each species based on its average body mass and digestive physiology. For foregut fermenters, $\epsilon^*_{\text{diet-bioapatite}} = 2.34 + 0.05(\text{BM})$, where (BM) is the natural log of body mass in kg. For hindgut fermenters, $\epsilon^*_{\text{diet-bioapatite}} = 2.42 + 0.032(\text{BM})$. Resulting $\epsilon^*_{\text{diet-bioapatite}}$ values range from 11.0 (*Neotragus batesi*, 3 kg) to 15.0‰ (*Hippopotamus amphibius*, 1500 kg). When comparing the calculated $\delta^{13}\text{C}_\text{diet}$ values, we use -17‰ to separate C_3 and C_4 vegetation, based on plant data collected since the late 20th century (Cerling and Ehleringer, 2000;

Sponheimer and Cerling, 2014). Mixed C_3 - C_4 feeders would have $\delta^{13}\text{C}_\text{diet}$ close to this value.

Comparing $\delta^{13}\text{C}_\text{diet}$ values among feeding categories and ecoregions

We assigned species to one of seven feeding categories based on published dietary information (Supplementary Table 3). The feeding categories include one omnivorous category (omnivore) and six herbivorous categories (frugivore, browser, browser-grazer intermediate, variable grazer, and obligate grazer). Assignment of species into herbivorous categories is based on the relative abundance of fruit, dicots, and monocots in the species' average diet, following criteria from Gagnon and Chew (2000) and Wang et al. (2022). The diets of frugivores and browsers consist of $>70\%$ fruit and $>70\%$ dicots, respectively. Variable grazers and obligate grazers have diets that include 60–90% and $>90\%$ monocots, respectively. Browser-grazer intermediates consume $<70\%$ dicots, $<60\%$ monocots, and $<20\%$ fruit, while generalists consumed $>20\%$ of all three food types. This six-category classification scheme captures more information about the dietary preference and dietary selectivity of herbivores than the traditional three-category classification of browsers, mixed feeders, and grazers.

Each sampled locality was assigned to one of the Global 200 terrestrial ecoregions, which were established on the bases of biodiversity dynamics and environmental conditions (Olson et al., 2001). Different ecoregions provide different habitats and different plants for artiodactyls to feed on. Therefore, $\delta^{13}\text{C}_\text{diet}$ values are expected to vary among ecoregions.

Box and whisker plots were used to illustrate the summary statistics for feeding categories (Figure 2) and for ecoregions (Figure 3). Histograms of $\delta^{13}\text{C}_\text{diet}$ values illustrate the total dataset for each feeding category and for each ecoregion with sufficiently large sample size (>100 samples, Figures 2–5). These diagrams allow for comparison of the differences and similarities in the range and frequency of $\delta^{13}\text{C}_\text{diet}$ values that each feeding category or ecoregion represents. Parametric (ANOVA) and non-parametric statistical tests (Kruskal–Wallis) were used to compare the difference between group-means, using PAST v4.03 (Hammer et al., 2001). Because some feeding categories and ecoregions are more geographically widespread than others, we also evaluate the composition of continental origin of the samples.

Since sampling is highly uneven among geographic regions (Figure 1) and among taxa (Table 2), the $\delta^{13}\text{C}_\text{diet}$ values of well-sampled species from certain locations could have an oversize impact on the overall distribution of $\delta^{13}\text{C}_\text{diet}$ values. Therefore, we repeated the comparison among feeding categories using mean $\delta^{13}\text{C}_\text{diet}$ values of species, both with and without controlling for phylogeny. Non-phylogenetic analyses are the same as detailed above. A phylogenetic ANOVA was

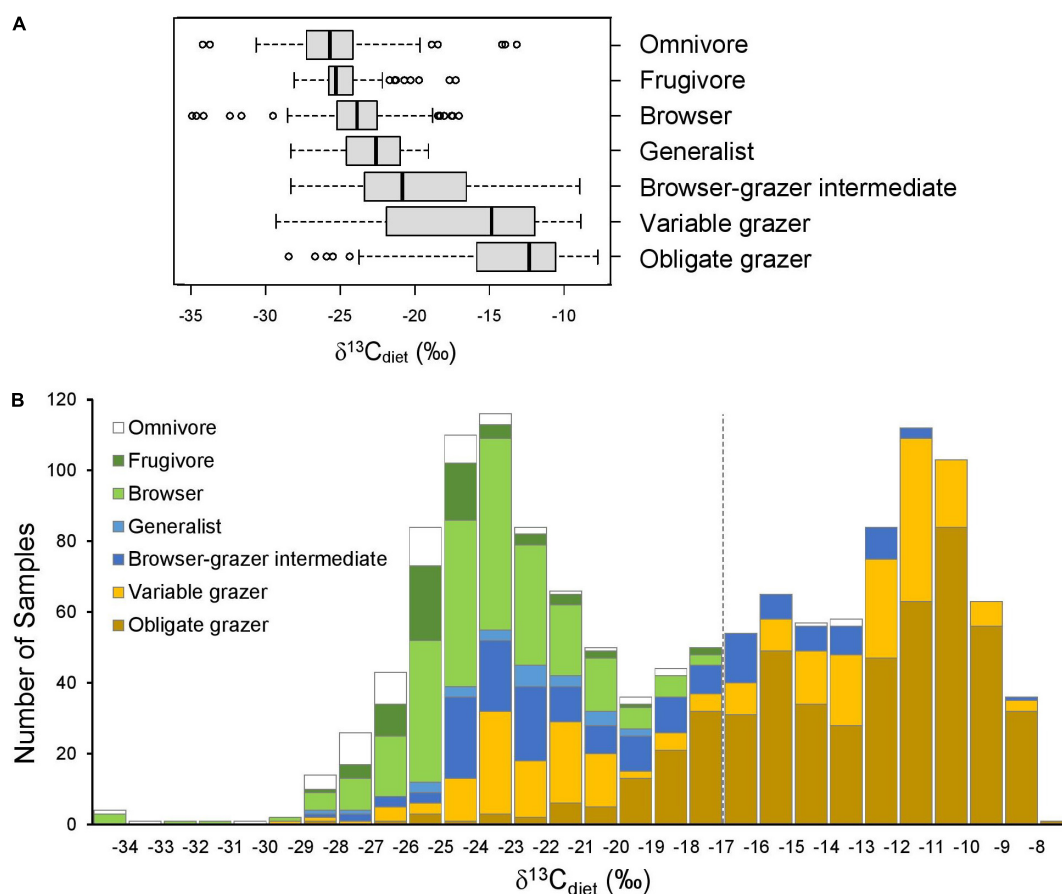


FIGURE 2

Comparison of $\delta^{13}\text{C}_{\text{diet}}$ values among seven artiodactyl feeding categories. (A) Boxplots showing the (non-outlier) range (whiskers), first and third quartiles (box), median (vertical line), and outliers (circles) of $\delta^{13}\text{C}_{\text{diet}}$ values in each ecoregion. (B) Histogram of $\delta^{13}\text{C}_{\text{diet}}$ values of the feeding categories. Dashed line is the C_3 - C_4 boundary.

conducted using the “*phylANOVA*” function from the R package “*phytools*” (Revell, 2012).

Phylogenetic signal of $\delta^{13}\text{C}_{\text{diet}}$ values

To examine the $\delta^{13}\text{C}_{\text{diet}}$ variation among phylogenetic groups, we obtained a sample of 1000 node-dated consensus trees of artiodactyls from Upham et al. (2019) and generated a maximum clade credibility tree using *TreeAnnotator* (Drummond et al., 2012). The phylogeny and the isotope dataset share 76 species. We then estimated the phylogenetic signal in species’ mean $\delta^{13}\text{C}_{\text{diet}}$ values with Blomberg’s K (1000 permutations) using the function “*phylosig*” from “*phytools*”. The K value can be either less than 1, equal to 1, or greater than 1. A $K < 1$ suggests that $\delta^{13}\text{C}_{\text{diet}}$ values are less similar in closely related species than expected under neutral Brownian model, while $K > 1$ suggests that $\delta^{13}\text{C}_{\text{diet}}$ values are more similar in phylogenetically closely related species than expected under a Brownian motion (Blomberg et al., 2003). We also mapped

the mean $\delta^{13}\text{C}_{\text{diet}}$ values of species onto the pruned artiodactyl phylogeny, using the function “*contMap*” from “*phytools*”. Because species with similar mean $\delta^{13}\text{C}_{\text{diet}}$ values could have different range and variance of $\delta^{13}\text{C}_{\text{diet}}$ values that reflect difference in dietary niche breadths, we additionally aligned box and whisker plots of species with the phenogram (Figure 6).

Results

Including the new samples from this study (Table 1), the $\delta^{13}\text{C}_{\text{diet}}$ compilation results in a dataset of 1366 carbon-isotope values from 25 primary sources (Table 2). The tooth-enamel samples come from 79 species of artiodactyls sampled from Africa, Eurasia, North America, and South America, with the highest number of samples from Africa (Figure 1). Thirteen of the 23 species sampled from UMMZ (Table 1) have not been previously analyzed for $\delta^{13}\text{C}_\text{E}$ values. Other specimens were chosen to expand the geographic range of sampled species.

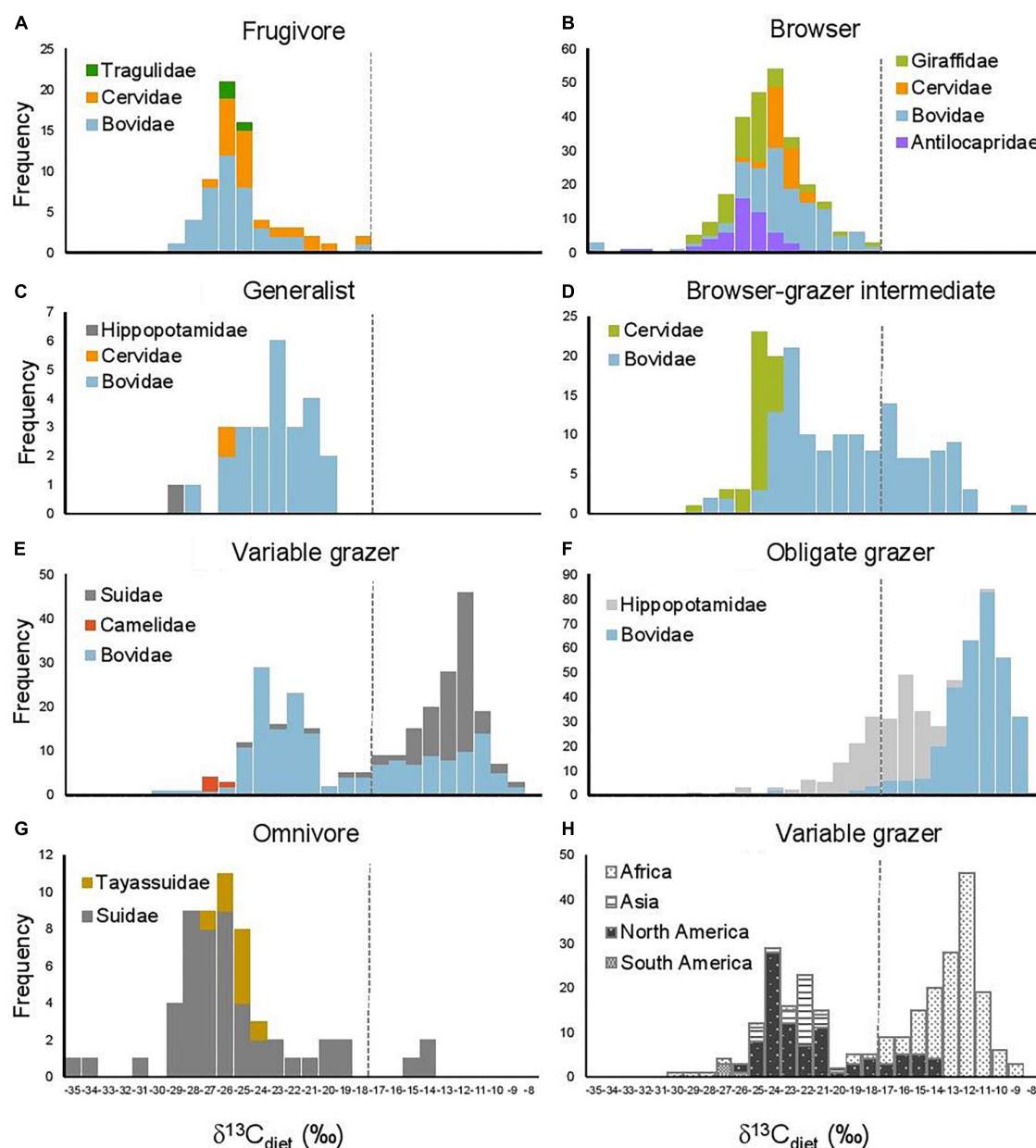


FIGURE 3
Histograms of $\delta^{13}\text{C}_{\text{diet}}$ values in seven artiodactyl feeding categories in relation to (A–G) taxonomic group and (H) continent. Dashed line is the C_3 - C_4 boundary.

The total dataset includes representatives from nine out of ten families of terrestrial artiodactyls, missing only the Moschidae (Table 2).

Variation in $\delta^{13}\text{C}_{\text{diet}}$ among feeding categories

As expected, the seven artiodactyl feeding categories exhibit different ranges, means, and medians of $\delta^{13}\text{C}_{\text{diet}}$ values.

Group means differ significantly from each other, using both parametric and non-parametric tests ($p < 0.001$). *Post hoc* tests show that group means differ significantly for most pairwise comparisons ($p < 0.05$), except for that between frugivores and browsers and a few comparisons that involve omnivores or generalists (Table 3B). When using mean $\delta^{13}\text{C}_{\text{diet}}$ values of species to reduce the bias introduced by sampling, we found that pairwise comparisons between obligate grazers and other feeding categories remain significantly different both with and without controlling for phylogeny (Tables 3C,D). Mean $\delta^{13}\text{C}_{\text{diet}}$

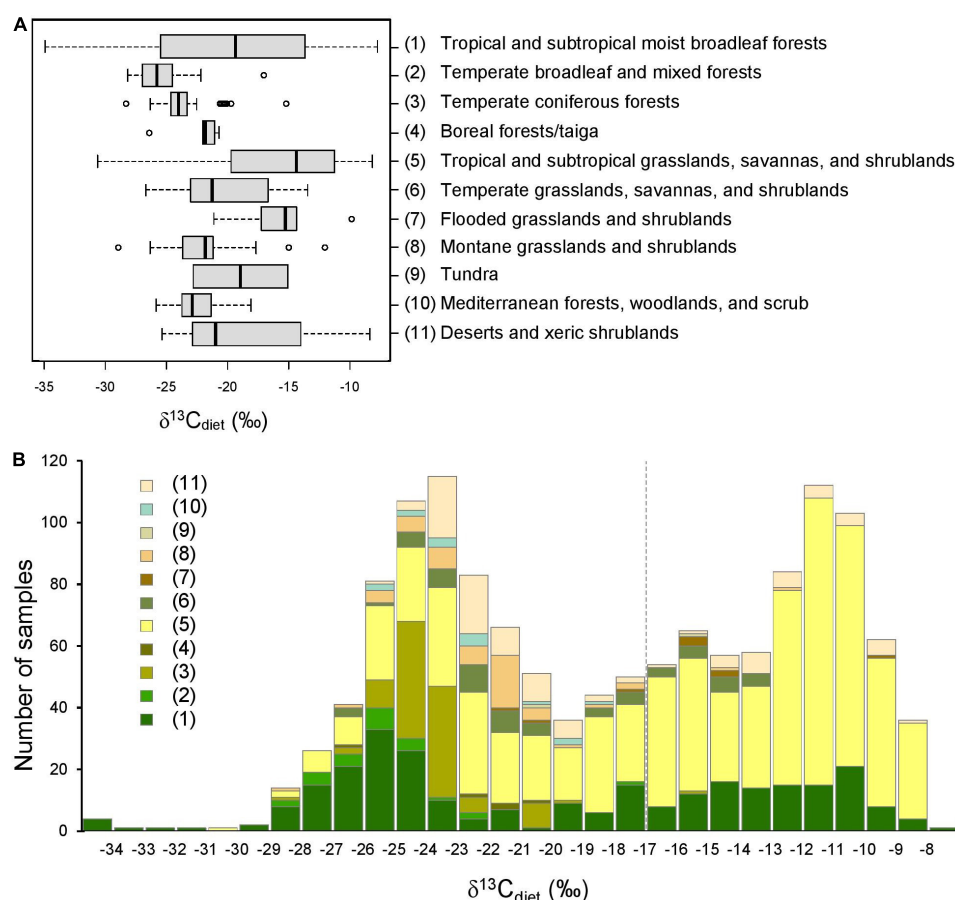


FIGURE 4
 Comparison of $\delta^{13}\text{C}_{\text{diet}}$ values among 11 terrestrial ecoregions. **(A)** Boxplots showing the (non-outlier) range (whiskers), first and third quartiles (box), median (vertical line), and outliers (circles) of $\delta^{13}\text{C}_{\text{diet}}$ values in each ecoregion. **(B)** Histogram of $\delta^{13}\text{C}_{\text{diet}}$ values of the ecoregions. Numbers in legend correspond to ecoregions in **(A)**, and the color scheme corresponds to that of **Figure 1**. Dashed vertical line is the C_3 - C_4 boundary.

values of variable grazer species also differ from those of most other groups, although the differences are not significant when controlling for phylogeny. Among the six herbivorous feeding categories, mean $\delta^{13}\text{C}_{\text{diet}}$ values increase along the dietary continuum from frugivores, through browsers, the mixed feeders (generalists and browser-grazer intermediates), variable grazers, to obligate grazers (**Figure 2A** and **Table 3A**). Generalists and omnivores have smaller sample sizes than other feeding categories, but omnivores still exhibit a wide range of $\delta^{13}\text{C}_{\text{diet}}$ values, reflecting their wide dietary niche breadth (**Table 3A**).

The entire dataset exhibits a generally bimodal distribution in $\delta^{13}\text{C}_{\text{diet}}$ values, with a saddle around -19‰ (**Figure 2B**). Grazers dominate the C_4 (enriched) mode of the distribution but extend considerably into the C_3 realm. Mixed feeders occupy the intermediate range of values. Frugivores, browsers, and omnivores are prevalent in the C_3 range. The most depleted and most enriched $\delta^{13}\text{C}_{\text{diet}}$ values are found in a browser

(*Neotragus batesi*, the dwarf antelope) and an obligate grazer (*Redunca redunca*, the bohor reedbuck), respectively (**Figure 2** and **Table 2**).

The bimodal distribution of $\delta^{13}\text{C}_{\text{diet}}$ values in the total dataset is comprised of several different patterns among artiodactyl feeding groups (**Figure 3**). Taxonomic composition also differs among feeding categories. Most feeding categories exhibit a unimodal distribution but vary in mean, median, mode, and peak frequency (**Figure 3** and **Table 3A**). Obligate grazers and variable grazers exhibit patterns that differ from those of the other feeding categories. Obligate grazers, which all occur in Africa, exhibit a left-skewed bimodal distribution, with the higher peak driven primarily by the high frequency of enriched $\delta^{13}\text{C}_{\text{diet}}$ values in bovids (**Figure 3F**). All but one sample of Hippopotamidae are from *Hippopotamus amphibius*; this species makes up roughly an eighth of the total sample size (**Table 2**), and their $\delta^{13}\text{C}_{\text{diet}}$ values contribute to a second, lower mode in the obligate-grazer data. Variable grazers

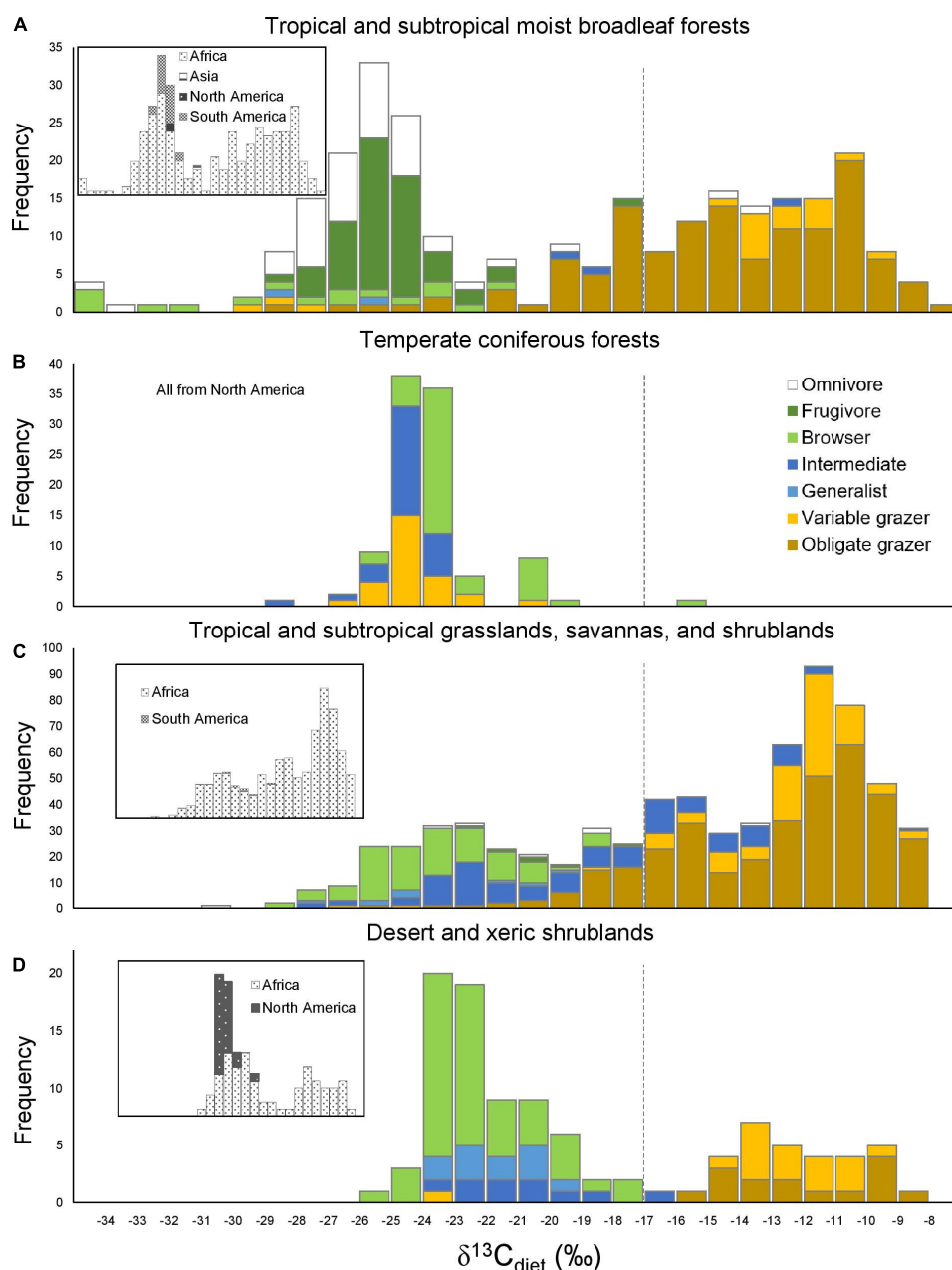


FIGURE 5

Histograms of $\delta^{13}\text{C}_{\text{diet}}$ values in the four best-sampled ecoregions in relation to feeding categories (A,B) (main panels) and continent (C,D) (inset panels). Dashed line is the C_3 - C_4 boundary.

exhibit a bimodal distribution of $\delta^{13}\text{C}_{\text{diet}}$ values (Figure 3E). Within this group, bovids are the most numerous (as is the case for all herbivorous feeding categories) and are the main contributor to the bimodal pattern. Other families in this feeding category are well separated between C_3 -feeding camelids (llamas) and primarily C_4 -feeding suids (warthogs). Associated with taxonomic differentiation, the C_3 - C_4 separation in variable grazers is strongly influenced by geography, with samples from North America being mostly in the C_3 range while

samples from Africa are mostly in the C_4 range (Figure 3H). Variable grazers in Asia and South America are also C_3 -feeders.

Variation in $\delta^{13}\text{C}_{\text{diet}}$ among ecoregions

Sample localities in the dataset are distributed among 11 terrestrial ecoregions of the world (Figure 4 and

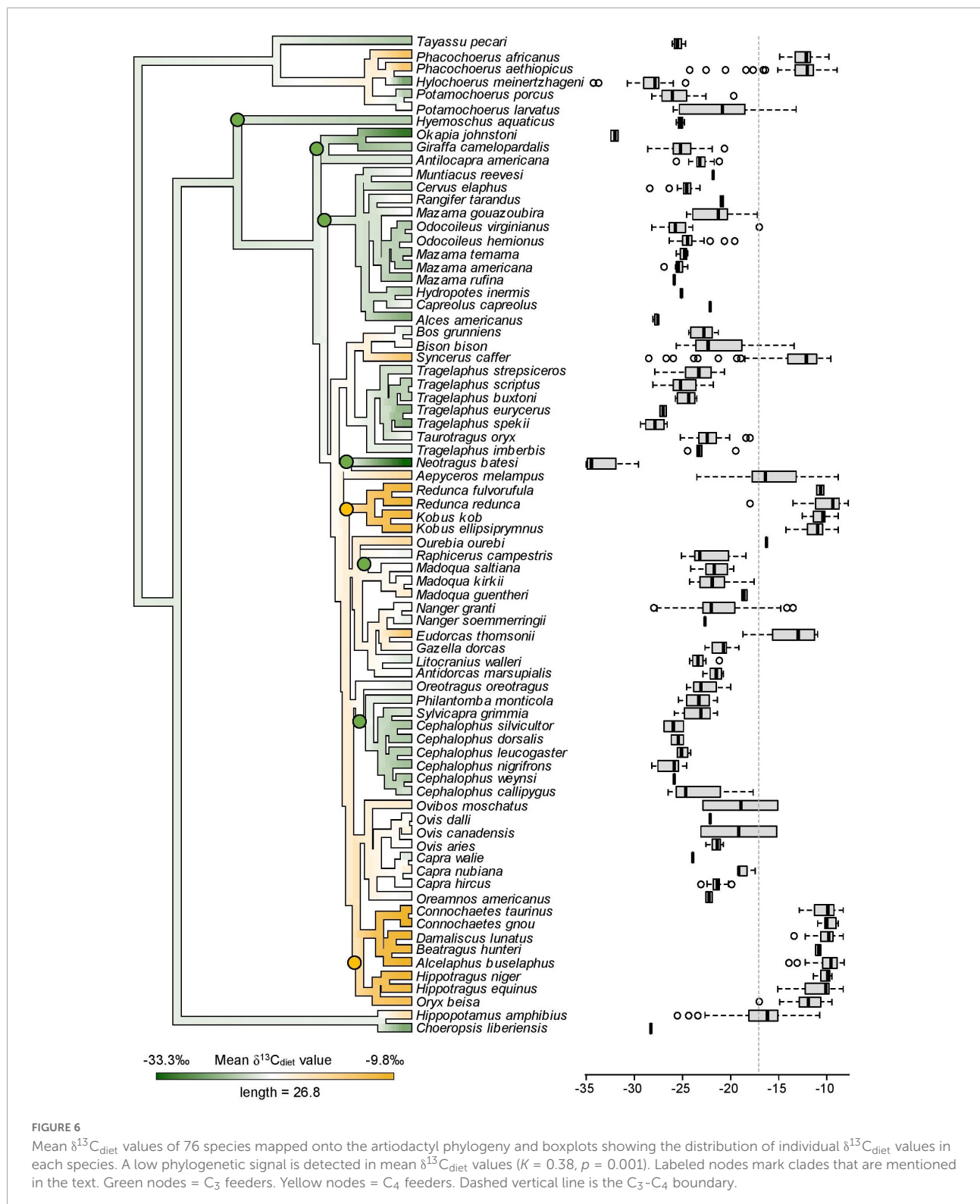


Table 4). The $\delta^{13}\text{C}_{\text{diet}}$ values of species in different ecoregions differ significantly from each other, using both parametric and non-parametric tests ($p < 0.001$). Pairwise

comparisons yielded significant differences ($p < 0.05$) among forest ecoregions, between grassland ecoregions and forest ecoregions, as well as between desert and xeric

shrublands and most other ecoregions (Table 4B). Mesic environments (forests and woodlands from a range of temperature conditions) are more prevalent in the lower values of the $\delta^{13}\text{C}_{\text{diet}}$ spectrum while intermediate to semiarid environments (grasslands) occupy the middle and higher values (Figure 4B).

Because sample size is highly variable among ecoregions (Table 3A), histograms were only generated for the four ecoregions with the largest sample sizes. Tropical and

subtropical moist broadleaf forests, mostly occurring in Africa, exhibit a generally bimodal distribution of $\delta^{13}\text{C}_{\text{diet}}$ values (Figure 5A). The peak in the C_3 range is well-established and consists mostly of frugivores and omnivores, although other feeding categories are also present. The broad low peak in the C_4 range is primarily from obligate grazers, specifically those from East Africa (Supplementary Table 1). Samples from the tropical and subtropical moist broadleaf forests of South America, North America, and

TABLE 3 Comparison of $\delta^{13}\text{C}_{\text{diet}}$ values among seven feeding categories of artiodactyls.

(A) Summary statistics of all $\delta^{13}\text{C}_{\text{diet}}$ values.

Feeding category	N	Min.	Max.	Mean	Median	S.D.
1) Frugivore	66	-28.1	-17.2	-24.7	-25.3	2.17
2) Browser	262	-35.0	-17.0	-23.9	-23.9	2.57
3) Generalist	26	-28.3	-19.1	-22.9	-22.6	2.36
4) Browser-grazer intermediate	168	-28.3	-8.9	-19.9	-20.9	4.28
5) Variable grazer	273	-29.3	-8.8	-16.7	-14.9	5.31
6) Obligate grazer	513	-28.5	-7.7	-13.4	-12.3	3.62
7) Omnivore	58	-34.2	-13.2	-25.0	-25.7	3.96

(B) P-values from *post hoc* pairwise tests of all $\delta^{13}\text{C}_{\text{diet}}$ values.

	1	2	3	4	5	6	7
1)		0.756	0.458	0.000	0.000	0.000	0.999
2)	0.000		0.900	0.000	0.000	0.000	0.414
3)	0.000	0.032		0.005	0.000	0.000	0.263
4)	0.000	0.000	0.002		0.000	0.000	0.000
5)	0.000	0.000	0.000	0.000		0.000	0.000
6)	0.000	0.000	0.000	0.000	0.000		0.000
7)	0.107	0.000	0.001	0.000	0.000	0.000	

(C) P-values from *post hoc* pairwise tests of species' mean $\delta^{13}\text{C}_{\text{diet}}$ values.

	1	2	3	4	5	6	7
1)		0.995	0.999	0.292	0.001	0.000	1.000
2)	0.079		1.000	0.465	0.000	0.000	0.998
3)	0.712	0.719		0.721	0.050	0.000	0.999
4)	0.003	0.056	0.194		0.772	0.000	0.504
5)	0.002	0.000	0.045	0.360		0.000	0.018
6)	0.000	0.000	0.002	0.001	0.001		0.000
7)	0.958	0.308	0.835	0.074	0.045	0.002	

(D) Results from phylogenetic ANOVA of species' mean $\delta^{13}\text{C}_{\text{diet}}$ values.

	1	2	3	4	5	6	7
1)		-0.569	-0.272	-2.197	-4.705	-9.360	0.161
2)	1.000		0.126	-1.977	-4.976	-10.386	0.559
3)	1.000	1.000		-1.564	-3.357	-7.065	0.359
4)	1.000	0.060	1.000		-1.800	-5.982	1.845
5)	0.090	0.021	0.090	1.000		-5.113	3.509
6)	0.021	0.021	0.021	0.021	0.021		6.930
7)	1.000	1.000	1.000	1.000	1.000	0.429	

Above diagonal line: Tukey's HSD *post hoc* test. Below diagonal line: Mann-Whitney U test. Both ANOVA and Kruskal-Wallis tests yielded $p < 0.001$ of significant differences among feeding categories.

The test yielded $p = 0.001$. Above diagonal line: pairwise t-values. Below diagonal line: adjusted P-values.

P-values < 0.05 are in bold.

Asia fall in the mid-range of the C_3 realm (Figure 5A). Samples from temperate coniferous forests are all from North America (Figure 5B). There, variable grazers, browser–grazer intermediates, and browsers form a unimodal distribution of $\delta^{13}C_{\text{diet}}$ values, primarily in the C_3 range. Tropical and subtropical grasslands, savannas, and shrublands are represented almost exclusively by samples from Africa (Figure 5C), showing a grazer-dominated (especially obligate grazer) distribution of $\delta^{13}C_{\text{diet}}$ values in the C_4 range. Some browsers and mixed feeders are also present, forming a small mode of $\delta^{13}C_{\text{diet}}$ values in the C_3 range. Desert and xeric shrublands also have a bimodal distribution of $\delta^{13}C_{\text{diet}}$ values (Figure 5D). There is a clear division between non-grazers (browsers and browser–grazer intermediates), which comprise $\delta^{13}C_{\text{diet}}$ values in the C_3 range, and the grazers, which contribute to $\delta^{13}C_{\text{diet}}$ values in the C_4 range. Within this ecoregion, samples from Africa include both C_3 - and C_4 -feeders, while those from North America are all C_3 -feeders.

Variation in $\delta^{13}C_{\text{diet}}$ among phylogenetic groups

The mean and range of $\delta^{13}C_{\text{diet}}$ values are more constrained in some artiodactyl clades than in others. Within the suborder Ruminantia, lineages with the oldest node ages (Tragulidae, Antilocapridae, Giraffidae, Cervidae) are exclusively C_3 feeders, while C_4 feeders appear in relatively young lineages (<13 million years old; Figure 6). Species with a pure C_4 diet, corresponding to their assignment in the obligate grazer category, belong in two bovid tribes, the Reduncini and the Hippotragini. Some groups within Bovidae maintained C_3 feeding, such as the Cephalophini, the Neotragini, and subgroups of the Antilopini. Other clades have a mixture of C_3 feeders, C_4 feeders, and mixed C_3 – C_4 feeders. There is low phylogenetic signal in the $\delta^{13}C_{\text{diet}}$ values of artiodactyls ($K = 0.38$, $p = 0.001$). Similar $\delta^{13}C_{\text{diet}}$ values occur in multiple artiodactyl clades and

TABLE 4 Comparison of $\delta^{13}C_{\text{diet}}$ values of artiodactyls among 11 ecoregions, each found on multiple continents.

(A) Summary statistics.

Ecoregion	N	Min.	Max.	Mean	Median	S.D.
1) Tropical and subtropical moist broadleaf forests	278	−35.0	−7.7	−19.6	−19.4	6.67
2) Temperate broadleaf and mixed forests	25	−28.2	−17.0	−25.4	−25.7	2.35
3) Temperate coniferous forests	101	−28.3	−15.2	−23.7	−24.0	1.66
4) Boreal forests/taiga	5	−26.4	−20.7	−22.4	−21.9	2.30
5) Tropical and subtropical grasslands, savannas, and shrublands	709	−30.7	−8.2	−15.6	−14.3	5.29
6) Temperate grasslands, savannas, and shrublands	58	−26.7	−13.4	−20.1	−21.3	3.94
7) Flooded grasslands and shrublands	9	−21.1	−9.8	−15.9	−15.2	3.36
8) Montane grasslands and shrublands	51	−29.0	−12.0	−22.1	−21.9	2.77
9) Tundra	2	−22.8	−15.1	−19.0	−19.0	5.47
10) Mediterranean forests, woodlands, and scrub	15	−25.9	−18.1	−22.5	−22.9	2.16
11) Deserts and xeric shrublands	103	−25.4	−8.3	−19.0	−21.0	4.83

(B) P-values from *post hoc* pairwise tests.

	1	2	3	4	5	6	7	8	9	10	11
1)		0.000	0.000	0.983	0.000	1.000	0.577	0.067	1.000	0.585	0.994
2)	0.000		0.934	0.985	0.000	0.001	0.000	0.237	0.839	0.824	0.000
3)	0.001	0.000		1.000	0.000	0.001	0.001	0.757	0.971	0.999	0.000
4)	0.458	0.019	0.095		0.124	0.997	0.476	1.000	0.999	1.000	0.938
5)	0.000	0.000	0.000	0.010		0.000	1.000	0.000	0.998	0.000	0.000
6)	0.980	0.000	0.000	0.430	0.000		0.484	0.632	1.000	0.877	0.974
7)	0.138	0.000	0.000	0.008	0.579	0.011		0.042	1.000	0.095	0.837
8)	0.130	0.000	0.000	0.852	0.000	0.023	0.000		0.999	1.000	0.022
9)	0.820	0.037	0.037	0.847	0.332	0.918	0.554	0.469		0.998	1.000
10)	0.304	0.000	0.012	0.631	0.000	0.030	0.000	0.506	0.264		0.340
11)	0.054	0.000	0.000	0.342	0.000	0.267	0.048	0.001	0.963	0.008	

Above diagonal line: Tukey's HSD *post hoc* test. Below diagonal line: Mann–Whitney U test. Both ANOVA and Kruskal–Wallis tests yielded $p < 0.001$ of significant differences among ecoregions.

P-values < 0.05 are in bold.

individual clades show broad to narrow variation in $\delta^{13}\text{C}_{\text{diet}}$ values.

Discussion

We compiled and evaluated a global dataset of $\delta^{13}\text{C}_{\text{diet}}$ (isotope values of ingested forage) of extant artiodactyls, which documents variation among feeding categories, ecoregions, and clades. Our data compilation shows that research on artiodactyl $\delta^{13}\text{C}_\text{E}$ has covered just over 30% of species richness of extant artiodactyls. In addition, sampling is highly uneven both phylogenetically and geographically (Figure 1 and Table 2). Only one species of tragulid has been sampled, and no data are available for moschids. Although both species of extant hippopotamid have been sampled, the hippopotamus (*Hippopotamus amphibius*) is represented by 182 samples, making up 13% of the total number of samples, while the pygmy hippopotamus (*Choeropsis liberiensis*) is only represented by one sample. Sampling is dense in sub-Saharan African ecosystems (Figures 1, 5), where C_4 grasslands and closed-canopy C_3 environments are both extensive and artiodactyl species-richness is high. In contrast, sampling is sparse across the Eurasian continent. In East Africa, where sampling is the densest, savanna ecosystems lie adjacent to expansive tropical rainforest. Riverine and montane forest habitats and xeric shrublands also occur in patchy areas surrounded by tropical and subtropical grasslands there. Samples from this region largely contribute to the bimodal distributions in Figure 5, indicating consumption of both C_3 and C_4 plants by resident artiodactyls.

The herbivore dietary spectrum is expressed through a wide range of $\delta^{13}\text{C}_{\text{diet}}$ values, with the most depleted mean and median values in frugivores and the most enriched in obligate grazers. In general, grazing taxa have a broader range of dietary isotope values than browsing taxa. Notably, variable grazers exhibit a bimodal distribution of $\delta^{13}\text{C}_{\text{diet}}$ values, with North American taxa consuming C_3 vegetation and African taxa consuming C_4 vegetation, reflecting the different amounts of C_4 biomass available in temperate versus tropical environments. Variation in $\delta^{13}\text{C}_{\text{diet}}$ values also occurs among ecoregions, taxonomic groups, and geographic regions. Grassland ecoregions differ significantly from forest ecoregions in $\delta^{13}\text{C}_{\text{diet}}$ values. Some of the oldest ruminant lineages have maintained C_3 feeding, and pure C_4 dietary signals are restricted to two bovid clades. The $\delta^{13}\text{C}_{\text{diet}}$ values of species and faunas also vary across geographic regions and may be related to amount of C_4 vegetation in the environment. Most of the observed patterns correspond broadly with existing knowledge about stable isotope ecology, but deviations from the general trend can be identified in well-sampled taxa and regions. Additionally, we detected low phylogenetic signal ($K = 0.38$, $p = 0.001$) in the mean $\delta^{13}\text{C}_{\text{diet}}$ values of artiodactyl species. It is important

to note, however, that ecology, phylogeny, biogeography, and environmental settings are often correlated, and the combination of available vegetation, ecological interactions, and physiological processes affects the $\delta^{13}\text{C}$ values recorded in artiodactyl tooth enamel.

The herbivore dietary spectrum

The frugivore–browser–grazer dietary spectrum corresponds to an increase in group-mean $\delta^{13}\text{C}_{\text{diet}}$ values over a range of 10‰ from frugivores (−24.7‰) to obligate grazers (−13.4‰) (Figure 2 and Table 3). Feeding groups have different dietary preferences as well as niche breadths. The two herbivore dietary extremes (frugivores and obligate grazers) have the narrowest range of species-mean $\delta^{13}\text{C}_{\text{diet}}$ values, and obligate grazers can be most readily distinguished from other feeding categories (Table 3). The intermediate feeding categories (i.e., generalist and browser–grazer intermediate), by their defining criteria, have inherently wider dietary variation than the dietary extremes. Considerable variation also exists in browsers and variable grazers. The lowest $\delta^{13}\text{C}_{\text{diet}}$ values occur in two subcanopy browsers, the dwarf antelope (*Neotragus batesi*) and the okapi (*Okapia johnstoni*) (Figure 6 and Table 2). Both species inhabit closed-canopy forests in equatorial Africa. Okapis are endemic to the forests in northeastern Congo Basin. The dwarf antelope has a discontinuous range in central and western equatorial Africa. The two specimens of *N. batesi* from Cameroon have more variable $\delta^{13}\text{C}_{\text{diet}}$ values (−29.5‰ and −34.7‰) than do the two specimens from the Ituri Forest (−34.2‰ and −35.0‰), and more variation may be present in this group across its geographic range than previously recognized. Variable grazers exhibit a bimodal distribution of $\delta^{13}\text{C}_{\text{diet}}$ values that is distinct from the other feeding categories, and the pattern can be best explained by a distinction between the North American species feeding primarily on C_3 vegetation and the African species feeding primarily on C_4 vegetation (Figure 3H). In North America, variable grazers include the bison (*Bison bison*), muskox (*Oreamnos americanus*), bighorn sheep (*Ovis canadensis*), and the Dall sheep (*Ovis dalli*). Bison are sampled from a range of latitudes in the western United States; their $\delta^{13}\text{C}_\text{E}$ values vary considerably and are correlated with mean annual temperature (Hoppe et al., 2006). In Africa, warthog (*Phacochoerus africanus*) makes up most of the variable-grazer sample; the rest are from oryx (*Oryx beisa*), oribi (*Ourebia ourebia*), and the marshbuck (*Tragelaphus spekii*). Species in both continental faunas consume over 60% monocots in their average diets. Their contrasting $\delta^{13}\text{C}_{\text{diet}}$ signatures likely reflect variation in the amount of C_4 biomass in the vegetation (Still et al., 2003), which is affected by both temperature and seasonality of precipitation (Boutton et al., 1980; Winslow et al., 2003; Kohn, 2010). Differentiating C_3 graze from C_3 browse in the fossil record would require incorporation of other kinds of data, such as morphological and use-wear traits.

Dietary breadth and flexibility

While sampled individuals may be categorized as a browser, a mixed feeder, or a grazer solely by their $\delta^{13}\text{C}_{\text{diet}}$ values (e.g., Cerling et al., 2015), it is evident from Figure 2B that there are no clear-cut boundaries among the three broad feeding types. Individuals belonging to the same phylogenetic group or feeding category can have a range of $\delta^{13}\text{C}_{\text{diet}}$ values. Consequently, the C_3 - C_4 cutoff is frequently crossed by clades and feeding groups (Figures 2, 6). Artiodactyls have been documented to shift their diets due to geographic variation in vegetation structure, seasonal climatic and environmental changes, and ecological interactions with sympatric species (Sponheimer et al., 2003; Djaloun et al., 2013; Radloff et al., 2013; Miranda et al., 2014). Such dietary changes increase the abundance of savanna herbivore species (Staver and Hempson, 2020).

Grazing species have wider dietary niche breadths than browsing species do, as represented by their $\delta^{13}\text{C}_{\text{diet}}$ values (Figure 2 and Table 3). The difference between maximum and minimum $\delta^{13}\text{C}_{\text{diet}}$ values in browsing species (including frugivores and browsers) is $\sim 18\text{‰}$ ($\sim 12\text{‰}$ if excluding the outliers from understory browsers), and no sample from browsing species plots in the C_4 range. Grazing species (including variable grazers and obligate grazers) have a total range of over 22‰ , with many samples extending well into the C_3 range. Variable grazers have the widest range of mean $\delta^{13}\text{C}_{\text{diet}}$ values, ranging from -27.9‰ (*Tragelaphus spekii*) to -9.8‰ (*Connochaetes gnou*). Corresponding to this difference in extant artiodactyls, findings in the North American fossil record show that species with grazing-adapted morphology have broader diets than browsing-adapted ones and consume more browse than previously anticipated, thus morphological specialization may result in ecological generalization (Feranec, 2003; Pardi and DeSantis, 2021). Herbivores with grazing adaptations, such as hypsodont teeth, are able to consume grass but can also eat other foods when they are available. This dietary flexibility would have implications for species duration over evolutionary time scales, especially during times of climate change. For example, in the Miocene Siwalik record of Pakistan, ungulate species that were able to alter their diet (from browsing to mixed feeding or grazing) in response to vegetation change persisted substantially longer than those that were not (Badgley et al., 2008).

Future research

More isotopic data are needed for currently understudied regions and taxa to further explore the research questions posed in this study. In the current data compilation, tragulids are represented by only one species and moschids are absent. Both families are important forest dwellers in Asia and have substantial fossil records, and their $\delta^{13}\text{C}_{\text{diet}}$ values can help us investigate the resource use and partitioning in artiodactyl

faunas in tropical, subtropical, and temperate forests, which may be important analogs for some paleo-ecosystems. Better sampling records from Eurasia in general are also needed. Although some isotope data from other body tissues (e.g., hair) have been reported, tooth enamel data are lacking for many regions of the continent. Due to variability in the carbon-isotope spacing between different body tissues, converting hair or bone collagen data to enamel equivalent values can confound paleodietary reconstructions (Codron et al., 2011, 2012, 2018; Bocherens et al., 2014). Therefore, $\delta^{13}\text{C}_\text{E}$ data are ideal for making direct comparisons between ungulate diets in modern and paleo ecosystems.

Incorporating different data types has proven valuable to studying paleoecology, and when reconstructing the diet of fossil species, more proxies are better than one. In addition to mandibular morphology and tooth-enamel isotopes, tooth-wear proxies should be incorporated (e.g., Codron et al., 2008; Luyt and Faith, 2014; Fillion et al., 2022). The microscopic wear patterns on the occlusal surface of teeth (microwear), for example, record feeding habits with the finest temporal resolution (daily or weekly) and can be used to detect subtle variations in broadly similar diets (e.g., Louail et al., 2021) as well as ecological responses to short-term environmental changes that would not be reflected in tooth-wear measurements (such as mesowear) or dental morphology (such as hypsodonty) (Mihlbachler et al., 2018). While carbon isotope analysis is limited in its ability to distinguish dicot fruits from leaves in a species' diet, microwear and mesowear analyses as well as mandibular morphology have proven useful for differentiating frugivores from browsers (e.g., Scott, 2012; Kaiser et al., 2013; Wang et al., 2022).

Our dataset is potentially useful for addressing many questions beyond this study. For example, how are the mean and range of $\delta^{13}\text{C}_{\text{diet}}$ values related to vegetation heterogeneity, topographic complexity, and climatic conditions? Do some species track the variation in environmental $\delta^{13}\text{C}$ values better than other species with similar geographic ranges? If so, what aspects of their ecology can explain the difference? How do species' $\delta^{13}\text{C}_{\text{diet}}$ values contract or expand from ecological interactions, such as co-occurrence with competitors for forage? What combination of isotopic signature and osteological characters can be used to improve paleoecological reconstructions? Some of these questions will need better sampling of targeted taxa, regions, or environmental settings, others will require more comparative data from plants.

Data availability statement

The original contributions presented in this study are included in the article/Supplementary material, further inquiries can be directed to the corresponding author.

Author contributions

BW and CB developed the research plan and wrote the manuscript. BW gathered and analyzed the data and produced the figures. Both authors contributed to the article and approved the submitted version.

Funding

This work was supported by a Graduate Student Research Grant from the Geological Society of America and a Wood Award from the Society of Vertebrate Paleontology to BW.

Acknowledgments

We thank Cody Thompson, Michael Cherney, and other members at the University of Michigan Museum of Zoology and the University of Michigan Museum of Paleontology for their kind assistance with museum access, data collection, and lab work. Isotope samples were analyzed by Lora Wingate and Kyger Lohmann at the University of Michigan Stable Isotope Laboratory in the Department of Earth and Environmental Sciences. Ethan Vanvalkenburg helped with the compilation of dietary data. This work benefited from discussions with Benjamin Passey, Laura MacLachy, John Kingston, Matt

Friedman, and Miriam Zelditch, reviews by AG and PH, and the editorial input from CM.

Conflict of interest

The authors declare that the research was conducted in the absence of any commercial or financial relationships that could be construed as a potential conflict of interest.

Publisher's note

All claims expressed in this article are solely those of the authors and do not necessarily represent those of their affiliated organizations, or those of the publisher, the editors and the reviewers. Any product that may be evaluated in this article, or claim that may be made by its manufacturer, is not guaranteed or endorsed by the publisher.

Supplementary material

The Supplementary Material for this article can be found online at: <https://www.frontiersin.org/articles/10.3389/fevo.2022.958859/full#supplementary-material>

References

- Badgley, C., Barry, J. C., Morgan, M. E., Nelson, S. V., Behrensmeyer, A. K., Cerling, T. E., et al. (2008). Ecological changes in Miocene mammalian record show impact of prolonged climatic forcing. *Proc. Natl. Acad. Sci. U.S.A.* 105, 12145–12149. doi: 10.1073/pnas.0805592105
- Blomberg, S. P., Garland, T. Jr., and Ives, A. R. (2003). Testing for phylogenetic signal in comparative data: Behavioral traits are more labile. *Evolution* 57, 717–745. doi: 10.1111/j.0014-3820.2003.tb00285.x
- Bocherens, H., Grandal-d'Anglade, A., and Hobson, K. A. (2014). Pitfalls in comparing modern hair and fossil bone collagen C and N isotopic data to reconstruct ancient diets: a case study with cave bears (*Ursus spelaeus*). *Isot. Environ. Health* 50, 291–299. doi: 10.1080/10256016.2014.890193
- Bocherens, H., Koch, P. L., Mariotti, A., Geraads, D., and Jaeger, J. J. (1996). Isotopic biogeochemistry (^{13}C , ^{18}O) of mammalian enamel from African Pleistocene hominid sites. *Palaio* 11, 306–318. doi: 10.2307/3515241
- Boisserie, J. R., Zazzo, A., Merceron, G., Blondel, C., Vignaud, P., Likies, A., et al. (2005). Diets of modern and late Miocene hippopotamids: evidence from carbon isotope composition and microwear of tooth enamel. *Palaeogeogr. Palaeoclimatol. Palaeoecol.* 221, 153–174. doi: 10.1016/j.palaeo.2005.02.010
- Boutton, T. W., Harrison, A. T., and Smith, B. N. (1980). Distribution of biomass of species differing in photosynthetic pathway along an altitudinal transect in southeastern Wyoming grassland. *Oecologia* 45, 287–298. doi: 10.1007/BF00540195
- Bradham, J. L., DeSantis, L. R. G., Jorge, M. L. S. P., and Keuroghlian, A. (2018). Dietary variability of extinct tayassuids and modern white-lipped peccaries (*Tayassu pecari*) as inferred from dental microwear and stable isotope analysis. *Palaeogeogr. Palaeoclimatol. Palaeoecol.* 499, 93–101. doi: 10.1016/j.palaeo.2018.03.020
- Burgin, C. J., Colella, J. P., Kahn, P. L., and Upham, N. S. (2018). How many species of mammals are there? *J. Mammal.* 99, 1–14. doi: 10.1093/jmammal/gyx147
- Cerling, T. E., Andanje, S. A., Blumenthal, S. A., Brown, F. H., Chritz, K. L., Harris, J. M., et al. (2015). Dietary changes of large herbivores in the Turkana Basin Kenya from 4 to 1 Ma. *Proc. Natl. Acad. Sci. U.S.A.* 112, 11467–11472. doi: 10.1073/pnas.1513075112
- Cerling, T. E., and Ehleringer, J. R. (2000). "Welcome to the C4 world," in *Phanerozoic Terrestrial Ecosystems*, eds R. A. Gastaldo and W. A. DiMichele (New Haven, CT: Yale University Press), 273–286. doi: 10.1017/S1089332600000802
- Cerling, T. E., Harris, J., MacFadden, B., Leakey, M. G., Quade, J., Eisenmann, V., et al. (1997). Global vegetation change through the Miocene/Pliocene boundary. *Nature* 389, 153–158. doi: 10.1038/38229
- Cerling, T. E., and Harris, J. M. (1999). Carbon isotope fractionation between diet and bioapatite in ungulate mammals and implications for ecological and paleoecological studies. *Oecologia* 120, 347–363. doi: 10.1007/s004420050868
- Cerling, T. E., Harris, J. M., Hart, J. A., Kaleme, P., Klingel, H., Leakey, M. G., et al. (2008). Stable isotope ecology of the common hippopotamus. *J. Zool.* 276, 204–212. doi: 10.1111/j.1469-7998.2008.00450.x
- Cerling, T. E., Harris, J. M., and Leakey, M. G. (1999). Browsing and grazing in modern and fossil proboscideans. *Oecologia* 120, 364–374. doi: 10.1007/s004420050869
- Cerling, T. E., Harris, J. M., Leakey, M. G., and Mudida, N. (2003). "Stable isotope ecology of Northern Kenya, with emphasis on the Turkana Basin, Kenya," in *Lothagam: the Dawn of Humanity in Africa*, eds M. G. Leakey and J. M. Harris (New York, NY: Columbia University Press), 583–603. doi: 10.7312/leak11870-023

- Cerling, T. E., Harris, J. M., Leakey, M. G., Passey, B. H., and Levin, N. E. (2010). "Stable carbon and Oxygen isotopes in east African mammals: Modern and fossil," in *Cenozoic Mammals of Africa*, ed. L. Werdelin (Oakland, CA: University of California Press), 941–952. doi: 10.1525/california/9780520257214.003.0048
- Cerling, T. E., Hart, J. A., and Hart, T. B. (2004). Stable isotope ecology in the Ituri Forest. *Oecologia* 138, 5–12. doi: 10.1007/s00442-003-1375-4
- Cerling, T. E., Mbuu, E., Kirera, F. M., Manthi, F. K., Grine, F. E., Leakey, M. G., et al. (2011). Diet of *Paranthropus boisei* in the early Pleistocene of East Africa. *Proc. Natl. Acad. Sci. U.S.A.* 108, 9337–9341. doi: 10.1073/pnas.1104627108
- Clauss, M., Lechner-Doll, M., and Streich, W. J. (2003). Ruminant diversification as an adaptation to the biomechanical characteristics of forage. *Oikos* 102, 253–262. doi: 10.1034/j.1600-0706.2003.12406.x
- Clementz, M. T. (2012). New insight from old bones: stable isotope analysis of fossil mammals. *J. Mammal.* 93, 368–380. doi: 10.1644/11-MAMM-S-179.1
- Codron, D., Brink, J. S., Rossouw, L., Clauss, M., Codron, J., Lee-Thorp, J. A., et al. (2008). Functional differentiation of African grazing ruminants: an example of specialized adaptations to very small changes in diet. *Biol. J. Linn. Soc.* 94, 755–764. doi: 10.1111/j.1095-8312.2008.01028.x
- Codron, D., Clauss, M., Codron, J., and Tütken, T. (2018). Within trophic level shifts in collagen-carbonate stablecarbon isotope spacing are propagated by diet and digestive physiology in large mammal herbivores. *Ecol. Evol.* 8, 3983–3995. doi: 10.1002/ece3.3786
- Codron, D., Codron, J., Sponheimer, M., Bernasconi, S. M., and Clauss, M. (2011). When animals are not quite what they eat: diet digestibility influences ^{13}C -incorporation rates and apparent discrimination in a mixed-feeding herbivore. *Can. J. Zool.* 89, 453–465. doi: 10.1139/z11-010
- Codron, D., Sponheimer, M., Codron, J., Newton, I., Lanham, J. L., and Clauss, M. (2012). The confounding effects of source isotopic heterogeneity on consumer-diet and tissue-tissue stable isotope relationships. *Oecologia* 169, 939–953. doi: 10.1007/s00442-012-2274-3
- Copeland, S. R., Sponheimer, M., Spinage, C. A., and Lee-Thorp, J. A. (2008). Bulk and intra-tooth enamel stable isotopes of waterbuck *Kobus ellipsiprymnus* from Queen Elizabeth National Park. *Uganda. Afr. J. Ecol.* 46, 697–701. doi: 10.1111/j.1365-2028.2008.00950.x
- Copeland, S. R., Sponheimer, M., Spinage, C. A., Lee-Thorp, J. A., Codron, D., and Reed, K. E. (2009). Stable isotope evidence for impala *Aepyceros melampus* diets at Akagera National Park, Rwanda. *Afr. J. Ecol.* 47, 490–501. doi: 10.1111/j.1365-2028.2008.00969.x
- DeSantis, L., Feranec, R., Southon, J., Binder, W. J., Cohen, J., Farrell, A., et al. (2020). "More tools and isotopes are better than one: Clarifying the ecology of ancient mammals at Rancho La Brea and beyond," in *Proceeding of the society of vertebrate paleontology program and abstracts meeting*.
- Djagoun, C. A. M. S., Kassa, B., Mensah, G. A., and Sinsin, B. A. (2013). Seasonal habitat and diet partitioning between two sympatric bovid species in Pendjari Biosphere Reserve (northern Benin): waterbuck and western kob. *Afr. Zool.* 48, 279–289. doi: 10.1080/15627020.2013.11407594
- Drummond, A. J., Suchard, M. A., Xie, D., and Rambaut, A. (2012). Bayesian phylogenetics with BEAUti and the BEAST 1.7. *Mol. Biol. Evol.* 29, 1969–1973. doi: 10.1093/molbev/mss075
- Ehrlinger, J. R., Sage, R. F., Flanagan, L. B., and Pearcy, R. W. (1991). Climate change and the evolution of C_4 photosynthesis. *Trends Ecol. Evol.* 6, 95–99. doi: 10.1016/0169-5347(91)90183-X
- Fenner, J. N. (2008). The use of stable isotope ratio analysis to distinguish multiple prey kill events from mass kill events. *J. Archaeol. Sci.* 35, 704–716. doi: 10.1016/j.jas.2007.06.010
- Feranec, R. S. (2003). Stable isotopes, hypsodonty, and the paleodiet of Hemiauchenia (Mammalia: Camelidae): a morphological specialization creating ecological generalization. *Paleobiology* 29, 230–242. doi: 10.1666/0094-8373(2003)029<0230:SIHATP>2.0.CO;2
- Feranec, R. S. (2007). Stable carbon isotope values reveal evidence of resource partitioning among ungulates from modern C_3 -dominated ecosystems in North America. *Palaeogeogr. Palaeoclimatol. Palaeoecol.* 252, 575–585. doi: 10.1016/j.palaeo.2007.05.012
- Feranec, R. S., and MacFadden, B. J. (2006). Evolution of the grazing niche in Pleistocene mammals from Florida: evidence from stable isotopes. *Palaeogeogr. Palaeoclimatol. Palaeoecol.* 162, 155–169. doi: 10.1016/S0031-0182(00)00110-3
- Fillion, E. N., Harrison, T., and Kwekason, A. (2022). A nonanalogue Pliocene ungulate community at Laetoli with implications for the paleoecology of *Australopithecus afarensis*. *J. Hum. Evol.* 167:103182. doi: 10.1016/j.jhevol.2022.103182
- Gagnon, M., and Chew, A. E. (2000). Dietary preferences in extant African Bovidae. *J. Mammal.* 81, 490–511. doi: 10.1644/1545-1542(2000)081<0490:DPiEAB>2.0.CO;2
- Gong, Y., Wang, Y., Wang, Y., Mao, F., Bai, B., Wang, H., et al. (2020). Dietary adaptations and palaeoecology of Lophiidae (Mammalia, Tapiroidea) from the Eocene of the Erlan Basin, China: combined evidence from mesowear and stable isotope analyses. *Palaeontology* 63, 547–564. doi: 10.1111/pala.12471
- Hammer, Ø., Harper, D. A. T., and Ryan, P. D. (2001). PAST: Paleontological statistics software package for education and data analysis. *Palaeontol. Electron.* 4, 1–9.
- Harris, J. M., and Cerling, T. E. (2002). Dietary adaptations of extant and Neogene African suids. *J. Zool.* 256, 45–54. doi: 10.1017/S0952836902000067
- Hillson, S. (2005). *Teeth*. Cambridge, MA: Cambridge University Press. doi: 10.1017/CBO9780511614477
- Hofmann, R. R., and Stewart, D. R. M. (1972). Grazer or browser: a classification based on the stomach-structure and feeding habits of East African ruminants. *Mammalia* 36, 226–240. doi: 10.1515/mamm.1972.36.2.226
- Hoppe, K. A., Paytan, A., and Chamberlain, P. (2006). Reconstructing grassland vegetation and paleotemperatures using carbon isotope ratios of bison tooth enamel. *Geology* 34, 649–652. doi: 10.1130/G22745.1
- Janis, C. M., and Ehrhardt, D. (1988). Correlation of relative muzzle width and relative incisor width with dietary preference in ungulates. *Zool. J. Linn. Soc.* 92, 267–284. doi: 10.1111/j.1096-3642.1988.tb01513.x
- Kaiser, T. M., Müller, D. W. H., Fortelius, M., Schulz, E., Codron, D., and Clauss, M. (2013). Hypsodonty and tooth facet development in relation to diet and habitat in herbivorous ungulates: implications for understanding tooth wear. *Mammal Rev.* 43, 34–46. doi: 10.1111/j.1365-2907.2011.00203.x
- Keeling, R. F., Graven, H. D., Welp, L. R., Resplandy, L., Bi, J., Piper, S. C., et al. (2017). Atmospheric evidence for a global secular increase in carbon isotopic discrimination of land photosynthesis. *Proc. Natl. Acad. Sci. U.S.A.* 114, 10361–10366. doi: 10.1073/pnas.1619240114
- Kingston, J. D. (2011). "Stable isotopic analyses of Laetoli fossil herbivores," in *Paleontology and Geology of Laetoli: Human Evolution in Context*, ed. T. Harrison (Dordrecht: Springer Netherlands), 293–328. doi: 10.1007/978-90-481-9956-3_15
- Kita, Z. A., Secord, R., and Boardman, G. S. (2014). A new stable isotope record of Neogene paleoenvironments and mammalian paleoecologies in the western Great Plains during the expansion of C_4 grasslands. *Palaeogeogr. Palaeoclimatol. Palaeoecol.* 399, 160–172. doi: 10.1016/j.palaeo.2014.02.013
- Koch, P. L. (1998). Isotopic reconstruction of past continental environments. *Annu. Rev. Earth Planet. Sci.* 26, 573–613. doi: 10.1146/annurev.earth.26.1.573
- Koch, P. L., Behrensmeyer, A. K., and Fogel, M. L. (1991). The isotopic ecology of plants and animals in Amboseli National Park. *Kenya. Annu. Rep. Dir. Geophys. Lab.* 23, 163–171.
- Koch, P. L., Tuross, N., and Fogel, M. L. (1997). The effects of sample treatment and diagenesis on the isotopic integrity of carbonate in biogenic hydroxylapatite. *J. Archaeol. Sci.* 24, 417–429. doi: 10.1006/jasc.1996.0126
- Kohn, M. J. (2010). Carbon isotope compositions of terrestrial C_3 plants as indicators of (paleo)ecology and (paleo)climate. *Proc. Natl. Acad. Sci. U.S.A.* 107, 19691–19695. doi: 10.1073/pnas.1004933107
- Lazzerini, N., Coulon, A., Simon, L., Marchina, C., Fiorillo, D., Turbat, T. S., et al. (2021). The isotope record ($\delta^{13}\text{C}$, $\delta^{18}\text{O}$) of vertical mobility in incremental tissues (tooth enamel, hair) of modern livestock: A reference set from the Mongolian Altai. *Quat. Int.* 595, 128–144. doi: 10.1016/j.quaint.2021.04.008
- Lee-Thorp, J. (2002). Two decades of progress towards understanding fossilization processes and isotopic signals in calcified tissue minerals. *Archaeometry* 44, 435–446. doi: 10.1111/1475-4754.t01-1-00076
- Lee-Thorp, J. A., and van der Merwe, N. J. (1987). Carbon isotope analysis of fossil bone apatite. *S. Afr. J. Sci.* 83, 712–715.
- Levin, N. E., Simpson, S. W., Quade, J., Cerling, T. E., and Frost, S. R. (2008). "Herbivore enamel carbon isotopic composition and the environmental context of *Ardipithecus* at Gona, Ethiopia," in *The Geology of Early Humans in the Horn of Africa: Geological Society of America Special Paper 446*, eds J. Quade and J. G. Wynn (Boulder, CO: Geological Society of America), 215–234. doi: 10.1130/2008.2446(10)
- Louail, M., Ferchaud, S., Souron, A., Walker, A. E. C., and Merceron, G. (2021). Dental microwear textures differ in pigs with overall similar diets but fed with different seeds. *Palaeogeogr. Palaeoclimatol. Palaeoecol.* 572:110415. doi: 10.1016/j.palaeo.2021.110415
- Louys, J., Ditchfield, P., Meloro, C., Elton, S., and Bishop, L. C. (2012). Stable isotopes provide independent support for the use of mesowear variables for inferring diets in African antelopes. *Proc. R. Soc. B* 279, 4441–4446. doi: 10.1098/rspb.2012.1473
- Luyt, J., and Faith, J. T. (2014). Phylogenetic topology mapped onto dietary ecospace reveals multiple pathways in the evolution of the herbivorous niche in African Bovidae. *J. Zool. Syst. Evol. Res.* 53, 140–154. doi: 10.1111/jzs.12080

- Luyt, J., and Sealy, J. (2018). Inter-tooth comparison of $\delta^{13}\text{C}$ and $\delta^{18}\text{O}$ in ungulate tooth enamel from south-western Africa. *Quat. Int.* 495, 144–152. doi: 10.1016/j.quaint.2018.02.009
- MacFadden, B. J., and Cerling, T. E. (1996). Mammalian herbivore communities, ancient feeding ecology, and carbon isotopes: a 10 million-year sequence from the Neogene of Florida. *J. Vertebr. Paleontol.* 16, 103–115. doi: 10.1080/02724634.1996.10011288
- Martin, J. E., Vance, D., and Balter, V. (2015). Magnesium stable isotope ecology using mammal tooth enamel. *Proc. Natl. Acad. Sci. U.S.A.* 112, 430–435. doi: 10.1073/pnas.1417792112
- Mendoza, M., Janis, C. M., and Palmqvist, P. (2002). Characterizing complex craniodental patterns related to feeding behavior in ungulates: A multivariate approach. *J. Zool.* 258, 223–246. doi: 10.1017/S0952836902001346
- Merceron, G., Zazzo, A., Spassov, N., Geraads, D., and Kovachev, D. (2006). Bovid paleoecology and paleoenvironments from the Late Miocene of Bulgaria: Evidence from dental microwear and stable isotopes. *Palaeogeogr. Palaeoclimatol. Palaeoecol.* 241, 637–654. doi: 10.1016/j.palaeo.2006.05.005
- Mihlbachler, M. C., Campbell, D., Chen, C., Ayoub, M., and Kaur, P. (2018). Microwear–mesowear congruence and mortality bias in rhinoceros mass-death assemblages. *Paleobiology* 44, 131–154. doi: 10.1017/pab.2017.13
- Miranda, M., Dalerum, F., and Parrini, F. (2014). Interaction patterns within a multi-herbivore assemblage derived from stable isotopes. *Ecol. Complex.* 20, 51–60. doi: 10.1016/j.ecocom.2014.08.002
- Nelson, S. V. (2013). Chimpanzee fauna isotopes provide new interpretations of fossil ape and hominin ecologies. *Proc. R. Soc. B* 280:20132324. doi: 10.1098/rspb.2013.2324
- O'Leary, M. H. (1988). Carbon isotopes in photosynthesis. *Bioscience* 38, 328–336. doi: 10.2307/1310735
- O'Leary, M. H., Madhavan, S., and Paneth, P. (1992). Physical and chemical basis of carbon isotope fractionation in plants. *Plant Cell Environ.* 15, 1099–1104. doi: 10.1111/j.1365-3040.1992.tb01660.x
- Olson, D. M., Dinerstein, E., Wikramanayake, E. D., Burgess, N. D., Powell, G. V. N., Underwood, E. C., et al. (2001). Terrestrial ecoregions of the world: a new map of life on Earth. *Bioscience* 51, 933–938. doi: 10.1641/0006-3568(2001)051[0933:TEOTWA]2.0.CO;2
- Pardi, M. I., and DeSantis, L. R. G. (2021). Dietary plasticity of North American herbivores: a synthesis of stable isotope data over the past 7 million years. *Proc. R. Soc. B* 288:20210121. doi: 10.1098/rspb.2021.0121
- Passey, B. H., and Cerling, T. E. (2002). Tooth enamel mineralization in ungulates: Implications for recovering a primary isotopic time-series. *Geochim. Cosmochim. Acta* 66, 3225–3234. doi: 10.1016/S0016-7037(02)00933-X
- Passey, B. H., Robinson, T. F., Ayliffe, L. K., Cerling, T. E., Sponheimer, M., Dearling, M. D., et al. (2005). Carbon isotope fractionation between diet, breath CO_2 , and bioapatite in different mammals. *J. Archaeol. Sci.* 32, 1459–1470. doi: 10.1016/j.jas.2005.03.015
- Radloff, F. G., van der Waal, C., and Bond, A. L. (2013). Extensive browsing by a conventional grazer? Stable carbon isotope analysis reveals extraordinary dietary flexibility among Sanga cattle of North Central Namibia. *Isotopes Environ. Health Stud.* 49, 318–324. doi: 10.1080/10256016.2013.789025
- Revell, L. J. (2012). phytools: An R package for phylogenetic comparative biology (and other things). *Methods Ecol. Evol.* 3, 217–223. doi: 10.1111/j.2041-210X.2011.00169.x
- Rivals, F., and Ziegler, R. (2018). High-resolution paleoenvironmental context for human occupations during the Middle Pleistocene in Europe (MIS 11, Germany). *Quat. Sci. Rev.* 188, 136–142. doi: 10.1016/j.quascirev.2018.03.026
- Rivera-Araya, M., and Birch, S. P. (2018). Stable isotope signatures in white-tailed deer as a seasonal paleoenvironmental proxy: A case study from Georgia, United States. *Palaeogeogr. Palaeoclimatol. Palaeoecol.* 505, 53–62. doi: 10.1016/j.palaeo.2018.05.025
- Rubino, M., Etheridge, D. M., Trudinger, C. M., Allison, C. E., Battle, M. O., Langenfelds, R. L., et al. (2013). A revised 1000-year atmospheric $\delta^{13}\text{C}$ - CO_2 record from Law Dome and South Pole, Antarctica. *J. Geophys. Res. Atmos.* 118, 8482–8499. doi: 10.1002/jgrd.50668
- Scott, J. R. (2012). Dental microwear texture analysis of extant African Bovidae. *Mammalia* 76, 157–174. doi: 10.1515/mammalia-2011-0083
- Secord, R., Wing, S. L., and Chew, A. (2008). Stable isotopes in early Eocene mammals as indicators of forest canopy structure and resource partitioning. *Paleobiology* 34, 282–300. doi: 10.1666/0094-8373(2008)034[0282:SIIEEM]2.0.CO;2
- Sewell, L., Merceron, G., Hopley, P. J., Zipfel, B., and Reynolds, S. C. (2019). Using springbok (*Antidorcas*) dietary proxies to reconstruct inferred palaeovegetational changes over 2?million?years in Southern Africa. *J. Archaeol. Sci. Rep.* 23, 1014–1028. doi: 10.1016/j.jasrep.2018.02.009
- Spencer, L. M. (1995). Morphological correlates of dietary resource partitioning in the African Bovidae. *J. Mammal.* 76, 448–471. doi: 10.2307/1382355
- Sponheimer, M., and Cerling, T. E. (2014). “Investigating ancient diets using stable isotopes in bioapatites,” in *Treatise on Geochemistry (Second Edition)*, eds H. D. Holland and K. K. Turekian (Amsterdam: Elsevier), 341–355. doi: 10.1016/B978-0-08-095975-7.01222-5
- Sponheimer, M., Lee-Thorp, J. A., DeRuiter, D. J., Smith, J. M., van der Merwe, N. J., Reed, K., et al. (2003). Diets of Southern African Bovidae: Stable isotope evidence. *J. Mammal.* 84, 471–479. doi: 10.1644/1545-1542(2003)084<0471:DOSABS>2.0.CO;2
- Sponheimer, M., Reed, K. E., and Lee-Thorp, J. A. (1999). Combining isotopic and ecomorphological data to refine bovid dietary reconstruction: A case study from the Makapansgat Limeworks hominin locality. *J. Hum. Evol.* 36, 705–718. doi: 10.1006/jhev.1999.0300
- Staver, A. C., and Hempson, G. P. (2020). Seasonal dietary changes increase the abundances of savanna herbivore species. *Sci. Adv.* 6:eabd2848. doi: 10.1126/sciadv.abd2848
- Still, C. J., Berry, J. A., Collatz, G. J., and DeFries, R. S. (2003). Global distribution of C_3 and C_4 vegetation: Carbon cycle implications. *Global Biogeochem. Cycles* 17:1006. doi: 10.1029/2001GB001807
- Tejada, J. V., Flynn, J. J., Antoine, P. O., Pacheco, V., Salas-Gismondi, R., and Cerling, T. E. (2020). Comparative isotope ecology of western Amazonian rainforest mammals. *Proc. Natl. Acad. Sci. U.S.A.* 117, 26263–26272. doi: 10.1073/pnas.2007440117
- Tejada-Lara, J. V., MacFadden, B. J., Bermudez, L., Rojas, G., Salas-Gismondi, R., and Flynn, J. J. (2018). Body mass predicts isotope enrichment in herbivorous mammals. *Proc. R. Soc. B* 285:20181020. doi: 10.1098/rspb.2018.1020
- Uno, K. T., Rivals, F., Bibi, F., Pante, M., Njau, M., and de la Torre, I. (2018). Large mammal diets and paleoecology across the Oldowan–Acheulean transition at Olduvai Gorge, Tanzania from stable isotope and tooth wear analyses. *J. Hum. Evol.* 120, 76–91. doi: 10.1016/j.jhev.2018.01.002
- Upham, N. S., Esselstyn, J. A., and Jetz, W. (2019). Inferring the mammal tree: Species-level sets of phylogenies for questions in ecology, evolution, and conservation. *PLoS Biol.* 17:e3000494. doi: 10.1371/journal.pbio.3000494
- van der Merwe, N. J. (2013). Isotopic ecology of fossil fauna from Olduvai Gorge at ca 1.8 Ma, compared with modern fauna. *S. Afr. J. Sci.* 109, 1–14. doi: 10.1590/sajs.2013/20130105
- Wang, B., and Secord, R. (2020). Paleoecology of *Aphelops* and *Teleoceras* (Rhinocerotidae) through an interval of changing climate and vegetation in the Neogene of the Great Plains, central United States. *Palaeogeogr. Palaeoclimatol. Palaeoecol.* 542:109411. doi: 10.1016/j.palaeo.2019.109411
- Wang, B., Zelditch, M., and Badgley, C. (2022). Geometric morphometrics of mandibles for dietary differentiation of Bovidae (Mammalia: Artiodactyla). *Curr. Zool.* 68, 237–249. doi: 10.1093/cz/zoab036
- Wang, Y., and Cerling, T. E. (1994). A model of fossil tooth and bone diagenesis: implications for paleodiet reconstruction from stable isotopes. *Palaeogeogr. Palaeoclimatol. Palaeoecol.* 107, 281–289. doi: 10.1016/0031-0182(94)90100-7
- Wang, Y., Cerling, T. E., and MacFadden, B. J. (1994). Fossil horses and carbon isotopes: new evidence for Cenozoic dietary, habitat, and ecosystem changes in North America. *Palaeogeogr. Palaeoclimatol. Palaeoecol.* 107, 269–279. doi: 10.1016/0031-0182(94)90099-X
- Wang, Y., Kromhout, E., Zhang, C., Xu, Y., Parker, W., Deng, T., et al. (2008). Stable isotopic variations in modern herbivore tooth enamel, plants and water on the Tibetan Plateau: Implications for paleoclimate and paleoelevation reconstructions. *Palaeogeogr. Palaeoclimatol. Palaeoecol.* 260, 359–374. doi: 10.1016/j.palaeo.2007.11.012
- West, J. B., Bowen, G. J., Cerling, T. E., and Ehleringer, J. R. (2006). Stable isotopes as one of nature's ecological recorders. *Trends Ecol. Evol.* 21, 408–414. doi: 10.1016/j.tree.2006.04.002
- Winslow, J. C., Hunt, E. R. Jr., and Piper, S. C. (2003). The influence of seasonal water availability on global C_3 versus C_4 grassland biomass and its implications for climate change research. *Ecol. Model.* 163, 153–173. doi: 10.1016/S0304-3800(02)00415-5



OPEN ACCESS

EDITED BY

Ferran Estebanaranz-Sánchez,
Milá y Fontanals Institution
for Research in Humanities (CSIC),
Spain

REVIEWED BY

Maria Ana Correia,
University of São Paulo, Brazil
Lisa Schunk,
University of Wrocław, Poland

*CORRESPONDENCE

Ryohei Sawaura
sawaura@gmail.com
Yuri Kimura
ykimura.research@gmail.com
Mugino O. Kubo
mugino@k.u-tokyo.ac.jp

†These authors have contributed
equally to this work

SPECIALTY SECTION

This article was submitted to
Paleoecology,
a section of the journal
Frontiers in Ecology and Evolution

RECEIVED 22 June 2022

ACCEPTED 16 September 2022

PUBLISHED 20 October 2022

CITATION

Sawaura R, Kimura Y and Kubo MO
(2022) Accuracy of dental microwear
impressions by physical properties
of silicone materials.
Front. Ecol. Evol. 10:975283.
doi: 10.3389/fevo.2022.975283

COPYRIGHT

© 2022 Sawaura, Kimura and Kubo.
This is an open-access article
distributed under the terms of the
[Creative Commons Attribution License
\(CC BY\)](https://creativecommons.org/licenses/by/4.0/). The use, distribution or
reproduction in other forums is
permitted, provided the original
author(s) and the copyright owner(s)
are credited and that the original
publication in this journal is cited, in
accordance with accepted academic
practice. No use, distribution or
reproduction is permitted which does
not comply with these terms.

Accuracy of dental microwear impressions by physical properties of silicone materials

Ryohei Sawaura^{1,2,3*†}, Yuri Kimura^{4,5*†} and Mugino O. Kubo^{6*†}

¹Okinawa Prefectural Museum and Art Museum, Naha, Japan, ²Department of Anthropology, National Museum of Nature and Science, Tsukuba, Japan, ³Division of Oral and Craniofacial Anatomy, Graduate School of Dentistry, Tohoku University, Sendai, Japan, ⁴Department of Geology and Paleontology, National Museum of Nature and Science, Tsukuba, Japan, ⁵Institut Català de Paleontologia Miquel Crusafont, Barcelona, Spain, ⁶Department of Natural Environmental Studies, Graduate School of Frontier Sciences, The University of Tokyo, Kashiwa, Japan

Dental microwear analysis is an oft-used paleodietary estimation method, and the impression molds or resin casts are often analyzed rather than the original tooth surfaces. A choice of silicone products for dental impressions is crucial because the quality of microwear data is affected by the impression accuracy of the molds. For this reason, microwear researchers have heavily depended on a few commercial products such as “President” (Coltene/Whaledent AG, Switzerland) to avoid analytical errors caused using different silicone materials. Considering that the production business might be terminated, however, heavy reliance on specific products could be a potential weakness in the field. In this study, we aimed at identifying specific indexes of physical properties of silicone materials with satisfactory accuracy. For this purpose, we measured dynamic viscoelasticity and shrinkage rates of various silicone compounds, including the standard impression material President and other eight affordable dental silicones. We scanned both original tooth surface and dental impression molds with a confocal laser microscope and conducted dental microwear texture analysis (DMTA) to quantitatively compare the scanned surfaces. The results showed relationships between the material properties of silicones and impression accuracy, indicating that the materials that cured slowly and began to shrink relatively early in the hardening process were less accurate. Some of these dental impression molds showed blurred surfaces, implying that molds were peeled off from the tooth surface at the microscopic level, as the shrinkage speed might exceed the curing speed. The following indices provided in the product information were found to be helpful in the search for substitutes: (1) medium viscosity, (2) short curing time after mixing (5–6 min), and (3) delayed change in shrinkage.

KEYWORDS

dental microwear texture (DMT), accuracy of silicone molds, material properties, dynamic viscoelasticity, shrinkage rate

Introduction

Microscopic use-wear marks on tooth surfaces (microwear) are important as a morphological indicator for estimating the diets of extinct and extant animals and have long been investigated using scanning electron microscopes or light microscopes (reviewed in Ungar, 2015). In the early stages of dental microwear research, optical microscopy and SEM were the main methods of observation. Even when the same area was analyzed, the observation settings and inter- or intra-observer errors were often problematic (Grine et al., 2002; Galbany et al., 2005; Purnell et al., 2006). So, dental microwear was difficult to evaluate quantitatively. However, the recent progress in the evaluation of microwear by optical profilometers has generated a new field of microwear research (Ungar et al., 2003; Scott et al., 2005; Schulz et al., 2010). Currently, an increasing number of studies reported characteristics of microscopic 3D topography, that is dental microwear texture (DMT), of various types of vertebrates (Krueger et al., 2008, 2017; Caporale and Ungar, 2016; DeSantis and Patterson, 2017; Aiba et al., 2019; Kubo and Fujita, 2021).

In the studies of 3D dental microwear texture analysis (DMTA) on anthropological and paleontological materials, impression molds and resin casts are analyzed rather than the original tooth surfaces. Two major reasons are considered. First, large specimens, such as teeth in the jawbone, cannot be placed properly on a microscope stage. Second, cultural and paleontological resources may be protected under laws and regulations, and thus casts and molds are the best alternatives for further analyses in laboratories. Therefore, the accuracy of dental silicones is crucial in DMTA. In previous studies, microwear researchers have utilized a few commercial products of silicone compounds such as President (Coltène/Whaledent AG, Switzerland) to avoid analytical errors caused by using different materials. However, such an effort of analytical quality control (i.e., relying on certain products) is a fundamental weakness in the field, considering that the production business might be terminated for miscellaneous reasons as in the case of President.

A few studies have tested the President silicone in the method of DMTA. Goodall et al. (2015) tested some substitutes for President and reported that silicone compounds with medium viscosity were more accurate than low viscosity (Speedex, MM913, and Accutrans) and high viscosity (Microset 101 RF and MM240TV). They detected a few differences of statistical significance between the original specimen and casts made with President. On the other hand, Mühlebacher et al. (2019) used President to examine differences between the original specimen and casts in higher magnification scans (150×) and reported many significant differences. Their contradictory conclusions indicate that different choices of molding and casting materials, the surface textures analyzed, and scanning magnifications may have affected the results.

In this study, we aim at identifying the physical properties of silicones to find appropriate silicones, which mold the tooth surface with satisfactory accuracy, by examining the reproducibility of DMT among various silicone compounds, including President and other affordable dental silicones. In addition to comparing the general properties of the tested silicones provided by product companies, we measured changes in viscosity and shrinkage over time, which are important properties in the process of making impression molds.

Materials

Tooth specimen

We used an isolated right mandibular second molar of a Pleistocene Japanese macaque (*Macaca fuscata*) (lower right of Figure 1). The analyzed specimen (NMNS PV 6166-7) was originally reported by Hasegawa et al. (1968) and is now stored in the Department of Geology and Paleontology at the National Museum of Nature and Science, Japan. Following the standard of primate dental microwear studies (Kay and Hiiemae, 1974), facet 9 of Phase II was observed for the analysis. Three arbitrary sites on facet 9 (f9-1, f9-2, and f9-3) were selected based on the accessibility to the focal points, which had characteristic landmarks (e.g., pits, scratches, and cracks) (Figure 1).

Silicone impression materials

We used the following nine dental silicone compounds including the standard silicone impression material (President Regular Body) in microwear research (Table 1): President Regular Body, Affinis regular body, Affinis light body (Coltène/Whaledent AG, Switzerland), Dr. Silicon regular (BSA Sakurai, Japan), Fusion II wash, EXAHIFLEX regular (GC, Japan), JM Silicone (Nissin Dental Products INC., Japan), IMPRINSIS regular (Tokuyama Dental Corporation, Japan), and SILDE FIT regular (Shofu INC., Japan). Dr. Silicon is a local product mainly in East Asia, whereas others are commercially available worldwide. However, President Regular Body was no longer available in Japan and was replaced by the subsequent product line called Affinis. Therefore, we imported it from the United Kingdom in 2017. Around that time, the “President” series became a new product line, “PRESIDENT The Original.” Since this material was not available (and still is not in Japan) at the time we initiated this study, we did not include it but used the older “President.”

All products are cartridge-type in dentistry quality, and their material properties such as shrinkage rate and cure time are provided by the companies. High-viscosity materials

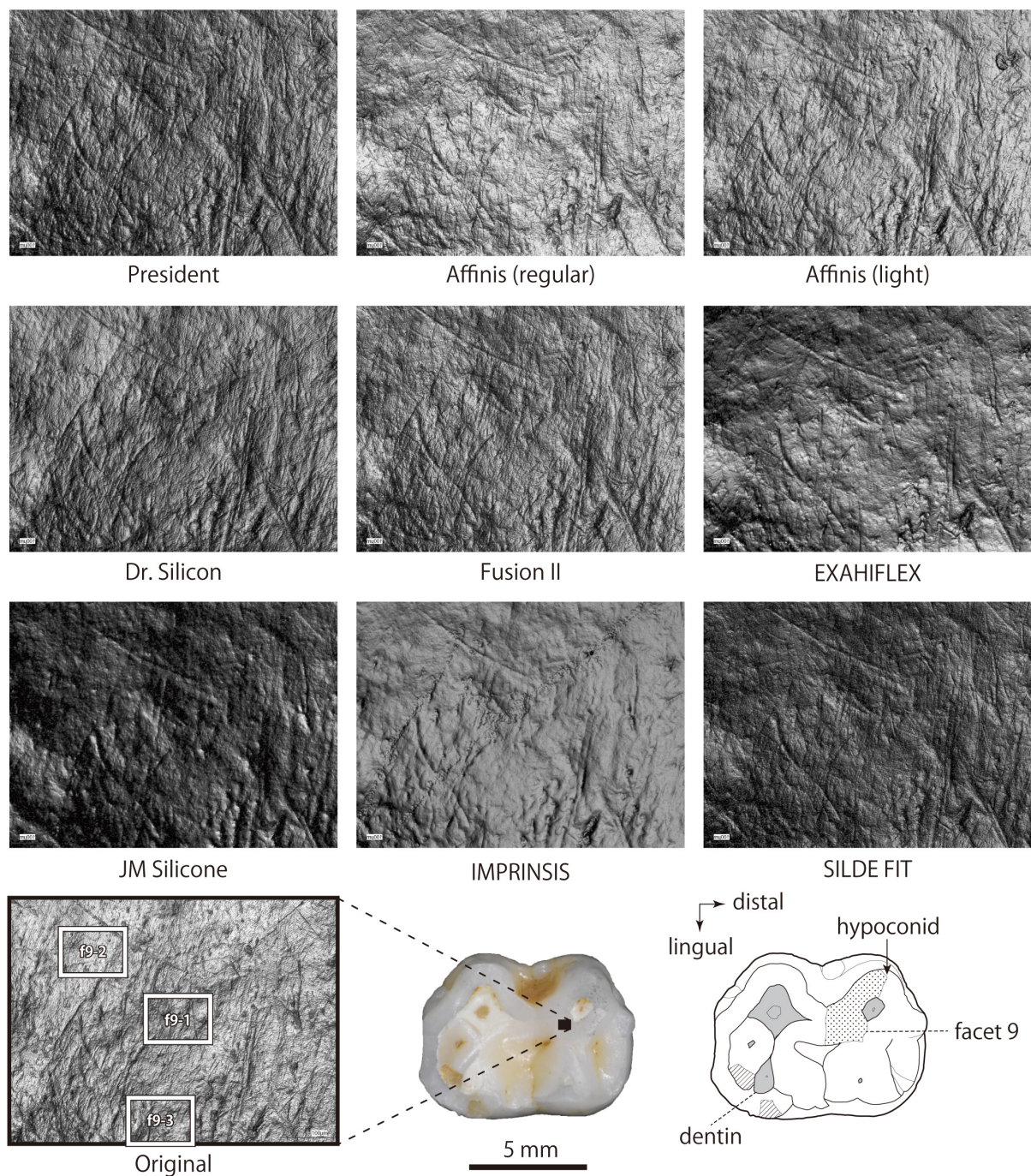


FIGURE 1

Comparison of dental impressions among nine impression materials. 2D images were obtained by a confocal laser microscope equipped with a 20× objective lens. The size of each image is 540 μm \times 725 μm . An occlusal view of the right lower second molar of the Japanese macaque used in this study is shown in the right lower photo and schema. The black rectangle on the tooth photo indicates the area where we obtained silicone impression molds. The white rectangles in the 20× tooth surface image obtained from the original tooth indicate the locations (f9-1, 2, and 3) where higher magnification images and 3D texture data were acquired. Wear state and location of facet 9 are shown in the schema.

were excluded in this study because [Goodall et al. \(2015\)](#) reported poor accuracy with high-viscosity materials. For mixing, we used a cartridge dispenser and mixing tips. We

made sure to apply the silicones well before their expiration date to avoid the impact of quality deterioration on the results.

TABLE 1 Silicone materials tested in this study and their physical properties shown in their product material safety data sheet (MSDS) and obtained through the measurements in this study.

Company	Product		Pot life (s) ^a	Cure time (s)		Hardness ^c	Final shrinkage (%)		Viscosity in product MSDS	Viscoelasticity at 500 s (log kPa/s) ^e
	Name	Type		Product MSDS ^a	This study ^b		Product MSDS ^a	This study ^d		
Coltène/Whaledent AG	President	Regular body	120*	180*	325	55	≤0.2*	0.65	Medium	47.4
	Affinis	Regular body	135*	120*	430	NA	0–1.5*	0.35	Medium	40.6
BSA sakurai		Light body	135*	120	415	NA	0–1.5*	0	Low	35.8
	Dr. Silicon	Regular	120	190	500	57	0.1	0.63	Medium	37.9
GC	Fusion II	Wash	120	180*	>600	NA	0.1	0.54	Low	7.4
	EXAHIFLEX	Regular	120	180	>600	NA	0.1	0.38	Medium	12.7
Nissin	JM Silicone	Regular	138	180	>600	NA	0.2	0.67	Low	19.9
Tokuyama	IMPLINSIS	Regular	120	180	>600	NA	0.1	0.74	Low	13.4
Shofu	SILDE FIT	Regular & denture	120	240	>600	40.5	0.2	0.82	Low	22.5

^aMeasured under JIS T6513:2005. ^bDefined as duration to reach constant viscosity in Figure 2A. ^cEnd hardness in Shore A. ^dSee Figure 2B. ^eSee Figure 2A. Asterisks (*) indicate that JIS is not mentioned in the product information. JIS T6513:2005 is a Japanese Industrial Standard based on the international standard ISO 4823:2000 Dentistry—Elastomeric impression materials and JIS and ISO have the same standard for pot life and final shrinkage (at the time this test was conducted).

Methods

Measurement of physical properties of silicones

To monitor the time-dependent elastic behaviors of the silicone materials after mixing, we measured the dynamic viscoelasticity and shrinkage rate of the silicone materials. Dynamic viscoelasticity was measured by a rheometer (HAAKE Mars III, Thermofisher Scientific) at the Tokyo Metropolitan Industrial Technology Research Institute. For every measurement, about 3 ml of silicone material was tested and monitored for 10 min. Nagrath et al. (2014) reported that humidity at curing affects impression accuracy. In this study, dynamic viscoelasticity measurements were performed under average room temperature and humidity conditions.

Time-sequential change of shrinkage was monitored under a room temperature of 25°C and ambient humidity by a Custron device (AcroEdge, Tokyo, Japan) for 10 min, starting 90 s after silicone materials were drawn on a discal pit (diameter = 10 mm and depth = 1 mm) in a glass plate.

Evaluation of impression accuracy

Preparation for microscope scanning

Each silicone was applied to the targeted area of the tooth surface and then pressed against its surface with a small ball of silicone putty (EXAFINE PUTTY TYPE, GC) to assure that details are imprinted on the silicone mold. This procedure was done as an imitation of the common one when taking dental impressions in clinical situations: (1) a dentist applies an impression material using a cartridge dispenser on the teeth of a patient, and (2) the patient bites a clinic tray filled with putty-type silicon. The mold was taken off from the specimen in 5–6.5 min. Before applying the next silicone material, we cleaned the specimen surface with 2% NaOCl-soaked cotton sheets followed by rubbing with acetone-soaked industrial cotton swabs. After taking off from the specimen, we trimmed the silicon mold to an appropriate size using a knife and attached it to a sliding glass using superglue for laser microscope observation.

Confocal laser microscope scanning

The original specimen and silicone molds were scanned with a confocal laser microscope (VK-9700, Keyence, Osaka, Japan) housed in the Department of Natural Environmental Studies, Graduate School of Frontier Sciences, the University of Tokyo. We used lower magnification lenses (20× and 50×) to identify the scan locations (i.e., f9-1, f9-2, and f9-3). Then we used a 100× long-distance lens (N.A. = 0.95) to scan the focal sites and generated 3D surface texture data by lateral (x , y) sampling with an interval of 0.138 μm and a vertical

resolution (z) of 0.001 μm . For each scan, 3D surface data of an area of 140 $\mu\text{m} \times 105 \mu\text{m}$ was obtained. Moreover, grayscale photographs of the tooth surfaces were procured for graphical comparison. We scanned both the original tooth surface and the silicone molds with dental impressions by the following procedures. We first placed the original specimen on the stage of the laser microscope and scanned the focal sites. To replicate the process, we took the specimen out of the stage and then replaced it on the stage to scan the same targeted area again. The relocation was done manually by finding common features (see [Supplementary Figures 1–3](#)), so this may have influenced the results to some extent. The scanning was repeated at least three times for each site. We scanned the silicone molds in the same way, but for every scanning, we made new impression molds to take the intrasample errors of impression molds into account. The original tooth was scanned repeatedly on different days to check intrapersonal variation in the choice of the targeted area. The accessibility to the focal scan points varied among the samples because it was difficult to find the same scan points in the molding samples with less precise surface replication. Therefore, the number of repeated scans differed among the molding materials ([Table 2](#)). Note that the scanning of molds was done within 1–2 weeks after molding, so there is little need to consider the effects of dimensional changes as reported in [Rodriguez and Bartlett \(2011\)](#) on the acquired data.

Qualitative evaluation of 2D image

For a simple evaluation of the accuracy and precision of the silicone impression molds, we first checked air bubble contamination and surface smoothing on 2D images obtained by the $100 \times$ lens.

Quantitative evaluation of 3D surface microtopography

We analyzed the 3D data obtained by the confocal laser microscope using Mountains Map Imaging Topography (version 9.0.9653, Digital Surf, Besançon, France). The 3D data were preprocessed to remove measurement noises and outliers by the following procedure described in [Aiba et al. \(2019\)](#), which included (1) mirroring (only for molds), (2) leveling (least square plane by subtraction), (3) application of S-filter (a robust Gaussian filter with a cutoff value of 0.8 μm , as defined in ISO 25178), (4) form removal function (polynomial of increasing power = 2) to remove large-scale curvature of enamel bands (F -operation in ISO 25178), (5) outlier removal with a slope $> 80^\circ$, (6) application of a threshold removing the upper and lower 0.1% of the data, and (7) filling of the non-measured points. After data cleaning, 30 parameters of ISO 25178-2 and two (fractal complexity $Asfc$ and length-scale anisotropy $epLsar$) from scale-sensitive fractal analysis (SSFA) were calculated ([Table 3](#)).

For non-parametric pair-wise tests between the parameter values from the original tooth surface and those from the

TABLE 2 The number of repeated scans for each sample and scan location.

Sample	Facet 9-1	Facet 9-2	Facet 9-3	Total
Original tooth	29	27	27	83
1. Affinis light body	12	12	12	36
2. Affinis regular body	3	3	3	9
3. Dr. Silicon regular type	4	4	4	12
4. Fusion II wash type	7	7	7	21
5. EXAHIFLEX regular type	3	3	3	9
6. JM Silicone regular type	3	3	3	9
7. President jet regular body	4	4	4	12
8. IMPRINSIS regular type	3	3	3	9
9. SILDE FIT regular & denture type	7	7	7	21
Total	75	73	73	221

silicone molds, Steel's multiple-comparison test was performed with the original surface scan as a control treatment. The number of significant differences was counted for each of the nine impression materials at each scan location (f9-1, f9-2, and f9-3). To visualize the variation of surface roughness among original tooth surfaces and the molds, we conducted principal component analysis (PCA) with Varimax rotation for the 32 DMT parameters (30 ISO and 2 SSFA parameters), which are presented as scatter plots along the principal component (PC) axes. All statistical analyses were conducted using JMP Pro 16.0.0 (SAS Institute Inc.).

Results

Dynamic viscoelasticity

[Figure 2A](#) shows the dynamic viscoelasticity (log kPa/s) of silicone materials measured by a rheometer. The analyzed silicone materials are categorized into two types based on viscoelastic behaviors during hardening.

Rapid completion type (i.e., steep changes in viscoelasticity)

Four products of silicone compounds are included, which are President, Affinis (regular), Dr. Silicon, and Affinis (light) in this order. Of these, Dr. Silicon, Affinis (regular), and Affinis (light) have low initial viscoelasticity. The hardening of President was completed 6 min after mixing of main and cure agents. The final viscosity of President is the highest of all. The hardening of Affinis (regular), Dr. Silicon, and Affinis (light) has completed about 7 min after mixing. Noticeably, these four products with rapid completion of hardening have high impression accuracy by qualitative evaluation of two-dimensional microscopic images ([Supplementary Figures 1–3](#)).

TABLE 3 Names and descriptions of dental microwear texture parameters used in this study.

Parameter	Description	Unit	Standard
<i>Sq</i>	Standard deviation of the height distribution	μm	ISO 25178-2
<i>Ssk</i>	Skewness of the height distribution	No unit	ISO 25178-2
<i>Sku</i>	Kurtosis of the height distribution	No unit	ISO 25178-2
<i>Sp</i>	Maximum peak height, height between the highest peak and the mean plane	μm	ISO 25178-2
<i>Sv</i>	Maximum pit height, depth between the mean plane and the deepest pit	μm	ISO 25178-2
<i>Sz</i>	Maximum height, sum of the maximum peak height and the maximum pit height ($Sp + Sv$)	μm	ISO 25178-2
<i>Sa</i>	Arithmetic mean height	μm	ISO 25178-2
<i>Smr</i>	Areal material ratio, ratio of the area of the material at a specified height c ($c = 1\mu\text{m}$ under the highest peak)	%	ISO 25178-2
<i>Smc</i>	Inverse areal material ratio, height at which a given areal material ratio ($p = 10\%$)	μm	ISO 25178-2
<i>Sdc</i> (Previously <i>Sxp</i>)	Peak extreme height, difference in height between the p and q material ratio ($p = 50\%$, $q = 97.5\%$)	μm	ISO 25178-2
<i>Sal</i>	Autocorrelation length ($s = 0.2$)	μm	ISO 25178-2
<i>Sdq</i>	Root mean square gradient	No unit	ISO 25178-2
<i>Sdr</i>	Developed interfacial area ratio	%	ISO 25178-2
<i>Vm</i>	Material volume at a given material ratio ($p = 10\%$)	$\mu\text{m}^3/\mu\text{m}^2$	ISO 25178-2
<i>Vv</i>	Void volume at a given material ratio ($p = 10\%$)	$\mu\text{m}^3/\mu\text{m}^2$	ISO 25178-2
<i>Vmc</i>	Material volume of the core at a given material ratio ($p = 10\%$, $q = 80\%$)	$\mu\text{m}^3/\mu\text{m}^2$	ISO 25178-2
<i>Vvc</i>	Void volume of the core ($p = 10\%$, $q = 80\%$)	$\mu\text{m}^3/\mu\text{m}^2$	ISO 25178-2
<i>Vvv</i>	Void volume of the dale at a given material ratio ($q = 80\%$)	$\mu\text{m}^3/\mu\text{m}^2$	ISO 25178-2
<i>Spd</i>	Density of peaks	$1/\mu\text{m}^2$	ISO 25178-2
<i>Spc</i>	Arithmetic mean peak curvature	$1/\mu\text{m}$	ISO 25178-2
<i>S10z</i>	Ten-point height	μm	ISO 25178-2
<i>S5p</i>	Five-point peak height	μm	ISO 25178-2
<i>S5v</i>	Five-point pit height	μm	ISO 25178-2
<i>Sda</i>	Closed dale area	μm^2	ISO 25178-2
<i>Sha</i>	Closed hill area	μm^2	ISO 25178-2
<i>Sdv</i>	Closed dale volume	μm^3	ISO 25178-2
<i>Shv</i>	Closed hill volume	μm^3	ISO 25178-2
<i>Sk</i>	Distance between the highest and lowest level of the core surface	μm	ISO 25178-2
<i>Spk</i>	Average height of the protruding peaks above the core surface	μm	ISO 25178-2
<i>Svk</i>	Average height of the protruding dales below the core surface	μm	ISO 25178-2
<i>epLsar</i>	Exact proportion of length scale anisotropy of relief	No unit	Scale sensitive fractal analysis (Ungar et al., 2003)
<i>Asfc</i>	Area-scale fractal complexity	No unit	Scale sensitive fractal analysis (Ungar et al., 2003)

Slow completion type (i.e., gradual changes in viscoelasticity)

The remaining five products are categorized in this type: SILDE FIT, JM Silicone, IMPRINSIS, EXAHIFLEX, and Fusion II had higher viscosity in this order. The hardening of these products did not complete perfectly even 10 min after mixing.

Shrinkage rate

Figure 2B shows the shrinkage rate changes of silicone materials during cure time. More complicated patterns are observed for shrinkage than for dynamic viscosity. However,

they are largely categorized into two types with a threshold of 0.2% in 200 seconds (s) as follows.

Delayed change in shrinkage

The shrinkage rates exceed 0.2% after 200 s, showing more gradual curves of shrinkage compared to the fast shrinkage type. This includes President (two-step slope with an initial shrinkage starting in 180 s after mixing and reaching 0.74% in 480 s), Affinis regular (one-step slope with an initial shrinkage starting in 200 s after mixing and reaching 0.35% in 330 s), and Dr. Silicon (one-step gradual slope, with an initial shrinkage starting in 280 s and reaching at 0.58% after 650 s). Final shrinkage rates fall between 0.35 and 0.65%. Irregularly, no shrinkage was

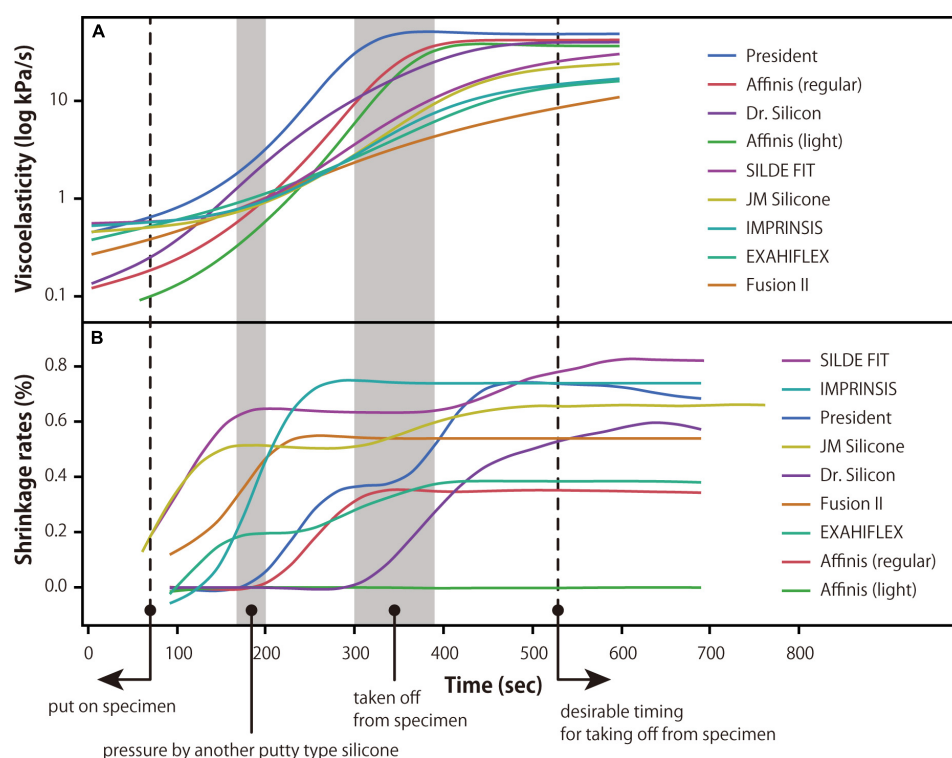


FIGURE 2

Dynamic viscoelastic properties and shrinkage rates of silicone materials. (A) Chronological change of viscoelasticity after mixing. (B) Chronological change of shrinkage rates after mixing. The dashed and gray areas in the figure show the timing of silicon application, pressing, and removal.

observed for Affinis light, which could be an unknown analytical error since its final shrinkage rate provided by the company was comparable to that of Affinis regular (Table 1). Alternatively, this result on Affinis light could be batch-dependent, but due to the budget and time available for this study, we were not able to repeat the measurements.

Fast change in shrinkage

The shrinkage rates exceed 0.2% within 200 s, showing increased shrinkage rates immediately after mixing. This group includes JM Silicone (1st slope, reaching a shrinkage rate of 0.5% in 200 s, followed by the 2nd gradual slope), SILDE FIT (1st slope, reaching 0.6% in 200 s, followed by the 2nd gradual slope), Fusion II (one-step steep slope, reaching 0.55% in 250 s), IMPRINSIS (one-step steep slope, reaching 0.74% in 280 s), and EXAHIFLEX (1st slope, staying at 0.2% until ~240 s and reaching at 0.38% after 420 s, followed by the 2nd gradual slope between 300 and 400 s). Final shrinkage rates range from 0.38 to 0.82%.

Impression accuracy judged by 2D images

Though it was confirmed that there were differences in impression accuracy of silicone materials even in the

lower magnification images (Figure 1), it was obvious in the higher magnification images that several impression molds (EXAHIFLEX, JM Silicone, and IMPRINSIS) had poor reproducibility of original DMT, that is, their microscopic images showed blurred surfaces and contamination of bubbles (Supplementary Figures 1–3). In all fields of f9-1, f9-2, and f9-3, blurring was observed in EXAHIFLEX, JM Silicone, and IMPRINSIS. Molds made by SILDEFIT roughly reproduced overall microwear features but had many traces of small bubbles contamination on the surfaces in all target views. Among other impression materials with relatively good accuracy, President and Dr. Silicon had the best accuracy with fine microwear features (e.g., very fine scratches).

Impression accuracy evaluated by dental microwear texture parameters

The difference between the original surface and molds was further evaluated by statistical comparisons of 32 DMT parameters. The raw values of the DMT parameters of all scans ($N = 221$) used in this study are listed in Supplementary Table 1. Summary statistics (sample size, mean, and S.D.) of the DMT parameters for scan targets (i.e., the original tooth and nine impression materials) are provided in Supplementary Table 2. Results of Steel's non-parametric test

comparing the original tooth surface and dental molds are presented in [Supplementary Table 3](#).

Figure 3 shows the number of significant differences in Steel's non-parametric test presented for each silicone material and scan location. Thus, lower values on the vertical axis are better, capturing morphological details of the original surface. President Jet Regular body and Dr. Silicon regular type are better (= the smallest number of significant differences) than other products. The accuracy of Affinis light and SILDE FIT follows President and Dr. Silicon, and the difference is small. To present the precision of dental molds, the deviation of the parameter value of the mold from the average parameter value of the original tooth surface was obtained for each parameter ([Supplementary Figure 4](#)). In [Supplementary Figure 4](#), the ranges of deviations (mold—original tooth surface) are wider for some impression materials (IMPRINSIS and JM Silicone), whereas others show equivalent ranges. Affinis light shows narrower ranges since it has a larger number of molding and scanning. In most cases, the ranges include zero, suggesting that there was no outstanding impression material and that all show decent levels of precision. However, as seen in the 100 × 2D images of [Supplementary Figures 1–3](#), SILDE FIT molds contain many bubbles. And the Affinis light molds are slightly blurred. Therefore, we evaluated them not as accurate as President and Dr. Silicon. IMPRINSIS regular type is the worst among all ([Figure 3](#)), which corresponds to visual observations of 2D images ([Supplementary Figures 1–3](#)).

PCA of the 32 DMT parameters clarified that the first and the second principal components explained 52.6 and 19.1% of the observed variation. The factor loadings of PC1 ([Table 4](#)) showed larger positive values of height and volume parameters

of ISO 25178-2, indicating that PC1 could be interpreted as overall surface roughness, in other words, the size of microwear features. On the other hand, PC2 had larger positive values for *Sdq*, *Sdr*, *Asfc*, and *Spd*, which were all related to the fineness of the surface. In addition, the parameters related to surface segmentation (*Sda*, *Sha*, *Svd*, and *Shv*) showed large negative values. Therefore, the larger PC2 values indicated that the surface was characterized by finer features and segmented into smaller hills and dales. The scatter plots of PCs are shown in [Figure 4](#). We found a non-negligible variation in repeated scans of the original tooth surface, which indicated uncontrolled errors associated with placing the tooth on the microscope stage, tilting the tooth, and searching and scanning the focal sites: all of them cannot be perfectly repeated and therefore this leads to data variation. Most of the scan data from the dental molds lay within the 90% confidence ellipses of the original tooth scans, though some departed even from the ellipses. Notably, the data of molds made by IMPRINSIS regular type, the material with the least replicability ([Supplementary Figures 1–3](#)), are placed beyond the ellipses for all three scan locations.

Discussion

Dynamic viscoelasticity as a good indicator to find suitable silicones for dental microwear texture analysis

Based on 2D observations and statistical results of the DMT parameters, we clearly showed dynamic viscoelasticity

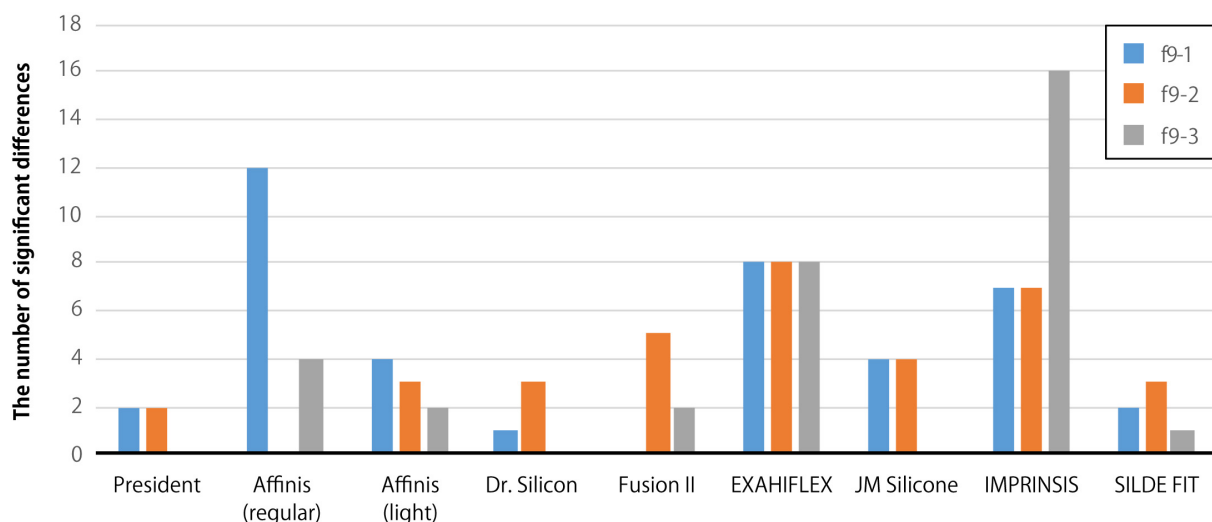


FIGURE 3
The number of significant differences in 32 DMT parameters between the original tooth surface and silicone molds. Pair-wise tests were conducted for each scan location on facet 9 (f9-1, f9-2, and f9-3).

TABLE 4 The factor loadings obtained from a PCA using 32 DMT parameters.

	PC1	PC2
Variance explained (%)	52.6	19.1
<i>Sq</i>	0.9860	−0.0872
<i>Ssk</i>	−0.3811	0.4047
<i>Sku</i>	0.1615	−0.2427
<i>Sp</i>	0.8890	0.1019
<i>Sv</i>	0.9415	−0.1742
<i>Sz</i>	0.9840	−0.0776
<i>Sa</i>	0.9813	−0.0780
<i>Smr</i>	−0.6484	−0.1563
<i>Smc</i>	0.9729	−0.0390
<i>Sdc</i>	0.9684	−0.1372
<i>Sal</i>	0.5220	−0.3105
<i>Sdq</i>	0.5495	0.7938
<i>Sdr</i>	0.4881	0.7770
<i>Vm</i>	0.8096	0.0160
<i>Vv</i>	0.9764	−0.0371
<i>Vmc</i>	0.9735	−0.0938
<i>Vvc</i>	0.9713	−0.0203
<i>Vvv</i>	0.9336	−0.1865
<i>Spd</i>	0.0902	0.8415
<i>Spc</i>	0.5694	0.5266
<i>S10z</i>	0.9674	0.1615
<i>S5p</i>	0.8451	0.3353
<i>S5v</i>	0.9435	0.0370
<i>Sda</i>	0.1007	−0.7624
<i>Sha</i>	0.1177	−0.7742
<i>Sdv</i>	0.0167	−0.5166
<i>Shv</i>	0.1496	−0.6440
<i>Sk</i>	0.7664	0.4959
<i>Spk</i>	0.5859	0.4824
<i>Svk</i>	0.6901	0.4659
<i>epLsar</i>	−0.2506	0.3188
<i>Asfc</i>	0.4542	0.7987

is the best indicator to find appropriate dental impression materials, which can mold accurately the tooth surface as President. In our study, dynamic viscoelasticity categorized the analyzed silicones into two types based on the hardening speed. Despite a wide range of initial values, the rapid completion type commonly shows steep viscoelastic curves. The silicones of this type include President, Affinis regular, Affinis light, and Dr. Silicone. They show better reproducibility of microwear features with less blurring and less air bubble contamination than the slow completion type (Figures 1, 3, 4). Especially, Dr. Silicone presents better reproducibility of fine microwear features than others. In contrast, the slow completion type, showing gradual viscoelastic curves, did not complete hardening in 600 s from the start. Nevertheless, according to the physical properties of

the silicones provided by the product companies (Table 1), the range of cure time of the slow completion type does not differ from that of the rapid completion type. This finding indicates that the most conclusive and quantitative way to find suitable silicones for DMTA is to measure dynamic viscoelasticity by a rheometer and identify the product with similar curves to those of the rapid completion type.

Criteria for silicones with the high impression accuracy

Although dynamic viscoelasticity is the best indicator, we suggest the following criteria for silicones as reliable as President.

Rapid completion of curing in 5–6 min after mixing

The silicones with rapid completion showed better impression accuracy. It may be related to the timing of removal of the impression molds from the specimen, which was set as 5–6.5 min after mixing. If the pressure with putty-type silicone had been continued until the completion of hardening, the slow completion type may have presented a better impression than the resultant impression of this study. Nevertheless, we suggest that the 5–6 min completion of curing is a reasonable time for DMTA research, considering the procedures for making many impression molds of tooth specimens in a limited working time (e.g., visiting museums). It must be noted that the data of cure time provided by companies were not concordant with dynamic viscoelasticity measured in this study; the provided cure time data of the slow completion type do not differ from those of the rapid completion type (Table 1). This is partly because the cure time in product material safety data sheet (MSDS) is idealized for the application of *in vivo* human dentition in the oral cavity, whose temperature is much higher than the ambient temperature condition of 25°C for measuring the dynamic viscoelasticity in this study. Also, there should be variability due to production batches. The divergence of acquired viscoelasticity and shrinkage data in the present study from product MSDS should be further investigated in future collaboration with professionals of dental materials and product manufacturers.

Delayed change in shrinkage, not exceeding 0.2% in 200 s after mixing

The analyzed silicones show more complicated patterns for the time-sequential shrinkage rate than for dynamic viscoelasticity. In our study, the silicones that do not exceed the 0.2% shrinkage in 200 s after mixing showed better impression accuracy. These products were also categorized as the rapid

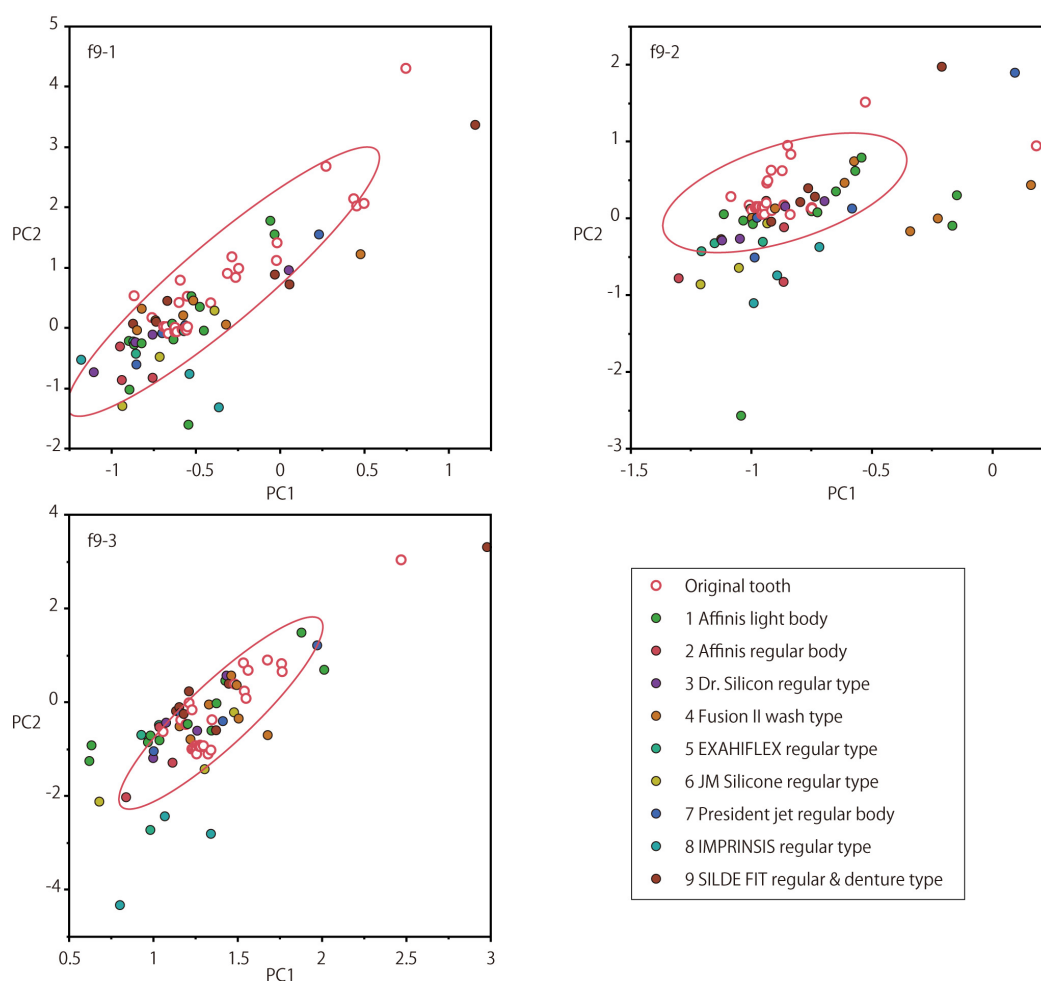


FIGURE 4

Scatter plots of the PC scores obtained from 32 DMT parameters, presented respectively for each scan location on facet 9 (f9-1, f9-2, and f9-3). Variation of repeated scanning of the original tooth surface was presented by the ellipses, within which 90% of the data lie. Symbols for the dental impression materials are shown in right lower corner.

completion type, which is also associated with better impression accuracy. In contrast, poor impression accuracy was observed for the products that began shrinking immediately after mixing.

Delayed change in shrinkage with better impression accuracy is related to the timing of applying the silicone to the specimen (approximately 70 s after mixing) and pressing it to the specimen with another putty-type silicone (approximately 180–200 s after mixing) (Figure 2B). The delayed start of shrinkage seemed to provide enough time for silicone compounds to extend over the microscopic details. On the other hand, the materials that cured slowly and began to shrink relatively early in the hardening process were less accurate and their molds showed blurred surfaces (JM Silicone and IMPRINSIS). This implies that the molds were peeled off from the tooth surface at the microscopic level before capturing details due to the shrinkage, as the shrinkage speed might exceed the curing speed.

Medium viscosity

Among the four products categorized as the type with rapid completion of curing through the measurements of dynamic viscoelasticity, President and Affinis (regular) are medium viscosity, whereas Affinis (light) is low viscosity in the ISO 4823 classification. Although the viscosity classification is unknown for Dr. Silicone, based on handling these materials, the product is assumed to be medium viscosity. These medium viscosity products show more accurate impressions of microwear features, which is concordant with the previous finding (Goodall et al., 2015). Affinis light body was overall good in parameter values, but from our experience, this material should contain a larger amount of oil than medium viscosity materials and the oil seems to be associated with the slightly blurred surfaces of the molds.

Air bubble contaminations

Adhesion of air bubbles was remarkable in the materials not only with relatively high viscosity immediately after the mixing but also with slow completion of curing (EXAHIFLEX, JM Silicone, IMPRINSIS, and SILDE FIT). Exceptionally, very few bubbles were observed in President molds despite the high initial viscosity. There may be some material characteristics or components that make it difficult for bubbles to be mixed. Anyway, the factors that contribute to bubble contamination and deaeration would need to be considered with other physical properties of materials and molding procedures.

As pointed above, the materials in combination of the rapid completion type and delayed change in shrinkage result in higher impression accuracy than other materials. This was supported not only by qualitative evaluation based on comparisons of 2D images but also by quantitative evaluation based on statistical analysis using 32 DMT parameters.

Conclusion

For seeking dental impression materials suitable for DMTA research, this study quantitatively evaluates the physical properties of silicone impression materials (changes of viscoelasticity and shrinkage over time) and the accuracy of dental impression molds by DMTA. Our results, show that dynamic viscoelasticity is strongly related to the accuracy of silicone impression materials. On the timing of the impression molding procedure, it is important for the impression accuracy that the curing of silicone occurs immediately after mixing and completes by the time the mold is removed from the specimen, while the shrinkage starts after application to the specimen. In addition, it is suggested that the physical property information supplied by the product companies is not practical in searching for impression materials suitable for DMTA, even if it is measured according to ISO standards. Further collecting and examining the data on physical properties of other dental impression materials, which are globally or locally purchasable, is to be of use for standardizing the methodology of DMTA.

Data availability statement

The original contributions presented in this study are included in the article/**Supplementary material**, further inquiries can be directed to the corresponding authors. In addition, we uploaded original raw scan data saved in “.vk3” format, all the analytical files in “.mnt” format, and processed surface 3D data in “.sur” format to the online repository Zenodo. DOI of the uploaded files is <https://doi.org/10.5281/zenodo.7052345>.

Ethics statement

Ethical review and approval were not required for this study as this study used a fossil museum specimen and the investigation of the fossil was officially approved by the curator.

Author contributions

YK conceived the experiments. RS and YK conducted the experiments. MOK and RS analyzed the results. All authors reviewed the manuscript.

Funding

This work was funded by JSPS grants No. 18K12567 (to RS), Nos. 18K13650 and 21K15176 (to YK), and Nos. 16K18615 and 22H00027 (to MOK).

Acknowledgments

We thank Tai Kubo (The University Museum, The University of Tokyo), Eisuke Yamada (Yamanashi Prefectural Museum), and Konoka Aiba (Japan Wildlife Research Center) for supporting our study.

Conflict of interest

The authors declare that the research was conducted in the absence of any commercial or financial relationships that could be construed as a potential conflict of interest.

Publisher's note

All claims expressed in this article are solely those of the authors and do not necessarily represent those of their affiliated organizations, or those of the publisher, the editors and the reviewers. Any product that may be evaluated in this article, or claim that may be made by its manufacturer, is not guaranteed or endorsed by the publisher.

Supplementary material

The Supplementary Material for this article can be found online at: <https://www.frontiersin.org/articles/10.3389/fevo.2022.975283/full#supplementary-material>

References

- Aiba, K., Miura, S., and Kubo, M. O. (2019). Dental microwear texture analysis in two ruminants, Japanese serow (*Capricornis crispus*) and sika deer (*Cervus nippon*), from Central Japan. *Mamm. Study* 44, 183–192. doi: 10.3106/ms2018-0081
- Caporale, S. S., and Ungar, P. S. (2016). Rodent incisor microwear as a proxy for ecological reconstruction. *Palaeogeogr. Palaeoclimatol. Palaeoecol.* 446, 225–233. doi: 10.1016/j.palaeo.2016.01.013
- DeSantis, L. R. G., and Patterson, B. D. (2017). Dietary behaviour of man-eating lions as revealed by dental microwear textures. *Sci. Rep.* 7:904. doi: 10.1038/s41598-017-00948-5
- Galbany, J., Martínez, L. M., López-Amor, H. M., Espurz, V., Horaldo, O., Romero, A., et al. (2005). Error rates in buccal-dental microwear quantification using scanning electron microscopy. *Scanning* 27, 23–29. doi: 10.1002/sca.4950270105
- Goodall, R., Darras, L., and Purnell, M. (2015). Accuracy and precision of silicon based impression media for quantitative areal texture analysis. *Sci. Rep.* 5:10800. doi: 10.1038/srep10800
- Grine, F. E., Ungar, P. S., and Teaford, M. F. (2002). Error rates in dental microwear quantification using scanning electron microscopy. *Scanning* 24, 144–153. doi: 10.1002/sca.4950240307
- Hasegawa, Y., Yamauti, H., and Okafuji, G. (1968). A fossil assemblage of *Macaca* and *Homo* from Ojikado-cave of Hiraodai karst plateau, northern Kyushu, Japan. *Trans. Proc. Paleontol. Soc. Japan New Ser.* 69, 218–229.
- Kay, R. F., and Hiiemae, K. M. (1974). Jaw movement and tooth use in recent and fossil primates. *Am. J. Phys. Anthropol.* 40, 227–256. doi: 10.1002/ajpa.1330400210
- Krueger, K. L., Scott, J. R., Kay, R. F., and Ungar, P. S. (2008). Technical note: dental microwear textures of 'Phase I' and 'Phase II' facets. *Am. J. Phys. Anthropol.* 137, 485–490. doi: 10.1002/ajpa.20928
- Krueger, K. L., Ungar, P. S., Guatelli-Steinberg, D., Hublin, J., Pérez-Pérez, A., Trinkaus, E., et al. (2017). Anterior dental microwear textures show habitat-driven variability in Neandertal behavior. *J. Hum. Evol.* 105, 13–23. doi: 10.1016/j.jhevol.2017.01.004
- Kubo, M. O., and Fujita, M. (2021). Diets of Pleistocene insular dwarf deer revealed by dental microwear texture analysis. *Palaeogeogr. Palaeoclimatol. Palaeoecol.* 562:110098. doi: 10.1016/j.palaeo.2020.110098
- Mihlbachler, M. C., Foy, M., and Beatty, B. L. (2019). Surface replication, fidelity and data loss in traditional dental microwear and dental microwear texture analysis. *Sci. Rep.* 9:1595. doi: 10.1038/s41598-018-37682-5
- Nagrath, R., Lahori, M., and Agrawal, M. (2014). A comparative evaluation of dimensional accuracy and surface detail reproduction of four hydrophilic Vinyl polysiloxane impression materials tested under dry, moist, and wet conditions-an in vitro study. *J. Indian Prosthodont. Soc.* 14, 59–66. doi: 10.1007/s13191-014-0365-z
- Purnell, M. A., Hart, P. J. B., Baines, D. C., and Bell, M. A. (2006). Quantitative analysis of dental microwear in threespine stickleback: a new approach to analysis of trophic ecology in aquatic vertebrates. *J. Ani. Ecol.* 75, 967–977. doi: 10.1111/j.1365-2656.2006.01116.x
- Rodriguez, J. M., and Bartlett, D. W. (2011). The dimensional stability of impression materials and its effect on in vitro tooth wear studies. *Dental Mater.* 27, 253–258. doi: 10.1016/j.dental.2010.10.010
- Schulz, E., Calandra, I., and Kaiser, T. M. (2010). Applying tribology to teeth of hoofed mammals. *Scanning* 32, 162–182. doi: 10.1002/sca.20181
- Scott, R. S., Ungar, P. S., Bergstrom, T. S., Brown, C. A., Grine, F. E., Teaford, M. F., et al. (2005). Dental microwear texture analysis shows within-species diet variability in fossil hominins. *Nature* 436, 693–695. doi: 10.1038/nature03822
- Ungar, P. S. (2015). Mammalian dental function and wear: a review. *Biosurf. Biotribol.* 1, 25–41. doi: 10.1016/j.bsbt.2014.12.001
- Ungar, P. S., Brown, C. A., Bergstrom, T. S., and Walker, A. (2003). Quantification of dental microwear by tandem scanning confocal microscopy and scale-sensitive fractal analyses. *Scanning* 25, 185–193. doi: 10.1002/sca.4950250405



OPEN ACCESS

EDITED BY

Larisa R. G. DeSantis,
Vanderbilt University, United States

REVIEWED BY

Frank Williams,
Georgia State University, United States
Brian Lee Beatty,
New York Institute of Technology,
United States

*CORRESPONDENCE

Daniela E. Winkler
daniela.eileen.winkler@k.u-tokyo.ac.jp

SPECIALTY SECTION

This article was submitted to
Paleoecology,
a section of the journal
Frontiers in Ecology and Evolution

RECEIVED 31 May 2022

ACCEPTED 20 September 2022

PUBLISHED 27 October 2022

CITATION

Winkler DE, Iijima M, Blob RW, Kubo T
and Kubo MO (2022) Controlled
feeding experiments with juvenile
alligators reveal microscopic dental
wear texture patterns associated with
hard-object feeding.
Front. Ecol. Evol. 10:957725.
doi: 10.3389/fevo.2022.957725

COPYRIGHT

© 2022 Winkler, Iijima, Blob, Kubo and
Kubo. This is an open-access article
distributed under the terms of the
[Creative Commons Attribution License](#)
(CC BY). The use, distribution or
reproduction in other forums is
permitted, provided the original
author(s) and the copyright owner(s)
are credited and that the original
publication in this journal is cited, in
accordance with accepted academic
practice. No use, distribution or
reproduction is permitted which does
not comply with these terms.

Controlled feeding experiments with juvenile alligators reveal microscopic dental wear texture patterns associated with hard-object feeding

Daniela E. Winkler ^{1*}, Masaya Iijima ^{2,3,4},
Richard W. Blob ², Tai Kubo ^{1,5,6} and Mugino O. Kubo ¹

¹Department of Natural Environmental Studies, Graduate School of Frontier Sciences, The University of Tokyo, Kashiwa, Japan, ²Department of Biological Sciences, Clemson University, Clemson, SC, United States, ³Nagoya University Museum, Nagoya, Japan, ⁴Department of Comparative Biomedical Sciences, The Royal Veterinary College, North Mymms, Hertfordshire, United Kingdom, ⁵The University Museum, The University of Tokyo, Tokyo, Japan, ⁶Marine Macroevolution Unit, Okinawa Institute of Science and Technology Graduate University, Onna-son, Japan

Dental wear analyses are classically applied to mammals because they have evolved heterodont dentitions for sophisticated mastication. Recently, several studies have shown a correlation between pre-assigned and analytically inferred diet preferences in extant reptiles through dental microwear texture analysis (DMTA), a method using quantitative assessment of microscopic wear marks to reconstruct the diet material properties. The first tentative applications of DMTA to extinct reptiles have followed. However, for large and small mammals, microwear analyses have undergone a long time of ground-truthing through direct feeding observations, stomach content analyses, and feeding experiments. Such data are currently lacking for reptiles, but are necessary to further extend DMTA, especially to Archosauria, as the application to dinosaurs could be of great interest to the scientific community. We herein present data from a pilot feeding experiment with five juvenile American alligators (*Alligator mississippiensis*). Each individual received a diet of assumed different hardness for ~4 months: crocodylian pellets (control), sardines, quails, rats, or crawfish. All individuals initially received the same pellet diet, and we found them to show similar dental microwear texture patterns before they were switched to their designated experimental diet. From the first feeding bout on, dental microwear textures differed across the diets. The crawfish-feeder showed consistently higher surface complexity, followed by the rat-feeder. Quail- and fish-feeding resulted in similar wear signatures, with low complexity. Fast tooth replacement and selective tooth use likely affected microwear formation, but we were able to detect a general hard (crawfish and rat) versus soft (quail and fish) DMTA signature. Such patterns can support the identification of hard-object feeding in the fossil record.

KEYWORDS

microwear, DMTA, diet reconstruction, crocodylia, dental wear, hard-object feeding

Introduction

The study of dental microwear texture (DMT) using standardized textural parameters for quantification of diet-related wear patterns has gained considerable interest in the last decade, particularly for application to non-mammalian species. With pioneering studies on fish (Purnell et al., 2012; Purnell and Darras, 2015), lepidosaurs and archosaurs (Bestwick et al., 2019; Winkler et al., 2019a), pterosaurs (Bestwick et al., 2020), phytosaurs (Bestwick et al., 2021a), and sauropods (Sakaki et al., 2022), it has been shown that diet-related DMT features are formed (and preserved) in species without heterodont, occluding teeth, and without sophisticated mastication. Many of these non-mammalian species exhibit frequent tooth replacement, but tooth-to-food contact still seems to be sufficient to result in significant DMT differences between diet preference groups, information that can be used for dietary discrimination in extant and extinct taxa. However, reptiles were also found to display non-diet-induced DMT patterns that may be related to tooth position, bite force, and behavioral differences in tooth use (Bestwick et al., 2021b), thus complicating the assessment of diet-related DMTs.

Because diet proxies based on tooth-wear patterns can enable inferences of niche partitioning among sympatric species (Fiorillo, 1998; Mallon and Anderson, 2014), they can enhance reconstructions of paleoecosystems. Several studies have linked microscopic (2D microwear) and macroscopic tooth wear to paleodiet in extinct archosauriforms (Schubert and Ungar, 2005; Williams et al., 2009; Varriale, 2016; Virag and Osi, 2017) and squamates (Holwerda et al., 2013; Gere et al., 2021). Therefore, comparisons of DMT observed in extant reptiles could also be helpful for the reconstruction of the paleoecology of taxa such as dinosaurs, with extant toothed archosaurs (crocodilians) likely being the best candidates to study as a model for theropod dental wear. Dental microwear texture analysis (DMTA) has undergone a long time of ground-truthing for large (Merceron et al., 2016; Ackermans et al., 2020; Schulz-Kornas et al., 2020) and small mammals (Schulz et al., 2013; Winkler et al., 2019b, 2020a,b, 2021) through feeding experiments. However, so far, no direct observations regarding diet and tooth wear exist for extant archosaurs that could validate our interpretation of diet-related wear marks. Instead, DMTA for reptiles still relies on dietary preference data compiled from the literature (from observations and stomach content analysis).

To observe a direct effect of ingested diet on dental microwear texture, we performed controlled feeding experiments with five juvenile American alligators (*Alligator mississippiensis*). Extant crocodilians are opportunistic carnivores, with most species having a generalistic diet of animal prey (Pooley, 1989). Still, dietary differences exist across crocodilian taxa. For example, the Indian gharial, the most slender-snouted of extant crocodilians, is primarily piscivorous (Thorbjarnarson, 1990; Stevenson and Whitaker,

2010; Grigg and Kirshner, 2015), whereas broader snouted crocodilians include harder prey in their diet, such as crustaceans (Taylor, 1979; Platt et al., 2006, 2013) and turtles (Taylor, 1986; Barr, 1997). Moreover, most crocodilians undergo distinct ontogenetic dietary changes. Juveniles often feed on invertebrates and small vertebrates (fish and amphibians), but switch to larger vertebrates (mammals and fish) as adults (Cott, 1961; Taylor, 1979; Delany and Abercrombie, 1986; Hutton, 1987; Wolfe et al., 1987; Webb and Manolis, 1989; Platt et al., 2006, 2013; Wallace and Leslie, 2008). If a specialized diet would result in distinct DMTA signatures, transitions in diet and the main components of diet might be detectable in crocodilians, such that microwear data could help to resolve ontogenetic dietary changes in fossil archosaurs.

For our comparisons, we selected four diet items assumed to be of different hardness, representing hypothetical, specialized feeding types, and compared DMTA patterns from shed teeth of alligators on each of these diets to those from a control alligator kept on the same pelleted diet received before our experiment. Pellets were provided as a control food item because we expected that their consumption would not leave distinct dental wear, as they are not seized or processed with the teeth, but instead only swallowed. Our four experimental foods included sardines (representing a piscivorous diet), quails (representing a “soft” vertebrate diet), rats (representing a “hard” vertebrate diet), and crawfish (representing a “hard” invertebrate diet). Consistent comparative data of mechanical and material properties of our selected diet items are difficult to compile, but several studies support our intuitive assessment of these diets being different in their “hardness” or differently mechanically challenging to process: Young’s modulus and bending strength of bones have been found to be lower in teleost fish when compared to rats and other mammals (Erickson and Catanese, 2002; Horton and Summers, 2009). Birds have overall thinner, pneumatized bones (Swartz et al., 1992; Cubo and Casinos, 2000) than mammals, while crawfish, as crustaceans, possess a resistant exoskeleton (Raabe et al., 2005) that needs to be fractured during prey processing.

While the exact interrelations between mechanical properties and DMT are unclear (Winkler et al., 2022), previous studies have shown that extant archosaurs with a presumed piscivorous diet had the lowest enamel surface roughness (Bestwick et al., 2019), whereas extant archosaurs and lepidosaurs assumed to feed on “hard” invertebrates (mollusks and crustaceans) exhibited higher surface roughness and surface complexity (Bestwick et al., 2019; Winkler et al., 2019a). Therefore, sardines and crawfish represent the two extreme endpoints of our experimental diet spectrum, with sardine-feeding expected to result in overall lower wear (low roughness and complexity), and crawfish expected to have the strongest effect on dental enamel wear (large roughness and complexity). Quails and rats were chosen as intermediate hardness samples in our dietary continuum because bird skeletons are generally

lightweight and delicate, in contrast to the skeletons of terrestrial mammals; therefore, it could be assumed that quails represent an overall softer diet than rats. There is some uncertainty in these assessments. For example, in birds and mammals of similar body mass, the skeleton contributes equally to total body mass (Prange et al., 1979); however, long bones of birds are often pneumatized, with significantly thinner walls than marrow-filled bones found in mammals (Cubo and Casinos, 2000). The surprisingly large skeletal mass of birds results from higher bone density compared to terrestrial rodents (Dumont, 2010), which gives bird skeletons a higher strength-to-weight and stiffness-to-weight ratio. Thus, our use of both quails and rats as samples should help to determine whether these prey items actually pose different mechanical challenges to alligators, or if these two tetrapod vertebrate diets might result in similar DMT patterns.

Materials and methods

Five juvenile American alligators (*Alligator mississippiensis*) were housed individually at Clemson University, South Carolina (USA), where they are part of a larger number of alligators kept for locomotion studies. Alligator husbandry and further experimental procedures were approved by the Clemson University IACUC (protocol 2019-037). The sex of the animals was unknown. In July 2020, the average initial body mass of the animals was 5,076.46 g (SD \pm 1,368.98 g), while the average snout-vent length was 612.00 mm (SD \pm 53.40 mm) (Table 1). For two individuals, weight and length were determined again in December 2021, resulting in an average weight of 6,484.30 g (SD \pm 1,252.00 g) and snout-vent length of 632.00 mm (SD \pm 56.57 mm). Further details about the individuals and their husbandry can be found in a study by (Iijima et al., 2021).

Before the start of the feeding experiments, all alligators were fed a diet of commercial pellets for crocodylians (Mazuri crocodylian diet, small) two times a week. The feeding experiment took place in two phases, from February/March until May/June 2021 (~4 months per diet) and from September to November/December 2021 (~2 months per diet). At the beginning of the feeding experiment, four out of five juvenile alligators were switched to their designated experimental diet, either receiving whole sardines (wild-caught, frozen sardines from Portugal, ordered through whole.com; alligator individual identifier #2), whole quails (frozen extra-large *Coturnix*, ordered through rodentpro.com; #4), whole crawfish (live red swamp crawfish *Procambarus clarkia*, ordered through lacrawfish.com, and frozen red swamp crawfish ordered through acadiacrawfish.com; #3), or whole rats (frozen medium feeder rats, ordered through rodentpro.com; #1). One individual was kept on the pelleted diet as a control during phase 1 (#6). The experimental feeds were first thawed, and then presented as whole items two times a week. During phase 1, quails and rats

were similar in body weight and size, while sardines were longer and more lightweight (Supplementary Table S1). Crawfish were much smaller than the vertebrate diets, and hence ~7 crawfish were given for each feeding bout (Supplementary Table S1). Phase 2 was a repetition of sardine- and crawfish-feeding, with alligators that had received different foodstuffs during the first period and were switched back to pellets from June to late September 2021. The individual receiving quails during phase 1 (#4) received crawfish and the one kept on the pellets (#6) received sardines. During phase 2, sardines were smaller and more lightweight than during phase 1, thus ~1.8 sardines were fed for each feeding bout. Details of the feeding schedule and observations of feeding behavior are given in Supplementary Table S1. After each feeding bout, shed teeth were collected from each individual tank and the source individual and date of the collection were recorded. Feeding events were captured on video, from which the number of bites and behavioral notes were derived.

Dental microwear texture sampling strategy

Collected teeth were shipped to the University of Tokyo with export permission from the United States Fish and Wildlife Service (CITES permit # 21US05232E/9). The original enamel surfaces of the shed alligator teeth were scanned using a confocal laser microscope (VK-9700, Keyence, Osaka, Japan) with a violet laser (408 nm), equipped with a long working distance 100x lens (N.A. = 0.95) (resolution in x, y = 0.138 μ m, step size in z = 0.001 μ m). Scans were obtained from the buccal side (which was identified through the curvature of the tooth) as close to the apex as possible, but always within the third of the tooth crown closest to the apex for several reasons. The enamel is thickest at the tooth tip (Kvam, 1959) and gets thinner along the tooth crown toward the root. Therefore, the apex is likely to preserve the enamel wear without exposing the dentine quickly. Additionally, the apex is most likely to get in contact with food items, either for seizing and holding them, or for processing the prey. The apex is therefore the focus area of a conical tooth (without a developed occlusal surface or visible wear facets) to show diet-related wear.

Teeth were cleaned with acetone-soaked cotton swaps. If teeth still showed attached dirt particles afterward, they were additionally subjected to cleaning in an ultrasound bath. First, teeth were individually placed in a 2% NaClO solution for 3 min, and then transferred to a milli-Q water bath for 3 min.

Up to four scans (141 \times 106 μ m) were taken for each tooth, and if several teeth were retrieved after the same feeding bout, these were treated as belonging to the same date. All scans were trimmed in MountainsMap v. 9.0.9878 to 100 \times 100 μ m to exclude peripheral damage. For each tooth, median parameter

TABLE 1 Overview of experimental animals, experimental period, and diets.

Experimental period	Individual #	Diet	Snout-vent length (mm)	Weight (g)
1 29. Jan. –31. May 2021	1	Rat	678	6,877
1 29. Jan. –31. May 2021	2	Sardine	570	4,335
1 10. Feb. –31. May 2021	3	Crawfish	590	4,265
1 04. Mar. –10. Jun. 2021	4	Quail	660	6,164
1 28. Jan. –08. Jun. 2021	6	Pellet (control)	562	3,711
2 27. Sep. –06. Dec. 2021	4	Crawfish	672	7,370
2 27. Sep. –25. Nov. 2021	6	Sardine	592	5,599

values were calculated from the obtained scans. Then, for each collection date, mean parameter values were calculated from all obtained teeth recovered on that date.

Teeth could not be assigned to a specific tooth position or jaw. However, because posterior teeth are broader and shorter, with blunter tips compared to anterior teeth, overall tooth shape could be used to designate teeth as having come from either posterior (molariform) or central/anterior (caniniform) positions (Berkovitz and Shellis, 2017). Similar to Bestwick et al. (2019), we avoided including molariform teeth, as they are used for crushing and might be used differently on food items of different hardness, and because they were more scarce among the collected teeth. Instead, we concentrated on sharp, conical teeth in our sample.

The teeth of alligators often show pronounced enamel wrinkles (Sander, 1999). Through dental wear, the wrinkles are worn away and enamel surfaces appear smoother (pers. observation, Supplementary Figures S1, S2). We found that the pellet-feeding individual as well as sardine- and quail-feeding individuals showed the most pronounced enamel wrinkles. These are problematic for assessing diet-related DMTs, as the commonly applied surface roughness parameters from ISO 25871 would record higher surface roughness from the natural enamel topography of relatively unworn teeth. In DMTA, filtering protocols are usually applied to account for the gross shape and waviness of the enamel surface. The commonly applied filtering procedure in MountainsMap v. 9.0.9878 for the employed microscope (compare Kubo and Fujita, 2021; Winkler and Kubo, 2022) did not result in the satisfactory removal of the enamel wrinkles (Supplementary Figures S1, S2). Thus, we tested stronger filtering algorithms until satisfied with the result (Supplementary Figures S1, S2), and settled on a robust Gaussian filter (with a cut-off value of 0.8 μm , using the resulting S-F surface) followed by a Gaussian filter (with a cut-off-value of 20 μm , using the resulting S-L surface). As this strong filtering procedure not only removed enamel wrinkles, but also reduced the height and depth of diet-induced wear features, we found that most of the commonly applied DMTA parameters from ISO 25178, motif, and furrow analysis did not detect differences between diet treatments. However, parameters

reflecting the complexity of the surface such as the scale-sensitive fractal analysis (SSFA) parameter area-scale fractal complexity ($Asfc$) and ISO 25178 developed interfacial area ratio (Sdr) were less influenced by the strong filter routine, and still showed significant differences between diets. Complexity is known to indicate hard-object feeding in primates (Scott et al., 2005, 2012; Ungar et al., 2008), carnivores (DeSantis et al., 2012), and reptiles (Winkler et al., 2019a), and hence we only concentrate on complexity parameters in this study. We note that $Asfc$ is calculated over the whole scale of a surface (Scott et al., 2006). Our approach uses filtered, scale-limited surfaces, because using the whole scale of the surface would result in misinterpretation of enamel wrinkles as wear-induced topography (hills and valleys). Thus, we are diverging from the common practice of SSFA-based DMTA, which makes our results less comparable to other studies. The range of $Asfc$, and the absolute values obtained, will be smaller in the current study as compared to previous studies. Still, we consider this approach justified due to the nature of the studied surfaces, i.e., the natural (unworn) enamel topography, and because the observed differences in $Asfc$ were also confirmed by the ISO 25178 parameter Sdr , which is applicable to describe surface geometry of the scale-limited surface.

Statistics

All statistical analyses were conducted in JMP v.16.0. We pooled data for each experimental diet starting with teeth collected after the first feeding bout. Thereby, teeth experiencing only one feeding event on an experimental diet and teeth experiencing several feeding events were grouped. A Shapiro–Wilk test indicated that mean food item weight ($p = 0.217$), mean bite count ($p = 0.652$), mean $Asfc$ ($p = 0.950$), and mean Sdr ($p = 0.931$) per diet were normally distributed, hence we analyzed their relationship using linear correlations (Pearson coefficient). We used a heteroscedastic pairwise comparison test (Wilcoxon test) to compare complexity patterns between all dietary pairs. Data were also visualized per tooth on the collection day over the course of the feeding experiment.

However, because on several days only one tooth was recovered, we did not statistically compare differences between individual dates within or between diets.

Results

Feeding observations

The pelleted diet was consumed slower and more reluctantly by individual #6. The four individuals on experimental diets displayed high levels of anticipation prior to and during feeding time, standing on their hindlegs, jumping, and frantically searching for the prey item once it was dropped into the water (see [Supplementary Videos](#)). They often missed the prey during the first seconds due to this turmoil and had to be pointed toward the food with a long stick.

During the first experimental phase, the mean bite count on the four experimental feeds was lowest on the rat diet, followed by quails, and highest on crawfish and sardines ([Figure 1](#), [Supplementary Figure S3](#), [Supplementary Table S1](#)). During the second phase, the bite count on crawfish was even higher than during the first phase, while the bite count on sardines was lower, even though most of the time two instead of one sardine were fed ([Supplementary Figure S3](#), [Supplementary Table S1](#)). Individual #4 received different diets during each experimental phase and displayed different mean bite counts, with many fewer bites on quails (23.96) than on crawfish (42.71) ([Supplementary Figure S3](#)). There was no significant correlation between the weight of the diet items and bite count ($p = 0.691$, [Figure 1](#)). Bite count was not recorded for the pellet-feeding individual, as the feeding motion did not include visible biting or processing of pellets.

Dental microwear texture analysis

Feeding on the pelleted diet resulted in overall smoother dental enamel surface textures ([Figure 2](#)). Visually, surfaces of teeth from pellet-feeders seem to show no or little wear marks. Sardine-feeding and quail-feeding resulted in similar surface wear as pellet-feeding, with only small visible wear marks. Rat- and crawfish-feeding, on the contrary, resulted in visible, deep wear marks (scratches).

The pelleted diet resulted in similar complexity (*Asfc* and *Sdr*) for all individuals ([Figure 3](#), [Supplementary Table S2](#)). Before being placed on their designated experimental diet, at least one shed tooth was collected from each individual. The DMT of these falls within the range of *Asfc* and *Sdr* values observed over the duration of the first experimental phase for the control individual which remained on the pelleted diet ([Figure 3](#)). Only one tooth collected for individual #6, before being switched to sardine-feeding, shows significantly lower

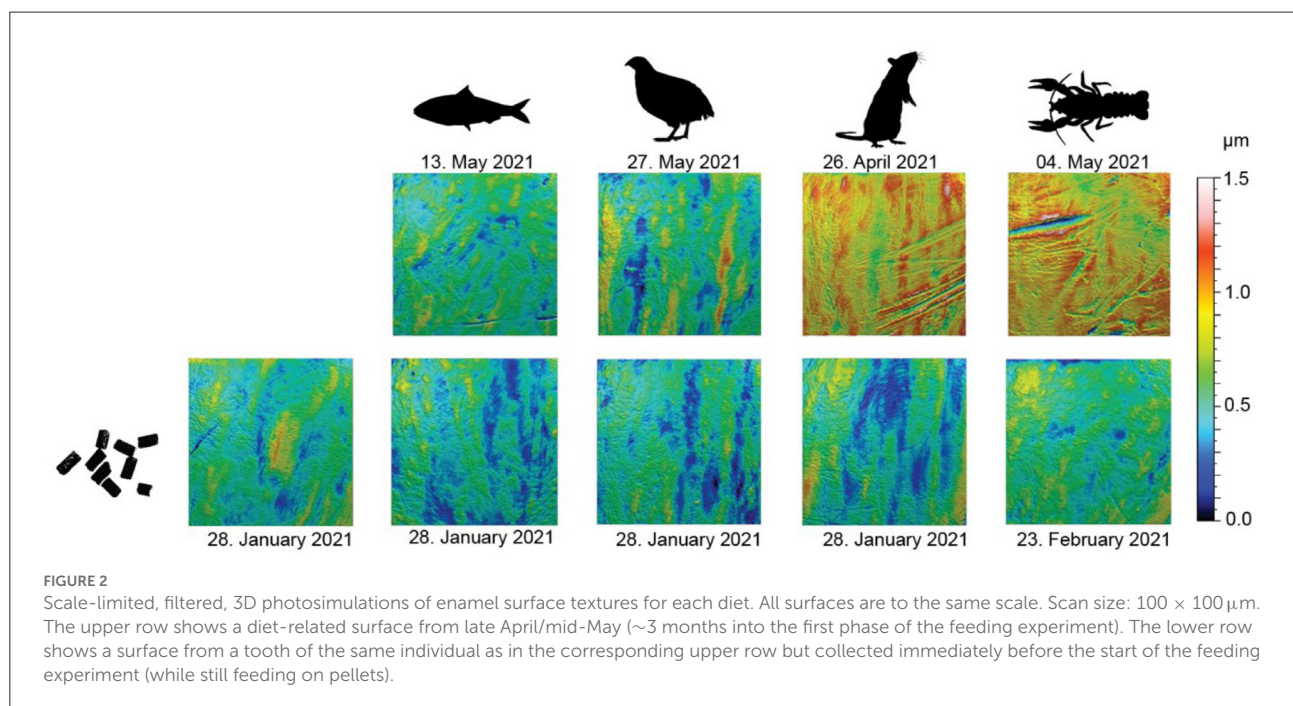
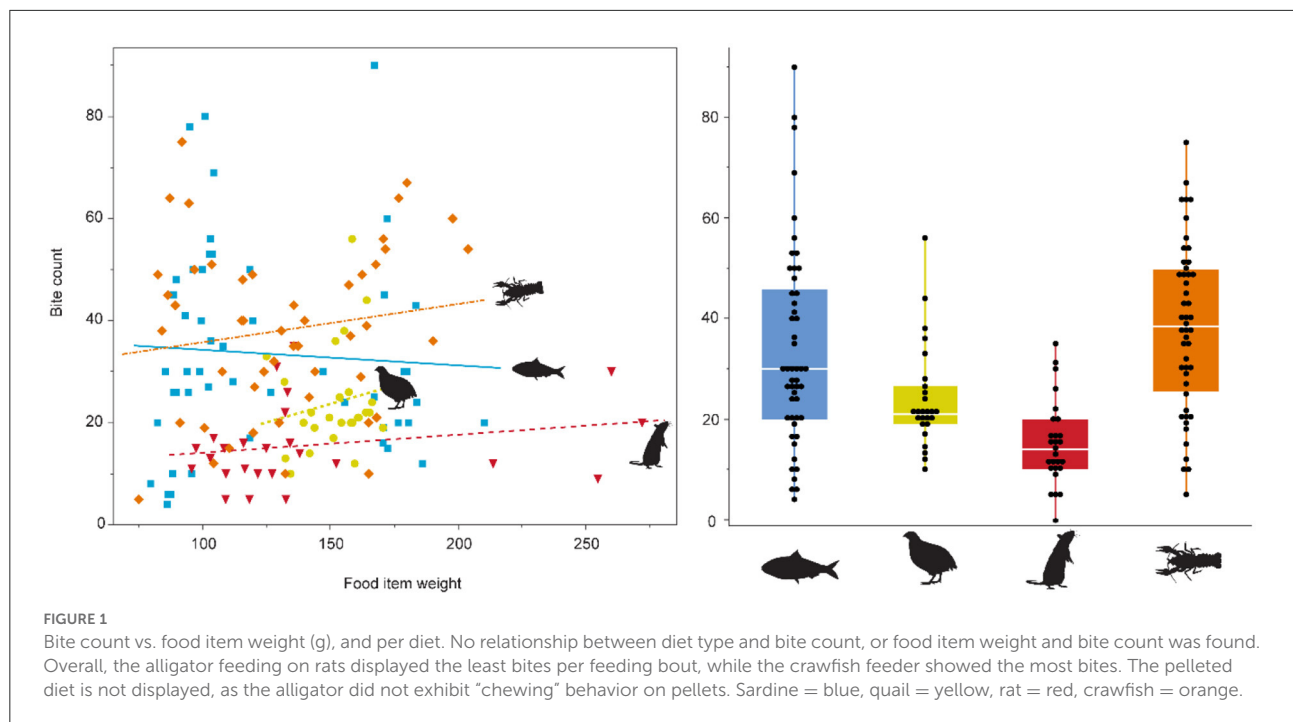
Asfc and *Sdr* values than teeth from the same individual when compared to the pooled data for itself over the course of phase 1, and individuals #2 (dedicated sardine-feeder) and #3 (dedicated crawfish-feeder).

Pooling of all data over the course of the experiment highlights that already after the first feeding bout, several experimental diets resulted in a change of DMT. Each experimental diet except for quails displays significantly higher *Asfc* and *Sdr* values than the control individual ([Figure 4](#)). Within experimental diets, complexity increases in the following order: quail \leq sardine $<$ rat \leq crawfish ([Supplementary Table S2](#)). The crawfish feeder showed significantly larger *Asfc* and *Sdr* values than the sardine and quail feeders, and non-significantly larger *Asfc* and *Sdr* values than the rat feeder. Between sardine and quail, or rat and crawfish, no significant differences in *Asfc* and/or *Sdr* values were found. It is evident that *Asfc* and *Sdr* reflect the same qualities of the surface. Hence, over the course of the experiment, we only displayed a change in *Asfc* ([Figure 5](#)). Mean complexity values were not significantly correlated to mean bite counts in any of the diets (*Asfc*: $p = 0.425$, *Sdr*: $p = 0.353$, [Supplementary Figure S3](#)).

All diets resulted in large variability in surface complexity over the first experimental phase ([Figure 5](#)). There was no distinct trend for increase or decrease of complexity values, but an undulating pattern was observed. During the second phase, variability seems to be lower for both the sardine- and crawfish-feeding individuals. Already for the first recovered teeth at the beginning of the feeding experiment, complexity increased on all diets, except for the crawfish-feeding individual during the second phase. For several dates during the feeding experiment, single teeth showed complexity values as low as before (when still feeding on a pelleted diet). Overall, rat- and crawfish-feeding resulted in complexity values that were two times as high as recorded for sardine- or quail-feeding.

Discussion

Though they do not truly chew, oral processing in young alligators includes rapid orthal biting movements of the lower jaw (Busbey, 1989). During initial prey acquisition, positioning, and these crushing bites, we observed that teeth contacted several times with the prey ([Supplementary Videos](#)). However, these contacts are of varying frequency and intensity, depending on the tooth position. We found that on diets of similar size and weight (quails and rats), on average 16–24 bites were used before the prey was swallowed ([Supplementary Figure S1](#), [Supplementary Table S1](#)). From seizing to swallowing, alligators used a highly variable number of bites for sardines. Alligators used more bites when being presented with one large sardine than when being presented with two smaller sardines. The total number of bites, however, does not seem to



affect the observed complexity of dental microwear textures (Supplementary Figure S3). Complexity values were higher for the individuals feeding on rats than for the individuals feeding on quails (Figure 4), but quails were on average consumed with more bites, and overall lower complexity values were observed when only one large sardine was consumed with more bites

than two small sardines (Supplementary Table S2). Crawfish-feeding resulted in the largest complexity values observed, and alligators also took the largest number of bites to process crawfish. However, for each feeding bout, ~7 crawfish were fed on average. Therefore, the large number of bites here is the total number of bites used to consume all crawfish.

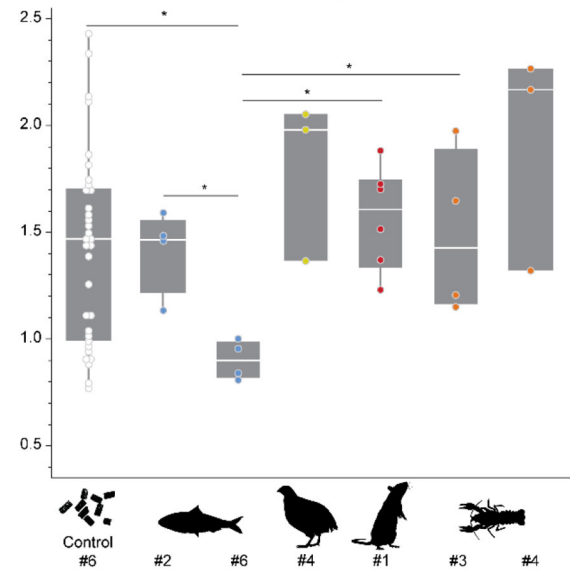
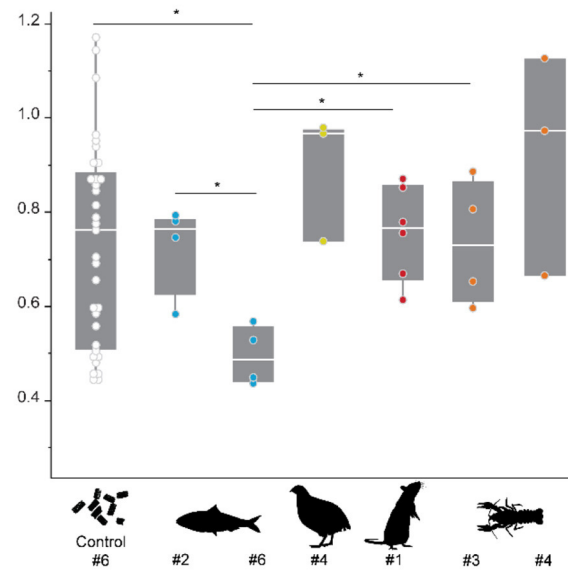
Asfc - (area-scale fractal) complexity*Sdr* - developed interfacial area ratio

FIGURE 3

Asfc and *Sdr* recorded in different individuals while feeding on the pelleted diet. The control animal (#6) received the pelleted diet over the course of the feeding experiment. For the other individuals, 1–2 teeth were collected immediately before starting the feeding experiment. Each scan is treated as an individual datapoint in this plot. Significance level: * = 0.05. Colored points indicate the diet which was assigned to each individual during the feeding experiment: sardine = blue, quail = yellow, rat = red, crawfish = orange.

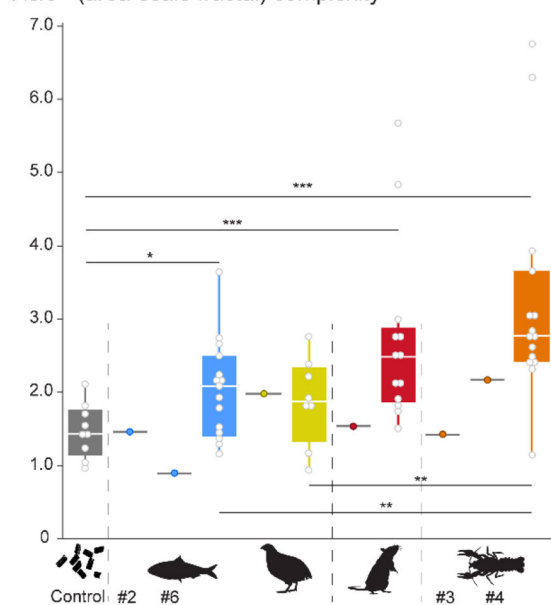
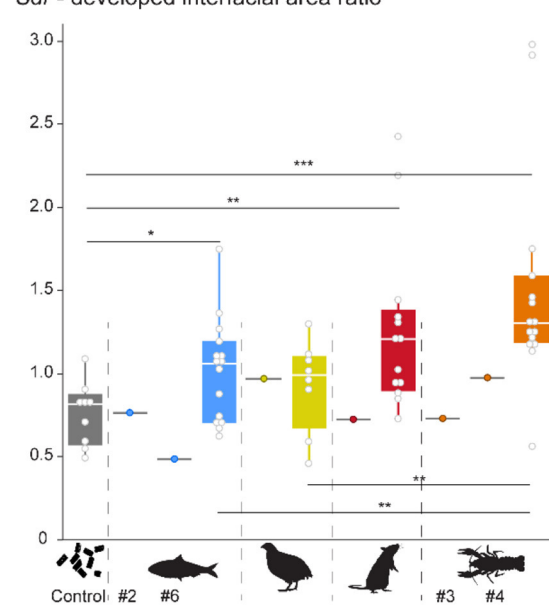
Asfc - (area-scale fractal) complexity*Sdr* - developed interfacial area ratio

FIGURE 4

Pooled *Asfc* and *Sdr* observed for all diets over the whole experimental duration. Significance level: * = 0.05, ** = 0.01, *** = 0.001. Sardine = blue, quail = yellow, rat = red, crawfish = orange. Gray boxplots with colored points indicate that teeth were collected before the start of the feeding experiments, while the alligator was still feeding on pellets. Pooled data were created by using the median from all scans per tooth, and then calculating a mean per collection date. Each collection date represents one point.

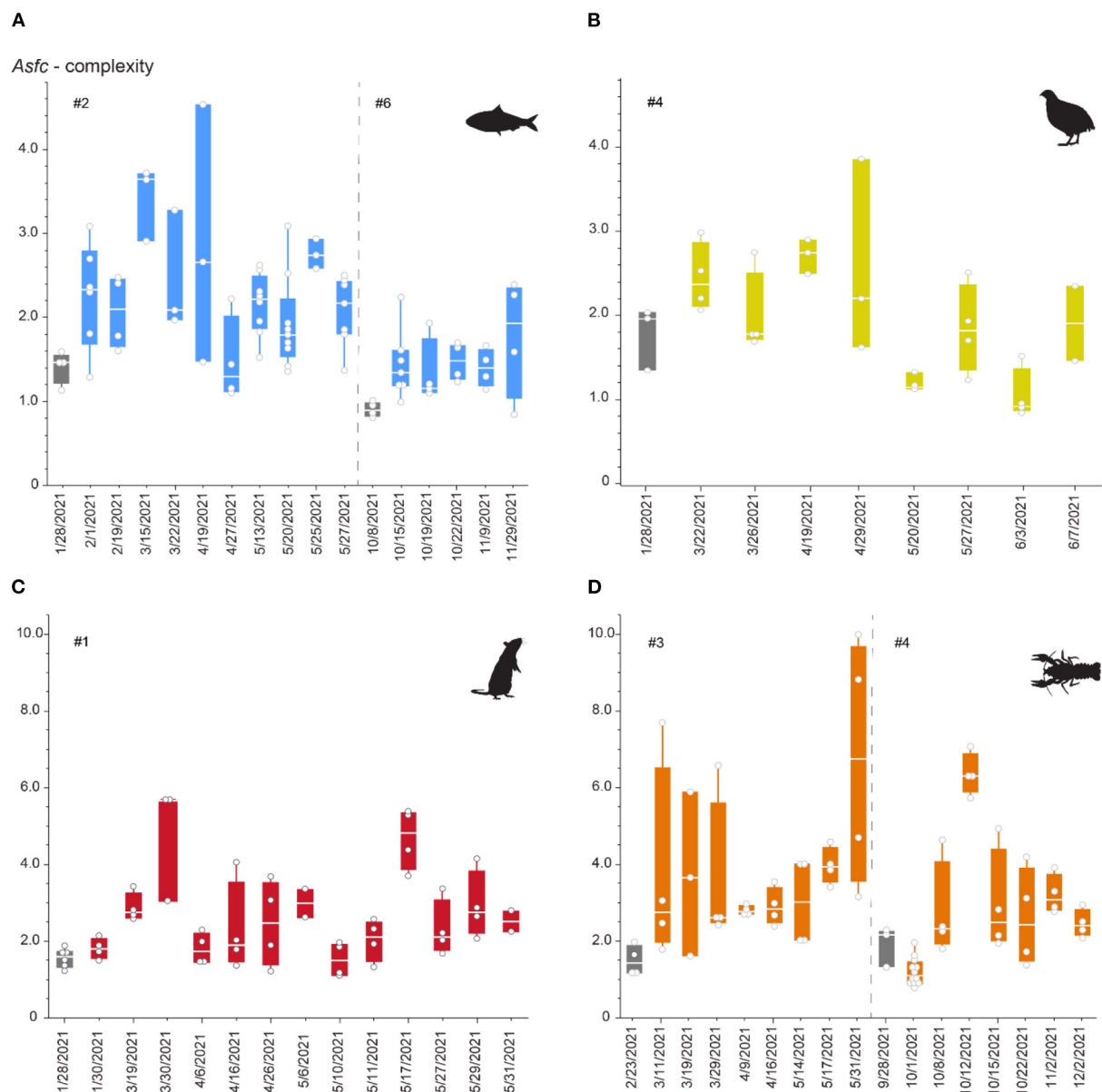


FIGURE 5
Asfc over the duration of the first and (for sardine and crawfish) second phase of the feeding experiment. Phases 1 and 2 are separated by a dashed line. Each datapoint represents one scan and can be derived from several teeth collected on the same date. **(A)** Sardine-feeder (alligators #2 and #6), **(B)** quail feeder (alligator #4), **(C)** rat-feeder (alligator #1), **(D)** crawfish-feeder (alligators #3 and #4). Gray boxplots mark teeth collected before switching to the experimental diet, when the alligator has only consumed pellets for at least 3 months. Note that different scales are used for pairs of sardine-/quail- and rat-/crawfish-feeding.

Dietary differences in dental microwear texture analysis

The pelleted control diet resulted in variable, but overall lowest complexity values and differed significantly from all experimental vertebrate and invertebrate diets except for quails (Figure 4). This is in accordance with our expectations, as the pelleted diet was not seized or processed with the teeth, but

instead swallowed whole. The low complexity observed for sardine-feeders and the high complexity observed for crawfish-feeders were also in accordance with our expectations that they would be on opposite ends of the DMT spectrum observed. Crawfish can be considered a “hard” invertebrate diet, because of their highly mineralized exoskeleton (Aiken and Waddy, 1992; Raabe et al., 2005). In mammals (including hominins, modern humans, and Neanderthals) and reptiles, high complexity has

been consistently associated with hard-object feeding, whether bones, nuts, seeds, or mollusks (Scott et al., 2005, 2012; Ungar et al., 2008; DeSantis et al., 2012; Schmidt et al., 2016, 2019; Williams et al., 2019, 2021; Winkler et al., 2019a, 2022). Alligators feeding on crustaceans fit within this pattern and emphasize the universal interrelation between complex DMT and hard objects in the diet.

The difference between surface complexity observed for teeth used on rat and quail prey is striking, with quail-feeding resulting in similar complexity values as sardine-feeding, whereas rat-feeding resulted in similarly high values as crawfish-feeding (though crawfish-feeding resulted in the highest complexity values observed). We can only speculate on the source of these differences, and of course with a sample size of one animal per diet, individual variability might also play a role in our observed patterns. However, as hypothesized, bird skeletons may exhibit different levels of resistance to breaking by alligator teeth than rat skeletons. The overall thinner but denser bird bone is optimized to withstand torsional stresses during flight (Swartz et al., 1992), while making the skeletal construction lightweight (Dumont, 2010). Bird bones, especially the skull and humeri, are pneumatized (Cubo and Casinos, 2000). Rat bones, however, have thicker walls and are marrow-filled, which makes them more resistant to bending under the localized impact (Currey and Alexander, 1985). Moreover, the skull is much heavier in relation to the rest of the body than in birds, and also bears teeth (Dumont, 2010). Teeth are composed of the hardest biological material, and it is plausible that during feeding, the alligator's teeth contact not only with the rat postcranial skeleton, but also with the skull several times. The observed distinct wear marks (Figure 2) and high surface complexity (Figure 4) might result from these contacts with the rat skull, their teeth, and the overall more bending-resistant bones.

Individual variability and limitations of the study

During capture, crocodylians use only the teeth of one side of their jaws (Cleuren and DeVree, 2000; Erickson et al., 2012), before repositioning the prey with inertial bites (Cleuren and DeVree, 2000). Bestwick et al. (2021b) found that the middle-distal and distal teeth of *Alligator mississippiensis* and *Caiman crocodilus*, for example, exhibit the roughest microwear textures (indicating higher abrasion due to more tooth-to-food contacts). This may stem from alligators using preferred teeth when acquiring, manipulating, and crushing prey (Busbey, 1989). As our experimental design did not allow to control for tooth position, some teeth may show less use due to such differences. Moreover, we do not know if the shed teeth were in use for the same duration, or if some individual tooth positions were

exchanged more frequently than others. Therefore, it is not surprising that our data show high intra-individual variability over the course of the experiment.

The surface structure of enamel in alligators, with distinct wrinkles that form small ridges, posed a challenge for evaluating DMTA as compared to other species with smooth enamel (Supplementary Figures S1, S2). This problem can likely occur in other crocodylian taxa, theropods, or possibly in other archosaurs with wrinkled or fluted enamel. Particularly, if teeth have newly erupted, or the diet is soft and less abrasive, the wrinkles do not wear down and present a topography that will result in high surface roughness, height, and volume. However, these large roughness, height, and volume values are not related to diet-induced wear marks, and therefore not comparable to the wear observed in mammals or non-mammalian species with smooth enamel. This problem can be overcome by choosing parameters that are less affected by the wrinkled enamel surface, and by using a strong filtering routine that eliminates the original enamel surface topography. However, such strong filters will also reduce or erase diet-induced wear features. Therefore, it is difficult to compare low abrasive diets to highly abrasive diets in very young individuals with frequent tooth replacement. In older specimens, when tooth replacement is slower, and thus teeth experience wear over a longer period, this problem seems not to occur. Bestwick et al. (2019) did not report such problems when analyzing DMTA in extant crocodylians. Due to this limitation, we can only report on two complexity parameters that seem to effectively reflect diet hardness in young alligators, as well as older individuals.

Our results confirm the expectations and encourage the idea that hard-object feeding can be detected in archosaurs, even in juveniles with frequent tooth replacement. It must be noted, however, that our sample size of one (two for crawfish and sardine) is too low to draw definitive conclusions. Individual variability and behavioral differences might influence feeding behavior, and thus dental wear. Still, the repetition of feeding two out of four experimental diets supports that the observed patterns are stable and repeatable, and in the pooled sample, we were able to analyze 8–20 teeth per diet. If these teeth would stem from different individuals, it would be an acceptable sample size. Hence, we may at least consider the DMT signature is representative, for each individual.

Captive alligator diets and behavior

We observed that alligators feeding on the four experimental diets displayed a great level of “excitement” during feeding time. They were actively searching for their food, standing on their hind legs, and jumping toward the food. Hence, including dietary items similar to their natural diets (small vertebrates and crustaceans) may be used as an

enrichment for captive crocodylians and promote their natural feeding behavior.

Outlook and conclusions

This experiment highlighted both challenges and opportunities when analyzing archosaur DMT. Unworn dental enamel surfaces are wrinkled, which biases the assessment of topography and requires strong surface filtering. Tooth position-specific usage of teeth during prey processing, for example posterior teeth being utilized for crushing, is known in alligators and might result in tooth position-specific wear patterns. Isolated teeth are difficult to assign to a certain tooth position (unless they are blunt, button-like posterior teeth). It would therefore be of great interest to explore tooth position-specific DMT in greater detail in archosaurs, along the jaw, and especially comparing caniniform and molariform teeth. Obviously, a continuation of similar feeding experiments with a larger number of individuals would be desirable, but may be impractical. Therefore, even though these results need to be treated with great caution, our feeding experiments provide unique data on how different food types affect DMT in alligators and support the universal interrelation of hard-object feeding and high surface complexity. Such patterns may also support the identification of hard-object feeding in the fossil record, and thus shed light on the paleodiet of extinct faunivorous taxa, including dinosaurs.

Data availability statement

The original contributions presented in the study are included in the article/[Supplementary material](#), and the original scan dataset (unfiltered surface scans) used in this study is published in the online repository Zenodo under the <https://www.doi.org/10.5281/zenodo.6597169>.

Ethics statement

The animal study was reviewed and alligator husbandry and further experimental procedures were approved by the Clemson University IACUC (protocol 2019-037).

Author contributions

DEW, TK, and MOK: conceptualization. DEW, MI, RWB, and MOK: methodology. DEW: formal analysis, writing of the original draft, and visualization. MI, RWB, MOK, and TK: resources. DEW and TK: funding acquisition. All authors:

reviewing and editing. All authors contributed to the article and approved the submitted version.

Funding

The research was funded by the Japan Society for the Promotion of Science (JSPS) under a grant-in-aid for DEW, No. 20F20325 and for MI, No. 19J00701.

Acknowledgments

We thank R. Elsey (Louisiana Department of Wildlife and Fisheries, Rockefeller Wildlife Refuge) for providing alligators, M. Hart (South Carolina Department of Natural Resources), R. Flynt (Mississippi Department of Wildlife, Parks and Fisheries), C. Threadgill and T. Ancelet (Alabama Department of Conservation and Natural Resources), and J. Hawkins (Georgia Department of Natural Resources) for granting permission to transport and house alligators, Kent Vliet (University of Florida) for his helpful suggestions regarding alligator husbandry and feeding, and D. Munteanu, K. Diamond, C. Kinsey, A. Palecek, and D. Adams (Clemson University) for assisting with animal care, and Kodai Usami (The University of Tokyo) for support in the cleaning of alligator teeth. We further thank two reviewers for their helpful comments and suggestions.

Conflict of interest

The authors declare that the research was conducted in the absence of any commercial or financial relationships that could be construed as a potential conflict of interest.

Publisher's note

All claims expressed in this article are solely those of the authors and do not necessarily represent those of their affiliated organizations, or those of the publisher, the editors and the reviewers. Any product that may be evaluated in this article, or claim that may be made by its manufacturer, is not guaranteed or endorsed by the publisher.

Supplementary material

The Supplementary Material for this article can be found online at: <https://www.frontiersin.org/articles/10.3389/fevo.2022.957725/full#supplementary-material>

References

- Ackermans, N. L., Winkler, D. E., Martin, L. F., Kaiser, T. M., Clauss, M., and Hatt, J. M. (2020). Dust and grit matter: abrasives of different size lead to opposing dental microwear textures in experimentally fed sheep (*Ovis aries*). *J. Exp. Biol.* 223, jeb220442. doi: 10.1242/jeb.220442
- Aiken, D. E., and Waddy, S. L. (1992). The growth process in crayfish. *Rev. Aquat. Sci.* 6, 335–381.
- Barr, B. R. (1997). *Food habits of the American alligator, Alligator mississippiensis, in the Southern Everglades* Ph.D. Thesis. University of Miami, Coral Gables, FL, United States.
- Berkovitz, B. K., and Shellis, R. P. (eds.). (2017). “Reptiles 3: crocodylia,” in *The Teeth of Non-Mammalian Vertebrates* (Amsterdam: Elsevier; Academic Press), 225–226.
- Bestwick, J., Jones, A. S., Purnell, M. A., and Butler, R. J. (2021a). Dietary constraints of phytosaurian reptiles revealed by dental microwear textural analysis. *Palaeontology* 64, 119–136. doi: 10.1111/pala.12515
- Bestwick, J., Unwin, D. M., Butler, R. J., and Purnell, M. A. (2020). Dietary diversity and evolution of the earliest flying vertebrates revealed by dental microwear texture analysis. *Nat. Commun.* 11, 1–9. doi: 10.1038/s41467-020-19022-2
- Bestwick, J., Unwin, D. M., Henderson, D. M., and Purnell, M. A. (2021b). Dental microwear texture analysis along reptile tooth rows: complex variation with non-dietary variables. *R. Soc. Open Sci.* 8, 201754. doi: 10.1098/rsos.201754
- Bestwick, J., Unwin, D. M., and Purnell, M. A. (2019). Dietary differences in archosaur and lepidosaur reptiles revealed by dental microwear textural analysis. *Sci. Rep.* 9, 1–11. doi: 10.1038/s41598-019-48154-9
- Busbey, A. B. (1989). Form and function of the feeding apparatus of *Alligator mississippiensis*. *J. Morphol.* 202, 99–12. doi: 10.1002/jmor.1052020108
- Cleuren, J., and DeVree, F. (2000). “Feeding in crocodilians,” in *Feeding: Form, Function, and Evolution in Tetrapod Vertebrates*, ed K. Schwenk (San Diego, CA, Academic Press), 337–358.
- Cott, H. B. (1961). Scientific results of an inquiry into the ecology and economic status of the Nile Crocodile (*Crocodilus niloticus*) in Uganda and northern Rhodesia. *Trans. Zool. Soc. Lond.* 29, 211–357. doi: 10.1111/j.1096-3642.1961.tb00220.x
- Cubo, J., and Casinos, A. (2000). Incidence and mechanical significance of pneumatization in the long bones of birds. *Zool. J. Linn. Soc.* 130, 499–510. doi: 10.1111/j.1096-3642.2000.tb02198.x
- Currey, J. D., and Alexander, R. M. (1985). The thickness of the walls of tubular bones. *J. Zool.* 206, 453–468. doi: 10.1111/j.1469-7998.1985.tb03551.x
- Delany, M. F., and Abercrombie, C. L. (1986). American alligator food habits in northcentral Florida. *J. Wildl. Manag.* 50, 348–353. doi: 10.2307/3801926
- DeSantis, L. R., Schubert, B. W., Scott, J. R., and Ungar, P. S. (2012). Implications of diet for the extinction of saber-toothed cats and American lions. *PLoS ONE* 7, e52453. doi: 10.1371/journal.pone.0052453
- Dumont, E. R. (2010). Bone density and the lightweight skeletons of birds. *Proc. R. Soc. B Biol. Sci.* 277, 2193–2198. doi: 10.1098/rspb.2010.0117
- Erickson, G. M., Catanese, J. III, and Keaveny, T. M. (2002). Evolution of the biomechanical material properties of the femur. *Anat. Rec.* 268, 115–124. doi: 10.1002/ar.10145
- Erickson, G. M., Gignac, P. M., Stepan, S. J., Lappin, A. K., Vliet, K. A., Brueggel, J. D., et al. (2012). Insights into the ecology and evolutionary success of crocodilians revealed through bite-force and tooth-pressure experimentation. *PLoS ONE* 7, e31781. doi: 10.1371/journal.pone.0031781
- Fiorillo, A. R. (1998). Dental microwear patterns of the sauropod dinosaurs. *Camarasaurus* and *Diplodocus*: Evidence for resource partitioning in the late Jurassic of North America. *Hist. Biol.* 13, 1–16. doi: 10.1080/08912969809386568
- Gere, K., Bodor, E. R., Makádi, L., and Osi, A. (2021). Complex food preference analysis of the Late Cretaceous (Santonian) lizards from Iharkút (Bakony Mountains, Hungary). *Hist. Biol.* 33, 3686–3702. doi: 10.1080/08912963.2021.1887862
- Grigg, G. C., and Kirshner, D. (2015). *Biology and Evolution of Crocodylians*. Clayton South, VIC, Australia: CSIRO Publishing, 672.
- Holwerda, F. M., Beatty, B. L., and Schulp, A. S. (2013). Dental macro- and microwear in *Carinodens belgicus*, a small mosasaur from the type Maastrichtian. *Neth. J. Geosci.* 92, 267–274. doi: 10.1017/S0016774600000202
- Horton, J. M., and Summers, A. P. (2009). The material properties of acellular bone in a teleost fish. *J. Exp. Biol.* 212, 1413–1420. doi: 10.1242/jeb.020636
- Hutton, J. M. (1987). Growth and feeding ecology of the Nile crocodile *Crocodilus niloticus* at Ngezi, Zimbabwe. *J. Anim. Ecol.* 56, 25–38. doi: 10.2307/4797
- Iijima, M., Munteanu, V. D., Elsey, R. M., and Blob, R. W. (2021). Ontogenetic changes in limb posture, kinematics, forces and joint moments in American alligators (*Alligator mississippiensis*). *J. Exp. Biol.* 224, jeb242990. doi: 10.1242/jeb.242990
- Kubo, M. O., and Fujita, M. (2021). Diets of Pleistocene insular dwarf deer revealed by dental microwear texture analysis. *Palaeogeogr. Palaeoclimatol. Palaeoecol.* 562, 110098. doi: 10.1016/j.palaeo.2020.110098
- Kvam, T. (1959). The Teeth of *Alligator mississippiensis* Daud.: V. *Morphol. Enamel. Acta Odontol. Scand.* 17, 45–59. doi: 10.3109/00016355909011232
- Mallon, J. C., and Anderson, J. S. (2014). The functional and palaeoecological implications of tooth morphology and wear for the megaherbivorous dinosaurs from the Dinosaur Park Formation (Upper Campanian) of Alberta, Canada. *PLoS ONE* 9, e98605. doi: 10.1371/journal.pone.0098605
- Merceron, G., Ramdarshan, A., Blondel, C., Boisserie, J.-R., Brunetiere, N., Francisco, A., et al. (2016). Untangling the environmental from the dietary: dust does not matter. *Proc. R. Soc. B* 283, 20161032. doi: 10.1098/rspb.2016.1032
- Platt, S. G., Rainwater, T. R., Finger, A. G., Thorbjarnarson, J. B., Anderson, T. A., and McMurry, S. T. (2006). Food habits, ontogenetic dietary partitioning and observations of foraging behaviour of Morelet's crocodile (*Crocodilus moreletii*) in northern Belize. *Herpetol. J.* 16, 281–290.
- Platt, S. G., Thorbjarnarson, J. B., Rainwater, T. R., and Martin, D. R. (2013). Diet of the American crocodile (*Crocodilus acutus*) in marine environments of coastal Belize. *J. Herpetol.* 47, 1–10. doi: 10.1670/12-077
- Pooley, A. C. (1989). “Food and feeding habits,” in *Crocodiles and Alligators*, eds Ross, C. A., New York: Facts on File, 76–91.
- Prange, H. D., Anderson, J. F., and Rahn, H. (1979). Scaling of skeletal mass to body mass in birds and mammals. *Am. Nat.* 113, 103–122. doi: 10.1086/283367
- Purnell, M., Seehausen, O., and Galis, F. (2012). Quantitative three-dimensional microtextural analyses of tooth wear as a tool for dietary discrimination in fishes. *J. R. Soc. Interface* 9, 2225–2233. doi: 10.1098/rsif.2012.0140
- Purnell, M. A., and Darras, L. P. (2015). 3D tooth microwear texture analysis in fishes as a test of dietary hypotheses of durophagy. *Surf. Topogr.: Metrol. Prop.* 4, 014006. doi: 10.1088/2051-672X/4/1/014006
- Raabe, D., Sachs, C., and Romano, P. J. A. M. (2005). The crustacean exoskeleton as an example of a structurally and mechanically graded biological nanocomposite material. *Acta Mater.* 53, 4281–4292. doi: 10.1016/j.actamat.2005.05.027
- Sakaki, H., Winkler, D. E., Kubo, T., Hirayama, R., Uno, H., Miyata, S., et al. (2022). Non-occlusal dental microwear texture analysis of a titanosauriform sauropod dinosaur from the Upper Cretaceous (Turonian) Tamagawa Formation, northeastern Japan. *Cretac. Res.* 136, 105218. doi: 10.1016/j.cretres.2022.105218
- Sander, P. M. (1999). *The Microstructure of Reptilian Tooth Enamel: Terminology, Function, and Phylogeny. Münchner Geowissenschaftliche Abhandlungen Reihe A: Geologie und Paläontologie Band 38*. Friedrich Pfeil Verlag.
- Schmidt, C. W., Beach, J. J., McKinley, J. I., and Eng, J. T. (2016). Distinguishing dietary indicators of pastoralists and agriculturalists via dental microwear texture analysis. *Surf. Topogr.: Metrol. Prop.* 4, 014008. doi: 10.1088/2051-672X/4/1/014008
- Schmidt, C. W., Remy, A., Van Sessen, R., Willman, J., Krueger, K., Scott, R., et al. (2019). Dental microwear texture analysis of *Homo sapiens sapiens*: foragers, farmers, and pastoralists. *Am. J. Phys. Anthropol.* 169, 207–226. doi: 10.1002/ajpa.23815
- Schubert, B. W., and Ungar, P. S. (2005). Wear facets and enamel spalling in tyrannosaurid dinosaurs. *Acta Palaeontol. Pol.* 50, 93–99. Available online at: <http://app.pan.pl/acta50/app50-093.pdf>
- Schulz, E., Piotrowski, V., Clauss, M., Mau, M., Merceron, G., and Kaiser, T. M. (2013). Dietary abrasiveness is associated with variability of microwear and dental surface texture in rabbits. *PLoS ONE* 8, e56167. doi: 10.1371/journal.pone.0056167
- Schulz-Kornas, E., Winkler, D. E., Clauss, M., Carlsson, J., Ackermans, N. L., Martin, L. F., et al. (2020). Everything matters: molar microwear texture in goats (*Capra aegagrus hircus*) fed diets of different abrasiveness. *Palaeogeogr. Palaeoclimatol. Palaeoecol.* 552, 109783. doi: 10.1016/j.palaeo.2020.109783

- Scott, R., Ungar, P., Bergstrom, T., et al. (2005). Dental microwear texture analysis shows within-species diet variability in fossil hominins. *Nature* 436, 693–695. doi: 10.1038/nature03822
- Scott, R. S., Teaford, M. F., and Ungar, P. S. (2012). Dental microwear texture and anthropoid diets. *Am. J. Phys. Anthropol.* 147, 551–579. doi: 10.1002/ajpa.22007
- Scott, R. S., Ungar, P. S., Bergstrom, T. S., Brown, C. A., Childs, B. E., Teaford, M. F., et al. (2006). Dental microwear texture analysis: technical considerations. *J. Hum. Evol.* 51, 339–349. doi: 10.1016/j.jhevol.2006.04.006
- Stevenson, C., and Whitaker, R. (2010). “Indian gharial *Gavialis gangeticus*,” in *Crocodiles Status Survey and Conservation Action Plan. Third Edn*, eds S. C. Manolis and C. Stevenson (Darwin, NT: Crocodile Specialist Group), 139–143.
- Swartz, S. M., Bennett, M. B., and Carrier, D. R. (1992). Wing bone stresses in free flying bats and the evolution of skeletal design for flight. *Nature* 359, 726–729. doi: 10.1038/359726a0
- Taylor, D. (1986). Fall foods of adult alligators from Cypress Lake habitat, Louisiana. *Proc. Annu. Conf. Southeast Fish and Wildl. Agencies* 40, 338–341.
- Taylor, J. A. (1979). The foods and feeding habits of subadult *Crocodylus porosus* Schneider in northern Australia. *Wildl. Res.* 6, 347–359. doi: 10.1071/WR9790347
- Thorbjarnarson, B. (1990). Notes on the feeding behavior of the gharial (*Gavialis gangeticus*) under semi-natural conditions. *J. Herpetol.* 24, 99–100. doi: 10.2307/1564301
- Ungar, P. S., Grine, F. E., and Teaford, M. F. (2008). Dental microwear and diet of the Plio-Pleistocene hominin *Paranthropus boisei*. *PLoS ONE* 3, e2044. doi: 10.1371/annotation/195120f0-18ee-4730-9bd6-0d6effd68fcf
- Varriale, F. J. (2016). Dental microwear reveals mammal-like chewing in the neoceratopsian dinosaur *Leptoceratops gracilis*. *PeerJ* 4, e2132. doi: 10.7717/peerj.2132
- Virag, A., and Osi, A. (2017). Morphometry, microstructure, and wear pattern of neornithischian dinosaur teeth from the upper cretaceous iharkut locality (Hungary). *Anat. Rec. Adv. Integr. Anat. Evol. Biol.* 300, 1439–1463. doi: 10.1002/ar.23592
- Wallace, K. M., and Leslie, A. J. (2008). Diet of the Nile crocodile (*Crocodylus niloticus*) in the Okavango Delta, Botswana. *J. Herpetol.* 42, 361–368. doi: 10.1670/07-1071.1
- Webb, G., and Manolis, C. (1989). *Crocodiles of Australia*. Sydney, NSW: New Holland Publishers, 160.
- Williams, F. L., Schmidt, C. W., Droke, J., Willman, J. C., Semal, P., Becam, G., et al. (2019). Dietary reconstruction of Spy I using dental microwear texture analysis. *C. R. Palevol* 18, 1083–1094. doi: 10.1016/j.crpv.2019.06.004
- Williams, F. L., Schmidt, C. W., Droke, J. L., Willman, J. C., Neruda, P., Becam, G., et al. (2021). Reconstructing the diet of Kulna 1 from the Moravian karst (Czech Republic). *J. Paleolit. Archaeol.* 4, 21. doi: 10.1007/s41982-021-00099-0
- Williams, V. S., Barrett, P. M., and Purnell, M. A. (2009). Quantitative analysis of dental microwear in hadrosaurid dinosaurs, and the implications for hypotheses of jaw mechanics and feeding. *Proc. Nat. Acad. Sci.* 106, 11194–11199. doi: 10.1073/pnas.0812631106
- Winkler, D. E., Clauss, M., Kubo, M. O., Schulz-Kornas, E., Kaiser, T. M., Tschudin, A., et al. (2022). Microwear textures associated with experimental near-natural diets suggest that seeds and hard insect body-parts cause high enamel surface complexity in small mammals. *Front. Ecol. Evol.* 10, 957427. doi: 10.3389/fevo.2022.957427
- Winkler, D. E., Clauss, M., Rölle, M., Schulz-Kornas, E., Codron, D., Kaiser, T. M., et al. (2021). Dental microwear texture gradients in guinea pigs reveal that material properties of the diet affect chewing behaviour. *J. Exp. Biol.* 224, jeb242446. doi: 10.1242/jeb.242446
- Winkler, D. E., and Kubo, M. O. (2022). Inter-microscope comparability of dental microwear texture data obtained from different optical profilometers. *bioRxiv [Preprint]*. doi: 10.1101/2022.03.08.483539
- Winkler, D. E., Schulz-Kornas, E., Kaiser, T. M., Codron, D., Leichter, J., Hummel, J., et al. (2020b). The turnover of dental microwear texture: testing the “last supper” effect in small mammals in a controlled feeding experiment. *Palaeogeogr. Palaeoclimatol. Palaeoecol.* 557, 109930. doi: 10.1016/j.palaeo.2020.109930
- Winkler, D. E., Schulz-Kornas, E., Kaiser, T. M., De Cuyper, A., Clauss, M., and Tütken, T. (2019b). Forage silica and water content control dental surface texture in guinea pigs and provide implications for dietary reconstruction. *Proc. Nat. Acad. Sci.* 116, 1325–1330. doi: 10.1073/pnas.1814081116
- Winkler, D. E., Schulz-Kornas, E., Kaiser, T. M., and Tütken, T. (2019a). Dental microwear texture reflects dietary tendencies in extant Lepidosauria despite their limited use of oral food processing. *Proc. R. Soc. B* 286, 20190544. doi: 10.1098/rspb.2019.0544
- Winkler, D. E., Tütken, T., Schulz-Kornas, E., Kaiser, T. M., Müller, J., Leichter, J., et al. (2020a). Shape, size, and quantity of ingested external abrasives influence dental microwear texture formation in guinea pigs. *Proc. Nat. Acad. Sci.* 117, 22264–22273. doi: 10.1073/pnas.2008149117
- Wolfe, J. L., Bradshaw, D. K., and Chabreck, R. H. (1987). Alligator feeding habits: new data and a review. *Northeast Gulf Sci.* 9, 1–8. doi: 10.18785/negs.0901.01



OPEN ACCESS

EDITED BY

Eduardo Jiménez-Hidalgo,
University of the Sea, Mexico

REVIEWED BY

Antoine Souron,
UMR5199 De la Préhistoire A l'actuel
Culture, Environnement et
Anthropologie (PACEA), France
Ivan Calandra,
Romano-Germanic Central
Museum, Germany

*CORRESPONDENCE

Mugino O. Kubo
mugino@k.u-tokyo.ac.jp

†PRESENT ADDRESS

Kohga Miyamoto,
Technology Research Institute,
Obayashi Co., Tokyo, Japan

†These authors have contributed
equally to this work and share first
authorship

SPECIALTY SECTION

This article was submitted to
Paleoecology,
a section of the journal
Frontiers in Ecology and Evolution

RECEIVED 31 May 2022

ACCEPTED 17 August 2022

PUBLISHED 28 October 2022

CITATION

Miyamoto K, Kubo MO and Yokohata Y
(2022) The dental microwear texture
of wild boars from Japan reflects inter-
and intra-populational feeding
preferences.
Front. Ecol. Evol. 10:957646.
doi: 10.3389/fevo.2022.957646

COPYRIGHT

© 2022 Miyamoto, Kubo and
Yokohata. This is an open-access
article distributed under the terms of
the [Creative Commons Attribution
License \(CC BY\)](#). The use, distribution
or reproduction in other forums is
permitted, provided the original
author(s) and the copyright owner(s)
are credited and that the original
publication in this journal is cited, in
accordance with accepted academic
practice. No use, distribution or
reproduction is permitted which does
not comply with these terms.

The dental microwear texture of wild boars from Japan reflects inter- and intra-populational feeding preferences

Kohga Miyamoto^{1†}, Mugino O. Kubo^{1*†} and Yasushi Yokohata²

¹Department of Natural Environmental Studies, Graduate School of Frontier Sciences, The University of Tokyo, Kashiwa, Japan, ²Faculty of Science, Academic Assembly, University of Toyama, Toyama, Japan

Dental microwear texture analysis (DMTA) is rapidly expanding for the dietary estimation of extinct animals. There has been an extensive accumulation of microwear texture data from herbivorous mammals, especially for ruminant artiodactyls, but suids are still underrepresented. Microwear varies depending on the diet, and suids are naturally more flexible than other artiodactyls. Thus, their microwear is prone to greater variability. In this study, we examine the tooth microwear texture of wild boars from Toyama Prefecture, Japan, for which detailed ecological and dietary information by stomach content analysis is available. We first investigated 205 individuals of wild-shot Toyama boars with known sex, age class, localities (the eastern high latitude region vs. the western low latitude region), and season of collection. The tooth surfaces of boarlets were rougher than those of juvenile and adult animals. The decrease in surface roughness with age implied that the frequency of tooth-tooth contact, which seemed to result in cracking of enamels and thus rough surfaces, decreased after the boars started feeding on solid foods (food-tooth contact), with progressive involvement of rooting behavior in mature adults. We further found that surface roughness showed significant differences between localities, with the western Toyama boars having flatter surfaces, possibly because they were involved in more rooting and feeding on soil-contaminated rhizomes than the eastern ones, as implied by the available stomach content data. The frequency of rooting was also evident in the broader comparison among Japanese boar populations with different habitat environments. The mainland boars inhabiting deciduous broad-leaved forests had a flatter and less rough tooth surfaces than those in the subtropical evergreen broad-leaved forests of the southern islands. This corresponds to the fact that above-ground dietary resources were more abundant in the habitat of the southern island boars, where crops like succulent vegetables and fruits, as well as naturally fallen acorns, were abundant, whereas underground plant parts were the dominant diet component for the mainland boars. This study proved that DMTA can identify the difference in foraging modes in suids and make it possible to estimate the frequency of rooting, which is informative for inferring breeding methods of boars/pigs from archaeological sites.

KEYWORDS

Sus scrofa, ISO 25178, tooth wear, rooting, diets, foraging ecology, boars, pigs

Introduction

The wild boar (*Sus scrofa*) is the most widely distributed terrestrial wild mammal globally and is currently distributed throughout Eurasia and northern Africa. It has been introduced to the North and South Americas and the Oceanian islands. The wild boar is highly adaptable to local environments and shows plasticity in feeding habits. Wild boars have been an important human food resource for a long time, possibly more than several hundred thousand years (Stiner et al., 2009), and boars excavated from archaeological sites have been a particular focus of zooarchaeological research to verify the process of domestication by humans (Larson et al., 2007, 2010). In recent years, in addition to the conventional comparative anatomy of bones and teeth [e.g., Evin et al., 2013 and the references therein], attempts have been made to investigate the domestication and husbandry practices of wild boars by clarifying the feeding habits of boars excavated from archaeological sites (Minagawa et al., 2005; Vanpoucke et al., 2013; Halley and Rosvold, 2014; Yamada et al., 2021). Isotopic analyses were conducted to reveal dietary differences among wild and reared boars/pigs from excavated historical sites and clarified in part that some pigs from historical sites were raised on human refuse and not on a diet predominated by terrestrial plants, which was indicative of outspan foraging (Minagawa et al., 2005; Halley and Rosvold, 2014). On the other hand, studies on dental use-wear analysis, which analyzes the microscopic wear (microwear) formed on tooth enamel surfaces, focused not only on a diet but also on the frequency of rooting behavior (Vanpoucke et al., 2013; Yamada et al., 2021). Because rooting and foraging on grit-contaminated foods could produce characteristic dental wear (Ward and Mainland, 1999; Souron et al., 2015; Yamada et al., 2018; Lazagabaster, 2019) (see below), husbandry practices, which keep boars/pigs within stalls and restrict rooting behavior, could be inferred from dental microwear. Therefore, analysis of microwear is anticipated to reveal the transition from free-ranging to rearing within stalls, which should have occurred in the domestication process.

Dental microwear texture analysis (DMTA) is one of the dietary estimation methods and has been developed since the 2000s (Scott et al., 2005, 2006; Schulz et al., 2010). DMTA has been applied to diverse vertebrates, including mammals, reptiles, and fish (Purnell et al., 2012, 2013; DeSantis et al., 2013; Desantis and Haupt, 2014; Gill et al., 2014; Calandra and Merceron, 2016; Bestwick et al., 2019; Winkler et al., 2019). The relationship between DMT and diet derived from extant species has been used to estimate the diet of fossil species. Among them, extensive DMT data of extant herbivorous mammals have been generated and accumulated, both for wild individuals (Merceron et al., 2010, 2014; Scott, 2012; Kubo et al., 2017; Aiba et al., 2019; Arman et al., 2019; Kubo and Fujita, 2021) and laboratory-reared, diet-controlled ones (Merceron et al., 2017; Winkler et al., 2019, 2020;

Ackermans et al., 2020, 2021). DMT data of the omnivorous species, however, have not been investigated rigorously, possibly because their flexible dietary preferences make the comparisons difficult and less interpretable. Yet, a few DMT studies of boars have been conducted, comparing DMT among multiple species with different foraging ecologies (Souron et al., 2015; Lazagabaster, 2019) and among populations of the same species in different habitats (Yamada et al., 2018). In the former studies, distinct differences in DMT were found between species that frequently forage on grasses and their roots and those that are more omnivorous and feed on rhizomes, nuts, leaves, grasses, and animal matter (Souron et al., 2015; Lazagabaster, 2019). The herbivorous species had tooth surfaces with more aligned scratches and, therefore, were less complex and more homogeneous than the omnivorous species. In the latter study, three populations of the same species (*Sus scrofa*) in Japan were compared: mainland boars, which were involved in frequent rooting behavior; boars from the southern island (Iriomote Island), which are thought to have a higher consumption rate of fruits, nuts, and cultivated plants in their diets; and boars that were raised in a concrete-floored stall and fed corn hay (Yamada et al., 2018). Significant differences in DMT were found between the mainland boars and the reared boars, and the island boars were placed between them. Ward and Mainland (1999) also found the same dental microwear differences, though not by the three-dimensional DMT but by a conventional method of counting microwear features from 2D images obtained by SEM, between free-ranging and stall-fed pigs. Yamada et al. (2021) further investigated the DMT of boars/pigs from archaeological sites in the southern islands (Ryukyu Islands) of Japan. They found chronological and/or locality differences in DMT among studied populations. The differences were interpreted by possible feeding on human leftovers and rearing in floored stalls: boars/pigs having lower surface roughness might be allowed to range freely around human settlements and thus forage on underground plant resources, whereas those having higher surface roughness were expected to be kept in floored stalls and fed on softer diets, possibly provided by humans. The above DMTA studies on extant suids (Ward and Mainland, 1999; Souron et al., 2015; Yamada et al., 2018; Lazagabaster, 2019) were based on information about “known” diets of populations, though quantitative data on their diets were not provided. To supplement these studies, a study examining the relationship between DMT and diet was conducted by running feeding experiments on pigs; the pigs were fed different seed-mixed diets among the groups (Louail et al., 2021). While seed foraging was shown to be associated with DMT, the control group feeding only on soy flour, the food item which was included in the diets of other seed feeding groups, showed a large variation of DMT parameters and overlapped with other seed-feeding groups, making dietary inference from DMT more complicated. Since wild boars feed on various items at varying proportions according to seasons, it is necessary to conduct

analyses of wild populations whose diet is more clearly defined by quantitative dietary analysis. It will be a crucial step toward a more quantitative estimation of wild diets by DMTA.

In this study, we aim to solve the above problem and clarify how locality, season, and age at the culling are related to DMT for wild boars hunted in Toyama Prefecture, Japan. Stomach content analysis has already been conducted for some of the boars analyzed in this study (Yasuda and Yokohata, 2015), and the quantitative dietary data can be used to correlate with DMT. The habitat environments were different between the eastern and western regions of Toyama Prefecture (see Materials and methods Section), which caused a difference in the food habits of wild boars between the localities. We also used the DMT data of Japanese wild boars obtained by Yamada et al. (2018, 2021), aiming to conduct a broader comparison and examine the relationship between the foraging ecology and the DMT of wild boars in Japan. From the preceding DMTA and conventional microwear studies, we specifically expect that both diets and frequency of rooting are associated with DMT even at finer scales among Japanese wild boars, aiming at providing a more solid background when discussing boar husbandry practice in the zooarchaeological context.

Materials and methods

Sus scrofa population from Toyama Prefecture

We used 205 individuals of wild boars collected by nuisance culls in Toyama Prefecture, central western Japan (Figure 1). The nuisance cull was done year-round, and sex, date of collection, and localities were recorded. In the present study, the boars were divided into two localities, i.e., the eastern and western Toyama, which were separated by the Jinzu River running across Toyama Prefecture in the north-south direction (Figure 1). The geological and environmental settings of the two localities were contrasting. The eastern region was characterized by high elevation areas (altitude of ca. 100–2,000 m) with natural vegetation of cool-temperate deciduous broad-leaved forest and secondary forest. On the other hand, the western region was in lower elevation areas (altitude of ca. 100–500 m), and both secondary and planted coniferous forests showed a mosaic distribution. Agricultural fields (rice and other crops) were more widely distributed in the western region. Mean annual temperature and annual precipitation were 11.8°C and 3020.7 mm for the eastern Toyama (Kamiichi-machi, 36°40′20″ N, 137°25′40″ E) and 13.4°C and 2597.3 mm for the western Toyama (Nanto-shi, 36°32′70″ N, 136°52′30″ E). The number of specimens used in the present study is given in Table 1.

The boars' age at death (in months) was assessed by tooth eruption and wear status according to the method of Koderá et al. (2012). Subsequently, we classified them into

three age classes: adults (older than 20 months), juveniles (12–20 months), and boarlets (younger than 12 months). The season of death was classified into spring (March, April, and May), summer (June, July, and August), autumn (September, October, and November), and winter (December, January, and February). Among the 205 individuals, the stomach contents of 36 wild boars were investigated (Yasuda and Yokohata, 2015). The dried weight of stomach contents was weighed for four dietary categories: above-ground plant parts (leaves and stems), underground plant parts (rhizomes, tubers, and roots), nuts, and rice. In the current samples, animal matters (vertebrates and invertebrates) were minor components; therefore, the boars in Toyama Prefecture had herbivorous feeding habits in general, similar to other Japanese mainland populations (Asahi, 1975; Koderá et al., 2013). The proportion of each category (weight of the dietary item/total weight of analyzed stomach content) was calculated, and the category that accounted for the largest part of stomach content was identified for each boar. Table 1 includes the number of samples of stomach content analysis, and the proportion of each dietary item in percent (%) is provided in Supplementary Table S1. Figure 1 includes bar charts showing the difference in stomach content between the eastern and western regions. All the skull specimens are stored in the Faculty of Science, University of Toyama.

Molding and obtaining microwear texture data

Dental impressions were obtained from the occlusal enamel surfaces of the lower 4th deciduous premolar (dp4) and the lower 1st, 2nd, or 3rd permanent molars. Following Souron et al. (2015) and Yamada et al. (2018, 2021), we investigated the lingual enamel bands (facets 1, 3, 5, and 7 in Figure 2), which act as Phase I shearing facets during mastication. When the lingual enamel band was broken ($N = 42$), we used the buccal enamel bands (facets 2, 4, 6, 8, and 10 in Figure 2). In the present dataset, we did not observe any significant differences in DMT parameters between the lingual and buccal enamel bands (see Supplementary Figure S1), therefore we combined the data from different enamel bands. Molding was conducted following the methodology of Kubo et al. (2017), in which the tooth occlusal surfaces were cleaned with cotton swabs soaked with acetone, and molds were taken using high-resolution A-silicone dental impression material (Dr. Silicon regular type, BSA Sakurai, Japan). We used a confocal laser microscope (VK-9700, Keyence, Japan) equipped with a 100 × long-distance lens ($N.A. = 0.95$) to scan the occlusal impressions. It uses a violet laser, and its wavelength is 408 nm. Generated 3D microwear texture data had point clouds with lateral (x, y) sampling with an interval of 0.137 μm and a vertical resolution (z) of 0.001 μm (the nominal value from the brochure). The field of view was 140

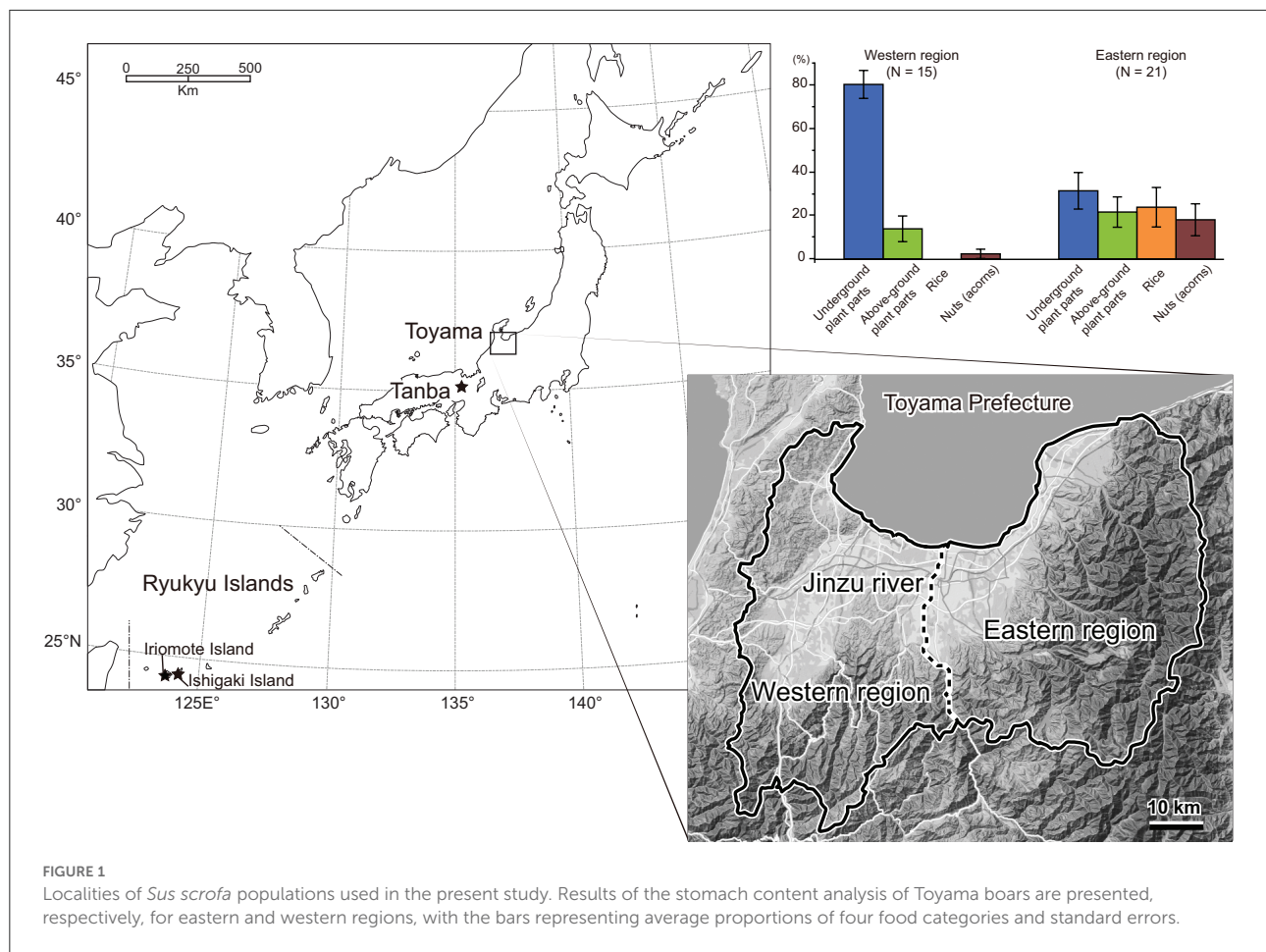


FIGURE 1

Localities of *Sus scrofa* populations used in the present study. Results of the stomach content analysis of Toyama boars are presented, respectively, for eastern and western regions, with the bars representing average proportions of four food categories and standard errors.

TABLE 1 The number of *Sus scrofa* specimens used in the present study.

Locality	Number of specimens used for DMTA															Source of DMT data	
	Boarlet					Juvenile					Adult						Unknown age
	Sp	Su	A	W	Total	Sp	Su	A	W	Total	Sp	Su	A	W	Total		
Eastern	8	9	30	24	71	1	11	7	6	25	4	5	5	18	32	This study	
Toyama	(0)	(0)	(7)	(1)	(8)	(0)	(0)	(4)	(2)	(6)	(0)	(0)	(3)	(4)	(7)		
Western	14	15	10	10	49	0	6	1	5	12	5	3	1	7	16	This study	
Toyama	(1)	(0)	(0)	(5)	(6)		(1)	(0)	(1)	(2)	(2)	(0)	(1)	(4)	(7)		
Tanba										4					9	Yamada et al., 2018	
Iriomote Island										5					4	Yamada et al., 2018	
Ishigaki Island															23*	Yamada et al., 2021	
Stall-fed										11						Yamada et al., 2018	

For the Tanba, Ishigaki, Iriomote, and stall-fed populations, we used the original surface scan data from Yamada et al. (2018, 2021). Abbreviations for seasons are Sp, spring; Su, summer; A, autumn; W, winter. The numbers in parentheses for Toyama boars are the sample size of the stomach content analyses.

*The age class of Ishigaki boar was not shown in Yamada et al. (2021), but the tooth surface data were obtained from either lower 1st or 2nd molars. Therefore, they were obtained from either juveniles or adults.

The numbers in parentheses for Toyama boars are the sample size of the stomach content analyses.

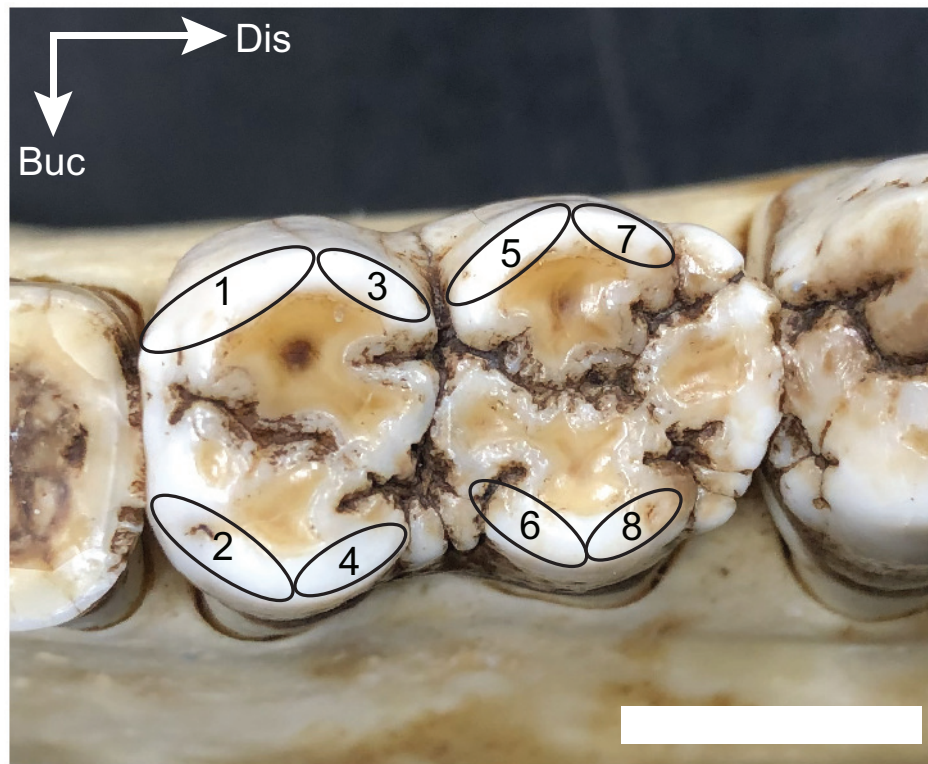


FIGURE 2

The occlusal surface of the left lower second molar and nomenclature of enamel bands. This study scanned the lingual enamel bands (facets 1, 3, 5, and 7). In case the lingual enamel bands were broken, we used the buccal enamel bands (facets 2, 4, 6, and 8). The scale bar is 10 mm. Abbreviations for orientation are Buc, buccal; Dis, distal.

$\times 105 \mu\text{m}$. We scanned four adjacent fields and combined them into one large field by using VK Assembler software (Keyence, Japan). The total acquired area was smaller than $280 \times 210 \mu\text{m}$ due to overlaps between adjacent fields and thus variable among the specimens. After trimmed into $208 \times 144 \mu\text{m}$ in size (see “Processing 3D surfaces and calculation of DMT parameters” below), DMT parameters were calculated from these combined fields by using surface roughness software (Mountains Map, Imaging Topography, ver. 9. 0. 9733, Digital Surf, France).

Comparative DMT data of extant *Sus scrofa* populations from Japan

Yamada et al. (2018, 2021) compared DMT data of extant and archaeological *S. scrofa* populations from Japan. We utilized the scan data of the four extant populations:

a wild mainland population from the Tanba region, Hyogo Prefecture, central Japan (hereafter referred to as Tanba), reared individuals in a concrete-floored stall (stall-fed), and two wild populations from the Ryukyu Islands (Iriomote Island and Ishigaki Island). Detailed information on these populations is given in Yamada et al. (2018, 2021), and dietary characteristics are summarized below. The boars from the Tanba population inhabited deciduous broad-leaved forests and fed mainly on roots, barks, and rhizomes during the winter season (Asahi, 1975). The boars from Iriomote Island lived in subtropical evergreen broad-leaved forests and consumed roots, rhizomes, fruits, and nuts throughout the year (Ishigaki et al., 2007). The boars from Ishigaki Island were not investigated in their feeding habits, but they also lived in subtropical evergreen broad-leaved forests and fed on crops (Ishigaki City, 2021). Both Iriomote and Ishigaki Island boars were known to feed on crops such as pineapples, bananas, mandarin oranges, sugar canes,

TABLE 2 Names and definitions of 30 parameters of ISO 25178-2.

Parameter	Description	Unit
Sq	The standard deviation of the height distribution	μm
Ssk	The skewness of the height distribution	no unit
Sku	Kurtosis of the height distribution	no unit
Sp	Maximum peak height, height between the highest peak and the mean plane	μm
Sv	Maximum pit height, depth between the mean plane and the deepest pit	μm
Sz	Maximum height is the sum of the maximum peak height and the maximum pit height ($Sp + Sv$)	μm
Sa	Arithmetic mean height	μm
Smr	Areal material ratio, the ratio of the area of the material at a specified height c ($c = 1 \mu\text{m}$ under the highest peak)	%
Smc	Inverse areal material ratio, height at which a given areal material ratio ($p = 10\%$)	μm
Sxp	Peak extreme height, difference in height between the p and q material ratio ($p = 50\%$, $q = 97.5\%$)	μm
Sal	Autocorrelation length ($s = 0.2$)	μm
Sdq	Root mean square gradient	no unit
Sdr	The developed interfacial area ratio	%
Vm	Material volume at a given material ratio ($p = 10\%$)	$\mu\text{m}^3/\mu\text{m}^2$
Vv	Void volume at a given material ratio ($p = 10\%$)	$\mu\text{m}^3/\mu\text{m}^2$
Vmc	Material volume of the core at a given material ratio ($p = 10\%$, $q = 80\%$)	$\mu\text{m}^3/\mu\text{m}^2$
Vvc	Void volume of the core ($p = 10\%$, $q = 80\%$)	$\mu\text{m}^3/\mu\text{m}^2$
Vvv	The void volume of the dale at a given material ratio ($q = 80\%$)	$\mu\text{m}^3/\mu\text{m}^2$
Spd	Density of peaks	$1/\mu\text{m}^2$
Spc	Arithmetic mean peak curvature	$1/\mu\text{m}$
$S10z$	Ten-point height	μm
$S5p$	Five-point peak height	μm
$S5v$	Five-point pit height	μm
Sda	Closed dale area	μm^2
Sha	Closed hill area	μm^2
Sdv	Closed dale volume	μm^3
Shv	Closed hill volume	μm^3
Sk	distance between the highest and lowest level of the core surface	μm
Spk	the average height of the protruding peaks above the core surface	μm
Svk	The average height of the protruding dales below the core surface	μm

and sweet potatoes (Ishigaki et al., 2007; Ishigaki City, 2021). The stall-fed boars were fed mainly on corn. Except for the Ishigaki population, the age at death in months was estimated by Yamada et al. (2018) following the method of Hayashi et al. (1977). There was a good correspondence between the methodologies of Hayashi et al. (1977) and Kadera et al. (2012). Therefore, the estimated ages were comparable to the Toyama populations. The number of specimens used for comparative analysis is shown in Table 1. Using a modified analytical template of the newer version of the software (Mountains Map) after the publications of Yamada et al. (2018, 2021), we reanalyzed the original scan data obtained by Yamada et al. (2018, 2021) rather than compared it to the published DMT parameter values. The method for obtaining 3D surfaces by Yamada et al. (2018, 2021) was identical to that was applied for the Toyama boars: i.e., the same tooth types and facets were scanned by the same laser microscope with the same settings; therefore, the DMTA

data are directly comparable after the application of the newer analytical template.

Processing 3D surfaces and calculation of DMT parameters

All the 3D surface data were processed following the procedures of Yamada et al. (2018) and Aiba et al. (2019) by Mountains Map Imaging Topography. The scanned impressions were mirror images of the actual tooth surfaces. Therefore, the coordinates were mirrored in the x- and z-axes. The surfaces were then leveled *via* the least-square plane by subtraction to remove the inclination of the molds, and a robust Gaussian filter was applied with a cutoff value of $0.8 \mu\text{m}$ to remove measurement noise (S-filter as defined in ISO 25178-2). The form removal function (polynomial of increasing power = 2)

was utilized to remove the large-scale curvature of the enamel bands (*F*-operation in ISO 25178-2). Because measurement noise appeared as spikes on the surface, we applied the automated outlier removal function, which removes any features with a slope of $> 80^\circ$ and a threshold that removes the upper and lower 0.1% of the data. These non-measured points were subsequently filled using the smoothing function of the Mountains Map. This workflow was similar to that of the preceding DMTA research (Arman et al., 2016; Kubo et al., 2017), but the difference was in filtering: i.e., a robust Gaussian with a $0.8\ \mu\text{m}$ threshold was used in the present study, whereas single, double, and triple usage of spline, Gaussian, and robust Gaussian filters with different threshold values were used in previous studies (Arman et al., 2016; Kubo et al., 2017). Finally, the scanned areas were trimmed to $208 \times 144\ \mu\text{m}$ to standardize the area size. After the above procedures, 30 parameters of ISO 25178-2 were calculated. The names and definitions of the parameters are shown in Table 2.

Statistical analyses

We conducted a principal component analysis (PCA) to summarize the 30 parameters into a few interpretable components. The PCA was applied to the whole dataset ($N = 261$). In the following statistical analyses, we focused on the principal components. Since the normal distribution of the principal components was rejected by the Shapiro–Wilk test ($P < 0.05$, see Supplementary materials), we transformed them using Johnson’s *Su* distribution to fulfill the normality. Hereafter, the transformed principal components are referred to as PCs for simplicity.

First, we compared PC1, PC2, and PC3 among Toyama boars to test the relationships between dietary and ecological characteristics and DMT. The following hypotheses were tested: (1) there are significant differences among the dietary groups based on the stomach contents, (2) there is an ontogenetic change in DMT from boarlets to adults, and (3) there are significant differences between localities (eastern Toyama vs. western Toyama) and among seasons of collection in DMT. In the first analysis, we conducted an ANOVA comparing the four dietary categories using 36 individuals with data on stomach contents: above-ground plant parts, $N = 7$; underground plant parts, $N = 21$; nuts, $N = 3$; and rice, $N = 5$. Due to the scarcity of samples, we grouped both localities, seasons, and age classes. In the second and third analyses, we used the whole Toyama dataset ($N = 205$) and conducted a stepwise model selection with the PCs being the response variables and age class, locality, season, and their interaction terms (age class*locality, age class*season, locality*season, and age class*locality*season) being the explanatory variables. Since we did not find a consistent difference between adults and juveniles in PCs (the Tukey–Kramer test, $P > 0.05$), we used a dichotomous age

TABLE 3 The factor loadings from the PCA of 30 ISO 25178-2 parameters.

Parameter	PC1	PC2	PC3
<i>Sq</i>	0.94491	0.23792	−0.08922
<i>Ssk</i>	−0.04061	0.30561	−0.83249
<i>Sku</i>	−0.07864	−0.36458	0.71585
<i>Sp</i>	0.90227	0.04394	−0.18948
<i>Sv</i>	0.89798	−0.07368	0.29806
<i>Sz</i>	0.96874	−0.02356	0.08975
<i>Sa</i>	0.92533	0.26467	−0.15181
<i>Smr</i>	−0.52860	−0.06517	0.00448
<i>Smc</i>	0.90078	0.30132	−0.22015
<i>Sxp</i>	0.91367	0.09729	0.17192
<i>Sal</i>	0.16170	0.48160	−0.24314
<i>Sdq</i>	0.84296	−0.49282	−0.08509
<i>Sdr</i>	0.83481	−0.48088	−0.11054
<i>Vm</i>	0.71334	0.20988	−0.27369
<i>Vv</i>	0.90253	0.30107	−0.22343
<i>Vmc</i>	0.89635	0.28138	−0.19591
<i>Vvc</i>	0.87386	0.32185	−0.28150
<i>Vvv</i>	0.85723	0.04733	0.30025
<i>Spd</i>	−0.39962	−0.63749	−0.28188
<i>Spc</i>	0.83996	−0.22180	−0.06605
<i>S10z</i>	0.85811	−0.33164	0.09577
<i>S5p</i>	0.78107	−0.30319	0.00562
<i>S5v</i>	0.83011	−0.31971	0.16049
<i>Sda</i>	0.40833	0.53991	0.40586
<i>Sha</i>	0.13575	0.72509	0.39891
<i>Sdv</i>	0.39155	0.28338	0.39700
<i>Shv</i>	0.29101	0.45430	0.53937
<i>Sk</i>	0.83817	−0.24701	−0.02094
<i>Spk</i>	0.83146	−0.45346	−0.00272
<i>Svk</i>	0.80094	−0.43389	0.10264

The absolute values larger than the threshold value (0.4) were shown in bold.

class (adult/juvenile vs. boarlet). We used Akaike’s information criterion for a small sample size (AICc) for model selection. The model was significantly different when the ΔAICc was > 2 . The model with the lowest AICc value and all included explanatory variables being statistically significant was selected as the best model (Burnham and Anderson, 1998).

Second, we compared the PCs of Toyama populations with other wild boar populations and the stall-fed ones. For this comparison, we only used juvenile and adult individuals of Toyama boars with combined collection seasons. We conducted a one-way ANOVA followed by pairwise comparisons with the Tukey–Kramer tests. All the statistical analyses were conducted with the statistical software JMP (ver 16.2, SAS Institute Inc., USA).

TABLE 4 Descriptive statistics of PCs of investigated boar populations.

Locality	Age class	Number of specimens	PC1		PC2		PC3	
			Mean	S.D.	Mean	S.D.	Mean	S.D.
Eastern Toyama	Adult/Juvenile	57	−0.307	0.793	0.137	1.036	0.127	0.941
	Boarlet	71	0.324	0.722	0.449	0.924	−0.229	1.122
Western Toyama	Adult/Juvenile	28	−0.903	0.719	−0.142	0.804	0.014	1.013
	Boarlet	49	−0.180	0.936	0.114	0.869	−0.362	0.889
Tanba	Adult/Juvenile	13	−0.570	0.928	−0.026	0.769	0.244	1.161
Iriomote Island	Adult/Juvenile	9	0.581	1.077	−0.813	1.317	0.401	0.853
Ishigaki Island	N.A.*	23	0.664	0.634	−0.863	0.944	0.537	1.034
Stall-fed	Juvenile	11	1.797	1.086	−1.223	1.073	0.026	0.869

*The age class of Ishigaki boar was not shown in Yamada et al. (2021), but the tooth surface data were obtained from either lower 1st or 2nd molars. Therefore, they were obtained from either juveniles or adults.

Results

Principal component analysis of DMT parameters

According to PCA of 30 ISO 25178-2 parameters, the first, second, and third PCs explained about 55.5, 12.7, and 9.2% of the total variance, respectively. Table 3 presents the factor loadings of the parameters. The first component (PC1) can be interpreted as the overall surface roughness or size of microwear features, as most of the height (e.g., *Sq*: standard deviation of the height distribution, *Sp*: maximum peak height, and *Sa*: arithmetic mean height) and volume parameters (e.g., *Vv*: void volume at a given material ratio, *Vmc*: material volume of the core at a given material ratio, and *Vvc*: void volume of the core) showed large values of the loadings. These were positively loaded; therefore, larger PC1 values indicated greater surface relief. The parameters which exerted a strong influence on the second component (PC2) are those which are related to surface segmentation. *Sda* (closed dale area) and *Sha* (closed hill area) have large positive loadings, whereas *Spd* (density of peaks) has a negative loading value. This indicates that larger values of PC2 represent tooth surfaces segmented into larger hills and dales, resulting in a lower number of segments (i.e., low density of peaks). The negative factor loadings of *Sdr* (developed interfacial area ratio) and *Sdq* (root mean square gradient) are related to the fineness of surface features, with the larger values indicating the dominance of finer features, are concordant to this interpretation. The third component (PC3) is related to height distribution. *Ssk* (skewness of the height distribution) and *Sku* (kurtosis of the height distribution) show large factor loadings. Therefore, the larger value of PC3 indicates the height distribution of the surface is skewed to a high elevation with the pointed peaks and valleys.

All the raw parameter values and PC scores are included in Supplementary Table S1. The descriptive statistics of PCs are presented in Table 4.

Correlation between stomach contents and DMT in Toyama boars

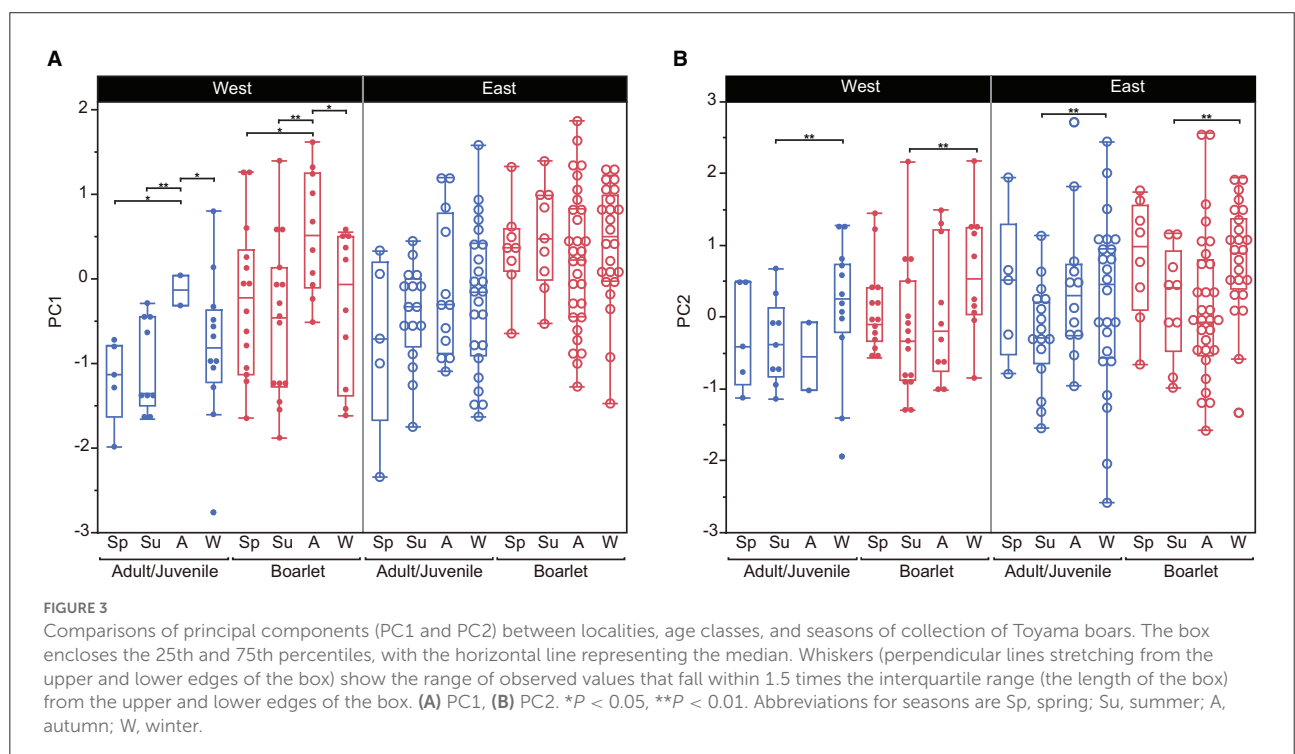
There are no significant differences in any of the PCs among the four dietary groups defined by stomach content analysis [one-way ANOVA; PC1: $F_{3,32} = 0.26$, $P = 0.85$; PC2: $F_{3,32} = 0.10$, $P = 0.96$; PC3: $F_{3,32} = 1.51$, $P = 0.23$; Supplementary Figure S2], refuting the correlation between the stomach content and DMT parameters in Toyama boars at the individual level.

Factors responsible for the variation of PCs in Toyama boars

We selected the best models explaining the variation of PC1–3 by stepwise model selection using AICc (Supplementary Table S2). The best model for PC1 includes four explanatory variables: age class, locality (east or west), season, and interaction of locality*season, whereas that for PC2 shares the same variables but lacks the interaction term (locality*season). On the other hand, only age class and season are included in the best model for PC3. The parameter estimates of the best models for PC1, PC2, and PC3 are presented in Table 5. These results indicate habitat-related differences in DMT are reflected in PC1 and PC2 but not in PC3. Considering the fact that PC3 contributed a smaller amount of total variation (9.2%) than PC1 and PC2, in the following analyses,

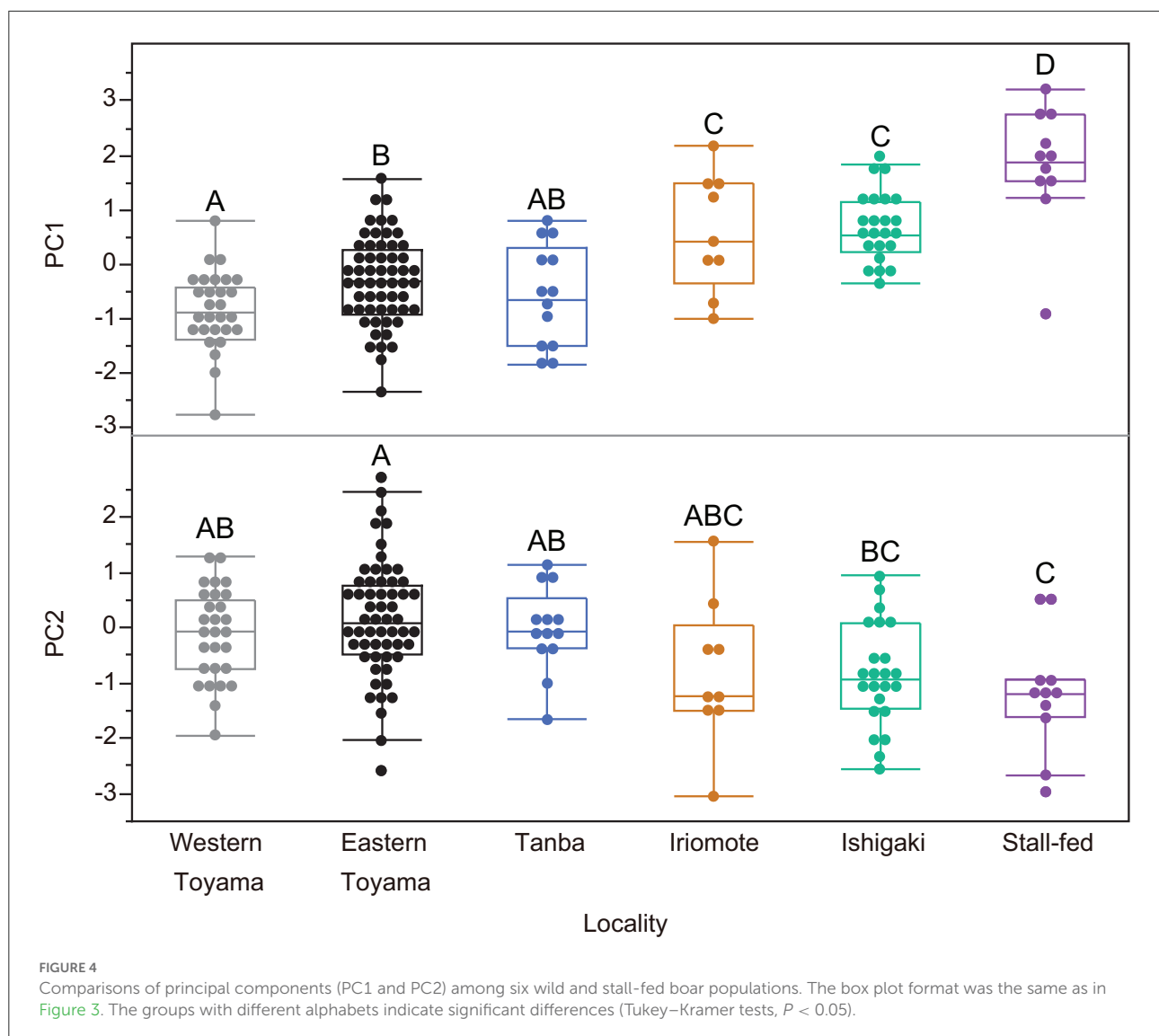
TABLE 5 Parameter estimates of the best models for PC1, PC2, and PC3.

	Parameter	Estimate	S.E.	<i>t</i> -value	<i>P</i> -value
PC1	Intercept	−0.23	0.06	−3.77	< 0.001
	Locality [East]	0.21	0.06	3.48	< 0.001
	Age class [Adult/Juvenile]	−0.32	0.06	−5.53	< 0.0001
	Season [Spring]	−0.16	0.12	−1.42	0.16
	Season [Summer]	−0.15	0.10	−1.52	0.13
	Season [Autumn]	0.33	0.11	3.04	< 0.01
	Locality [East]*Season [Spring]	0.04	0.12	0.39	0.70
	Locality [East]*Season [Summer]	0.17	0.10	1.72	0.09
	Locality [East]*Season [Autumn]	−0.33	0.11	−3.01	< 0.01
PC2	Intercept	0.12	0.07	1.78	0.08
	Age class [Adult/Juvenile]	−0.16	0.07	−2.37	0.02
	Season [Spring]	0.12	0.13	0.89	0.37
	Season [Summer]	−0.28	0.11	−2.46	0.01
	Season [Autumn]	−0.12	0.11	−1.01	0.31
	Locality [West]	−0.15	0.07	−2.16	0.03
	Locality [East]	0.04	0.07	0.57	0.58
PC3	Intercept	−0.09	0.07	−1.26	0.21
	Age class [Adult/Juvenile]	0.21	0.07	2.85	< 0.01
	Season [Spring]	0.19	0.14	1.35	0.18
	Season [Summer]	−0.37	0.12	−3.02	< 0.01
	Season [Autumn]	0.05	0.12	0.39	0.70



we only focused on PC1 and PC2. PC1, the proxy of overall surface roughness or size and depth of microwear features, is significantly larger in boarlets than adults/juveniles and larger in eastern Toyama than in western Toyama. Seasonal differences

were detected only in western Toyama. In both age classes, the individuals collected in autumn showed significantly higher PC1 scores than in other seasons (Figure 3A). PC2 is the proxy of surface fineness, with larger values indicating that the surfaces



were segmented into larger hills and dales. The parameter estimate of age class “adult/juvenile” has a negative value on PC2 (Table 5), which means the tooth surfaces of adult/juvenile are characterized by fine features. The differences between localities are also statistically significant, with the boars in the western region having lower PC2 scores (i.e., finer microwear features) than those in the eastern region. There is a significant seasonal difference only between summer and winter, i.e., the tooth surfaces of individuals collected in summer have finer features (Figure 3B).

Comparisons of Toyama boars with other wild and stall-fed boar populations

After we combined all seasons for the east and west Toyama populations, a one-way ANOVA was conducted to

test for differences among the six boar populations. Both PC1 and PC2 are significantly different among the populations [PC1: $F_{(5, 135)} = 24.26$, $P < 0.0001$; PC2: $F_{(5, 135)} = 6.53$, $P < 0.0001$; PC3: $F_{(5, 135)} = 0.95$, $P = 0.44$]. Subsequent pairwise comparisons by the Tukey-Kramer method reveal both disparities and similarities among the populations (Figure 4). There is an explicit difference in PC1: the stall-fed boars display the highest PC1 scores, followed by two southern island populations (Iriomote and Ishigaki populations) and three mainland populations (eastern and western Toyama and Tanba). On the other hand, PC2 scores of groups overlap each other except for the stall-fed and eastern Toyama populations (Figure 4). A scatter plot of PC1 and PC2 illustrates the similarity between populations (Figure 5). The three mainland populations (eastern and western Toyama and Tanba) overlap each other, whereas the two island populations and the stall-fed show considerable overlap. The overlap between the mainland

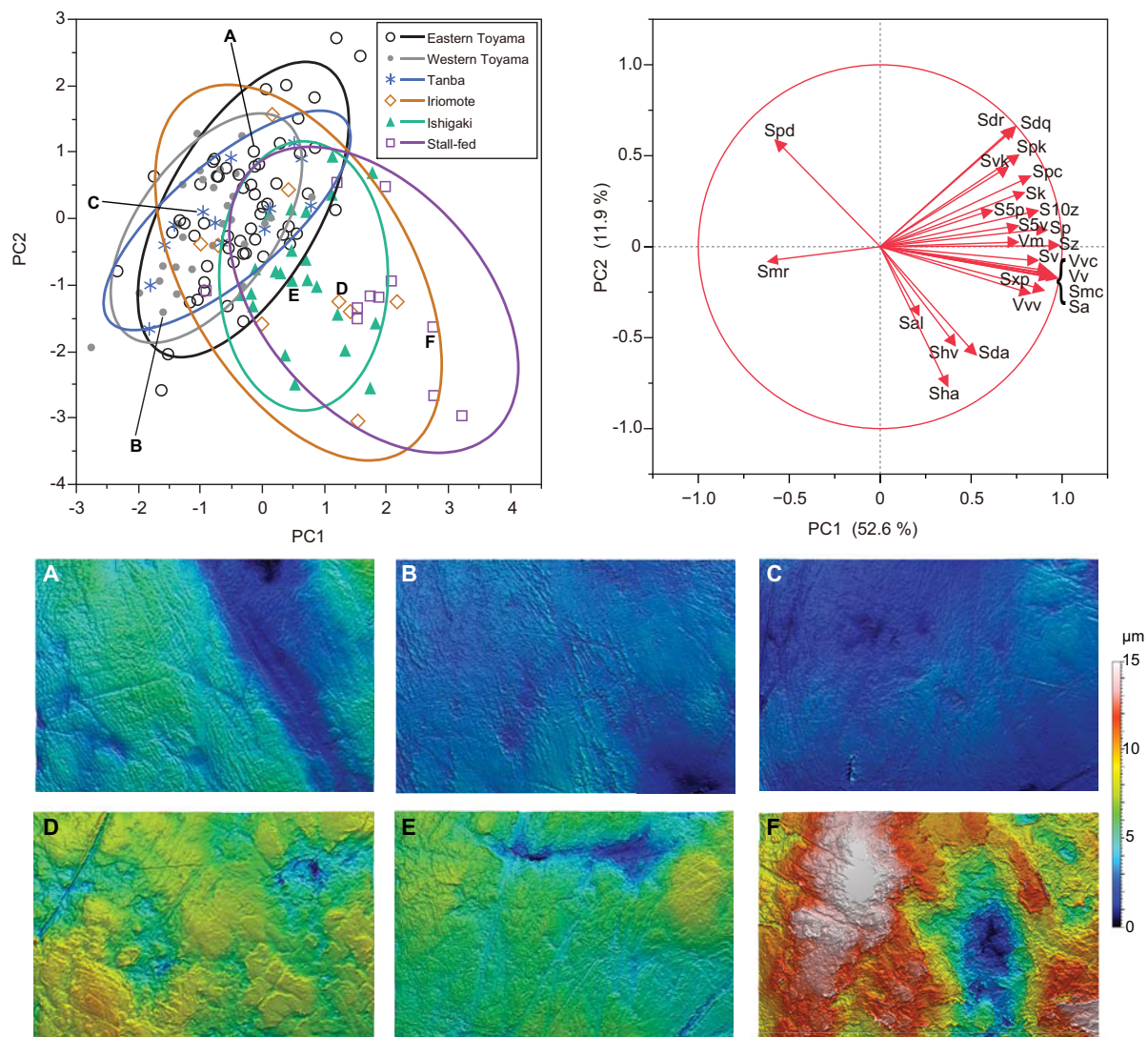


FIGURE 5

A scatter plot of PC1 and PC2 accompanied by the representative 3D surface models of wild and stall-fed boars. The 90% confidence ellipse is drawn for each population. DMTA variables with factor loadings higher than 0.4 in absolute values are shown as arrows in vector mapping. Surface models are presented with the same height (z) scale. (A) Eastern Toyama (2008S-45), (B) western Toyama (2007S-11), (C) Tanba (No. 75q), (D) Iriomote Island (M31148), (E) Ishigaki Island (OPM-102), (F) stall-fed (Ishii-16).

populations and the island ones is relatively small. This is exemplified by the representative 3D surface models (Figure 5). The boars from the mainland populations have overall flat and homogeneous surfaces with abundant scratches (Figures 5A–C), and the island populations have more heterogeneous surfaces with high relief (Figures 5D,E). The stall-fed individuals show high relief with heterogeneity (Figure 5F).

Discussion

Through the intensive sampling of wild-shot boars in Toyama Prefecture and comparison to other wild and stall-fed populations, this study clarified the difference in DMT

of *S. scrofa*, both at the finer and broader geographical scales. In the following discussion, we start with the comparison between geographically and ecologically different populations, then continue to the discussion on DMT differences observed within Toyama boars.

Variation among the wild boar populations in different habitat environments

As shown in Figures 4, 5, the DMT of six populations showed differentiation among the ecologically different groups,

i.e., those in temperate deciduous broad-leaved forests (eastern and western Toyama and Tanba), those in subtropical evergreen broad-leaved forests (Ishigaki and Iriomote Islands), and stall-fed, and similarity within each group. The stall-fed boars have the largest PC1 scores, shown on their tooth surfaces with large and deep depressions (Figure 5F). As discussed in Yamada et al. (2018), the characteristic tooth surfaces of the stall-fed boars resulted from their feeding on corn hay in the concrete-floored stall. Crushing of hard seeds without contamination of soils is responsible for their extremely rough tooth surfaces. On the other hand, the boars from deciduous broad-leaved forests had flatter tooth surfaces with abundant scratches (Figures 5A–C). As discussed in previous studies (Ward and Mainland, 1999; Souron et al., 2015; Yamada et al., 2018), this reflects the frequent rooting of these populations. In addition to feeding on rhizomes and roots, above-ground plant parts, like bamboo shoots in spring and leaves and stems of dicots and monocots from spring to summer, were important food items for mainland boars in deciduous forests (Kodera et al., 2013; Yasuda and Yokohata, 2015). The shearing of tough and fibrous plant tissues causes dental wear with numerous scratches and more homogeneous tooth surfaces in primates (Grine and Kay, 1988; Scott et al., 2005). Therefore, it is expected that both feedings on soil-contaminated underground storage organs and fibrous above-ground plant tissues caused relatively flat and homogeneous tooth surfaces of the mainland boar populations.

Contrary to the results of Yamada et al. (2018), in which they did not find statistically significant differences between the island boars in subtropical evergreen broad-leaved forests and the stall-fed ones, we found significant differences between the two groups (Figure 4). This is probably due to our current statistical procedure, transforming PC scores to achieve normality and using parametric tests, which are more sensitive to detecting the differences than the non-parametric tests (Wilcoxon rank-sum tests) applied by Yamada et al. (2018) for most of the ISO parameter comparisons. Both island populations were not significantly different in PC scores, and their PC1 values were located between the stall-fed and the mainland populations. Based on the limited information on the feeding habits of the island boars, they feed on fruits, seeds, nuts, and crops throughout the year (Ishigaki et al., 2007; Ishigaki City, 2021). Therefore, it is expected that their mode of mastication was more inclined to crushing hard objects and pulping the succulent vegetable tissues, both of which would cause more pitted tooth surfaces. The boars from the southern islands might also be involved in rooting and feeding on leaves and stems, but the high availability of nutritionally preferred foods (fruits, seeds, and crops) in their habitats might offer them more opportunities for feeding on these items.

Variation in DMT in Toyama boars and its interpretation

In the current samples of Toyama boars, for which stomach contents were analyzed ($N = 36$), we did not find a clear relationship between DMT and the dietary groups defined by the major items in the stomach contents. This is not surprising because of the opportunistic feeding of the boars and the different timescales at which the two dietary signals are recorded (Davis and Pineda Munoz, 2016). Through experimental feeding trials, Winkler et al. (2020) estimated how long the turnover of DMT takes place in laboratory-reared rats. It was shown to be ~16–24 days, after which the later diets overwrote dietary signals. Therefore, the association between the stomach contents (the “last supper”) and DMT should not be apparent unless the animals had continuously been fed on the same diet for a while. In addition, the sample size of stomach content analysis might not be large enough to average and represent the dietary groups, failing to detect the group differences.

The differences between the two localities (eastern vs. western Toyama) are notable. The boars in the west of the Toyama region showed lower PC1 values than those from the eastern region (Figure 3A, Table 5), even in the broader comparison with other populations (Figure 4). This indicates that the boars in the eastern region have overall rougher tooth surfaces than the western boars. Though we did not find a direct association between the stomach content and DMT at the individual scale, this regional difference can be interpretable from the viewpoint of the habitat environment and feeding habits. Nakajima and Kobayashi (2014) investigated the distribution of forest types in Toyama Prefecture and reported that in the eastern region, natural forests, secondary forests, and planted forests tend to be distributed sequentially in this order from the mountainous areas to the low elevation areas, whereas in the western region, these different forests show a mosaic distribution. The Toyama boars preferably consumed rhizomes of Japanese yam (*Dioscorea japonica*) and kudzu (*Pueraria lobata*) (Yasuda and Yokohata, 2015), which are more abundant in the secondary forests. Due to the mosaic distribution of the secondary forest in the western region, the boars could use the secondary forests frequently. Together with the current data of stomach content analysis (Figure 1), it suggests that the boars in the western region were involved in more frequent rooting during foraging, possibly in the secondary forests, which resulted in a flatter and more homogeneous tooth surfaces, presumably by the abrading effect of grit as suggested by Souron et al. (2015). On the other hand, the boars in the eastern region foraged on the four dietary categories in approximately equal amounts (Figure 1). A higher rate of nut consumption compared to the western boars is notable, and this corresponds to the

distribution of acorn-bearing trees (*Fagus crenata*, *Quercus crispula*, and *Quercus serrata*) in the eastern region (Nakajima and Kobayashi, 2014). Feeding on acorns requires a high bite force for crushing kernels, which may induce the generation of large pits (Scott et al., 2005; Ungar et al., 2008; Daegling et al., 2011). In addition, rice husks were abundantly detected in the stomachs of some eastern Toyama boars (Yasuda and Yokohata, 2015). Ramdarshan et al. (2016) pointed out by their experimental feeding that the highest surface complexity was observed in a group of ewes fed with clover and barley. Therefore, it is possible that ingestion of rice husks may cause strong abrasive wear. These food items might be potential causes of the higher surface roughness in the eastern boars during the seasons when they were available (summer and autumn for rice and autumn and winter for acorns). Acorns were utilized by boars until mid-winter (December) but might disappear in late winter (Yasuda and Yokohata, 2015).

The seasonal difference in PC1 was detected only in the western region (Figure 3A, Table 5). The western boars culled in autumn showed significantly rougher tooth surfaces than those culled in other seasons. The PC1 scores of the autumn-culled individuals from the western region are comparable to those of the eastern boars: both western boarlets and juveniles/adults culled in autumn show higher PC1 scores than western boars in other seasons, but their values are similar to those of the eastern boars (Figure 3A). That means the western boars show overall less rough surfaces than the eastern boars, but the surface roughness increases to the level of the eastern boars in autumn. Therefore, it is possible that in the autumn season, the boars in the western region are involved in less rooting than in other seasons and might more frequently feed on acorns and rice, which are mostly available in autumn. Intensive rooting and feeding on underground plant parts in winter might quickly reduce the roughness of the surface in western boars.

We found significant differences between the age classes (adult/juvenile vs. boarlet). The tooth surfaces of boarlets are characterized by larger and deeper microwear features and are segmented into larger hills and dales (i.e., coarser surface texture) than adults and juveniles. This may reflect a higher frequency of tooth-tooth (= attrition) contact, which seemed to result in cracking of enamels and thus rough surfaces in sucklings and weanlings. After the boars start feeding on solid foods, food-tooth (= abrasion) contact becomes predominant and decreases overall surface roughness (i.e., flatter tooth surfaces). It is possible that progressive involvement of rooting behavior in adults also reduces surface roughness due to a polishing effect of contaminated soils. This perspective, i.e., rough and non-homogeneous tooth surfaces by frequent tooth-tooth contacts, would explain why the stall-fed boars (Yamada et al., 2018 and data shown in Figure 4) and the pigs experimentally fed on flour as the control feeding group (Louail et al., 2021) have similarly rough tooth surfaces.

We provided the first evidence of significant differences in DMT reflecting the frequency of rooting and foraging on underground plant parts at scales finer than interspecific comparisons, i.e., among populations in ecologically diverse habitats in Japan and even between geographically close but slightly different habitats. Therefore, the current data can be a reference for the foraging ecology of excavated boars/pigs from archaeological sites. As boar skeletal remains are abundantly yielded from Holocene archaeological sites in Japan (Nishimoto, 1994), investigation of DMT of these dental boar remains will shed light on their palaeoecology and human–animal relationships that have changed through time.

Further technical considerations of DMTA

We used 30 ISO 25178-2 parameters and resultant PCs in this study to detect DMT differences among boar populations. Though PCA successfully extracted the trends in DMT, further application of scale-sensitive fractal analysis (SSFA) would be beneficial for evaluating the more heterogeneous tooth surfaces of suids (Souron et al., 2015; Lazagabaster, 2019; Louail et al., 2021). This is reserved in the present study because of our past experiences based on ruminant DMTA, in which we found SSFA was less powerful in detecting dietary differences (Kubo et al., 2017; Kubo and Fujita, 2021), and the fact that analytical software formerly used in SSFA (Toothfrax or Sfrax) and the SSFA module now integrated into MountainsMap produce significantly different values (Calandra et al., 2021). Reanalysis of published DMT of suids analyzed by older SSFA software is mandatory when integrative comparisons are made.

Another technical issue is the replication of surface scans from the same tooth facet. In the present study, we used four single scans of $140 \times 100 \mu\text{m}$ and combined them into a larger area of $208 \times 144 \mu\text{m}$. It is equivalent to the commonly used total scan size (e.g., Scott et al., 2012: single scan size of $102 \times 138 \mu\text{m}$ and combined four into $204 \times 276 \mu\text{m}$; Louail et al., 2021: single scan of $200 \times 200 \mu\text{m}$ per a facet; Ramdarshan et al., 2016: single scan of $333 \times 251 \mu\text{m}$ was segmented into four $140 \times 100 \mu\text{m}$ areas). Therefore, we consider that total areas of $208 \times 144 \mu\text{m}$ can fulfill the requirements of the DMTA standard. Nevertheless, intra-facet variability in DMT exists in various mammals (e.g., Bas et al., 2020 in humans; Sawaaura et al., 2022 in macaques; Ramdarshan et al., 2017 in sheep); therefore, it may also have strong effects on tooth facets of omnivorous suids. Additional scans from different spots in the same facet can increase the sample size, control the intra-facet variability, and then make the statistical tests more sensitive, especially when we apply statistical tests with nested structures.

Conclusion

In this study, we compared the tooth microwear texture of wild boars from six populations in Japan. Detailed ecological and dietary information from stomach content analysis was available for Toyama populations, allowing us to test the effects of ecological variables on DMT. As expected, we did not find a correlation between stomach content and DMT at the individual level, but the dietary difference between localities was detected, even between locations with geographical proximity. The tooth surfaces of boarlets are rougher than those of juvenile and adult animals, which cautions against the mixed usage of deciduous and permanent molars of fossil or archaeological specimens in dental microwear studies. The decrease in surface roughness with age implies that the frequency of tooth-tooth contact, which seems to result in cracking of enamels and thus rough surfaces, decreases after the boars start feeding on solid foods (food-tooth contact), with progressive involvement of rooting behavior in mature adults. We further found that surface roughness showed significant differences among localities, with the western boars having flatter surfaces, possibly due to their more intense involvement in rooting and feeding on soil-contaminated rhizomes than the eastern ones, as evidenced by the available stomach content data. The difference in rooting frequency is also evident in the broader comparison among populations with different habitat environments. The mainland boars inhabiting deciduous broad-leaved forests have flatter tooth surfaces than those in the subtropical evergreen broad-leaved forests of the southern islands. This corresponds to the fact that above-ground dietary resources are more abundant in the habitat of the southern island boars, where crops like succulent vegetables and fruits, as well as naturally fallen acorns, are abundant, whereas underground plant parts are the dominant diet component for the mainland boars. Together with the data of the boars reared under dietary control, this study suggests that DMTA can identify the difference in foraging modes in suids with great dietary variability and paves the way to estimate the frequency of rooting in semi-domesticated and free-ranging boars from archaeological sites.

Data availability statement

The original data presented in the study are included in the main text and the [Supplementary materials](#). We also uploaded 1) the original scan data of all individuals in common 3D surface format (“sur” format) and 2) 3D surface analytical files including raw scans and procedures of analyses in DMTA standard format (“mnt”) to online repository (Zenodo). DOI of the scan data files is: <https://doi.org/10.5281/zenodo.6965607>.

Ethics statement

Ethical review and approval were not required for this study because we used the stored skeletal specimens of boars collected by nuisance culls and the published resources of the previous studies.

Author contributions

KM: conceptualization, investigation, formal analysis, and writing—original draft preparation. MOK: conceptualization, investigation, formal analysis, data curation, visualization, and writing—original draft preparation. YY: resources, data curation, and writing—review and editing. All authors contributed to the article and approved the submitted version.

Funding

This study was partially funded by the JSPS KAKENHI Grant (No. 16K18615) to MOK.

Acknowledgments

We are grateful to the following people for their assistance during this study: Yamada, E. for sharing the published DMT data of wild boars, Yasuda, A., and the members of Yokohata Laboratory, and the University of Toyama for valuable assistance with collections of skull specimens of wild boars. The comments from two reviewers (AS and IC) improved the manuscript greatly, and we appreciate their constructive comments.

Conflict of interest

The authors declare that the research was conducted in the absence of any commercial or financial relationships that could be construed as a potential conflict of interest.

Publisher’s note

All claims expressed in this article are solely those of the authors and do not necessarily represent those

of their affiliated organizations, or those of the publisher, the editors and the reviewers. Any product that may be evaluated in this article, or claim that may be made by its manufacturer, is not guaranteed or endorsed by the publisher.

References

- Ackermans, N. L., Winkler, D. E., Martin, L. F., Kaiser, T. M., Clauss, M., Hatt, J. M., et al. (2020). Dust and grit matter: abrasives of different size lead to opposing dental microwear textures in experimentally fed sheep (*Ovis aries*). *J. Exp. Biol.* 223, jeb.220442. doi: 10.1242/jeb.220442
- Ackermans, N. L., Winkler, D. E., Schulz-Kornas, E., Kaiser, T. M., Martin, L. F., Hatt, J. M., et al. (2021). Dental wear proxy correlation in a long-term feeding experiment on sheep (*Ovis aries*). *J. R. Soc. Interface* 18, 20210139. doi: 10.1098/rsif.2021.0139
- Aiba, K., Miura, S., and Kubo, M. O. (2019). Dental Microwear texture analysis in two ruminants, Japanese Serow (*Capricornis crispus*) and Sika Deer (*Cervus nippon*), from Central Japan. *Mammal Study* 44, 183–192. doi: 10.3106/ms2018-0081
- Arman, S. D., Prowse, T. A. A., Couzens, A. M. C., Ungar, P. S., and Prideaux, G. J. (2019). Incorporating intraspecific variation into dental microwear texture analysis. *J. R. Soc. Interface* 16, 20180957. doi: 10.1098/rsif.2018.0957
- Arman, S. D., Ungar, P. S., Brown, C. A., DeSantis, L. R. G., Schmidt, C., Prideaux, G. J., et al. (2016). Minimizing inter-microscope variability in dental microwear texture analysis. *Surface Topogr. Metrol. Propert.* 4, 024007. doi: 10.1088/2051-672X/4/2/024007
- Asahi, M. (1975). Stomach contents of wild boars (*Sus scrofa leucomystax*) in winter. *J. Mammal. Soc. Jpn.* 6, 115–120.
- Bas, M., Le Luyer, M., Kanz, F., Rebay-Salisbury, K., Queffelec, A., Souron, A., et al. (2020). Methodological implications of intra- and inter-facet microwear texture variation for human childhood paleo-dietary reconstruction: insights from the deciduous molars of extant and medieval children from France. *J. Archaeol. Sci. Rep.* 31, 102284. doi: 10.1016/j.jasrep.2020.102284
- Bestwick, J., Unwin, D. M., and Purnell, M. A. (2019). Dietary differences in archosaur and lepidosaur reptiles revealed by dental microwear textural analysis. *Sci. Rep.* 9, 11691. doi: 10.1038/s41598-019-48154-9
- Burnham, K. P., and Anderson, D. R. (1998). *Model Selection and Inference: A Practical Information-Theoretic Approach*. New York, NY: Springer. doi: 10.1007/978-1-4757-2917-7
- Calandra, I., Bob, K., Merceron, G., Blateyron, F., Hildebrandt, A., Schulz-Kornas, E., et al. (2021). Dental microwear texture analysis in Toothfrax and Mountains Map® SSFA module: different software packages, different results? *bioRxiv [Preprint]*. doi: 10.5281/zenodo.6669276
- Calandra, I., and Merceron, G. (2016). Dental microwear texture analysis in mammalian ecology. *Mamm. Rev.* 46, 215–228. doi: 10.1111/mam.12063
- Daegling, D. J., McGraw, W. S., Ungar, P. S., Pampush, J. D., Vick, A. E., Bitty, E. A., et al. (2011). Hard-object feeding in sooty mangabeys (*Cercocebus atys*) and interpretation of early hominin feeding ecology. *PLoS ONE* 6, e23095. doi: 10.1371/journal.pone.0023095
- Davis, M., and Pineda Munoz, S. (2016). The temporal scale of diet and dietary proxies. *Ecol. Evol.* 6, 1883–1897. doi: 10.1002/ece3.2054
- Desantis, L. R., and Haupt, R. J. (2014). Cougars' key to survival through the Late Pleistocene extinction: insights from dental microwear texture analysis. *Biol. Lett.* 10, 20140203. doi: 10.1098/rsbl.2014.0203
- DeSantis, L. R., Scott, J. R., Schubert, B. W., Donohue, S. L., McCray, B. M., Van Stolk, C. A., et al. (2013). Direct comparisons of 2D and 3D dental microwear proxies in extant herbivorous and carnivorous mammals. *PLoS ONE* 8, e71428. doi: 10.1371/journal.pone.0071428
- Evin, A., Cucchi, T., Cardini, A., Strand Vidarsdottir, U., Larson, G., Dobney, K., et al. (2013). The long and winding road: identifying pig domestication through molar size and shape. *J. Archaeol. Sci.* 40, 735–743. doi: 10.1016/j.jas.2012.08.005
- Gill, P. G., Purnell, M. A., Crumpton, N., Brown, K. R., Gostling, N. J., Stapanoni, M., et al. (2014). Dietary specializations and diversity in feeding ecology of the earliest stem mammals. *Nature* 512, 303–305. doi: 10.1038/nature13622
- Grine, F. E., and Kay, R. F. (1988). Early hominid diets from quantitative image analysis of dental microwear. *Nature* 333, 765–768. doi: 10.1038/333765a0
- Halley, D. J., and Rosvold, J. (2014). Stable isotope analysis and variation in medieval domestic pig husbandry practices in northwest Europe: absence of evidence for a purely herbivorous diet. *J. Archaeol. Sci.* 49, 1–5. doi: 10.1016/j.jas.2014.04.006
- Hayashi, Y., Nishida, T., and Mochizuki, K. (1977). Sex and age determination of the Japanese wild boar (*Sus scrofa leucomystax*) by the lower teeth. *Jpn. J. Vet. Sci.* 39, 165–174. doi: 10.1292/jvms1939.39.165
- Ishigaki City (2021). *Management plan for prevention of agricultural damage by wild animals in Ishigaki City*. Ishigaki City: Ishigaki City, 12.
- Ishigaki, C., Shinzato, T., Aramoto, M., and Wu, L. (2007). Feed plant, dressing and utilization of carcass of Ryukyuan wild boar in Iriomote Island. *Sci. Bull. Faculty Agric. Univ. Ryukyus* 54, 23–27.
- Kodera, Y., Kanzaki, N., Ishikawa, N., and Minagawa, A. (2013). Food habits of wild boar (*Sus scrofa*) inhabiting Iwami District, Shimane Prefecture, western Japan. *Honyurui Kagaku* 53, 279–287. doi: 10.11238/mammaliancience.53.279
- Kodera, Y., Takeda, T., Tomaru, S., and Sugita, S. (2012). The estimation of birth periods in wild boar by detailed aging. *Honyurui Kagaku* 52, 185–191. doi: 10.11238/mammaliancience.52.185
- Kubo, M. O., and Fujita, M. (2021). Diets of Pleistocene insular dwarf deer revealed by dental microwear texture analysis. *Palaeogeogr. Palaeoclimatol. Palaeoecol.* 562, 110098. doi: 10.1016/j.palaeo.2020.110098
- Kubo, M. O., Yamada, E., Kubo, T., and Kohno, N. (2017). Dental microwear texture analysis of extant sika deer with considerations on inter-microscope variability and surface preparation protocols. *Biosurface Biointerface* 3, 155–165. doi: 10.1016/j.bsbt.2017.11.006
- Larson, G., Albarella, U., Dobney, K., Rowley-Conwy, P., Schibler, J., Tresset, A., et al. (2007). Ancient DNA, pig domestication, and the spread of the Neolithic into Europe. *Proc. Nat. Acad. Sci. U. S. A.* 104, 15276–15281. doi: 10.1073/pnas.0703411104
- Larson, G., Liu, R., Zhao, X., Yuan, J., Fuller, D., Barton, L., et al. (2010). Patterns of East Asian pig domestication, migration, and turnover revealed by modern and ancient DNA. *Proc. Natl. Acad. Sci. U. S. A.* 107, 7686–7691. doi: 10.1073/pnas.0912264107
- Lazagabaster, I. A. (2019). Dental microwear texture analysis of Pliocene Suidae from Hadar and Kanapoi in the context of early hominin dietary breadth expansion. *J. Hum. Evol.* 132, 80–100. doi: 10.1016/j.jhevol.2019.04.010
- Louail, M., Ferchaud, S., Souron, A., Walker, A. E. C., and Merceron, G. (2021). Dental microwear textures differ in pigs with overall similar diets but fed with different seeds. *Palaeogeogr. Palaeoclimatol. Palaeoecol.* 572, 110415. doi: 10.1016/j.palaeo.2021.110415
- Merceron, G., Blondel, C., Brunetiere, N., Francisco, A., Gautier, D., Ramdarshan, A., et al. (2017). Dental microwear and controlled food testing on sheep: the TRIDENT project. *Biosurface Biointerface* 3, 174–183. doi: 10.1016/j.bsbt.2017.12.005
- Merceron, G., Escarguel, G., Angibault, J. M., and Verheyden-Tixier, H. (2010). Can dental microwear textures record inter-individual dietary variations? *PLoS ONE* 5, e9542. doi: 10.1371/journal.pone.0009542
- Merceron, G., Hofman-Kamińska, E., and Kowalczyk, R. (2014). 3D dental microwear texture analysis of feeding habits of sympatric ruminants in

Supplementary material

The Supplementary Material for this article can be found online at: <https://www.frontiersin.org/articles/10.3389/fevo.2022.957646/full#supplementary-material>

the Bialowieza Primeval Forest, Poland. *For. Ecol. Manag.* 328, 262–269. doi: 10.1016/j.foreco.2014.05.041

Minagawa, M., Matsui, A., and Ishiguro, N. (2005). Patterns of prehistoric boar *Sus scrofa* domestication, and inter-islands pig trading across the East China Sea, as determined by carbon and nitrogen isotope analysis. *Chem. Geol.* 218, 91–102. doi: 10.1016/j.chemgeo.2005.01.019

Nakajima, H., and Kobayashi, H. (2014). Distribution of forest types classified by vegetation map and distribution of private and national forest in Toyama Prefecture, Japan. *Bull. Toyama For. Res. Instit.* 6, 1–12.

Nishimoto, T. (1994). Differences of concept of animals between the Jomon people and the yayoi people. *Bull. Natl. Museum Japanese Hist.* 61, 73–86.

Purnell, M., Seehausen, O., and Galis, F. (2012). Quantitative three-dimensional microtextural analyses of tooth wear as a tool for dietary discrimination in fishes. *J. R. Soc. Interface* 9, 2225–2233. doi: 10.1098/rsif.2012.0140

Purnell, M. A., Crumpton, N., Gill, P. G., Jones, G., and Rayfield, E. J. (2013). Within-guild dietary discrimination from 3-D textural analysis of tooth microwear in insectivorous mammals. *J. Zool.* 291, 249–257. doi: 10.1111/jzo.12068

Ramdarshan, A., Blondel, C., Brunetière, N., Francisco, A., Gautier, D., Surault, J., et al. (2016). Seeds, browse, and tooth wear: a sheep perspective. *Ecol. Evol.* 6, 5559–5569. doi: 10.1002/ece3.2241

Ramdarshan, A., Blondel, C., Gautier, D., Surault, J., and Merceron, G. (2017). Overcoming sampling issues in dental tribology: insights from an experimentation on sheep. *Palaeontol. Electron.* 19.3.53A, 1–19. doi: 10.26879/762

Sawaura, R., Kimura, Y., and Kubo, M. O. (2022). Accuracy of dental microwear impressions by physical properties of silicone materials. *Front. Ecol. Evol.* 10: 975283. doi: 10.3389/fevo.2022.975283

Schulz, E., Calandra, I., and Kaiser, T. M. (2010). Applying tribology to teeth of hoofed mammals. *Scanning* 32, 162–182. doi: 10.1002/sca.20181

Scott, J. R. (2012). Dental microwear texture analysis of extant African Bovidae. *Mammalia* 76, 157–174. doi: 10.1515/mammalia-2011-0083

Scott, R. S., Teaford, M. F., and Ungar, P. S. (2012). Dental microwear texture and anthropoid diets. *Am. J. Phys. Anthropol.* 147, 551–579. doi: 10.1002/ajpa.22007

Scott, R. S., Ungar, P. S., Bergstrom, T. S., Brown, C. A., Childs, B. E., Teaford, M. F., et al. (2006). Dental microwear texture analysis: technical considerations. *J. Hum. Evol.* 51, 339–349. doi: 10.1016/j.jhevol.2006.04.006

Scott, R. S., Ungar, P. S., Bergstrom, T. S., Brown, C. A., Grine, F. E., Teaford, M. F., et al. (2005). Dental microwear texture analysis shows within-species

diet variability in fossil hominins. *Nature* 436, 693–695. doi: 10.1038/nature03822

Souron, A., Merceron, G., Blondel, C., Brunetière, N., Colyn, M., Hofman-Kamińska, E., et al. (2015). Three-dimensional dental microwear texture analysis and diet in extant Suidae (Mammalia: Cetartiodactyla). *Mammalia* 79, 279–291. doi: 10.1515/mammalia-2014-0023

Stiner, M. C., Barkai, R., and Gopher, A. (2009). Cooperative hunting and meat sharing 400–200 kya at Qesem Cave, Israel. *Proc. Natl. Acad. Sci. U. S. A.* 106, 13207–13212. doi: 10.1073/pnas.0900564106

Ungar, P. S., Grine, F. E., and Teaford, M. F. (2008). Dental microwear and diet of the Plio-Pleistocene hominin *Paranthropus boisei*. *PLoS ONE* 3, e2044. doi: 10.1371/annotation/195120f0-18ee-4730-9bd6-0d6effd68fcf

Vanpoucke, S., Mainland, I., De Cupere, B., and Waelkens, M. (2013). Dental microwear study of pigs from the classical site of Sagalassos (SW Turkey) as an aid for the reconstruction of husbandry practices in ancient times. *Environ. Archaeol.* 14, 137–154. doi: 10.1179/146141009X12481709928328

Ward, J., and Mainland, I. L. (1999). Microwear in modern rooting and stall-fed pigs: the potential of dental microwear analysis for exploring pig diet and management in the past. *Environ. Archaeol.* 4, 25–32. doi: 10.1179/env.1999.4.1.25

Winkler, D. E., Schulz-Kornas, E., Kaiser, T. M., Codron, D., Leichliter, J., Hummel, J., et al. (2020). The turnover of dental microwear texture: testing the “last supper” effect in small mammals in a controlled feeding experiment. *Palaeogeogr. Palaeoclimatol. Palaeoecol.* 557, 109930. doi: 10.1016/j.palaeo.2020.109930

Winkler, D. E., Schulz-Kornas, E., Kaiser, T. M., and Tutken, T. (2019). Dental microwear texture reflects dietary tendencies in extant Lepidosauria despite their limited use of oral food processing. *Proc. Biol. Sci.* 286, 20190544. doi: 10.1098/rspb.2019.0544

Yamada, E., Hongo, H., and Endo, H. (2021). Analyzing historic human-suid relationships through dental microwear texture and geometric morphometric analyses of archaeological suid teeth in the Ryukyu Islands. *J. Archaeol. Sci.* 132, 105419. doi: 10.1016/j.jas.2021.105419

Yamada, E., Kubo, M. O., Kubo, T., and Kohno, N. (2018). Three-dimensional tooth surface texture analysis on stall-fed and wild boars (*Sus scrofa*). *PLoS ONE* 13, e0204719. doi: 10.1371/journal.pone.0204719

Yasuda, A., and Yokohata, Y. (2015). Stomach content analysis of wild boars collected in autumn and winter in Toyama Prefecture, Japan. *Bull. Toyama Biol. Soc.* 54, 101–106.



OPEN ACCESS

EDITED BY

Michael Anthony Berthume,
London South Bank University,
United Kingdom

REVIEWED BY

Marina Melchionna,
University of Naples Federico II, Italy
Elizabeth St. Clair,
Johns Hopkins University,
United States

*CORRESPONDENCE

Laura Mónica Martínez
lmartinez@ub.edu

SPECIALTY SECTION

This article was submitted to
Paleoecology,
a section of the journal
Frontiers in Ecology and Evolution

RECEIVED 14 June 2022

ACCEPTED 28 October 2022

PUBLISHED 11 November 2022

CITATION

Avià Y, Romero A,
Estebaranz-Sánchez F, Pérez-Pérez A,
Cuesta-Torralvo E and Martínez LM
(2022) Dental topography and dietary
specialization in Papionini primates.
Front. Ecol. Evol. 10:969007.
doi: 10.3389/fevo.2022.969007

COPYRIGHT

© 2022 Avià, Romero,
Estebaranz-Sánchez, Pérez-Pérez,
Cuesta-Torralvo and Martínez. This is
an open-access article distributed
under the terms of the [Creative
Commons Attribution License \(CC BY\)](#).
The use, distribution or reproduction in
other forums is permitted, provided
the original author(s) and the copyright
owner(s) are credited and that the
original publication in this journal is
cited, in accordance with accepted
academic practice. No use, distribution
or reproduction is permitted which
does not comply with these terms.

Dental topography and dietary specialization in Papionini primates

Yasmina Avià^{1,2}, Alejandro Romero^{3,4},
Ferran Estebaranz-Sánchez⁵, Alejandro Pérez-Pérez^{1,6},
Elisabeth Cuesta-Torralvo² and Laura Mónica Martínez^{1,6*}

¹Departament de Biologia Evolutiva, Ecologia i Ciències Ambientals (BEECA), La Secció de Zoologia i Antropologia Biològica, Facultat de Biologia, Universitat de Barcelona (UB), Barcelona, Spain,

²Departament de Biologia Animal, Vegetal i Ecologia, Facultat de Biociències, Universitat Autònoma de Barcelona, Barcelona, Spain, ³Departamento de Biotecnología, Facultad de Ciencias, Universidad de Alicante, Alicante, Spain, ⁴Instituto Universitario de Investigación en Arqueología y Patrimonio Histórico (INAPH), Universidad de Alicante, Alicante, Spain, ⁵Archaeology of Social Dynamics, Institución Milá y Fontanals de Investigación en Humanidades (CSIC), Barcelona, Spain, ⁶Institut d'Arqueologia de la Universitat de Barcelona (IAUB), Barcelona, Spain

Our understanding of primate adaptive evolution depends on appreciating the way in which dental functional morphology affects food processing. The Papionini tribe of *Cercopithecoidea* primates shows great dietary versatility and ecological adaptations to resource seasonality across the African and Asian ecosystems, however, there are few studies focusing on the occlusal topography of the bilophodont teeth and the effect of tooth wear in the crown shape. Here, we explore the relationship between wear-related dental functional morphology and dietary ecological constraints within the Papionini. Three-dimensional (3D) polygonal meshes of the upper permanent molar row (M1-3) were obtained in a large papionine sample (838 specimens) of known dietary preferences including species from six genera (*Cercocebus*, *Lophocebus*, *Macaca*, *Mandrillus*, *Papio*, and *Theropithecus*). All the sample was classified in four diet categories and four topographic metrics (orientation patch count rotated, OPCR; Dirichlet normal energy, DNE; occlusal relief, OR; and ambient occlusion, portion de ciel visible, PCV) were measured for each tooth-type according to wear stage (lightly and moderately worn) to determine diet-related interspecific morphological changes with long-term functionality. The results indicate that hard-object feeders (*Cercocebus* and *Lophocebus*) and grass eaters (*Theropithecus gelada*) exhibit a pattern of occlusal complexity (OPCR), surface curvature (DNE), relief (OR), and morphological wear resistance (PCV) that is significantly different from the omnivores and folivore-frugivore species (*Mandrillus* and *Macaca*) despite the overall homogeneity of the bilophodont dentition. A multifactorial ANOVA showed that the topographic metrics were sensitive to tooth wear as expected. The results also indicate that the interspecific variability of dental topography of the upper molars reflects dietary specializations rather than phylogenetic proximity. These findings

support the hypothesis that evolutionary convergence processes could have affected the Papionini, clustering the hard-object feeders (*Lophocebus* and *Cercocebus*) together in the morphospace, and clearly discriminating this group from the graminivorous and frugivores-folivores.

KEYWORDS

dental topography, diet, wear, *Cercopithecoidea*, Papionini

Introduction

The Papionini tribe (Family Cercopithecidae; Subfamily Cercopithecinae) has the greatest geographical range of extant non-human primates across Africa and Asia, demonstrating broad adaptability and evolutionary success (Perelman et al., 2011; Monson and Hlusko, 2014). Extant Papionini primates include the mangabeys (genera *Lophocebus* and *Cercocebus*), which occupy regions of eastern and central Africa (Daegling and McGraw, 2007), the macaques (*Macaca*), which inhabit Asia and some regions in North Africa (Ménard et al., 2014), the mandrills and drills (*Mandrillus*) from West Africa (Tutin et al., 1997), the baboons (*Papio*), distributed throughout the sub-Saharan savannahs (Kamilar, 2006), and the geladas (*Theropithecus*), from the highlands of Ethiopia (Jablonski, 1993). This wide ecological distribution reflects a great dietary diversity and different behavioral responses to resource seasonality, including the intake of foods with different mechanical and physical properties that vary according to microhabitats (Brugiere et al., 2002; Swindler, 2002).

The species of the Papionini tribe show great morphological diversity according to its wide range of ecological exploitation. Notable morphological similarities previously lead researchers to conclude that the small-bodied mangabeys (*Cercocebus* and *Lophocebus*) and the large-bodied taxa such as *Papio*, *Theropithecus* and *Mandrillus* formed potential subclades in the Papionini (Jolly, 1972; Szalay and Delson, 1979; Strasser and Delson, 1987). This morphological phenetic classification prevailed until molecular studies showed that the mangabeys might not constitute a monophyletic group (Disotell et al., 1992; Disotell, 1994, 2000; Harris and Disotell, 1998; Harris, 2000). Within the mangabeys, *Lophocebus* may be more closely related to the savannah (*Papio*) and the gelada (*Theropithecus*) baboons, whereas *Cercocebus* was more closely related to the mandrills (Figure 1). Dental and postcranial similarities between the *Cercocebus*/*Mandrillus* and *Lophocebus*/*Papio* groups were shown to support the hypothesis of paraphyly for this clade (Fleagle and McGraw, 1999, 2002; McGraw and Fleagle, 2006; Gilbert, 2007). Reappraisals of allometry-corrected cranial anatomy suggest that the craniodental anatomy is a valuable source of phylogenetic information (Gilbert, 2013). There is not yet a consensus, however, about the relationships among *Theropithecus*, *Papio* and *Lophocebus* (Perelman et al., 2011;

Gilbert, 2013; Zinner et al., 2013; Pugh and Gilbert, 2018), since high levels of craniomorph homoplasy are present (Fleagle and McGraw, 1999; Lockwood and Fleagle, 1999; Collard and O'Higgins, 2002; Gilbert and Rossie, 2007; Gilbert et al., 2009). Convergence and divergence in morphological traits are likely to have hindered determination of the actual phylogenetic proximity within the Papionini, resulting in the ambiguous evolutionary scenario of morphological and genetic signatures (Strasser and Delson, 1987; Harris and Disotell, 1998; Harris, 2000; Gilbert, 2007).

The Cercopithecidae share an ancestral bilophodont molar occlusal cusp pattern (Swindler, 1976; Lucas, 2004) consisting of four marginal cusps connected by two transverse lophs or ridges that define three foveas with a reduced lingual cingulum (Delson, 1975). The occlusal bite contact between the maxillary and mandibular bilophodont molars allows both shearing and tooth-to-tooth grinding contacts, which may represent an adaptation to increased seed consumption and folivory (Delson, 1975; Ungar, 2010). The Papionini primates show a common, although greatly variable, morphology of molar teeth (Figure 1) reflecting species-specific evolutionary adaptations to food processing (Swindler, 2002). They widen outwards, laterally from the cusp apexes to the cervix, especially on the buccal face of the lower and on the lingual face of the upper molars (Delson, 1975). This morphology results in differences between the cervical and apical width dimensions, and varies among the Papionini. It is least pronounced in *Cercocebus* and *Papio* and least in *Theropithecus* (Swindler, 2002). *Theropithecus* differs among the Papionini, with a higher molar crown relief, longer mediobuccal distance, and a wider central basin, which is deeper than the other two somewhat elongated basins (Delson, 1975).

This morphological dental variability may reflect specific dietary adaptations within the different taxa of the Papionini group. Although *Cercopithecoidea* primates are mostly fruit eaters that inhabit seasonal ecosystems, their dietary spectra vary from leaves, bark, grass, nuts and flowers to mammals and lizards (Swindler, 2002). For instance, *Theropithecus gelada* from the Ethiopian Highlands is specialized in the exploitation of a graminivorous niche (Dunbar and Bose, 1991), with slight variation in diet composition between dry and wet seasons (Mau et al., 2009; Moges and Balakrishnan, 2014). A multi-year study at Guassa Plateau –an intact, tall-grass ecosystem in the

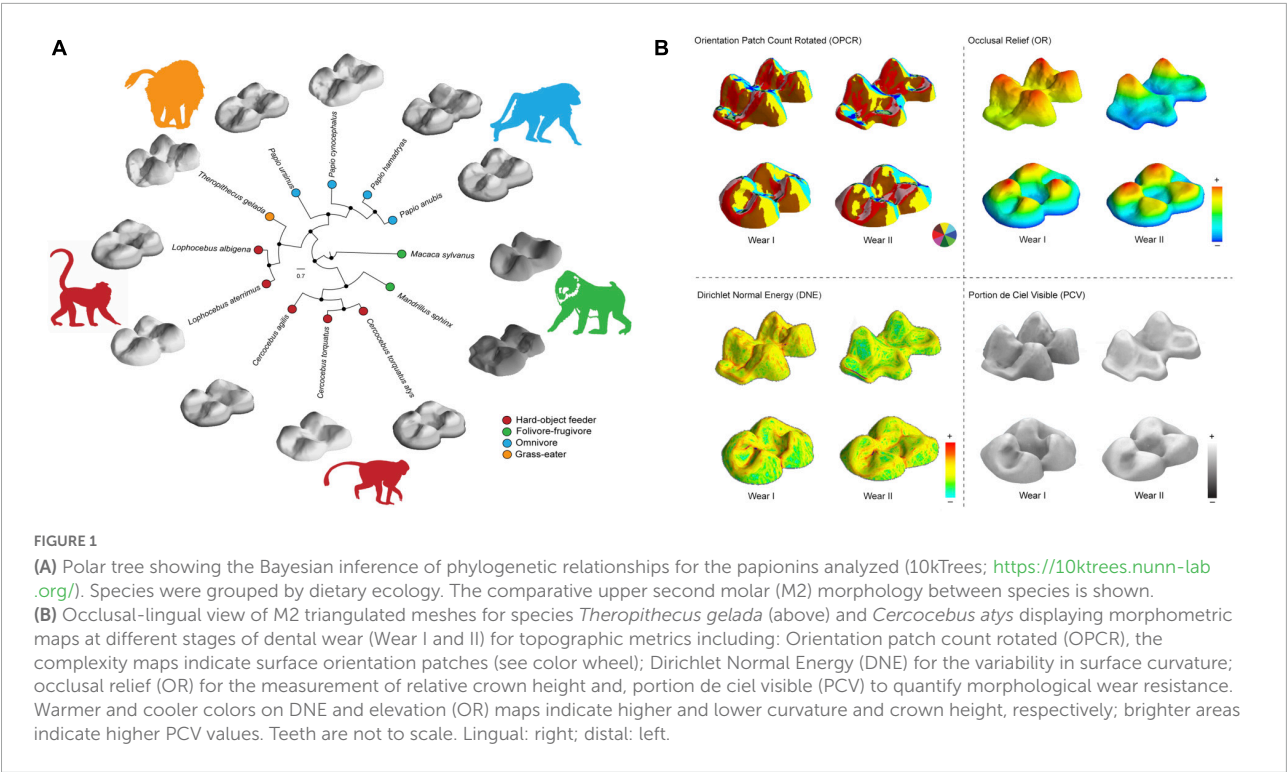


TABLE 1 Papionini dental sample studied.

Dietary category ^a	Species	M1	M2	M3	n(M/F)	Museum ^b
Hard-object feeder	<i>Cercocebus atys</i>	44	44	17	105 (49/56)	IMAZ
	<i>Cercocebus torquatus</i>	11	11	5	27 (14/13)	IRScNB, IMAZ
	<i>Cercocebus agilis</i>	16	16	5	37 (25/12)	RMCA
	<i>Lophocebus albigena</i>	53	53	19	125 (58/67)	IMAZ, RMCA, IRScNB
	<i>Lophocebus aterrimus</i>	34	37	15	86 (56/30)	RMCA
Total		158	161	61	380 (202/178)	
Folivore and frugivore	<i>Mandrillus sphinx</i>	26	28	4	58 (43/15)	NMK, IMAZ
	<i>Macaca sylvanus</i>	9	8	5	22 (10/12)	NMK, IRScNB, IMAZ
	<i>Macaca nemestrina</i>	2			2 (1/1)	IRScNB
	<i>Macaca mulatta</i>	1			1 (1/0)	IRScNB
Total		38	36	9	83 (55/28)	
Omnivore	<i>Papio hamadryas</i>	25	24	12	61 (52/9)	RMCA, IMAZ, IRScNB
	<i>Papio anubis</i>	39	38	13	90 (48/42)	RMCA, IMAZ
	<i>Papio ursinus</i>	12	9	4	25 (16/9)	RMCA
	<i>Papio cynocephalus</i>	37	38	15	90 (66/24)	NMK, IRScNB, RMCA, IMAZ
Total		113	109	44	266 (182/84)	
Grass eater	<i>Theropithecus gelada</i>	39	40	30	109 (40/69)	MNHN, IMAZ

ⁿ number of total teeth studied including M1, M2, and M3; M number of males and F number of females. ^aDietary categorization based on feeding preferences (see “Materials and Methods” section). ^bMuseum abbreviation correspond to University of Zurich (IMAZ), Zurich; National Museum of Kenya (NMK), Nairobi; Royal Museum for Central Africa (RMCA), Tervuren; Institut Royal des Sciences Naturelles de Belgique (IRScNB) Brussels; Muséum National d’Histoire Naturelle (MNHN), Paris.

Ethiopian Central highlands– has shown that specimens from Guassa rely heavily on forbs and invertebrates, however, and less on graminoids, expanding the documented diversity of gelada diets (Fashing et al., 2014). Occlusal microwear texture analyses have also shown a wide range of ecological adaptations to

diet and feeding in *Theropithecus*, reflecting population-specific dietary variability (Fashing et al., 2014; Shapiro et al., 2016).

The highly variable, species- and season-specific dietary regimes observed in the Papionini require primary diets, consisting of the preferred and most abundant foods consumed

year-round, to be differentiated from secondary diets (i.e., fallback foods). Derived dental morphology specializations, such as thick enamel and well-developed marginal crests, are likely to suggest the consumption of mechanically demanding fallback foods, at least for a short period when the preferred, year-round, less demanding foods are scarce. For instance, the two species of mangabeys, the terrestrial *Cercocebus* and the arboreal *Lophocebus*, adapted to feed on hard objects, both showing very thick-enamelled molar teeth (Kay, 1981), large incisors (Hylander, 1975), powerful jaws (Hylander, 1979), and a facial configuration that provides a mechanical advantage for producing large occlusal bite forces (Singleton, 2005). Although various species of both genera can be described as seed eaters and frugivores with a strong dependence on hard foods, numerous studies have shown significant differences in food preference (Lambert et al., 2004; McGraw et al., 2014; Ungar et al., 2018). *Cercocebus atys* depends strongly on fruits and seeds with very hard covers, such as the nut of *Sacoglottis gabonensis*, which they consume all-year round in different proportions (Daegling et al., 2011). Both the primary and secondary diets of *Cercocebus atys* are based on this type of fruit as a key resource. The *Lophocebus* species are all highly frugivorous, however, mainly consuming fleshy fruits, while hard fallback foods, such as seeds and bark, are consumed when there are shortages of preferred foods (Lambert et al., 2004). Although the enamel of both genera of mangabeys is some of the hardest enamel within the order of primates (McGraw et al., 2012), *Lophocebus* relies only on dry hard seeds and barks during the dry season or extreme El Niño events (Lambert et al., 2004; Daegling et al., 2011). Some authors argue that preferred foods have the greatest selective effect and are responsible for these morphological differences (Kay, 1975), however, it has also been suggested that the dependence on fallback foods during times of shortage can place much stronger selective pressure on dental anatomy (Fleagle and McGraw, 2002; Ungar et al., 2018). Other authors have suggested that preferred foods may be associated with adaptations for food procurement (efficient locomotion and food detection), while fallback foods, which are more abundant during dry seasons, involve challenging mechanical properties (hardness of food items) that require prolonged processing in the mouth, which promotes the development of food processing capacities that facilitate the efficient chewing and digestion of these foods (Marshall and Wrangham, 2007).

Analyses of dental topography and the shape of surface features in primates have explored the dynamic relationship between occlusal morphology, diet, and dental occlusal wear (M'Kirera and Ungar, 2003; Ungar and M'Kirera, 2003; Dennis et al., 2004; Ungar et al., 2018; Berthaume et al., 2020), including some *Cercopithecoidea* primates (Bunn and Ungar, 2009; Thierry et al., 2017a). During mastication the biomechanical action of teeth is based on the relationship between the mechanical properties of the foods and the dental action, defined as how teeth are used to access or fragment food (Kay, 1981; Lucas,

2004; Daegling et al., 2011; McGraw et al., 2014; Berthaume, 2016). In primates, these mechanical properties include toughness (resistance to crack propagation) and hardness (local resistance to elastic deformation) (Berthaume, 2016). Dental actions may vary among species, despite eating similar foods, due to the use of different motions or loads. Topographic variables thus quantify different aspects of tooth shape in relation to diet. For instance, frugivores with low-cusped crowns have a lower relief index, computed as the ratio between the 3D tooth surface area and its 2D projection area on the occlusal plane, than folivores, which have high cusped molars (Teaford and Ungar, 2000; Allen et al., 2015; Pampush et al., 2018). The curvature of the crown, however, calculated as Dirichlet normal energy (DNE; Bunn et al., 2011), is expected to be higher in folivores. DNE measures surface variability, meaning teeth with curvy surfaces, such as taller cusps, are generally sharper and have a higher DNE. Therefore, we may expect that frugivores and hard fruit eaters show a lower curvature and relief index than folivores or omnivores. Tooth occlusal complexity, which corresponds to the average number of dental elements, has been correlated with the significance of herbivory (Evans et al., 2007). These dental elements or triangles can be computed as the sum of the changes in triangle patch directions (OPCR; orientation patch count). Occlusal surfaces with greater patch counts have been connected to the enamel edges involved in shearing fibrous food (Pineda-Muñoz et al., 2017), however, large overlapping levels of OPCR values have been documented in primate species with distinct diets (Berthaume et al., 2020). Ambient occlusion (PCV; portion de ciel visible), has recently been introduced as a dental topographic metric (Berthaume et al., 2019a, 2020), that measures the exposure of a surface to ambient lighting when it come from the occlusal direction. Cusp tips, crest and blade edges tend to be more exposed to light and have higher PCV values, while the foveae, or sides of enamel caps, tend to be less exposed and have lower PCV values. PCV has been correlated with the efficiency of hard object feeding; primates with more fibrous diets (i.e., folivores) will have lower PCV values than frugivores or hard-object feeders that have low cusps highly exposed to light (Berthaume, 2016; Berthaume et al., 2020).

Although worn teeth are underrepresented in functional analysis, selective pressures are active throughout the entire functional life of teeth, modifying the morphology of the crowns. Some authors have suggested that wear, and the subsequent dentine exposure, may contribute to maintaining the functional efficiency of dental mastication (M'Kirera and Ungar, 2003; Ulhaas et al., 2004; King et al., 2005; Ungar, 2015; Glowacka et al., 2016), and, worn teeth could therefore be used to discriminate dietary specializations. Topographic variables change throughout wear stages. For instance, occlusal surface curvature (DNE) shows greater values in unworn molars with sharp cusps than in molar caps showing worn cusps and flatter occlusal surfaces (Bunn et al., 2011). Primates have flat dental crowns (non-hypsodont) compared to some other

mammals, and dental wear significantly changes tooth shape, from the initial appearance of wear facets to a complete dentine exposure in occlusal surfaces, which may affect food chewing, and compromise structural integrity. The relationship between enamel and the underlying dentine also plays a role in the tooth's functional efficiency that it is retained as tooth wears (Ungar, 2015). Natural selection shapes animal teeth to cope with wear and to retain dental functionality to fracture foods throughout a lifetime. In this context, some studies have found that wear patterns within primate taxa tend to maintain relatively high values of relief on occlusal surfaces, for example in folivorous compared to frugivorous species (M'Kirera and Ungar, 2003; Ungar, 2004; Bunn and Ungar, 2009; Ungar et al., 2018). This implies that teeth continue to maintain differences in occlusal morphologies with wear, or change their shapes in different ways as they wear (Ungar and M'Kirera, 2003). Diverse aspects of tooth shape can change throughout the wear process, such as cusp relief and slope, both of which can be measured by using topographic metrics. Examining topographic parameters is therefore a good approach to studying gross occlusal form, as teeth wear distinctively among primates in different species in relation to diet (Ungar, 2015). Several authors agree, however, that additional studies are needed to explore the dietary implications of dental sculpting in primates, and especially in the bilophodont teeth of the Papionini, which exploited a wide range of resources (Ulhaas et al., 2004; Bunn and Ungar, 2009; Pampush et al., 2018).

The present study focuses on the association between molar crown topography of the three upper molars (M1, M2, and M3) and the known dietary specializations of the Papionini specimens, which are analyzed to test the relationship between crown shape with different stage of wear and diet. If natural selection shapes primate teeth and retains their functionality as tooth wears, then the occlusal morphology of worn teeth will maintain these differences in order to also retain chewing efficiency throughout lifetime. Dental studies have shown significant levels of homoplasy in dental morphology in mammal lineages (Evans et al., 2007), as well as within the Papionini (Lockwood and Fleagle, 1999), and, so as a proxy of molar functional morphology, molar topography would be expected to reflect feeding strategies regarding the mechanical properties of food, rather than the phylogenetic proximity derived from molecular data alone. If confirmed, this could offer an important insight into the potential use of molar topography when studying the evolution of primate teeth.

Materials and methods

Studied samples

A total of 838 well-preserved, *in situ* (only molars that were placed in the maxillary row) first (M1; $n = 345$), second (M2;

$n = 347$), and third (M3; $n = 146$) permanent upper molars were selected from maxillary tooth rows from the dry skulls of adult (third molar erupted and in full occlusion) specimens belonging to the Papionini tribe (Table 1), including six genera and fourteen species: *Cercocebus* (*C. agilis*, *C. atys*, *C. torquatus*), *Lophocebus* (*L. albigena*, *L. aterrimus*), *Macaca* (*M. sylvanus*, *M. mulatta* and *M. nemestrina*), *Mandrillus* (*Ma. sphinx*), *Papio* (*P. anubis*, *P. cynocephalus*, *P. hamadryas*, *P. ursinus*), and *Theropithecus* (*T. gelada*). The specimens were sexed according to available museum records. Maxillary molars were selected for analyses because they exhibit a stable bilophodont cusp pattern of four main cusps, with minor size differences compared to mandibular molars, and also lack the distinct morphology of the extended talonid of the lower third molars (Delson, 1975).

The species considered were grouped into four primary diet categories (hard-object feeders, folivore-frugivores, omnivores, and grass-eaters) on the basis of the percentage of fruits and seeds vs. leaves and underground storage organs (USOs) consumed (Quris, 1975; Hoshino, 1985; Lahm, 1986; Mitani, 1989; Maisels et al., 1994; Tutin et al., 1997; Hill and Dunbar, 2002; Shah, 2003; Thierry, 2007; McGraw et al., 2011; Fashing et al., 2014; Jarvey et al., 2018). The *Lophocebus* (*L. albigena*, *L. aterrimus*) and *Cercocebus* mangabeys (*C. agilis*, *C. t. torquatus*, *C. torquatus atys*) species are hard-object feeders, mainly consuming hard fruits and seeds, and sharing habitats and dietary preferences (Quris, 1975; Waser, 1975; Mitani, 1989; Olupot et al., 1997; Shah, 2003; McGraw et al., 2011; DeCasien et al., 2017). *Mandrillus sphinx* and *Macaca* sp. are folivore-frugivore taxa, mainly consuming leaves, and fruits, but also seeds and herbs during the fruit-scarce season (Hoshino, 1985; Ménard and Vallet, 1986; Lucas and Corlett, 1991; Tutin et al., 1997; DeCasien et al., 2017; Powell et al., 2017). *Papio* species (*P. anubis*, *P. cynocephalus*, *P. hamadryas*, *P. ursinus*) are generalized omnivores with greatly variable diets dominated by fruits, leaves, and underground items (Hill and Dunbar, 2002), and they also consume invertebrates and small mammals. Finally, *Theropithecus gelada* has been traditionally described as a graminivorous specialist (Dunbar and Bose, 1991), although their diet might be significantly broader (Fashing et al., 2014; Shapiro et al., 2016; Souron, 2018).

Dental wear scoring

Both unworn and lightly worn-out teeth were studied to test for the effect of occlusal wear on dental topography (Berthaume et al., 2018; Pampush et al., 2018). All the teeth were scored and classified using a five-stages dental wear template for cercopithecoid species (Meikle, 1977) as follow: unworn (Grade 1), in erupted, though not yet full occlusion, molars; lightly worn (Grade 2), showing wear facets at or toward the top of the cusps but no part of the crown worn enough to expose the underlying dentine; moderate wear (Grade 3), circles of dentine exposure at

the cusp apices, the protocone cusp and the lingual cusps being affected before other cusps, lacking connections between them; medium wear (Grade 4), buccal and lingual areas of dentine start to merge along the lophs, although dentine exposure is still greater on the lingual half of the lophs, and dentine contact between the mesial and distal areas is still lacking; marked wear (Grade 5), with larger and similar dentine exposure areas on the buccal and lingual halves, with an incipient mesio-distal dentine contact affecting the talon. These occlusal wear scores were then grouped into two gross-wear categories following previous procedures (Berthaume et al., 2018): Wear I (Meikle's Grades 1 and 2), unworn or lightly worn molars without visible dentine exposure in the lingual cusps; Wear II (Meikle's Grade 3, 4), molars with moderate cusp removal with exposed dentine and a coalescence of dentine areas (Supplementary Figure 1). Molars in the advanced wear stage (Grade 5) were excluded of the sample in this study.

Sample processing

Maxillary *in situ* tooth rows of original specimens were cleaned with cotton swabs moistened with pure ethanol prior to molding. Silicone-base molds were made using Affinis® Regular body (Coltène-Whaledent™) polyvinylsiloxane, and high-resolution casts were produced from the molds using the two-base component polyurethane Feropur PR-55 (FeroCa® Composites, Spain) following standardized procedures (Galbany et al., 2006). Three-dimensional (3D) polygonal meshes of the dental casts were generated, using a structured light scanner (DAVID™ SLS-2) at a resolution of 0.05 mm, and were exported to polygon file format files (PLY). Meshes were post-processed using Geomagic™ Studio 2014 (3D Systems, Morrisville, USA) to isolate molar crowns by cropping the dental crown along the cervical and the interproximal rims. The meshes were slightly smoothed to reduce noise and cropped to the lowest point on the occlusal basin (BCO method; see Berthaume et al., 2019b), and finally simplified down to 10,000 polygons (Winchester, 2016). The processed polygonal models were imported into Meshlab (ISTI—CNR Research Centre, University of Pisa) and oriented to maximize the crown-base projection by placing the occlusal surfaces perpendicular to the Z-axis (Pampush et al., 2016).

Acquisition of three-dimensional dental topography

Dental topographic metrics were recorded from 3D polygonal meshes (Berthaume et al., 2018; Pampush et al., 2018) including the complexity (OPCR; Orientation Patch Count Rotated), the curvature (DNE; Dirichlet Normal Energy), and the occlusal relief (OR), using the MorphoTester software

(Winchester, 2016), as well as the ambient occlusion (PCV; Percentage du Ciel Visible) using the CloudCompare 3D software following the outlined procedures (Berthaume et al., 2019a). Briefly, occlusal complexity (OPCR) quantifies the number of enamel patches with distinct surface orientation (Evans et al., 2007). It was calculated using a minimum patch size of five polygons and averaging the oriented patch values of eight rotations around the Z-axis, with a 45° mesh rotation of each iteration (Winchester, 2016). DNE was calculated as the sum of energy values across a polygonal mesh surface, and the algorithm was invariant to mesh size and orientation (Bunn et al., 2011; Winchester, 2016). Surface bending was proportional to the number of mesh polygons, however, thus requiring the 10,000-polygon standardization (Winchester, 2016; Berthaume et al., 2018); a 0.1% (99.9th percentile) energy × area outlier removal was used to prevent changes in energy output due to polygon vertices (Winchester, 2016). The occlusal relief (OR) was estimated as the ratio of the 3D surface area of the cropped mesh to the projected 2D planimetric surface area (Berthaume et al., 2019b). Finally, the average PCV was calculated for each tooth using the PCV command in the Portion of Visible Sky plugin following Berthaume et al. (2019a, 2020) procedure.

Statistical analyses

Dental topographic variables were non-normally distributed by species (Shapiro–Wilk test; $p < 0.01$). Rank-transformed data was, thus, used for all the statistical analyses. A factorial ANOVA was run to test for the interaction effects of tooth-type (M1, M2, M3), sex (female, male), wear stages (I, II), and diet (hard-object feeders, folivore-frugivores, omnivores, grass-eaters) on crown shape descriptors (OPCR, DNE, OR and PCV). One-way ANOVAs on each variable by tooth-type and dietary groups were used to determine sources of significant variation by wear stages using Tukey's honestly significance test (HSD) for the paired comparisons. Finally, a principal component analysis (PCA) was performed on the correlation matrix to determine patterns of topographic variation that accounted for variation in dietary groups. Descriptive and statistical procedures were performed in SPSS™ Statistics 22.0 (IBM, Armonk, NY, USA) and PAST 4.02. The significance level was set at $\alpha = 0.05$.

Results

The multifactorial ANOVA showed that the effects of tooth-type, occlusal wear stage, and diet were highly significant ($p < 0.001$) for all the topographic metrics (Table 2), while the sex factor only showed a significant effect for OR ($p = 0.018$). Accordingly, sex was not considered for subsequent analyses. Significant interactions between factors (tooth, wear and diet)

were observed only when the diet factor was included, which suggest that differences between dietary categories remained when tooth and wear are considered. The interactions of the model showed that there were significant differences for all the topographic variables for each tooth and dietary category tested and there were significant differences for complexity ($p < 0.001$) and OR ($p = 0.021$) when both wear stages and dietary categories were considered.

Effect of wear on dental shape

Overall, occlusal wear was shown to be a highly significant factor affecting dietary-specific dental shape descriptors (Tables 3–6). One-way ANOVA comparisons of OPCR by tooth-type and dietary groups showed that complexity increased with wear stages (I to II) except for the higher-crowned grass eater *T. gelada*. There were significant differences in complexity values between wear stages in all dietary groups for the first molar (M1), and for hard-object feeders and folivore-frugivores for the second (M2) and third (M3) molars (Table 3). DNE significantly decreased with wear for M1 ($r = -0.343$; $p < 0.01$) and M2 ($r = -0.408$; $p < 0.01$) in hard-object feeders, and for M2 ($r = -0.219$; $p = 0.021$) and M3 ($r = -0.475$; $p < 0.01$) in omnivorous primates (Table 4). Relative cusp height loss (OR) was associated with tooth wear resistance (PCV) as a general trend. OR significantly decreased with wear for all the teeth in all the four dietary groups (Table 5), while PCV significantly increased with wear in all the dietary groups except for *T. gelada* for M1, and folivore-frugivore for M3, despite the fact that some sample sizes were small (Table 6). Overall, wear caused an increase in crown complexity (OPCR), not related to dentin exposure and probably due to the formation of wear facets, a reduction in crown curvature (DNE), due to increased flatness of occlusal enamel surfaces, a reduction of crown relief (OR) due to the loss of cusp heights, and an increase in ambient occlusion (PCV) as horizontal surfaces increase with wear.

Dental shape patterns by dietary groups

The dental shape metrics showed significant differences among the four dietary groups. More differences in tooth shape existed between hard-object feeders and other dietary groups than between other dietary groups for both unworn and worn teeth (Tukey's HSD; $p < 0.05$; Tables 6, 7). The topographic variables that most differed in hard-object feeders were PCV, OR and DNE, and their crowns showed the lowest curvature and OR values, and the highest PCV, characteristic of low rounded cusps. OPCR was also significant lower in this group ($p < 0.01$).

Graminivorous *T. gelada* showed the highest DNE and OR values and the lowest PCV values for all three teeth (Tables 3–6), a trend demonstrated by the paired, *post hoc* comparisons

(Table 7). The *post hoc* pairwise differences (Tukey's HSD; $p < 0.05$; Table 7) for the wear score I, showed that *T. gelada* differed significantly from all other diet groups in exhibiting higher OPCR and DNE values for M1, and differed significantly for OR and PCV from the hard-object feeders. The DNE and OPCR of the second lower molars of the graminivorous group also differed significantly from the frugivore/folivores, the former having a higher curvature and complexity, when the tooth crown was unworn or slightly worn. Greater OR values from graminivorous species denoted high-crowned molars and an expected inverse trend for PCV which differed significantly from the other dietary groups (Table 7).

The omnivores showed significantly higher complexities in all tooth crowns, but especially so in the second upper molar, which differed from the hard-object feeders and the folivore/frugivores groups ($p < 0.01$; Table 7). The DNE of the omnivores was significantly lower than that of the folivore/frugivore and hard-object feeders' groups for the unworn M2.

Lastly, the folivore/frugivore group showed few significant differences from the rest of the groups. The topographic parameters that differed significantly in this group compared to the hard-object feeders for the M1, M2 and M3, were OR and PCV, a trend similar to that observed between the omnivores and graminivorous groups.

In general, the between-diet comparisons of the worn teeth (wear score II) showed less inter-group differences, although they were similar in the M1 (Table 8). Dental complexity decreased as wear increased and, non-significant differences between diet groups were therefore observed for OPCR for the three teeth. DNE, OR and PCV showed similar trends to those seen in the unworn (wear score I) teeth, however *T. gelada* preserved the highest DNE and OR values, albeit smaller than those of the unworn teeth (Tables 3–6). Hard-object feeders showed the lowest values of DNE and OR compared to the rest of the groups while the PCV maintained the highest value despite the wear. These differences in M2 were significant for the hard-object eater group compared to the rest of the groups considered (except for the PCV comparison between folivore-frugivores, which was not significantly different).

The PCA summarized the trends in the topographic metrics of the dietary defined groups (Table 9 and Figure 2). The first two principal components (PC1-2) derived for each tooth (M1, M2, and M3) explained $> 85\%$ of the total variance in molar topography of the Papionini for the dietary preferences factor (Table 9). DNE and OR loaded positively ($r > 0.6$; $p < 0.01$) onto the PC1 ($> 45\%$ of total variance), while PCV showed strong negative loading ($r < -0.88$; $p < 0.01$) with PC1. This component clearly separated the hard-object feeders (negative PC1 values) from the omnivores and *T. gelada* (positive PC1 values) for all three molars, and a greater extent in the wear score I group compared to the II group (Figure 2). PC2 explained $< 45\%$ of total variance and was strongly and

TABLE 2 Factorial ANOVA model for the effects of tooth-type, wear stage, sex, and diet on topographic metrics.

Effects	OPCR		DNE		OR		PCV	
	<i>F</i>	<i>p</i>	<i>F</i>	<i>p</i>	<i>F</i>	<i>p</i>	<i>F</i>	<i>p</i>
Model	12.147	0.000**	23.715	0.000**	21.832	0.000**	30.246	0.000**
Tooth	13.850	0.000**	31.745	0.000**	14.081	0.000**	66.823	0.000**
Wear	29.459	0.000*	16.273	0.000**	112.391	0.000**	67.056	0.000**
Sex	2.651	0.104	0.707	0.401	5.578	0.018*	2.931	0.087
Diet	18.719	0.000**	86.406	0.000**	43.879	0.000**	70.492	0.000**
Tooth × wear	1.538	0.215	1.346	0.261	0.773	0.462	0.990	0.372
Tooth × sex	0.367	0.693	0.591	0.554	1.962	0.141	1.614	0.200
Wear × sex	0.254	0.615	0.480	0.489	0.983	0.322	2.061	0.152
Tooth × wear × sex	0.394	0.674	0.259	0.772	1.825	0.162	1.295	0.275
Tooth × diet	4.857	0.000**	4.849	0.000**	5.295	0.000**	4.737	0.000**
Wear × diet	7.624	0.000**	1.398	0.242	3.255	0.021*	1.691	0.167
Tooth × wear × diet	2.232	0.038*	0.622	0.713	0.525	0.790	1.953	0.070
Sex × diet	2.445	0.063	2.044	0.106	0.702	0.551	2.708	0.054
Tooth × sex × diet	0.611	0.722	1.690	0.121	0.606	0.726	1.505	0.174
Wear × sex × diet	2.383	0.068	1.740	0.157	0.571	0.634	0.013	0.998
Tooth × wear × sex × diet	0.762	0.550	0.355	0.840	0.538	0.708	0.596	0.666

Significant differences at $p < 0.05$ (*) and $p < 0.01$ (**).

TABLE 3 Descriptive statistics and differences (one-factor ANOVA) for orientation patch count rotated (OPCR) among dietary grouping species by tooth-type and wear stage.

Tooth	Dietary group	<i>n</i>	Wear	Mean	SD	<i>F</i>	<i>p</i>
M1	Hard-object feeder	93	I	89.23	19.62	25.732	0.000**
		65	II	104.66	21.49		
	Folivore-frugivore	14	I	83.34	20.76	5.312	0.027*
		24	II	98.71	24.37		
	Omnivore	47	I	93.43	19.28	18.307	0.000**
		63	II	110.53	22.04		
M2	Grass-eater	8	I	115.34	20.45	5.981	0.019*
		31	II	99.43	13.20		
	Hard-object feeder	97	I	86.10	13.84	148.671	0.000**
		64	II	114.10	19.70		
	Folivore-frugivore	19	I	100.55	19.18	12.423	0.000**
		17	II	121.91	15.78		
M3	Omnivore	88	I	112.15	17.54	1.157	0.284
		22	II	118.78	22.68		
	Grass-eater	27	I	112.13	15.64	3.339	0.076
		13	II	102.91	15.02		
	Hard-object feeder	59	I	77.48	14.12	10.019	0.002**
		2	II	103.88	6.72		
	Folivore-frugivore	5	I	95.18	17.59	3.654	0.098
		4	II	120.85	25.97		
	Omnivore	40	I	118.82	18.07	0.860	0.359
		6	II	122.34	7.36		
	Grass-eater	25	I	111.58	18.88	0.056	0.815
		5	II	112.73	19.56		

Significant differences at $p < 0.05$ (*) and $p < 0.01$ (**).

TABLE 4 Descriptive statistics and differences (one-factor ANOVA) for Dirichlet normal energy (DNE) among dietary grouping species by tooth-type and wear stage.

Tooth	Dietary group	<i>n</i>	Wear	Mean	SD	<i>F</i>	<i>p</i>
M1	Hard-object feeder	93	I	170.71	34.42	19.845	0.000**
		65	II	144.26	37.61		
	Folivore-frugivore	14	I	194.03	46.68	0.000	0.999
		24	II	192.41	66.66		
	Omnivore	47	I	205.52	35.41	0.295	0.588
		63	II	218.55	62.64		
	Grass-eater	8	I	265.05	60.44	3.573	0.067
		31	II	224.08	61.51		
M2	Hard-object feeder	97	I	180.79	33.91	34.462	0.000**
		64	II	150.13	33.53		
	Folivore-frugivore	19	I	241.20	64.93	0.001	0.980
		17	II	231.93	46.00		
	Omnivore	88	I	274.26	57.80	9.598	0.002**
		22	II	240.36	71.60		
	Grass-eater	27	I	306.04	60.61	0.913	0.345
		13	II	288.74	63.02		
M3	Hard-object feeder	59	I	180.88	38.23	2.981	0.090
		2	II	139.22	7.07		
	Folivore-frugivore	5	I	298.50	69.24	4.221	0.079
		4	II	214.30	48.96		
	Omnivore	40	I	342.96	52.66	28.554	0.000**
		6	II	256.03	73.48		
	Grass-eater	25	I	340.49	73.38	3.690	0.065
		5	II	247.05	36.38		

Significant differences at ** $p < 0.01$.

positively correlated with OPCR and ($r = 0.971$; $p < 0.01$) and DNE ($r = 0.735$; $p < 0.01$) for M1 (Table 9). As expected, the PCV for PC2 showed positive loadings with PC2 while OR showed negative loadings for all three teeth and the two wear groups (I and II) smaller OR values result in larger PCV values as the tooth wears down. Similar loadings were obtained between the topographic metrics and the PCs for all the teeth considered, and for both wear categories (Figure 2), which is consistent with the hypothesis that wear tends to decrease crown shape among dietary groups.

Discussion

The 3D crown topography of the upper molars (M1-3) of the studied Papionini shows a clear diet-related signal despite the overall homogeneity of the bilophodont dentition. The observed, dietary related among groups differences in crown topography reflect distinct adaptations to resource exploitation. The unworn dental crowns show a stronger dietary signal than the worn teeth, but the analyzed worn teeth still retained an overall dietary signal, which

may allow to gather larger samples than if only unworn teeth are considered.

Tooth shape and diet

The dental crowns of hard-object feeders tend to have lower and less complex cusps with more horizontally oriented enamel surfaces (Berthaume et al., 2019a) as an adaptation for breaking and grinding hard and brittle foods, such as seeds and nuts (Lucas, 2004; Ungar, 2004). Within the Papionini, the bilophodont morphology varies from hard object consumers to grass-eaters in relation to the amount of hard, brittle food particles chewed. Although OPCR has been applied to both extant and fossil taxa, Pineda-Muñoz et al. (2017) have suggested that it may have a reliable discriminating power only when applied to disparate tooth morphologies. We found, however, significant differences for the first molar (M1) between the high-crowned teeth of grass eaters and the rest of dietary groups. Moreover, most of the dietary groups showed significant differences in complexity for the second (M2) and third (M3) upper molar, suggesting that complexity varied between tooth type and the diet considered.

TABLE 5 Descriptive statistics and differences (one-factor ANOVA) for occlusal relief (OR) among dietary grouping species by tooth-type and wear stage.

Tooth	Dietary group	<i>n</i>	Wear	Mean	SD	<i>F</i>	<i>p</i>
M1	Hard-object feeder	93	I	1.44	0.09	94.889	0.000**
		65	II	1.28	0.13		
	Folivore-frugivore	14	I	1.57	0.13	24.343	0.000**
		24	II	1.39	0.09		
	Omnivore	47	I	1.50	0.10	11.895	0.001**
		63	II	1.43	0.16		
	Grass-eater	8	I	1.59	0.18	6.423	0.016*
		31	II	1.45	0.09		
M2	Hard-object feeder	97	I	1.46	0.10	145.001	0.000**
		64	II	1.27	0.10		
	Folivore-frugivore	19	I	1.54	0.17	25.902	0.000**
		17	II	1.35	0.07		
	Omnivore	88	I	1.55	0.12	36.920	0.000**
		22	II	1.40	0.12		
	Grass-eater	27	I	1.74	0.16	6.785	0.013*
		13	II	1.59	0.13		
M3	Hard-object feeder	59	I	1.50	0.09	11.238	0.001**
		2	II	1.28	0.10		
	Folivore-frugivore	5	I	1.77	0.14	6.981	0.033*
		4	II	1.44	0.22		
	Omnivore	40	I	1.67	0.10	35.267	0.000**
		6	II	1.49	0.16		
	Grass-eater	25	I	1.83	0.20	14.071	0.001**
		5	II	1.56	0.12		

Significant differences at $p < 0.05$ (*) and $p < 0.01$ (**).

Among sympatric African apes, the DNE of the second lower molar failed to differentiate folivores from frugivores except when dietary competition (between large bodied primates) was considered due to character displacement (Berthaume and Schroer, 2017). We showed that the curvature, complexity and morphological wear resistance of the upper molars (M1-3) of hard-object feeders differs among the Papionini from the other dietary groups considered. The multivariate analyses shown clearly differentiates the hard-object feeders Papionini from the omnivores and grass eaters, represented here by *Papio* and *T. gelada*, respectively. *Theropithecus* have dental crowns with high cusps and deep valleys, as shown by their high crown curvatures and reliefs which reflects an adaptation for increased chewing surface areas to facilitate the food processing activity of digestive enzymes (Szalay and Delson, 1979; Dunbar and Bose, 1991). Among *Papio* species, the dietary habits of *P. ursinus*, who inhabit heterogeneous ecosystems in Southern Africa, include the consumption of up to 30–50% of grasses in their diet, which is a higher value than that reported for baboons from African savanna environments (Codron et al., 2005). A 56% intake of graminoid grasses has been reported for *T. gelada* from Guassa (Fashing et al., 2014). These similarities in DNE

values between omnivores and grass-eaters could be related to similar dietary preferences, although *Papio* diet is more diverse than *Theropithecus* diet (Hill and Dunbar, 2002; Souron, 2018). Moreover, high crown cap curvatures have also been related to the consumption of fibers, leaves and foods of low digestibility, as well as insects, both in platyrrhine and in Hominoidea primates (Bunn et al., 2011; Winchester et al., 2014; Berthaume and Schroer, 2017).

Shape and wear in relation to diet

All the topographic metrics studied showed significant differences in relation to both wear and diet factors, suggesting that dental crown shape differences remain between dietary types despite an increased loss of dental crown through wear, at least in the upper bilophodont teeth analyzed. The OPCR, PCV and OR were the topographic metrics most sensitive to wear in all dietary groups considered. Overall, dental crown shape varies as cusps begin to decrease in height. Dentine is exposed in bilophodont teeth from the cusp tip, gradually developing an enamel ridge around the dentine pool. Unworn or slightly worn teeth show lower morphological wear resistance

TABLE 6 Descriptive statistics and differences (one-factor ANOVA) for portion de ciel visible (PCV) among dietary grouping species by tooth-type and wear stage.

Tooth	Dietary group	n	Wear	Mean	SD	F	p
M1	Hard-object feeder	93	I	0.70	0.03	31.411	0.000**
		65	II	0.75	0.05		
	Folivore-frugivore	14	I	0.68	0.03	30.572	0.000**
		24	II	0.73	0.03		
	Omnivore	47	I	0.67	0.03	14.208	0.000**
		63	II	0.70	0.04		
M2	Grass-eater	8	I	0.67	0.04	0.190	0.665
		31	II	0.66	0.03		
	Hard-object feeder	97	I	0.68	0.03	100.741	0.000**
		64	II	0.73	0.03		
	Folivore-frugivore	19	I	0.64	0.03	6.999	0.012*
		17	II	0.67	0.03		
	Omnivore	88	I	0.63	0.03	21.029	0.000**
		22	II	0.67	0.03		
	Grass-eater	27	I	0.60	0.03	6.499	0.015*
		13	II	0.62	0.03		
M3	Hard-object feeder	59	I	0.67	0.03	7.141	0.010*
		2	II	0.72	0.03		
	Folivore-frugivore	5	I	0.62	0.03	3.536	0.102
		4	II	0.68	0.06		
	Omnivore	40	I	0.61	0.02	25.986	0.000**
		6	II	0.64	0.04		
	Grass-eater	25	I	0.58	0.04	10.530	0.003**
		5	II	0.65	0.06		

Significant differences at $p < 0.05$ (*) and $p < 0.01$ (**).**TABLE 7** Tukey matrices of pairwise mean differences between dietary groups for topographic metrics by tooth-type (wear I).

		M1			M2			M3		
OPCR		HO	FF	OM	HO	FF	OM	HO	FF	OM
Hard-object feeder	HO									
Folivore-frugivore	FF	42.54			−177.45**			−204.03*		
Omnivore	OM	−59.32	−101.86		−309.38**	177.45**		−471.30**	−267.26**	
Grass-eater	GE	−307.72**	−350.26**	−248.40*	−309.03**	−131.93*	0.35	−389.81**	−185.78	81.48
DNE		HO	FF	OM	HO	FF	OM	HO	FF	OM
Folivore-frugivore	FF	−107.79			−201.72**			−356.13**		
Omnivore	OM	−162.63**	−54.84		−308.55**	−106.83*		−435.65**	−79.51	
Grass-eater	GE	−343.27**	−235.48**	−180.63*	−374.67**	−172.95**	−66.12	−406.49**	−50.36	29.15
OR		HO	FF	OM	HO	FF	OM	HO	FF	OM
Folivore-frugivore	FF	−200.66**			−92.22			−279.63**		
Omnivore	OM	−111.80**	88.86		−138.25**	−46.03		−221.48**	58.15	
Grass-eater	GE	−196.81**	3.85	−85.01	−318.62**	−226.40**	−180.37**	−272.03**	7.60	−50.55
PCV		HO	FF	OM	HO	FF	OM	HO	FF	OM
Folivore-frugivore	FF	141.73*			174.13**			232.59**		
Omnivore	OM	182.01**	40.28		224.24**	50.10		285.41**	52.82	
Grass-eater	GE	176.88*	35.15	−5.131	356.65**	182.52**	132.41**	314.90**	82.32	29.49

Significant differences at $p < 0.05$ (*) and $p < 0.01$ (**).

TABLE 8 Tukey matrices of pairwise mean differences between dietary groups for topographic metrics by tooth-type (wear II).

		M1			M2			M3		
OPCR		HO	FF	OM	HO	FF	OM	HO	FF	OM
Hard-object feeder	HO									
Folivore-frugivore	FF	27.67			−87.20			−140.12		
Omnivore	OM	−63.75	−91.43		−37.99	49.21		−220.58	−80.45	
Grass-eater	GE	46.23	18.55	109.98	120.87	208.08*	158.86	−92.35	47.77	128.23
DNE		HO	FF	OM	HO	FF	OM	HO	FF	OM
Folivore-frugivore	FF	−217.08**			−346.85**			−350.12		
Omnivore	OM	−292.08**	−75.00		−333.70**	13.14		−468.00**	−117.87	
Grass-eater	GE	315.56**	−98.51	−23.51	−477.23**	−130.38	−143.52	−479.80**	−129.67	−11.80
OR		HO	FF	OM	HO	FF	OM	HO	FF	OM
Folivore-frugivore	FF	−145.25*			−103.51			−275.25		
Omnivore	OM	215.77**	−70.52		−189.83**	−86.31		−305.16	−29.91	
Grass-eater	GE	−267.37**	−122.11	−51.59	−499.55**	−396.03**	−309.72**	−452.95	−177.70	−147.78
PCV		HO	FF	OM	HO	FF	OM	HO	FF	OM
Folivore-frugivore	FF	14.30			263.83**			212.62		
Omnivore	OM	189.23**	174.93**		280.15**	16.32		397.58	184.95	
Grass-eater	GE	346.92**	332.63**	157.69**	496.15**	232.32**	216.00**	351.80	139.17	−45.78

Significant differences at $p < 0.05$ (*) and $p < 0.01$ (**).

TABLE 9 Factor loadings of the first two principal components (PC1-2) on dental topographic metrics for the teeth analyzed by wear stage.

Wear I		M1		M2		M3	
PC		PC1	PC2	PC1	PC2	PC1	PC2
Eigenvalue		1.946	1.614	2.779	1.034	3.283	0.589
% Variance		48.656	40.361	69.488	25.848	82.09	14.728
Metric		<i>r</i>	<i>r</i>	<i>r</i>	<i>r</i>	<i>r</i>	<i>r</i>
OPCR		−0.017	0.971**	0.582**	0.800**	0.806**	0.579**
DNE		0.620**	0.735**	0.954**	0.199**	0.974**	0.123
OR		0.885**	−0.312**	0.807**	−0.550**	0.877**	−0.443**
PCV		−0.882**	0.186*	−0.938**	0.227**	−0.957**	0.207*
Wear II		M1		M2		M3	
PC		PC1	PC2	PC1	PC2	PC1	PC2
Eigenvalue		2.226	1.228	2.683	1.119	2.685	1.046
% Variance		55.652	30.703	67.075	27.98	67.146	26.151
Metric		<i>r</i>	<i>r</i>	<i>r</i>	<i>r</i>	<i>r</i>	<i>r</i>
OPCR		−0.031	0.969**	−0.147	0.981**	−0.169	0.982**
DNE		0.828**	0.451**	0.901**	0.360**	0.920**	0.275
OR		0.922**	−0.140	0.947**	−0.160	0.969**	−0.078
PCV		−0.830**	0.258**	−0.976**	0.029	−0.934**	0.012

Correlation (Pearson's r) PCs and metrics at $p < 0.05$ (*) and $p < 0.01$ (**).

(PCV), as has already been suggested for bunodont teeth (Berthaume et al., 2018), while DNE and OPCR tend to show lower values in worn teeth. It has been suggested that DNE increases with macrowear (Pampush et al., 2016), especially in

folivorous primates (Pampush et al., 2018), which is consistent with the dental sculpting hypothesis, suggesting that DNE could be used to study wear-related variability in different primate groups, including cercopithecoids. Overall, our results show that

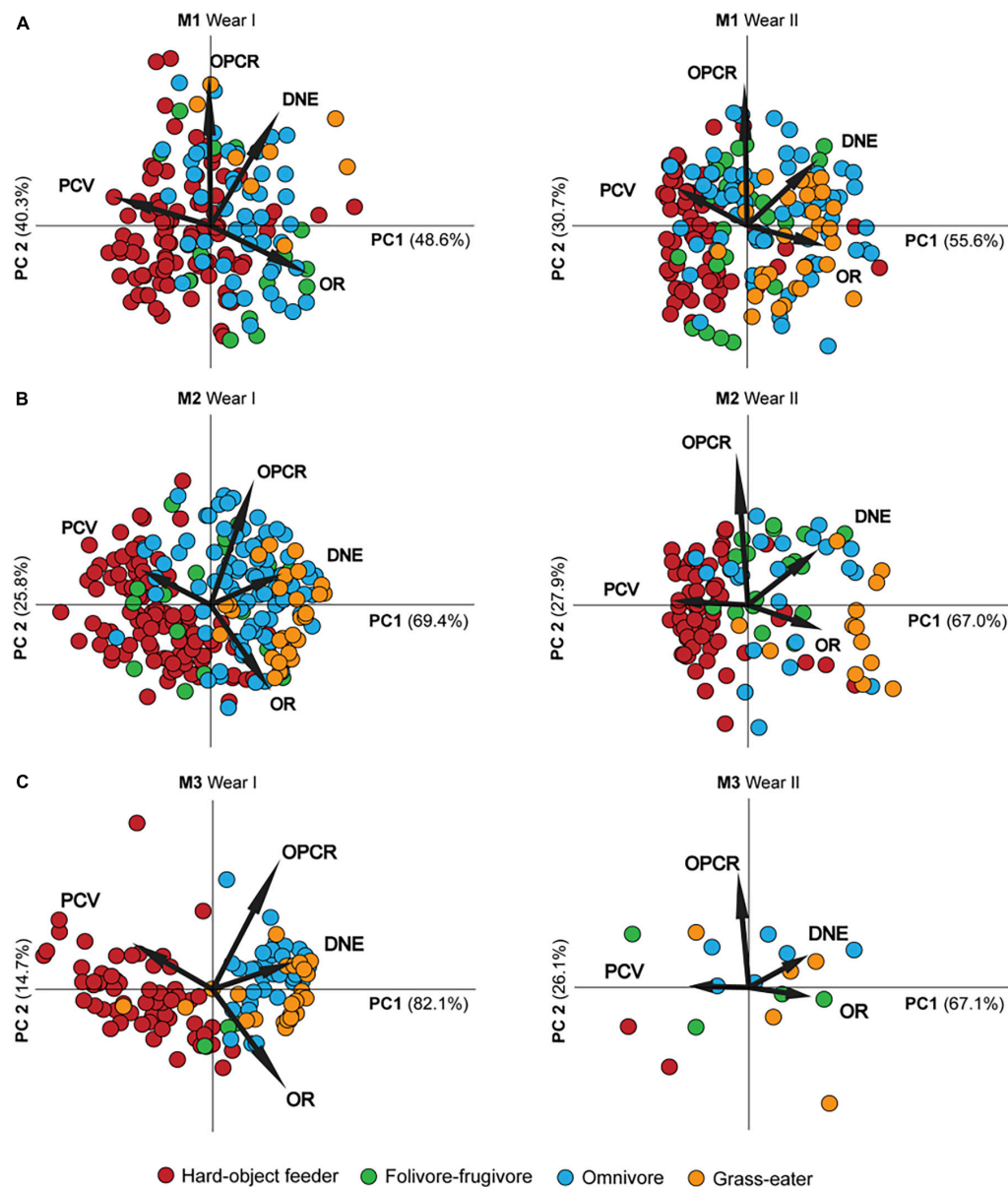


FIGURE 2

Scatter plot of the first two principal components (PC1–2) for first (A), second (B) and third (C) permanent maxillary molars by wear stage (Wear I and II) accounting for > 85% of the shape descriptor metrics variance between dietary groups. The labeled rays show the loadings of the topographic metrics onto PCs. Note the differences in molar topographic patterns despite wear clearly reflecting the adaptive variation of feeding habits.

DNE decreases with wear, but significant differences were only observed in the hard-object feeders and the omnivores, which suggests that the dental sculpting hypothesis is not evident in these dietary groups for the first stages of wear, in line with the hypothesis proposed by [Bunn et al. \(2011\)](#) and [Winchester et al. \(2014\)](#).

On the other hand, OPCR and OR showed a significant interaction with wear. OR demonstrated significant interaction for M1 and M2 in all dietary groups, and for M2. These

results suggest that there were differences in complexity along wear stages specifically for the M1 of all dietary groups, and for the M2 in hard-object feeders and folivore-frugivore. The occlusal relief decreased significantly with wear, which was an expected association since tooth height decreases as enamel and dentine tissue is lost ([M'Kirera and Ungar, 2003](#); [Ungar, 2015](#); [Ungar et al., 2018](#); [Romero et al., 2022](#)). High OPCR values, indicative of a complex surface topography, may be indicative of a great ability to shear fibrous foods ([Evans et al., 2007](#);

Evans and Janis, 2014). OPCR showed increased values along wear stages in the upper bilophodont molars in all the dietary groups except in the grass-eater *Theropithecus*. This suggests that *T. gelada* maintains the functional complexity of occlusal morphology with wear. Although a dental sculpting hypothesis was initially described for hypsodont taxa (Fortelius, 1985; Jablonski, 1994) proposed a similar ungulate-like secondary morphology for *Theropithecus*, which has high-crowned molars with deep and widely separated basins showing long shearing blades apparently adapted to a predominantly grass-eating diet (Jolly, 1970; Teaford, 1993). Our results, however, denote that the crown cap of *Theropithecus* did not show significantly increased OPCR values in worn out teeth consistent with the dental sculpting hypothesis. On the contrary, the complexity tended to decrease between wear stages in the upper first and second molars. Occlusal relief (OR) tends to be maintained regardless of wear patterns in both folivore and hard-object feeder primates, the folivores showing a higher relief, sharp edges and sloping surfaces at a given stage of wear (M'Kirera and Ungar, 2003; Ungar and M'Kirera, 2003; Bunn and Ungar, 2009), while omnivores and hard object eaters show lower shearing crests, similar to frugivores (Winchester et al., 2014; Allen et al., 2015). The distribution of both the unworn and worn tooth crowns caps in the morphospace was practically the same in the present study, and hard-object and grass feeders were clearly distinct from the other dietary groups. Although topographic metrics might differ between wear stages, the differences in cap topography among dietary groups remained for DNE, PCV and OR, suggesting that dental shape changes due to wear did not obscure the distinct dietary-related topographies, at least for the lightly worn teeth considered in this study.

Tooth shape and phylogeny

The dental topography of the upper molars (M1-3) seems to better reflect dietary specializations than phylogenetic proximity. *Lophocebus* and *Cercocebus*, which both have a hard-object dietary regime, cluster together in our topographic morphospace, and genetic evidence shows that *Lophocebus* is more closely related to baboons (Disotell et al., 1992; Disotell, 1994, 2000; Harris and Disotell, 1998; Harris, 2000). As some authors have suggested, this is consistent with processes of evolutionary convergence affecting the Papionini (Lockwood and Fleagle, 1999; Lycett and Collard, 2005; Collard and Wood, 2007), as also shown by inconsistencies between molecular and morphological inferences (Guevara and Steiper, 2014; Liedigk et al., 2014; Pugh et al., 2018). Skeletal structures that are subject to great biomechanical stress are prone to homoplasies compared to regions with reduced stress (Lycett and Collard, 2005; Collard and

Wood, 2007). The masticatory apparatus in the skull has great biomechanical constraints related to craniofacial bone tensions during the chewing cycle (Wall, 1999; Vinyard et al., 2003), resulting in a greater phenotypic plasticity that means the associated structures are less reliable indicators of phylogeny (Lieberman, 1995) compared to a dietary-related proxy.

The dietary classifications used in the present study represent year-round resource exploitation groups, however, seasonal fallback foods may play a more important role in shaping tooth morphology when favored items are inaccessible for primate species (Thiery et al., 2017b; Ungar et al., 2018). In order to use dental topography as a proxy for functional morphology to infer dietary strategies, it is important to understand such ecological and dietary determinants in the Papionini clade. Our findings may contribute to understanding the evolution of dental crown morphology in relation with environmental changes and dietary resources in the Papionini lineage along the Plio-Pleistocene, and thus to the study of the isolated teeth, both unworn and worn, that are abundant in the fossil record. The Papionini model may be an analogous model with which to interpret the evolutionary trend of the Hominini lineage, as both the Papionini and Hominini lineages emerged during the Pliocene in African sites, and, therefore, confronted the same ecological constraints and seasonal shifts in resource acquisition. Understanding functional adaptations to different ecological strategies may be a clue to allowing us to infer diet in fossil taxa.

Data availability statement

The original contributions presented in this study are included in the article/Supplementary material, further inquiries can be directed to the corresponding author.

Author contributions

LM, AR, FE-S, and AP-P conceived the research and approach and led the manuscript writing. YA, AR, and LM conducted the analyses. AP-P and AR acquired the funding. YA, LM, FE-S, and EC-T collected the material. All authors contributed to the writing of the manuscript and approved it for publication.

Funding

Grants PID2020-112963GB-I00 to APP and PID2020-114517GB-I00 to AR, funded by MCIN/AEI/10.13039/501100011033 and by "ERDF A way

of making Europe”, by the “European Union”.
www.paleobaboonproject.science.

Acknowledgments

We are grateful to all the curators and technical personnel of the different institutions where the specimens were molded. We thank all the work of the reviewers and the editor that help to improve the manuscript.

Conflict of interest

The authors declare that the research was conducted in the absence of any commercial or financial relationships that could be construed as a potential conflict of interest.

References

- Allen, K. L., Cooke, S. B., Gonzales, L. A., and Kay, R. F. (2015). Dietary inference from upper and lower molar morphology in platyrrhine primates. *PLoS One* 10:e0118732. doi: 10.1371/journal.pone.0118732
- Berthaume, M. A. (2016). On the relationship between tooth shape and masticatory efficiency: a finite element study. *Anat. Rec.* 299, 679–687. doi: 10.1002/ar.23328
- Berthaume, M. A., Delezenne, L. K., and Kupczik, K. (2018). Dental topography and the diet of *Homo naledi*. *J. Hum. Evol.* 118, 14–26. doi: 10.1016/j.jhevol.2018.02.006
- Berthaume, M. A., Lazzari, V., and Guy, F. (2020). The landscape of tooth shape: over 20 years of dental topography in primates. *Evol. Anthropol.* 29, 245–262. doi: 10.1002/evan.21856
- Berthaume, M. A., and Schroer, K. (2017). Extant ape dental topography and its implications for reconstructing the emergence of early Homo. *J. Hum. Evol.* 112, 15–29. doi: 10.1016/j.jhevol.2017.09.001
- Berthaume, M. A., Winchester, J., and Kupczik, K. (2019a). Ambient occlusion and PCV (portion de ciel visible): a new dental topographic metric and proxy of morphological wear resistance. *PLoS One* 14:e0215436. doi: 10.1371/journal.pone.0215436
- Berthaume, M. A., Winchester, J., and Kupczik, K. (2019b). Effects of cropping, smoothing, triangle count, and mesh resolution on 6 dental topographic metrics. *PLoS One* 14:e0216229. doi: 10.1371/journal.pone.0216229
- Brugiere, D., Gautier, J. P., Moungazi, A., and Gautier-Hion, A. (2002). Primate diet and biomass in relation to vegetation composition and fruiting phenology in a rain forest in Gabon. *Am. J. Primatol.* 23, 999–1024.
- Bunn, J. M., Boyer, D. M., Lipman, Y., St. Clair, E. M., Jernvall, J., and Daubechies, I. (2011). Comparing Dirichlet normal surface energy of tooth crowns, a new technique of molar shape quantification for dietary inference, with previous methods in isolation and in combination. *Am. J. Phys. Anthropol.* 145, 247–261. doi: 10.1002/ajpa.21489
- Bunn, J. M., and Ungar, P. S. (2009). Dental topography and diets of four old world monkey species. *Am. J. Primatol.* 71, 466–477. doi: 10.1002/ajp.20676
- Codron, J., Codron, D., Lee-Thorp, J. A., Sponheimer, M., Bond, W. J., de Ruiter, D., et al. (2005). Taxonomic, anatomical, and spatio-temporal variations in the stable carbon and nitrogen isotopic compositions of plants from an African savanna. *J. Archaeol. Sci.* 32, 1757–1772. doi: 10.1016/j.jas.2005.05.005
- Collard, M., and O’Higgins, P. (2002). Ontogeny and homoplasy in the papionin monkey face. *Evol. Dev.* 3, 322–331. doi: 10.1046/j.1525-142x.2001.01042.x
- Collard, M., and Wood, B. (2007). “Defining the genus homo,” in *Handbook of Paleoanthropology*, eds W. Henke and I. Tattersall (New York, NY: Springer), 1575–1610. doi: 10.1007/978-3-642-39979-4_51
- Daegling, D. J., and McGraw, W. S. (2007). Functional morphology of the mangabey mandibular corpus: relationship to dental specializations and feeding behavior. *Am. J. Phys. Anthropol.* 134, 50–62. doi: 10.1002/ajpa.20621
- Daegling, D. J., McGraw, W. S., Ungar, P. S., Pampush, J. D., Vick, A. E., and Bitty, E. A. (2011). Hard-Object feeding in sooty mangabeys (*Cercocebus atys*) and interpretation of early hominin feeding ecology. *PLoS One* 6:e23095. doi: 10.1371/journal.pone.0023095
- DeCasien, A. R., Williams, S. A., and Higham, J. P. (2017). Primate brain size is predicted by diet but not sociality. *Nat. Ecol. Evol.* 1, 1–7.
- Delson, E. (1975). “Evolutionary history of the Cercopithecidae,” in *Approaches to Primate Paleobiology: Contributions to Primatology*, ed. F. Szalay (Basel: S. Karger).
- Dennis, J. C., Ungar, P. S., Teaford, M. F., and Glander, K. E. (2004). Dental topography and molar wear in *Alouatta palliata* from Costa Rica. *Am. J. Phys. Anthropol.* 125, 152–161. doi: 10.1002/ajpa.10379
- Disotell, T. R. (1994). Generic level relationships of the *Papionini* (Cercopithecoidea). *Am. J. Phys. Anthropol.* 94, 47–57. doi: 10.1002/ajpa.1330940105
- Disotell, T. R. (2000). “Molecular systematics of the Cercopithecidae,” in *Old World Monkeys*, eds P. F. Whitehead and C. J. Jolly (New York, NY: Cambridge University Press), doi: 10.1111/j.1096-3642.2006.00253.x
- Disotell, T. R., Honeycutt, R. L., and Ruvulo, M. (1992). Mitochondrial DNA phylogeny of the Old-World monkey tribe *Papionini*. *Mol. Biol. Evol.* 9, 1–13. doi: 10.1093/oxfordjournals.molbev.a040700
- Dunbar, R. I. M., and Bose, U. (1991). Adaptation to grass-eating in gelada baboons. *Primates* 32, 1–7. doi: 10.1007/BF02381596
- Evans, A. R., and Janis, C. M. (2014). The evolution of high dental complexity in the horse lineage. *Ann. Zool. Fenn.* 51, 73–79. doi: 10.5735/086.051.0209
- Evans, A. R., Wilson, G. P., Fortelius, M., and Jernvall, J. (2007). High-level similarity of dentitions in carnivores and rodents. *Nature* 445, 78–81. doi: 10.1038/nature05433
- Fashing, P. J., Nguyen, N., Venkataraman, V. V., and Kerby, J. T. (2014). Gelada feeding ecology in an intact ecosystem at Guassa, Ethiopia: variability over time and implications for theropit and hominin dietary evolution. *Am. J. Phys. Anthropol.* 155, 1–16. doi: 10.1002/ajpa.22559
- Feagle, J. G., and McGraw, W. S. (1999). Skeletal and dental morphology supports diphyletic origin of baboons and mandrills. *PNAS* 96, 1157–1161. doi: 10.1073/pnas.96.3.1157
- Feagle, J. G., and McGraw, W. S. (2002). Skeletal and dental morphology of African papionins: unmasking a cryptic clade. *J. Hum. Evol.* 42, 267–292. doi: 10.1006/jhevol.2001.0526

Publisher’s note

All claims expressed in this article are solely those of the authors and do not necessarily represent those of their affiliated organizations, or those of the publisher, the editors and the reviewers. Any product that may be evaluated in this article, or claim that may be made by its manufacturer, is not guaranteed or endorsed by the publisher.

Supplementary material

The Supplementary Material for this article can be found online at: <https://www.frontiersin.org/articles/10.3389/fevo.2022.969007/full#supplementary-material>

- Fortelius, M. (1985). Ungulate cheek teeth: developmental, functional, and evolutionary interrelations. *Acta Zool. Fenn.* 180, 1–76.
- Galbany, J., Esteban, F., Martínez, L. M., Romero, A., De Juan, J., Turbón, D., et al. (2006). Comparative analysis of dental enamel polyvinylsiloxane impression and polyurethane casting methods for SEM research. *Microsc. Res. Tech.* 69, 246–252. doi: 10.1002/jemt.20296
- Gilbert, C. C. (2007). Identification and description of the first *Theropithecus* (Primates: Cercopithecidae) material from Bolt's Farm, South Africa. *Ann. Transvaal Mus.* 44, 1–10.
- Gilbert, C. C. (2013). Cladistic analysis of extant and fossil African papionins using craniodental data. *J. Hum. Evol.* 64, 399–433. doi: 10.1016/j.jhevol.2013.01.013
- Gilbert, C. C., Frost, S. R., and Strait, D. S. (2009). Allometry, sexual dimorphism, and phylogeny: a cladistic analysis of extant African papionins using craniodental data. *J. Hum. Evol.* 57, 298–232. doi: 10.1016/j.jhevol.2009.05.013
- Gilbert, C. C., and Rossie, J. B. (2007). Congruence of molecules and morphology using a narrow allometric approach. *PNAS* 104, 11910–11914. doi: 10.1073/pnas.0702174104
- Glowacka, H., McFarlin, S. C., Catlett, K. K., Mudakikwa, A., Bromage, T. G., Cranfield, M. R., et al. (2016). Age-related changes in molar topography and shearing crest length in a wild population of mountain gorillas from Volcanoes National Park, Rwanda. *Am. J. Phys. Anthropol.* 160, 3–15. doi: 10.1002/ajpa.22943
- Guevara, E. E., and Steiper, M. E. (2014). Molecular phylogenetic analysis of the *Papionina* using concatenation and species tree methods. *J. Hum. Evol.* 66, 18–28. doi: 10.1016/j.jhevol.2013.09.003
- Harris, E. E. (2000). Molecular systematics of the Old World monkey tribe *Papionini*: analysis of the total available genetic sequences. *J. Hum. Evol.* 38, 235–256. doi: 10.1006/jhev.1999.0318
- Harris, E. E., and Disotell, T. R. (1998). Nuclear gene trees and the phylogenetic relationships of the mangabeys (Primates: Papionini). *Mol. Biol. Evol.* 15, 892–900. doi: 10.1093/oxfordjournals.molbev.a025993
- Hill, R. A., and Dunbar, R. I. M. (2002). Climatic determinants of diet and foraging behaviour in baboons. *Evol. Ecol.* 16, 579–593. doi: 10.1023/A1021625003597
- Hoshino, J. (1985). Feeding ecology of mandrills (*Mandrillus sphinx*) in campo animal reserve, cameroon. *Primates* 26, 248–273. doi: 10.1007/BF02382401
- Hylander, W. L. (1975). Incisor size and diet in anthropoids with special reference to Cercopithecidae. *Science* 189, 1095–1098. doi: 10.1126/science.808855
- Hylander, W. L. (1979). Mandibular function in *Galago crassicaudatus* and *Macaca fascicularis*, an in vivo approach to stress analysis of the mandible. *J. Morphol.* 159, 253–296. doi: 10.1002/jmor.1051590208
- Jablonski, N. G. (1993). “Evolution of the masticatory apparatus in *Theropithecus*”, in *Theropithecus: the Rise and Fall of a Primate Genus*, ed N. G. Jablonski (Cambridge: Cambridge University Press).
- Jablonski, N. G. (1994). Convergent evolution in the dentitions of grazing macropodine marsupials and the grass-eating cercopithecine primate *Theropithecus gelada*. *J. R. Soc. West. Aust.* 77, 37–43.
- Jarvey, J. C., Low, B. S., Pappano, D. J., Bergman, T. J., and Beehner, J. C. (2018). Graminivory and fallback foods: annual diet profile of geladas (*Theropithecus gelada*) living in the simien Mountains National Park, Ethiopia. *Int. J. Primatol.* 39, 105–126. doi: 10.1007/s10764-018-0018-x
- Jolly, C. J. (1970). The seed-eaters: a new model of hominid differentiation based on a baboon analogy. *Man* 5, 5–26.
- Jolly, C. J. (1972). The classification and natural history of *Theropithecus* (Simopithecus) (Andrews, 1916), baboons of the African Plio-pleistocene. *Bull. Br. Mus. Nat.* 22, 1–123.
- Kamilar, J. M. (2006). “Geographic variation in savanna baboon (*Papio*) ecology and its taxonomic and evolutionary implications”, in *Primate Biogeography*, eds S. M. Lehman and J. G. Fleagle (New York, NY: Springer Press), 169–200.
- Kay, R. F. (1975). Allometry and early hominids. *Science* 189, 63.
- Kay, R. F. (1981). The nut-crackers: a new theory of the adaptations of the Ramapithecinae. *Am. J. Phys. Anthropol.* 55, 141–151. doi: 10.1002/ajpa.1330550202
- King, S. J., Arrigo-Nelson, S. J., Pochron, S. T., Semprebon, G. M., Godfrey, L. R., Wright, P. C., et al. (2005). Dental senescence in a long-lived primate links infant survival to rainfall. *PNAS* 102, 16579–16583. doi: 10.1073/pnas.0508377102
- Lahm, S. A. (1986). Diet and habitat preference of *Mandrillus sphinx* in gabon: implications of foraging strategy. *Am. J. Primatol.* 11, 9–26. doi: 10.1002/ajp.1350110103
- Lambert, J. E., Chapman, C. A., Wrangham, R. W., and Conklin-Brittain, N. L. (2004). Hardness of cercopithecine foods: implications for the critical function of enamel thickness in exploiting fallback foods. *Am. J. Phys. Anthropol.* 125, 363–368. doi: 10.1002/ajpa.10403
- Lieberman, D. E. (1995). Testing hypotheses about recent human evolution from skulls: integrating morphology, function, development, and phylogeny. *Curr. Anthropol.* 36, 159–197.
- Liedigk, R., Roos, C., Brameier, M., and Zinner, D. (2014). Mitogenomics of the old world monkey tribe Papionini. *BMC Evol. Biol.* 14:176. doi: 10.1186/s12862-014-0176-1
- Lockwood, C. A., and Fleagle, J. G. (1999). The recognition and evaluation of homoplasy in primate and human evolution. *Yearb. Phys. Anthropol.* 42, 189–232.
- Lucas, P. (2004). *Dental Functional Morphology. How Teeth Work*. Cambridge: Cambridge University Press.
- Lucas, P. W., and Corlett, R. T. (1991). Relationship between the diet of *Macaca fascicularis* and forest phenology. *Folia Primatol.* 57, 201–215. doi: 10.1159/000156587
- Lycett, S. J., and Collard, M. (2005). Do homologies impede phylogenetic analyses of the fossil hominids? an assessment based on extant papionin craniodental morphology. *J. Hum. Evol.* 49, 618–642. doi: 10.1016/j.jhevol.2005.07.004
- Maisels, F., Gautier-Hion, A., and Gautier, J.-P. (1994). Diets of two sympatric colobines in Zaire: more evidence on seed-eating in forests on poor soils. *Int. J. Primatol.* 15, 681–701. doi: 10.1007/BF02737427
- Marshall, A. J., and Wrangham, R. W. (2007). Evolutionary consequences of fallback foods. *Int. J. Primatol.* 28, 1219–1235. doi: 10.1007/s10764-007-9218-5
- Mau, M., Südekum, K.-H., Johann, A., Sliwa, A., and Kaiser, T. M. (2009). Saliva of the graminivorous *Theropithecus gelada* lacks proline-rich proteins and tannin-binding capacity. *Am. J. Primatol.* 71, 663–669. doi: 10.1002/ajp.20701
- McGraw, W. S., and Fleagle, J. G. (2006). “Biogeography of cercocebus-mandrillus clade: evidence from the face”, in *Primate Biogeography*, eds S. Lehman and J. G. Fleagle (New York, NY: Springer).
- McGraw, W. S., Pampush, J. D., and Daegling, D. J. (2012). Brief communication: Enamel thickness and durophagy in mangabeys revisited. *Am. J. Phys. Anthropol.* 147, 326–333.
- McGraw, W. S., Vick, A. E., and Daegling, D. J. (2011). Sex and age differences in the diet and ingestive behaviors of sooty mangabeys (*Cercocebus atys*) in the Tai Forest, Ivory Coast. *Am. J. Phys. Anthropol.* 144, 140–1153. doi: 10.1002/ajpa.21402
- McGraw, W. S., Vick, A. E., and Daegling, D. J. (2014). Dietary variation and food hardness in sooty mangabeys (*Cercocebus atys*): implications for fallback foods and dental adaptation. *Am. J. Phys. Anthropol.* 154, 413–423. doi: 10.1002/ajpa.22525
- Meikle, W. E. (1977). Molar Wear Stages in *Theropithecus gelada*. *Pap. Kroeber Anthropol. Soc.* 50, 21–26.
- Ménard, N., Rantier, Y., Foulquier, A., Qarro, M., Chillasse, L., Vallet, D., et al. (2014). Impact of human pressure and forest fragmentation on Moroccan Barbary macaque (*Macaca sylvanus*) populations. *Oryx* 48, 276–284. doi: 10.1017/S0030605312000312
- Ménard, N., and Vallet, D. (1986). Le régime alimentaire de *Macaca sylvanus* dans différents habitats d'Algérie: régime en forêt sempervirente et sur les sommets rocheux. *Rev. Ecol-Terre Vie* 41, 173–192.
- Mitani, M. (1989). *Cercocebus torquatus*: adaptive feeding and ranging behaviors related to seasonal fluctuations of food resources in the tropical rain forest of Southwestern Cameroon. *Primates* 30, 307–323. doi: 10.1007/BF02381257
- M'Kirera, F., and Ungar, P. S. (2003). Occlusal relief changes with molar wear in Pan troglodytes and Gorilla. *Am. J. Primatol.* 60, 31–41. doi: 10.1002/ajp.10077
- Moges, E., and Balakrishnan, M. (2014). Nutritional composition of food plants of geladas (*Theropithecus gelada*) in Guassa Community Protected Area, Ethiopia. *J. Biol. Agric. Healthc.* 4, 38–45.
- Monson, T. A., and Hlusko, L. J. (2014). Identification of a derived dental trait in the papionini relative to other old world monkeys. *Am. J. Phys. Anthropol.* 155, 422–429. doi: 10.1002/ajpa.22586
- Olupot, W., Chapman, C. A., Waser, P. M., and Isabirye-Basuta, G. (1997). Mangabey (*Cercocebus albigena*) ranging patterns in relation to fruit availability and the risk of parasite infection in Kibale National Park, Uganda. *Am. J. Primatol.* 43, 65–78. doi: 10.1002/(SICI)1098-2345(1997)43:1<65::AID-AJP5>3.0.CO;2-W
- Pampush, J., Spradley, J., Morse, P., Griffith, D., Gladman, J., Gonzales, L., et al. (2018). Adaptive wear-based changes in dental topography associated with

- atelid (Mammalia: Primates) diets. *Biol. J. Linn. Soc.* 124, 84–606. doi: 10.1093/biolinnean/bly069
- Pampush, J. D., Spradley, J. P., Morse, P. E., Harrington, A. R., Allen, K. L., Boyer, D. M., et al. (2016). Wear and its effects on dental topography measures in howling monkeys (*Alouatta palliata*). *Am. J. Phys. Anthropol.* 161, 705–721. doi: 10.1002/ajpa.23077
- Perelman, P., Johnson, W. E., Roos, C., Seuánez, H. N., Horvath, J. E., Moreira, M. A. M., et al. (2011). A molecular phylogeny of living primates. *PLoS Genetics* 7:e1001342. doi: 10.1371/journal.pgen.1001342
- Pineda-Muñoz, S., Lazagabaster, I. A., Alroy, J., and Evans, A. R. (2017). Inferring diet from dental morphology in terrestrial mammals. *Methods Ecol. Evol.* 8, 481–491. doi: 10.1111/2041-210X.12691
- Powell, L. E., Isler, K., and Barton, R. A. (2017). Re-evaluating the link between brain size and behavioural ecology in primates. *Proc. R. Soc. B: Biol. Sci.* 284:20171765. doi: 10.1098/rspb.2017.1765
- Pugh, K. D., and Gilbert, C. C. (2018). Phylogenetic relationships of living and fossil African papionins: combined evidence from morphology and molecules. *J. Hum. Evol.* 123, 35–51. doi: 10.1016/j.jhevol.2018.06.002
- Pugh, K. D., Gilbert, C. C., Patel, B. A., Campisano, C. J., Singh, N. P., Singleton, M., et al. (2018). A small-bodied catarrhine from the Miocene of India: additional evidence of an undersampled radiation. *Am. J. Phys. Anthropol.* 165, S66–S215.
- Quirós, R. (1975). Ecologie et organisation sociale de *Cercopithecus galeritis agilis* dans le nord-est du Gabon. *Rev. Ecol-Terre Vie* 3, 337–398.
- Romero, A., Pérez-Pérez, A., García Atiénzar, G., Martínez, L. M., and Macho, G. A. (2022). Do rates of dental wear in extant African great apes inform the time of weaning? *J. Hum. Evol.* 163:103126. doi: 10.1016/j.jhevol.2021.103126
- Shah, N. (2003). *Foraging Strategies in Two Sympatric Mangabey Species (Cercopithecus agilis and Lophocebus albigena)*. PhD dissertation, New York, NY: State University of New York.
- Shapiro, A. E., Venkataraman, V. V., Nguyen, N., and Fashing, P. J. (2016). Dietary ecology of fossil Theropithecus: inferences from dental microwear textures of extant geladas from ecologically diverse sites. *J. Hum. Evol.* 99, 1–9. doi: 10.1016/j.jhevol.2016.05.010
- Singleton, M. (2005). “Functional shape variation in the cercopithecine masticatory complex,” in *Modern Morphometrics In Physical Anthropology*, ed. D. E. Slice (Boston: Springer), doi: 10.1007/0-387-27614-9
- Souron, A. (2018). Morphology, diet, and stable carbon isotopes: on the diet of Theropithecus and some limits of uniformitarianism in paleoecology. *Am. J. Phys. Anthropol.* 166, 261–267. doi: 10.1002/ajpa.23414
- Strasser, E., and Delson, E. (1987). Cladistic analysis of cercopithecoid relationships. *J. Hum. Evol.* 16, 81–99. doi: 10.1016/0047-2484(87)90061-3
- Swindler, D. R. (1976). *Dentition of Living Primates*. London: Academic Press.
- Swindler, D. R. (2002). *Primate Dentition: An Introduction to the Teeth of Non-Human Primates*. Cambridge: Cambridge University Press.
- Szalay, F. S., and Delson, E. (1979). *Evolutionary History of the Primates*. New York, NY: Academic Press, doi: 10.1002/ajpa.1330600122
- Teaford, M. (1993). “Dental microwear and diet in extant and extinct Theropithecus: preliminary analyses,” in *Theropithecus: The Rise and Fall of a Primate Genus*, ed. N. G. Jablonski (Cambridge: Cambridge University Press), 331–349.
- Teaford, M. F., and Ungar, P. S. (2000). Diet and the evolution of the earliest human ancestors. *PNAS* 97, 13506–13511. doi: 10.1073/pnas.260368897
- Thierry, B. (2007). “The macaques: a double-layered social organization,” in *Primates in Perspective*, eds C. J. Campbell, A. Fuentes, K. C. MacKinnon, M. Panger, and S. K. Bearder (New York, NY: Oxford University Press), 224–239.
- Thierry, G., Gillet, G., Lazzari, V., Merceron, G., and Guy, F. (2017a). Was Mesopithecus a seed eating colobine? assessment of cracking, grinding and shearing ability using dental topography. *J. Hum. Evol.* 112, 79–92. doi: 10.1016/j.jhevol.2017.09.002
- Thierry, G., Guy, F., and Lazzari, V. (2017b). Investigating the dental toolkit of primates based on food mechanical properties: feeding action does matter. *Am. J. Primatol.* 79:e22640. doi: 10.1002/ajp.22640
- Tutin, C. E. G., Ham, R. M., White, L. J. T., and Harrison, M. J. S. (1997). The primate community of the Lope Reserve, Gabon: diets, responses to fruit scarcity, and effects on biomass. *Am. J. Primatol.* 42, 1–24. doi: 10.1002/(SICI)1098-2345(1997)42:1<1::AID-AJP1>3.0.CO;2-0
- Ulhaas, L., Kullmer, O., Schrenk, F., and Henke, W. (2004). A new 3D approach to determine functional morphology of cercopithecoid molars. *Ann. Anat.* 186, 487–493. doi: 10.1016/S0940-9602(04)80090-6
- Ungar, P. S. (2004). Dental topography and diets of Australopithecus afarensis and early Homo. *J. Hum. Evol.* 46, 605–622. doi: 10.1016/j.jhevol.2004.03.004
- Ungar, P. S. (2010). *Mammal Teeth: Origin, Evolution, and Diversity*. Baltimore, MD: Johns Hopkins University Press.
- Ungar, P. S. (2015). Mammalian dental function and wear: a review. *Biosurf. Biotribol.* 1, 25–41. doi: 10.1016/j.bsbt.2014.12.001
- Ungar, P. S., Healy, C., Karme, A., Teaford, M. F., and Fortelius, M. (2018). Dental topography and diets of platyrrhine primates. *Hist. Biol.* 30, 64–75. doi: 10.1080/08912963.2016.1255737
- Ungar, P. S., and M'Kirera, F. (2003). A solution to the worn tooth conundrum in primate functional anatomy. *PNAS* 100, 3874–3877. doi: 10.1073/pnas.0637016100
- Vinyard, C. J., Wall, C. E., Williams, S. H., and Hylander, W. L. (2003). Comparative functional analysis of skull morphology of tree-gouging primates. *Am. J. Phys. Anthropol.* 120, 153–170. doi: 10.1002/ajpa.10129
- Wall, C. E. (1999). A model of temporomandibular joint function in anthropoid primates based on condylar movements during mastication. *Am. J. Phys. Anthropol.* 109, 67–88. doi: 10.1002/(SICI)1096-8644(199905)109:1<67::AID-AJPA7>3.0.CO;2-F
- Waser, P. M. (1975). Monthly variations in feeding and activity patterns of the mangabey, *Cercopithecus albigena* (Lydekker). *East Afr. Wildl. J.* 13, 249–263. doi: 10.1111/j.1365-2028.1975.tb00138.x
- Winchester, J. M. (2016). MorphoTester: an open source application for morphological topographic analysis. *PLoS One* 11:e0147649. doi: 10.1371/journal.pone.0147649
- Winchester, J. M., Boyer, D. M., St Clair, E. M., Gosselin-Ildari, A. D., Cooke, S. B., and Ledogar, J. A. (2014). Dental topography of platyrrhines and prosimians: convergence and contrasts. *Am. J. Phys. Anthropol.* 153, 29–44. doi: 10.1002/ajpa.22398
- Zinner, D., Fickenscher, G. H., and Roos, C. (2013). “Family cercopithecidae (Old World monkeys),” in *Handbook of the Mammals of the World, Primates*, eds R. A. Mittermeier, A. B. Rylands, and D. E. Wilson (Barcelona: Lynx Edicions).



OPEN ACCESS

EDITED BY

Anna Maria Mercuri,
University of Modena and Reggio
Emilia, Italy

REVIEWED BY

Juan López Cantalapiedra,
Museum of Natural History Berlin
(MfN), Germany
Ellen Schulz-Kornas,
University of Leipzig, Germany

*CORRESPONDENCE

Melissa I. Pardi
melissa.pardi@illinois.gov

SPECIALTY SECTION

This article was submitted to
Paleoecology,
a section of the journal
Frontiers in Ecology and Evolution

RECEIVED 08 October 2022

ACCEPTED 09 November 2022

PUBLISHED 25 November 2022

CITATION

Pardi MI and DeSantis LRG (2022)
Interpreting spatially explicit variation
in dietary proxies through species
distribution modeling reveals foraging
preferences of mammoth
(*Mammuthus*) and American
mastodon (*Mammuth americanum*).
Front. Ecol. Evol. 10:1064299.
doi: 10.3389/fevo.2022.1064299

COPYRIGHT

© 2022 Pardi and DeSantis. This is an
open-access article distributed under
the terms of the [Creative Commons
Attribution License \(CC BY\)](#). The use,
distribution or reproduction in other
forums is permitted, provided the
original author(s) and the copyright
owner(s) are credited and that the
original publication in this journal is
cited, in accordance with accepted
academic practice. No use, distribution
or reproduction is permitted which
does not comply with these terms.

Interpreting spatially explicit variation in dietary proxies through species distribution modeling reveals foraging preferences of mammoth (*Mammuthus*) and American mastodon (*Mammuth americanum*)

Melissa I. Pardi^{1,2,3*} and Larisa R. G. DeSantis^{2,3}

¹Illinois State Museum, Springfield, IL, United States, ²Department of Biological Sciences, Vanderbilt University, Nashville, TN, United States, ³Department of Earth and Environmental Sciences, Vanderbilt University, Nashville, TN, United States

Introduction: The end Pleistocene was a time of considerable ecological upheaval. Recent work has explored the megafauna extinction's role in altering ecosystem processes. Analyses of functional traits within communities reveal hidden consequences of the megafauna extinction beyond declines in taxonomic diversity. Functional diversity analyses offer new insight into our understanding of past ecosystems and may even inform future rewilding efforts. However, the utility of functional diversity may be hampered by the use of discrete, taxon-level functional traits, such as dietary categories, that mask variation in functional diversity over space and time.

Methods: We present an approach in which species distribution modeling, in Maxent, provides context for interpreting variation in two widely used proxies for diet among fossil taxa: stable isotope analysis and dental microwear texture analysis. We apply this approach to two ecologically distinct taxa, the American mastodon (*Mammuth americanum*) and mammoths (*Mammuthus*) and investigate their resource use over space and time from the last glacial maximum to the end Pleistocene (25–11.7 thousand years before present).

Results: Mammoth dietary behavior varies by context across their geographic distribution, despite possessing evolutionary adaptations that facilitate grazing. Mammoths exhibit a preference for grazing where species distribution modeling predicts the highest likelihood of occurrence but engage in more mixed-feeding outside of core likelihood areas. In contrast, dietary preferences for mastodon are less resolved and our analyses were unable to identify significant differences in diet across their distribution.

Discussion: The ecological roles of some species are context specific and need to be critically evaluated when planning for management of reintroductions or introducing novel species to restore lost ecological function.

KEYWORDS

carbon, Maxent, *Mammuthus*, *Mammut*, stable isotope analysis (SIA), dental microwear texture analysis (DMTA)

Introduction

The end Pleistocene was a time of considerable environmental upheaval (Rule et al., 2012; Malhi et al., 2016), with the extinction of most megafauna (species weighing > 45 kg) (Lyons et al., 2004) occurring on the backdrop of a rapidly changing climate (Severinghaus et al., 1998; Alley, 2003). While the loss of megafauna reduced taxonomic richness more broadly, recent work has explored the megafauna extinction's role in altering ecosystem processes through the analysis of functional traits within communities. These studies have found that not only does functional diversity decline (Davis, 2017), but resilience declines with the loss of megafauna that filled unique ecological roles (Hedberg et al., 2022), highlighting the hidden consequences of species diversity loss. This work is timely, as the idea to rewild landscapes with so-called modern “functional equivalents” of Pleistocene megafauna is increasingly presented as a viable solution for restoring degraded ecosystems (Donlan et al., 2006; Svenning et al., 2016).

The search for modern functional equivalents relies on having a clear understanding of the biological roles of extinct species, and therein lies the rub. Much of our understanding of the ecological function of extinct animals has been inferred through comparisons with living analogs (Janis and Ehrhardt, 1988; Janis, 1995; Mendoza et al., 2002) and community-level paleoecological analyses are often conducted using discrete taxon-level traits and characteristics (Gladstone-Gallagher et al., 2019; Hedberg et al., 2022). Trait resolution can affect interpretation of functional structure (Kohli and Jarzyna, 2021) and the use of coarse categorizations, such as dietary group assignments (e.g., “grazer,” “mixed-feeder,” “browser,” “omnivore,” and “carnivore”) also does not account for variation in behavior within communities or across a taxon's geographic distribution. By ignoring variation, we risk limiting our understanding of the ecology of extinct species and masking community-level differences in functional diversity (Violle et al., 2012), which poses a hindrance to the possibility of rewilding.

Here, we ask how dietary function varies over the distributions of two iconic ice age taxa: mammoth (*Mammuthus*) and American mastodon (*Mammut*

americanum). There are many reasons that we expect landscape-scale patterns in intraspecific variation in diet. Within the niche of a species, and reflected by its geographic range, there are conditions that are most optimal for persistence and less optimal conditions near boundaries (Hutchinson, 1957). Variation in niche fitness is reflected in patterns of population densities across geographic ranges, which exhibit a pattern of central tendency across many organisms (Brown, 1984). Additionally, there is an interrelatedness between the niche, environmental conditions, and patterns of biological responses such as predation and competition (MacArthur and Levins, 1967; Maguire, 1973). Because the types and abundance of plants are constrained along gradients of temperature and precipitation (Whittaker, 1967) we predict that variation in the dietary behavior of mammoth and mastodon follow climate, and that diets consumed in the most environmentally suitable parts of the distribution, or “core areas,” differ from diets consumed closer to geographic boundaries, or “edges” (Hutchinson, 1957; Maguire, 1973; Brown, 1984).

Individual-level trait data can provide useful information regarding variation in ecological function between individuals, across populations, and across landscapes. Stable isotope analysis (SIA) of $\delta^{13}\text{C}$ from enamel ($\delta^{13}\text{C}_{\text{enamel}}$) is an individual-level proxy for the relative consumption of C_3 - and C_4 -based resources (e.g., Cerling et al., 1997; MacFadden et al., 1999; Secord et al., 2012; DeSantis et al., 2019). In environments where C_4 grasses are favored, $\delta^{13}\text{C}_{\text{enamel}}$ can differentiate between the consumption of C_4 grass and C_3 browse to quantify degrees of browsing, mixed-feeding, and grazing behavior in herbivores (Teeri and Stowe, 1976; Cerling et al., 1998) and quantify variation across these feeding strategies within a taxon (Pardi and DeSantis, 2021; DeSantis et al., 2022).

Often as a complement to SIA, dental microwear texture analysis (DMTA) is another tool that can provide information on the diets of individual animals (DeSantis, 2016). DMTA using scale-sensitive fractal analysis measures the following attributes: anisotropy ($epLsar$), complexity ($Asfc$), textural fill volume (Tfv), and heterogeneity of complexity compared among surfaces in a 3×3 grid ($HAsfc_3$) and in a 9×9 grid ($HAsfc_9$) (Ungar et al., 2003; Scott et al., 2005, 2006;

Scott, 2012; DeSantis, 2016). Through DMTA, microscopic tooth wear is used to characterize diets of differing hardness and toughness (Scott et al., 2006). High anisotropy is characteristic of individuals consuming tough food item such as flesh, in the case of carnivores, or grass, in the case of herbivores. High complexity distinguishes individuals consuming hard and brittle food items, while low complexity is characteristic of consuming soft items. In herbivores, DMTA has been successfully used to differentiate between diets ranging from obligate grazers to browsers to frugivores (Scott, 2012), including diets that are isotopically similar (DeSantis, 2016; DeSantis et al., 2017).

Our aim is to place intraspecific variation from SIA and DMTA into a geographic context to identify landscape-scale patterns in diet of mammoths and mastodons. Species distribution modeling (SDM) has been increasingly used to study the distribution of species over space and time, especially in response to climate change, including among fossil taxa (Martínez-Meyer et al., 2004; Elith and Leathwick, 2009; Maguire and Stigall, 2009; Wang et al., 2021). Such analyses leverage the availability of detailed paleoclimate reconstructions (e.g., Collins et al., 2006; Brown et al., 2018) as well as fossil occurrence data that are now widely accessible through databases (e.g., Williams et al., 2018). Presence-only methods, such as Maxent, are especially useful for analyzing the likely distributions of extinct species for which occurrences can be verified, but absences are uncertain or unknown (Phillips and Dudík, 2008; Elith et al., 2011). By modeling the distribution of species, relationships between climatic variables and likelihood of occurrence can be established, and geographic regions can be assessed as being more or less, suitable to a taxon.

Species distribution modeling and individual-level dietary proxies are useful tools for understanding the ecology of species. Here, we combine these approaches to explore how multiple aspects of the niche contribute to dietary variation. Mammoth and mastodon were selected for this study because they are broadly distributed, are well represented in the late Quaternary fossil record, and have diets that have been well described. Mammoth have morphological adaptations (Maglio, 1972) that permit a broad diet ranging from mixed-feeding to grazing (Smith and DeSantis, 2018, 2020; Pardi and DeSantis, 2021; DeSantis et al., 2022). In contrast, mastodon are browsers with a more narrow breadth in $\delta^{13}\text{C}$ (Green et al., 2017; Smith and DeSantis, 2018, 2020; Pardi and DeSantis, 2021; DeSantis et al., 2022), but the type of browse that is consumed can come from a variety of sources (Lepper et al., 1991; Newsom and Mithlacher, 2006) and can vary over time and space (Green et al., 2017). Our approach is to model their distributions using Maxent, and then compare variation in dietary proxies (via SIA or DMTA) over space. We ask if the diets of mammoth and mastodon living in the core areas of their distributions (and niches) differ from those living closer to the edges.

Materials and methods

Training and tuning of species distribution models

Our study treats mammoth (*Mammuthus*) at the genus level and mastodon (*Mammuth americanum*) at the species level. This choice was deliberate as a means to be congruent with (1) the treatment of dietary proxy data in the literature and (2) what genetic studies indicate is reasonable treatment of these taxa. Much of the dietary proxy data available are presented at the genus level. This is true not just for mammoth and mastodon, but across herbivores more broadly (see Pardi and DeSantis, 2021). Multiple species are currently recognized within *Mammuthus*, but study of their genetics casts doubt on current species designations; while there is phylogeographic structure in mammoth matriline, there is also introgression, potentially extensive, between nominal mammoth species and there are non-linear associations between genetics and morphological attributes that have been used to distinguish mammoth taxa (Enk et al., 2016). Mastodon taxonomy suffers in a different manner. While all of the mastodon records in our study are *M. americanum* and exclude *M. pacificus* (Dooley et al., 2019), recent genetic analyses of *M. americanum* identifies six distinct clades across the North American continent (Karpinski et al., 2020). Thus, taxonomic revisions to split *Mammuth* may be in order and the taxonomic resolution of our analyses between mammoth and mastodon are comparable.

Records identified as *Mammuthus* and *Mammuth americanum* were downloaded from the Neotoma Database¹ (Williams et al., 2018) and supplemented with a literature search (Supplementary Table 1). A record was included as an occurrence in the Maxent model if its location could be estimated with at least 20 km precision and if a high-quality date was made directly on the taxon of interest (Barnosky and Lindsey, 2010), or if there was reasonable stratigraphic evidence to accept an associated age. Radiocarbon dates were calibrated using the Intcal20 calibration curve (Reimer et al., 2020) using the “calibrate” function in the *rcarbon* package (version 1.4.3) in R (version 4.2.0) (Crema and Bevan, 2021; R Core Team, 2022). Median ages were used to place occurrences into one of the following time bins: the Last Glacial Maximum (LGM; 25,000–18,000 yr B.P.), Heinrich Stadial 1 (HS1; 17,000–14,700 yr B.P.), Bølling-Allerød (BA; 14,700–12,900 yr B.P.), and the Younger Dryas Stadial (YD; 12,900–11,700 yr B.P.).

A species distribution model was trained in Maxent², version 3.4.4 (Phillips et al., 2020) for each taxon using collective occurrences spanning the time periods of our study. Each occurrence was spatially associated with raster coverages of 19

¹ <http://neotomadb.org>

² http://biodiversityinformatics.amnh.org/open_source/maxent/

bioclimatic variables modeled for the YD, BA, and HS1 from Paleoclim (Brown et al., 2018), and the LGM (ca. 21,000 yr B.P) from the CHELSA algorithm (Karger et al., 2017). Climate rasters had a resolution of 20 km, and occurrences were spatially thinned such that no grid cell was shared by two or more occurrences within the same time bin to reduce potential issues of autocorrelation (Legendre, 1993).

Background points in the Maxent model represent the areas accessible to a species and the climatic conditions that are present at those locations. The experimentally determined minimum number of background points required to represent the available environment is 10,000 (Phillips and Dudík, 2008). Temporally balanced background points were randomly sampled by location and time period from within a seven-degree buffer surrounding each thinned occurrence, with the proportion of background points selected to match the proportion of occurrences in each time bin (Pendleton et al., 2012; Pardi and Smith, 2016). Background points were not sampled from regions covered by glaciers or large lakes (Dyke et al., 2003).

Model tuning was conducted using the function “ENMevaluate” in the R package *ENMeval* (version 2.0.3) (Kass et al., 2021) and followed a “ $n-1$ ” or “leave one out” jackknife procedure (Shcheglovitova and Anderson, 2013) varying two Maxent settings that regulate model complexity: feature class and regularization multiplier. Each omitted occurrence was used as a test case for each model trained with $n-1$ occurrences. Models were run with combinations of linear, hinge, linear with quadratic, and linear with hinge and quadratic features, and regularization multipliers ranging from 0.5 to 5.0, at 0.25 intervals. We compared a total of 76 model combinations across n iterations, each, for mammoths and mastodon. The average test omission [using the tenth percentile training presence threshold (TPT)] and average area under the receiver operating characteristic curve (AUC) across model runs was calculated for each combination. AUC is the probability that a random training occurrence will be ranked higher than a random background point (Phillips and Dudík, 2008; Elith et al., 2011). The combination that (1) minimized average omission rates and then (2) maximized average AUC values was selected for each taxon to minimize overfitting (Shcheglovitova and Anderson, 2013) while maximize predictability.

To model likely distributions for each time bin and identify geographic areas of differing likelihood of occurrence, the tuned models were projected onto gridded climate variables for each time period (Dyke et al., 2003; Karger et al., 2017; Brown et al., 2018) and categorized at different likelihood thresholds. Grid cells with modeled likelihood values above the TPT were categorized as “Core” areas. Cells below the TPT were categorized as “Edge” areas. For purposes of discussion, we further subdivided Edge areas as “intermediate” and of “lowest/least” likelihood of occurrence using the minimum training threshold (MTT). The aim of this classification was to identify geographic locations of differing likelihoods of

occurrence for each time period. Multivariate environmental similarity surfaces (MESS) were used to omit predicted areas from further analyses that fell outside of the range of climate variables used to train the models (Elith et al., 2010).

Spatial analyses of dietary proxies across regions of differing suitability

To assess how mammoth and mastodon diets varied across their niches and distributions, published dietary proxies were collected from the literature, and were then spatially and temporally compared across Core areas and Edge areas as defined by the Maxent models. Our expectation is that mammoth and mastodon vary their diets according to the suitability of the environment, as regions of the highest suitability may have greater availability of preferred resources.

Prior analyses of $\delta^{13}\text{C}_{\text{enamel}}$ have identified high variation within mammoth and characterized them as grazers that can mixed-feed; in contrast, there is low variation in $\delta^{13}\text{C}_{\text{enamel}}$ within mastodon, which are browsers (Figure 1). SIA is, therefore, unlikely to capture significant landscape-scale differences in dietary behavior within mastodon. However, DMTA has identified significant differences in the consumption of distinct browse resources by mastodons across sites of differing vegetation types (Green et al., 2017; Smith and DeSantis, 2018). We, therefore, focus our analyses of spatial variation in diets using SIA of mammoth and DMTA of mastodon. Mammoth SIA and mastodon DMTA samples were from published georeferenced specimens that had ages confirming they were from the latest Pleistocene, after the LGM (Supplementary Tables 2, 3).

We compared $\delta^{13}\text{C}_{\text{enamel}}$ values sampled from mammoth between Core and Edge areas. Analyses were geographically restricted to samples collected from occurrences from below 37° latitude (MacFadden and Cerling, 1996; Connin et al., 1998; Koch et al., 1998, 2004; Hoppe, 2004; Hoppe and Koch, 2006; Vetter, 2007; Metcalfe et al., 2011; Lundelius et al., 2019), where $\delta^{13}\text{C}_{\text{enamel}}$ values more directly reflect the relative consumption of C_3 browse and C_4 grass resources. Specifically, C_3 vegetation is likely trees, forbs, and shrubs ($\delta^{13}\text{C}_{\text{enamel}}$ values $< -9\text{‰}$) and C_4 resources are likely grasses ($\delta^{13}\text{C}_{\text{enamel}}$ values $> -2\text{‰}$) below 37° latitude (Teeri and Stowe, 1976; Cerling et al., 1997; Kohn, 2010). The temporal resolution of some SIA samples was coarser than our niche models, with the age estimates of some localities spanning time bins. We retained less temporally refined samples where the age estimate spanned time bins if they had the same suitability classification (Core vs. Edge). However, if a site spanned time bins where modeled suitabilities were different, the sample was removed from our analyses. The null hypothesis is that isotopic samples from Core areas and Edge areas are from the same distribution and indistinguishable.

Similarly, we compared DMTA values from mastodon across suitability regions. We did not employ any geographic

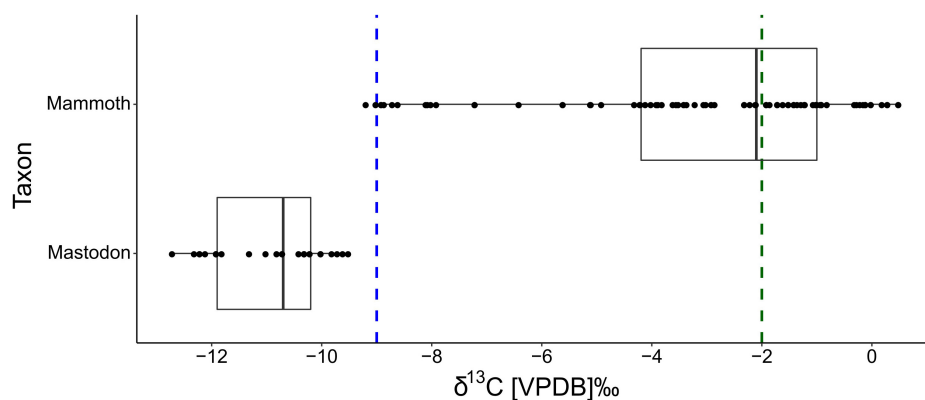


FIGURE 1

Isotopic breadth of mammoth (*Mammuthus*) and mastodon (*Mammot americanum*) during the Late Pleistocene (25–11.7 ka). Data are from latitudes below 37° North (MacFadden and Cerling, 1996; Connin et al., 1998; Koch et al., 1998, 2004; Hoppe, 2004; Hoppe and Koch, 2006; Vetter, 2007; Metcalfe et al., 2011; Lundelius et al., 2019; Pardi and DeSantis, 2021; DeSantis et al., 2022). Values are calibrated to the Vee Pee Dee Belemnite (V-PDB) standard.

constraints in these analyses; however, temporal constraints were treated the same as in mammoths. Higher complexity (*Asfc*) would be indicative of consuming harder foods, high anisotropy (*epLsar*) indicates softer and tougher foods, and low heterogeneity (*HAsfc*₃, *HAsfc*₉) may indicate specialized browsing (Scott et al., 2005; Scott, 2012). The null hypothesis is that DMTA parameters measured from Core area samples and Edge samples are from the same distribution and indistinguishable.

Results

Occurrences and model tuning

A literature search of occurrences with dates resulted in $n = 70$ occurrences of *Mammuthus* ($n = 16, 10, 28$, and 16 for the LGM, HS1, BA, and YD, respectively) and $n = 37$ occurrences of *Mammot americanum* ($n = 4, 2, 26$, and 5 , respectively) (Supplementary Table 1). The model that minimized average omission rates and maximized average validation AUC values for each taxon was selected: for mammoth, linear features with a regularization multiplier of 4.5 resulted in an average omission rate of 0.1142 and average validation AUC of 0.6661; for mastodon, hinge features and a regularization multiplier of 2.75 resulted in an average omission rate of 0.1111 and average validation AUC of 0.7948. Given these parameter settings, the final model training AUCs were 0.6842 for mammoths and 0.8436 for mastodon. An AUC of 0.7 or higher is generally considered good, however, a lower AUC may be reflective of greater difficulty in distinguishing suitable and unsuitable habitat for widespread and more generalist species (Dobrowski et al., 2011). The environmental variable with the greatest percent contribution to the mammoth model was

mean temperature of the driest quarter (85.5% contribution; Supplementary Table 4). The environmental variables with the greatest percent contribution to the mastodon model were mean temperature of the driest quarter (46.3%), maximum temperature of the warmest month (15.4%), precipitation of the coldest quarter (14.6%), and precipitation of the driest month (12.1%; Supplementary Table 5).

Modeled suitability of mammoths and interpretation of the dietary niche using stable isotope analysis

Models were projected onto climate raster layers to estimate where suitable regions for mammoth existed for each time bin in our study and classified into Core and Edge areas (Figure 2). Edge areas were further subdivided into areas that were of intermediate and lowest likelihood of occurrence. The tenth percentile training threshold was 0.3424 and the MTT was 0.2218. Projections onto the five time periods of the study indicate changes in the distribution of areas of relative likelihood (Figure 2). With the retreat of glaciers, the leading edge of Core areas for mammoth expand north but the trailing edge is displaced by Intermediate and Least Likely areas in the south, southwest, and along the west coast.

To test whether mammoth diets varied predictably with likelihood of occurrence, $\delta^{13}\text{C}_{\text{enamel}}$ values were categorized as being either from Core areas or Edge areas by age and location (Figures 2, 3). The Maxent model correctly predicted SIA sample locations as places of occurrence for mammoth: none of the SIA samples were found to be from areas modeled to be least likely, or below the MTT of the model. Within Core areas $\delta^{13}\text{C}_{\text{enamel}}$ values ranged from -8.7 to 0.5‰ with a median value of -1.5‰ ($n = 32$, $n_{\text{sites}} = 10$; Table 1). Samples from

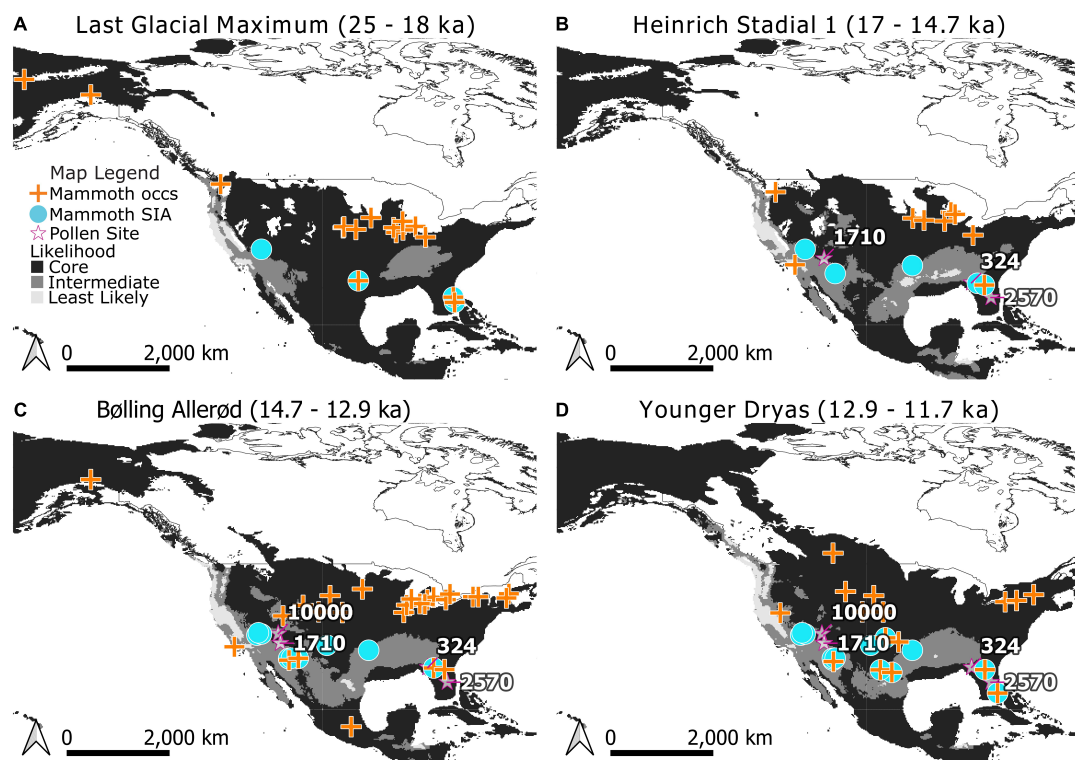


FIGURE 2

Modeled distributions for mammoth (*Mammuthus*) during the Last Glacial Maximum (A), Heinrich Stadial 1 (B), Bølling-Allerød (C), and Younger Dryas (D). Core areas are indicated in black, Edge areas are subdivided into Intermediate (medium gray) and Least Likely (light gray) categories. Occurrences used in training the Maxent models are indicated by crosses. Stable isotope analysis (SIA) sample locations are indicated by circles. Note that when a location for dietary proxy samples has age estimates spanning time bins it has been mapped across those bins for visualization purposes. Pollen records referenced in the text (stars) are labeled with their Neotoma site ID: Lake Tulane (2570), Camel Lake (324), Montezuma Well (1710), and Bear Lake (10000). The extent of North American ice sheets are shown for 18,000, 14,500, 13,000, and 11,500 radiocarbon years B.P. following Dyke et al. (2003).

Edge areas ranged from -9.0 to -0.9‰ with a median value of -2.8‰ ($n = 17$, $n_{\text{sites}} = 11$; Table 1). $\delta^{13}\text{C}_{\text{enamel}}$ sampled from Core areas were significantly less negative and reflective of the consumption of proportionally more C_4 resources (Wilcoxon rank sum and signed rank test; $W = 149$, $p = 0.01004$; Figure 3). To explore the possible effects of a larger sample size from Core areas, we applied a bootstrap analysis and plotted the distribution of resulting p -values from the Wilcoxon rank sum and signed rank test (Supplementary Figure 1). This analysis produced a median p -value of 0.03 and an interquartile range from 0.01 to 0.05, and we reject the null hypothesis on this basis.

Modeled suitability of mastodon and interpretation of the dietary niche using dental microwear texture analysis

Models were projected to estimate where regions for mastodon existed for each time bin in our study and classified into Core and Edge areas (Figure 4) using the tenth percentile

training threshold (0.4162). Edge areas were further subdivided into areas that were of Intermediate and Lowest Likelihood of occurrence using the MTT (0.1457). Projections onto the five time periods of the study indicate changes in the distribution of areas of relative likelihood (Figure 4). With the retreat of glaciers, the leading edge of Core areas for mastodon move northwards, while the trailing edge is displaced by Intermediate and Least Likely areas across the south and west.

To test whether diets of mastodon varied predictably with likelihood of occurrence, DMTA samples were categorized as being either from Core areas or from Edge areas based on their age and where they were sampled from Figures 4, 5 and compared. The Maxent model correctly predicted most of the DMTA sample locations as places of occurrence for mastodon: only one out of the 14 DMTA sample localities (Friesenhahn Cave) was from an area modeled to be least likely, meaning most were found to be at least within the MTT of the model. No significant differences were found in complexity ($Asfc$), anisotropy ($epLsar$), textural fill volume (Tfv), or heterogeneity ($Hasfc_3$ and $Hasfc_9$) between samples taken from Core areas ($n = 32$, $n_{\text{sites}} = 12$; Table 2) and Edge areas ($n = 10$, $n_{\text{sites}} = 2$;

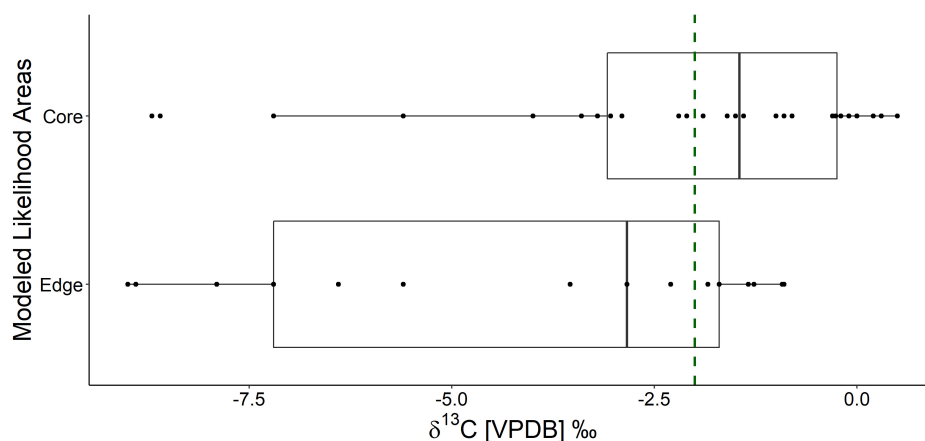


FIGURE 3

Boxplots of $\delta^{13}\text{C}_{\text{enamel}}$ from mammoth (*Mammuthus*) collected below 37° latitude. Samples from Core areas of the distribution (highest likelihood of occurrence) are compared to those in Edge areas (intermediate and lowest likelihood of occurrence). Raw values are plotted in addition to the distributions given by the boxplots. The dashed green line indicates a $\delta^{13}\text{C}_{\text{enamel}}$ value of -2.0‰ which is the threshold between a mixed-feeding versus grazing diet. Samples from Core areas are significantly less negative (Wilcoxon rank sum and signed rank test; $W = 149$, $p = 0.01004$).

Table 2). While a Wilcoxon rank sum and signed rank test of *Asfc* failed to reject the null hypothesis when evaluated at $\alpha = 0.05$ ($W = 100$, $p = 0.0788$), samples from Core areas had *Asfc* values that ranged from 0.537 to 5.926 and had a median value that was higher (1.904) than samples from Edge areas ranging 0.429 to 2.759 (median = 1.055; **Figure 5**). A comparison of the summary statistics across DMTA textures suggests that individuals are most differentiated by complexity (*Asfc*) over space when compared to any other texture variable (**Table 2**).

Discussion

Rather than attempt to strictly define geographic ranges of mammoth (*Mammuthus*) and mastodon (*Mammot americanum*), which SDMs often over- or under-predict (Mellert et al., 2011; Marcer et al., 2013; Lee-Yaw et al., 2022), our aim was to compare dietary function within Core areas of greatest likelihood to dietary function in Edge areas of lower likelihood (Peterson et al., 2018; **Figures 2, 4**). We established correlative relationships between climatic variables and likelihood of occurrence to test the hypothesis that mammoth and mastodon consume variable diets at the landscape scale according to relative suitability of the environment using the maximum-entropy approach of species distribution modeling. We found evidence for significant dietary preferences of mammoth (**Figure 3** and **Table 1**), while preference in mastodon was less resolved (**Figure 5** and **Table 2**).

Despite the cosmopolitan distribution of mammoth and their apparent high variation of dietary breadth (Smith and DeSantis, 2018), greater consumption of grass in Core areas across their modeled distribution suggests a preference for grass

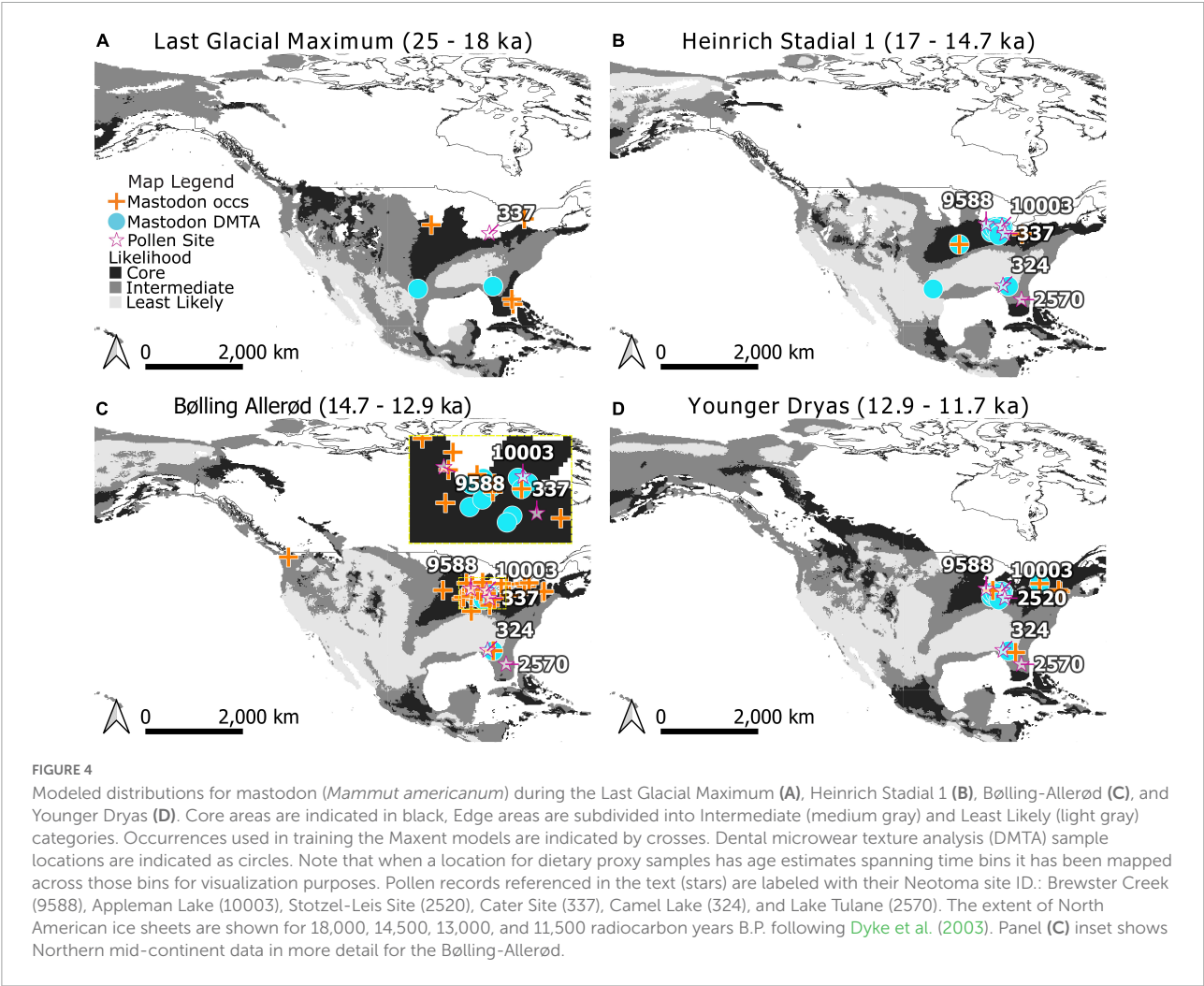
(**Figure 3**) as would be expected from both their morphology (Maglio, 1972) and as a requirement for adequate rates of tooth wear (Fagan et al., 1999). These preferences resemble those of *Elephas maximus* (Asian elephants) which are variable mixed-feeders with a preference for grazing (Sukumar et al., 1987; Baskaran et al., 2010; Koirala et al., 2016).

As a dietary proxy, $\delta^{13}\text{C}_{\text{enamel}}$ can discriminate between browse and graze consumption at low latitudes (below 37°) because most low-latitude grasses use the C_4 photosynthetic pathway and have tissues that are isotopically distinct from those of C_3 trees, forbs, and shrubs (Teeri and Stowe, 1976; Paruelo and Lauenroth, 1996; Cerling et al., 1997, 1998; Macfadden et al., 1999). High $\delta^{13}\text{C}_{\text{enamel}}$ values from individuals sampled at low latitudes in our study indicate greater consumption of C_4 grass by mammoths where they are most likely to occur. Preference is exhibited when a resource is utilized at a higher frequency than it occurs, and these individuals are from landscapes of mixed, but C_3 -browse dominant, resources. Local pollen records from Camel Lake (Watts et al., 1992; Wang et al., 2019) and Lake Tulane (Grimm et al., 1993; Wang et al., 2019; **Figure 2**) confirm the presence of mixed-parkland and deciduous forest environments coincident with SIA samples during Heinrich Stadial 1 through the Younger Dryas (**Supplementary Table 6**). Where, then, are these mammoth grazing?

Elephants typically maintain small home ranges (<250 km) (Bonhof and Pryor, 2022) but exhibit variable nomadic behavior that is influenced by seasonal change of habitat, the availability of food and water, as well as sex (Sukumar et al., 1987; Baskaran et al., 2010; Koirala et al., 2016). Similar movement patterns in mammoths have been inferred from $^{87}\text{Sr}/^{86}\text{Sr}$ analyses, although longer treks to other geographic areas are feasible (Bonhof and Pryor, 2022). If grasses are distributed heterogeneously in

TABLE 1 Summary statistics of $\delta^{13}\text{C}_{\text{enamel}}$ for mammoth (*Mammuthus*) in this study.

Modeled area	<i>n</i>	<i>n</i> -sites	$\delta^{13}\text{C}_{\text{enamel}}$ V-PDB (‰)					
			Mean	Median	SD	Min	Max	Range
Core area	32	10	−2.2	−1.5	2.6	−8.7	0.5	9.2
Edge area	17	11	−4.3	−2.8	3.1	−9	−0.9	9.9



patches within a browse-dominated environment, mammoth could have selectively made use of these resources by traveling between patches. However, enriched $\delta^{13}\text{C}_{\text{enamel}}$ values signaling the use of C_4 resources indicate that grazing was primarily at lower latitudes, as the relative abundance of C_3 to C_4 grasses increases with latitude (Teeri and Stowe, 1976; Paruelo and Lauenroth, 1996; Cerling et al., 1997, 1998; Macfadden et al., 1999).

Mammoth sampled from Edge areas of lower likelihood made greater use of mixed C_3 and C_4 resources (Figure 3). These individuals may be consuming the local vegetation. Pollen from Montezuma Well (Davis and Shafer, 1992) documents

predominantly desert vegetation which includes on average ~5% diversity from grasses during Heinrich Stadial 1 through the Younger Dryas, near SIA samples in the Southwest (Figure 2 and Supplementary Table 6). Another nearby pollen site is Bear Lake (Weng and Jackson, 1999), which documents predominantly spruce parkland with on average <1% grasses and sedges during the Bølling-Allerød and the Younger Dryas. Alternatively, these individuals could be acquiring a mixed signal by consuming C_3 grasses from higher latitudes: future studies of individual movement can help clarify where these animals are foraging.

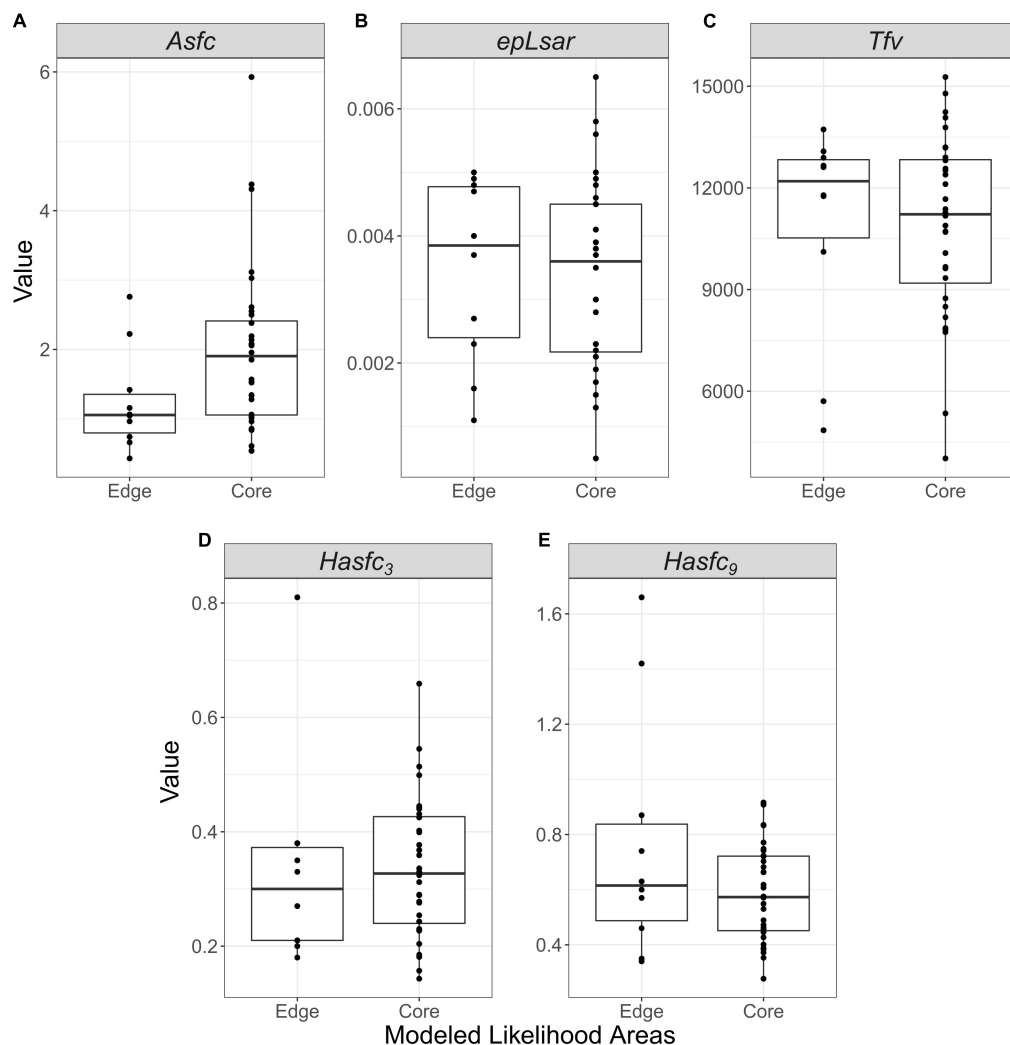


FIGURE 5

Boxplots of *epLsar* (A), *Asfc* (B), *Tfv* (C), *Hasfc₃* (D), and *Hasfc₉* (E) for mastodon (*Mammot americanum*). Individuals sampled from Core areas of the distribution (highest likelihood of occurrence) are compared to those in Edge areas (intermediate and lowest likelihood of occurrence). Raw values are plotted in addition to the distributions given by the boxplots. A Wilcoxon rank sum and signed rank test found no significant differences between groups for any dental microwear texture analysis (DMTA) texture parameter.

Dietary preferences are less clearly defined for mastodon. Their isotopic breadth is, overall, relatively low and indicates restricted use of C₃ resources (Figure 1; Pardi and DeSantis, 2021). However, analyses a coprolites demonstrate that they consumed a broad variety of C₃ plants (Lepper et al., 1991; Newsom and Muhlbachler, 2006). We therefore analyzed published DMTA values to explore variance in food texture across their modeled distribution. Mastodon from Core areas of highest likelihood of occurrence have somewhat higher complexity (*Asfc*) values (median = 1.904, Figure 5 and Table 2) than Edge areas (median = 1.055) which hints at greater consumption of brittle or hard food items (bark, nuts, and seeds) in Core areas, although this difference is non-significant ($p = 0.0788$). The bulk of what is known about mastodon

diets inferred through DMTA comes from a handful of studies comparing regional and temporal variation across sites of differing habitats (Green et al., 2017; Smith and DeSantis, 2018, 2020) and age demographics (Smith and DeSantis, 2018). Sampling for mastodon DMTA does not have nearly the breadth of geographic coverage as SIA for mammoth (Figures 2, 3). Future analyses of DMTA from samples collected outside of the Core areas of highest likelihood will help to clarify dietary preferences.

Although we were unable to identify significant differences in mastodon diets according to their likelihood of occurrence using DMTA, contemporaneous pollen records point to habitat types that may have been more suitable. Core areas of high likelihood of occurrence are consistently present for mastodon

TABLE 2 Summary statistics of dental microwear texture analysis (DMTA) texture attributes for mastodon (*Mammuth americanum*) in this study.

Modeled area	Statistic	<i>n</i>	<i>n</i> -sites	<i>Asfc</i>	<i>epLsar</i>	<i>Tfv</i>	<i>HAsfs</i> 3 × 3	<i>HAsfc</i> 9 × 9
Core area	Mean	32	12	1.977	0.0034	10891.8	0.337	0.586
	Median			1.904	0.0036	11221.0	0.327	0.573
	SD			1.200	0.0015	2682.3	0.122	0.173
	Min			0.537	0.0005	4016.0	0.143	0.277
	Max			5.926	0.0065	15271.0	0.659	0.916
	Range			5.389	0.0060	11255.0	0.516	0.639
Edge area	Mean	10	2	1.246	0.0035	10916.6	0.332	0.764
	Median			1.055	0.0039	12197.1	0.300	0.615
	SD			0.723	0.0015	3135.1	0.185	0.444
	Min			0.429	0.0011	4846.8	0.180	0.340
	Max			2.759	0.0050	13724.6	0.810	1.660
	Range			2.330	0.0039	8877.8	0.630	1.320

in the northern midcontinent during the late Pleistocene (Figure 4). Numerous pollen records from this region (Brewster Lake, Appleman Lake, Stotzel-Leis Site, and Carter Site) indicate the presence of mixed-parkland and prairie throughout the this time (Shane, 1987; Curry et al., 2007; Gill et al., 2009; Figure 4; Supplementary Table 6). This contrasts with pollen records near mastodon in Edge areas in the southeast, such as Camel Lake (Watts et al., 1992; Wang et al., 2019) and Lake Tulane (Grimm et al., 1993; Wang et al., 2019; Figure 4) which confirm the presence of mixed-parkland and deciduous forest.

When considering the scale and temporal grain of different dietary proxies, $\delta^{13}\text{C}_{\text{enamel}}$ and microwear can reasonably be applied to questions of habitat tracking and behavioral plasticity (Davis and Pineda-Munoz, 2016). $\delta^{13}\text{C}_{\text{enamel}}$ integrates the isotopic signal of the resources being used over the weeks to months of life during which the enamel mineralizes, which could also mean an integration of resources used across a geographic area for a highly mobile animal. For this reason, SIA is a reasonable proxy for what an animal is eating at the scale of a landscape (Davis and Pineda-Munoz, 2016) as we have applied it here. In contrast, microwear records properties of the food consumed during the days to weeks leading up to death (Grine, 1986). It therefore has high fidelity to the specific location where an individual is found as a fossil. DMTA has been applied to characterize interspecific dietary variation (Scott, 2012; DeSantis, 2016) as well as intraspecific variation over time and space (Rivals et al., 2007).

The mastodons sampled for DMTA from Friesenhahn Cave warrant further comment. These individuals are juveniles and have low complexity values (Supplementary Table 3). It is unclear if these low values represent ontogenetic niche partitioning or dietary differences that are reflective of the environment, and the question of whether there are ontogenetic shifts in mastodon diet, more generally, is still open (Smith and DeSantis, 2018). The megafaunal remains at Friesenhahn Cave span a dynamic time (15–20 ka) (Graham et al., 2013)

where the region experienced a shift from high likelihood of mastodon occurrence to low likelihood (Figure 4). The local vegetation around Friesenhahn Cave is described in other studies as C_4 open grassland with some riparian forests (Hoppe, 2004; Koch et al., 2004; Graham et al., 2013), consistent with our classification of this locality as outside the Core niche of mastodon.

There are refinements that could be made to our models that should be considered before any application beyond the scope of our study. High likelihood of occurrence is not equivalent to presence (Elith and Leathwick, 2009), and we do not account for physical barriers to dispersal. Doing so, however, would not qualitatively affect our results, as we are only concerned with drawing interpretations from dietary proxies from known occurrences. Our models are explicitly limited to relating climate variables with occurrence, which assumes climate is adequately correlated with resources that are required by Proboscideans (e.g., water and vegetation) (Sukumar et al., 1987; Baskaran et al., 2010; Koirala et al., 2016; Bonhof and Pryor, 2022). Realized niches are impacted by variables beyond climate, including biotic interactions (Hutchinson, 1957; Leibold, 1995; Chase and Leibold, 2009), which our models do not account for.

A potentially strong biotic interaction that warrants future investigation is competition. As some of the very largest animals on the landscape, Proboscideans function as ecosystem engineers (Owen-Smith, 1992). Today, African elephants (*Loxodonta africana*) compete with mesobrowsers and mesomixed feeders, but facilitate mesograzers (Fritz et al., 2002). The presence of megaherbivores, such as modern elephants, impacts the feeding of smaller sympatric herbivores; however, Pleistocene environments supported a much more diverse megaherbivore community. Were sympatric megaherbivores competing with each other, or partitioning resources? DMTA analyses of three middle/late Miocene Proboscideans (*Gomphotherium subtapiroideum*, *Gomphotherium steinheimense*, and *Deinotherium giganteum*)

from the Molasse Basin in Southern Germany supports niche partitioning rather than competition for resources (Calandra et al., 2008). In contrast, competitive exclusion imposed by *Mammut* and *Mammuthus* is a plausible cause for the eventual extinction of gomphotheres (*Cuvieronius*) in North America (Smith and DeSantis, 2020).

Mammoth and mastodon sometimes do co-occur, at least regionally. In the Northern, North American mid-continent, they exhibit partial isotopic niche overlap in their use of C_3 resources (Widga et al., 2021), although whether this represents consumption of C_3 browse or graze within these mammoth is not resolved. The influence these taxa have on each other more generally when they share a landscape remains to be clarified. Do they partition resources, and if so, how is this impacted by geographic variation in environmental suitability as we have identified in the present study? Our models identify geographic locations where there is overlap of Core niche areas for mammoth and mastodon, as well as areas where one is more likely to occur over the other. For example, the Core area of mammoth overlaps with the Edge areas for mastodon in Florida. In contrast, there appear to be few regions where the Core area of mastodon overlaps where mammoth are at the edge of their niche. Our current dataset is not extensive enough to directly compare diets within and outside of areas of sympatry, but our models could provide context for future comparisons.

Our study is unique in that it aims to explore dietary preference and spatially explicit variation within the context of the ecological niches of extinct taxa. Dietary proxy data alone can be incredibly useful for quantifying how resources are being used by individuals and populations over time and space (MacFadden and Cerling, 1996; Scott et al., 2005, 2006; DeSantis, 2016). Our approach provides a means for contextualizing proxy data by the suitability of the environment across the geographic distribution of a taxon. This context matters because ecological interactions and factors influencing populations at geographic range margins are not the same as in the center of the range—boundaries exist because of limiting conditions preventing persistence that are not so limiting elsewhere (Hutchinson, 1957; Brown, 1984).

The approach presented here provides a means for applying distributional context to interpretation of paleoecological data, where occurrences are known but boundaries of geographic ranges are poorly defined. This may be particularly useful when considering the potential causes and consequences of extinctions across landscapes. For example, one could reasonably point to climate and environmental change as a possible cause for late Pleistocene declines and extirpation of mastodon and mammoth in the Central and Southern Great Plains, as likelihood of occurrence decreases with climate change over time (Figures 2, 4). However, losses in the Core area of their distributions may have other causes, such as hunting and landscape changes caused by humans, which is supported by synchronous patterns of extinction and the timing and trajectory

of human dispersal (Surovell et al., 2005, 2016; Hamilton and Buchanan, 2007).

Analyses of functional diversity can reveal hidden consequences of taxonomic diversity loss. However, applying taxon-level traits in functional diversity analyses may mask variation that arises from plastic behavior. Specifically, dietary behavior can vary due to the non-uniform distribution of resources and biotic interactions over space. Here, we illustrate this point by exploring how diet, measured through proxies, varies over the modeled distributions of mammoths and mastodon. Mammoth dietary behavior varies by context across their geographic distribution, despite having evolutionary adaptations for grazing and exhibiting a preference for grass overall as a taxon. In contrast, specific dietary preferences for mastodon are less resolved and our analyses were unable to identify significant differences in the selection of browse across their distribution as it relates to likelihood of occurrence. The ecological roles of some species may be context specific and need to be critically evaluated when planning for the management of reintroductions or introducing novel species to restore lost ecological function.

Data availability statement

The original contributions presented in this study are included in the article/Supplementary material, further inquiries can be directed to the corresponding author.

Author contributions

MP collected data, conducted analyses, and wrote the first draft of the manuscript. LD collected data, aided in the development of the research, and helped with revisions to the manuscript. Both authors contributed to the article and approved the submitted version.

Funding

This work was funded by the National Science Foundation (EAR 1725154) and Vanderbilt University.

Acknowledgments

We are thankful to all who have contributed to the Neotoma database and all of the museum staff who have collected, curated, and managed the specimens used in this manuscript. We also thank C. Widga and A. Jukar for valuable discussions about Proboscideans and the feedback provided by two anonymous reviewers.

Conflict of interest

The authors declare that the research was conducted in the absence of any commercial or financial relationships that could be construed as a potential conflict of interest.

Publisher's note

All claims expressed in this article are solely those of the authors and do not necessarily represent those of their affiliated

organizations, or those of the publisher, the editors and the reviewers. Any product that may be evaluated in this article, or claim that may be made by its manufacturer, is not guaranteed or endorsed by the publisher.

Supplementary material

The Supplementary Material for this article can be found online at: <https://www.frontiersin.org/articles/10.3389/fevo.2022.1064299/full#supplementary-material>

References

- Alley, R. B. (2003). Abrupt climate change. *Science* 299, 2005–2010. doi: 10.1126/science.1081056
- Barnosky, A. D., and Lindsey, E. L. (2010). Timing of quaternary megafaunal extinction in South America in relation to human arrival and climate change. *Q. Int.* 217, 10–29. doi: 10.1016/j.quaint.2009.11.017
- Baskaran, N., Balasubramanian, M., Swaminathan, S., and Desai, A. A. (2010). Feeding ecology of the Asian elephant *Elephas maximus* Linnaeus in the Nilgiri biosphere reserve, Southern India. *J. Bombay Nat. Hist. Soc.* 107, 3–13.
- Bonhof, W. J., and Pryor, A. J. E. (2022). Proboscideans on parade: A review of the migratory behaviour of elephants, mammoths, and mastodons. *Quat. Sci. Rev.* 277:107304. doi: 10.1016/j.quascirev.2021.107304
- Brown, J. H. (1984). On the relationship between abundance and distribution of species. *Am. Nat.* 124, 255–279. doi: 10.1086/284267
- Brown, J. L., Hill, D., Dolan, A. M., and Carnaval, A. C. (2018). PaleoClim, high spatial resolution paleoclimate surfaces for global land areas. *Sci. Data* 5:180254. doi: 10.1038/sdata.2018.254
- Calandra, I., Göhlich, U. B., and Merceron, G. (2008). How could sympatric megaherbivores coexist? Example of niche partitioning within a proboscidean community from the Miocene of Europe. *Naturwissenschaften* 95, 831–838. doi: 10.1007/s00114-008-0391-y
- Cerling, T. E., Ehleringer, J. R., and Harris, J. M. (1998). Carbon dioxide starvation, the development of C4 ecosystems, and mammalian evolution. *Philos. Trans. R. Soc. B Biol. Sci.* 353, 159–171. doi: 10.1098/rstb.1998.0198
- Cerling, T. E., Harris, J. M., MacFadden, B. J., Leakey, M. G., Quade, J., Eisenmann, V., et al. (1997). Global vegetation change through the Miocene/Pliocene boundary. *Nature* 389, 153–158. doi: 10.1038/38229
- Chase, J. M., and Leibold, M. A. (2009). *Ecological niches: Linking classical and contemporary approaches*. Chicago, IL: University of Chicago Press.
- Collins, W. D., Bitz, C. M., Blackmon, M. L., Bonan, G. B., Bretherton, C. S., Carton, J. A., et al. (2006). The community climate system model version 3 (CCSM3). *J. Clim.* 19, 2122–2143. doi: 10.1175/JCLI3761.1
- Connin, S. L., Betancourt, J., and Quade, J. (1998). Late pleistocene C4 plant dominance and summer rainfall in the Southwestern United States from isotopic study of herbivore teeth. *Quat. Res.* 50, 179–193. doi: 10.1006/qres.1998.1986
- Crema, E. R., and Bevan, A. (2021). Inference from large sets of radiocarbon dates: Software and methods. *Radiocarbon* 63, 23–39. doi: 10.1017/RDC.2020.95
- Curry, B. B., Grimm, E. C., Slate, J., and Hansen, B. C. (2007). *The late-glacial and early Holocene geology, paleoecology, and paleohydrology of the Brewster Creek site, a proposed wetland restoration site, Pratt's Wayne woods forest preserve, and James "Pate" Philip State Park, Bartlett, Illinois*. Champaign, IL: Illinois State Geological Survey.
- Davis, M. (2017). What North America's skeleton crew of megafauna tells us about community disassembly. *Proc. R. Soc. B Biol. Sci.* 284:20162116. doi: 10.1098/rspb.2016.2116
- Davis, M., and Pineda-Munoz, S. (2016). The temporal scale of diet and dietary proxies. *Ecol. Evol.* 6, 1883–1897. doi: 10.1002/ece3.2054
- Davis, O. K., and Shafer, D. S. (1992). A Holocene climatic record for the Sonoran Desert from pollen analysis of Montezuma Well, Arizona, USA. *Palaeogeogr. Palaeoclimatol. Palaeoecol.* 92, 107–119. doi: 10.1016/0031-0182(92)90137-T
- DeSantis, L. R. (2016). Dental microwear textures: Reconstructing diets of fossil mammals. *Surface Topogr.* 4:023002. doi: 10.1088/2051-672X/4/2/023002
- DeSantis, L. R. G., Crites, J. M., Feranec, R. S., Fox-Dobbs, K., Farrell, A. B., Harris, J. M., et al. (2019). Causes and consequences of pleistocene megafaunal extinctions as revealed from rancho La Brea mammals. *Curr. Biol.* 29, 2488–2495.e2. doi: 10.1016/j.cub.2019.06.059
- DeSantis, L. R. G., Field, J. H., Wroe, S. W., and Dodson, J. R. (2017). Dietary responses of Sahul (Pleistocene Australia–New Guinea) megafauna to climate and environmental change. *Paleobiology* 43, 181–195. doi: 10.1017/pab.2016.50
- DeSantis, L. R. G., Pardi, M. I., Du, A., Greshko, M. A., Yann, L. T., Hulbert, R. C., et al. (2022). Global long-term stability of individual dietary specialization in herbivorous mammals. *Proc. R. Soc. B Biol. Sci.* 289:20211839. doi: 10.1098/rspb.2021.1839
- Dobrowski, S. Z., Thorne, J. H., Greenberg, J. A., Safford, H. D., Mynsberge, A. R., Crimmins, S. M., et al. (2011). Modeling plant ranges over 75 years of climate change in California, USA: Temporal transferability and species traits. *Ecol. Monogr.* 81, 241–257. doi: 10.1890/10-1325.1
- Donlan, C. J., Berger, J., Bock, C. E., Bock, J. H., Burney, D. A., Estes, J. A., et al. (2006). Pleistocene rewilding: An optimistic agenda for twenty-first century conservation. *Am. Nat.* 168, 660–681. doi: 10.1086/508027
- Dooley, A. C. Jr., Scott, E., Green, J., Springer, K. B., Dooley, B. S., and Smith, G. J. (2019). *Mammot pacificus* sp. nov., a newly recognized species of mastodon from the Pleistocene of western North America. *PeerJ* 7:e6614. doi: 10.7717/peerj.6614
- Dyke, A. S., Moore, A., and Robertson, L. (2003). *Deglaciation of North America, open file 1574*. Ottawa: Natural Resources Canada.
- Elith, J., Kearney, M., and Phillips, S. (2010). The art of modelling range-shifting species. *Methods Ecol. Evol.* 1, 330–342.
- Elith, J., and Leathwick, J. R. (2009). Species distribution models: Ecological explanation and prediction across space and time. *Annu. Rev. Ecol. Syst.* 40, 677–697. doi: 10.1146/annurev.ecolsys.110308.120159
- Elith, J., Phillips, S. J., Hastie, T., Dudik, M., Chee, Y. E., and Yates, C. J. (2011). A statistical explanation of MaxEnt for ecologists. *Divers. Distrib.* 17, 43–57.
- Enk, J., Devault, A., Widga, C., Saunders, J., Szpak, P., Southon, J., et al. (2016). Mammuthus population dynamics in late pleistocene North America: Divergence, phylogeography, and introgression. *Front. Ecol. Evol.* 4:42. doi: 10.3389/fevo.2016.00042
- Fagan, D. A., Oosterhuis, J. E., and Roocroft, A. (1999). Significant dental disease in elephants. *Verh. Ber. Erkr. Zootiere* 39, 15–133.
- Fritz, H., Duncan, P., Gordon, I. J., and Illius, A. W. (2002). Megaherbivores influence trophic guilds structure in African ungulate communities. *Oecologia* 131, 620–625. doi: 10.1007/s00442-002-0919-3
- Gill, J. L., Williams, J. W., Jackson, S. T., Lininger, K. B., and Robinson, G. S. (2009). Pleistocene megafaunal collapse, novel plant communities, and enhanced fire regimes in North America. *Science* 326, 1100–1103. doi: 10.1126/science.1179504

- Gladstone-Gallagher, R. V., Pilditch, C. A., Stephenson, F., and Thrush, S. F. (2019). Linking traits across ecological scales determines functional resilience. *Trends Ecol. Evol.* 34, 1080–1091. doi: 10.1016/j.tree.2019.07.010
- Graham, R. W., Lundelius, E. L., and Meissner, L. (2013). "Friesenhahn cave: Late pleistocene paleoecology and predator-prey relationships of mammoths with an extinct scimitar cat," in *Late cretaceous to quaternary strata and fossils of Texas: Field excursions celebrating 125 years of GSA and Texas geology*, GSA South-central section meeting, Austin, Texas, April 2013, eds B. B. Hunt and E. J. Catlos (Boulder, CO: Geological Society of America), 15–31. doi: 10.1130/2013.0030(02)
- Green, J. L., DeSantis, L. R. G., and Smith, G. J. (2017). Regional variation in the browsing diet of pleistocene *Mammot americanum* (Mammalia, Proboscidea) as recorded by dental microwear textures. *Palaeogeogr. Palaeoclimatol. Palaeoecol.* 487, 59–70. doi: 10.1016/j.palaeo.2017.08.019
- Grimm, E. C., Jacobson, G. L. Jr., Watts, W. A., Hansen, B. C., and Maasch, K. A. (1993). A 50,000-year record of climate oscillations from Florida and its temporal correlation with the Heinrich events. *Science* 261, 198–200. doi: 10.1126/science.261.5118.198
- Grine, F. E. (1986). Dental evidence for dietary differences in *Australopithecus* and *Paranthropus*: A quantitative analysis of permanent molar microwear. *J. Hum. Evol.* 15, 783–822. doi: 10.1016/S0047-2484(86)80010-0
- Hamilton, M. J., and Buchanan, B. (2007). Spatial gradients in Clovis-age radiocarbon dates across North America suggest rapid colonization from the north. *Proc. Natl. Acad. Sci. U.S.A.* 104, 15625–15630. doi: 10.1073/pnas.0704215104
- Hedberg, C. P., Lyons, S. K., and Smith, F. A. (2022). The hidden legacy of megafaunal extinction: Loss of functional diversity and resilience over the Late Quaternary at Hall's Cave. *Glob. Ecol. Biogeogr.* 31, 294–307. doi: 10.1111/geb.13428
- Hoppe, K. A. (2004). Late Pleistocene mammoth herd structure, migration patterns, and Clovis hunting strategies inferred from isotopic analyses of multiple death assemblages. *Paleobiology* 30, 129–145.
- Hoppe, K. A., and Koch, P. L. (2006). "The biogeochemistry of the Aucilla river fauna," in *First floridians and last mastodons: The page-ladson site in the Aucilla river*, ed. S. D. Webb (Dordrecht: Springer Netherlands), 379–401.
- Hutchinson, G. E. (1957). Concluding remarks. *Cold Spring Harb. Symp. Quant. Biol.* 22, 415–427.
- Janis, C. M. (1995). "Correlations between craniodental morphology and feeding behavior in ungulates: Reciprocal illumination between living and fossil taxa," in *Functional morphology in vertebrate paleontology*, ed. J. J. Thomasson (Cambridge: Cambridge University Press), 76–98.
- Janis, C. M., and Ehrhardt, D. (1988). Correlation of relative muzzle width and relative incisor width with dietary preference in ungulates. *Zool. J. Linn. Soc.* 92, 267–284. doi: 10.1111/j.1096-3642.1988.tb01513.x
- Karger, D. N., Conrad, O., Böhrer, J., Kawohl, T., Kreft, H., Soria-Auza, R. W., et al. (2017). Climatologies at high resolution for the earth's land surface areas. *Sci. Data* 4:170122. doi: 10.1038/sdata.2017.122
- Karpinski, E., Hackenberger, D., Zazula, G., Widga, C., Duggan, A. T., Golding, G. B., et al. (2020). American mastodon mitochondrial genomes suggest multiple dispersal events in response to Pleistocene climate oscillations. *Nat. Commun.* 11:4048. doi: 10.1038/s41467-020-17893-z
- Kass, J. M., Muscarella, R., Galante, P. J., Bohl, C. L., Pinilla-Buitrago, G. E., Boria, R. A., et al. (2021). ENMeval 2.0: Redesigned for customizable and reproducible modeling of species' niches and distributions. *Methods Ecol. Evol.* 12, 1602–1608. doi: 10.1111/2041-210X.13628
- Koch, P. L., Diffenbaugh, N. S., and Hoppe, K. A. (2004). The effects of late Quaternary climate and pCO₂ change on C4 plant abundance in the south-central United States. *Palaeogeogr. Palaeoclimatol. Palaeoecol.* 207, 331–357. doi: 10.1016/j.palaeo.2003.09.034
- Koch, P. L., Hoppe, K. A., and Webb, S. D. (1998). The isotopic ecology of late Pleistocene mammals in North America, Part 1: Florida. *Chem. Geol.* 152, 119–138. doi: 10.1016/S0009-2541(98)00101-6
- Kohli, B. A., and Jarzyna, M. A. (2021). Pitfalls of ignoring trait resolution when drawing conclusions about ecological processes. *Glob. Ecol. Biogeogr.* 30, 1139–1152. doi: 10.1111/geb.13275
- Kohn, M. J. (2010). Carbon isotope compositions of terrestrial C3 plants as indicators of (paleo)ecology and (paleo)climate. *Proc. Natl. Acad. Sci. U.S.A.* 107, 19691–19695. doi: 10.1073/pnas.1004933107
- Koirala, R. K., Raubenheimer, D., Aryal, A., Pathak, M. L., and Ji, W. (2016). Feeding preferences of the Asian elephant (*Elephas maximus*) in Nepal. *BMC Ecol.* 16:54. doi: 10.1186/s12898-016-0105-9
- Lee-Yaw, J., McCune, J., Pironon, S., and Sheth, S. (2022). Species distribution models rarely predict the biology of real populations. *Ecography* 2022:e05877. doi: 10.1111/ecog.05877
- Legendre, P. (1993). Spatial autocorrelation: Trouble or new paradigm? *Ecology* 74, 1659–1673. doi: 10.2307/1939924
- Leibold, M. A. (1995). The niche concept revisited: Mechanistic models and community context. *Ecology* 76, 1371–1382.
- Lepper, B. T., Frolking, T. A., Fisher, D. C., Goldstein, G., Sanger, J. E., Wymer, D. A., et al. (1991). Intestinal contents of a late Pleistocene mastodont from midcontinental North America. *Quat. Res.* 36, 120–125. doi: 10.1016/0033-5894(91)90020-6
- Lundelius, E. L. Jr., Thies, K. J., Graham, R. W., Bell, C. J., Smith, G. J., and DeSantis, L. R. G. (2019). Proboscidea from the big cypress creek fauna, Deweyville formation, Harris County, Texas. *Quat. Int.* 530–531, 59–68. doi: 10.1016/j.quaint.2019.11.018
- Lyons, S. K., Smith, F. A., and Brown, J. H. (2004). Of mice, mastodons and men: Human-mediated extinctions on four continents. *Evol. Ecol. Res.* 6, 339–358.
- Macarthur, R., and Levins, R. (1967). The limiting similarity, convergence, and divergence of coexisting species. *Am. Nat.* 101, 377–385. doi: 10.1086/282505
- MacFadden, B. J., and Cerling, T. E. (1996). Mammalian herbivore communities, ancient feeding ecology, and carbon isotopes: A 10 million-year sequence from the Neogene of Florida. *J. Vertebr. Paleontol.* 16, 103–115.
- MacFadden, B. J., Cerling, T. E., Harris, J. M., and Prado, J. (1999). Ancient latitudinal gradients of C3/C4 grasses interpreted from stable isotopes of new world pleistocene horse (*Equus*) teeth. *Glob. Ecol. Biogeogr.* 8, 137–149.
- MacFadden, B. J., Solounias, N., and Cerling, T. E. (1999). Ancient diets, ecology, and extinction of 5-million-year-old horses from Florida. *Science* 283, 824–827.
- Maglio, V. J. (1972). Evolution of mastication in the Elephantidae. *Evolution* 26, 638–658. doi: 10.1111/j.1558-5646.1972.tb01970.x
- Maguire, B. (1973). Niche response structure and the analytical potentials of its relationship to the habitat. *Am. Nat.* 107, 213–246. doi: 10.1086/282827
- Maguire, K. C., and Stigall, A. L. (2009). Using ecological niche modeling for quantitative biogeographic analysis: A case study of Miocene and Pliocene Equinae in the Great Plains. *Paleobiology* 35, 587–611. doi: 10.1666/0094-8373-35.4.587
- Malhi, Y., Doughty, C. E., Galetti, M., and Terborgh, J. W. (2016). Megafauna and ecosystem function from the Pleistocene to the Anthropocene. *Proc. Natl. Acad. Sci. U.S.A.* 113, 838–846. doi: 10.1073/pnas.1502540113
- Marcen, A., Sáez, L., Molowny-Horas, R., Pons, X., and Pino, J. (2013). Using species distribution modelling to disentangle realised versus potential distributions for rare species conservation. *Biol. Conserv.* 166, 221–230. doi: 10.1016/j.biocon.2013.07.001
- Martinez-Meyer, E., Peterson, A. T., and Hargrove, W. W. (2004). Ecological niches as stable distributional constraints on mammal species, with implications for pleistocene extinctions and climate change projections for biodiversity. *Glob. Ecol. Biogeogr.* 13, 305–314.
- Mellert, K. H., Fensterer, V., Küchenhoff, H., Reger, B., Kölling, C., Klemmt, H. J., et al. (2011). Hypothesis-driven species distribution models for tree species in the Bavarian Alps. *J. Veg. Sci.* 22, 635–646. doi: 10.1111/j.1654-1103.2011.01274.x
- Mendoza, M., Janis, C. M., and Palmqvist, P. (2002). Characterizing complex craniodental patterns related to feeding behaviour in ungulates: A multivariate approach. *J. Zool.* 258, 223–246. doi: 10.1017/S0952836902001346
- Metcalfe, J. Z., Longstaffe, F. J., Ballenger, J. A., and Haynes, C. V. Jr. (2011). Isotopic paleoecology of Clovis mammoths from Arizona. *Proc. Natl. Acad. Sci. U.S.A.* 108, 17916–17920. doi: 10.1073/pnas.1113881108
- Newsom, L. A., and Mithlacher, M. C. (2006). "Mastodons (*Mammot americanum*) diet foraging patterns based on analysis of dung deposits," in *First floridians and last mastodons: The page-ladson site in the Aucilla river*, ed. S. D. Webb (Dordrecht: Springer Netherlands), 263–331. doi: 10.1007/978-1-4020-4694-0_10
- Owen-Smith, R. N. (1992). *Megaherbivores: The influence of very large body size on ecology*. Cambridge: Cambridge University Press.
- Pardi, M. I., and DeSantis, L. R. G. (2021). Dietary plasticity of North American herbivores: A synthesis of stable isotope data over the past 7 million years. *Proc. R. Soc. B Biol. Sci.* 288:20210121. doi: 10.1098/rspb.2021.0121
- Pardi, M. I., and Smith, F. A. (2016). Biotic responses of canids to the terminal Pleistocene megafauna extinction. *Ecography* 39, 141–151. doi: 10.1111/ecog.01596

- Paruelo, J. M., and Lauenroth, W. K. (1996). Relative abundance of plant functional types in grasslands and shrublands of North America. *Ecol. Appl.* 6, 1212–1224. doi: 10.2307/2269602
- Pendleton, D. E., Sullivan, P. J., Brown, M. W., Cole, T. V. N., Good, C. P., Mayo, C. A., et al. (2012). Weekly predictions of North Atlantic right whale *Eubalaena glacialis* habitat reveal influence of prey abundance and seasonality of habitat preferences. *Endanger. Species Res.* 18, 147–161.
- Peterson, A. T., Navarro-Sigüenza, A. G., and Gordillo, A. (2018). Assumption-versus data-based approaches to summarizing species' ranges. *Conserv. Biol.* 32, 568–575. doi: 10.1111/cobi.12801
- Phillips, S. J., and Dudík, M. (2008). Modeling of species distributions with Maxent: New extensions and a comprehensive evaluation. *Ecography* 31, 161–175.
- Phillips, S. J., Dudík, M., and Schapire, R. E. (2020). *Maxent software for modeling species niches and distributions (Version 3.4.3)*. Available Online at: http://biodiversityinformatics.amnh.org/open_source/maxent/ (accessed October 26, 2022).
- R Core Team (2022). *R: A language and environment for statistical computing*. Vienna: R Foundation for Statistical Computing.
- Reimer, P. J., Austin, W. E. N., Bard, E., Bayliss, A., Blackwell, P. G., Bronk Ramsey, C., et al. (2020). The IntCal20 northern hemisphere radiocarbon age calibration curve (0–55 cal kBP). *Radiocarbon* 62, 725–757. doi: 10.1017/RDC.2020.41
- Rivals, F., Solounias, N., and Mithlacher, M. C. (2007). Evidence for geographic variation in the diets of late Pleistocene and early Holocene *Bison* in North America, and differences from the diets of recent *Bison*. *Quat. Res.* 68, 338–346. doi: 10.1016/j.yqres.2007.07.012
- Rule, S., Brook, B. W., Haberle, S. G., Turney, C. S., Kershaw, A. P., and Johnson, C. N. (2012). The aftermath of megafaunal extinction: Ecosystem transformation in pleistocene Australia. *Science* 335, 1483–1486. doi: 10.1126/science.1214261
- Scott, J. R. (2012). Dental microwear texture analysis of extant African Bovidae. *Mammalia* 76, 157–174. doi: 10.1515/mammalia-2011-0083
- Scott, R. S., Ungar, P. S., Bergstrom, T. S., Brown, C. A., Childs, B. E., Teaford, M. F., et al. (2006). Dental microwear texture analysis: Technical considerations. *J. Hum. Evol.* 51, 339–349. doi: 10.1016/j.jhevol.2006.04.006
- Scott, R. S., Ungar, P. S., Ungar, T. S., Brown, C. A., Grine, F. E., Teaford, M. F., et al. (2005). Dental microwear texture analysis shows within-species diet variability in fossil hominins. *Nature* 436, 693–695. doi: 10.1038/nature03822
- Secord, R., Bloch, J. I., Chester, S. G., Boyer, D. M., Wood, A. R., Wing, S. L., et al. (2012). Evolution of the earliest horses driven by climate change in the paleocene-eocene thermal maximum. *Science* 335, 959–962. doi: 10.1126/science.1213859
- Severinghaus, J. P., Sowers, T., Brook, E. J., Alley, R. B., and Bender, M. L. (1998). Timing of abrupt climate change at the end of the Younger Dryas interval from thermally fractionated gases in polar ice. *Nature* 391, 141–146.
- Shane, L. C. K. (1987). Late-glacial vegetational and climatic history of the Allegheny Plateau and the Till Plains of Ohio and Indiana, U.S.A. *Boreas* 16, 1–20. doi: 10.1111/j.1502-3885.1987.tb00750.x
- Shcheglovitova, M., and Anderson, R. P. (2013). Estimating optimal complexity for ecological niche models: A jackknife approach for species with small sample sizes. *Ecol. Modell.* 269, 9–17. doi: 10.1016/j.ecolmodel.2013.08.011
- Smith, G. J., and DeSantis, L. R. G. (2018). Dietary ecology of Pleistocene mammoths and mastodons as inferred from dental microwear textures. *Palaeogeogr. Palaeoclimatol. Palaeoecol.* 492, 10–25. doi: 10.1016/j.palaeo.2017.11.024
- Smith, G. J., and DeSantis, L. R. G. (2020). Extinction of North American *Cuvieronius* (Mammalia: Proboscidea: Gomphotheriidae) driven by dietary resource competition with sympatric mammoths and mastodons. *Paleobiology* 46, 41–57. doi: 10.1017/pab.2020.7
- Sukumar, R., Bhattacharya, S. K., and Krishnamurthy, R. V. (1987). Carbon isotopic evidence for different feeding patterns in an Asian elephant population. *Curr. Sci.* 56, 11–14.
- Surovell, T., Waguespack, N., and Brantingham, P. J. (2005). Global archaeological evidence for proboscidean overkill. *Proc. Natl. Acad. Sci. U.S.A.* 102, 6231–6236. doi: 10.1073/pnas.0501947102
- Surovell, T. A., Pelton, S. R., Anderson-Sprecher, R., and Myers, A. D. (2016). Test of Martin's overkill hypothesis using radiocarbon dates on extinct megafauna. *Proc. Natl. Acad. Sci. U.S.A.* 113, 886–891. doi: 10.1073/pnas.1504020112
- Svenning, J.-C., Pedersen, P. B., Donlan, C. J., Ejrnæs, R., Faurby, S., Galetti, M., et al. (2016). Science for a wilder Anthropocene: Synthesis and future directions for trophic rewilding research. *Proc. Natl. Acad. Sci. U.S.A.* 113, 898–906. doi: 10.1073/pnas.1502556112
- Teeri, J. A., and Stowe, L. G. (1976). Climatic patterns and the distribution of C4 grasses in North America. *Oecologia* 23, 1–12.
- Ungar, P. S., Brown, C. A., Bergstrom, T. S., and Walkers, A. (2003). Quantification of dental microwear by tandem scanning confocal microscopy and scale-sensitive fractal analyses. *Scanning* 25, 185–193. doi: 10.1002/sca.4950250405
- Vetter, L. (2007). *Paleoecology of Pleistocene megafauna in Southern Nevada, USA: Isotopic evidence for browsing on halophytic plants*. Master's thesis. Reno, NV: University of Nevada.
- Violle, C., Enquist, B. J., McGill, B. J., Jiang, L., Albert, C. H., Hulshof, C., et al. (2012). The return of the variance: Intraspecific variability in community ecology. *Trends Ecol. Evol.* 27, 244–252. doi: 10.1016/j.tree.2011.11.014
- Wang, Y., Goring, S. J., and McGuire, J. L. (2019). Bayesian ages for pollen records since the last glaciation in North America. *Sci. Data* 6:176. doi: 10.1038/s41597-019-0182-7
- Wang, Y., Widga, C., Graham, R. W., McGuire, J. L., Porter, W., Wärlind, D., et al. (2021). Caught in a bottleneck: Habitat loss for woolly mammoths in central North America and the ice-free corridor during the last deglaciation. *Glob. Ecol. Biogeogr.* 30, 527–542. doi: 10.1111/geb.13238
- Watts, W. A., Hansen, B. C., and Grimm, E. C. (1992). Camel Lake: A 40 000-yr record of vegetational and forest history from northwest Florida. *Ecology* 73, 1056–1066.
- Weng, C., and Jackson, S. T. (1999). Late glacial and Holocene vegetation history and paleoclimate of the Kaibab Plateau, Arizona. *Palaeogeogr. Palaeoclimatol. Palaeoecol.* 153, 179–201. doi: 10.1016/S0031-0182(99)00070-X
- Whittaker, R. H. (1967). Gradient analysis of vegetation. *Biol. Rev.* 42, 207–264. doi: 10.1111/j.1469-185X.1967.tb01419.x
- Widga, C., Hodgins, G., Kolis, K., Lengyel, S., Saunders, J., Walker, J. D., et al. (2021). Life histories and niche dynamics in late Quaternary proboscideans from Midwestern North America. *Quat. Res.* 100, 224–239. doi: 10.1017/qua.2020.85
- Williams, J. W., Grimm, E. C., Blois, J. L., Charles, D. F., Davis, E. B., Goring, S. J., et al. (2018). The Neotoma paleoecology database, a multiproxy, international, community-curated data resource. *Quat. Res.* 89, 156–177. doi: 10.1017/qua.2017.105



OPEN ACCESS

EDITED BY

Florent Rivals,
Catalan Institution for Research and
Advanced Studies (ICREA), Spain

REVIEWED BY

Hervé Bocherens,
University of Tübingen,
Germany
Rachel E. B. Reid,
Virginia Tech, United States
Victor Manuel Bravo-Cuevas,
Autonomous University of the State of
Hidalgo, Mexico

*CORRESPONDENCE

Larisa R. G. DeSantis
larisa.desantis@vanderbilt.edu

SPECIALTY SECTION

This article was submitted to
Paleoecology,
a section of the journal
Frontiers in Ecology and Evolution

RECEIVED 29 August 2022

ACCEPTED 28 October 2022

PUBLISHED 20 December 2022

CITATION

DeSantis LRG, Feranec RS, Southon J,
Cerling TE, Harris J, Binder WJ, Cohen JE,
Farrell AB, Lindsey EL, Meachen J, Robin
O'Keefe F and Takeuchi GT (2022) On the
relationship between collagen- and
carbonate-derived carbon isotopes with
implications for the inference of carnivore
dietary behavior.
Front. Ecol. Evol. 10:1031383.
doi: 10.3389/fevo.2022.1031383

COPYRIGHT

© 2022 DeSantis, Feranec, Southon,
Cerling, Harris, Binder, Cohen, Farrell,
Lindsey, Meachen, O'Keefe and Takeuchi.
This is an open-access article distributed
under the terms of the [Creative Commons
Attribution License \(CC BY\)](#). The use,
distribution or reproduction in other
forums is permitted, provided the original
author(s) and the copyright owner(s) are
credited and that the original publication in
this journal is cited, in accordance with
accepted academic practice. No use,
distribution or reproduction is permitted
which does not comply with these terms.

On the relationship between collagen- and carbonate-derived carbon isotopes with implications for the inference of carnivore dietary behavior

Larisa R. G. DeSantis^{1,2,3*}, Robert S. Feranec⁴, John Southon⁵,
Thure E. Cerling⁶, John Harris³, Wendy J. Binder^{3,7}, Joshua E.
Cohen^{3,7,8}, Aisling B. Farrell³, Emily L. Lindsey^{3,9,10}, Julie
Meachen^{3,11}, Frank Robin O'Keefe^{3,12} and Gary T. Takeuchi³

¹Department of Biological Sciences, Vanderbilt University, Nashville, TN, United States,

²Department of Earth and Environmental Sciences, Vanderbilt University, Nashville, TN, United

States, ³La Brea Tar Pits, Los Angeles, CA, United States, ⁴Research and Collections, New York

State Museum, Albany, NY, United States, ⁵Department of Earth System Science, University of

California, Irvine, Irvine, CA, United States, ⁶Department of Geology and Geophysics, University of

Utah, Salt Lake City, UT, United States, ⁷Department of Biology, Loyola Marymount University, Los

Angeles, CA, United States, ⁸Department of Biology, Pace University, New York City, NY, United

States, ⁹Institute of the Environment and Sustainability, University of California, Los Angeles, Los

Angeles, CA, United States, ¹⁰Department of Earth Sciences, University of Southern California, Los

Angeles, CA, United States, ¹¹Department of Anatomy, Des Moines University, Des Moines, IA,

United States, ¹²Department of Biological Sciences, Marshall University, Huntington, WV, United

States

Studies of Rancho La Brea predators have yielded disparate dietary interpretations when analyzing bone collagen vs. enamel carbonate—requiring a better understanding of the relationship between stable carbon isotopes in these tissues. Stable carbon isotope spacing between collagen and carbonate ($\Delta_{\text{ca-co}}$) has also been used as a proxy for inferring the trophic level of mammals, with higher $\Delta_{\text{ca-co}}$ values indicative of high carbohydrate consumption. To clarify the stable isotope ecology of carnivores, past and present, we analyzed bone collagen (carbon and nitrogen) and enamel carbonate (carbon) of extinct and extant North American felids and canids, including dire wolves, sabertooth cats, coyotes, and pumas, supplementing these with data from African wild dogs and African lions. Our results reveal that $\Delta_{\text{ca-co}}$ values are positively related to enamel carbonate values in secondary consumers and are less predictive of trophic level. Results indicate that the foraging habitat and diet of prey affects $\Delta_{\text{ca-co}}$ in carnivores, like herbivores. Average $\Delta_{\text{ca-co}}$ values in Pleistocene canids ($8.7 \pm 1\%$) and felids ($7.0 \pm 0.7\%$) overlap with previously documented extant herbivore $\Delta_{\text{ca-co}}$ values suggesting that trophic level estimates may be relative to herbivore $\Delta_{\text{ca-co}}$ values in each ecosystem and not directly comparable between disparate ecosystems. Physiological differences between felids and canids, ontogenetic dietary differences, and diagenesis at Rancho La Brea do not appear to be primary drivers of $\Delta_{\text{ca-co}}$ offsets. Environmental influences affecting protein and fat consumption in prey

and subsequently by predators, and nutrient routing to tissues may instead be driving $\Delta_{\text{ca-co}}$ offsets in extant and extinct mammals.

KEYWORDS

bone, carbon isotopes, carnivora, carnivores, enamel, nitrogen isotopes, Rancho La Brea

Introduction

Rancho La Brea (RLB) is one of the best preserved and studied fossil localities in the world, providing insight into the ecology of ancient mammals over the past ~50,000 years in southern California (e.g., Merriam and Stock, 1932; Stock and Harris, 1992; Van Valkenburgh and Hertel, 1993; DeSantis et al., 2012, 2019; Meachen and Samuels, 2012). Herbivorous mammals trapped in asphalt seeps (“pits”) attracted carnivores that also became trapped, resulting in one of the world’s best localities for studying ancient predators and their prey (Stock and Harris, 1992). As predators normally occur in lower numbers than their prey in modern ecosystems, they are also typically rare in fossil accumulations. However, because of their abundance in these deposits, Rancho La Brea provides unique insight into predator and prey dynamics in the Late Pleistocene—a time characterized by dramatic climatic change and the arrival of humans in North America (Stock and Harris, 1992; Barnosky et al., 2004). One productive avenue of research has been the inference of diet based on stable isotopes, allowing deep insight into the ecosystem dynamics of Late Pleistocene Rancho La Brea (e.g., Coltrain et al., 2004). However, recent work on isotopic values from RLB carnivores has revealed a clear discrepancy between values derived from collagen vs. enamel carbonate (DeSantis et al., 2019, 2020), complicating dietary inferences from either tissue. The goals of this study are to quantify and test potential drivers responsible for collagen/carbonate offsets generally, and to use these understandings to clarify dietary inference at RLB.

Stable isotopes and dietary inference

Stable isotope analyses of bone and/or tooth enamel have clarified the dietary ecology of numerous animals across the globe, past and present (e.g., Cerling et al., 1997; DeSantis et al., 2009; Secord et al., 2012). While studies of extant animals benefit from the ability to sample different tissues (including hair, feathers, scales, blood, etc.), archeological and paleontological studies of ancient life are limited to the analysis of tissues that preserve original biogenic stable isotope signatures in the fossil record (e.g., bones and teeth). Enamel is primarily inorganic (Teruel et al., 2015; Kendall et al., 2018) and stable isotopes of carbon and oxygen have been used to infer diet and climate, respectively, through time (e.g., DeNiro and Epstein, 1978; Cerling et al., 1997;

Levin et al., 2006; DeSantis et al., 2009; Secord et al., 2012). Bone and dentin collagen, which are organic, also provide insights into the diets of ancient animals (e.g., Schoeninger et al., 1983; Bocherens et al., 1994; Finucane et al., 2006; Fuller et al., 2006; Kellner and Schoeninger, 2007; Lee-Thorp, 2008; Tung et al., 2016). Specifically, carbon isotope values measured in collagen (bone or dentin) provide information about the protein component of an animal’s diet (Ambrose and Norr, 1993) and nitrogen isotope values clarify trophic level with higher values indicative of feeding at higher trophic levels and/or more meat or fish consumption (Schoeninger et al., 1983). In archeological studies, both tooth enamel (or bone apatite) and bone collagen are analyzed to infer differences between whole diet (e.g., carbohydrates, fat, and protein) and protein components of diet, respectively (e.g., Ambrose and Norr, 1993). However, paleontological studies often employ only one tool, due to a lack of preserved collagen, interest in only isotopes associated with a particular tissue (e.g., $\delta^{18}\text{O}$ in carbonate, $\delta^{15}\text{N}$ in collagen; Bocherens et al., 1994; DeSantis et al., 2009), and/or the need to minimize destructive sampling. Therefore, direct comparisons between data types from the same specimens are rare.

Those studies that have examined both tooth enamel and bone collagen stable isotopes from the same individual specimens (e.g., Krueger and Sullivan, 1984; Lee-Thorp et al., 1989; Ambrose and Norr, 1993; Clementz et al., 2007, 2009; Murphy et al., 2007; Bocherens et al., 2017; Codron et al., 2018) indicate that isotope values from the different tissues record different aspects of their diet. There is broad consensus that $\delta^{13}\text{C}_{\text{collagen}}$ reflects the protein component of diet, while $\delta^{13}\text{C}_{\text{carbonate}}$ reflects whole diet (e.g., protein, carbohydrates, and fats; Ambrose and Norr, 1993) and that the isotopic spacing between carbonate and collagen ($\Delta_{\text{ca-co}}$, $\delta^{13}\text{C}_{\text{carbonate}} - \delta^{13}\text{C}_{\text{collagen}}$) varies depending on trophic category (Krueger and Sullivan, 1984; Lee-Thorp et al., 1989; Clementz et al., 2009). Specifically, the lowest $\Delta_{\text{ca-co}}$ values occur in carnivores (averaging $4.3 \pm 1.0\text{‰}$ to $4.8 \pm 0.4\text{‰}$; Lee-Thorp et al., 1989; Clementz et al., 2009) while herbivores have higher $\Delta_{\text{ca-co}}$ values ($6.8 \pm 1.4\text{‰}$ to $7.6 \pm 0.5\text{‰}$; Lee-Thorp et al., 1989; Clementz et al., 2009). Animals with lower $\Delta_{\text{ca-co}}$ values are often attributed as having more meat and/or fat in their diet than animals with higher $\Delta_{\text{ca-co}}$ values— $\Delta_{\text{ca-co}}$ values are therefore used to infer degree of meat and/or fat consumption in ancient mammals (Lee-Thorp et al., 1989; Clementz et al., 2009). In *Canis lupus*, $\Delta_{\text{ca-co}}$ increases with increased $\delta^{13}\text{C}_{\text{carbonate}}$ values ($p = 0.016$, $R = 0.51$; per our analysis of the supplemental data in Clementz et al., 2009);

however, there is no predictable relationship between $\Delta_{\text{ca-co}}$ in bone apatite or bone collagen $\delta^{13}\text{C}$ values in African carnivores (Codron et al., 2018). Further, the significant positive-relationship between $\Delta_{\text{ca-co}}$ values and $\delta^{13}\text{C}_{\text{carbonate}}$ values in a sample of dire wolves (*Aenocyon dirus*, previously known as *Canis dirus*) at Rancho La Brea is similar to the relationship between $\Delta_{\text{ca-co}}$ and $\delta^{13}\text{C}_{\text{collagen}}$ values in the African mammals included in Codron et al. (2018; DeSantis et al., 2020, see Figure 1B).

Offset values between carbonate and collagen can be highly variable among herbivores, specifically African mammals (primarily ungulates, especially bovids) and Australian kangaroos (Murphy et al., 2007; Codron et al., 2018). Murphy et al. (2007) demonstrated a significant negative relationship between $\Delta_{\text{ca-co}}$ in herbivorous kangaroos and aridity (i.e., water availability index; higher $\Delta_{\text{ca-co}}$ values when less water is available). Codron et al. (2018) instead documented higher $\Delta_{\text{ca-co}}$ values with increased $\delta^{13}\text{C}_{\text{collagen}}$ values in African mammals, which they attribute to both physiological differences between ruminants and non-ruminants and dietary differences between grass and browse (e.g., effects of higher amounts of protein in ^{13}C deplete browse and higher amounts of CH_4 produced when consuming grass). In closely related ruminant taxa (i.e., members of the family Bovidae), $\Delta_{\text{ca-co}}$ values calculated from teeth (enamel carbonate and dentin collagen) span the full range of values from 3.6 to 14.8‰; the second lowest offset value (4.3‰) and highest offset value (14.8‰) also occur with the same species—springbok (*Antidorcas marsupialis*). Further, when re-analyzing and comparing just tooth data (enamel carbonate and dentin collagen) from Codron et al. (2018) from ruminants in the family Bovidae and hindgut fermenters (in the families Equidae and Rhinocerotidae), the slopes and R^2 values are indistinguishable (slopes are 0.21 and 0.20, R^2 values are 0.41 and 0.43, respectively). Thus, it is unlikely that ruminant or non-ruminant physiology is the primary driver of $\Delta_{\text{ca-co}}$ values; instead, the proportion of grass and browse may be a larger driver of herbivore $\Delta_{\text{ca-co}}$ values. Specifically, higher amounts of protein enriched browse with ^{13}C deplete values yield both lower $\delta^{13}\text{C}$ carbonate values and smaller $\Delta_{\text{ca-co}}$ values, while

protein deplete C_4 grasses also result in more methane production (that is isotopically depleted in ^{13}C , leaving behind more ^{13}C enriched carbon from which tissues are synthesized, in both ruminants and hind-gut fermenters) and are correlated with higher $\delta^{13}\text{C}$ carbonate values and higher $\Delta_{\text{ca-co}}$ values. Discrepancies between how herbivore and carnivore $\Delta_{\text{ca-co}}$ values correlate with stable isotope values of collagen and enamel are apparent and more work on carbonate-collagen relationships is needed to elucidate potential drivers of $\Delta_{\text{ca-co}}$ values and the efficacy of using $\Delta_{\text{ca-co}}$ values to infer ecological information such as trophic level in extinct and extant mammals.

Stable isotopes and dietary inferences in RLB carnivores

Despite extensive study of Rancho La Brea carnivores, there are differences between the dietary interpretations of Late Pleistocene mammals at Rancho La Brea as inferred from bone collagen versus enamel carbonate stable isotope values (Coltrain et al., 2004; Feranec et al., 2009; Fuller et al., 2014, 2020; DeSantis et al., 2019, 2020; Van Valkenburgh et al., 2020). Seminal work analyzed the carbon and nitrogen isotope ratios of bone collagen from Rancho La Brea carnivores and concluded that sampled individuals of *Smilodon fatalis* (the sabertooth cat) and *Aenocyon dirus* (the dire wolf, previously known as *Canis dirus*) had indistinguishable carbon and nitrogen isotope values and were therefore competing for similar prey (Coltrain et al., 2004). This idea persisted until dietary interpretations based on tooth enamel carbonate indicated the consumption of different prey (DeSantis et al., 2019, 2020). Specifically, DeSantis et al. (2019, 2020) found that *A. dirus* yielded statistically greater $\delta^{13}\text{C}_{\text{carbonate}}$ values than *S. fatalis*—which was interpreted as *S. fatalis* primarily having consumed prey that occupied denser forests/shrubland ecosystems, while *A. dirus* consumed prey from more open grassland environments. The reasons for this discrepancy between the two tissues remain unclear (Fuller et al., 2014, 2020; DeSantis

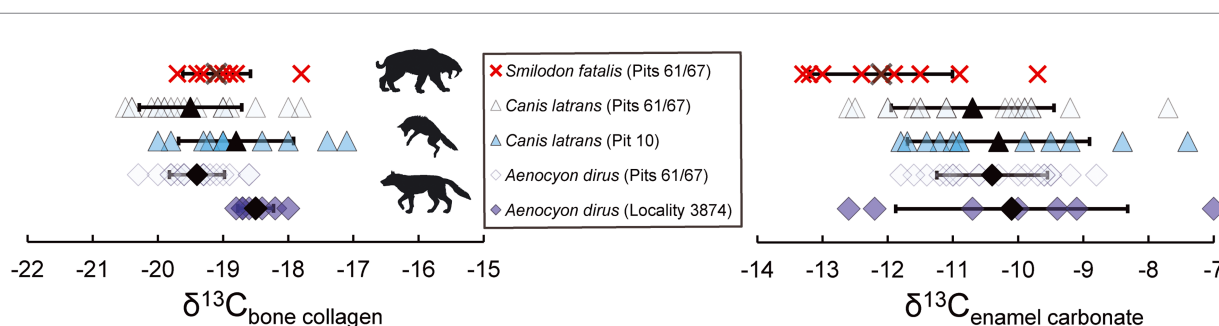


FIGURE 1

Stable carbon isotope data (collagen and carbonate) for all fossil specimens examined from Rancho La Brea ($n=71$). Mean values are denoted in bold (bars indicate 1 standard deviation, $n=1$). All collagen data are from bone collagen and carbonate data are from tooth enamel (lower first molars), with the exception of *A. dirus* from Locality 3,874 which are from incisor dentin collagen and incisor enamel, respectively. The felid *S. fatalis* is noted in red, with all canids noted in blue; the same shade of light blue is used for canids from pits 61/67. The scales on the x-axis are of the same magnitude for the two tissues.

et al., 2019, 2020), and have led some to question the recent dietary interpretations of Rancho La Brea carnivores (Van Valkenburgh et al., 2020). While DeSantis et al. (2019, 2020) speculate on some of these discrepancies, they concentrated on an enamel-based interpretation of diet.

To clarify the paleobiology of Rancho La Brea carnivores and resolve relationships between enamel carbonate and bone collagen in both extinct and extant mammals, tooth enamel and bone collagen were examined in extant canids and felids from C_3 and C_4 ecosystems in North America and Africa, in addition to Rancho La Brea carnivores. Specifically, we examined Late Pleistocene specimens from Rancho La Brea (*A. dirus*, *C. latrans*, *S. fatalis*), modern specimens from predominately C_3 ecosystems in southern California (*C. latrans* and *Puma concolor*), and modern specimens from predominately C_4 ecosystems throughout Africa (*Lycaon pictus* and *Panthera leo*). We test the hypotheses that Δ_{ca-co} values in carnivorous mammals (1) are largely consistent and independent of either $\delta^{13}C_{carbonate}$ or $\delta^{13}C_{collagen}$ values ($\sim 4.3 \pm 1.0\%$ to $4.8 \pm 0.4\%$; Lee-Thorp et al., 1989; Clementz et al., 2009), and (2) are indicative of trophic level. We also further clarify relationships between carbonate (enamel, bone, and dentin) and collagen (bone and dentin) in extant African canids and felids.

Statistical considerations of isotopic data from different tissues

We recognize that the correlations between Δ_{ca-co} values and $\delta^{13}C_{carbonate}$ or $\delta^{13}C_{collagen}$ may, in part, be influenced by plotting these values against each other; but these plots and correlations permit comparison to other studies, and provide information regarding the source of these isotopic data. As Auerwald et al. (2010) demonstrated, if pairs of values are drawn randomly from populations of variables A and B of equal variance, the difference A-B will be biased to high values when A is high and to low values when A is low. Hence an A-B vs. A correlation with a slope of +1 is generated; conversely A-B vs. B will yield a slope of -1. In the unrealistic scenario that $\delta^{13}C$ variations in the two tissues were completely independent (i.e., if their responses to environmental and physiological changes were totally uncoupled) the slopes of these relationships would approach +1 and -1 respectively, whereas if the isotopic responses of the two tissues were identical the slopes would both be zero. Since Δ_{ca-co} is defined as $\delta^{13}C_{carbonate} - \delta^{13}C_{collagen}$, all other things being equal one expects to see a positive correlation between Δ_{ca-co} and $\delta^{13}C_{carbonate}$ and a negative correlation between Δ_{ca-co} and $\delta^{13}C_{collagen}$. Additionally, if these relationships were a product of random sampling, we would not expect $\delta^{13}C$ values of different tissues to yield different relationships with Δ_{ca-co} values. See Caut et al. (2010) for a detailed reply to Auerwald et al. (2010) and discussion regarding the rationale for these sorts of comparisons that are prevalent in paleobiology and archeology (e.g., Krueger and Sullivan, 1984; Lee-Thorp et al., 1989;

Ambrose and Norr, 1993; Murphy et al., 2007; Clementz et al., 2009; Codron et al., 2018).

Differences in isotopic variance of tissue types are evident from our data set and the extensive data sets of Murphy et al. (2007) and Codron et al. (2018). However, this is not necessarily an intrinsic property of these tissues; studies have shown that $\delta^{13}C_{collagen}$ ranges are greater than those in $\delta^{13}C_{carbonate}$ in humans when their diets include protein sources with disparate $\delta^{13}C$ values (e.g., marine protein enriched in ^{13}C in addition to terrestrial C_3 resources that are ^{13}C deplete; Tung et al., 2020).

Materials and methods

To decipher the conflicting data interpretations between the stable isotope values of bone collagen and tooth enamel carbonate in Rancho La Brea carnivores, jawbone specimens containing teeth ($n=71$) were obtained for stable isotope analysis of both bone collagen and tooth enamel carbonate in the same specimen. Lower first molars were sampled in all taxa due to the larger size of these carnassial teeth and the need to minimize specimen destruction. In the case of *Aenocyon dirus* from the University of California Museum of Paleontology (UCMP) Locality 3,874, enamel was from incisors while collagen was from dentin (both near the enamel/dentin junction and down through the root, due to the need for appropriately large amounts of this tissue, as these teeth were isolated and lacked associated bone for bone collagen analysis; as noted in Supplementary Table S1, Supplemental Tables 1, 2). Rancho La Brea specimens comprised *Aenocyon dirus* (Pits 61/67, $n=21$; Locality 3,874, $n=8$), *Canis latrans* (Pits 61/67, $n=19$; Pit 10, $n=12$), and *Smilodon fatalis* (Pit 61/67, $n=11$; Supplementary Table S1, Supplemental Table 1). Modern predators from southern California ($n=19$; *Canis latrans*, *Puma concolor*) and from Africa ($n=18$; *Lycaon pictus*, *Panthera leo*) were also analyzed for both bone collagen and tooth enamel (Supplementary Tables S1, S2, Supplemental Table 2). The African specimens were also analyzed for bone (carbonate) and dentin (carbonate and collagen), in addition to enamel (carbonate) and bone (collagen). When more than one analysis was run on the same tissue, the sample was first homogenized and then split up after drilling to reduce temporal variability that could otherwise occur if tissues were not homogenized after sampling. While we would have liked to have sampled dentin carbonate and collagen from all Rancho La Brea specimens, this was not possible due to the scale and scope of this study and need to minimize specimen destruction on the fossil specimens (collagen analyses require significantly more sample as compared to carbonate). As tooth enamel carbonate and bone collagen are the most commonly analyzed tissues at Rancho La Brea and other Late Pleistocene fossil sites, we concentrated on these tissues for the bulk of our analyses. The addition of dentin carbonate and collagen and bone carbonate of modern African specimens can provide insights that can be followed up with future studies. Rancho La Brea specimens are housed at the University of California, Berkeley (UCMP Locality

3,874) and the La Brea Tar Pits and Museum (LACMHC). Modern specimens from southern California are from the Santa Barbara Museum of Natural History (SBMNH) and modern specimens from Africa are from the American Museum of Natural History (Mammalogy Collections; AMNH).

Carbonate samples from both teeth and bone were drilled with a low-speed dental-style drill and carbide dental burs (<1 mm burr width). The resulting carbonate powder samples (enamel, dentin, bone) were pretreated with 30% hydrogen peroxide for 24 h, and 0.1 N acetic acid for 18 h, to remove organics and secondary carbonates, respectively (Koch et al., 1997; DeSantis et al., 2009). Sample preparation followed procedures outlined in DeSantis et al. (2019) and included the rinsing of samples with ultra-pure water and subsequently centrifuging them between all treatment steps. Approximately 1 mg of each sample was then analyzed on a VG Prism stable isotope ratio mass spectrometer with an in-line ISOCARB automatic sampler in the Department of Geological Sciences at the University of Florida. All bone or dentin samples analyzed for collagen carbon or nitrogen isotope ratios were cut with a Dremel® UltraSaw™ cutting wheel or a diamond coring drill (dentin samples also sampled for carbonate were subsequently drilled, i.e., a subset of the sample was removed for carbonate analysis).

Clean collagen was recovered from the asphalt-impregnated bones using a modified procedure based on the protocol developed by Fuller et al. (2014). Samples of crushed bone were sonicated in a solvent sequence of increasing polarity to remove bulk asphalt, demineralized overnight with HCl, rinsed with ultrapure water, and gelatinized overnight at pH 2, at an elevated temperature (75°C) sufficient to break up collagen molecules into fragments of a molecular weight on the order of 10's of kDa, while leaving massive residual asphalt aggregates intact. The gelatin solution was then purified using two sequential ultrafiltrations to select an intermediate molecular weight fraction (5–100 kDa) which was frozen with liquid nitrogen and lyophilized overnight. Elemental analyses (‰C and ‰N) and stable isotope ratios were determined by flash combustion of ~0.7 mg samples of collagen in tin capsules, and analysis of the gas products using a Fisons NA1500NC elemental analyzer/Finnigan Delta Plus isotope ratio mass spectrometer combination at the Keck AMS laboratory at University of California Irvine. Stable isotope data are reported in conventional delta (δ) notation for carbon (δ¹³C), oxygen (δ¹⁸O), and nitrogen (δ¹⁵N), where δ¹³C (parts per thousand, ‰) = [(R_{sample}/R_{standard}) - 1] * 1,000, and R = ¹³C/¹²C; and, δ¹⁵N (parts per mil, ‰) = [(R_{sample}/R_{standard}) - 1] * 1,000, and R = ¹⁵N/¹⁴N on the VPDB (for carbon and oxygen; Pee Dee Belemnite, Vienna Convention; Coplen, 1994) and AIR (for nitrogen; Mariotti, 1983) scales. The analytical precision for carbonate δ¹³C and δ¹⁸O is ±0.1‰, based on replicate analyses of samples and standards (NBS-19). The analytical precisions for δ¹³C and δ¹⁵N from bone collagen are ±0.1‰, and ±0.2‰ respectively, based on replicate analyses of samples and standards.

Studies utilizing carbonate-collagen spacing use “capital delta notation” values, calculated as follows: Δ_{ca-co} = δ¹³C_{carbonate} - δ¹³C_{collagen} (e.g., Krueger and Sullivan, 1984; Lee-Thorp et al., 1989; Ambrose and Norr, 1993; Clementz et al., 2007; Murphy et al., 2007; Clementz et al., 2009; Bocherens et al., 2017; Codron et al., 2018). While we use these calculations to be directly comparable with prior analyses, we also calculated the fractionation factor (α) and isotopic enrichment (ε; Supplemental Table 1) similar to Passey et al. (2005), based on Friedman and O'Neil (1977). Specifically, α_{carbonate-collagen} = (1,000 + δ_{carbonate}) / (1,000 + δ_{collagen}), and ε_{carbonate-collagen} = (α_{carbonate-collagen} - 1)1000 (Friedman and O'Neil, 1977). Differences between Δ_{ca-co} and ε_{carbonate-collagen} are small within the ~10‰ range here noted (Cerling and Harris, 1999); of all specimens examined here, the average difference is 0.133‰ ±0.0518 SD, n-1 (ranging from 0.029 to 0.207‰). These differences are minor (approximately the error of the mass spectrometers), do not significantly affect the patterns observed, and the use of Δ_{ca-co} is important for consistency with published works (e.g., Krueger and Sullivan, 1984; Lee-Thorp et al., 1989; Ambrose and Norr, 1993; Murphy et al., 2007; Clementz et al., 2009; Codron et al., 2018); however, we suggest that α and ε be reported and discussed moving forward, as noted by Passey et al. (2005; all values are reported in the Supplemental information).

Parametric statistical tests were employed to compare stable isotope values among taxa, between tissues, and assess relationships between isotopic values and Δ_{ca-co} values (e.g., Student's *t*-tests, including paired *t*-tests when comparing tissues in the same individuals, linear regressions). No corrections (including the Suess correction) were made to reported and analyzed data (Supplementary Tables S1, S2, Supplemental Tables 1, 2). While we recognize that δ¹³C values today are approximately 1.5‰ lower than during the Late Pleistocene (Cerling et al., 1997; Cerling and Harris, 1999; Passey et al., 2005), we are focused on assessing relationships between δ¹³C values from disparate tissues within individuals (e.g., relationships between δ¹³C_{carbonate} and Δ_{ca-co}), as opposed to comparing diets of extant and extinct predators) and the majority of comparisons are done within modern or within Late Pleistocene samples. Further, it is possible that the δ¹³C values of the atmosphere (which are a function of CO₂ levels; Keeling, 1979; Keeling et al. 1979) affect how δ¹³C values are incorporated into various tissues *via* plants and prey, as we suggest in the discussion. All things being equal, plants exposed to higher atmospheric CO₂ levels have lower nutrients and lower nitrogen content/lower protein content but more carbon per unit biomass, and C₄ grasses have lower nutritional quality (Conroy, 1992; Barbehenn et al., 2004). This can impact nutrient routing to tissues in consumers and have downstream impacts on carnivores. Further, all studies to date have examined relationships between δ¹³C_{carbonate} and Δ_{ca-co} in modern taxa with no Suess corrections applied (e.g., Lee-Thorp et al., 1989; Ambrose and Norr, 1993; Murphy et al., 2007; Clementz et al., 2009; Codron et al., 2018), and we aimed to produce data directly comparable to those data sets.

Results

Bone collagen and enamel carbonate $\delta^{13}\text{C}$ values from Rancho La Brea

Stable carbon isotopes measured in bone collagen of *S. fatalis* (Pits 61/67) are indistinguishable from *A. dirus* (Pits 61/67; $p = 0.141$; Figure 1), consistent with prior work (Coltrain et al., 2004; Fuller et al., 2014, 2020). In contrast, stable carbon isotopes measured in enamel carbonate of *S. fatalis* (Pits 61/67) are significantly lower than in *A. dirus* (Pits 61/67; $p < 0.0001$; Figure 1), which is also consistent with prior analyses of enamel carbonate (DeSantis et al., 2019, 2020). When comparing the three most abundant carnivores at Rancho La Brea from the same deposit (*A. dirus*, *C. latrans*, and *S. fatalis* from Pits 61/67), bone collagen carbon isotope values are indistinguishable ($p = 0.187$), while enamel carbon isotope values of the canids *A. dirus* and *C. latrans* are significantly greater than *S. fatalis* ($p = 0.0002$, $p = 0.004$, respectively). Further, stable nitrogen isotopes ratios measured in the morphologically inferred hypercarnivores *A. dirus* and *S. fatalis* are significantly greater than *C. latrans* ($p < 0.0001$ for both), while *A. dirus* and *S. fatalis* are indistinguishable from one another ($p = 0.332$). Despite the fact that bone collagen and enamel carbonate integrate information about different portions of animal diets (protein component versus whole diet; Ambrose and Norr, 1993), there is a significant positive relationship between enamel $\delta^{13}\text{C}_{\text{carbonate}}$ and $\delta^{13}\text{C}_{\text{collagen}}$ from bone in both the fossil Rancho La Brea specimens ($p < 0.0001$, $R^2 = 0.25$, $R = 0.5$ in Rancho La Brea taxa, Figure 2A) and modern southern California ($p = 0.0002$, $R^2 = 0.57$, $R = 0.75$; Supplemental Table 1) specimens examined here.

Collagen-carbonate $\delta^{13}\text{C}$ spacing in carnivorans from southern California

There is a strong and significant positive relationship between $\Delta_{\text{ca-co}}$ and $\delta^{13}\text{C}_{\text{carbonate}}$ in enamel from both extant and extinct southern California canids and felids ($R^2 = 0.88$, $R = 0.94$; $p < 0.0001$; Figure 2D; Supplementary Table S3). This relationship additionally holds true when modern and fossil specimens are evaluated separately (modern: $R^2 = 0.58$, $R = 0.76$, $p = 0.0002$; fossil: $R^2 = 0.72$, $R = 0.85$, $p < 0.0001$). Because modern specimens of the canid *C. latrans* and the felid *P. concolor* have lower $\delta^{13}\text{C}_{\text{carbonate}}$ values than the extinct felids and canids from Rancho La Brea, likely due to their consumption of prey from ecosystems with increased canopy cover or denser shrubs (Feranec and DeSantis, 2014; DeSantis et al., 2019) and the Suess effect that accounts for $\sim 1.5\text{‰}$ lower $\delta^{13}\text{C}_{\text{carbonate}}$ values (Cerling et al., 1997; Cerling and Harris, 1999; Passey et al., 2005); we graphically present the results of linear regressions for fossil and modern specimens separately (see Materials and Methods, Figure 2). However, all relationships between enamel $\delta^{13}\text{C}_{\text{carbonate}}$ and $\Delta_{\text{ca-co}}$ were examined and reported (Supplementary Table S3). $\Delta_{\text{ca-co}}$ values and $\delta^{13}\text{C}_{\text{collagen}}$ values

exhibit no significant correlation when including either Rancho La Brea specimens ($R = 0.03$, $p = 0.767$) or modern specimens from southern California ($R = 0.14$, $p = 0.531$); however, there is a weak but significant positive relationship when both Rancho La Brea specimens and modern C_3 specimens are included (Figure 2B; Supplementary Table S4). In contrast to $\delta^{13}\text{C}_{\text{collagen}}$ values, $\delta^{13}\text{C}_{\text{carbonate}}$ values can be used to predict $\Delta_{\text{ca-co}}$ values; thus, $\delta^{13}\text{C}_{\text{collagen}}$ values can be estimated within 0.5‰.

Rancho La Brea specimens have average $\Delta_{\text{ca-co}}$ values of $8.5 \pm 1.2\text{‰}$ (ranging from 6 to 11‰, $n = 71$) and modern specimens from southern California have average $\Delta_{\text{ca-co}}$ values of $4.6 \pm 1\text{‰}$ (ranging from 3.2 to 7‰, $n = 19$). Rancho La Brea canid and felid $\Delta_{\text{ca-co}}$ values ($8.7 \pm 1.0\text{‰}$, $7.0 \pm 0.7\text{‰}$, respectively) overlap with modern herbivore $\Delta_{\text{ca-co}}$ values (Lee-Thorp et al., 1989; Murphy et al., 2007; Clementz et al., 2009; Codron et al., 2018) and are higher than modern carnivores based on the literature (averaging $4.3 \pm 1.0\text{‰}$ to $4.8 \pm 0.4\text{‰}$; Lee-Thorp et al., 1989; Clementz et al., 2009).

Most notably, $\Delta_{\text{ca-co}}$ values of both Rancho La Brea carnivores and modern carnivores from southern California are not significantly (negatively) correlated with $\delta^{15}\text{N}_{\text{collagen}}$ values as was expected (Figure 3C; Supplementary Table S4), based on prior research that documents higher $\Delta_{\text{ca-co}}$ values in more omnivorous or herbivorous taxa (e.g., Lee-Thorp et al., 1989; Clementz et al., 2009). *C. latrans* from Pits 61/67 at Rancho La Brea exhibit significantly lower $\delta^{15}\text{N}_{\text{collagen}}$ values than both *A. dirus* ($p < 0.0001$) and *S. fatalis* ($p < 0.0001$) from the same location, suggesting that coyotes were more omnivorous than the larger, more abundant, and inferred hypercarnivores (*A. dirus* and *S. fatalis*; Merriam and Stock, 1932; Stock and Harris, 1992). Yet, the mean $\Delta_{\text{ca-co}}$ value of *C. latrans* is indistinguishable from *A. dirus* ($p = 0.411$, Mann–Whitney U).

Collagen-carbonate $\delta^{13}\text{C}$ spacing and tissue specific enrichment in carnivorans from Africa

As in southern California, there is a strong ($R^2 = 0.65$, $R = 0.81$) and significant positive relationship ($p = 0.0001$; Supplementary Table S3) between $\delta^{13}\text{C}_{\text{carbonate}}$ in enamel and $\Delta_{\text{ca-co}}$ in African canids and felids from predominantly C_4 ecosystems. One individual with a $\delta^{13}\text{C}_{\text{enamel carbonate}}$ value of -12.3‰ , interpreted as consuming significant C_3 prey (and ~ 3 standard deviations from the mean) fell on the regression line from southern California extant and extinct taxa (Figure 2A) and was not included in the analysis of exclusively African (C_4) carnivores; however, it was included in the regression of C_3 taxa in Figures 2B,D, and relevant regressions of all carnivores (or modern carnivores; per Materials and Methods). $\delta^{13}\text{C}_{\text{collagen}}$ and $\Delta_{\text{ca-co}}$ values are not significantly correlated to one another in exclusively C_4 carnivorans ($R^2 = 0.13$, $p = 0.158$; Figure 2B; Supplementary Table S4), while $\delta^{15}\text{N}_{\text{collagen}}$ and $\Delta_{\text{ca-co}}$ values exhibit a significant positive

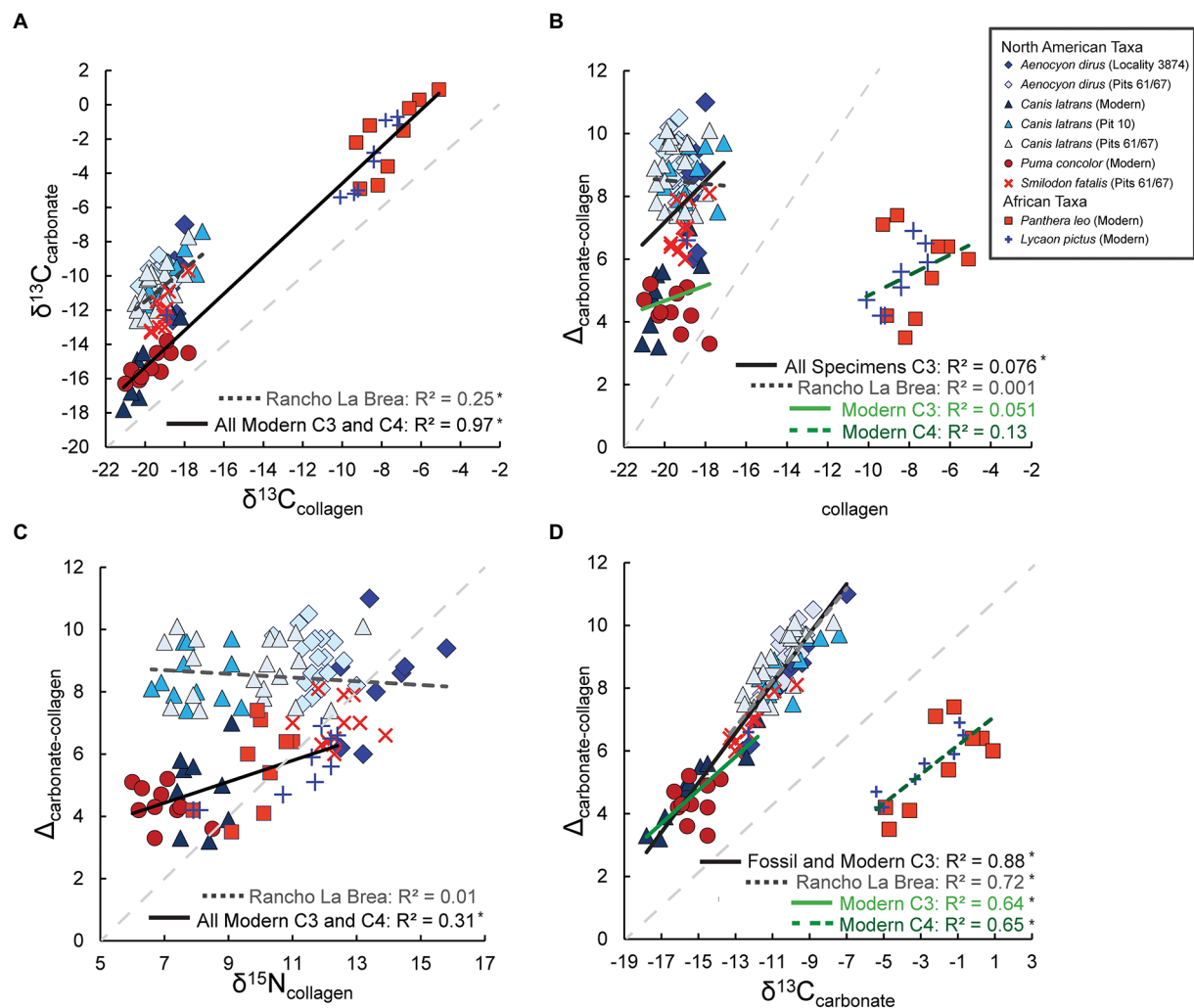


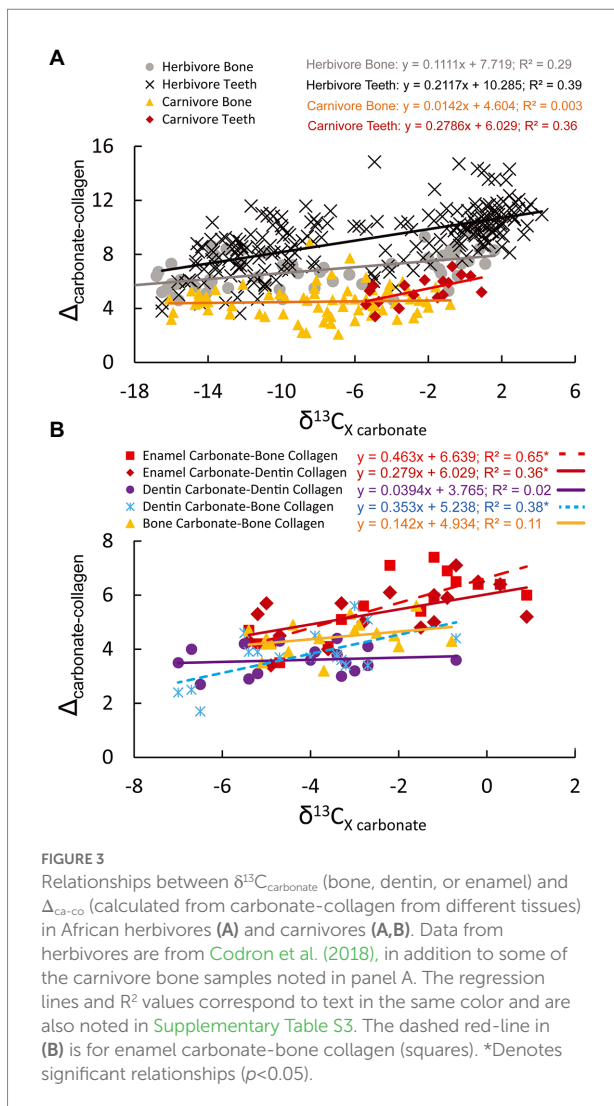
FIGURE 2

Relationship between $\delta^{13}\text{C}_{\text{carbonate}}$ and $\delta^{13}\text{C}_{\text{collagen}}$ values (A), and $\Delta_{\text{ca-co}}$ and $\delta^{13}\text{C}_{\text{collagen}}$ values (B), $\delta^{15}\text{N}_{\text{collagen}}$ values (C), and $\delta^{13}\text{C}_{\text{carbonate}}$ values (D; $n=108$). The regression lines and R^2 values correspond to text in the same color and are also noted in Supplementary Table S3. Note, the modern C₃ regression lines in (A) and (B) includes modern North American taxa and one African wild dog with a C₃ value (Supplementary Tables S3, S4 only include geographically similar taxa). The legend in (B) applies to all (A–D). A light-gray dashed-line with a slope of 1 is present in the background of each panel for reference. *Denotes significant relationships ($p < 0.05$).

relationship ($R^2 = 0.31$, $p = 0.021$; Supplementary Table S4, all data located in Supplementary Table 2).

There are differences among stable carbon isotope values measured in different tissues (Supplementary Table S5). Collagen consistently has lower $\delta^{13}\text{C}$ values than carbonate samples by 3.6–5.5‰, which is consistent with prior work (e.g., Lee-Thorp et al., 1989; Ambrose and Norr, 1993). Enamel $\delta^{13}\text{C}_{\text{carbonate}}$ values are significantly higher than both dentin $\delta^{13}\text{C}_{\text{carbonate}}$ values ($p < 0.001$) and bone $\delta^{13}\text{C}_{\text{carbonate}}$ values ($p = 0.004$), though mean differences are low (1.7 and 1.1‰, respectively; Supplementary Table S5). Further, dentin $\delta^{13}\text{C}_{\text{carbonate}}$ values are significantly lower than bone $\delta^{13}\text{C}_{\text{carbonate}}$ values ($p = 0.029$; Supplementary Table S5). All carbon isotopes signatures from all tissues sampled (enamel, dentin, and bone) yield significantly different values from one another (all p -values ≤ 0.001 ;

Supplementary Table S5). Only dentin and bone $\delta^{13}\text{C}_{\text{collagen}}$ values yield mean values indistinguishable from one another ($p = 0.504$; Supplementary Table S5). Mean $\delta^{15}\text{N}_{\text{collagen}}$ values from dentin are significantly higher than bone collagen ($p < 0.001$; Supplementary Table S5); however, the mean difference is quite small (0.9 ± 0.7 ‰; Supplementary Table S5). Further, the tissues with the strongest correlations between $\delta^{13}\text{C}$ values (dentin carbonate-dentin collagen, and bone carbonate-bone collagen) exhibit no significant relationships between apatite (dentin or bone) $\delta^{13}\text{C}_{\text{carbonate}}$ values and $\Delta_{\text{ca-co}}$ in African carnivores (Supplementary Table S4). Enamel $\delta^{13}\text{C}_{\text{carbonate}}$ values are consistently positively correlated with $\Delta_{\text{ca-co}}$ values (whether $\Delta_{\text{ca-co}}$ is based on dentin or bone collagen; Supplementary Table S3). Dentin $\delta^{13}\text{C}_{\text{carbonate}}$ values are also significantly related to $\Delta_{\text{ca-co}}$ values when bone collagen is used; however, neither bone nor



dentin exhibit any significant relationships between carbonate $\delta^{13}C$ values and $\Delta_{\text{ca-co}}$ values when calculated from just bone or just dentin tissues (carbonate/collagen; Figure 3). Further, African carnivores from C_4 ecosystems have average $\Delta_{\text{ca-co}}$ values of $5.5 \pm 1.2\text{‰}$ when comparing enamel and bone, however $\Delta_{\text{ca-co}}$ values are lower when bone carbonate and bone collagen are used ($4.4 \pm 0.6\text{‰}$ for C_4 carnivores, $4.7 \pm 0.6\text{‰}$ for *Lycaon pictus*, and $4.2 \pm 0.5\text{‰}$ for *Panthera leo*) and closer to values reported in the literature (averaging $4.3 \pm 1.0\text{‰}$ to $4.8 \pm 0.4\text{‰}$; Lee-Thorp et al., 1989; Clementz et al., 2009).

Collagen-carbonate $\delta^{13}C$ and $\delta^{18}O$ variances in carnivorans

Carbonate and collagen tissues do vary to different extents, with $\delta^{13}C_{\text{carbonate}}$ values having greater variances than $\delta^{13}C_{\text{collagen}}$ values ($p < 0.0001$ for both Levene's Median test and Bartlett's test) and a standard deviation almost double that of collagen (1.3 vs.

0.7‰) in Rancho La Brea samples. Modern specimens from C_3 and C_4 ecosystems were equivocal (C_3 specimens, $p = 0.111$ and $p = 0.039$ for Levene's Median test and Bartlett's test; C_4 specimens, $p = 0.025$ and $p = 0.081$ for Levene's Median test and Bartlett's test, respectively), but sample sizes were significantly lower ($n = 20$, $n = 17$, respectively) than Rancho La Brea specimens ($n = 71$).

Stable oxygen isotope ratios were measured and compared among all carbonate samples from southern California to assess if Rancho La Brea fossils had anomalously low $\delta^{18}O$ values, potentially due to diagenesis. Modern canid and felid (i.e., *Canis latrans* and *Puma concolor*, respectively) enamel $\delta^{18}O$ values ranged from -5.0 to 0.6 (mean = $-2.6 \pm 1.3\text{‰}$, $n = 19$) and were indistinguishable in both mean value ($p = 0.336$) and variance ($p = 0.955$) from $\delta^{18}O$ values of fossil specimens that include *C. latrans*, *A. dirus*, and *S. fatalis* from Rancho La Brea ($\delta^{18}O$ values ranged from -5.3 to 2.3 ; mean = $-2.3 \pm 1.3\text{‰}$, $n = 71$).

Discussion

Identifying the primary drivers of collagen-carbonate spacing in carnivores requires the testing of numerous hypotheses. Below we evaluate hypotheses pertaining to ontogenetic dietary differences, diagenesis, and physiological differences between canids and felids, eliminating these as potential drivers with data provided from this paper and published studies. We are unable to eliminate hypotheses pertaining to tissue and environmental/dietary differences, and their downstream impacts on $\Delta_{\text{ca-co}}$ spacing. Further work is needed to clarify the exact mechanism(s) responsible for $\Delta_{\text{ca-co}}$ spacing (including the role of trophic level in different ecosystems); regardless, this work helps to advance our understanding of a challenging problem and cautions the use of static offset values between collagen and carbonates in future work (as has become a more common practice; e.g., Clementz et al., 2009; Smith et al., 2022).

The absence of significant ontogenetic dietary differences and diagenetic effects on collagen-carbonate $\delta^{13}C$ spacing

Tissues such as bone collagen and enamel carbonate mineralize at different times and undergo significant to no remodeling, respectively. While it is possible that ontogenetic differences in diet are responsible for the isotopic differences between bone collagen (representing a later in life signal due to continuous remodeling) and enamel carbonate (occurring earlier in life when the teeth mineralized and representing a discrete interval of time) in the carnivores examined, this would require dramatic dietary changes over time that are possible but not probable. The canids studied would need to eat prey from more open grassland environments as young individuals and then shift to eating forest-dwelling prey as adults, in a manner that predictably correlates with $\delta^{13}C_{\text{carbonate}}$ values in all felids and

canids studied. This depiction of canid and felid ecology also does not align with morphological interpretations of extinct taxa or our knowledge of extant felid and canid behavior in the wild (Elliot et al., 1977; Bekoff and Wells, 1982). Specifically, the morphology of *S. fatalis* and *A. dirus* suggests terrestrial and cursorial hunting in these taxa, respectively (Samuels et al., 2013), while observational data suggests that extant felids typically use vegetation as cover to ambush prey while extant canids rarely utilize cover (Elliot et al., 1977; Bekoff and Wells, 1982). Additionally, both *A. dirus* and *S. fatalis* are interpreted as social predators (Carbone et al., 2009; McHorse et al., 2012); in extant social carnivores, juveniles typically consume the same prey as adults (i.e., meat and/or carcasses are shared, as observed in African lions; Schaller, 1972). Published adult $\delta^{13}\text{C}_{\text{collagen}}$ values that span multiple pits (Fuller et al., 2014, 2020) prepared *via* ultrafiltration (as was done here), were indistinguishable from juvenile $\delta^{13}\text{C}_{\text{collagen}}$ values from Locality 3,874 ($p = 0.378$; means of -18.4 and -18.5‰ respectively), indicating that juvenile dire wolves are eating similar prey as adults. Juvenile $\delta^{13}\text{C}_{\text{collagen}}$ values are from tooth dentin in *A. dirus* (Supplemental Table 1) and bone collagen from one juvenile humerus (Fuller et al., 2020). While $\delta^{13}\text{C}_{\text{collagen}}$ values from tooth dentin (laid down during the animal's youth) in *A. dirus* (Locality 3,874; no published radiocarbon dates, a general locality name for material collected by the University of California Museum of Paleontology; Feranec et al., 2009) are significantly greater than $\delta^{13}\text{C}_{\text{collagen}}$ values from bone collagen from *A. dirus* deposited in Pits 61/67 ($\sim 11,581 \pm 3,768$ years before present, calibrated; O'Keefe et al., 2009), these differences may be a result of different ecologies during different sampling periods (i.e., Locality 3,874 may represent a much broader, narrower, or different span of time than Pits 61/67; Feranec et al., 2009; O'Keefe et al., 2009). Further, extant African canids and felids reveal only minor differences in $\delta^{13}\text{C}_{\text{carbonate}}$ values between bone (a more recent diet) and both enamel (1.1‰) or dentin (0.7‰ ; both enamel and dentin are laid down earlier in life; also see Figure 6 from Bocherens, 2015), suggesting that 'whole diet' ontogenetic differences are minor through time, with such minor differences potentially due to weaning. It should also be noted that $\delta^{13}\text{C}_{\text{collagen}}$ are indistinguishable between dentin and bone collagen in extant African carnivores (Supplementary Table S5), indicative of similar dietary protein sources through ontogeny in African canids and felids.

A case could be made that the difference in variance at Rancho La Brea is due to bone turnover smoothing out differences that appear in $\delta^{13}\text{C}$ values of the enamel, the latter of which is laid down over a relatively short period of the animal's lifespan and is not subject to reworking (as is the case with bone; Hedges et al., 2007). However, this cannot explain the dire wolf data from Locality 3,874, where enamel $\delta^{13}\text{C}$ is compared with collagen from dentin (which like enamel, does not turn over; Helfman and Bada, 1976) though it is of course possible that the sampling geometry of enamel and dentin represent slightly different times (separated by days to month, not years; Bocherens, 2015). Further, the tooth dentin analyzed from Locality 3,874 has significantly higher

$\delta^{15}\text{N}_{\text{collagen}}$ values than *A. dirus* from Pit 61/67 where bone collagen (not dentin collagen) was analyzed; suggesting that the dentin analyzed was laid down early in the life of the animal when it was still consuming a significant portion of its mother's milk (i.e., $13.7 \pm 1.1\text{‰}$ SD in dentin from Locality 3,874, $11.8 \pm 0.5\text{‰}$ in bone collagen from Pits 61/67; $p < 0.0001$). At locality 3,874, $\delta^{13}\text{C}_{\text{carbonate}}$ values range from -12.6 to -7.0‰ while $\delta^{13}\text{C}_{\text{collagen}}$ values of the same individuals range from -18.8 to -18‰ , in the same teeth. Therefore, differences in $\delta^{13}\text{C}$ variability likely stems from difference in $\delta^{13}\text{C}$ variability of protein and whole diet sources, and not the timing or turnover of tissues. As mentioned above, lipids can be extremely ^{13}C depleted relative to protein (Ramsay and Hobson, 1991) and may contribute to larger $\delta^{13}\text{C}_{\text{carbonate}}$ ranges as compared to $\delta^{13}\text{C}_{\text{collagen}}$ ranges. Hence, understanding relationships between $\delta^{13}\text{C}$ values from different tissues and $\Delta_{\text{ca-co}}$ values derived from those tissues has unique challenges. This highlights the importance of experimental studies and the benefits of obtaining data from multiple tissue types (especially from fossils) when possible—both to best understand protein and whole diet sources while also providing further resolution to understanding relationships between $\delta^{13}\text{C}$ and $\Delta_{\text{ca-co}}$ values.

If a nursing/weaning signal was apparent, we would expect both enamel and dentin to have significantly lower $\delta^{13}\text{C}_{\text{carbonate}}$ values than bone $\delta^{13}\text{C}_{\text{carbonate}}$ values (due to the consumption of fattier milk with lower $\delta^{13}\text{C}$ values while nursing and/or weaning earlier in life; e.g. Richards et al., 2002; Fuller et al., 2006; Tsutaya and Yoneda, 2015), and this is not the case. Contributions from weaning are also less likely due to early weaning of canids (by ~ 5 – 8 weeks of age; Mech, 1974; Ewer, 1998; Nowak and Walker, 1999) while weaning occurs later in large felids (e.g., African lions, weaning by ~ 8 – 9 months; Haas et al., 2005). Further, studies that examined the effect of weaning on $\delta^{13}\text{C}$ values in tissues, including plasma, hair, and tooth enamel in humans and other mammals, showed its effect was minimal ($< 1\text{‰}$; Tsutaya and Yoneda, 2015). Studies of non-primate taxa, including herbivores and carnivores, showed no evidence of ^{13}C enrichment in the plasma of offspring ($0.0 \pm 0.6\text{‰}$; Jenkins et al., 2001), while ^{13}C enrichment of $\sim 1\text{‰}$ was observed in the tissues (hair, fingernails, and/or ribs) of exclusively breastfed human infants (Richards et al., 2002; Fuller et al., 2006). Further, serial sampling of the enamel of two adult upper canines from *S. fatalis* from Rancho La Brea (which developed and mineralized from near birth up to 25 months of age) did not exhibit a weaning signal or any trend in $\delta^{13}\text{C}$ values over time (Feranec, 2004; Wysocki et al., 2015).

Other possible reasons for the difference between collagen and carbonate $\delta^{13}\text{C}$ values include differences in tissue formation and/or post-mortem differences in diagenesis between tissues. Bone collagen is organic, while enamel is primarily inorganic (only ~ 6 – 10‰ organic content; Teruel et al., 2015; Kendall et al., 2018). It is possible that the bone collagen values were altered in some way that homogenized the isotopic values of the taxa examined, either *in situ* or during collection and cleaning (which included boiling in kerosene in the historical early twentieth

century collections); or conversely that the larger spread in the enamel $\delta^{13}\text{C}$ values (Figure 1) is due to variable diagenesis or contamination that affected the carbonate. However, the fact that $\Delta_{\text{ca-co}}$ values in modern taxa are predictable from $\delta^{13}\text{C}_{\text{carbonate}}$ values, like those from Rancho La Brea (Figure 2A), suggests that neither of these processes is likely and that the origin of the greater variability of $\delta^{13}\text{C}_{\text{carbonate}}$ values relative to $\delta^{13}\text{C}_{\text{collagen}}$ is biogenic. Furthermore, isotopic difference in $\delta^{13}\text{C}_{\text{collagen}}$ values is apparent between other taxa that co-occurred in Rancho La Brea (e.g., bison, horses, and camels as compared to *A. dirus*, *C. latrans*, and *S. fatalis*; Coltrain et al., 2004), again suggesting that bone collagen values were not homogenized due to taphonomic factors; and samples with C:N ratios of 3.1–3.4 (well within the range of 2.9–3.6 indicative of biogenic values; Ambrose et al., 1997) were included in this study. Similarly, $\delta^{13}\text{C}_{\text{carbonate}}$ values of extinct taxa from Rancho La Brea are similar in both $\delta^{13}\text{C}_{\text{carbonate}}$ values and in variability as other Pleistocene sites in North America (e.g., DeSantis et al., 2009, 2019, 2020; Feranec et al., 2009; Feranec and DeSantis, 2014; Jones and DeSantis, 2017). If the $\delta^{13}\text{C}_{\text{carbonate}}$ values were diagenetically altered, we might expect anomalously low oxygen isotope values as oxygen isotopes are more susceptible to post-mortem alteration than $\delta^{13}\text{C}$ values from structural carbonates from bioapatite (Wang and Cerling, 1994). However, oxygen isotope values measured in enamel carbonate from fossil material are neither more variable nor anomalously lower than $\delta^{18}\text{O}$ values from extant *C. latrans* and *P. concolor* from southern California (collected during the 20th and 21st centuries). Finally, a large set of published literature demonstrates that tooth enamel is inherently less prone to diagenetic alteration than other tissues like bone apatite, bone collagen, dentin apatite, and dentin collagen (e.g., Wang and Cerling, 1994; Collins et al., 2002; Koch, 2007; Lee-Thorp, 2008; MacFadden et al., 2010). Hence while diagenesis is possible at any fossil locality, several lines of evidence suggest that both types of tissues sampled in this study (i.e., enamel and bone) record biogenic isotope signals and that diagenesis is not a likely driver of the carbonate-collagen discrepancies we observe here.

Physiological similarities in collagen-carbonate $\delta^{13}\text{C}$ spacing between canids and felids and the need for caution in making trophic level assessments

$\Delta_{\text{ca-co}}$ spacing has been previously used to identify differential dietary sources as well as trophic level, however data from this study suggest that such determinations should be made with caution. For example, larger values indicate when protein and carbohydrates come from different sources while smaller values indicate that both protein and carbohydrates are from similar sources. The work of Ambrose et al. (1997) documents that when ancient humans have $\Delta_{\text{ca-co}}$ spacing $>4.4\text{‰}$ they consumed C_4 carbohydrates and C_3 protein, while values under this threshold suggest that both carbohydrates and proteins

originate from similar sources (e.g., marine protein). In herbivores, it is thought that consumption of C_4 vegetation and rumination contribute to higher $\Delta_{\text{ca-co}}$ values; ^{13}C deplete methane produced *via* fermentation results in ^{13}C enriched CO_2 , which is subsequently incorporated into the body *via* blood bicarbonate (Hedges, 2003; Clementz et al., 2009; Codron et al., 2018). Thus, herbivorous mammals exhibit variability in $\Delta_{\text{ca-co}}$ values, even when consuming only primary productivity—with values ranging from 3.6 to 14.8‰ in African bovids, likely due to differences in the amounts of ^{13}C depleted methane produced *via* digestion and subsequently removed from the remaining nutrient pool *via* expulsion of methane gas by the animal (Codron et al., 2018). Further, it should be noted that all bovids are ruminants, so differences in $\Delta_{\text{ca-co}}$ values likely have more to do with disparate diets than differences in digestive physiology—especially when one species (*Antidorcas marsupialis*) has $\Delta_{\text{ca-co}}$ values that range more than 10‰ (from 4.3 to 14.8‰; these wide ranging values may be related to stark differences in protein content in C_3 and C_4 plants consumed as discussed later). In hypercarnivorous mammals, fats, proteins, and carbohydrates (minimal to no consumption) should largely come from the same source, so that larger $\Delta_{\text{ca-co}}$ spacing would suggest individuals with more plant biomass in their diets (Clementz et al., 2009; Bocherens et al., 2017). It was presumed that higher lipid consumption by carnivores (especially hypercarnivores) was responsible for lower $\Delta_{\text{ca-co}}$ values (Krueger and Sullivan, 1984; Lee-Thorp et al., 1989; O'Connell and Hedges, 2017) and thus $\Delta_{\text{ca-co}}$ values would be predictive of trophic level (Clementz et al., 2009; Bocherens et al., 2017). However, the hypercarnivores examined here—including *P. concolor*, *S. fatalis* and *A. dirus*—have average offset values that range from 4.4 ± 0.6 in *P. concolor* to 8.8 ± 1.1 in *A. dirus* (when calculated from enamel carbonate and bone collagen) and are thus unrelated to trophic level (as inferred from $\delta^{15}\text{N}_{\text{collagen}}$ values) in Rancho La Brea carnivores and extant carnivores from C_3 ecosystems (Supplementary Table S4). Contrary to expectations, extant hypercarnivores from C_4 ecosystems exhibit higher (not lower) $\Delta_{\text{ca-co}}$ values with higher $\delta^{15}\text{N}_{\text{collagen}}$ values (Supplementary Table S4). Data from extant and extinct carnivores here suggest that the C_3 or C_4 environment the prey are foraging in has an impact on not only the $\delta^{13}\text{C}_{\text{carbonate}}$ values, but also the offset between collagen and carbonate when $\Delta_{\text{ca-co}}$ is calculated from enamel carbonate and bone collagen (Figure 2)—though this may be related to fat consumption and/or digestive physiology *via* effects of vegetation on fat accumulation in prey or digestion of those prey in carnivores. Thus, trophic level estimations may be more nuanced and not directly comparable between disparate ecosystems.

Codron et al. (2018) documented a positive relationship between $\delta^{13}\text{C}_{\text{carbonate}}$ and $\Delta_{\text{ca-co}}$ values in herbivores, combining teeth and bones into one data set and focusing on the relationship between $\delta^{13}\text{C}_{\text{collagen}}$ and $\Delta_{\text{ca-co}}$ values ($R^2 = 0.09$, $p < 0.0001$). Our recalculation of their published data also yields significant (and stronger) relationships between $\delta^{13}\text{C}_{\text{carbonate}}$ and $\Delta_{\text{ca-co}}$ values ($R^2 = 0.34$, $R = 0.58$, $p < 0.0001$ when calculated *via* enamel carbonate and dentin collagen in teeth; $R^2 = 0.29$, $R = 0.54$, $p < 0.0001$ when calculated *via* bone carbonate and bone collagen; and $R^2 = 0.35$, $R = 0.59$, $p < 0.0001$ when combined), though these

results are weaker than those observed in carnivores (Supplementary Table S3). Within trophic-level difference in herbivores were attributed to physiology or environmental factors, to differences in methane production that result from grass vs. browse consumption, and to differences between ruminants and hindgut fermenters (Cerling and Harris, 1999; Clauss et al., 2020). However, as we noted with the springbok example generated from data by Codron et al. (2018)—its ‘environment’ (i.e., the composition of its diet, as browse or grass) is likely the driving factor of $\Delta_{\text{ca-co}}$ values in this bovid as all members of the species (*Antidorcas marsupialis*) share the same physiology.

Differences in canid and felid physiology are not likely the primary cause of $\Delta_{\text{ca-co}}$ variability. Canid and felid $\Delta_{\text{ca-co}}$ values are indistinguishable when feeding in similar environments (e.g., individuals of both *P. concolor* and *C. latrans* with similar $\delta^{13}\text{C}_{\text{carbonate}}$ values have similar $\Delta_{\text{ca-co}}$ values in C_3 ecosystems, and the same is true for *P. leo* and *L. pictus* in C_4 ecosystems) but do vary with $\delta^{13}\text{C}_{\text{carbonate}}$ values and both within and between C_3 or C_4 dominated environments. The fact that *S. fatalis* $\Delta_{\text{ca-co}}$ values are significantly lower than both canids at Rancho La Brea may stem from consuming prey that foraged in disparate environments (based on $\delta^{13}\text{C}_{\text{carbonate}}$ values). In contrast, the $\Delta_{\text{ca-co}}$ values of the modern felid *P. concolor* and canid *C. latrans* that consume prey that forage in similar environments (as inferred from indistinguishable $\delta^{13}\text{C}_{\text{carbonate}}$ values, $p = 0.964$) are indistinguishable from each other ($p = 0.762$). Thus, it does not appear that differences in canid and felid physiology are the primary cause of $\Delta_{\text{ca-co}}$ variability (see Figure 2). If physiological differences between canids and felids were a primary driver of $\Delta_{\text{ca-co}}$ variability, we would expect similar $\delta^{13}\text{C}_{\text{carbonate}}$ values to yield disparate $\Delta_{\text{ca-co}}$ values in canids and felids, especially when feeding on similar prey. Accordingly, these data (Figures 2, 4) can help us rule out physiological differences between canids and felids as the primary driver. It therefore appears that the foraging habitats of prey have a substantial influence on $\Delta_{\text{ca-co}}$ values in carnivores, as documented here, and in herbivores as documented by Murphy et al. (2007) and Codron et al. (2018).

Tissue and environmental/dietary drivers of collagen-carbonate $\delta^{13}\text{C}$ spacing

Tissue specific differences, including processes governing how macronutrients such as amino acids and fats (including types and lengths of fatty acids) are incorporated into tooth enamel and bone collagen, may contribute to differences between $\delta^{13}\text{C}_{\text{carbonate}}$ and $\delta^{13}\text{C}_{\text{collagen}}$ and $\Delta_{\text{ca-co}}$ values. Earlier work by Ambrose and Norr (1993) established that $\delta^{13}\text{C}_{\text{carbonate}}$ values reflect whole diet (carbohydrates, proteins, and fats), while $\delta^{13}\text{C}_{\text{collagen}}$ reflects protein consumption. In carnivores, especially hypercarnivores, it is expected that carbohydrates would be a minor component of their diet and that the ‘whole diet’ most likely reflects proteins and fats, in contrast to primarily protein being routed into bone collagen (Ambrose and Norr, 1993). Further, as fat is depleted in ^{13}C

compared to either protein or carbohydrates (Ramsay and Hobson, 1991), one would expect $\delta^{13}\text{C}_{\text{carbonate}}$ values to be more ^{13}C depleted when consuming prey with a higher fat content (all else being equal; though research in this area is needed). Fats are ^{13}C depleted compared to muscle to an astonishing degree, differing by as much as 7–8‰ in polar bears and ringed seals, with muscle and fat being even more ^{13}C depleted than bone collagen (Tieszen et al., 1983; Ramsay and Hobson, 1991). The ^{13}C depleted nature of fat is the primary reason why carnivores were thought to have lower $\Delta_{\text{ca-co}}$ values (due to the consumption of ^{13}C depleted fat relative to other sources (Lee-Thorp et al., 1989; Clementz et al., 2009). However, an observation of Ambrose and Norr (1993) is often overlooked; when $\delta^{13}\text{C}$ values of protein are higher than $\delta^{13}\text{C}$ values of whole diet (regardless of the amount of protein in the diet; i.e., whether the diet consists of 6% protein or 77% protein) then $\Delta_{\text{ca-co}}$ values are low, when $\delta^{13}\text{C}$ values of protein are lower than $\delta^{13}\text{C}$ values of whole diet then $\Delta_{\text{ca-co}}$ values are high (again, regardless of the amount of protein in the diet, i.e., whether the diet consists of 6, 25, or 76% protein). Monoisotopic diets (where protein and whole diet are similar) yield intermediate $\Delta_{\text{ca-co}}$ values (i.e., 5.7 ± 0.4 ‰, as compared to a range of 1.2 to 11.3‰; Ambrose and Norr, 1993). Thus, the isotopic composition of carbohydrates and fat relative to protein can influence $\Delta_{\text{ca-co}}$ values, and $\Delta_{\text{ca-co}}$ values are far from predictable based on trophic level or the amount of protein in one’s diet, alone.

Observed larger offsets in $\Delta_{\text{ca-co}}$ values in carnivores could stem from either increased consumption of more ^{13}C enriched carbohydrates, the consumption of leaner prey, and/or different amounts of methane production. One possibility is that the canids consume more terrestrial resources that are not meat, and the higher $\Delta_{\text{ca-co}}$ values are a result of more non-meat sources. Alternatively, even limited non-protein sources with higher $\Delta_{\text{ca-co}}$ values (including fat) could result in higher $\Delta_{\text{ca-co}}$ values. Ambrose and Norr (1993) demonstrated that large $\Delta_{\text{ca-co}}$ values occur (i.e., $\Delta_{\text{ca-co}}$ values of 10.8 ± 0.38 , 10.8 ± 0.36 , and 11.3 ± 0.40) when rats were fed protein that was significantly isotopically lighter than whole diet values (by ~ 10 ‰); in contrast, much smaller $\Delta_{\text{ca-co}}$ values occur (i.e., $\Delta_{\text{ca-co}}$ values of 1.2 ± 0.10 , 2.1 ± 0.24) when rats were fed protein that was isotopically heavier than whole diet values. As the canids have the highest $\Delta_{\text{ca-co}}$ values, as compared to the felids (from North America), increased C_4 whole diet values (which can include protein, carbohydrates, and fats) in canids could also cause this pattern. *Aenocyon dirus* has been interpreted as a hypercarnivore (Van Valkenburgh, 1991), making the source of the non-protein components less likely to be terrestrial plants and nuts, though even a small amount of supplemental foods that are isotopically heavier could drive this pattern (based on data from Ambrose and Norr, 1993) in addition to $\delta^{15}\text{N}_{\text{collagen}}$ values providing only a ‘minimum estimate’ of trophic level (per Bocherens, 2015). Alternatively, the consumption of fat in prey from more open grassland ecosystems could also result in larger $\Delta_{\text{ca-co}}$ values that correlate with $\delta^{13}\text{C}_{\text{carbonate}}$ values (per the discussion of Ambrose and Norr, 1993, above). Literature from the livestock industry demonstrates that free-ranging elk and bison

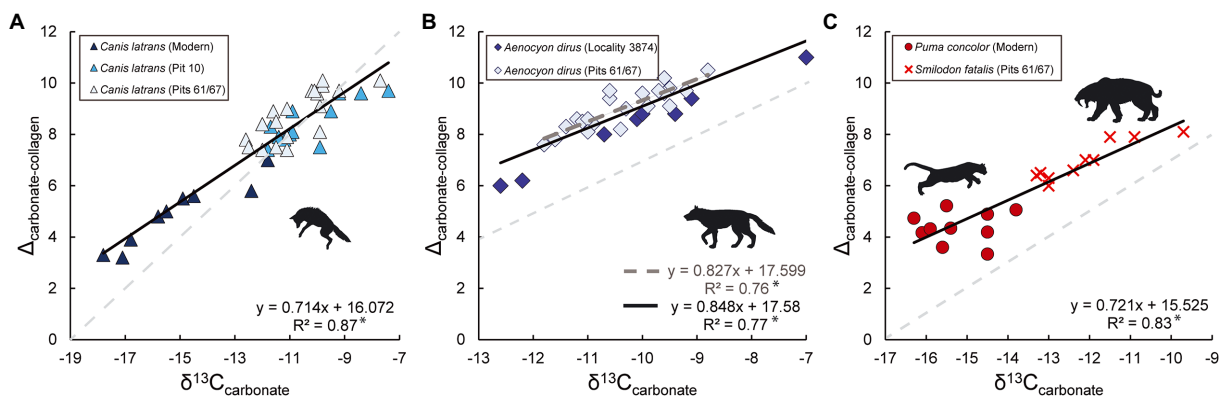


FIGURE 4

Relationships between $\delta^{13}\text{C}_{\text{carbonate}}$ values and $\Delta_{\text{ca-co}}$ values for North American canid and felid specimens examined. Relationships between $\delta^{13}\text{C}_{\text{carbonate}}$ values and $\Delta_{\text{ca-co}}$ values and in *Canis latrans* (A), *Aenocyon dirus* (B), and the felids (C; both *Puma concolor* and *Smilodon fatalis*). Black lines and subsequent regression equations and R^2 values reflect the inclusion of all data per taxon. The dark-gray dashed line in panel B denotes the regression line and equations specific to *A. dirus* based on $\delta^{13}\text{C}_{\text{collagen}}$ from bone collagen, while the solid black line includes $\delta^{13}\text{C}_{\text{collagen}}$ data from tooth dentin from *A. dirus* from Locality 3,874. A light-gray dashed-line with a slope of 1 is present in the background of each panel for reference. *denotes significant relationships ($p < 0.05$).

can yield disparate fat and fatty acid compositions (Rule et al., 2002; e.g., elk have higher n-6 fatty acids than bison or beef cattle), which can have downstream impacts on the isotopic values observed in predators. Further, carnivores are known to increase fat oxidation when consuming a high-fat diet (Lester et al., 1999), which may also influence resulting $\Delta_{\text{ca-co}}$ values, though this has not yet been documented. While methane production is more pronounced in herbivores than carnivores (and most pronounced in grass-rich diets; Cerling and Harris, 1999), methane production could also play a role in carnivores if greater methane production occurs when digesting leaner prey (this could also yield higher $\Delta_{\text{ca-co}}$ values in carnivores that correlate with the foraging habitat of prey); however, this is not well understood.

Environmental differences, including water deficits may also contribute to isotopic offsets, as suggested by Murphy et al. (2007). Water deficits are positively correlated with $\Delta_{\text{ca-co}}$ values in kangaroos (Murphy et al., 2007); thus, as it gets wetter $\Delta_{\text{ca-co}}$ values decrease. While plants need adequate water to grow (zero rainfall results in no growth), excess rainfall beyond a certain threshold can reduce the nutritional quality of foliage (increased rainfall results in increased growth, and subsequently lower nitrogen per unit biomass, which is less nutritious; Austin and Vitousek, 1998). Similar effects are observed when growing plants under higher atmospheric CO_2 conditions. Plants grown under higher atmospheric CO_2 levels (which also have lower $\delta^{13}\text{C}$ values when grown in growth chambers) also yield more growth (structural carbon, and often associated tissues like lignin and cellulose) while per unit biomass is subsequently less nutritious (nitrogen content is lower; Conroy, 1992; Barbehenn et al., 2004). All things being equal, herbivores that consume plants with relatively lower nitrogen/protein content may utilize protein differently and have different amounts of fat stores that are subsequently transferred to predators. More work is needed to clarify if and how

environmental factors (e.g., precipitation, atmospheric CO_2) play a role in affecting herbivore and carnivore $\Delta_{\text{ca-co}}$ values.

Future research directions

It is not yet clear why $\Delta_{\text{ca-co}}$ and $\delta^{13}\text{C}_{\text{carbonate}}$ from bone apatite are unrelated in African carnivores collectively (when combining canids and felids), both here and in Codron et al. (2018), in contrast to enamel apatite. However, there is clear evidence that bone apatite and enamel apatite tissues are not equal and vary quite dramatically in their mineralogy and crystal size (Wopenka and Pasteris, 2005). Bone apatite crystals typically lack the hydroxyl ion (OH^-) and are about 10 to 100 times smaller than in enamel, both of which can affect carbonate concentration (with bone apatite having higher carbonate concentration and thus also greater solubility; Wopenka and Pasteris, 2005). Therefore, bone is well suited for being resorbed/re-precipitated and interacting with organic material, while enamel is well suited to resisting dissolution (Wopenka and Pasteris, 2005). While herbivores do exhibit positive relationships between $\delta^{13}\text{C}_{\text{carbonate}}$ and $\Delta_{\text{ca-co}}$ in both bone apatite and enamel apatite, bone apatite has significantly lower $\Delta_{\text{ca-co}}$ values and $\delta^{13}\text{C}_{\text{carbonate}}$ values than enamel ($p < 0.0001$, based on the analysis of data from Codron et al., 2018; mean $\Delta_{\text{ca-co}}$ in bone and enamel is $6.7 \pm 1.4\%$ and $9.3 \pm 2.1\%$, respectively; mean $\delta^{13}\text{C}_{\text{carbonate}}$ values of $-8.5 \pm 6.5\%$, and $-5.1 \pm 6.2\%$, respectively). Further, our analysis of African carnivores also demonstrates no relationship between $\delta^{13}\text{C}_{\text{carbonate}}$ in bone and $\Delta_{\text{ca-co}}$ and no relationship between $\delta^{13}\text{C}_{\text{carbonate}}$ in dentin and $\Delta_{\text{ca-co}}$ when calculated from dentin carbonate and dentin collagen (Supplementary Table S3). The lack of a relationship between dentin $\delta^{13}\text{C}_{\text{carbonate}}$ and dentin $\delta^{13}\text{C}_{\text{collagen}}$, similar to bone yet different from enamel, indicates that while differences in tissue routing may be at play, they likely do not stem from differences in

routing due to ontogeny (e.g., using more amino acids for bone growth while young but not while older). Instead, these differences may have more to do with differences in the inorganic content of enamel versus both dentin and bone (and dentin vs. bone) and/or the mineralogy of these tissues (Wang and Cerling, 1994; Wopenka and Pasteris, 2005). Further, wolves (*Canis lupus*) document a significant positive relationship between $\delta^{13}\text{C}_{\text{carbonate}}$ in bone and $\Delta_{\text{ca-co}}$ (based on data from Clementz et al., 2009), as do African wild dogs noted here, but in contrast to African lions (Supplementary Table S3). Thus, future work is needed to examine mechanisms behind these tissue specific discrepancies in $\Delta_{\text{ca-co}}$ values in carnivores, including differences between specific taxa.

More work is also needed to determine the precise mechanism responsible for the correlation between increased $\Delta_{\text{ca-co}}$ values and higher $\delta^{13}\text{C}_{\text{carbonate}}$ values, and why this pattern is not apparent in bone apatite and dentin apatite of African carnivores (Codron et al., 2018, and noted here). Further, a re-evaluation of the potential drivers of relationships between herbivore $\Delta_{\text{ca-co}}$ and $\delta^{13}\text{C}_{\text{carbonate}}$ values may be necessary. Codron et al. (2018) outlined two potential drivers of the positive relationship between $\Delta_{\text{ca-co}}$ values and $\delta^{13}\text{C}_{\text{carbonate}}$ values in herbivores: environmental differences in food sources; and physiological differences between hindgut fermenters and ruminants. As carnivores did not exhibit the above relationship in their data set (which was primarily composed of bone and not teeth), it was assumed that environmental factors were not at play, as it was expected that environmental influences would similarly affect relationships between both herbivore and carnivore $\Delta_{\text{ca-co}}$ values and $\delta^{13}\text{C}_{\text{carbonate}}$ values. Considering data presented here, carnivores clearly demonstrate a significant positive relationship between $\Delta_{\text{ca-co}}$ values and $\delta^{13}\text{C}_{\text{carbonate}}$ values in tooth enamel, but not bone apatite (weakly in some; see Clementz et al., 2009). Thus, macronutrient routing in these disparate tissues (biochemically and structurally) may also play a role. These drivers are not mutually exclusive and may both contribute to the isotopic disparities outlined here. Further, we clearly document that carnivores in both C_3 and C_4 ecosystems demonstrate positive relationships between $\Delta_{\text{ca-co}}$ and $\delta^{13}\text{C}_{\text{carbonate}}$ values (Figure 2), yet the reasons for ecosystem-associated differences between these lines and their intercepts is unclear—though may stem from differences in rainfall and/or CO_2 over time (and effects on protein and fat content in plants and prey). Thus, until the precise mechanisms driving the highly predictable $\Delta_{\text{ca-co}}$ values are identified, the examination of multiple tissues and isotopes may reveal a more complete understanding of the dietary ecology of both extinct and extant mammals.

Advances and challenges of relevance to paleobiology and archeology

The $\Delta_{\text{ca-co}}$ spacing in extinct and extant carnivores is predictable based on $\delta^{13}\text{C}_{\text{carbonate}}$ values—indicating that the

foraging behavior of prey consumed by predators is the best predictor of $\Delta_{\text{ca-co}}$ spacing. This positive relationship negates the idea that within trophic-level $\Delta_{\text{ca-co}}$ spacing is constant in carnivores and calls into question our ability to interpret degrees of carnivory, omnivory, or herbivory from $\Delta_{\text{ca-co}}$ values, alone. In the case of carnivores, felids and canids have similar $\Delta_{\text{ca-co}}$ values when consuming similar prey today (in both C_3 and C_4 environments), while felids and canids only differ in the past when consuming prey that foraged in different habitats. Thus, physiological differences between canids and felids do not appear to be drivers of $\Delta_{\text{ca-co}}$ spacing. While either ontogenetic differences in diet or diagenesis have been invoked as potential reasons for differences in $\delta^{13}\text{C}_{\text{carbonate}}$ and $\delta^{13}\text{C}_{\text{collagen}}$ values, neither of these hypotheses have much support. These data allow us to rule out many hypotheses and indicates that $\Delta_{\text{ca-co}}$ spacing is likely driven by the foraging habitat of prey, environmental influences, and/or tissue specific differences that affect how macronutrients are allocated and incorporated into mineralized tissues.

More work is needed to better understand the drivers of increased $\Delta_{\text{ca-co}}$ spacing in individuals with higher $\delta^{13}\text{C}_{\text{carbonate}}$ values and why these relationships are weaker or absent when comparing certain tissues. Further, not all tissues can be treated similarly. For example, bone apatite and enamel apatite were combined in Codron et al. (2018) as $\delta^{13}\text{C}$ values were similar; however, the resulting $\Delta_{\text{ca-co}}$ values are significantly higher when enamel carbonate and bone collagen were used to calculate $\Delta_{\text{ca-co}}$ ($p < 0.0001$, y-intercepts/mean differences of 2.6‰; Figure 3). While sampling from multiple tissues from the same specimens can be costly and potentially more destructive, more work that examines these relationships in different ecosystems and through time is necessary to better understand if and how a taxon's habitat contributes to nutrient routing to different tissues.

Our understanding of Rancho La Brea carnivores has benefited from sampling both enamel and bone collagen. Isotopes from different tissues are not “right” or “wrong” but rather provide different insights into the dietary ecology of carnivores. Nitrogen isotope ratios demonstrate that *C. latrans* likely consumed less meat than either *A. dirus* or *S. fatalis*. Stable carbon isotope values measured in bone collagen from Coltrain et al. (2004), Fuller et al. (2020), and here indicate that the protein component of Rancho La Brea carnivore diets are similar, while carbon isotope ratios from carbonate enamel indicate stark differences in the whole diet of *S. fatalis* as compared to *A. dirus* (DeSantis et al., 2019, 2020, and here) and *C. latrans* (at Pits 61/67). Differences in the stable carbon isotope signatures from whole diet indicate that *A. dirus* and *S. fatalis* are not consuming similar proportions of the same prey species and are instead consuming prey with disparate isotopic signatures—suggesting that these prey may forage in more open grasslands and more wooded areas, respectively; and/or may exhibit differences in fat content which can influence whole diet. As C_3 grasses have higher amounts of protein than C_4 grasses (Barbehenn et al., 2004); protein in prey-species may be biased toward C_3 protein sources, which may be responsible for similar carbon isotope values of bone collagen in herbivores and

carnivores. The dominance of protein from C_3 plants can be further amplified in drier ecosystems, where C_3 plants can have even more protein per unit biomass than in higher rainfall regions (Austin and Vitousek, 1998). Fat is an important component of hypercarnivore diets (e.g., polar bears; Ramsay and Hobson, 1991), and many hypercarnivores preferentially consume fat (Nowak and Walker, 1999). However, the isotopic source of fat is primarily reflected in the carbonate portion of tooth enamel, dentin, or bone, but not in collagen (Ambrose and Norr, 1993). Thus, whole diet differences are apparent between *S. fatalis* and *A. dirus* (DeSantis et al., 2019, 2020, and here), and *C. latrans* from Pits 61/67. Protein component of one's diet does not necessarily equal prey source, and we argue here that whole diet indicators (e.g., carbonate) are necessary to elucidating diets of extinct and extant carnivores. Our work here suggests potential drivers of the differences between stable carbon isotopes in enamel and collagen in Rancho La Brea taxa that include tissue and/or environmental differences (while challenging others including trophic level, ontogenetic dietary differences, physiological differences between canids and felids, and diagenesis), and outlines areas of future research that can bring further clarity to our understanding of the dietary ecology of predators and prey, today and in the past.

Data availability statement

The original contributions presented in the study are included in the article/Supplementary material, further inquiries can be directed to the corresponding author.

Ethics statement

Ethical review and approval was not required for the animal study because all of the animals studied were from museum collections. They were killed previously and not for the purpose of this study.

Author contributions

LD and RF conceptualized the study. All co-authors contributed to study design. LD, JS, JC, RE, and GT collected, prepared, and produced specimen/isotope data. LD analyzed stable isotope data. LD wrote the paper with significant editorial input from RE, JS, and JH, and additional feedback from all co-authors. All authors contributed to the article and approved the submitted version.

Funding

This work was supported by the National Science Foundation (1757545, 1758110, 1758116, 1758117, 1757236, and 1758108), Vanderbilt University, and the NY State Museum.

Acknowledgments

We thank L. Chiappe, P. Collins, P. Holroyd, E. Holt, and K. Fahy for access to materials, KF-D for discussions about stable isotopes and Rancho La Brea, J. Curtis for isotopic analysis, J. Olsson for the shadow drawings in Figures 1, 4, S. DeSantis for assistance with Figures 2, 4, and D. Fox, H. Bocherens, V. M. Bravo-Cuevas and additional reviewers for detailed feedback on earlier versions of this manuscript.

Conflict of interest

The authors declare that the research was conducted in the absence of any commercial or financial relationships that could be construed as a potential conflict of interest.

Publisher's note

All claims expressed in this article are solely those of the authors and do not necessarily represent those of their affiliated organizations, or those of the publisher, the editors and the reviewers. Any product that may be evaluated in this article, or claim that may be made by its manufacturer, is not guaranteed or endorsed by the publisher.

Supplementary material

The Supplementary material for this article can be found online at: <https://www.frontiersin.org/articles/10.3389/fevo.2022.1031383/full#supplementary-material>

SUPPLEMENTARY TABLE S1

Descriptive statistics of stable carbon and nitrogen isotope ratios from bone collagen and enamel carbonate of all taxa examined from North America.

SUPPLEMENTARY TABLE S2

Descriptive statistics of stable carbon and nitrogen isotope ratios from bone, dentin, and enamel in African carnivores.

SUPPLEMENTARY TABLE S3

Descriptive statistics of differences between carbon isotope values in carbonate and collagen (carbonate-collagen, $\Delta\text{ca-co}$) in all North American and African carnivores examined in this study.

SUPPLEMENTARY TABLE S4

Descriptive statistics of relationships between isotope values in carbonate and collagen and offset values in North American and African carnivores.

SUPPLEMENTARY TABLE S5

Descriptive statistics of relationships between isotope ratios in carbonate and collagen from enamel, dentin, and bone in African carnivores from C_4 ecosystems ($n=17$).

SUPPLEMENTAL TABLE 1

Stable isotope values and associated calculations for all individual samples (modern and fossil) from Rancho La Brea, southern California, and throughout Africa.

SUPPLEMENTAL TABLE 2

Stable isotope data and associated calculations for all tissues (enamel, dentin, bone) from individual samples (modern) from Africa, housed in the American Museum of Natural History (AMNH).

References

- Ambrose, S. H., Butler, B. M., Hanson, D. B., Hunter-Anderson, R. L., and Krueger, H. W. (1997). Stable isotopic analysis of human diet in the Marianas archipelago, Western Pacific. *Am. J. Phys. Anthropol.* 104, 343–361. doi: 10.1002/(SICI)1096-8644(199711)104:3<343::AID-AJPA5>3.0.CO;2-W
- Ambrose, S. H., and Norr, L. (1993). “Experimental evidence for the relationship of the carbon isotope ratios of whole diet and dietary protein to those of bone collagen and carbonate,” in *Prehistoric human bone: Archaeology at the molecular level*. eds. J. B. Lambert and G. Grupe (Heidelberg, German: Springer), 1–37.
- Auerswald, K., Wittmer, M. H. O. M., Zazzo, A., Schaefele, R., and Schnyder, H. (2010). Biases in the analyses if stable isotope discrimination in food webs. *J. Appl. Ecol.* 47, 936–941. doi: 10.1111/j.1365-2664.2009.01764.x
- Austin, A. T., and Vitousek, P. M. (1998). Nutrient dynamics on a precipitation gradient in Hawai'i. *Oecologia* 113, 519–529. doi: 10.1007/s004420050405
- Barbehenn, R. V., Chen, Z., Karowe, D. N., and Spickard, A. (2004). C₃ grasses have higher nutritional quality than C₄ grasses under ambient and elevated atmospheric CO₂. *Glob. Chang. Biol.* 10, 1565–1575. doi: 10.1111/j.1365-2486.2004.00833.x
- Barnosky, A. D., Koch, P. L., Feranec, R. S., Wing, S. L., and Shabel, A. B. (2004). Assessing the causes of late Pleistocene extinctions on the continents. *Science* 306, 70–75. doi: 10.1126/science.1101476
- Bekoff, M., and Wells, M. C. (1982). Behavioral ecology of coyotes: social organization, rearing patterns, space use, and resource defense. *Ethology* 60, 281–305.
- Bocherens, H. (2015). Isotopic tracking of large carnivore palaeoecology in the mammoth steppe. *Quat. Sci. Rev.* 117, 42–71. doi: 10.1016/j.quascirev.2015.03.018
- Bocherens, H., Cotte, M., Bonini, R. A., Straccia, P., Scian, D., Soibelzon, L., et al. (2017). Isotopic insight on paleodiet of extinct Pleistocene megafaunal Xenarthrans from Argentina. *Gondwana Res.* 48, 7–14. doi: 10.1016/j.gr.2017.04.003
- Bocherens, H., Fizet, M., and Mariotti, A. (1994). Diet, physiology and ecology of fossil mammals as inferred from stable carbon and nitrogen isotope biogeochemistry: implications for Pleistocene bears. *Palaeogeogr. Palaeoclimatol. Palaeoecol.* 107, 213–225. doi: 10.1016/0031-0182(94)90095-7
- Carbone, C., Maddox, T., Funston, P. J., Mills, M. G., Grether, G. F., and Van Valkenburgh, B. (2009). Parallels between playbacks and Pleistocene tar seeps suggest sociality in an extinct sabretooth cat, *Smilodon*. *Biol. Lett.* 5, 81–85. doi: 10.1098/rsbl.2008.0526
- Caut, S., Angulo, E., Courchamp, F., and Figuerola, J. (2010). Trophic experiments to estimate isotope discrimination factors. *J. Appl. Ecol.* 47, 948–954. doi: 10.1111/j.1365-2664.2010.01832.x
- Cerling, T. E., and Harris, J. M. (1999). Carbon isotope fractionation between diet and biopapatite in ungulate mammals and implications for ecological and paleoecological studies. *Oecologia* 120, 347–363. doi: 10.1007/s004420050868
- Cerling, T. E., Harris, J. M., MacFadden, B. J., Leakey, M. G., Quade, J., Eisenmann, V., et al. (1997). Global vegetation change through the Miocene/Pliocene boundary. *Nature* 389, 153–158. doi: 10.1038/38229
- Clauss, M., Dittmann, M. T., Vendl, C., Hagen, K. B., Frei, S., Ortmann, S., et al. (2020). Comparative methane production in mammalian herbivores. *Animal* 14, s113–s123. doi: 10.1017/S1751731119003161
- Clementz, M. T., Fox-Dobbs, K., Wheatley, P. V., Koch, P. L., and Doak, D. F. (2009). Revisiting old bones: coupled carbon isotope analysis of biopapatite and collagen as an ecological and palaeoecological tool. *Geol. J.* 44, 605–620. doi: 10.1002/gj.1173
- Clementz, M. T., Koch, P. L., and Beck, C. A. (2007). Diet induced differences in carbon isotope fractionation between sirenians and terrestrial ungulates. *Mar. Biol.* 151, 1773–1784. doi: 10.1007/s00227-007-0616-1
- Codron, D., Clauss, M., Codron, J., and Tütken, T. (2018). Within trophic level shifts in collagen–carbonate stable carbon isotope spacing are propagated by diet and digestive physiology in large mammal herbivores. *Ecol. Evol.* 8, 3983–3995. doi: 10.1002/ece3.3786
- Collins, M. J., Nielsen-Marsh, C. M., Hiller, J., Smith, C. I., Roberts, J. P., Prigodich, R. V., et al. (2002). The survival of organic matter in bone: a review. *Archaeometry* 44, 383–394. doi: 10.1111/1475-4754.t01-1-00071
- Coltrain, J. B., Harris, J. M., Cerling, T. E., Ehleringer, J. R., Dearing, M.-D., Ward, J., et al. (2004). Rancho La Brea stable isotope biogeochemistry and its implications for the paleoecology of the late Pleistocene coastal southern California. *Palaeogeogr. Palaeoclimatol. Palaeoecol.* 205, 199–219. doi: 10.1016/j.palaeo.2003.12.008
- Conroy, J. P. (1992). Influence of elevated atmospheric CO₂ concentrations on plant nutrition. *Aust. J. Bot.* 40, 445–456. doi: 10.1071/BT9920445
- Coplen, T. B. (1994). Reporting of stable hydrogen carbon and oxygen isotopic abundances. *Pure Appl. Chem.* 66, 273–276. doi: 10.1351/pac199466020273
- DeNiro, M. J., and Epstein, S. (1978). Influence of diet on the distribution of carbon isotopes in animals. *Geochim. Cosmochim. Acta* 42, 495–506. doi: 10.1016/0016-7037(78)90199-0
- DeSantis, L. R. G., Crites, J. M., Feranec, R. S., Fox-Dobbs, K., Farrell, A. B., Harris, J. M., et al. (2019). Causes and consequences of Pleistocene megafaunal extinctions as revealed from rancho La Brea mammals. *Curr. Biol.* 29, 2488–2495.e2. doi: 10.1016/j.cub.2019.06.059
- DeSantis, L. R., Feranec, R. S., Fox-Dobbs, K., Harris, J. M., Cerling, T. E., Crites, J. M., Farrell, A. B., and Takeuchi, G. T. (2020). Reply to Van Valkenburgh et al. *Curr. Biol.* 30:R151–R152, doi: 10.1016/j.cub.2020.01.011.
- DeSantis, L. R. G., Feranec, R. S., and MacFadden, B. J. (2009). Effects of global warming on ancient mammalian communities and their environments. *PLoS One* 4:e5750. doi: 10.1371/journal.pone.0005750
- DeSantis, L. R. G., Schubert, B. W., Scott, J. R., and Ungar, P. S. (2012). Implications of diet for the extinction of saber-toothed cats and American lions. *PLoS One* 7:e5245. doi: 10.1371/journal.pone.0052453
- Elliot, J. P., Cowan, I. M., and Holling, C. S. (1977). Prey capture by the African lion. *Can. J. Zool.* 55, 1811–1828. doi: 10.1139/z77-235
- Ewer, R. F. (1998). *The carnivores* Ithaca, NY: Cornell University Press.
- Feranec, R. S. (2004). Isotopic evidence of saber-tooth development, growth rate, and diet from the adult canine of *Smilodon fatalis* from rancho La Brea. *Palaeogeogr. Palaeoclimatol. Palaeoecol.* 206, 303–310. doi: 10.1016/j.palaeo.2004.01.009
- Feranec, R. S., and DeSantis, L. R. G. (2014). Understanding specifics in generalist diets of carnivores by analyzing stable carbon isotope values in Pleistocene mammals of Florida. *Paleobiology* 40, 477–493. doi: 10.1666/13055
- Feranec, R. S., Hadly, E. A., and Paytan, A. (2009). Stable isotopes reveal seasonal competition for resources between late Pleistocene bison (Bison) and horse (Equus) from rancho La Brea, southern California. *Palaeogeogr. Palaeoclimatol. Palaeoecol.* 271, 153–160. doi: 10.1016/j.palaeo.2008.10.005
- Finucane, B., Agurto, P. M., and Isbell, W. H. (2006). Human and animal diet at Conchopata, Peru: stable isotope evidence for maize agriculture and animal management practices during the middle horizon. *J. Archaeol. Sci.* 33, 1766–1776. doi: 10.1016/j.jas.2006.03.012
- Friedman, I., and O'Neil, J. R. (1977). *Compilation of stable isotope fractionation factors of geochemical interest*, vol. 440 US Government Printing Office.
- Fuller, B. T., Fahrni, S. M., Harris, J. M., Farrell, A. B., Coltrain, J. B., Gerhart, L. M., et al. (2014). Ultrafiltration for asphalt removal from bone collagen for radiocarbon dating and isotopic analysis of Pleistocene fauna at the tar pits of rancho La Brea, Los Angeles, California. *Quat. Geochronol.* 22, 85–98. doi: 10.1016/j.quageo.2014.03.002
- Fuller, B. T., Fuller, J. L., Harris, D. A., and Hedges, R. E. M. (2006). Detection of breastfeeding and weaning in modern human infants with carbon and nitrogen stable isotope ratios. *Am. J. Phys. Anthropol.* 129, 279–293. doi: 10.1002/ajpa.20249
- Fuller, B. T., Southon, J. R., Fahrni, S. M., Farrell, A. B., Takeuchi, G. T., Nehlich, O., et al. (2020). Pleistocene paleoecology and feeding behavior of terrestrial vertebrates recorded in a pre-LGM asphaltic deposit at rancho La Brea, California. *Palaeogeogr. Palaeoclimatol. Palaeoecol.* 537:109383. doi: 10.1016/j.palaeo.2019.109383
- Haas, S. K., Hayssen, B., and Krausman, P. R. (2005). *Panthera leo*. *Mamm. Species* 762, 1–11. doi: 10.1644/1545-1410(2005)762[0001:PL]2.0.CO;2
- Hedges, R. E. (2003). On bone collagen—apatite-carbonate isotopic relationships. *Int. J. Osteoarchaeol.* 13, 66–79. doi: 10.1002/oa.660
- Hedges, R. E., Clement, J. G., Thomas, C. D., and O'Connell, T. C. (2007). Collagen turnover in the adult femoral mid-shaft: modelled from anthropogenic radiocarbon tracer measurements. *Am. J. Phys. Anthropol.* 133, 808–816. doi: 10.1002/ajpa.20598
- Helfman, P. M., and Bada, J. L. (1976). Aspartic acid racemisation in dentine as a measure of ageing. *Nature* 262, 279–281. doi: 10.1038/262279b0
- Jenkins, S. G., Partridge, S. T., Stephenson, T. R., Farley, S. D., and Robbins, C. T. (2001). Nitrogen and carbon isotope fractionation between mothers, neonates, and nursing offspring. *Oecologia* 129, 336–341. doi: 10.1007/s004420100755
- Jones, D. B., and DeSantis, L. R. G. (2017). Dietary ecology of ungulates from the La Brea tar pits in southern California: a multi-proxy approach. *Palaeogeogr. Palaeoclimatol. Palaeoecol.* 466, 110–127. doi: 10.1016/j.palaeo.2016.11.019
- Keeling, C. D. (1979). The Suess effect: 13Carbon-14Carbon interrelations. *Environ. Int.* 2, 229–300. doi: 10.1016/0160-4120(79)90005-9
- Keeling, C. D., Mook, W. G., and Tans, P. P. (1979). Recent trends in the 13C/12C ratio of atmospheric carbon dioxide. *Nature* 277, 121–123. doi: 10.1038/277121a0
- Kellner, C. M., and Schoeninger, M. J. (2007). A simple carbon isotope model for reconstructing prehistoric human diet. *Am. J. Phys. Anthropol.* 133, 1112–1127. doi: 10.1002/ajpa.20618

- Kendall, C., Eriksen, A. M., Kontopoulos, I., Collins, M. J., and Gordon, T.-W. (2018). Diagenesis of archaeological bone and tooth. *Palaeogeogr. Palaeoclimatol. Palaeoecol.* 491, 21–37. doi: 10.1016/j.palaeo.2017.11.041
- Koch, P. L. (2007). "Isotopic study of the biology of modern and fossil vertebrates," in *Stable isotopes in ecology and environmental science*. eds. R. Michener and K. Lajtha. Second ed (Malden, MA: Blackwell), 99–154.
- Koch, P. L., Tuross, N., and Fogel, M. L. (1997). The effects of sample treatment and diagenesis on the isotopic integrity of carbonate in biogenic hydroxylapatite. *J. Archaeol. Sci.* 24, 417–429. doi: 10.1006/jasc.1996.0126
- Krueger, H. W., and Sullivan, C. H. (1984). "Models for carbon isotope fractionation between diet and bone," in *Stable isotopes in nutrition. ACS symposium series 258*. eds. J. F. Turnland and P. E. Johnson (Washington D.C: American Chemical Society), 205–222.
- Lee-Thorp, J. A. (2008). On isotopes and old bones. *Archaeometry* 50, 925–950. doi: 10.1111/j.1475-4754.2008.00441.x
- Lee-Thorp, J. A., Sealy, J. C., and van der Merwe, N. J. (1989). Stable carbon isotope ratio differences between bone collagen and bone apatite, and their relationship to diet. *J. Archaeol. Sci.* 16, 585–599. doi: 10.1016/0305-4403(89)90024-1
- Lester, T., Czarnecki-Maulden, G., and Lewis, D. (1999). Cats increase fatty acid oxidation when isocalorically fed meat-based diets with increasing fat content. *Regul. Integr. Physiol.* 277, R878–R886. doi: 10.1152/ajpregu.1999.277.3.R878
- Levin, N. E., Cerling, T. E., Passey, B. H., Harris, J. M., and Ehleringer, J. R. (2006). A stable isotope aridity index for terrestrial environments. *Proc. Natl. Acad. Sci.* 103, 11201–11205. doi: 10.1073/pnas.0604719103
- MacFadden, B. J., DeSantis, L. R. G., Hochstein, J. L., and Kamenov, G. D. (2010). Physical properties, geochemistry, and diagenesis of xenarthran teeth: prospects for interpreting the paleoecology of extinct species. *Palaeogeogr. Palaeoclimatol. Palaeoecol.* 291, 180–189. doi: 10.1016/j.palaeo.2010.02.021
- Mariotti, A. (1983). Atmospheric nitrogen is a reliable standard for natural ^{15}N measurements. *Nature* 303, 685–687. doi: 10.1038/303685a0
- McHorse, B. K., Orcutt, J. D., and Davis, E. B. (2012). The carnivore fauna of rancho La Brea: average or aberrant? *Palaeogeogr. Palaeoclimatol. Palaeoecol.* 329–330, 118–123. doi: 10.1016/j.palaeo.2012.02.022
- Meachen, J. A., and Samuels, J. X. (2012). Evolution in coyotes (*Canis latrans*) in response to the megafaunal extinctions. *Proc. Natl. Acad. Sci. U.S.A.* 109, 4191–4196. doi: 10.1073/pnas.1113788109
- Mech, L. D. (1974). *Canis lupus*. *Mamm. Species* 37, 1–6. doi: 10.2307/3503924
- Merriam, J. C., and Stock, C. (1932). *The Felidae of rancho la Brea*. No. 422. Carnegie Institute, Washington.
- Murphy, B. P., Bowman, D. M. J. S., and Gagan, M. K. (2007). Sources of carbon isotope variation in kangaroo bone collagen and tooth enamel. *Geochim. Cosmochim. Acta* 71, 3847–3858. doi: 10.1016/j.gca.2007.05.012
- Nowak, R. M., and Walker, E. P. (1999). *Walker's mammals of the world* Baltimore, MD: John Hopkins University Press.
- O'Keefe, F. R., Fet, E. V., and Harris, J. M. (2009). Compilation, calibration, and synthesis of faunal and floral radiocarbon dates, Rancho La Brea, California. *Cont. Sci.* 518, 1–16. doi: 10.5962/p.226783
- O'Connell, T. C., and Hedges, R. E. M. (2017). Chicken and egg: testing the carbon isotopic effects of carnivory and herbivory. *Archaeometry* 59, 302–315. doi: 10.1111/arc.12253
- Passey, B. H., Robinson, T. F., Ayliffe, L. K., Cerling, T. E., Sponheimer, M., Dearing, M. D., et al. (2005). Carbon isotope fractionation between diet, breath CO_2 , and bioapatite in different mammals. *J. Archaeol. Sci.* 32, 1459–1470. doi: 10.1016/j.jas.2005.03.015
- Ramsay, M. A., and Hobson, K. A. (1991). Polar bears make little use of terrestrial food webs: evidence from stable-carbon isotope analysis. *Oecologia* 86, 598–600. doi: 10.1007/BF00318328
- Richards, M. P., Mays, S., and Fuller, B. T. (2002). Stable carbon and nitrogen isotope values of bone and teeth reflect weaning age at the Medieval Wharram Percy site, Yorkshire, UK. *Am. J. Phys. Anthropol.* 119, 205–210. doi: 10.1002/ajpa.10124
- Rule, D. C., Broughton, K. S., Shellito, S. M., and Maiorano, G. (2002). Comparison of muscle fatty acid profiles and cholesterol concentrations of bison, beef cattle, elk, and chicken. *J. Anim. Sci.* 80, 1202–1211. doi: 10.2527/2002.8051202x
- Samuels, J. X., Meachen, J. A., and Sakai, S. A. (2013). Postcranial morphology and the locomotor habits of living and extinct carnivores. *J. Morphol.* 274, 121–146. doi: 10.1002/jmor.20077
- Schaller, G. B. 1972. *The Serengeti lion, a study of predator-prey relationships*. Chicago: University of Chicago Press.
- Schoeninger, M. J., DeNiro, M. J., and Tauber, H. (1983). Stable nitrogen isotope ratios of bone collagen reflect marine and terrestrial components of prehistoric human diet. *Science* 220, 1381–1383. doi: 10.1126/science.6344217
- Secord, R., Bloch, J. I., Chester, S. G., Boyer, D. M., Wood, A. R., Wing, S. L., et al. (2012). Evolution of the earliest horses driven by climate change in the Paleocene-Eocene thermal maximum. *Science* 335, 959–962. doi: 10.1126/science.1213859
- Smith, F. A., Elliott Smith, E. A., Villaseñor, A., Tomé, C. P., Lyons, S. K., and Newsome, S. D. (2022). Late Pleistocene megafauna extinction leads to missing pieces of ecological space in a north American mammal community. *Proc. Natl. Acad. Sci.* 119:e2115015119. doi: 10.1073/pnas.2115015119
- Stock, C., and Harris, J. M. 1992. *Rancho La Brea: A record of Pleistocene life in California Los Angeles: Natural History Museum of Los Angeles*. Natural History Museum of Los Angeles County, Los Angeles.
- Teruel, J. D., Alcolea, A., Hernández, A., and Ruiz, A. J. O. (2015). Comparison of chemical composition of enamel and dentine in human, bovine, porcine and ovine teeth. *Arch. Oral Biol.* 60, 768–775. doi: 10.1016/j.archoralbio.2015.01.014
- Tieszen, L. L., Boutton, T. W., Tesdahl, K. G., and Slade, N. A. (1983). Fractionation and turnover of stable carbon isotopes in animal tissues: implications for $\delta^{13}\text{C}$ analysis of diet. *Oecologia* 57, 32–37. doi: 10.1007/BF00379558
- Tsutaya, T., and Yoneda, M. (2015). Reconstruction of breastfeeding and weaning practices using stable isotope and trace element analyses: a review. *Am. J. Phys. Anthropol.* 156, 2–21. doi: 10.1002/ajpa.22657
- Tung, T. A., Dillehay, T. D., Feranec, R. S., and DeSantis, L. R. G. (2020). Early specialized maritime and maize economies of the north coast of Peru. *Proc. Natl. Acad. Sci. U.S.A.* 117, 32308–32319. doi: 10.1073/pnas.2009121117
- Tung, T. A., Miller, M., DeSantis, L., Sharp, E. A., and Kelly, J. (2016). "Patterns of violence and diet among children during a time of imperial decline and climate change in the ancient Peruvian Andes," in *The archaeology of food and warfare*, eds. E. Amber, M. VanDerwarker and G. D. Wilson (Cham, Switzerland: Springer), 193–228.
- Van Valkenburgh, B. (1991). Iterative evolution of hypercarnivory in canids (Mammalia: Carnivora): evolutionary interactions among sympatric predators. *Paleobiology* 17, 340–362. doi: 10.1017/S0094837300010691
- Van Valkenburgh, B., Clementz, M. T., and Ben-David, M. (2020). Problems with inferring a lack of competition between rancho La Brea dire wolves and sabertooth cats based on dental enamel. *Curr. Biol.* 30, R149–R150. doi: 10.1016/j.cub.2020.01.009
- Van Valkenburgh, B., and Hertel, F. (1993). Tough times at La Brea: tooth breakage in large carnivores of the late Pleistocene. *Science* 261, 456–459. doi: 10.1126/science.261.5120.456
- Wang, Y., and Cerling, T. E. (1994). A model of fossil tooth and bone diagenesis: implications for paleodiet reconstruction from stable isotopes. *Palaeogeogr. Palaeoclimatol. Palaeoecol.* 107, 281–289. doi: 10.1016/0031-0182(94)90100-7
- Wopenka, B., and Pasteris, J. D. (2005). A mineralogical perspective on the apatite in bone. *Mater. Sci. Eng. C* 25, 131–143. doi: 10.1016/j.msec.2005.01.008
- Wysocki, M. A., Feranec, R. S., Tseng, Z. J., and Björnsson, C. S. (2015). Using a novel absolute ontogenetic age determination technique to calculate the timing of tooth eruption in the saber-toothed cat, *Smilodon fatalis*. *PLoS One* 10:e0129847. doi: 10.1371/journal.pone.0129847



OPEN ACCESS

EDITED BY

Maciej Tomasz Krajcarz,
Institute of Geological Sciences (PAN),
Poland

REVIEWED BY

Paweł Dąbrowski,
Wrocław Medical University,
Poland
Yuichi Naito,
Central Research Institute of
Electric Power Industry (CRIEPI),
Japan

*CORRESPONDENCE

Almudena Estalrich
✉ aestalrichalbo@gmail.com

[†]These authors have contributed equally to this work

SPECIALTY SECTION

This article was submitted to
Paleoecology,
a section of the journal
Frontiers in Ecology and Evolution

RECEIVED 11 October 2022

ACCEPTED 05 December 2022

PUBLISHED 23 December 2022

CITATION

Estalrich A and Krueger KL (2022)
Behavioral strategies of prehistoric and
historic children from dental microwear
texture analysis.
Front. Ecol. Evol. 10:1066680.
doi: 10.3389/fevo.2022.1066680

COPYRIGHT

© 2022 Estalrich and Krueger. This is an
open-access article distributed under the
terms of the [Creative Commons Attribution
License \(CC BY\)](#). The use, distribution or
reproduction in other forums is permitted,
provided the original author(s) and the
copyright owner(s) are credited and that
the original publication in this journal is
cited, in accordance with accepted
academic practice. No use, distribution or
reproduction is permitted which does not
comply with these terms.

Behavioral strategies of prehistoric and historic children from dental microwear texture analysis

Almudena Estalrich^{1,2*†} and Kristin L. Krueger^{3†}

¹Grupo de I+D+i EVOADAPTA (Evolución Humana y Adaptaciones Económicas y Ecológicas durante la Prehistoria), Departamento Ciencias Históricas, Universidad de Cantabria, Santander, Spain, ²Ungar Lab, Department of Anthropology, University of Arkansas, Fayetteville, AR, United States, ³Department of Anthropology, Loyola University Chicago, Chicago, IL, United States

Introduction: Reconstructing the dietary and behavioral strategies of our hominin ancestors is crucial to understanding their evolution, adaptation, and overall way of life. Teeth in general, and dental microwear specifically, provide a means to examine these strategies, with posterior teeth well positioned to tell us about diet, and anterior teeth helping us examine non-dietary tooth-use behaviors. Past research predominantly focused on strategies of adult individuals, leaving us to wonder the role children may have played in the community at large. Here we begin to address this by analyzing prehistoric and historic children through dental microwear texture analysis of deciduous anterior teeth.

Materials and Methods: Four sample groups were used: Neandertals ($N=8$), early modern humans ($N=14$), historic Egyptians from Amarna ($N=19$) and historic high-Arctic Inuit from Point Hope, Alaska ($N=6$). Anterior deciduous teeth were carefully cleaned, molded, and cast with high-resolution materials. Labial surfaces were scanned for dental microwear textures using two white-light confocal microscopes at the University of Arkansas, and a soft filter applied to facilitate data comparisons.

Results and Discussion: Results show that dental microwear texture analysis successfully differentiated the samples by all texture variables examined (anisotropy, complexity, scale of maximum complexity, and two variants of heterogeneity). Interestingly, the Neandertal and Point Hope children had similar mean values across all the texture variables, and both groups were significantly different from the Amarna, Egyptian children. These differences suggest diversity in abrasive load exposure and participation in non-dietary anterior tooth-use behaviors. Further analyses and an expanded sample size will help to strengthen the data presented here, but our results show that some prehistoric and historic children took part in similar behaviors as their adult counterparts.

KEYWORDS

labial surface, deciduous enamel, dietary reconstruction, prehistoric children, historic populations, Neandertal

1. Introduction

Dental microwear texture analysis (DMTA) is widely recognized as a useful method to highlight differences in both dietary and behavioral strategies of fossil and modern hominins (Scott et al., 2005, 2006; Ungar et al., 2008, 2010, 2012; El Zaatari, 2010; Krueger and Ungar, 2010, 2012; El Zaatari et al., 2011; Estalrich et al., 2017). While molar microwear have demonstrated to be especially valuable as a dietary proxy (e.g., Scott et al., 2005; El Zaatari, 2007; Ungar et al., 2008, 2010), incisor microwear texture analyses are useful in understanding behavioral and dietary strategies, as well as abrasive load exposure (Krueger, 2006; Krueger and Ungar, 2010, 2012).

The majority of dental microwear research has focused on adult individuals using permanent enamel. Only a few examples have examined children and their deciduous dentition (Bullington, 1991; Toussaint et al., 2010; Hlusko et al., 2013; El Zaatari et al., 2014; Mahoney et al., 2016; Bas et al., 2020; Kelly et al., 2020). Examinations of children's diet and behavior are usually limited to weaning and other types of dietary stress, as shown by skeletal indicators of malnutrition, dental enamel defects, and other feeding-practice studies (Skinner, 1997; Lewis, 2007; Prowse et al., 2008; Clement and Freyne, 2012). Even basic dental microwear analyses in children are limited and are then only used for age estimation or social status purposes (Lewis, 2007; Dawson and Brown, 2013). Why is this the case?

The first difference is the number of teeth, with fewer deciduous than permanent teeth. This is important when considering available sample sizes between child and adult remains. Another distinction is the composition of deciduous and permanent enamel. Deciduous enamel is not only less mineralized than permanent enamel (92% vs. 96%), but also has a higher water content (De Menezes Oliveira et al., 2010). These composition variations make deciduous enamel softer. Moreover, the mean thickness of deciduous enamel is less than half that of its permanent counterpart (1.14 mm vs. 2.58 mm, De Menezes Oliveira et al., 2010). Collectively, these differences cause greater susceptibility to fracture, chipping, and wear in deciduous teeth. Add the limited sample size to these other differences, and it is unsurprising that research has focused on the dietary and behavior reconstruction of adult individuals.

However, there is another important reason dietary and behavioral reconstructions have favored adults and their permanent teeth: the under-representation of children in the archaeological and paleoanthropological record. This is due not only to the lower mortality rates in children, but also to taphonomic processes, which affect the preservation of fragile sub-adult bones and teeth (Lewis, 2007; McFadden et al., 2021). For example, a child's body skeletonizes faster, becomes readily disarticulated, and the smaller size makes them more attractive to scavengers, allowing for dispersal of body parts (Lewis, 2007). Due to these phenomena, analyses of sub-adult bones and teeth are not as common as in adult individuals, and are limited to those specific, unique sites where children are present, and preservation is exceptional.

Challenges in studying deciduous teeth (and children in general) exist; however, there is evidence that significant information can be gleaned from what is preserved in the archaeological and fossil record. For example, a recent study on the anterior tooth-use behavior of Paleolithic children (Estalrich and Marín-Arroyo, 2021) revealed comparable behavioral patterns as their adult counterparts, despite these known differences between the deciduous and permanent enamel. These data, along with those demonstrating the efficacy of microwear textures in differentiating hominin anterior tooth-use behaviors in different ecological zones (Krueger et al., 2017, 2019), show we need to push the boundaries of what we know – or thought we could know – about children in the past. The goal of this paper is to present and analyze the largest microwear texture dataset of deciduous anterior teeth of both fossil (Neandertals and early modern humans) and recent individuals (Amarna Egyptians and Point Hope Inuit), and, ultimately, to better recognize the role these children played in daily life.

2. Materials and methods

2.1. Materials

Statistical analyses have previously indicated that microwear textures do not differ significantly across anterior permanent dentition (Krueger et al., 2017). Thus, we included all anterior tooth types to maximize the sample. We analyzed a sample of 47 deciduous incisor and canine teeth, including, based on their cultural context, Neandertal ($N = 8$); early modern humans ($N = 14$), and recent modern humans from the historic Egyptians from Amarna ($N = 19$), and historic high-Arctic Inuit from Point Hope, Alaska ($N = 6$). [Supplementary Table S1](#) provides details of the studied samples. All the samples studied here are samples curated at different museums, and each museum complies with the ethical issues addressed by each country. By us accessing those samples in order to make the molds and the study, we signed and agreed to follow the required ethical issues.

2.2. Dental microwear texture analysis

The high-resolution replicas were used for analysis of both the fossil and recent human comparative samples. All molds and casts were prepared following standard microwear analysis protocols (Bromage, 1987; Teaford and Oyen, 1989). The labial surface of each specimen was gently cleaned with acetone using cotton swabs. President Jet regular body polysiloxane (Coltene-Whaledent) and Epotek 301 epoxy base and hardener (Epoxy Technologies) were used as the mediums for mold and cast production, respectively. Each tooth was examined for antemortem microwear on the labial surface, next to the incisal edge, using a Sensofar Plμ white-light confocal profiler, *Connie* (Solarius Development Inc., Sunnyvale, California) and Sensofar Plμ Neox confocal profiler, *Wall-e*,

(Sensofar, Barcelona, Spain) both found at the Department of Anthropology of the University of Arkansas in Fayetteville.

With the Sensofar Plμ white-light confocal profiler four adjacent scans of the enamel surface were taken using a 100x objective lens, yielding a lateral point spacing of 0.18 mm and individual fields of view of $138 \times 102 \mu\text{m}$, following Scott et al. (2006). We also used Sensofar Plμ Neox confocal profiler in white-light mode with a 100x objective to analyze some specimens. A stitched point cloud of $242 \times 181 \mu\text{m}$ with a lateral spacing of $0.17 \mu\text{m}$ and a published vertical resolution $<1 \text{ nm}$ was obtained for each surface.

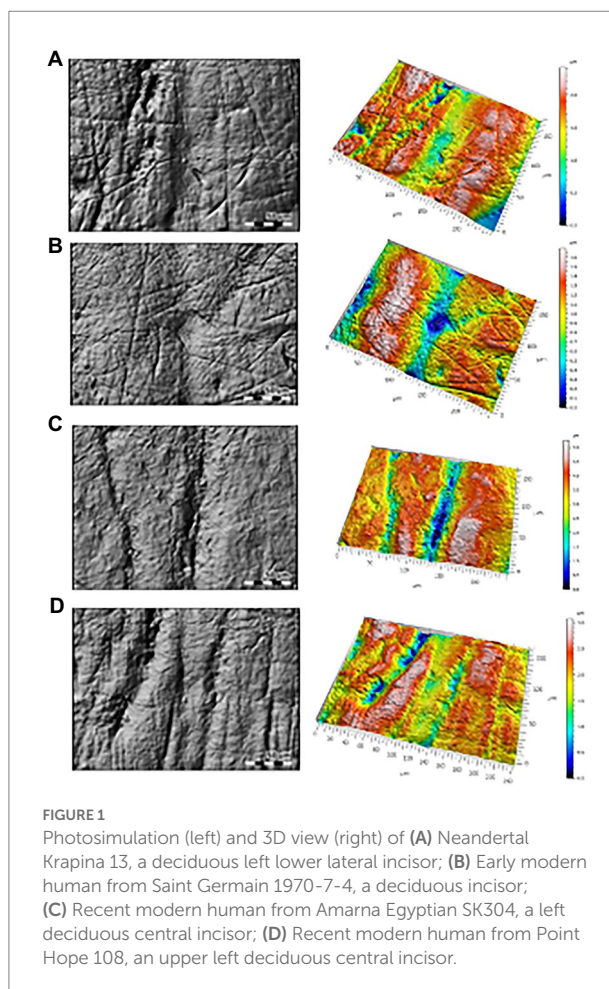
Data from each specimen were then imported to MountainsMap software version 8 (DigitalSurf, Besançon, France), where the scans were processed and calibrated applying the soft filter (Arman et al., 2016) to ensure a standard data collection across different profilers. After this, the scale-sensitive fractal variables were calculated with the same software. Briefly, the variables considered are complexity, scale of maximum complexity, anisotropy, and two variants of heterogeneity (Scott et al., 2006). Complexity or area-scale fractal complexity ($Asfc$) measures the change in surface roughness at different scales. Scale of maximum complexity (Smc) measures the fine scale limit of the steepest part of the curve described for the $Asfc$ measure. Surfaces dominated by large features on a microscopic scale would have a high Smc . Anisotropy ($epLsar$) measures the degree of directionality in surface roughness at a fine scale. Heterogeneity of area-scale fractal complexity ($HAsfc$) reflects variability of complexity across the surface. More heterogeneous surfaces will have higher values. Two forms of this variable are used here: $HAsfc_{3 \times 3}$ ($HAsfc_9$) and $HAsfc_{9 \times 9}$ ($HAsfc_{81}$).

2.3. Statistical analyses

Independent-Samples Kruskal-Wallis tests were completed with the four groups (Neandertal, early modern humans, and recent modern humans from Amarna Egyptians, and Point Hope Inuit) as independent variables and microwear texture variables ($epLsar$, $Asfc$, Smc , $HAsfc_9$ and $HAsfc_{81}$) as dependent. Non-parametric pairwise comparisons to find sources of significant differences in the Kruskal-Wallis tests were then completed. Significance values have been adjusted by the Bonferroni correction for multiple comparisons tests in Supplementary Tables S5a–e. These non-parametric tests were selected as they do not assume normality, are less sensitive to outliers, and appropriate given our limited sample sizes (G. Matthews, pers. comm.). It is important to note we found the same results with both parametric and non-parametric tests.

3. Results

Photosimulations of the occlusal surfaces of selected teeth are shown in Figure 1. Kruskal-Wallis and pairwise comparisons are represented visually in Figure 2. Descriptive statistics for each group are provided in Table 1. Individual microwear texture values are provided in Supplementary Table S2, as well as the test for



normality of the microwear data (Supplementary Table S3), Kruskal–Wallis results (Supplementary Table S4), and pairwise comparisons (Supplementary Tables S5a–e).

Tests for normality were completed, and except for anisotropy, the microwear texture data were not normally distributed (Supplementary Table S3). As a result, nonparametric tests were used. The Independent-Samples Kruskal–Wallis tests found statistically significant differences at the 0.05 level among the groups in all five microwear texture variables (Figure 2; Supplementary Table S4).

In every microwear texture variable analyzed here, the Neandertal and Point Hope children were significantly different from their Amarna counterparts (Figure 2; Supplementary Tables S5a–S5e).

4. Discussion and conclusions

This study examined a large sample of prehistoric and historic deciduous teeth to better understand the role children played within society. Were children behaving like their adult counterparts? If so, can we glean what those teeth-as-tools behaviors could have been? If not, at what age were they expected to contribute to the community at large? While this study has answered some of these questions, we also need to continue searching for more evidence.

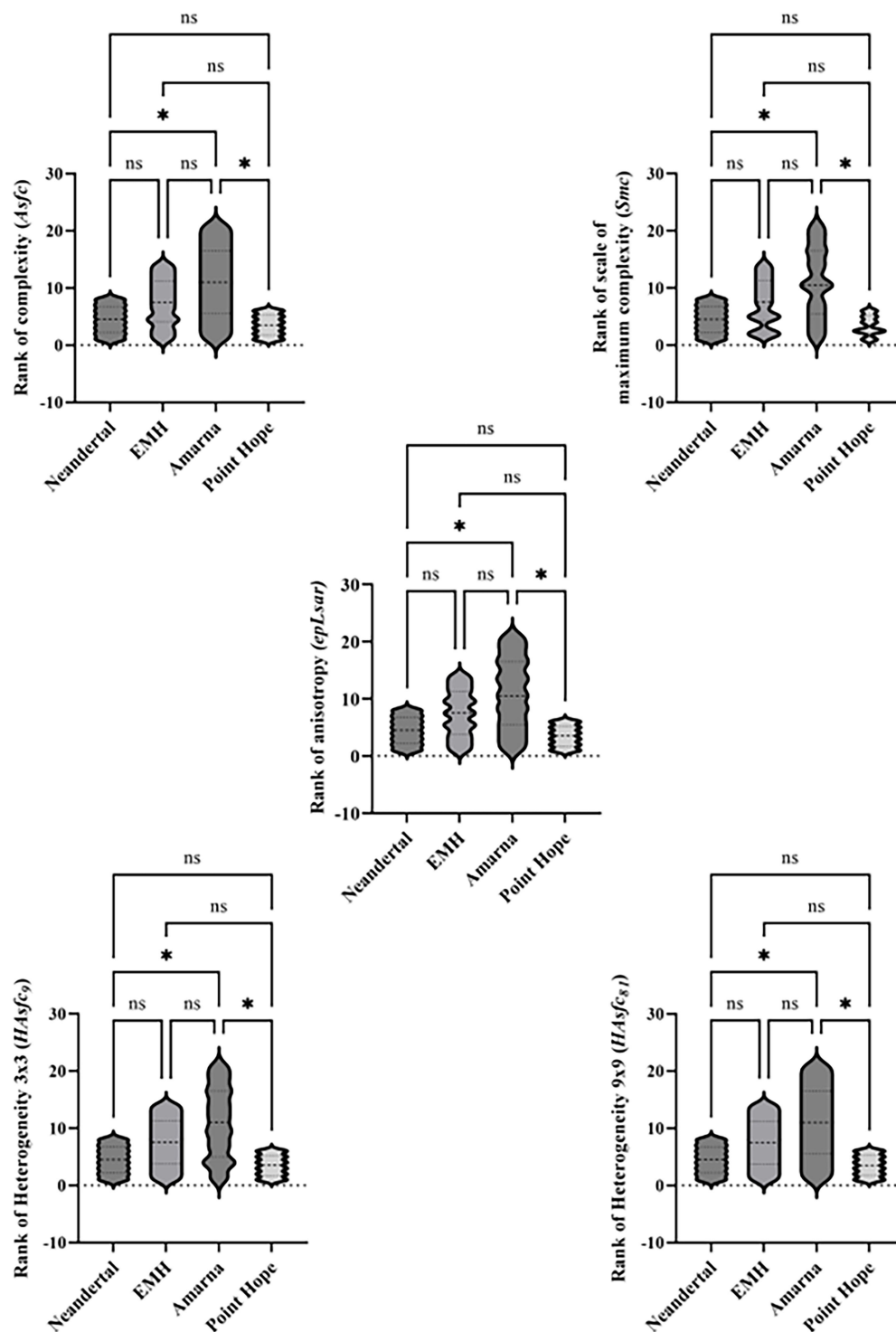


FIGURE 2

Violin plots with pairwise comparisons of ranked microwear data by variable. Two dotted lines and one single dashed line within each violin plot represent quartiles and median, respectively. *=significant difference and ns=no significant difference between the two groups.

The samples studied here include Neandertal and early modern human children from various sites and a wider time range, whereas the historic Point Hope and Amarna samples are from the same site and time (see [Supplementary Table S1](#)). We would expect more variability within the fossil microwear

values, as they are geographically and temporally distinct. Interestingly, our data show that when analyzing these groups, every dental microwear texture variable used here distinguish the Neandertal and Point Hope children from those of the Amarna Egyptians.

TABLE 1 Summary descriptive statistics for the groups studied.

Group	epLsar	Asfc Median	Smc	HAsfc9	HAsfc81
NEAN MEAN	0.017775	2.1725	124.5487	0.4588	0.8988
NEAN SD	0.0010634	1.63835	198.82129	0.30334	0.42273
EMH MEAN	0.017186	1.4479	11.5193	0.4029	0.8164
EMH SD	0.0004944	0.86935	19.44259	0.20838	0.8091
AMARNA MEAN	0.016952	3.2281	8.2043	0.4686	0.8819
AMARNA SD	0.0010755	3.61266	4.10336	0.23627	0.33603
POINT HOPE MEAN	0.016967	1.5833	6.5483	0.3967	0.7417
PONT HOPE SD	0.0019086	0.73666	3.35328	0.16.269	0.23819

This certainly is not the first time that Neandertal and high-Arctic aboriginal samples have been [El Zaatari et al., 2011](#). Indeed, decades of research, especially regarding anterior tooth-use behaviors, heavily associated Neandertals and their unique anterior tooth wear patterns with Arctic groups who used their anterior teeth as a clamp or third hand during animal hide processing ([Brace, 1967, 1975, 1979](#); [Brace and Molnar, 1967](#); [Ryan, 1980](#); [Brace et al., 1981](#)). However, all these analyses focus on adult individuals. This is the first that links similar microwear textures between Neandertal and high-Arctic children. This suggests that the Neandertal and Point Hope Inuit children, at least those sampled here, were completing similar anterior tooth-use behaviors. Whether that means they were eating similar dietary items, had similar abrasive loads, and/or were completing tooth-use behaviors requires a deeper look at the values.

The microwear texture values presented here were collected using two different white-light confocal profilers, and a filter was applied to make these data comparable ([Arman et al., 2016](#)); however, we have not applied that filter to other published microwear texture datasets. Even if we did, there are limited available datasets of deciduous teeth from which to make comparisons. A confounding issue is understanding if microwear forms similarly or differently between permanent and deciduous enamel, as studies have found conflicting results ([Krueger, 2016](#); [Mahoney et al., 2016](#); [Kelly et al., 2020](#)). Therefore, our interpretations should be viewed with caution, and seen as preliminary until these issues are resolved.

Largely viewed within the realm of “hunter-gatherers,” Neandertals relied on a mixed diet and were highly dependent on the ecogeographic setting in which they lived ([El Zaatari et al., 2011](#); [Fiorenza et al., 2011](#)). It is parsimonious to assume that their children relied on a similar diet and were also constrained by their environment. Indeed, stable isotope research of prehistoric juveniles in California suggests some were foraging independently, in addition to parent-provided resources, especially during high-stress times associated with social or climate change ([Greenwald et al., 2016](#); [Fournier et al., 2022](#)). It is not unreasonable to assume that Neandertal children were subsisting on similar diets as their adult counterparts, and perhaps were even able to forage independently when the need arose.

Neandertal adults were found to perform different non-dietary anterior tooth-use behaviors based on their habitat ([Krueger et al., 2017](#)). Using a comparative approach, it was found that Neandertals

in cold, open environments had similar microwear textures to high-Arctic Alaskan aboriginal groups who used their anterior teeth in clamping and grasping behaviors related to animal hide preparation for clothing production. Other Neandertals in more mixed environments were using their anterior teeth for other behaviors, such as wood softening or cordage production ([Krueger et al., 2017](#)). Interestingly, a preliminary study of Pleistocene deciduous teeth from northern Spain indicated they too showed the characteristic dental wear features associated to para-masticatory or cultural-related dental wear, including toothpick use ([Estalrich and Marin-Arroyo, 2021](#)). When previous analyses on diet and tooth-use behaviors are considered, they suggest that Neandertal adults and children were subsisting on similar dietary and behavioral strategies that are heavily influenced by their eco-geographic setting.

The Point Hope Inuit were also considered “hunter-gatherers,” and their diet largely consisted of land and sea mammals (especially caribou, whale, walrus, and seal), fish, and edible plants ([Larsen and Rainey, 1948](#); [Lester and Shapiro, 1968](#); [Dabbs, 2009](#); [Brubaker et al., 2010](#); [El Zaatari, 2014](#)). They took part in non-dietary anterior tooth-use behaviors in the form of wood softening, clamping and grasping tasks related to hide preparation, and sinew cord production, and were, at times, subjected to high abrasive loads ([Burch, 1981](#); [Foote, 1992](#)). Some of these individuals lived seasonally at Point Hope, while others lived there year-round, which is located 125 miles north of the Arctic Circle ([Larsen and Rainey, 1948](#); [Dabbs, 2009](#)).

On the other hand, the Amarna Egyptians were not “hunter-gatherers,” but were excavated from the non-elite South Tombs Cemetery and date from 3,300 to 3,280 BP ([Rose, 2006](#)). This cemetery is composed of an estimated 5,000 individuals from different occupations and/or socio-economic positions but did not hold elite or royal status ([Dabbs et al., 2015](#)). The excavated individuals showed high rates of subadult death, workload stress, trauma, and nutritional deficiencies ([Rose and Zabecki, 2009](#); [Dabbs et al., 2015](#)). Adult microwear analysis suggests this sample was reliant on tough food, most likely bread, and the desert environment at Amarna would make sand a likely adherent abrasive ([Krueger and Scott, in press](#)).

The Neandertal and Point Hope children, both from “hunter-gatherer” groups, had significantly lower complexity (*Asfc*), scale of maximum complexity (*Smc*) and heterogeneity (*HAsfc₉* and *HAsfc₈₁*) than their Amarna counterparts ([Table 1](#), [Supplementary Table S2](#),

Figure 2). While these variables are not often used in texture analyses of anterior teeth, they are useful for molar analyses, especially regarding the fracture properties of foods and abrasive loads. Here, we propose that the significantly lower values of these three variables for the Neandertal and Point Hope Inuit children show differences in abrasive loads from the Amarna children. While the Amarna children were subjected to a desert environment with little-to-no tree cover, their higher values may indicate their increased exposure to diverse types of abrasives that were adherent to their food. On the other hand, the lower values of the Neandertal and Point Hope Inuit children suggest more limited exposure to abrasives, which could be due to their reliance on a mixed diet.

The Neandertal and Point Hope children had significantly lower anisotropy (*epLsar*) than their Amarna counterparts. This variable is more heavily used in anterior tooth texture analyses and indicates the use of these teeth in non-dietary behaviors (e.g., clamping, grasping, tool retouching, etc.; Krueger and Ungar, 2012; Krueger et al., 2017, 2019). These results suggest both Neandertal and Point Hope children were taking part in non-dietary anterior tooth-use behaviors, while the Amarna children were not. While we are hesitant to suggest what specific types of behaviors in which these children may have been engaging, perhaps it was related to clamping and grasping behaviors like those found in their adult counterparts; however, an expanded sample size and comparative datasets are necessary to strengthen this idea.

It is worth noting that no statistically significant differences were found between the early modern human children and neither the Neandertal nor historic modern human counterparts (see Supplementary Tables S5a–S5e). Perhaps this is simply a reflection of our limited sample size, and building this dataset is necessary to recognize potential differences. Or, perhaps this reflects a more diverse diet, abrasive load exposure, or landscape in which these children lived. However, these data provide the largest dataset from which to work in the future, and we look forward to continued analyses to reinforce or refute the ideas posited here.

In conclusion, these datasets provide a crucial pathway to understanding the role children played in the Paleolithic and beyond. Perhaps this is a starting point to investigating complex issues like independent foraging in Paleolithic children, especially considering the stress that climate change may have had on their dietary and behavioral strategies. It also helps us understand how teaching and learning may have transpired between adults and children, especially if the latter are performing non-dietary anterior tooth-use behaviors similar to their adult counterpart. We hope this creates a larger platform for additional analyses surrounding Paleolithic children, so that we may better recognize an entire community's contribution to survival.

Data availability statement

The original contributions presented in the study are included in the article/Supplementary material, further inquiries can be directed to the corresponding author.

Author contributions

AE and KK designed the research, analyzed data, and wrote the manuscript. All authors contributed to the article and approved the submitted version.

Funding

The work was supported by the AE is supported by H2020-MSCA-IF project No. 891529 (3DFOSSILDIET).

Acknowledgments

We are sincerely grateful to Peter S. Ungar for allowing us the use of the microscope facilities at the Department of Anthropology in the University of Arkansas and encouraging discussions on microwear and diet. We also acknowledge Greg Matthews for his advice on statistical analyses and Emily Hallett and Jacopo Cerasoni for their input on data visualization. Thank you to Jean-Jacques Hublin, Manuel R. González Morales, David Frayer, Antonio Rosas, Sireen El Zaatari, F. Igor Gutiérrez Zugasti, Cristina Vega Maeso and Borja González Rabanal for access to some of the fossils sampled here. We thank Barry Kemp and Anna Stevens for permission to mold the Amarna individuals, Museo de Prehistoria y Arqueología de Cantabria (Spain) for permission to mold the El Castillo tooth, and the American Museum of Natural History for permission to mold the Point Hope sample.

Conflict of interest

The authors declare that the research was conducted in the absence of any commercial or financial relationships that could be construed as a potential conflict of interest.

Publisher's note

All claims expressed in this article are solely those of the authors and do not necessarily represent those of their affiliated organizations, or those of the publisher, the editors and the reviewers. Any product that may be evaluated in this article, or claim that may be made by its manufacturer, is not guaranteed or endorsed by the publisher.

Supplementary material

The Supplementary material for this article can be found online at: <https://www.frontiersin.org/articles/10.3389/fevo.2022.1066680/full#supplementary-material>

References

- Arman, S. D., Ungar, P. S., Brown, C. A., DeSantis, L. R. G., Schmidt, C., and Prideaux, G. J. (2016). Minimizing inter-microscope variability in dental microwear texture analysis. *Surf. Topogr. Metrol. Prop.* 4:024007. doi: 10.1088/2051-672X/4/2/024007
- Bas, M., Le Luyer, M., Kanz, F., Rebay-Salisbury, K., Queffelec, A., Souron, A., et al. (2020). Methodological implications of intra- and inter-facet microwear texture variation for human childhood paleo-dietary reconstruction: insights from the deciduous molars of extant and medieval children from France. *J. Archaeol. Sci. Rep.* 31:102284. doi: 10.1016/j.jasrep.2020.102284
- Brace, C. L. (1967). Environment, tooth form and size in the Pleistocene. *J. Dent. Res.* 46, 809–816. doi: 10.1177/00220345670460053501
- Brace, C. L. (1975). Comment on: did La Ferrassie I use his teeth as a tool? *Curr. Anthropol.* 16, 396–397.
- Brace, C. L. (1979). Krapina, “classic” Neanderthals, and the evolution of the European face. *J. Hum. Evol.* 8, 527–550. doi: 10.1016/0047-2484(79)90043-5
- Brace, C. L., and Molnar, S. (1967). Experimental studies in human tooth wear: I. *Am. J. Phys. Anthropol.* 27, 213–221. doi: 10.1002/ajpa.1330270210
- Brace, C. L., Ryan, A. S., and Smith, B. H. (1981). Comment: tooth wear in La Ferrassie man. *Curr. Anthropol.* 22, 426–430.
- Bromage, T. (1987). The scanning electron microscopy replica technique and recent applications to the study of fossil bone. *Scanning Microsc.* 1, 607–613. PMID: 3112936
- Brubaker, M., Berner, J., Bell, J., Warren, J., and Rolin, A. (2010). *Climate Change in Point Hope, Alaska: Strategies for Community Health* ANTHC Center for Climate and Health, 1–40.
- Bullington, J. (1991). Deciduous dental microwear of prehistoric juveniles from the lower Illinois River valley. *Am. J. Phys. Anthropol.* 84, 59–73. doi: 10.1002/ajpa.1330840106
- Burch, E. S. (1981). *The Traditional Eskimo Hunters of Point Hope, Alaska: 1800–1875*. North Slope Borough, Barrow, AK.
- Clement, A. F., and Freyne, A. (2012). A revised method for assessing tooth wear in deciduous dentition. in *Proceedings of the twelfth annual conference of the British Association for Biological Anthropology*, 119–129.
- Dabbs, G. R. (2009). Health and nutrition at prehistoric point Hope, Alaska: Application and critique of the Western hemisphere health index. Ph.D. Dissertation. Fayetteville, AR: University of Arkansas.
- Dabbs, G. R., Rose, J. C., and Zabecki, M. (2015). “The bioarchaeology of Akhenaten: unexpected results from a capital city,” in *Egyptian Bioarchaeology: Humans, Animals, and the Environment*. eds. S. Ikram, J. Kaiser and R. Walker (Leiden: Sidestone Press), 43–52.
- Dawson, H., and Brown, K. R. (2013). Exploring the relationship between dental wear and status in late medieval subadults from England. *Am. J. Phys. Anthropol.* 150, 433–441. doi: 10.1002/ajpa.22221
- De Menezes Oliveira, M. A. H., Torres, C. P., Gomez-Silva, J. M., Chinelatti, M. A., De Menezes, F. C. H., Palma-Dibb, R. G., et al. (2010). Microstructure and mineral composition of dental enamel of permanent and deciduous teeth. *Microsc. Res. Tech.* 73, 572–577. doi: 10.1002/jemt.20796
- El Zaatari, S. (2007). *Ecogeographic variation in Neandertal dietary habits: Evidence from microwear texture analysis*. [Ph.D. Dissertation]. [New York, NY]: Stony Brook University.
- El Zaatari, S. (2010). Occlusal microwear texture analysis and the diets of historical/prehistoric hunter-gatherers. *Int. J. Osteoarchaeol.* 20, 67–87.
- El Zaatari, S. (2014). “The diets of the Ipiutak and Tigara (point Hope, Alaska): evidence from occlusal molar microwear texture analysis,” in *The foragers of point Hope: Bioarchaeology on the edge of the Alaskan Arctic*. eds. C. E. Hilton, B. M. Auerbach and L. W. Cowgill (Cambridge: Cambridge University Press), 120–137. doi: 10.1017/CBO9781139136785.011
- El Zaatari, S., Grine, F. E., Ungar, P. S., and Hublin, J. J. (2011). Ecogeographic variation in Neandertal dietary habits: evidence from occlusal microwear texture analysis. *J. Hum. Evol.* 61, 411–424. doi: 10.1016/j.jhevol.2011.05.004
- El Zaatari, S., Krueger, K. L., and Hublin, J. J. (2014). “Dental microwear texture analysis and the diet of the Scladina child,” in *The Juvenile Neandertal Facial Remains from Scladina cave (Belgium)*. eds. M. Tausant and D. Bonjean (Liège (Belgium): Etudes et Recherches Archeologiques de l’Université de Liège), 363–368.
- Estalrich, A., El Zaatari, S., and Rosas, A. (2017). Dietary reconstruction of the El Sidrón Neandertal familial group (Spain) in the context of other Neandertal and modern hunter-gatherer groups. A molar microwear texture analysis. *J. Hum. Evol.* 104, 13–22. doi: 10.1016/j.jhevol.2016.12.003
- Estalrich, A., and Marin-Arroyo, A. B. (2021). Evidence of habitual behavior from non-alimentary dental wear on deciduous teeth from the middle and upper Paleolithic Cantabrian region, Northern Spain. *J. Hum. Evol.* 158:103057. doi: 10.1016/j.jhevol.2021.103047
- Fiorenza, L., Benazzi, S., Tausch, J., Kullmer, O., Bromage, T. G., and Schrenk, F. (2011). Molar microwear reveals Neandertal eco-geographic dietary variation. *PLoS One* 6:e14769. doi: 10.1371/journal.pone.0014769
- Foot, B. A. (1992). *The Tigara Eskimos and Their Environment*. North Slope Borough, Commission on Inupiat history, Language, and Culture, Point Hope.
- Fournier, N. A., Thornton, E. K., Arellano, M. W., and Leventhal, A. (2022). Stable isotope reconstruction of weaning and childhood diet during times of change: an examination of life history and health of san Francisco Bay Area juveniles. *J. Archaeol. Sci. Rep.* 44:103495
- Greenwald, A. M., Eerkens, J. W., and Bartelink, E. J. (2016). Stable isotope evidence of juvenile foraging in prehistoric Central California. *J. Archaeol. Sci. Rep.* 7, 146–154. doi: 10.1016/j.jasrep.2016.04.003
- Hlusko, L., Carlson, J. P., Guatelli-Steinberg, D., Krueger, K. L., Mersey, B., Ungar, P. S., et al. (2013). Neandertal teeth from Moula-Guercy, Ardèche, France. *Am. J. Phys. Anthropol.* 151, 477–491. doi: 10.1002/ajpa.22291
- Kelly, C. D., Schmidt, C. W., and D’Anastasio, R. (2020). *Dental microwear texture analysis in deciduous teeth*. In: *Dental Wear in Evolutionary and Biocultural Contexts*. 169–186.
- Krueger, K. L. (2006). *Incisal dental microwear of the prehistoric point Hope communities: A dietary and cultural synthesis*. MA Thesis. Kalamazoo, MI: Western Michigan University.
- Krueger, K. L. (2016). Dental microwear texture differences between permanent and deciduous enamel. *Am. J. Phys. Anthropol.* 159 (S62), 196–197.
- Krueger, K. L., and Scott, J. R. (in press). “Dietary and behavioral trends in the south tombs cemetery individuals at Amarna,” in *Amarna: The South Tombs Cemetery*. eds. G. R. Dabbs, J. C. Rose and A. Stevens, Vol. 2 (Egypt Exploration Society: Cairo)
- Krueger, K. L., and Ungar, P. S. (2010). Incisor microwear textures of five bioarchaeological groups. *Int. J. Osteoarchaeol.* 20, 549–560. doi: 10.1002/oa.1093
- Krueger, K. L., and Ungar, P. S. (2012). Anterior dental microwear texture analysis of the Krapina Neandertals. *Cent. Eur. J. Geosci.* 4, 651–662.
- Krueger, K. L., Ungar, P. S., Guatelli-Steinberg, D., Hublin, J.-J., Pérez-Pérez, A., Trinkaus, E., et al. (2017). Anterior dental microwear textures show habitat-driven variability in Neandertal behavior. *J. Hum. Evol.* 105, 13–23. doi: 10.1016/j.jhevol.2017.01.004
- Krueger, K. L., Willman, J. C., Matthews, G. J., Hublin, J. J., and Pérez-Pérez, A. (2019). Anterior tooth-use behaviors among early modern humans and Neandertals. *PLoS One* 14:e0224573. doi: 10.1371/journal.pone.0224573
- Larsen, H., and Rainey, F. (1948). Ipiutak and the Arctic whale hunting culture. *Anthropological Papers of the American Museum of Natural History*, vol. 42, New York: Nabu Press.
- Lester, C. W., and Shapiro, H. L. (1968). Vertebral arch defects in the lumbar vertebrae of pre-historic American Eskimos. *Am. J. Phys. Anthropol.* 28, 43–47. doi: 10.1002/ajpa.1330280113
- Lewis, M. E. (2007). *The bioarchaeology of children*. Cambridge: Cambridge University Press.
- Mahoney, P., Schmidt, C. W., Deter, C., Remy, A., Slavin, P., Johns, S. E., et al. (2016). Deciduous enamel 3D microwear texture analysis as an indicator of childhood diet in medieval Canterbury, England. *J. Archaeol. Sci.* 66, 128–136. doi: 10.1016/j.jas.2016.01.007
- McFadden, C., Muir, B., and Oxenham, M. F. (2021). Determinants of infant mortality and representation in bioarchaeological samples: a review. *Am. J. Bio. Anthropol.* 177, 196–206. doi: 10.1002/ajpa.24406
- Prowse, T. L., Saunders, S. R., Schwarcz, H. P., Garnsey, P., Macchiarelli, R., and Bondioli, L. (2008). Isotopic and dental evidence for infant and young child feeding practices in an imperial roman skeletal sample. *Am. J. Phys. Anthropol.* 137, 294–308. doi: 10.1002/ajpa.20870
- Rose, J. C. (2006). Paleopathology of the commoners at tell Amarna, Egypt, Akhenaten’s capital city. *Mem. Inst. Oswaldo Cruz* 101, 73–76. doi: 10.1590/S0074-02762006001000013
- Rose, J. C., and Zabecki, M. (2009). “The commoners of tell el-Amarna,” in *Beyond the horizon: Studies in Egyptian art, archaeology and history in honour of Barry J. eds. S. Ikram and A. Dodson, Kemp*, vol. 2 (Cairo: Supreme Council of Antiquities Press), 408–422.
- Ryan, A. S. (1980). Anterior dental microwear in hominid evolution: Comparisons with human and nonhuman primates. PhD Dissertation. Ann Arbor (MI): University of Michigan.

- Scott, R. S., Ungar, P. S., Bergstrom, T. S., Brown, C. A., Childs, B. E., Teaford, M. F., et al. (2006). Dental microwear texture analysis: technical considerations. *J. Hum. Evol.* 51, 339–349. doi: 10.1016/j.jhevol.2006.04.006
- Scott, R. S., Ungar, P. S., Bergstrom, T. S., Brown, C. A., Grine, F. E., Teaford, M. F., et al. (2005). Dental microwear texture analysis reflects diets of living primates and fossil hominins. *Nature* 436, 693–695. doi: 10.1038/nature03822
- Skinner, M. (1997). Dental wear in immature late Pleistocene hominines. *J. Archaeol. Sci.* 24, 677–700. doi: 10.1006/jasc.1996.0151
- Teaford, M. F., and Oyen, O. (1989). Live primates and dental replication: new problems and new techniques. *Am. J. Phys. Anthropol.* 80, 73–81. doi: 10.1002/ajpa.1330800109
- Toussaint, M., Olejniczak, A. J., El Zaatari, S., Cattelain, P., and Pirson, S. (2010). The Neandertal lower right deciduous second molar from the “Trou de l’Abime” at Couvin, Belgium. *J. Hum. Evol.* 58, 56–67. doi: 10.1016/j.jhevol.2009.09.006
- Ungar, P. S., Grine, F. E., and Teaford, M. F. (2008). Dental microwear and diet of the PlioPleistocene hominin *Paranthropus boisei*. *PLoS One* 3, 1–6. doi: 10.1371/journal.pone.0002044
- Ungar, P. S., Krueger, K. L., Blumenshine, R. J., Njau, J., and Scott, R. S. (2012). Dental microwear texture analysis of hominins recovered by the Olduvai landscape paleoanthropology project, 1995–2007. *J. Hum. Evol.* 63, 429–437. doi: 10.1016/j.jhevol.2011.04.006
- Ungar, P. S., Scott, R. S., Grine, F. E., and Teaford, M. F. (2010). Molar microwear textures and the diets of *Australopithecus anamensis* and *Australopithecus afarensis*. *Philos. Trans. R. Soc. B* 365, 3345–3354. doi: 10.1098/rstb.2010.0033



OPEN ACCESS

EDITED BY

Eduardo Jiménez-Hidalgo,
University of the Sea, Mexico

REVIEWED BY

Ruth Blasco,
Institut Català de Paleoecologia
Humana i Evolució Social
(IPHES), Spain
Marie-Hélène Moncel,
Director of Research
CNRS-MNHN, France

*CORRESPONDENCE

William Rendu
✉ william.rendu@cnrs.fr
Svetlana Shnaider
✉ sveta.shnayder@gmail.com

SPECIALTY SECTION

This article was submitted to
Paleoecology,
a section of the journal
Frontiers in Ecology and Evolution

RECEIVED 31 October 2022

ACCEPTED 30 November 2022

PUBLISHED 20 January 2023

CITATION

Rendu W, Renou S, Kolasnikova A,
Baumann M, Plisson H, Discamps E,
Soulier M-C, Gicqueau A, Augoyard M,
Bocquel M, Guerin G, Shnaider S and
Kolobova K (2023) Neanderthal
subsistence at Chez-Pinaud Jonzac
(Charente-Maritime, France): A kill site
dominated by reindeer remains, but
with a horse-laden diet?
Front. Ecol. Evol. 10:1085699.
doi: 10.3389/fevo.2022.1085699

COPYRIGHT

© 2023 Rendu, Renou, Kolasnikova,
Baumann, Plisson, Discamps, Soulier,
Gicqueau, Augoyard, Bocquel, Guerin,
Shnaider and Kolobova. This is an
open-access article distributed under
the terms of the [Creative Commons
Attribution License \(CC BY\)](#). The use,
distribution or reproduction in other
forums is permitted, provided the
original author(s) and the copyright
owner(s) are credited and that the
original publication in this journal is
cited, in accordance with accepted
academic practice. No use, distribution
or reproduction is permitted which
does not comply with these terms.

Neanderthal subsistence at Chez-Pinaud Jonzac (Charente-Maritime, France): A kill site dominated by reindeer remains, but with a horse-laden diet?

William Rendu^{1,2*}, Sylvain Renou³, Anastasiia Kolasnikova¹,
Malvina Baumann^{4,5}, Hugues Plisson⁵, Emmanuel Discamps⁶,
Marie-Cécile Soulier⁶, Arthur Gicqueau^{1,6}, Mathilde Augoyard⁵,
Manon Bocquel⁵, Guillaume Guerin⁷, Svetlana Shnaider^{1*} and
Kseniya Kolobova⁸

¹ZooSCAn (IRL 2013) CNRS - IAET SB RAS, Novosibirsk, Russia, ²Institut français d'études sur l'Asie
centrale (IFEAC), UAR3140 (CNRS), Bishkek, Kyrgyzstan, ³HADES, Agence Atlantique, Bordeaux,
France, ⁴TRACEOLAB, University of Liège, Liège, Belgium, ⁵UMR5199 De la Préhistoire A l'actuel
Culture, Environnement et Anthropologie (PACEA), Pessac, Aquitaine, France, ⁶UMR5608 Travaux de
Recherches Archéologiques sur les Cultures, les Espaces et les Sociétés (TRACES), Toulouse,
Midi-Pyrénées, France, ⁷UMR6118 Géosciences Rennes, Rennes, Brittany, France, ⁸Institute of
Archaeology and Ethnography (RAS), Novosibirsk, Novosibirsk Oblast, Russia

During the MIS 4 in Southwestern France, Quina Neanderthal from the north of the Aquitaine was characterized by a hunting specialization on the reindeer and the lack of diversity in their diet. They developed task-specific locations dedicated to the capture, the butchery, and the consumption of reindeer, and the whole society seems, in this region, to be dependent on this food resource. In this context, the site of Chez-Pinaud at Jonzac (France) occupies a specific place. First, interpreted as a reindeer kill and butchery site, the recent recovery of the site underlines the importance of the large ungulate (horse and bison) to the faunal spectrum (30% of the NISP). Considering the quantity of meat and grease that these species can provide to hunters, the new zooarchaeological analyses suggest that at least the horse may have played a major role in the diet of the Neanderthal population. Since Jonzac is one of the largest sites for this period, these results relativize the importance of reindeer specialization of the Quina population and the lack of diversity in their diet.

KEYWORDS

Neanderthal, hunting strategy, zooarchaeology, Middle Paleolithic, site function

Introduction

In the last decades, considerable input on Neanderthal subsistence has been acquired on a particular period of the Middle Paleolithic record, the Quina Mousterian (Discamps and Royer, [Costamagno et al., 2006](#)). In southwestern France, the Quina Mousterian techno-complex, dated from the MIS 4 or early MIS 3 ([Figure 1](#)), is notably characterized by its recurrent association with reindeer hunting ([Discamps and Royer, 2017](#);

[Rendu et al., 2022](#)). In fact, out of the 32 Quina stratigraphic units that yielded sufficiently large faunal assemblages (i.e., with a total NISP of ungulates >100), 28 are dominated by the arctic deer's remains.

The probable abundance of reindeer in the environment during the Quina has been purportedly correlated to the major climatic pejoration of the Heinrich Stadial 6 ([Discamps et al., 2011](#); [Discamps and Royer, 2017](#)). During this period, several indicators also point to a major drop in the ungulate biomass

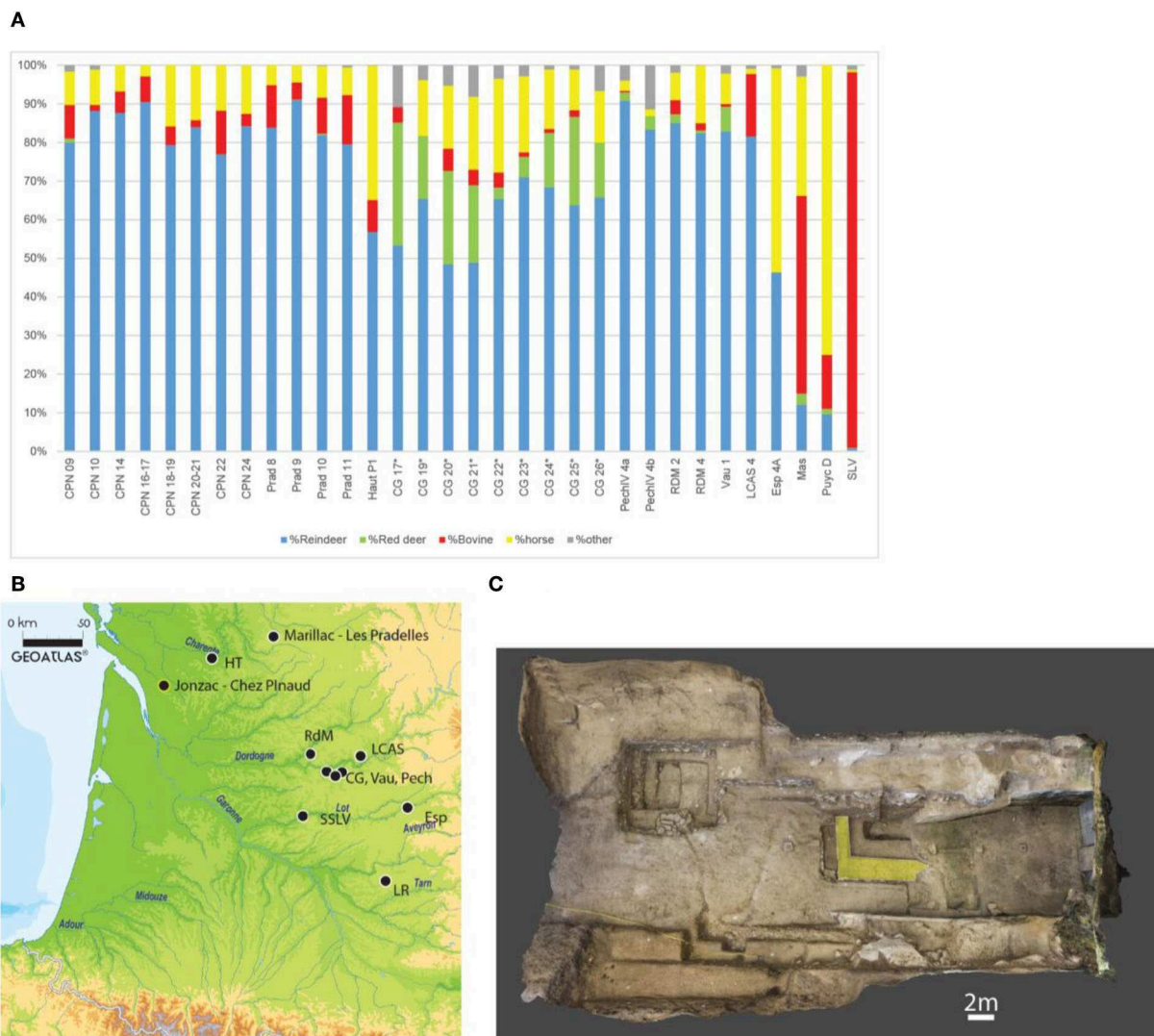


FIGURE 1

(A, B) Distribution of the main Quina sites yielding faunal assemblages in Southwestern France, and contribution of the main prey to the faunal spectra (in %NR; Blue, reindeer; green, red deer; Red, Bison; Yellow, Horse; Gray, other). (A) CG, Combe Grenal ([Laquay, 1981](#); [Guadelli, 1987](#); Vau, Vaufray ([Delpech, 1996](#)); PechIV, Pech de l'Azé IV ([Niven, 2013](#)); RdM, Roc de Marsal ([Castel et al., 2017](#)); LP, Les Pradelles ([Costamagno et al., 2006](#)); CPN, Chez-Pinaud-Jonzac ([Airvaux, 2004](#); [Jaubert et al., 2008b](#); [Niven, 2013](#)); LCAS, La Chapelle-aux-Saints ([Rendu et al., 2014](#)); Haut, Hauteroche ([Paletta, 2005](#)); LR, La Rouquette ([Rendu et al., 2011](#)); SLV, Sous les Vignes ([Turq et al., 1999](#)); ESP, Espagnac ([Jaubert, 2001](#)). Numbers correspond to the different stratigraphic units. For Combe Grenal Reindeer was under-evaluated in the previous excavation due to selective sampling. Derived from [Discamps and Royer, 2017](#). Map from Geoatlas. (C) Orthophotography of the site, extracted from the 3D model. In yellow, the 2019–2021 excavation area.

available for large game hunters (Discamps, 2014). In addition, sedentary prey that was present just before this event was replaced by reindeer, identified as a migratory species at that time (Britton et al., 2011).

This over-representation of reindeer in faunal spectra and the development of different task-specific locations (Binford, 1980) dedicated to subsistence activities [kill and first butchery sites (Niven et al., 2012) and secondary butchery sites (Costamagno et al., 2006)] conducted scholars to propose the strong dependence of Quina groups on reindeer, which would have occupied a central place in the Neanderthal diet at the time (Delagnes and Rendu, 2011; Rendu et al., 2022).

In this model, the Chez-Pinaud site at Jonzac plays a major role along with Les Pradelles (Costamagno et al., 2006), one of the best examples of these task-specific locations dedicated to the exploitation of reindeer herds (Niven et al., 2012; Rendu et al., 2022). We here report on new zooarchaeological data acquired on this key site, concerning notably the importance of reindeer and other prey in Neanderthal diets throughout the Quina period.

Material: The Chez-Pinaud Jonzac site

Excavated between 1999 and 2002 by a team led by Airvaux (Airvaux, 2004), and between 2004 and 2007 by Jaubert, Hublin, et al. (Jaubert et al., 2008a), Chez-Pinaud is situated at the bottom of a 10-m cliff. More than 24 stratigraphic units were identified, eight of them yielding artifacts attributed to the Quina Mousterian (Airvaux, 2004; Jaubert et al., 2008a; Niven et al., 2012).

Among them, Stratigraphic Unit (SU) 22 is a 1-m thick bone bed with excellent preservation of the bones and their spatial distribution (Jaubert et al., 2008a; Niven et al., 2012). During the Jaubert-Hublin excavations (2004–2007), a significant number of anatomical articulations were uncovered identifying “snapshots” on-site, allowing for discussing the carcass processing and the organization of activities within a specialized site dedicated to predation with high resolution (Rendu et al., 2022). Since 2019, the site is under a new excavation program focusing on the US22 bone bed directed by the CNRS, the IAET SB RAS, and Bordeaux University (dir. W. Rendu, K. Kolobova, and S. Shnaider). The excavation area covers a surface of $\sim 8 \text{ m}^2$. We applied the common “decapage” method consisting of removing the sediment over the complete excavated area without moving the artifacts to have a better view of their relative organization. Each decapage is followed by a photogrammetric model of the whole surface using a Canon EOS 600 D. Raw pictures were processed through Agisoft Metashape software to obtain a 3D model of the excavated area. Artifacts (lithics bigger than 1 cm and all the identifiable faunal remains or remains larger than 2 cm) were

then piece-plotted using a Nikon Nivo total station. The different analytical databases were linked to the 3D model using ArcGIS for studying spatial distribution. In total, nine decapages (C1–C9) were realized between 2019 and 2021 by conducting the collection of almost 5,000 faunal remains (including 4% of teeth remains) and 2,000 lithics.

All the faunal remains were identified on the site (with the help of the portable comparative collection), and potential anatomical articulations were looked for by two zooarchaeologists (WR, SR) during the excavation and before any collecting session. Numerous anatomical articulations were identified during the excavations (NR = 46), some of them imply several bones such as a complete reindeer carp in articulation with its radio-ulna and metacarpal (Figure 2).

Zooarchaeological data

Previous zooarchaeological analyses demonstrate that reindeer, which dominate largely the assemblage (>80% of total NISP, Supplementary Table 1), were killed in the direct vicinity of the site and partially processed there before exportation toward a secondary consumption camp (Beauval, 2004; Niven et al., 2012). The 18 individuals, including males, females, and juveniles (based on a dental MNI), present a catastrophic mortality profile. Based on cementum increment analyses, tooth eruption sequences, and fetal bone abundances, the exploitation of the site in winter has been proposed (Niven et al., 2012; Rendu et al., 2022).

However, while the zooarchaeological analyses of the Jaubert and Hublin collection brought significant information about reindeer exploitation, largely used to discuss the Quina diet (Discamps and Royer, 2017; Faivre et al., 2017; Rendu et al., 2022), the exploitation of large ungulates was not described in detail. Throughout, C. Beauval (Beauval, 2004) demonstrated on the large collection of Airvaux excavation (Airvaux, 2004) the fluctuation of the relative contribution of horse and bison through the thickness of US 22.

The exact place of large ungulates in the subsistence of Quina Neanderthals has been left mostly undiscussed. The importance of large ungulates might have been underestimated in previous studies, notably if one considers that their carcasses provide between 3 and 5 times more food than a reindeer carcass. At a regional scale, if we consider that Chez-Pinaud has been a central piece in our perception of the Quina diet, new results could lead us to ponder or even change our perception of the Neanderthal diet and subsistence at the time. Based on the material from the new excavation and our high-resolution control on the field, we propose to evaluate how a better inclusion of large ungulates in zooarchaeological interpretation and horse, in particular, can modify our perception of the use of the Chez-Pinaud site and the diet of the Quina population.

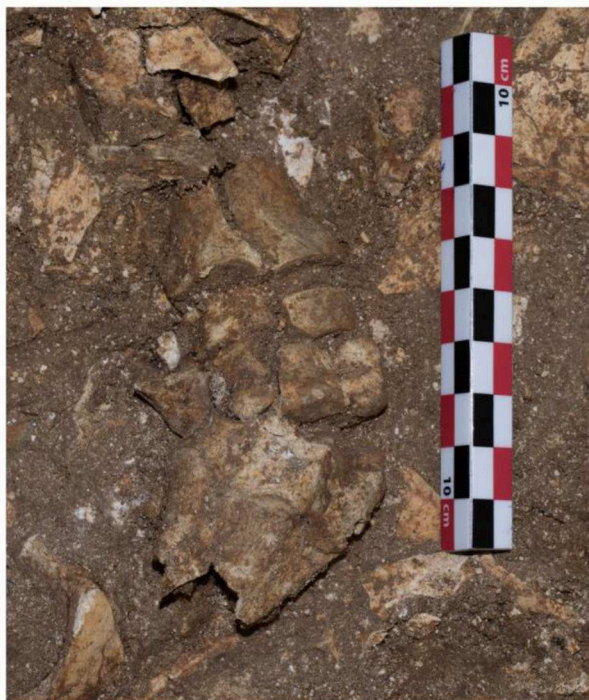
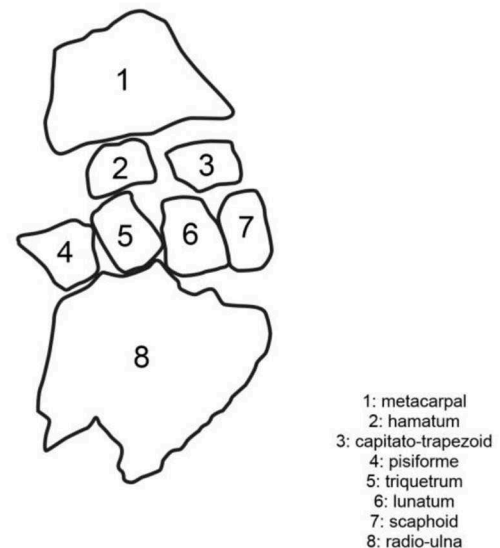


FIGURE 2
Remains 6,218–6,225 in anatomical articulation found during decapage 8.



Methods

All the faunal remains were observed. For taxonomic and anatomical identifications, we used the reference skeletal collections from the IRL 2013 ZoSCAN (CNRS—IAET SB RAS) and the one from PACEA Laboratory (CNRS—Bordeaux University—MCC), sometimes complemented by the *Virtual Faunal Comparative Collection* from the Max Planck Institute (Niven et al., 2009). Pieces were identified at the most precise level and, when it was not possible to propose a specific attribution, ungulate size classes were used (adapted from Brain, 1981). With regard to the skeletal part profiles, all identifiable specimens (including shaft fragments) were taken into account and recorded following the “element, portion, segment” method (Gifford and Crader, 1977). Shaft fragmentation was evaluated using the shaft length and shaft circumference indexes (Villa and Mahieu, 1991). Analyses of the bone surfaces were conducted on all the identified remains and part of the non-identified ones. The bone surfaces were observed under a low-angled light systematically using a hand lens (enlargement: 20x) for the taphonomic and zooarchaeological observations. Weathering, root etching, and anthropogenic and carnivore modifications were systematically looked for

(Behrensmeyer, 1978; Olsen and Shipman, 1988; Blumenshine et al., 1996; D’Errico and Villa, 1997; Pickering and Egeland, 2006). Oxide colorations of the bone cortical surfaces were also recorded. The proportion of preserved cortical surface was estimated per quartile (Rendu, 2010). When unclear modifications were detected, specimens were subjected to a more thorough evaluation with a 20–80x microscope. Percentage values were calculated based on the number of analyzed remains (NRa). Bones with unobservable surfaces were excluded from the calculation of the percentages of modified bones, thus NRa can change depending on the analysis type. Skeletal part representations were established for the reindeer and the horse using both %NNISP (Grayson and Frey, 2004) and %MAU index (Binford, 1978, 1981). Differential preservation has been tested for the reindeer and the horse by confronting frequencies of skeletal elements (in %NNISP) and their respective densities (Lyman, 1994; Lam et al., 1999). The possibility of a selective transport based on the nutritive value of the elements was tested using the SFUI (Metcalfé and Jones, 1988; Outram and Rowley-Conwy, 1998). Statistical tests of correlation (Spearman’s rank r_s) and Fisher exact tests were performed using the R stats package, and 95% confidence intervals for

TABLE 1 Fauna spectrum per decapage (C1 to C9) expressed in number of remains (NR). MNIc was calculated on the combination of bone and teeth.

	C1	C2	C3	C4	C5	C6	C7	C8	C9	TotalNISP	NMI
Leporid								3		3	1
Fox	1			1						2	1
Wolf									1	1	1
Carnivore NID							2			2	
Horse	39	45	27	28	60	67	83	75	88	512	
Bovine	13	20	13	10	42	28	23	40	55	244	
Reindeer	202	159	151	149	247	239	399	403	483	2,432	
Red Deer								1	2	3	1
Total NISP	255	224	191	188	349	334	507	522	629	3,199	
				2	9		1	1	3	16	
Small size ungulate	90	51	47	49	104	32	60	74	65	572	
Medium size ungulate										377	
Large size ungulate	72	47	40	46	85	87	92	120	116	328	
NID	97	31	42	34	47	44	40	55	49	439	
Total NR	514	353	320	319	594	497	700	772	862	4,931	

percentages were calculated using the BinomCI function of the R DescTools package using the Wilson method. Plots were carried out in QGIS (QGIS Development Team, 2022).

Results

Faunal spectrum

Due to good bone preservation (see *infra*) and a limited number of taxa identified in the faunal spectrum (7 species), 65% of the remains were taxonomically identified (Table 1). As expected, reindeer dominates largely the assemblages (76%), followed by horses (16%) and large bovids (8%). Red deer, leporids, foxes, and wolves complete the faunal spectrum.

An evolution through the deposit can be observed with, in particular, the fluctuation of the Bovinae contribution as identified by C. Beauval on the Airvaux collections (Beauval, 2004). Fisher exact tests identify differences between the C4 and C5 decapages, and between the C6 and C7 decapages (Figure 3). The visualization of these fluctuations with confidence intervals (Figure 3), however, ponders these rather small differences between the decapages.

The contribution of the horse is however significantly higher in our assemblage than what Niven et al. (Niven et al., 2012) identified (16% of the NISP vs. 9%; Fisher exact test: $p < 0,001$), but closer to Beauval results (11.67% NISP; Beauval, 2004). If the MNI is taken into account, this trend is slightly less pronounced

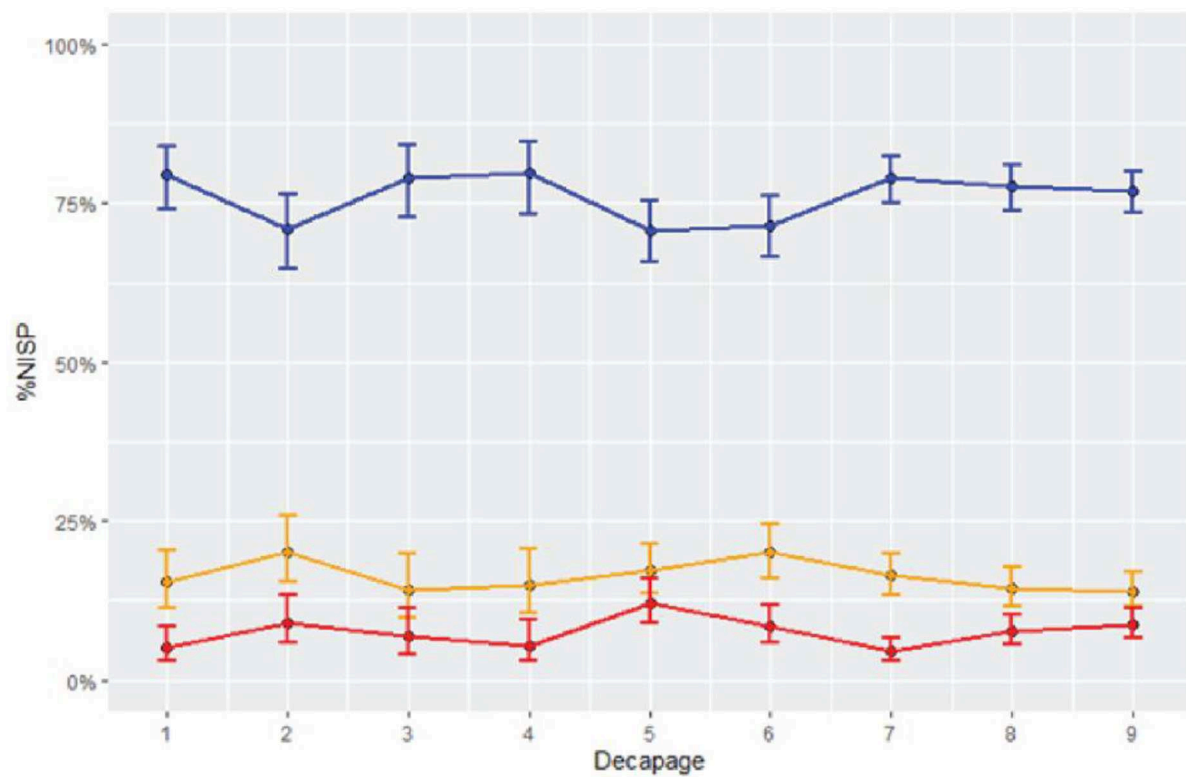
with reindeer (MNI = 28) dominating the assemblage followed by horse (MNI = 8) and bovinæ (MNI = 4).

A detailed spatial analysis of the Chez-Pinaud dataset will be carried out in the future, but Figure 4 proposes a first general overview of the distribution and density of the three main taxa identified: no specific clustering by species is apparent. Remains do not tend to be clustered by species but, rather, mixed all together.

The comparison of ungulate size classes allows to overcome the greater difficulty of horse and bison identification. Indeed, the reindeer is almost the only member of the medium size ungulate category creating a bias in its advantage and leading to an overestimation of its remains and a tendency to attribute the anatomically identified remains of this category to this taxon. Table 2 clearly underlines that reindeer is overestimated in the faunal spectrum and that the large ungulates contribute to about one-third of the assemblage. This point is crucial: it tempers the presentation generally made of the deposit as being specialized [sensu (Mellars, 2004)] on reindeer exploitation (Jaubert et al., 2008a; Delagnes and Rendu, 2011; Niven et al., 2012; Rendu et al., 2022).

Taphonomy

The faunal stock is globally well preserved. The impact of weathering is particularly limited in intensity but not in frequency (Table 3). Nearly half of the material was affected by these changes. On the other hand, the advanced stages

A**B**

FISHER EXACT TEST	P
C1-C2	0,07839
C2-C3	0,1676
C3-C4	0,8537
C4-C5	0,02259
C5-C6	0,2281
C6-C7	0,02111
C7-C8	0,08802
C8-C9	0,8152

FIGURE 3

(A) Variations in Reindeer (blue), Bovine (red), and Horse (yellow) %NISP per decapage, with 95% confidence intervals; (B) Paired Fisher exact tests by decapage, performed on NISP of reindeer, large bovines, and horses. Statistically significant differences in values are highlighted in bold.

(stage 3 and stage 4) are visible on <8% of the total number of bones. This supports the idea of rapid burial of the remains.

While there is no significant variation between bison and horse remains, the reindeer appears to be less affected by the weathering.

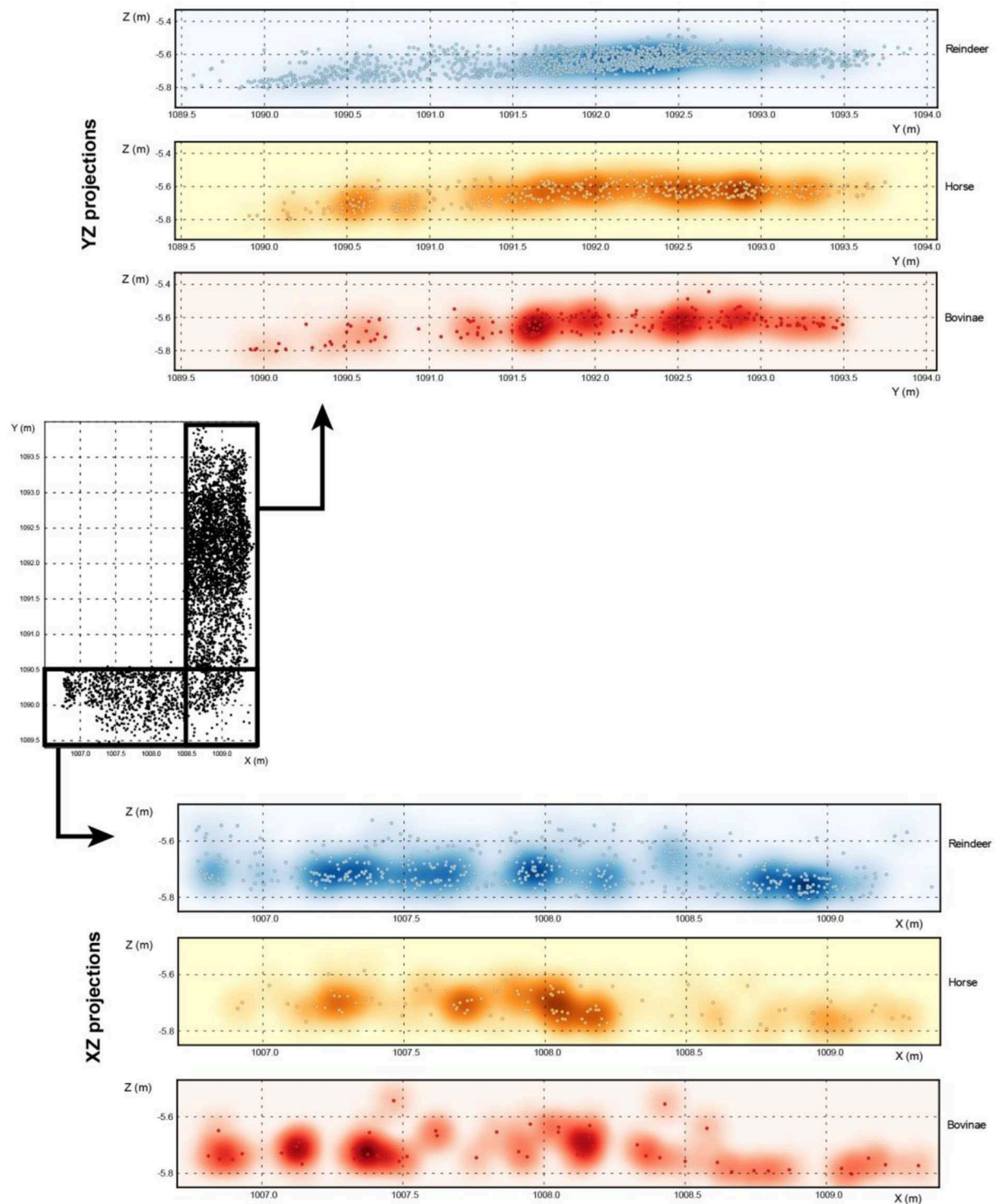




FIGURE 4
Spatial distribution of the three main taxa on sagittal (YZ) and frontal (XZ) projections (dots: identified remains, color background: density).

In detail (Supplementary Table 2), it is mainly the longitudinal cracking of the bones or cracks that are visible

on the material with the exfoliations that correspond to the detachment of the outermost cortical layers. They are generally

TABLE 2 Relative contribution of the different ungulate size classes to the Fauna spectrum per decapage (C1 to C9).

Taxa	C1 (%)	C2 (%)	C3 (%)	C4 (%)	C5 (%)	C6 (%)	C7 (%)	C8 (%)	C9 (%)	Total (%)
	70	65	71	70	66	60	70	67	68	67
	30	35	29	30	34	40	30	33	32	33

found on the same remains. The cracks within the thickness of the bones are rare. Since this taphonomic attack is generally associated with freeze alternations (Guadelli and Ozouf, 1994), and considering that the deposition took place in a per-arctic climate (Jaubert et al., 2008b), it is possible that its low representation of frost modifications attests that the bone bed remained frozen most of the time (or at least did not undergo much freeze/thaw alternations) before its complete embedding.

Once again, it is possible to see a difference between the reindeer and the two large ungulates (Supplementary Table 3).

These different modifications had a limited impact on the preservation of the cortical surface of the bone. Indeed, more than 80% of the remains show preservation of at least 50% of their cortical surfaces (Figure 5), but reindeer remains appear to have been more altered.

The carnivore damages are almost absent from the assemblage and affect only 1.2% of the remains. This low carnivore impact is coherent with what was observed previously in the Airvaux and Jaubert and Hublin collections (Beauval, 2004; Niven et al., 2012). Associated with their very limited presence in the faunal spectrum, their low impact strongly suggests that they had no major influence on bone accumulations. In addition, cut marks on the remains of the three carnivore taxa identified in the different collections evidence their exploitation by Neanderthals [a fox tibia (Niven et al., 2012); metacarpals of cave lion (Beauval, 2004); and a wolf tibia (this study)].

On the contrary, the human impact on the collection is particularly pronounced (Table 4), affecting 29% of the analyzed remains (Table 4).

The anthropogenic modifications affect all the taxa with the exception of the leporid (Table 5). If we did not identify any modification on the fox remains, Niven and collaborators identified cut marks on a distal extremity of a tibia (Niven et al., 2012). In addition, a longitudinal cut mark on a shaft fragment of a wolf tibia attests to defleshing activities on carnivores.

The very low quantity of burnt bones was already highlighted in the previous analysis (Niven et al., 2012) and is something very common in most Quina contexts, such as Les Pradelles or Roc de Marsal, for instance, where their frequency is largely below 1% (Costamagno et al., 2006; Castel et al., 2017).

The skeletal profiles

The post-depositional fragmentation of the assemblage is limited and 91% of identified breaks were realized on green bone. In addition, more than 5% of the remains (teeth excluded) are found complete, including some of the ribs. This limited fragmentation is also highlighted by the relatively high frequency of long bones extremities: they represent more than 13% (217/1709) of the long bones NISP, though they are known to be usually under-represented on archaeological sites due to preservation issues or specific human or carnivore exploitation (Lyman, 1994; Marean and Assefa, 1999). For instance, at the contemporaneous Les Pradelles Quina site, their proportion is under 1% and it is interpreted as resulting from the destruction of these extremities by humans for recovering the grease within (Costamagno et al., 2006).

Skeletal profiles have been established for the reindeer and horse (Figure 6), and they show two different patterns: while all the reindeer skeletal parts are found at the site, the horse skeletal profile shows a greater discrepancy between meaty long bones and head than axial skeleton and griddles. Also, on the horse, it is worth noting the quasi-absence of the lower-leg elements.

As highlighted previously by Niven et al. (2012), there is a weak but significant correlation ($r_s = 0.4343$, $p < 0.001$; $ddl = 46$, Figure 7) between the frequency of the reindeer skeletal elements and their relative density (Lyman, 1994; Lam et al., 1999) while none exists for the horse elements ($r_s = 0.0181$; $ddl = 46$, Figure 7). This taxonomic difference in the preservation of the bone finds an interesting echo with the difference in the preservation of the cortical surfaces (cf. supra). It suggests that the existence of density-mediated destruction has influenced the skeletal part profile of the reindeer (such as proposed by Niven et al., 2012) but cannot explain the variations observed on the horse skeletal profile.

Simultaneously, there is no correlation ($r_s = 0.093$) between the frequency of the reindeer skeletal elements (Supplementary Table 4) and their nutritive values expressed in SFUI (Metcalf and Jones, 1988), as illustrated by Figure 7. This attests to the absence of evidence of selective transport by the human population for the cervid and confirms the results of

TABLE 3 Impact of the weathering (C1 to C9) on the three main taxa.

stage	C1 (%)	C2 (%)	C3 (%)	C4 (%)	C5 (%)	C6 (%)	C7 (%)	C8 (%)	C9 (%)	Total (%)		Bison (%)		Horse (%)		Reindeer (%)	
	%NR	%NR	%NR	%NR	%NR	%NR	%NR	%NR	%NR	%NR	%NR	NR	%NR	NR	%NR	NR	%NR
0	54	41	52	46	39	51	34	43	33	41	55	25	116	26	977	43	43
1	17	19	15	38	38	26	46	47	58	41	99	45	200	45	962	42	42
2	11	19	19	11	17	19	16	9	8	13	53	24	94	21	229	10	10
3	14	15	7	4	6	3	4	1	1	4	9	4	27	6	85	4	4
4	5	5	8	1	0	0	0	0	0	1	6	3	7	2	23	1	1

Niven and collaborators, who concluded that the whole carcasses were brought to the site (Niven et al., 2012).

The comparison of the horse skeletal part representation (Supplementary Table 5) with the Standardized Food Utility Index [SFUI; Figure 7, (Outram and Rowley-Conwy, 1998)] underlines a statistically significant negative correlation ($r_s = -0.54033$; DDL = 14; $p < 0.05$). In other words, the poorest an element is, the more common it is in the assemblage. It would attest to the selective exportation of the richest skeletal parts of the horse carcasses to a consumption site and the discarding at Chez-Pinaud of the less interesting parts. Figure 7 underlines the existence of a gourmet strategy (Binford, 1981), which could explain the relatively weak correlation.

The site would have been used as an acquisition site for horse raw material, confirming a task-specific location dedicated to hunting activities (Jaubert et al., 2008a; Delagnes and Rendu, 2011; Niven et al., 2012).

Exploitation of the horse

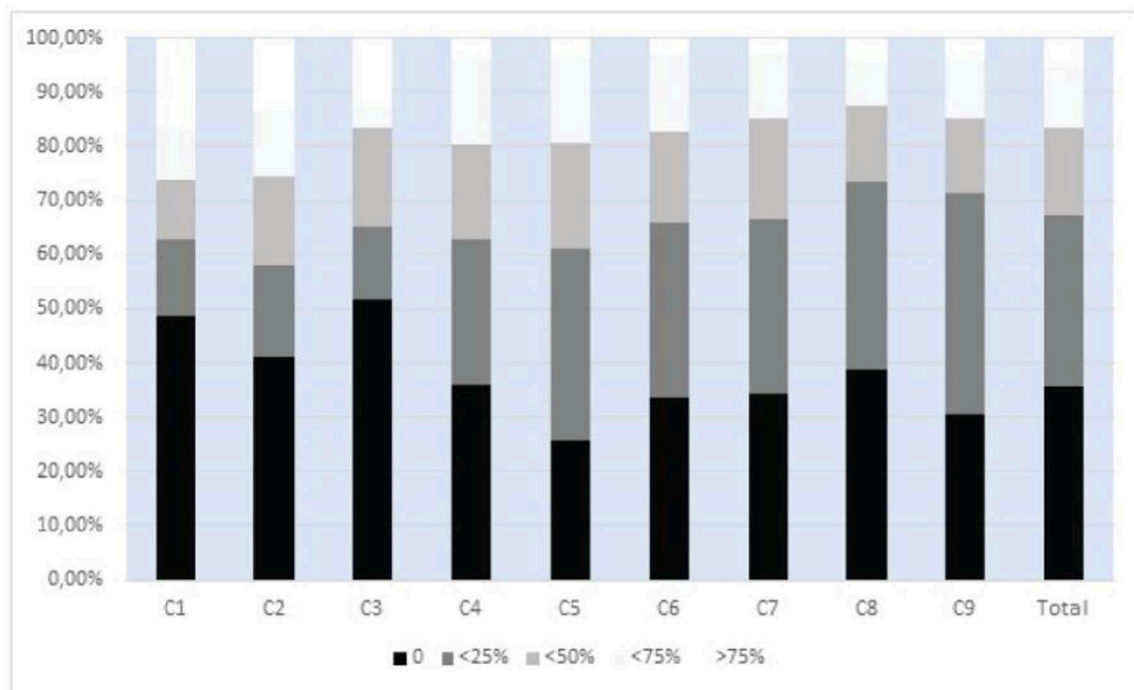
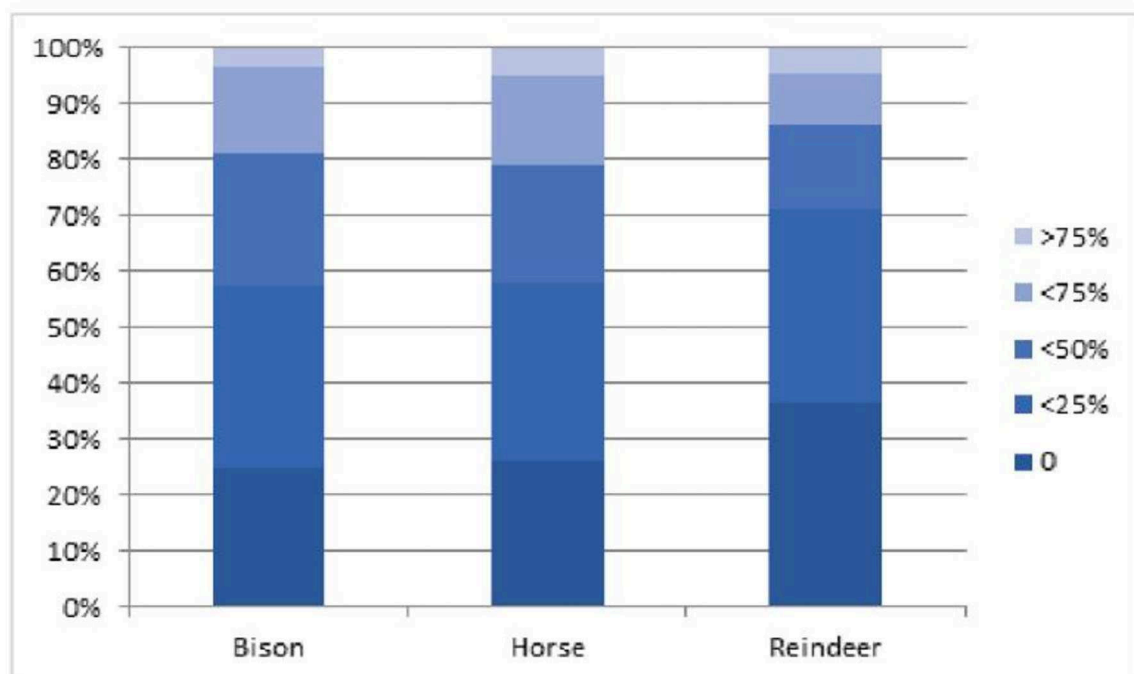
Horse carcasses were intensively exploited during the Quina occupation. Indeed, 44% of the remains exhibit evidence of anthropogenic modifications, mostly cut marks (39% of the total remains, 43% of the remain with good preservation, and <50% of the cortical surfaces destroyed) being largely more frequent than the exploitation marks observable on the reindeer remains. This difference is statistically highly significant ($\text{Khi}^2 = 10.262$, $\text{ddl} = 1$; $p < 0.01$).

The distribution of the cut marks on the horse skeleton attests to skinning, dismembering, and defleshing activities (Soulier and Costamagno, 2017; Soulier et al., 2022).

Skinning activities are identified for now by only circular marks at the base of two metatarsals, while this activity was documented on the reindeer elements (Beauval, 2004; Jaubert et al., 2008a; Claud et al., 2012; Niven et al., 2012).

The rib dismembering shows an interesting pattern: 9 out of the 17 articular heads exhibit the same transversal repetitive short disarticulations marks. The fact that these rib heads may come from the same individual and bear traces of the same gesture cannot be excluded. The two observable atlases attest to their separation from the cranium.

The defleshing activities are well identified on the collection, with at least 39 occurrences out of the 383 remains (teeth excluded; out of 247 remains if only the remains with very good preservation are considered [$<25\%$ of the cortical surface is altered]). These occurrences are preferentially found on the axial skeleton (15 ribs and 7 vertebrae) compared to the long bone remains (NISP = 12), while these elements are more frequent. Associated with the exportation of the elements rich in meat, it shows the strong interest of the Quina Neanderthal from Chez-Pinaud for horsemeat. Two occurrences of tongue extraction have also been identified by cut marks on the inner part of

A**B****FIGURE 5**

(A) Preservation of the cortical surfaces (per quartile) following (Rendu, 2010; Rendu et al., 2019): Stage 0: no destruction; Stage1: <25% destroyed; stage2: <50%; stage 3: <75%; Stage 4: >75% destroyed. (B) Preservation of the cortical surfaces for the three main taxa, (per quartile) following (Rendu, 2010; Rendu et al., 2019) (Stage 0: no destruction; Stage1: <25% destroyed; stage2: <50%; stage 3: <75%; Stage 4: >75% destroyed).

TABLE 4 Anthropogenic modifications. NRA: Number of analyzed remains.

		C1	C2	C3	C4	C5	C6	C7	C8	C9	Total
NR A		207	207	193	183	394	343	661	751	829	3,768
NR with anthropogenic modifications	NR	63	66	72	79	153	173	263	279	270	1,418
	%Nra	30%	32%	37%	43%	39%	50%	40%	37%	33%	38%
Cut marks	NR	50	57	59	62	134	151	194	187	217	1,111
	%Nra	24%	28%	31%	34%	34%	44%	29%	25%	26%	29%
Scrapping	NR	8	9	9	3	4		2	9	4	48
	%Nra	4%	4%	5%	2%	1%	0%	0%	1%	0%	1%
Notches	NR	11	16	20	17	32	33	57	42	50	278
	%Nra	5%	8%	10%	9%	8%	10%	9%	6%	6%	7%
Cortical notches	NR	1	1	3	6	7	2	12	29	17	
	%Nra	0%	0%	2%	3%	2%	1%	2%	4%	2%	0%
Burnt bones	NR	4	2	2	2		1	3	3	2	19
	%Nra	2%	1%	1%	1%	0%	0%	0%	0%	0%	1%

TABLE 5 Anthropogenic modifications par taxa and their details.

	NRA	Anthropogenic		Cut Marks		Scrapping		Notches		Retouchers		Total
		NR	%NR	NR	%NR	NR	%NR	NR	%NR	NR	%NR	
Wolf	1	1	100	1	100		0		0		0	1
Horse	383	167	44	139	36	5	1	25	7	35	9	383
Bovine	194	79	41	67	35	3	2	8	4	20	10	194
Reindeer	2,120	743	35	621	29	31	1	182	9	52	2	2,120
Red deer	3	2	67	1	33		0	1	33	1	33	3

NRA, number of analyzed remains.

mandibles. In addition, the gutting is attested by several cut marks in the inner part of the six ribs.

Notches have been recorded on 29% (22/74 NISP) of the long-bone shaft fragments, evidencing the intense long-bone breakage to recover the grease and marrow and probably also to extract blank for the bone tool industry (see below). It is noteworthy that horse bones are more difficult to break than reindeer bones and they contain proportionally less marrow because of the large amount of spongy tissue, characteristic of equids (Outram and Rowley-Conwy, 1998). On the other hand, horse marrow is richer in linoleic acid (Levine 1998), a substance of great interest to human groups living in cold environments.

The exploitation of the carcasses was not limited to the soft tissues, but the bone themselves were used as blanks for the production of bone tools. A large number of retouchers is produced on horse remains (NR = 35) and more generally on large ungulate remains (NR = 72), representing 8% of the number of remains of these taxa. This proportion is significantly higher than the frequency of retouchers (2.5%) made from

medium-size ungulate blanks ($\text{Khi}^2 = 38.177$, $\text{ddl} = 1$; $p < 0.0001$), confirming a strong selection on the nature of the support. This interest in large ungulates, in general, and horses, in particular, is clearly identified by the use of an upper horse incisor as a retoucher (Figure 8).

Discussion

A zooarchaeological analysis of material from new excavations at Chez-Pinaud brings new insights into the subsistence activities and the diet of the Quina Mousterian that exploited the site around 60,000 years ago.

First and foremost, the importance of large ungulates, and especially horses, seems higher than previously thought. When remains identified by ungulate size classes are taken into account, a large contribution of horse and bison can be highlighted (33% of the NISP). However, the dominance of the reindeer in the faunal spectrum does not necessarily imply

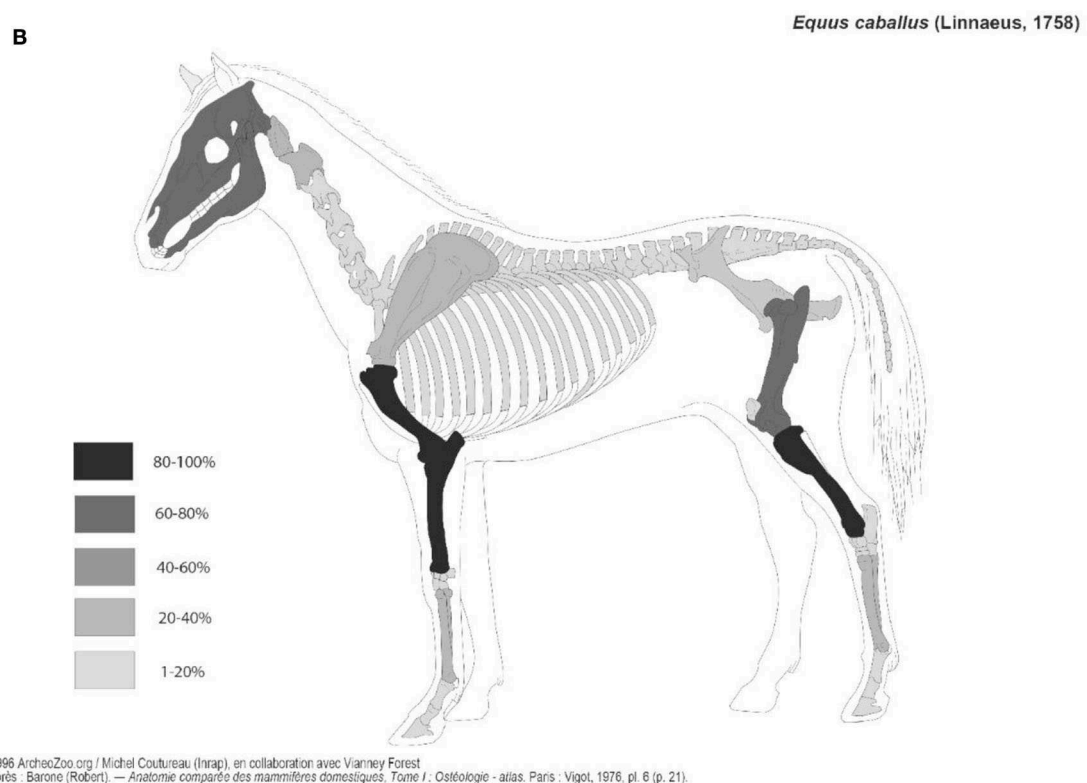
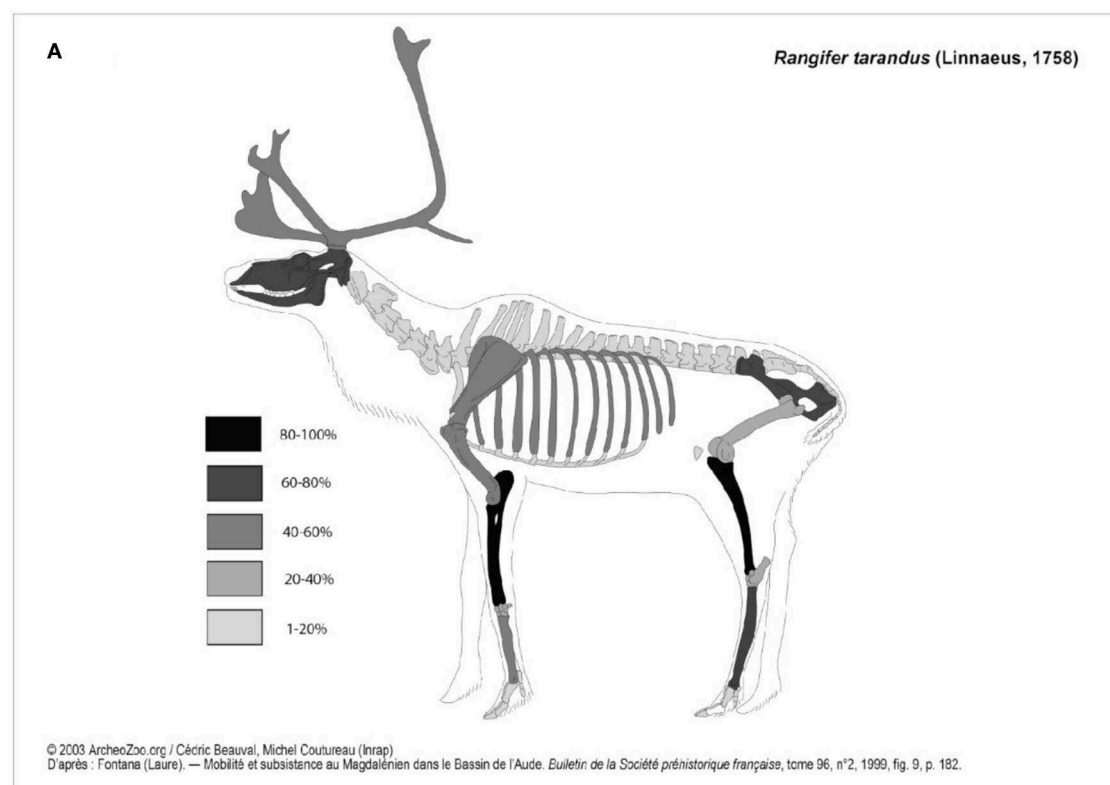
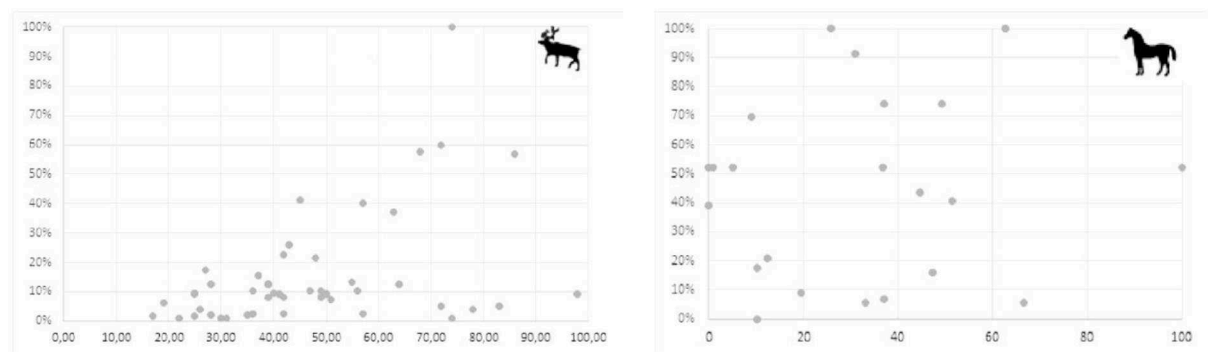


FIGURE 6

(A) Reindeer skeletal part representation of Chez-Pinaud horse remains expressed in %MAU, image modified from © 2003 ArcheoZoo.org / Cédric Beauval, Michel Coutureau (Inrap) D'après : Fontana (Laure). — Mobilité et subsistance au Magdalénien dans le Bassin de l'Aude. *Bulletin de la Société préhistorique française*, tome 96, n°2, 1999, fig. 9, p. 182. (B) Horse skeletal part representation of Chez-Pinaud horse remains expressed in %MAU, Modified from © 1996 ArcheoZoo.org / Michel Coutureau (Inrap), en collaboration avec Vianney Forest D'après : Barone (Robert). — Anatomie comparée des mammifères domestiques, Tome I : Ostéologie - atlas. Paris : Vigot, 1976, pl. 6 (p. 21).

A %MAU compared to the bone density



B %MAU compared to the SFUI

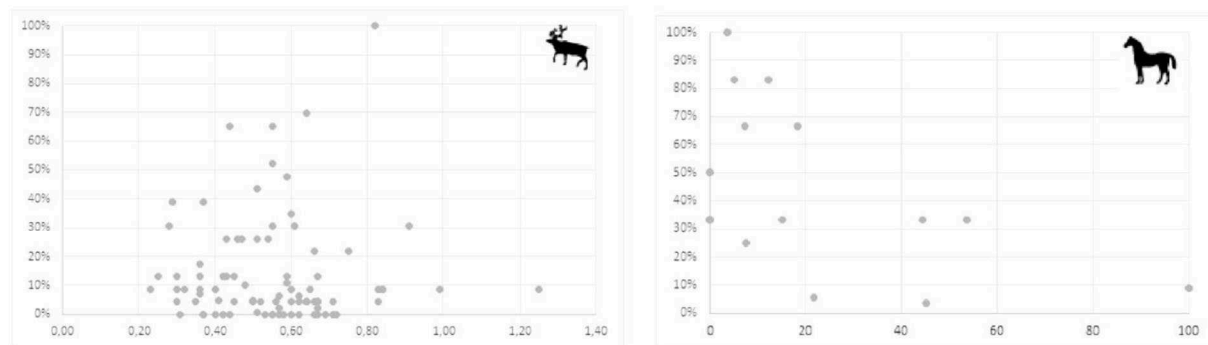


FIGURE 7

(A) Differential preservation test: for Reindeer (left) and horse (Right) relative skeletal representation (%NNISP) compared to the bone density (Lam et al., 1999). (B) reindeer (left) and horse (Right) skeletal part representation (y) [in %MAU see Binford (1978, 1981)] compared to their nutritive value (x) expressed in SFUI (Outram and Rowley-Conwy, 1998).

its dominance in the Neanderthal diet. Indeed, medium and large size ungulates do not provide the same quantity of animal raw material to the hunters, and if we consider the quantity of meat available on reindeer [35–40 kg (Klokov, 2000)] and horse [150kg (Outram and Rowley-Conwy, 1998)], the ratio (around 4) is more or less equivalent to the reindeer/horse MNI ratio ($28/8 = 3.5$). Thus, considering that the site is in the direct vicinity of the kill site and consequently the whole carcasses were available, the Quina Neanderthal of Chez-Pinaud would have had access to the same quantity of reindeer and horse meat.

For now, while there are multiple pieces of evidence of seasonal winter hunting of the reindeer (Beauval, 2004; Niven et al., 2012; Rendu et al., 2022), no seasonal information are available for the horse, and we can only mention the absence of fetal remains. Thus, it is not possible to establish if the two taxa were hunted in the same season or not. The ongoing seasonal analyses should be able to solve this issue. Simultaneously, the limited number of individuals does not allow us to discuss deeply

the hunted populations, but the presence of juvenile horses attests that matriarchal groups were exploited.

Part of the horse carcasses seems to have been intensively butchered, as was evidenced for the reindeer by Niven and colleagues. There is in addition a statistically significant difference in the frequency of cut marks between horse and reindeer remains ($\text{Khi}^2 = 3.873$, $\text{ddl} = 1$; $p < 0.05$), an interesting pattern, even if such a distinction could be due to differences in handling larger carcasses during the butchering process (Soulier et al., 2022). Differences can also be seen in the anatomical articulations found during excavations: on the 44 bones found in articulated groups during the 2019–2021 excavation, 40 belong to reindeer, two to bison, and two to horse, the difference being statistically significant ($\text{Khi}^2 = 5.01$, $\text{ddl} = 3$; $p < 0.02$). During the Jaubert and Hublin excavations, only reindeer connections were attested. This difference implies that the reindeer carcasses were dismembered more expediently, in larger parts, while the large ungulates would have been more



FIGURE 8
Piece #4061, decapage 6. Upper horse incisor used as retoucher. Photo and DAO: Malvina Baumann.

systematically processed. This found an interesting echo in the fact that horse carcasses were more selectively transported than the reindeer ones, maybe due to the difference in weight between the two animals. Seasonal data on large ungulates will also provide discussion on this point, allowing access to the health status of prey, potentially different between reindeer and large ungulates (generating a more or less intense search for marrow for example).

The zooarchaeological analysis underlines a specific interest in the meat on the horse carcasses, whatever we consider the skeletal profiles or the human impact on the bones, confirming the specific place of this taxon in the Neanderthal diet. At the same time, the preferential use of horse bone remains a blank for the bone tool industry, suggesting that horses occupied a specific place in the whole Quina economy (Costamagno et al., 2018). At Les Pradelles, it has been suggested that the preference for large ungulate diaphysis as blanks for retouchers may result from the density constraints necessary to manufacture Quina scrapers (Costamagno et al., 2018); this selection toward large ungulates has also been noticed for several other Quina assemblages (e.g., Soulier, 2007; Daujeard et al., 2014; Jéquier et al., 2018). This particular place is notably underlined by the use of a horse incisor as a retoucher, a unique case in the Middle Paleolithic record.

Thus, the interpretation of the site as a site devoted to the capture and process of reindeer has to be reconsidered or, at least, pondered. The Neanderthals did not come specifically to hunt reindeer herds but rather to hunt reindeer and horses, at least (the place of bison remains to be explored in more detail). This has an important resonance in the discussion of the specialization of the Quina economy on the reindeer since US22 is the most important of the Quina unit from Chez-Pinaud, and Chez-Pinaud itself represents almost one-third of the units used in the different models to discuss the Quina population diet.

While the reindeer is the most common taxa in the Quina faunal spectra of Southwestern France, the horse is the second most common one, sometimes even dominating the spectra such as at La Rouquette L3 (Griggo in Rendu et al. (2011)] and Espagnac Level 2, 3, and 4a (Jaubert, 2001). Its frequency is also notable at Hauteroche (Paletta, 2005), Roc de Marsal Level 4 (Castel et al., 2017), and Combe Grenal Level 21 and 22 (Laquay, 1981; Guadelli, 1987). However, precautions have to be taken when dealing with old collections from Combe Grenal, as some selective sampling occurred during the 50–60s excavations creating a bias in favor of the large ungulates (Discamps and Faivre, 2017). Thus, if we reconsider the whole Quina spectrum through the lens of our current

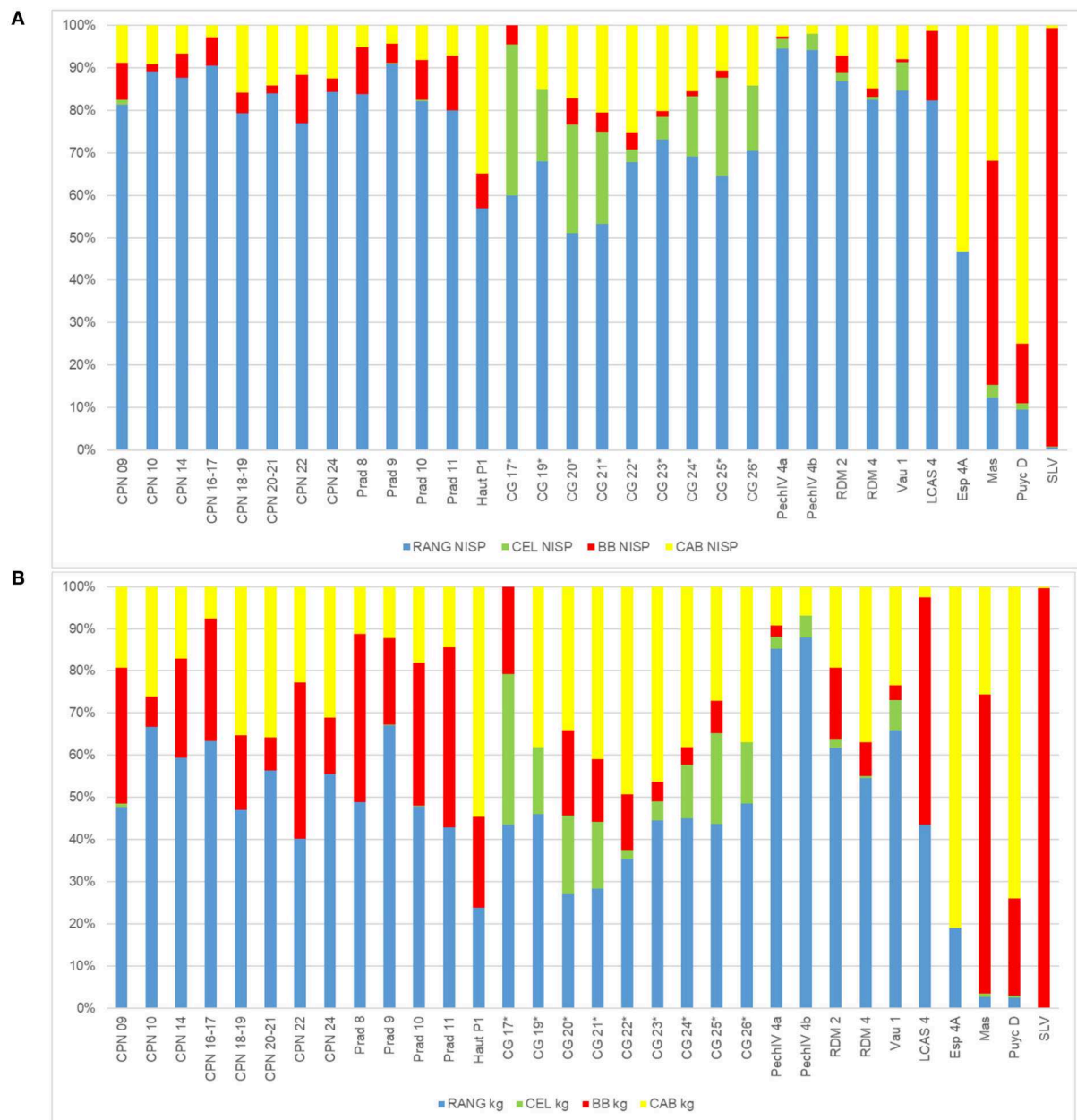


FIGURE 9

Spectra (A) in %NISP, (B) in kg of meat; Blue, reindeer; green, red deer; Red, bison; Yellow, horse; Gray, other). References used for data CG, Combe Grenal (Laquay, 1981; Guadelli, 1987); Vau, Vaufray (Delpech, 1996); PechIV, Pech de l'Azé IV (Laquay, 1981; Niven, 2013); Rdm, Roc de Marsal (Castel et al., 2017); LP, Les Pradelles (Costamagno et al., 2006); CPN, Chez-Pinaud-Jonzac (Airvaux, 2004; Jaubert et al., 2008b; Niven, 2013); LCAS, La Chapelle-aux-Saints (Rendu et al., 2014); Haut, Hauteroche (Paletta, 2005); LR, La Rouquette (Rendu et al., 2011); SLV, Sous les Vignes (Turq et al., 1999); ESP, Espagnac (Jaubert, 2001). Numbers correspond to the different stratigraphic units. *For Combe Grenal Reindeer was under-evaluated in the previous excavation due to selective sampling.

results, we can assume that the role of large ungulates in the Quina diet might have been under-evaluated. Figure 9 proposes the rebalancing of the faunal spectra from Figure 1 using the meat weight of the different taxa [for reindeer: 40 kg, after (Klokov, 2000); red deer: 55 kg, after (Varin, 1980);

bison: 250 kg, after (Wheat, 1967; Berger and Cunningham, 1991); horse: 150 kg, (Outram and Rowley-Conwy, 1998)]. It underlines that while reindeer remains the dominant faunal spectrum in 28 out of 32 cases, it constituted the main resource of ungulate meat acquired by the Quina Mousterian

in only 22 cases out of 32 and more than 50% in only 11 cases.

Naturally, numerous biases here are directly affecting these comparisons (the weight reference selected, the variation between males and females, the use of NISP and not MNI, the problem of transport strategies, the preservation, etc ...). Keeping these different limitations in mind, it appears that although the reindeer might have dominated the number of animals killed by Quina Neanderthals (Discamps and Royer, 2017), other taxa might have significantly contributed to their diet.

Thus, the Quina subsistence pattern might have been more complex than previously described, and if Chez-Pinaud at Jonzac was also recurrently used as a horse kill and butchery site, it would suggest that the large ungulate predation, and more specifically the horse, played a role in the annual organization of the activities within the territory.

Conclusion

This article completes the data we have about the subsistence strategies developed at Chez-Pinaud during the late MIS4. The horse remains attest to the intense exploitation of the carcasses for the meat and the blank of the bone industry and confirms the use of the site as a kill site/primarily butchery site. Without changing the interpretation of the site function and its specific place in the Quina territory, it proposes a more accurate vision of the role of the Horse for the Neanderthals from Chez-Pinaud. In a broader view, by extrapolating our interpretations to the rest of the Quina records, we assume here that large ungulates (horses and bovines) were an important part of the protein resources for the Quina population, which has been presented as specialized by the reindeer. However, due to the lack of seasonal data for the horse, it is not possible for now to discuss a potential seasonal complementarity in the hunting between the horse and the reindeer. The ongoing project should soon clarify this issue and new data will be needed for the rest of the Quina record.

Data availability statement

The raw data supporting the conclusions of this article will be made available by the authors, without undue reservation.

Author contributions

WR, KK, and SS designed the research and directed the scientific team and the field research. AG, MA, MBo, and SR were responsible of part of the excavation. SS realized the spatial analysis of the site, the post field treatment of the data and the 3D modeling, and submitted the manuscript. ED made the

spatial analysis of the faunal remains for this article. WR, SR, and AK collected the zooarchaeological data. WR, SR, AK, M-CS, and ED performed the zooarchaeological analyses. MBa and HP conducted the bone tool industry analysis. KK performed the lithic analysis. GG the discussion on the chronological attribution. WR wrote the article with the help of SS, SR, and AK. All the authors contributed to the editing and correction of it.

Funding

The excavation is part of the IRL 2013 ZooSCAN activity, a joint project between the CNRS and the Institute of Archaeology and Ethnography of the Siberian Branch of the Russian Academy of Sciences. The excavation is funded by the French Ministry of Cultural Heritage under the supervision of the Service Régional d'Archéologie de Nouvelle Aquitaine, Poitiers. We are grateful to the Conseil Général of the Charente-Maritime for its financial and logistic support. Our fieldwork would not have been possible without the major help of the Communauté de Commune de Haute Saintonge and Jonzac Municipality. The LIA Artemir and then the IRL Artemir were essential for their financial and logistic support. The study of the bone industry was supported by the Marie Skłodowska-Curie actions under the European Union's Horizon 2020 research and innovation programme (#839528, MBa). The HADES society supported us by funding part of the field and analytical time of SR. This article is part of the QuinaWorld project that has received funding from the European Research Council (ERC) under the European Union's Horizon 2020 research and innovation program ERC Grant agreement No. 851793.

Acknowledgments

We are thankful to Mr. Belot, Président of the Communauté de Commune de Haute Saintonge for his help and support. We thank Mrs. Annie Gendre for her help and support, and her friendship was essential; the team is really missing her. We are thankful to the UMR 5199 PACEA for its help during the field and the storage of the material.

Conflict of interest

The authors declare that the research was conducted in the absence of any commercial or financial relationships that could be construed as a potential conflict of interest.

Publisher's note

All claims expressed in this article are solely those of the authors and do not necessarily represent those

of their affiliated organizations, or those of the publisher, the editors and the reviewers. Any product that may be evaluated in this article, or claim that may be made by its manufacturer, is not guaranteed or endorsed by the publisher.

References

- Airvaux, J. (2004). Le site paléolithique de chez-Pinaud à Jonzac, Charente-Maritime. *Préhistoire du Sud-Ouest* 8, 180p.
- Beauval, C. (2004). La faune des niveaux Mousteriens de 'Chez-Pinaud' (Jonzac, Charente-Maritime, France). *Première analyse. Le Site Paléolithique de Chez-Pinaud à Jonzac, Charente-Maritime. Préhistoire du Sud Ouest* 8, 125e156.
- Behrensmeier, A. K. (1978). Taphonomic and ecologic information from bone weathering. *Paleobiology* 4, 150–162. doi: 10.1017/S0094837300005820
- Berger, J., and Cunningham, C. (1991). Bellows, copulations, and sexual selection in bison (Bison bison). *Behav. Ecol.* 2, 1–6. doi: 10.1093/beheco/2.1.1
- Binford, L. R. (1978). *Nunamiut: Ethnoarchaeology*. New York, NY: Academic Press.
- Binford, L. R. (1980). Willow Smoke and Dogs' Tails: Hunter-Gatherer Settlement Systems and Archaeological Site Formation. *Am. Antiquity* 45, 4–20. doi: 10.2307/279653
- Binford, L. R. (1981). *Bones: Ancient Men and Modern Myths*.
- Blumenschine, R. J., Marean, C. W., and Capaldo, S. D. (1996). Blind tests of inter-analyst correspondence and accuracy in the identification of cut marks, percussion marks, and carnivore tooth marks on bone surfaces. *J. Archaeol. Sci.* 23, 493–507. doi: 10.1006/jasc.1996.0047
- Brain, C. K. (1981). *The Hunter or the hunted. An Introduction to African Cave Taphonomy*. Chicago, London: The University of Chicago press.
- Britton, K., Grimes, V., Niven, L., Steele, T. E., McPherron, S., Soressi, M., et al. (2011). Strontium isotope evidence for migration in late Pleistocene Rangifer: Implications for Neanderthal hunting strategies at the Middle Palaeolithic site of Jonzac, France. *J. Hum. Evol.* 61, 176–185. doi: 10.1016/j.jhevol.2011.03.004
- Castel, J. C., Discamps, E., Soulier, M.-C., Sandgathe, D., and Dibble, H. L., McPherron, S. P., et al. (2017). Neandertal subsistence strategies during the Quina Mousterian at Roc de Marsal (France). *Quatern. Int.* 431, 216–222. doi: 10.1016/j.quaint.2015.12.033
- Claud, É., Soressi, M., Jaubert, J., and Hublin, J.-J. (2012). Étude tracéologique de l'outillage moustérien de type Quina du bonebed de Chez-Pinaud à Jonzac (Charente-Maritime). Nouveaux éléments en faveur d'un site de boucherie et de traitement des peaux. *Gallia Préhistoire* 54, 3–32. doi: 10.3406/galip.2012.2492
- Costamagno, S., Bourguignon, L., Soulier, M.-C., Meignen, L., and Beauval, C., Rendu, W., et al. (2018). Bone retouchers and site function in the Quina Mousterian: The case of Les Pradelles (Marillac-le-Franc, France), in *The Origins of Bone Tool Technology, Mainz, Verlag des Römisch-Germanisches Zentralmuseums*, dir. J. Hutson, 165–195.
- Costamagno, S., Meignen, L., Beauval, C., Vandermeersch, B., and Maureille, B. (2006). Les Pradelles (Marillac-le-Franc, France): A mousterian reindeer hunting camp? *J. Anthropol. Archaeol.* 25, 466–484. doi: 10.1016/j.jaa.2006.03.008
- Daujeard, C., Moncel, M.-H., Fiore, I., Tagliacozzo, A., Bindon, P., Raynal, J.-P., et al. (2014). Middle Paleolithic bone retouchers in Southeastern France: variability and functionality. *Quatern. Int.* 326–327, 492–518. doi: 10.1016/j.quaint.2013.12.022
- Delagnes, A., and Rendu, W. (2011). Shifts in Neandertal mobility, technology and subsistence strategies in western France. *J. Archaeol. Sci.* 38, 1771–1783. doi: 10.1016/j.jas.2011.04.007
- Delpech, F. (1996). L'environnement animal des Moustériens Quina du Périgord. *Paléo* 8, 31–46. doi: 10.3406/pal.1996.905
- D'Errico, F., and Villa, P. (1997). Holes and grooves: the contribution of microscopy and taphonomy to the problem of art origins. *J. Hum. Evol.* 33, 1–31. doi: 10.1006/jhev.1997.0141
- Discamps, E. (2014). Ungulate biomass fluctuations endured by Middle and Early Upper Paleolithic societies (SW France, MIS 5-3): The contributions of modern analogs and cave hyena paleodemography. *Quat. Int.* 337, 64–79. doi: 10.1016/j.quaint.2013.07.046
- Discamps, E., and Faivre, J.-P. (2017). Substantial biases affecting Combe-Grenal faunal record cast doubts on previous models of Neanderthal subsistence and environmental context. *J. Archaeol. Sci.* 81, 128–132. doi: 10.1016/j.jas.2017.03.009
- Discamps, E., Jaubert, J., and Bachellerie, F. (2011). Human choices and environmental constraints: deciphering the variability of large game procurement from Mousterian to Aurignacian times (MIS 5-3) in southwestern France. *Quatern. Sci. Rev.* 30, 2755–2775. doi: 10.1016/j.quascirev.2011.06.009
- Discamps, E., and Royer, A. (2017). Reconstructing palaeoenvironmental conditions faced by Mousterian hunters during MIS 5 to 3 in southwestern France: A multi-scale approach using data from large and small mammal communities. *Quatern. Int.* 433, 64–87. doi: 10.1016/j.quaint.2016.02.067
- Faivre, J.-P., Gravina, B., Bourguignon, L., Discamps, E., and Turq, A. (2017). Late Middle Palaeolithic lithic technocomplexes (MIS 5–3) in the northeastern Aquitaine Basin: Advances and challenges. *Quatern. Int.* 433, 116–131. doi: 10.1016/j.quaint.2016.02.060
- Gifford, D. P., and Crader, D. C. (1977). A computer coding system for archaeological faunal remains. *Am. Antiq.* 42, 225–238. doi: 10.2307/278983
- Grayson, D. K., and Frey, C. F. (2004). Measuring Skeletal Part Representation in Archaeological Faunas. *J. Taphon.* 2, 27–42.
- Guadelli, J.-L. (1987). *Contribution à l'étude des zooécénoses préhistoriques en Aquitaine (Würm ancien et interstade würmien)* (PhD thesis). Université Bordeaux I.
- Guadelli, J.-L., and Ozouf, J.-C. I. (1994). "Étude expérimentale de l'action du gel sur les restes fauniques. Premiers résultats," in *Outillage peu élaboré en os et bois de cervidés. IV Table ronde taphonomie/bone modification no 6 (Paris: Artefact)*, 47–56.
- Jaubert, J. (2001). Un site moustérien de type Quina dans la vallée du Célé: Pailhès à Espagnac-Sainte-Eulalie. *Gallia Préhistoire* 43, 1–100. doi: 10.3406/galip.2001.2312
- Jaubert, J., Hublin, J.-J., McPherron, S. P., and Soressi, M. (2008a). *CHEZ-PINAUD, JONZAC (CHARENTE-MARITIME) Fouille programmée triennale 2005-2007 3ème année 2007, Service régional de l'archéologie de Poitou-Charentes, Poitiers*. ed.
- Jaubert, J., Hublin, J.-J., McPherron, S. P., Soressi, M., Bordes, J.-G., Claud, É., et al. (2008b). *Paléolithique moyen récent et Paléolithique supérieur ancien à Jonzac (Charente-Maritime)*.
- Jéquier, C., Livraghi, A., Romandini, M., and Peresani, M. (2018). "Same but different: 20,000. years of bone retouchers from northern Italy A diachronologic approach from Neanderthals to anatomically modern humans," in *The Origins of Bone Tool Technology, Mainz, Verlag des Römisch-Germanisches Zentralmuseums*, dir. J. Hutson, 269–285.
- Klokov, K. B. (2000). Nenets reindeer heders on the lower Yenisei River: Traditional economy under current conditions are responses to economic change. *Polar Res.* 19, 39–47. doi: 10.1111/j.1751-8369.2000.tb00326.x
- Lam, Y., Chen, X., and Pearson, O. (1999). Intertaxonomic variability in patterns of bone density and the differential representation of bovid, cervid, and equid elements in the archaeological record. *Am. Antiq.* 64, 343–362. doi: 10.2307/2694283
- Laquay, G. (1981). *Recherches sur les faunes du Würm I en Périgord* (PhD thesis). Université Bordeaux I.
- Lyman, R. L. (1994). *Vertebrate Taphonomy*. Cambridge: Cambridge University Press.

Supplementary material

The Supplementary Material for this article can be found online at: <https://www.frontiersin.org/articles/10.3389/fevo.2022.1085699/full#supplementary-material>

- Marean, C. W., and Assefa, Z. (1999). Zooarcheological evidence for the faunal exploitation behavior of Neandertals and early modern humans. *Evol. Anthropol. Issues News Rev.* 8, 22–37. doi: 10.1002/(SICI)1520-6505(1999)8:1<22::AID-EVAN7>3.0.CO;2-F
- Metcalf, D., and Jones, K. T. (1988). A Reconsideration of Animal Body-Part Utility Indices. *Am. Antiq.* 53, 486–504. doi: 10.2307/281213
- Niven, L. (2013). “A diachronic evaluation of Neanderthal cervid exploitation and site use at Pech de l’Azé IV, France,” in *Zooarchaeology and Modern Human Origins*, eds. J. L. Clark, J. D. Speth, 151–161.
- Niven, L., Steele, T. E., Finke, H., Gernat, T., and Hublin, J.-., J. (2009). Virtual skeletons: using a structured light scanner to create a 3D faunal comparative collection. *J. Archaeol. Sci.* 36, 2018–2023. doi: 10.1016/j.jas.2009.05.021
- Niven, L., Steele, T. E., Rendu, W., Mallye, J.-B., and McPherron, S. P., Soressi, M., et al. (2012). Neandertal mobility and large-game hunting: the exploitation of reindeer during the Quina Mousterian at Chez-Pinaud Jonzac (Charente-Maritime, France). *J. Hum. Evol.* 63, 624–635. doi: 10.1016/j.jhevol.2012.07.002
- Olsen, S. L., and Shipman, P. (1988). Surface modification on bone: Trampling versus butchery. *J. Archaeol. Sci.* 15, 535–553. doi: 10.1016/0305-4403(88)90081-7
- Outram, A., and Rowley-Conwy, P. (1998). Meat and Marrow Utility Indices for Horse (Equus). *J. Archaeol. Sci.* 25, 839–849. doi: 10.1006/jasc.1997.0229
- Paletta, A. (2005). *L'évolution des comportements de subsistance des hommes du Moustérien au Solutrén dans la région Poitou-Charentes (France)* (PhD thesis). Muséum national d'histoire naturelle, Paris.
- Pickering, T. R., and Egeland, C. P. (2006). Experimental patterns of hammerstone percussion damage on bones: implications for inferences of carcass processing by humans. *J. Archaeol. Sci.* 33, 459–469. doi: 10.1016/j.jas.2005.09.001
- QGIS Development Team. (2022). *QGIS Geographic Information System, and the Open Source Geospatial Foundation Project*. Available online at: <http://qgis.osgeo.org>.
- Rendu, W. (2010). Hunting behavior and Neanderthal adaptability in the Late Pleistocene site of Pech-de-l’Azé I. *J. Archaeol. Sci.* 37, 1798–1810. doi: 10.1016/j.jas.2010.01.037
- Rendu, W., Beauval, C., Crevecoeur, I., Bayle, P., Balzeau, A., Bismuth, T., et al. (2014). Evidence supporting an intentional Neandertal burial at La Chapelle-aux-Saints. *Proc. Natl. Acad. Sci. U. S. A.* 111, 81. doi: 10.1073/pnas.1316780110
- Rendu, W., Bourguignon, L., Costamagno, S., Meignen, L., Soulier, M.-C., Armand, D., et al. (2011). “Mousterian hunting camps: Interdisciplinary approach and methodological considerations,” in *Hunting Camps in Prehistory. Current Archaeological Approaches, Proceedings of the International Symposium*, eds F. Bon, S. Costamagno, and N. Valdeyron (University Toulouse II - Le Mirail), 61–76.
- Rendu, W., Pubert, E., and Discamps, E. (2022). “Using cementochronology to discuss the organization of past neanderthal societies,” in *Dental Cementum in Anthropology*, eds. S. Naji, W. Rendu, L. Gourichon (Cambridge: Cambridge University Press), 275–287.
- Rendu, W., Renou, S., Soulier, M.-C., Rigaud, S., and Roussel, M., Soressi, M., et al. (2019). Subsistence strategy changes during the Middle to Upper Paleolithic transition reveals specific adaptations of Human Populations to their environment. *Sci. Rep.* 9, 15817. doi: 10.1038/s41598-019-50647-6
- Soulier, M.-., C. (2007). *Étude archéozoologique du carré M16 de la couche 2 du gisement moustérien du Roc-de-Marsal (Dordogne)*, Mémoire de Master I, Université de Toulouse-Le Mirail 110p.
- Soulier, M.-., C., Costamagno, S., Claud, E., and Deschamps, M. (2022). “Tracing the past: butchering a bison with Middle Palaeolithic stone tools,” in *Recreating Artefacts and Ancient Skills: From Experiment to Interpretation*, Targoviste, Cetatea de Scaun Publishing, eds. M. Mărgărit, and A. Boronean? 13–31.
- Soulier, M. C., and Costamagno, S. (2017). Let the cutmarks speak! Experimental butchery to reconstruct carcass processing. *J. Archaeol. Sci. Rep.* 11, 782–802. doi: 10.1016/j.jasrep.2016.12.033
- Turq, A., Guadelli, J.-., L., and Quintard, A. (1999). “A propos de deux sites d’habitat moustérien de type Quina à exploitation du bison: l’exemple du Mas-Viel et de Sous-les-Vignes,” in J. P. Brugal, F. David, J. G. Enloe, J. Jaubert, Antibes, eds. *Le Bison: Gibier et Moyen de Subsistance Des Hommes Du Paléolithique Aux Paléindiens Des Grandes Plaines*, 143–158.
- Varin, E. (1980). Chevreuil, cerf, sanglier: Etudes et récits d’un chasseur. les Editions de l’Orée. 270p.
- Villa, P., and Mahieu, E. (1991). Breakage patterns of human long bones. *J. Hum. Evol.* 21, 27–48. doi: 10.1016/0047-2484(91)90034-S
- Wheat, J. B. (1967). A Paleo-Indian bison kill. *Sci. Am.* 216, 44–53. doi: 10.1038/scientificamerican0167-44



OPEN ACCESS

EDITED BY

Brooke Crowley,
University of Cincinnati,
United States

REVIEWED BY

Gina Marie Semperebon,
Bay Path University,
United States
Mugino O. Kubo,
The University of Tokyo, Japan

*CORRESPONDENCE

Iván Ramírez-Pedraza
✉ ramirezpedrazaivan@gmail.com
Laura M. Martínez
✉ lmartinez@ub.edu

SPECIALTY SECTION

This article was submitted to
Paleoecology,
a section of the journal
Frontiers in Ecology and Evolution

RECEIVED 03 August 2022

ACCEPTED 25 January 2023

PUBLISHED 28 February 2023

CITATION

Ramírez-Pedraza I, Martínez LM, Aouraghe H,
Rivals F, Tornero C, Haddoumi H,
Estebaranz-Sánchez F, Rodríguez-Hidalgo A,
van der Made J, Oujaa A, Ibáñez JJ, Mhamdi H,
Souhir M, Aissa AM, Chacón MG and
Sala-Ramos R (2023) Multiproxy approach to
reconstruct fossil primate feeding behavior:
Case study for macaque from the Plio-
Pleistocene site Guefaït-4.2 (eastern Morocco).
Front. Ecol. Evol. 11:1011208.
doi: 10.3389/fevo.2023.1011208

COPYRIGHT

© 2023 Ramírez-Pedraza, Martínez, Aouraghe,
Rivals, Tornero, Haddoumi, Estebaranz-
Sánchez, Rodríguez-Hidalgo, van der Made,
Oujaa, Ibáñez, Mhamdi, Souhir, Aissa, Chacón
and Sala-Ramos. This is an open-access article
distributed under the terms of the [Creative
Commons Attribution License \(CC BY\)](#). The
use, distribution or reproduction in other
forums is permitted, provided the original
author(s) and the copyright owner(s) are
credited and that the original publication in this
journal is cited, in accordance with accepted
academic practice. No use, distribution or
reproduction is permitted which does not
comply with these terms.

Multiproxy approach to reconstruct fossil primate feeding behavior: Case study for macaque from the Plio-Pleistocene site Guefaït-4.2 (eastern Morocco)

Iván Ramírez-Pedraza^{1,2*}, Laura M. Martínez^{3,4*}, Hassan Aouraghe⁵,
Florent Rivals^{1,2,6}, Carlos Tornero^{1,7}, Hamid Haddoumi⁵,
Ferran Estebaranz-Sánchez^{4,8}, Antonio Rodríguez-Hidalgo^{1,2,9},
Jan van der Made¹⁰, Aïcha Oujaa¹¹, Juan José Ibáñez⁸,
Hicham Mhamdi⁵, Mohamed Souhir⁵, Al Mahdi Aissa⁵,
M. Gema Chacón^{1,2,12} and Robert Sala-Ramos^{1,2}

¹Institut Català de Paleoecologia Humana i Evolució Social (IPHES-CERCA), Tarragona, Spain, ²Departament d'Història i Història de l'Art, Universitat Rovira i Virgili (URV), Tarragona, Spain, ³Departament de Biologia Evolutiva, Ecologia i Ciències Ambientals, Secció de Zoologia i Antropologia Biològica, Universitat de Barcelona, Barcelona, Spain, ⁴Institut d'Arqueologia de la Universitat de Barcelona, Barcelona, Spain, ⁵Faculté des Sciences, Département de Géologie, Université Mohamed Premier, Oujda, Morocco, ⁶Institució Catalana de Recerca i Estudis Avançats (ICREA), Barcelona, Spain, ⁷Department of Prehistory, Autonomous University of Barcelona (UAB), Bellaterra, Spain, ⁸Archaeology of Social Dynamics (ASD), Institución Milá y Fontanals (IMF), Spanish National Research Council (CSIC), Barcelona, Spain, ⁹Instituto de Evolución en África (IDEA, Madrid), Madrid, Spain, ¹⁰Consejo Superior de Investigaciones Científicas (CSIC), Museo Nacional de Ciencias Naturales, Departamento de Paleobiología, Madrid, Spain, ¹¹Institut National des Sciences de l'Archéologie et du Patrimoine (INSAP), Rabat, Morocco, ¹²UMR 7194 - Histoire Naturelle de l'Homme Préhistorique (CNRS/MNHN/UPVD), Paris, France

The genus *Macaca* belongs to Cercopithecidae (Old World monkeys), Cercopithecinae, Papionini. The presence of *Macaca* in North Africa is well known from the Late Miocene to the Late Pleistocene. However, the diet of fossil *Macaca* has been poorly described in the literature. In this study, we investigated the feeding habits of *Macaca* cf. *sylvanus* ($n=4$) from the Plio-Pleistocene site Guefaït-4.2 in eastern Morocco through multiproxy analysis combining analyses of stable carbon and oxygen isotopes from tooth enamel, buccal microtexture, and low-magnification occlusal dental microwear. For both microwear analyses, we compared the macaques with a new reference collection of extant members of Cercopithecoidea. Our occlusal microwear results show for the fossil macaque a pattern similar to the extant *Cercocebus atys* and *Lophocebus albigena*, African forest-dwelling species that are characterized by a durophagous diet based mainly on hard fruit and seed intake. Buccal microtexture results also suggest the consumption of some grasses and the exploitation of more open habitats, similar to that observed in *Theropithecus gelada*. The $\delta^{13}\text{C}$ of *M. cf. sylvanus* indicates a C_3 based-diet without the presence of C_4 plants typical of the savanna grassland in eastern Africa during this period. The high $\delta^{18}\text{O}$ values of *M. cf. sylvanus*, compared with the contemporary ungulates recovered from Guefaït-4.2, could be associated with the consumption of a different resource by the primate such as leaves or fresh fruits from the upper part of trees. The complementarity of these methods allows for a dietary reconstruction covering a large part of the individual's life.

KEYWORDS

habitat, paleodiet, Africa, buccal microtexture, occlusal microwear, stable isotopes

Introduction

Modern Cercopithecoidea primates inhabit a wide range of habitats, including tropical forests, high-altitude woodlands, and savanna grasslands (Jablonski et al., 2000). This adaptability across a range of environments began with a radiation within and beyond Africa, probably due to the increasingly open and fragmented environments of the Late Miocene and the Plio-Pleistocene (Elton, 2007; Hughes et al., 2008; Roos et al., 2019). For example, the closing of the Tethys Ocean and subsequent aridification of northern Africa (Zhang et al., 2014), and fluctuations in Milankovitch cycles (DeMenocal, 1995), formed intermittent biogeographical barriers. It is hypothesized that these ecological barriers diversified Cercopithecoidea, specifically the Papionini tribe, into different genera. *Theropithecus* adapted to wet lowlands, *Papio*, *Cercocebus*, *Lophocebus*, and *Mandrillus* filled niches within more forested environments, while *Macaca* became more-generalized and settled a wide variety of habitats within higher latitudes (Delson, 1980). Paleontological and molecular evidence indicates that the macaque lineage originated during the Miocene in Africa and diverged from other African Papionini around 7–5.5 Ma (Delson, 1980; Tosi et al., 2005; Roos et al., 2019). According to the fossil record, macaques dispersed throughout Eurasia during the Late Miocene, inhabiting primarily the Mediterranean region 6–5 Ma (Alba et al., 2014; Piñero et al., 2017) and then in the Late Pliocene, eastern Asia (~4 Ma; Szalay and Delson, 1979; Elton, 2007; Meloro and Elton, 2012). In this radiation, macaques experienced a rapid diversification into several species (Elton and O'Regan, 2014; Roos et al., 2019). The genus *Macaca* consists of approximately 23 extant species and occupies more diverse ecological environments and geographical ranges (from 10° south to over 40° north latitude) than any other genus of nonhuman primates. In fact, the expansion of this genus in Africa and Eurasia is one of the most successful among primates (Jablonski, 2002; Jablonski and Frost, 2010; Fleagle, 2013; Roos et al., 2019), and its ecological distribution and adaptive capacity reflect great dietary diversity and interspecific behavioral responses to seasonality (Kato et al., 2014).

The oldest macaque fossils in Africa have been found in the Miocene paleontological sites of Menacer (Algeria, *Macaca* sp.; Arambourg, 1959) and Wadi Natrum (Egypt, *Macaca lybica*; Stromer, 1913, 1920). Other *Macaca* fossil remains have been recorded in the Pliocene Tunisian sites of Garaet Ichkeul (Szalay and Delson, 1979; Delson, 1993; Alemseged and Geraads, 1998) and Ain Brimba (Arambourg and Coque, 1959; Arambourg, 1979; Szalay and Delson, 1979). Contemporaneous to the remains of *Macaca* cf. *sylvanus* from the Guefait-4.2 (GFT-4.2) site in eastern Morocco analyzed in this work, fossil remains of *Macaca* sp. have been found in the Plio-Pleistocene site of Ahl al Oughlam in western Morocco (Geraads, 2006). *Macaca sylvanus* has also been described from the Late Pleistocene sites of Chrafate and Ez Zarka in Morocco (Ouahbi et al., 2001; Fooden, 2007), and in the Middle and Late Pleistocene sites of Traras, Monts des Nedroma, Afalou bou Rhummel, and Tamar Hat in Algeria (Pomel, 1892; Joleaud, 1926; Delson, 1974; Szalay and Delson, 1979; Geraads, 1987; Fooden, 2007).

At present, there is only one species of the genus *Macaca* in Africa, *M. sylvanus* (Barbary macaques) from Algeria (Chiffa, Tigounatine, Ictecifère, Akfadou, and Kherrata) and Morocco (High Atlas, Middle Atlas, and Rif; Fooden, 2007). Field observations have defined feeding

habits as varied and to include an important seasonal component, with diet consisting of more than 100 species of plants, fungi, lichens, mosses, and animal prey (Deag, 1983; Ménard, 1985; Ménard and Vallet, 1986). Studies that have taken into account the annual composition of the diet indicate that seeds, leaves, and herbs are the main foods of Barbary macaques in Akfadou and Tigounatine (Algeria; Ménard, 1985; Ménard and Vallet, 1986, 1996). However, in the Rif mountains of northern Morocco, more than 50% of their diet is based on seeds (Mehlman, 1988), and some studies of the populations that inhabit the Middle Atlas suggest that fruits could constitute a significant part of their diet (Deag, 1983; Drucker, 1984; Ménard and Mohamed, 1999), demonstrating high intra-species local variation at the population level. Nevertheless, the diet of fossil *M. cf. sylvanus* is virtually unknown, with the exception of a study on dental microwear of *Macaca* sp. from the Pliocene of northwestern China, which suggests a hard-object feeder or extractive forager, without grass consumption (Williams and Holmes, 2011).

Previous work on the feeding habits of African Plio-Pleistocene Cercopithecidae, through analysis of stable isotopes and dental microwear, have mainly focused on Eastern Africa (Teaford, 1993; Ungar and Teaford, 1996; Cerling et al., 2011, 2013a,b; Sponheimer et al., 2013; Levin et al., 2015; Shapiro et al., 2016; Robinson et al., 2017; Ungar et al., 2017; Martin et al., 2018; Souron, 2018; Manthi et al., 2020; Merceron et al., 2021) and Southern Africa (Lee-Thorp et al., 1989, 2010; Daegling and Grine, 1999; Codron et al., 2005; El-Zaatari et al., 2005; Scott et al., 2005; Fourie et al., 2008; Williams and Patterson, 2010; Williams and Holmes, 2011; Sponheimer et al., 2013; Grine et al., 2020). In these studies, the most represented genera are *Theropithecus*, *Parapapio*, and *Papio*, among which there is a consensus on the predominance of a graminivore diet with a high component of C₄-based resources for *Theropithecus* (Lee-Thorp et al., 1989; Cerling et al., 2013a; Levin et al., 2015; Souron, 2018) and more diverse food intake with a proportion of C₃ plants in the diet of *Parapapio* and *Papio* (Lee-Thorp et al., 1989; Codron et al., 2005; Fourie et al., 2008; Williams and Patterson, 2010; Levin et al., 2015). In Northern Africa, analysis of the feeding behavior of *Theropithecus oswaldi leakeyi* (Jolly, 1972; Delson, 1993) from Tighennif (ca. 1 Ma) and *Theropithecus atlanticus* (Alemseged and Geraads, 1998) from Ahl al Oughlam (ca. 2.5 Ma) suggest a different pattern in carbon values, with a clear domination of C₃ plants, although other authors suggest bulk-feeding graminivory (Fannin et al., 2021).

Many cercopithecoid fossils have been recovered from the same sites where Hominin fossils have been found (Delson, 1980). The genus *Homo* experienced a similar out-of-Africa dispersion during the Pleistocene and inhabited the same ecosystems as members of Papionini. Therefore, both lineages had to confront the same climatic constrictions and habitat partitioning. Understanding the ecology of the fossil Cercopithecoidea primates is of interest for interpreting the paleoecology and niche partitioning of both groups. Consequently, we aimed to analyze the feeding strategies of *M. cf. sylvanus* from GFT-4.2 on different timescales using, for the first time, a multi-proxy approach. On the one hand, the isotopic signal ($\delta^{18}\text{O}$ and $\delta^{13}\text{C}$) of tooth enamel bioapatite provides dietary information during the first years of the animal's life following the tooth mineralization times proposed by Sirianni and Swindler (1985) for the extant *Macaca nemestrina*. On the other hand, dental microwear analysis, combining buccal (microtexture analysis) and occlusal (low magnification) surfaces, provides dietary information over the long term (weeks to

months; Romero et al., 2012; Hernando et al., 2021) and short term (last days; Semperebon et al., 2004), respectively, but always toward the end of the animal's life. Occlusal microwear studies in primates have suggested that mechanical properties of food items are the primary cause of different microwear pattern among primates. For instance, primates that incorporate hard objects, such as seeds and nuts, have more pitted surfaces than folivores primates that exhibit heavily scratched areas (Ungar, 1996; Scott et al., 2006). Occlusal microwear has a short-term turnover therefore, occlusal microwear patterns provide information on the nature of food intake during the last days prior to death (Teaford and Oyen, 1989). On the other hand, buccal surfaces should only interact with the food items consumed while they are being processed in the oral cavity (Ungar and Teaford, 1996; Romero et al., 2012), and experimental studies have shown that the buccal pattern is more stable through time, at least in the absence of significant dietary shift (Romero et al., 2012).

We hypothesize that combining occlusal and buccal microwear analyses will strengthen the dietary discrimination among these species. Based on the dietary information of extant *M. sylvanus* from Morocco and Algeria, we expect, for the GFT-4.2 specimens, a buccal and occlusal pattern similar to folivore-frugivore primates with the incorporation of seeds during the dry season. In the case of stable carbon and oxygen isotopes, we expect values similar to those of the *Theropithecus* from Ahl al Oughlam (Morocco). That is, a predominance of C₃ plants in the diet and high oxygen values in relation to ungulates. To compare the dental microwear of *M. cf. sylvanus* from GFT-4.2, we present a new reference collection of wild modern cercopithecines including the same individuals for both microwear methods. The integration of the data obtained from these three high-resolution techniques has allowed us to obtain a more precise and robust picture of the feeding habits of *M. cf. sylvanus* from GFT-4.2.

Site: GUEFAÏT-4.2

An interdisciplinary Spanish–Moroccan project started in 2006 as an international cooperation between the Université Mohamed Premier Oujda (UMP, Eastern Morocco) and the Catalan Institute for Human Palaeoecology and Social Evolution from Tarragona (IPHES-CERCA, Catalonia, Spain). The aim of this cooperation is to establish the geochronological and archeo-paleontological context of the Ain Beni Mathar/Guefaït fluvio-lacustrine basin, in the northern part of the High Plateaus (Jerada Province, Eastern Morocco; Aouraghe et al., 2016; Chacón et al., 2016; Sala-Ramos et al., 2022). One of the systematic surveys in the region revealed the fossiliferous level of Guefaït-4. This horizon yielded a rich and diverse faunal assemblage of vertebrates, which was systematically excavated at the GFT-4.2 site (reptiles, amphibians, and both small and large mammals), including the macaque fossil remains analyzed in this work (Alba et al., 2021). The fossil remains were concentrated in a palustrine level constituted of clay and marls, at the base of Unit 2, within the Dhar Iroumyane stratigraphic section (Aouraghe et al., 2019b). The fieldwork carried out between 2017 and 2019 recovered more than 3,000 fossil remains in an excavated area of 28 m². Biostratigraphic correlations with other sites in Northern Africa, such as the lower levels of the Ain Boucherit site in Algeria (Sahnouni et al., 2018) and Ahl al Oughlam in Morocco (Geraads, 2006), suggest an age close to the Plio-Pleistocene boundary (2.58 Ma). The absence of the genus *Equus* (despite the abundance of

Hipparion equid remains; Aouraghe et al., 2019a,b) indicates an age older than ~2.4 Ma (Sahnouni et al., 2018). This chronological limit is supported by the study of the murid assemblage (Agustí et al., 2017; Piñero et al., 2019), the carnivore assemblage (Madurell-Malapeira et al., 2021), and preliminary paleomagnetism studies (Parés et al., 2020).

Materials

A total of six teeth of *M. cf. sylvanus* were recovered from GFT-4.2 during the fieldwork in 2018 and 2019 (Alba et al., 2021). The materials are housed in the Faculty of Science, Mohammed I University in Oujda, Morocco. We discarded two of them for the final analysis because they correspond to dental germ fragments (GFT4.2018-1-P13-191, right M2 or M3, and GFT4.2019-1-R15-45, right M2).

The studied teeth ($n = 4$) correspond to a left upper central incisor (I¹, GFT4.2018-1-Q14-70), a right lower first molar (M₁, the lingual crown fragment of GFT4.2018-1-Q14-13), a right second lower molar (M₂, GFT4.2019-1-S15-65), and a left lower third molar (M₃, GFT4.2019-1-R13-63). All four available fossil teeth (M₁, M₂, M₃, and I¹) were sampled for stable isotope analysis, three (M₁—GFT140, M₂—GFT138, and M₃—GFT137) were sampled for buccal dental microtexture analysis, and two (M₁—GFT140 and M₂—GFT138) were samples for occlusal dental microwear analysis. M₃ was discarded for the occlusal dental microwear analysis due to the absence of wear facets on this surface. Metrical comparisons suggests that the incisor would belong to a different individual than the lower molars. However, it cannot be ruled out that the lower molars were from the same individual (Alba et al., 2021).

The extant Cercopithecoidea comparative sample for the buccal microtexture and occlusal microwear analyses correspond to a total of 41 well-preserved left second lower molars (M₂; Supplementary Table 1). We excluded 10 samples from occlusal microwear analysis and 12 samples from buccal microtexture due to bad preservation or other taphonomic defects on the analyzed surface. The selected species have well-defined habitat and dietary preferences and include five extant species (*Theropithecus gelada*, *Mandrillus sphinx*, *Lophocebus albigena*, *Cercocebus atys*, and *Macaca mulatta*). Whenever possible, we chose specimens of the same taxa from close localities to minimize the variability of their dietary regime. We selected the extant species based on the criteria of phylogenetic affinity (Perelman et al., 2011) and the dental morphology that characterizes all cercopithecines, namely bilophodont molars (Kay and Hylander, 1978; Monson and Hlusko, 2014). This comparative sample served to establish a broad spectrum of ecological and dietary diversity.

1. *Theropithecus gelada* specimens from Ethiopia have a plant-based dietary regime (Dunbar and Bose, 1991), with more than 80% consisting of blades (Mau et al., 2009). However, those *T. gelada* living on the Guassa Plateau also incorporate large quantities of forbs into their diet (Fashing et al., 2014), and are often selective of tender forbs that are rare on the plateau (Souron, 2018).
2. *Mandrillus sphinx* is a frugivore primate that usually lives in gallery forest. Fruits, supplemented with various plant parts like leaves and flowers, constitute the *Mandrillus* diet. However, when fruit is scarce due to seasonality, *M. sphinx* fallback on

mechanically challenging items like seeds and hard-shell fruits from the forest floor (Hoshino, 1985; Lahm, 1986; Tutin et al., 1997; Powell et al., 2017).

3. *Cercocebus atys* forages on the forest's floor and shrub layers, relying on hard-shelled nuts like *Sacoglottis gabonensis* year-round. Yet, due to seasonal fluctuations, the total contribution of *S. gabonensis* can range anywhere from 19% to 80% of the monthly diet (Daegling et al., 2011; McGraw et al., 2014).
4. *Lophocebus albigena* is classified as a hard object feeder (Lambert et al., 2004; McGraw et al., 2011) that consumes a significant portion of hard seeds and nuts (Lambert et al., 2004). In actuality, due to seasonal fluctuations, *L. albigena* is a generalist that consumes a high (40%) percentage of soft ripe fruit (Lambert et al., 2004) in addition to seeds, flowers and young leaves (Poulsen et al., 2001). During seasons with low fruit availability, *L. albigena* will eat bark that, although hard, is rich in protein and soluble sugars (Rogers et al., 1994; Olupot, 1998). This fall-back feeding strategy has also been described for Barbary macaques (*Macaca sylvanus*; Ménard and Mohamed, 1999).
5. *Macaca mulatta* has the largest geographical distribution with its ranges spanning from Afghanistan to India, Pakistan, China, Thailand and Vietnam, among others (Sengupta et al., 2014). Its wide distribution reflects highly opportunistic feeding strategy, even though fruits may constitute as much as 70% of their diet in some regions (Fooden, 2007), yet less than 9% in other ecosystems, such as Pakistan (Goldstein and Richard, 1989). They are semi-terrestrial primates that can also feed up with species that are in different strata of the forest (Albert et al., 2013).

We have not included extant *M. sylvanus* specimens because they have a narrow distribution, and some populations are fed by humans like those of Gibraltar (Spain). Therefore, the baseline samples included in the present study consist of wild specimens with well-defined diet and habitat. To contextualize the oxygen and carbon values of *M. cf. sylvanus*, we have also included contemporaneous herbivore samples from GFT-4.2 corresponding to the same paleontological level 1. These samples include the remains of Tragelaphini ($n = 4$), *Gazella* sp. ($n = 4$), and *Hipparion* sp. ($n = 4$). The list of specimens sampled and analyzed and the raw data for stable isotope analysis are provided in Supplementary Table 2.

Methods

Stable isotope analysis

Tooth surfaces were cleaned with a tungsten abrasive drill bit to remove any adhering external material. Enamel powder for bulk isotope analysis was then obtained using a diamond-tipped drill, passed along the full length of the buccal surface to ensure a representative measurement for the entire period of enamel formation.

Powdered enamel samples (2–6 mg) were chemically treated at the Biomolecular Laboratory of IPHES. Chemical treatment of samples was based on protocols originally proposed by Koch et al. (1997) and later modified by Tornero et al. (2013). The samples were treated for 4 h in 0.1 M acetic acid [CH_3COOH] (0.1 mL solution/0.1 mg of sample), neutralized with distilled water, and freeze-dried.

The $\delta^{18}\text{O}$ and $\delta^{13}\text{C}$ values of tooth enamel bioapatite were measured using an automated carbonate preparation device (KIEL-III) coupled to a

gas-ratio mass spectrometer (Finnigan MAT 252) at the Environmental Isotope Laboratory, University of Arizona, United States. Samples were reacted with dehydrated phosphoric acid under a vacuum at 70°C. The accuracy and precision of the measurements were checked and calibrated using the calcium carbonate international standards (NBS-19 and NBS-18). Replicate measurements of the standards during analysis had errors of $\pm 0.1\text{‰}$ for $\delta^{18}\text{O}$ and $\pm 0.08\text{‰}$ for $\delta^{13}\text{C}$ (1 sigma). Carbon isotope composition is reported in δ notation, where $\delta^{13}\text{C} = [(R_{\text{sample}}/R_{\text{standard}}) - 1]$, $R = {}^{13}\text{C}/{}^{12}\text{C}$, and δ is expressed as per mil notation (‰). Carbon and oxygen values are reported relative to PDB (Vienna Pee Dee Belemnite).

In terrestrial ecosystems there is a marked isotopic distinction between the two photosynthetic pathways in plants, C_3 (Calvin cycle) and C_4 (Hatch-Slack cycle), which differ mainly in their discrimination against ${}^{13}\text{C}$ during the fixation of CO_2 (Farquhar et al., 1989). Modern plants that use the C_3 photosynthetic pathway (including most trees, woody shrubs, bushes, herbs and temperate grasses) have an average isotopic composition of -28.5‰ (global range -20 to -37‰), with -23‰ as the maximum value recommended for typical C_3 plants and a cutoff of -31.5‰ for closed-canopy forests (Kohn, 2010). Due to the fact that we discarded the presence of that environment in GFT-4.2. For this study, we use the average $\delta^{13}\text{C}$ value of -27‰ for modern C_3 plants, excluding analyses from the understory of closed-canopy forests below -31.5‰ (Kohn, 2010). Modern plants that use the C_4 photosynthetic pathway (primarily tropical grasses and sedges) have an average isotopic composition of -12‰ (global range -10 to -14‰ ; Cerling and Harris, 1999; Kohn and Cerling, 2002). Crassulacean Acid Metabolism (CAM) plants can have $\delta^{13}\text{C}$ values corresponding to both C_3 and C_4 plants. However, such plants do not seem to be consumed by primates (Cerling et al., 2013a). The $\delta^{13}\text{C}$ values of atmospheric CO_2 have fluctuated over time and this impacts $\delta^{13}\text{C}$ values in plants (Fiedli et al., 1986; Keeling et al., 2017). We have corrected by $\sim +1.5$ the $\delta^{13}\text{C}$ values of modern plants, due to the difference between the pre-Industrial $\delta^{13}\text{C}_{\text{CO}_2}$ value of $\sim -6.5\text{‰}$ established for the Plio-Pleistocene (Tippie et al., 2010) and the $\delta^{13}\text{C}_{\text{CO}_2}$ value of $\sim -8\text{‰}$ corresponding to the time at which the plants were collected (Kohn, 2010). In this paper, we have used the enamel-diet enrichment factor of $+11.8 \pm 0.3\text{‰}$ calculated for chimpanzees (*Pan troglodytes*) at Ngogo in Kibale National Park in Uganda for macaques (Malone et al., 2021) and the enamel-diet enrichment factor of $+14.1 \pm 0.5\text{‰}$ for ungulates (Cerling and Harris, 1999; Passey et al., 2005) to interpret tooth enamel $\delta^{13}\text{C}$ values and estimate potential consumption of C_3 - or C_4 -plant. These isotopic enrichment factor values for C_3 and C_4 plants are assumed to provide tooth enamel values of $< -18.2\text{‰}$ for closed canopy diets, $< -13.7\text{‰}$ for pure C_3 diets, $< -9.7\text{‰}$ for C_3 -dominated diets, from -9.7 to -0.7‰ for C_3 - C_4 mixed feeders, $> -0.7\text{‰}$ for C_4 -dominated diets and $> +1.3\text{‰}$ for pure C_4 diets in primates and tooth enamel values of $< -15.9\text{‰}$ for closed canopy diets, $< -11.4\text{‰}$ for pure C_3 diets, $< -7.4\text{‰}$ for C_3 -dominated diets, from -7.4 to $+1.6\text{‰}$ for C_3 - C_4 mixed feeders, $> +1.6\text{‰}$ for C_4 -dominated diets and $> +3.6\text{‰}$ for pure C_4 diets in ungulates.

The $\delta^{18}\text{O}$ values in enamel bioapatite is directly related to the drinking water (i.e., springs, rivers, lakes, water holes), plant/food water (i.e., leaves, grass, fruit) and metabolic water by reaction with carbohydrates. Consequently, the precipitation, altitude, humidity/aridity and local temperatures will have an effect on the $\delta^{18}\text{O}$ of locally available water and food (Longinelli, 1984; Luz and Kolodny, 1985; Bryant and Froelich, 1995; Pederzani and Britton, 2019). Oxygen values can also vary within the same habitat, especially in tropical forest

environments, depending on where the species forages. Species feeding in the upper part of the canopy tend to have higher $\delta^{18}\text{O}$ values as opposed to species feeding in the understory which tend to have lower $\delta^{18}\text{O}$ values (Krigbaum et al., 2013; Crowley, 2014; Fannin and McGraw, 2020).

The approximate initial and final mineralization estimated for the extant *Macaca nemestrina* (Sirianni and Swindler, 1985), in relation to the teeth analyzed in fossil *M. cf. sylvanus*, is ca. birth to 1 year for M_1 , I^1 ca. 1 to 2 years for I^1 , ca. 1 to 2.5 years for M_2 and ca. 3 to 4 years for M_3 . Related to dental development, the only permanent tooth to begin development prenatally in the non-human primates is the first molar, which may have one to three cusps mineralized at birth and a complete development of the crown for about 1 year (Sirianni and Swindler, 1985). Relatively recent studies in *Macaca mulatta* suggest that the longest weaning periods are ca. 10 months and the shortest weaning period, between 2 and 5 months (Reitsemma et al., 2015). Considering the data on nursing and mineralization timing in extant *Macaca*, we assume that the I^1 , M_2 and M_3 enamel apatite should reflect a post-weaning signal and the M_1 enamel apatite could therefore reflect a pre-weaning signal for the *M. cf. sylvanus* from GFT-4.2. This allows us to reconstruct the diet from birth to approximately 4 years of age.

The bivariate graphs were made with the Past 4.02 software (Hammer et al., 2001).

Occlusal microwear analysis (low magnification)

Enamel microwear features were observed *via* standard light microscopy using a Zeiss Stemi 2000C stereomicroscope at 35× magnification on high-resolution epoxy casts of teeth, following the cleaning, molding, casting, and examination protocol developed by Solounias and Sempredon (2002) and Sempredon et al. (2004). We used the wear facets of the mesiobuccal cusp of M_2 (normally the paracone of M_2). Before molding, the occlusal surface of each specimen was cleaned using acetone and then 96% ethanol. The surface was molded using high-resolution silicone (Heraeus Kulzer, PROVIL novo Vinylpolysiloxane, Light C.D. 2 regular set), and transparent casts were created using clear epoxy resin (C.T.S. Spain, EPO 150 + K151). A standard 0.16 mm² ocular reticle was employed to quantify the number of small pits (round scars—relatively shallow, refract light easily and consequently appear bright and shiny) and large pits (round scars—deeper, wider, and consequently less refractive), coarse scratches (elongated scars with parallel sides—narrow, and barely etched into the enamel surfaces) and fine scratches (elongated scars with parallel sides—wider and more obviously etched into the enamel surface), gouges (features with irregular edges and much larger and deeper than large pits), puncture pits (craterlike features with regular margins), and cross scratches (oriented perpendicularly to the majority of scratches; Supplementary Figure 1). The scratch width score (SWS) was obtained by giving a score of “0” to teeth with predominantly fine scratches per tooth surface, “1” to those with a mixture of fine and coarse types of textures, and “2” to those with predominantly coarse scratches. We took microphotographs using a Blackfly S digital camera and the Kivv Mic Capture Z software. We used the Helicon Focus 7 software to merge images from various focal planes and to produce a single image with a greater depth of field. We added scale bars using ImageJ. We compared the quantitative results with the reference dataset of the extant

Cercopithecidae species. A single observer (IRP) analyzed all specimens to avoid inter-observer errors. We used the Addinsoft™ XLSTAT-3.02 statistical packages to generate the linear discriminant analysis (LDA) and the correspondence analysis (CA).

Buccal microtexture analysis

The original specimens (Supplementary Table 1) were cleaned with acetone and alcohol-soaked cotton swabs, and vinyl impressions were made using President's Jet Regular Body (Coltène-Whaledent). Positive casts were made with Ferropur (Feroce®) polyurethane (Martínez et al., 2022). Buccal areas were obtained using a Sensofar Plu Neox laser scanning confocal microscope, with a 20× (0.45NA) objective, a spatial sampling of 0.83 μm, an optical resolution of 0.31 μm, a vertical resolution of 20 nm, and a z-step interval of 1 μm (Ibáñez et al., 2020; Martínez et al., 2022). Buccal surfaces were placed perpendicular to the objective in a horizontal position and an image of the field of view of the microscope (600 μm × 500 μm) was obtained (see 3D photosimulations in Supplementary Figure 3). From this image, four subsamples of 138 μm × 102 μm (a standard area in DMTA studies) were cropped using the Mountain 7® software from Digital Surf.¹ We have tested the S-filter prior to the obtention of the 38 parameters, following (Winkler et al., 2022). The workflow included leveling the surface to remove plane inclination, eliminating the curvature applying a 2nd degree polynomial, removing the anomalous points by applying upper and lower 0.5% (a total of 1% of threshold values), following the threshold operator included in the same software and applying a Spatial filter (Gaussian 3 × 3). The Gaussian filter was applied because is widely used for technical surfaces and was applied after the trimming because it is sensitive to outliers (Schulz et al., 2013). Surface roughness was later quantified according to 38 ISO 25178/ISO 12781 parameters (Martínez et al., 2022; Supplementary Table 5).

To standardize the measured area on the buccal surface, we calculated the median of the parameters derived from the several (one to four) measurements of a single buccal surface (Scott et al., 2006; Calandra et al., 2012; Martínez et al., 2022), and used the median per specimen for analysis. We used log-transformed texture data for analyses because some texture parameters have non-normal distributions (Shapiro–Wilk, $p < 0.05$). To ensure we did not exclude any parameter (e.g., Ssk has negative values), we log transformed the data as log [1 + parameter] (Supplementary Table 6). We identified the outliers for both original and log-transformed variables according to their Studentized residual values (absolute value > 3) and removed them from the final data set (Schulz et al., 2013; Martínez et al., 2022). To test the null hypothesis that microwear textures do not differ between teeth from different species, we applied analysis of variance (ANOVA) with pairwise testing (Tukey's honest significant difference [HSD]) to each texture parameter for each species. Where homogeneity of variance test (Levene's test) revealed evidence of unequal variances, we used Welch's ANOVA. We selected the parameters that showed significant differences between species and applied a linear discriminant analysis (LDA). Descriptive statistics, tests and graphs were performed using Addinsoft™ XLSTAT-3.02 statistical packages.

¹ www.digitalsurf.com

Results

Stable isotope analysis

The $\delta^{13}\text{C}$ values of all samples measured in GFT-4.2 range from -12.5 to -8.1‰ ($n = 16$; [Supplementary Table 2](#)). *Macaca cf. sylvanus* carbon values range from -12.5 to -11.8‰ ($n = 4$), with a mean of $-12.3 \pm 0.3\text{‰}$. The values for the herbivore samples from GFT-4.2 are: *Hipparion* sp. ($n = 4$; range = -10.4 to -9.2‰ ; mean = $-9.5 \pm 1\text{‰}$), *Tragelaphini* ($n = 4$; range = -11.3 to -8.1‰ ; mean = $-10 \pm 1.5\text{‰}$), and *Gazella* sp. ($n = 4$; range = -12.2 to -9.4‰ ; mean = $-10.9 \pm 1.1\text{‰}$). The $\delta^{13}\text{C}$ values of the *M. cf. sylvanus* and ungulates from GFT-4.2 range from -12.5 to -8.1‰ , these values correspond to a C_3 -dominated diets for macaques and ungulates.

The $\delta^{18}\text{O}$ values range from -3.5 to 1.8‰ ($n = 16$; [Supplementary Table 2](#)). *Macaca cf. sylvanus* oxygen values range from 0.6 to 1.8‰ , with a mean of $1 \pm 0.5\text{‰}$. The values for the herbivore samples from GFT-4.2 are: *Hipparion* sp. ($n = 4$; range = -3.6 to -0.3‰ ; mean = $-1.8 \pm 0.7\text{‰}$), *Tragelaphini* ($n = 4$; range = -1.4 to 0.3‰ ; mean = $-0.5 \pm 0.4\text{‰}$), and *Gazella* sp. ($n = 4$; range = -1.7 to 1.8‰ ; mean = $-0.4 \pm 0.8\text{‰}$).

The mineralization of M_1 in non-human primates starting from birth of the individual may reflect the nursing signal and thus affecting carbon and oxygen isotope values. However, our results do not indicate a ^{13}C depletion or ^{18}O enrichment in relation to the other *M. cf. sylvanus* teeth analyzed with a post-weaning isotopic signal ([Supplementary Table 2](#)).

Occlusal microwear analysis (low magnification)

The *M. cf. sylvanus* dental microwear pattern is characterized by a high number of pits (NP = 28.5) and a medium number of scratches (NS = 16). The extant cercopithecids show a similar pattern, namely a higher number of pits than scratches ([Table 1](#)). *Lophocebus albigena*

has the highest number of pits (NP = 40.6; raw data in [Supplementary Table 3](#)). The exception is *T. gelada* with a microwear pattern dominated by scratches. Considering the SWS, all species show a high proportion of coarse scratches, and gouges are present in all species except *T. gelada*. *L. albigena* (G = 4.3), *M. sphinx* (G = 3.8), and the fossil macaque (G = 4) have a high abundance of gouges. *L. albigena* (PP = 5.4), *M. mulatta* (PP = 4.3), and the fossil macaque (PP = 4.5) have the highest number of puncture pits; this trait is absent in *T. gelada* and *M. sphinx*. All extant and fossil primates analyzed have a few hyper-coarse scratches and lack cross scratches ([Table 1](#)).

We performed correspondence analysis to compare four microwear variables (pits, scratches, puncture pits, and gouges) of the extant species and macaque from GFT-4.2 ([Figure 1](#)). We plot the results for discriminant functions 1 and 2 (DF1 and DF2, respectively) because they explain a higher percentage of the variance than the other axes ([Supplementary Table 4](#)). Three groups are well defined in the graph. The first group is located on the left and comprises *T. gelada*. The second group, located in the middle, includes *M. sphinx*. The third group, on the right, includes *L. albigena*, *C. atys*, and *M. mulatta*. *T. gelada* falls far from the other species because it has the highest number of scratches (NS = 25.9), the smallest number of pits (NP = 10.1), and the absence of puncture pits and gouges. *M. sphinx* has intermediate microwear values relative to the other two groups. This species has more pits than *T. gelada*, but also more scratches than the components of the third group. *M. sphinx* does not have puncture pits. The last group (*L. albigena*, *C. atys*, and *M. mulatta*) is characterized by a high number of pits (NP > 30) and a small number of scratches (NS < 12). The two specimens of the fossil macaque are located near the third group.

We performed LDA including the four microwear variables (pits, scratches, puncture pits, and gouges) to predict group membership of the fossil *M. cf. sylvanus* specimens from GFT-4.2. The LDA showed significant between-species differences (Wilks' $\lambda = 0.05$; $F = 20.826$; $p < 0.0001$) and correctly classified 90.48% of the species. The two first discriminant functions explained 96.68% of the total variance. DF1 (85.88%) was positively correlated with scratches and negatively correlated with the presence of puncture pits and pits. DF2 (10.80%) was

TABLE 1 Summary of tooth microwear data of the extant and fossil Cercopithecidae analyzed.

Species		Occlusal microwear analysis (low magnifications)							
		N	NS	NP	SWS	PP	HC	G	XS
Extant— <i>Theropithecus gelada</i>	M	7	25.9	10.1	1.6	0	0.4	0	0
	SD		0.8	3.3		0		0	
Extant— <i>Lophocebus albigena</i>	M	5	11.6	40.6	2	5.4	0	4.3	0
	SD		1.5	4.4		1.8		2.2	
Extant— <i>Cercocebus atys</i>	M	7	10.8	31.9	2	3.7	0	3	0
	SD		2.2	2.7		1.3		0.6	
Extant— <i>Macaca mulatta</i>	M	5	11.7	38.5	2	4.3	0	1.9	0
	SD		1	2.6		0.8		1.1	
Extant— <i>Mandrillus sphinx</i>	M	5	15.4	20	2	0	0	3.8	0
	SD		0.7	1.3		0		0.9	
Fossil <i>Macaca cf. sylvanus</i>	M	2	16	28.5	1.5	4.5	0	4	0
	SD		4.2	3.5		0		0	

N, number of specimens; SD, standard deviation; M, mean; NS, average number of scratches; NP, average number of pits; SWS, scratch width score; PP, average number of puncture pits; HC, average number of hypercoarse scratches; G, average number of gouges; XS, average number of cross scratches; (Raw microwear data in [Supplementary Table 3](#)).

negatively correlated with the presence of gouges. GFT140 was classified as *C. atys* (99% of predicted classification probability) and GFT138 was classified as *L. albigena* (83% of predicted probability).

Buccal microtexture analysis

A total of 15 buccal enamel microtexture parameters out of the 38 (39.47%) showed significant differences (ANOVA and Tukey's HSD *post hoc* procedure $p < 0.05$ and Welch correction, see [Supplementary Table 7](#)) among the Cercopithecoidea species. The main significant differences are between the folivore-frugivore *M. mulatta* and the graminivorous *T. gelada* and the hard fruit eater *C. atys* and the folivore-frugivore *M. sphinx*. *T. gelada* mainly differentiates from *M. mulatta* in volume parameters, functional and flatness (V_v , V_{mc} , V_{vc} , S_{xp} , S_{mc} , $FLTp$, $FLTv$, and $FLTq$ $p < 0.05$) while the hard fruit eater differentiates from *M. sphinx* in spatial, feature and flatness parameters (Sal , Shv , $FLTp$, $FLTt$, $FLTv$, and $FLTq$; [Supplementary Figure 4](#)). No significant differences are found between hard fruit eaters taxa, the arboreal *L. albigena* and terrestrial *C. atys* and, only one difference was found between the hard fruit eaters and the graminivorous *T. gelada* (the feature parameter *Spc* between *L. albigena* and *T. gelada* $p < 0.05$).

The LDA includes the 15 parameters to classify the extinct GFT-4.2 samples. DF1 and DF2 account for the 82.51% of the total original variance (Wilks' $\lambda = 0.014$; $F = 1.371$; p -value = 0.143). DF1 (57.15%) is positively correlated with flatness and volume parameters and negatively with *Shv* (mean hill volume) DF2 (25.36%) was positively correlated with all the parameters except for *Spc* ([Figure 2](#); see [Supplementary Table 8](#) for the r values and significance). Overall, 86.21% of the teeth were correctly classified in their taxonomic category. Mixed feeders that incorporate more seeds and leaves compared to the other of species, such as *M. sphinx* and *M. mulatta*, have the highest loadings for DF2. Their buccal surfaces show the greatest texture relief, with sharp features and different slopes and heights compared to hard fruit eaters and *T. gelada*. *M. sphinx* and *M. mulatta* incorporate more seeds and leaves in their diets compared to the rest of species and their buccal surfaces show coarse features (high *Sal*) that is significantly flatter than *T. gelada* and *C. atys*. Moreover, *T. gelada* has the lowest loading for DF1, differing from *L. albigena*, because these features are rounded (lower *Spc*).

The extant LDA model have been used to predict group membership of the fossil specimens from GFT-4.2. GFT-137 is classified as *T. gelada* (74.9% of probability as *T. gelada* and 25.1% as

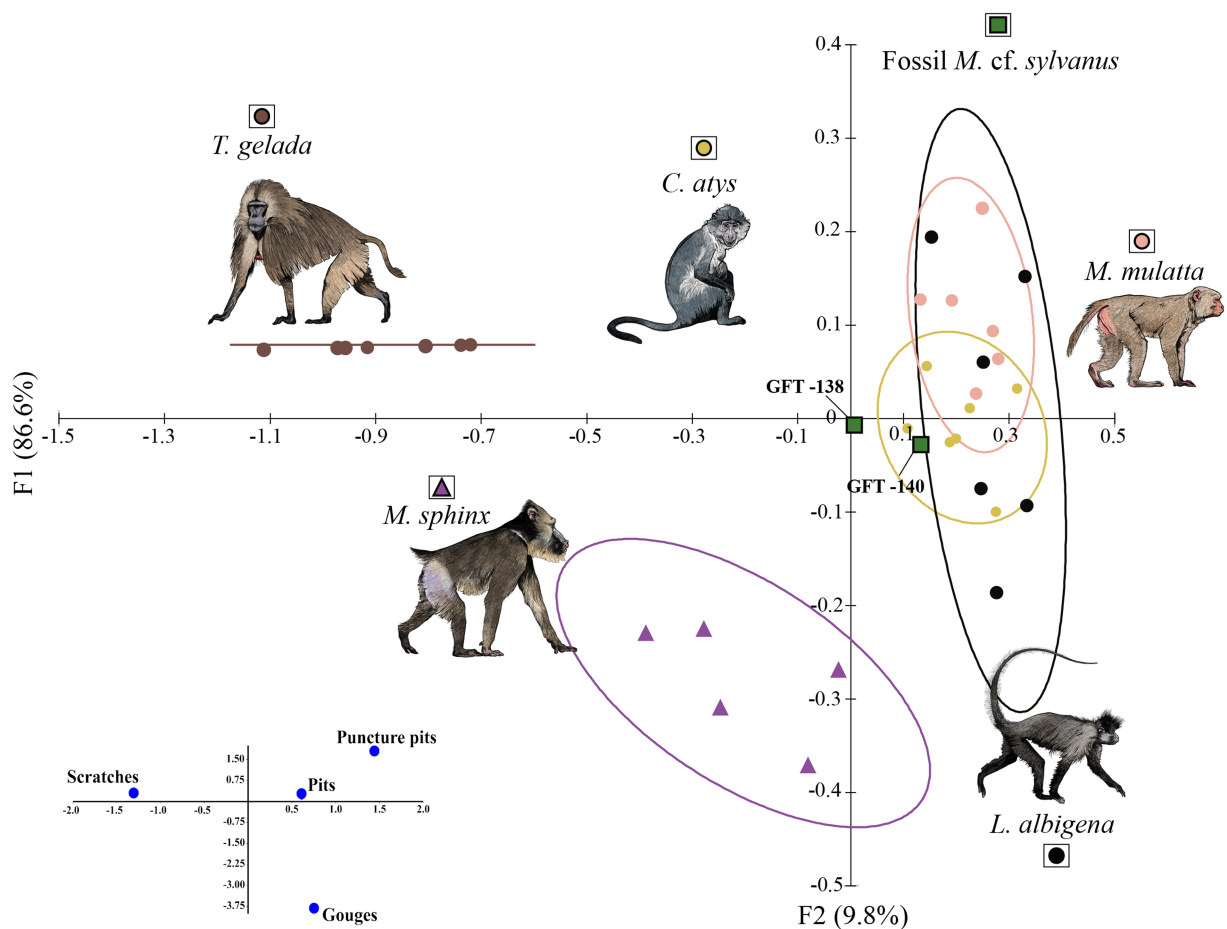


FIGURE 1

Correspondence analysis based on four occlusal microwear variables (number of puncture pits, number of gouges, number of scratches, and number of pits). Ellipses show 68% confidence limits for means (one standard deviation). Eigenvalues, percentages of variance and cumulative percentages of each axis in [Supplementary Table 4](#) (illustrations by Diego Rodríguez-Robredo).

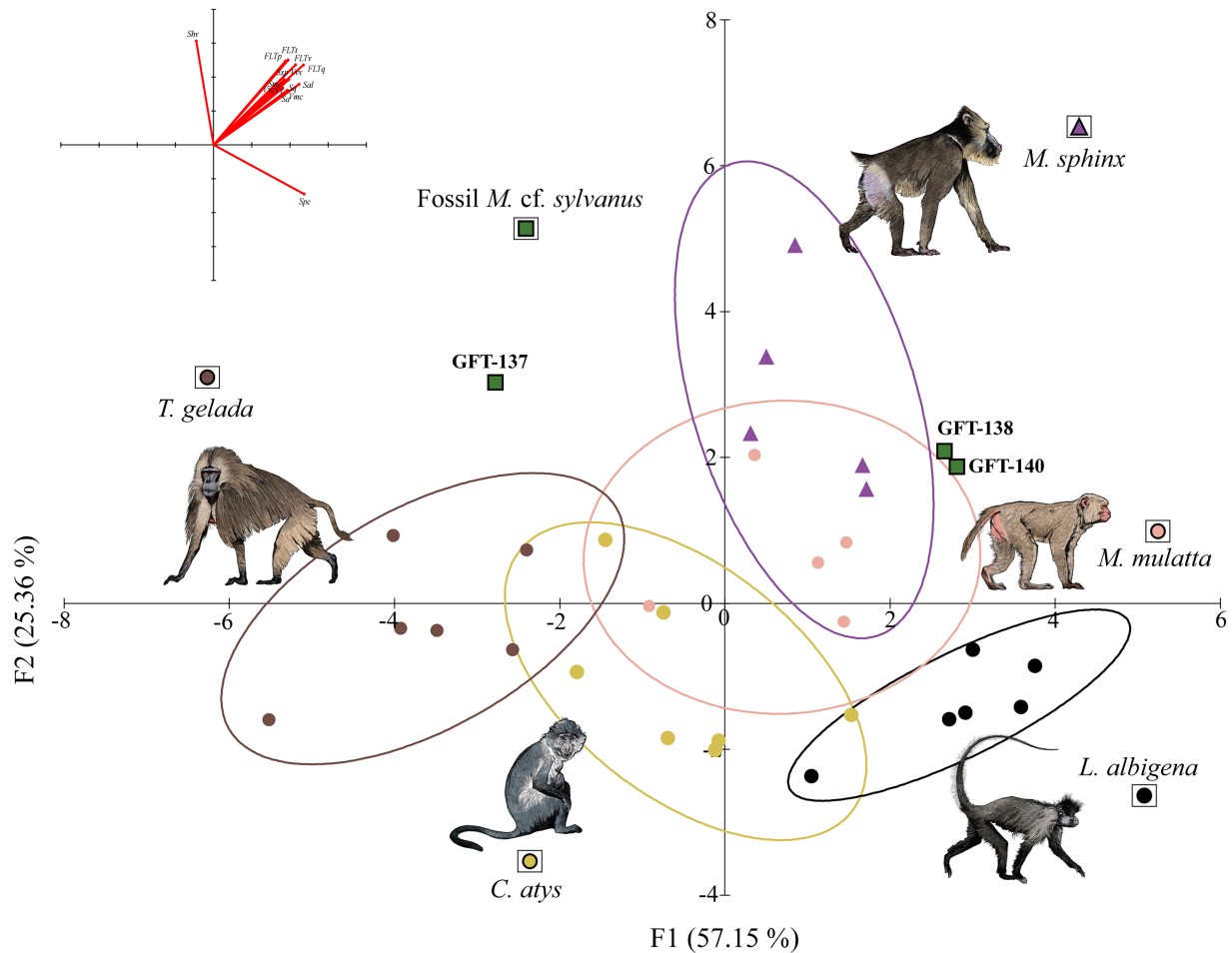


FIGURE 2

Plot of the two first discriminant functions (DF1-2) of buccal-dental microtextural parameters. Ellipses show 68% confidence limits for means (one standard deviation). On the top left are the loadings of the ISO texture parameters onto DFs. Raw data in [Supplementary Table 8](#) (illustrations by Diego Rodríguez-Robredo).

M. sphinx), GFT-138 (Figure 3) as *M. mulatta* (97.5% of probability) and GFT140 as *M. sphinx* (69.8% of probability as *M. sphinx* and 26.7% as *L. albigena*). The mean height, volume and flatness parameters of the three specimens from GFT-4.2 differ significantly ($p < 0.05$) from both *C. atys* and *T. gelada*, and were similar to folivores and seed eaters. Two GFT-4.2 specimens, therefore, resemble to primates that exploit seasonally leaves, fruits and seeds in major proportion, on the ground of mixed forest. GFT137, however, is classified as *T. gelada* a graminivorous primate that exploit also forbs in open ecosystems, due to similarities on buccal microtexture feature parameters.

Discussion

Our multiproxy analysis suggests a different short-term (occlusal) and long-term (buccal) feeding habits of *M. cf. sylvanus* from GFT-4.2, but with an overall dominance of abrasive, tough and brittle food items in an environment dominated by C_3 plants. The most commonly consumed foods would be fruit, seeds and leaves but also some grasses (Table 2). This dietary variety reflects the ability and flexibility of fossil macaques to consume different foods. As well as the richness of

resources, and probably microhabitats, present in the GFT-4.2 area during the Plio-Pleistocene.

Based on short-term resolution, the occlusal microwear analysis classifies the *M. cf. sylvanus* specimens (GFT138 and GFT140) as *L. albigena* and *C. atys*, which have a diet rich in hard fruit and seeds (Poulsen et al., 2001; Shah, 2003; Lambert et al., 2004; Daegling et al., 2011; McGraw et al., 2011, 2012, 2014). The extant *L. albigena* and *C. atys* species and the fossil *M. cf. sylvanus* have puncture pits and gouges, which is a distinctive microwear feature of hard-object feeders (Godfrey et al., 2004; Semperebon et al., 2004; Williams and Geissler, 2014). Both *Cercocebus* and *Lophocebus* have thicker enamel compared to other primate groups, which allows both genera to rely on hard foods throughout the year (McGraw et al., 2012). *Macaca cf. sylvanus* occlusal surfaces differs significantly from the extant *T. gelada*, which is characterized by an almost exclusively graminivorous diet with seasonal incorporation of forbs (Fashing et al., 2014; Jarvey et al., 2018). The occlusal microwear pattern of *T. gelada* is dominated by a high number of scratches and the absence of puncture pits and gouges. This surface is characteristic of animals with grass-dominated feeding habits (Godfrey et al., 2004; Semperebon et al., 2004). Even if it was not the dominant food item in their diet, we cannot exclude that *M. cf. sylvanus* consumed

some grasses due to the large number of scratches found in specimen GFT138.

Occlusal microwear and buccal microtexture analysis group fossil *M. cf. sylvanus* with different extant species, an outcome that is explained by differences in the temporal resolution and turnover of the analyzed tooth surfaces. Buccal microtexture analysis provides medium long-term, compared to occlusal microwear, from weeks to months (Romero et al., 2012) temporal resolution classifying two of the three *M. cf. sylvanus* specimens (GFT 138, and GFT 140) from GFT-4.2 as *M. sphinx* and *M. mulatta*. These species primarily consume fruits, leaves, and seeds in closed and riparian forests during the wet season, and seeds foraged from the ground year-round. The sample included in the present analysis comes from the population that inhabit Pakistan where *M. mulatta* rely primarily on leaves and fruits depending on their availability (Goldstein and Richard, 1989; Sengupta and Radhakrishna,

2016). Both taxa, therefore, consume abrasive items from the ground in mixed forest. *Mandrillus sphinx* and *M. mulatta* diet also includes herbs such as piths and blades and occasionally woody tissue during seasons of heightened fruit scarcity (Sengupta and Radhakrishna, 2016; Hongo et al., 2017). Based on observations of *M. sphinx* from Gabon, more seeds are consumed during the dry season than in the peak fruit season. Moreover, finely crushed seeds in fecal samples indicate that *M. sphinx* uses the occlusal surface to fracture seeds (Hongo et al., 2017), and this mechanical action correlates with gouges on these surfaces (Figure 3; Supplementary Figure 2). *M. sphinx* consumes large nuts, like *S. gabonensis*, during seasons of heightened fruit scarcity (Hongo et al., 2017). Hard items are consumed habitually by *L. albigena* and *C. atys* year-round (McGraw et al., 2012). The microtexture buccal pattern of *M. sphinx*, characterized by higher relief, with peaks and dales and coarse features compared with the rest of analyzed species, may correlate with the presence of more abrasive fractured seeds or phytoliths from the leaves that are processed in the oral cavity while being fractured along occlusal surfaces. The similarity in the microtexture pattern of the two GFT-4.2 specimens with *M. sphinx* and *M. mulatta* suggests that *M. cf. sylvanus* regularly consumed abrasives food items. The LDA of the buccal microtexture plot two specimens (GFT138 and GFT140) close to each other and to the hard fruit eaters (Figures 1,2). All these species rely on hard-shelled fruits and seeds with seasonal fluctuations. Specially, *M. mulatta* diet resembles *M. sphinx* (Sengupta and Radhakrishna, 2016) with more soft fruit ingestion in the former. Both *M. mulatta* and *M. sphinx* incorporate hard and brittle dietary resources but, this is dependent on fruit availability during the year (Sengupta and Radhakrishna, 2016). When fruit is scarce, *M. mulatta* relies heavily on seeds. However, the buccal microtexture pattern of the GFT137 is also similar to *T. gelada* (Figure 2). *Theropithecus gelada* is a graminivorous primate that inhabit the open highlands of Ethiopia and consume grasses and forbs (Jarvey et al., 2018; Souron, 2018).

Three out of four extant species in which the microwear classifies the macaque of GFT-4.2 are species whose diet is related to the presence of trees. In this sense, oxygen values could also reinforce this link. The four *M. cf. sylvanus* specimens (GFT137, GFT138, GFT139, and GFT140) from GFT-4.2 show high $\delta^{18}\text{O}$ values compared with the contemporary ungulates recovered from the same site. The same pattern occurs with other fossil cercopithecines (*T. atlanticus* and *T. oswaldi*) from North Africa (Figure 4). Extant *M. sylvanus* are highly adaptable and have an eclectic diet which adds to the variables that can affect their oxygen isotope values. A significant amount of their water ingestion comes from leaf, fruit and vegetable consumption, especially during the rainy season. Meanwhile, during the dry season, they drink more water from open water sources (Fooden, 2007). In the case of *M. cf. sylvanus*

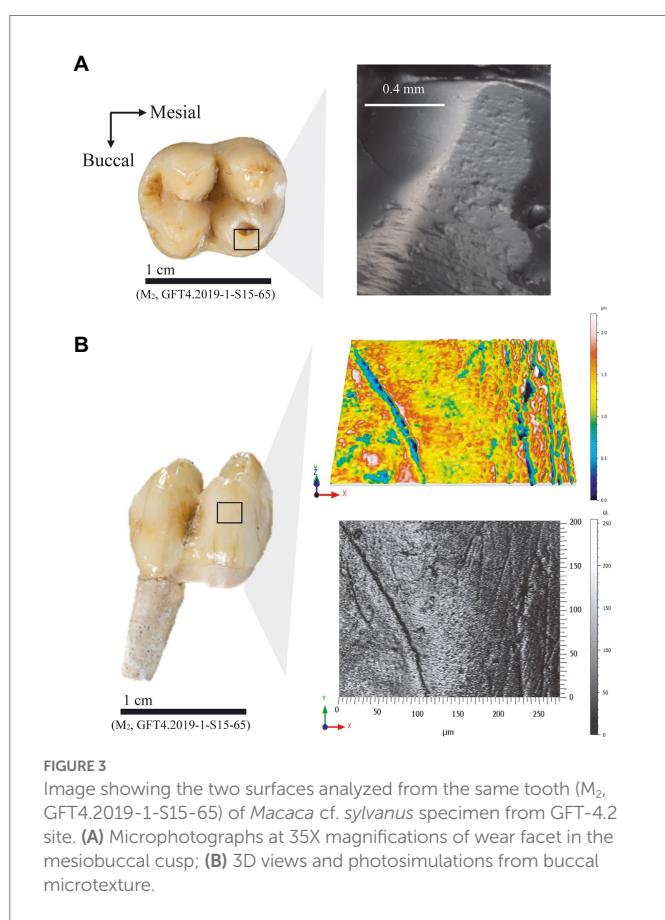
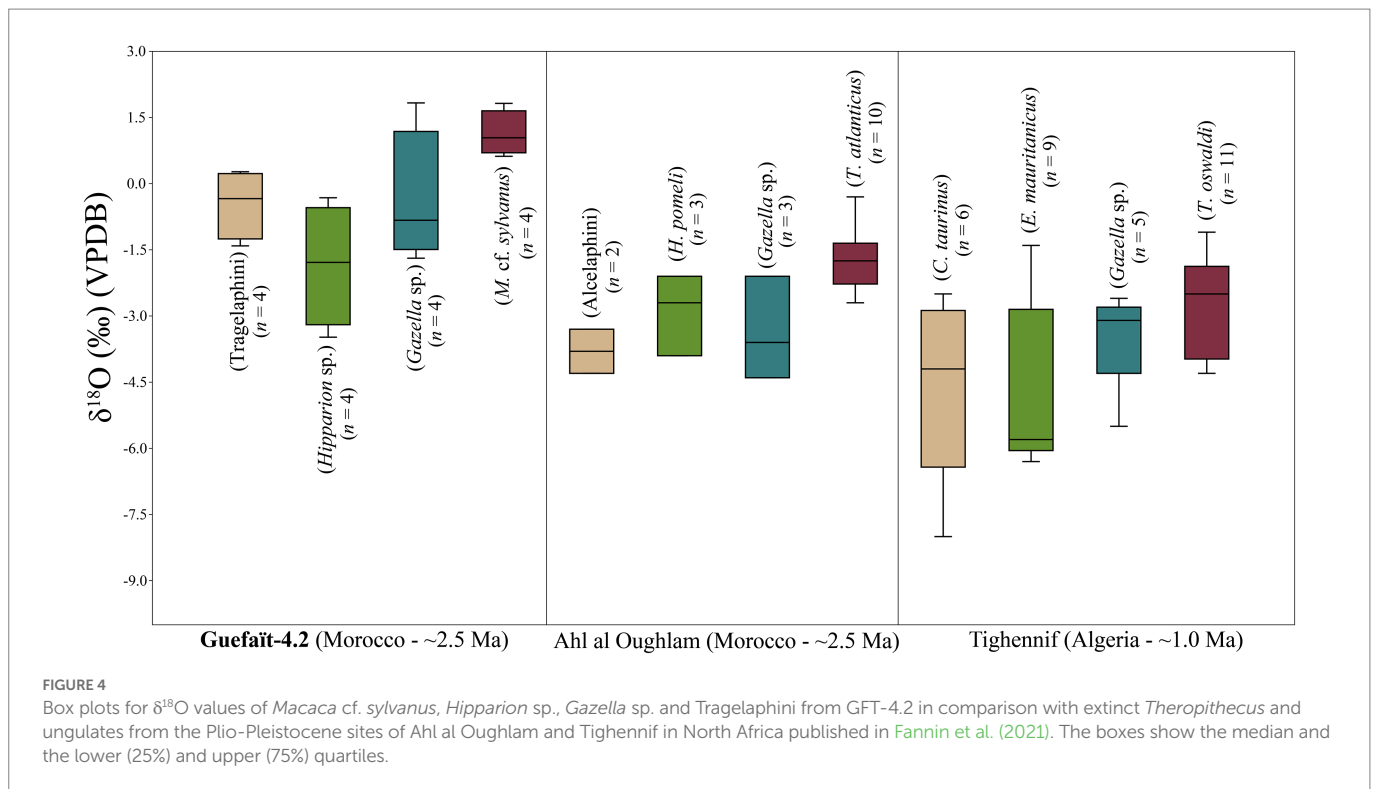


FIGURE 3
Image showing the two surfaces analyzed from the same tooth (M_2 , GFT4.2019-1-S15-65) of *Macaca cf. sylvanus* specimen from GFT-4.2 site. (A) Microphotographs at 35X magnifications of wear facet in the mesiobuccal cusp; (B) 3D views and photosimulations from buccal microtexture.

TABLE 2 Summary of the results provided by the three methods used to reconstruct the diet and habitat of *Macaca cf. sylvanus* from GFT-4.2.

Methods	Diet and habitat reconstruction	Timescales
$\delta^{13}\text{C}$ values	C_3 resource-based diet. Woodland ecosystem.	The first ~4 years of life. Possible nursing signal: M_1 Post-weaning: I^1 , M_2 , M_3
$\delta^{18}\text{O}$ values	Folivore-frugivore foraging in the canopy (Woodland).	The first ~4 years of life. Possible nursing signal: M_1 Post-weaning: I^1 , M_2 , M_3
Buccal microtexture	Folivore-frugivore with hard item consumption and some grass intake (Similar to extant <i>Mandrillus sphinx</i> , <i>Macaca mulatta</i> , and <i>Theropithecus gelada</i>).	Toward the end of the animal's life (Long-term/weeks to months)
Occlusal microwear	Hard-fruit eater with leaf and seed intake (Similar to extant <i>Lophocebus albigena</i> and <i>Cercocebus atys</i>).	Toward the end of the animal's life (short-term/last days)

The timescale represented by the enamel isotopic signature has been defined following the work of dental development in the species *Macaca nemestina* (Sirianni and Swindler, 1985) and the weaning period defined for *M. mulatta* (Reitsema et al., 2015).



from GFT-4.2, the differences in oxygen values in relation to contemporary ungulates could be associated with differential access to and consumption of certain food resources by the primates, such as fresh fruits and leaves from trees. Sun-exposed leaves, especially in arid conditions, are particularly sensitive to evaporative fractionation that could lead to ^{18}O enrichment (Gonfiantini et al., 1965; Barbour, 2007; Crowley et al., 2015; Carter and Bradbury, 2016; Fannin and McGraw, 2020). Other authors argue that this enrichment by evapotranspiration also occurs in other parts of the plant like fruits (Yakir, 1997; McCarroll and Loader, 2004). Paleoenvironmental data of GFT-4.2 based on the study of paleoherpetological and small mammal records, suggest dry conditions in an open woodland habitat with a permanent water body nearby (Agustí et al., 2017; Piñero et al., 2019; Alba et al., 2021).

Considering that aridity affects all GFT-4.2 taxa, we suggest that the oxygen enrichment of *M. cf. sylvanus* may be due to the ingestion of some different foods. An example in extant primates is the one exposed by Moritz et al. (2012) that measured the $\delta^{18}\text{O}_{\text{hair}}$ from two baboon species (*Papio anubis* and *Papio hamadryas*) which inhabit the arid hybrid zone of Awash National Park (Ethiopia). The diets of the two species in this area are similar and both obtain their meteoric water from the same source (Awash River). However, the oxygen values of *P. hamadryas* are relatively enriched due to the ingestion of a greater proportion of ^{18}O -enriched leaf water in the arid thornbush. Krigbaum et al. (2013) show how $\delta^{18}\text{O}_{\text{ap}}$ values of different cercopithecids covary depending on foraging position in the closed tropical canopy forest (Taï forest, Côte d'Ivoire). Higher humidity on the forest floor is associated with low $\delta^{18}\text{O}_{\text{ap}}$ values, with enrichment of ^{18}O observed along a vertical gradient. The *C. atys* exhibits low $\delta^{18}\text{O}_{\text{ap}}$ values relative to guenons and colobines, which reflects the *C. atys* terrestrial foraging habits. Although we do not have a tropical canopy forest in GFT-4.2, these differences in $\delta^{18}\text{O}$ values between feeding on the ground and in the upper parts of the tree could explain the ^{18}O enrichment of macaques compared to ungulates.

The ^{18}O enrichment points to a diet based on tree foraging in a forest ecosystem. These findings are consistent with the microtexture and low magnification signals and support the carbon isotope results of *M. cf. sylvanus* from GFT-4.2. The $\delta^{13}\text{C}$ values indicate consumption of C_3 plants (i.e., trees, shrubs, fruit/seeds, and C_3 -grass adapted to a mild growth season). *M. cf. sylvanus*, *Hipparion* sp., *Gazella* sp. and *Tragelaphini* from GFT-4.2 have been compared with the fossil *T. atlanticus* from Ahl al Oughlam, Morocco (ca. 2.5 Ma) and *T. oswaldi* from Tighennif, Algeria (ca. 1 Ma) and other ungulates from the same sites (Fannin et al., 2021; Figure 5; Supplementary Table 2). The *M. cf. sylvanus* ($n = 4$) mean is $-12.3 \pm 0.3\text{‰}$, the *T. atlanticus* ($n = 10$) mean is $-12.4 \pm 0.8\text{‰}$, and the *T. oswaldi* ($n = 11$) mean is $-11.3 \pm 1.9\text{‰}$ (Figure 5). These three fossil species show similar median carbon values and no consumption of C_4 plants. Except for one individual of *T. oswaldi* from Tighennif with a $\delta^{13}\text{C}$ value of -5.9‰ that includes some C_4 plant consumption.

Our data differ from the mean $\delta^{13}\text{C}$ values of $1.9 \pm 1.8\text{‰}$ ($n = 49$) from Plio-Pleistocene fossils of *Theropithecus* from Eastern Africa, 3.5 to 1.5 Ma. In Southern Africa, *Theropithecus* living 2.8 and 1.6 Ma have mean value of $-2.4 \pm 1.4\text{‰}$ ($n = 13$). In both areas, these species indicate a strongly C_4 -based diet composed mostly of grasses (Cerling et al., 2011; Souron, 2018), especially after the 2 Ma (Figure 6). The carbon values of *M. cf. sylvanus* from GFT-4.2 are similar to the $\delta^{13}\text{C}$ values of C_3 consumers *Papio* (2.1 to 1.6 Ma; $-9.8 \pm 2.3\text{‰}$; $n = 26$), *Parapapio* (2.8 to 1.7 Ma; $-8.4 \pm 2\text{‰}$; $n = 38$), and *Cercopithecoides* (2.8 to 1.7 Ma; $-9.8 \pm 3.6\text{‰}$; $n = 12$) from the Plio-Pleistocene of Southern Africa (Figure 6; Lee-Thorp et al., 1989; Codron et al., 2005). The largest proportion of Southern African cercopithecids fall into the C_3 – C_4 mixed feeders' area, suggesting a consumption of some C_4 plants (Figure 6). Cercopithecids with carbon values resembling those of GFT-4.2 macaques are the *Cercopithecoides haasgati* (2.1 Ma; $-12.3 \pm 1.4\text{‰}$; $n = 2$) from Haasgat HGD, *Papio robinsoni* (1.85 Ma; $-11.2 \pm 0.9\text{‰}$; $n = 5$) and *Parapapio jonesi* (1.85 Ma; $-11.2 \pm 2.3\text{‰}$; $n = 2$) from Swartkrans (Figure 6). The $\delta^{13}\text{C}$ values of *C. haasgati* could

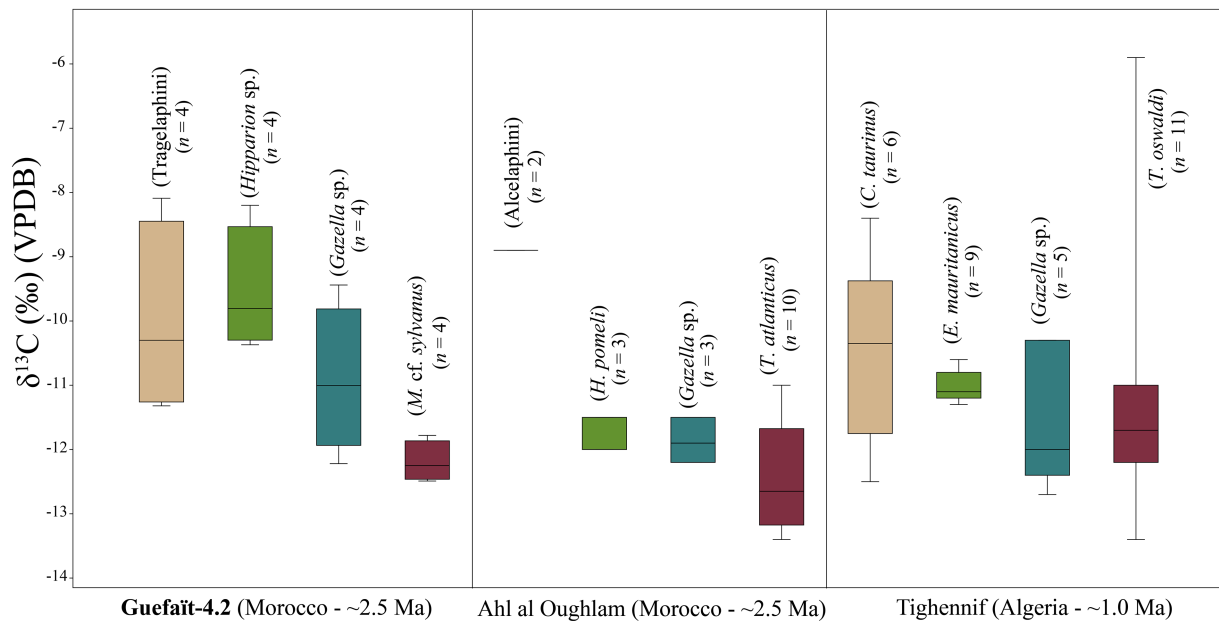


FIGURE 5

Box plots for $\delta^{13}\text{C}$ values of *Macaca cf. sylvanus*, *Hipparion* sp., *Gazella* sp. and *Trachelaphini* from GFT-4.2 in comparison with extinct *Theropithecus* and ungulates from the Plio-Pleistocene sites of Ahl al Oughlam and Tighennif in North Africa published in Fannin et al. (2021). The boxes show the median and the lower (25%) and upper (75%) quartiles.

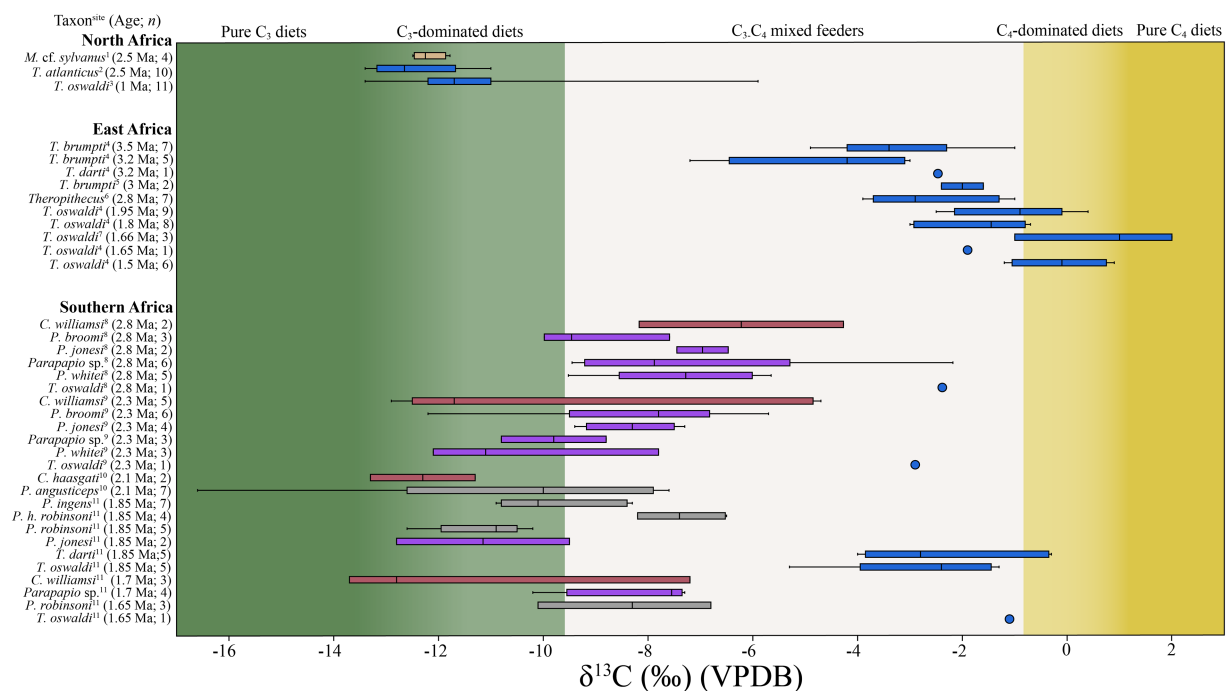


FIGURE 6

Box plots comparing the $\delta^{13}\text{C}$ values of Plio-Pleistocene fossil cercopithecids (3.5 to 1 Ma) from North Africa (data from this study and Fannin et al., 2021). Sites: 1=Guefaït 4.2; 2=Ahl al Oughlam; 3=Tighennif, East Africa [data from Levin et al. (2015), Robinson et al. (2017), and Uno et al. (2018)]. Sites: 4=Koobi Fora, East Turkana; 5=Nachuki, West Turkana; 6=Ledi-Geraru, Gurumaha; 7=Bed II, Olduvai and Southern Africa [data from Levin et al. (2015)]. Sites: 8=Makapansgat, 3 and 4; 9=Sterkfontein; 10=Haasgat HGD; 11=Swartkrans. The boxes show the median and the lower (25%) and upper (75%) quartiles. The colors of the box plots represent the different genus (beige for *Macaca*, blue for *Theropithecus*, red for *Cercopithecoides*, purple for *Parapapio*, and gray for *Papio*).

indicate a preference toward food sources associated with closed woodland environments (Adams et al., 2013). This interpretation is consistent with the carbon values of all of them, including the fossil macaque. Feeding habits of *P. robinsoni* and *P. jonesi* from Swartkrans have been reconstructed as a frugivore-folivore on the basis of cusp form (Benefit, 2000). We also propose this using the occlusal and buccal microwear for *M. cf. sylvanus* from GFT-4.2, although the exploitation of grasses and forbs in a more open habitats cannot rule out due to the buccal microtexture pattern of GFT137 and the high number of scratches on the occlusal surface of GFT138. Carbon isotopic signal of the *Macaca* from GFT-4.2 would indicate that these consumed grasses would be C_3 . Consumption of C_3 grasses has also been identified in the diet of *T. oswaldi* from the Plio-Pleistocene site of Ahl al Oughlam (Morocco), as well as in extant *T. gelada* at Guassa Plateau (Ethiopia; Fannin et al., 2021).

The microwear analysis shows that the diet of the fossil macaque is close, among others, to that of extant *M. sphinx*, *L. albigena*, and *C. atys*, species that live in dense tropical forests. Isotopic studies on extant *M. sphinx* and *C. atys* have shown carbon values strongly affected by canopy effect. According to Oelze et al. (2020), the $\delta^{13}C$ values of *M. sphinx* hair sections from Gabon are within the range ($-25.1\text{‰} \pm 0.3\text{‰}$) of those obtained from the hair of chimpanzees and gorillas in Loango National Park. Like these species, mandrills live in dense forest habitats. Another study by Krigbaum et al. (2013) on bone apatite from seven sympatric cercopithecine species, including *C. atys*, in the Taï forest (Côte d'Ivoire) obtained carbon values range between -19.9‰ and -17.9‰ for all species. In contrast, the carbon values of *M. cf. sylvanus* from GFT-4.2 ($-12.3 \pm 0.3\text{‰}$) do not correspond to those of a species foraging in a closed canopy forest. Considering the enamel-diet enrichment factor for primates ($+11.8 \pm 0.3\text{‰}$; Malone et al., 2021) and the cutoff of -30‰ ($\delta^{13}C_{CO_2}$ corrected by $\sim +1.5$) for closed-canopy forests (Kohn, 2010), the $\delta^{13}C$ values of tooth enamel for a diet in a closed-canopy forest should be lower than $\sim -18\text{‰}$ for fossil *Macaca*. The carbon values of the taxa analyzed are compatible with an open woodland. This is in line with the paleoherpetological and small mammal work in which taxa characteristic of open woodland have been defined (Agustí et al., 2017; Piñero et al., 2019).

The use of these three methods has allowed us to produce a paleodietary reconstruction at different times in the life of the individuals, although we cannot discard that the analyzed molars belong to the same specimen. The isotopic signal, corresponding to approximately the first 4 years of life, is in agreement with the data of the two dental microwear proxies in the diet-tree relationship for *M. cf. sylvanus*, and the absence of C_4 typical of open grassland. Buccal and occlusal microwear turnover is a dynamic process; however, the buccal signal is more stable in the long term and may indicate the diet consumed year-round (Romero et al., 2012). Whereas the low magnification occlusal microwear results may indicate the consumption of hard fruit and seeds similar to mangabeys the last days or weeks prior to death (Semperebon et al., 2004), perhaps representing the diet of a single season. The buccal microtexture analysis suggest that the abrasiveness of their diet was similar to primates (*M. sphinx* and *M. mulatta*) that consumes hard, tough, and brittle food items year round with the incorporation of leaves, and the consumption of grasses as *T. gelada* does. The complementarity of these proxies helps to differentiate between seasonal, short-term durophagous species from those that exploit tough and brittle items actively in a long term, broadening the dietary range of consumed resources throughout the year.

Conclusion

Our research represents the first report related to the feeding ecology of fossil *Macaca* during the Plio-Pleistocene in Africa. Our results highlight a tight correlation between the fossil *M. cf. sylvanus* specimens from GFT-4.2 and extant primates with a predominant abrasive, tough and brittle food items. Evidence from the multiproxy analysis suggests that the macaques foraged for food in a wooded habitat, but also foraging in more open environments. The versatility of macaques to occupy wide habitat ranges makes them a useful candidate for analogies with hominins and for understanding how they adapted to different environments. Evidence of early hominins in North Africa is dated close to the Plio-Pleistocene boundary (ca. 2.4 Ma) at the Ain Boucherit site in Algeria. The ecological context of this first human population is a key question to understand the dispersions of humans and other mammals in these territories. Considering the proximity of GFT to Ain Boucherit, understanding the feeding ecology of *M. cf. sylvanus* from GFT may provide clues about some of the ecological resources that these early humans may have had. This initial investigation is only one step toward understanding the feeding habits of *M. cf. sylvanus*. More data are needed from additional individuals to be able to confidently interpret foraging ecology of this species.

Data availability statement

The original contributions presented in the study are included in the article/Supplementary material, further inquiries can be directed to the corresponding authors. The surface data are available from the corresponding author upon reasonable request.

Author contributions

IR-P, LM, FR, CT, and FE-S conceived and designed this research. IR-P and LM performed the laboratory analyses and collected and analyzed the data. JI provided access to the laser scanning confocal microscope. AA, AR-H, JM, HA, AO, HH, IR-P, HM, MS, RS-R and MC participated in the fieldwork and provided materials and background for the research. MC, RS-R, and HA are in charge of the project administration and the funding acquisition. AR-H supervised the excavation. AR-H, HA, and JM identified the faunal remains. All authors contributed to the article and approved the submitted version.

Funding

This work has been funded by Palarq Foundation, Spanish Ministry of Culture and Sport (Ref: 42-T002018N0000042853 and 170-T002019N0000038589), Direction of Cultural Heritage (Ministry of Culture and Communication, Morocco), Faculty of Sciences (Mohamed 1r University of Oujda, Morocco), INSAP (Institut National des Sciences de l'Archéologie et du Patrimoine), Spanish Ministry of Science, Innovation and Universities (Ref: CGL2016-80975-P, CGL2016-80000-P, PGC2018-095489-B-I00, and PID2021-122355NB-C33), Research Groups Support of the Generalitat de Catalunya (2017 SGR 836, 2017 SGR 1040, 2017 SGR 102, and 2017 SGR 859) and PDC2021-121613-I00 and PID2020-112963GB-I00 by ERDF A way of making Europe, by the European Union. RS-R, MC,

AR-H, and CT research was funded by CERCA Programme Generalitat de Catalunya. IR-P is beneficiary of predoctoral fellowship (2020-FI-B-00731) funded by AGAUR and the Fons Social Europeu (FSE). AA and is beneficiary of a fellowship from the Erasmus Mundus Program to do the Master in Quaternary and Prehistory at the Universitat Rovira i Virgili (Tarragona, Spain). CT was supported by the Spanish Ministry of Science and Innovation through the “Ramón y Cajal” program (RYC2020-029404-I). The Institut Català de Paleoeologia Humana i Evolució Social (IPHES-CERCA) has received financial support from the Spanish Ministry of Science and Innovation through the “María de Maeztu” program for Units of Excellence (CEX2019-000945-M), including the postdoctoral fellowships of AR-H.

Acknowledgments

We thank the Direction of Cultural Heritage (Ministry of Culture and Communication, Morocco), the Jerada Government and Local Authorities of Ain Béni Mathar and Guefait for local permits to develop geological, archeological and paleontological fieldwork in the region. Lastly, we want to thank the local population for their support, collaboration and help in the discovery of some of the fossils and certain archeo-paleontological sites and above all for their hospitality and welcome. We also acknowledge the two reviewers, the editor Brooke E. Crowley and Robert Patalano for the constructive comments raised, which considerably helped to improve this research and Diego

Rodríguez-Robredo for the illustrations of extant primates. We are grateful to all the curators and technical personnel of the different institutions where the extant specimens were molded.

Conflict of interest

The authors declare that the research was conducted in the absence of any commercial or financial relationships that could be construed as a potential conflict of interest.

Publisher's note

All claims expressed in this article are solely those of the authors and do not necessarily represent those of their affiliated organizations, or those of the publisher, the editors and the reviewers. Any product that may be evaluated in this article, or claim that may be made by its manufacturer, is not guaranteed or endorsed by the publisher.

Supplementary material

The Supplementary material for this article can be found online at: <https://www.frontiersin.org/articles/10.3389/fevo.2023.1011208/full#supplementary-material>

References

- Adams, J. W., Kegley, A. D. T., and Krigbaum, J. (2013). New faunal stable carbon isotope data from the Haasgat HGD assemblage, South Africa, including the first reported values for *Papio angusticeps* and *Cercopithecoides haasgati*. *J. Hum. Evol.* 64, 693–698. doi: 10.1016/j.jhevol.2013.02.009
- Agustí, J., Piñero, P., Blain, H.-A., Aouraghe, H., Haddoumi, H., El Hammouti, K., et al. (2017). “The early Pleistocene small vertebrates from Guefait 4 (Jerada, Morocco)” in *III Jornadas de Prehistoria Africana. Book of abstracts*. eds. M. G. Chacón, I. Caceres, V. Altés, M. Soto, and R. Sala (Tarragona), 49.
- Alba, D. M., Delson, E., Carnevale, G., Colombero, S., Delfino, M., Giuntelli, P., et al. (2014). First joint record of *Mesopithecus* and cf. *Macaca* in the Miocene of Europe. *J. Hum. Evol.* 67, 1–18. doi: 10.1016/j.jhevol.2013.11.001
- Alba, D. M., Rodríguez-hidalgo, A., Aouraghe, H., Van Der Made, J., Oujaa, A., Haddoumi, H., et al. (2021). New macaque fossil remains from Morocco. *J. Hum. Evol.* 153, 102951–102958. doi: 10.1016/j.jhevol.2021.102951
- Albert, A., Hambuckers, A., Culot, L., Savini, T., and Huynen, M. C. (2013). Frugivory and seed dispersal by northern pigtailed macaques (*Macaca leonina*), in Thailand. *Int. J. Primatol.* 34, 170–193. doi: 10.1007/s10764-012-9649-5
- Alemseged, Z., and Geraads, D. (1998). *Theropithecus atlanticus* (Thomas, 1884) (primates: Cercopithecidae) from the late Pliocene of Ahl al Oughlam, Casablanca, Morocco. *J. Hum. Evol.* 34, 609–621. doi: 10.1006/jhev.1998.9999
- Aouraghe, H., Haddoumi, H., Hajji, N.-E., Sala, R., Rodríguez-Hidalgo, A., Van der Made, J., et al. (2019a). “Découverte d’un nouveau site paléontologique plio-quaternaire dans le Maroc oriental (Guefait 4, province de Jerada),” in *Recueil des Résumés, 23ème Colloque des Bassins Sédimentaires. Fès, 21–23 novembre*, 34–35.
- Aouraghe, H., Haddoumi, H., Rodríguez-Hidalgo, A., Van der Made, J., Piñero, P., Agustí, J., et al. (2019b). “Nouvelles données sur le site du Pliocène Final/Pléistocène Inférieur de Guefait 4: Mission 2019,” in *10ème Rencontre des Quaternaristes Marocains, Kénitra. Recueil des Résumés*, 47–48.
- Aouraghe, H., Sala, R., and Chacón, M. (2016). “Bilan de dix ans de recherches archéologiques dans la région de Jerada (Maroc Oriental),” in *10 Ans de Recherches & de Coopération Scientifiques Maroc-Espagne dans la Province de Jerada (Maroc Oriental). Séminaire International sur le Patrimoine Archéologique de la Province de Jerada. Recueil du Séminaire, Jerada*, 8–9.
- Arambourg, C. (1959). Vertébrés continentaux du Miocene Supérieur de l’Afrique du Nord. *Publ. du Serv. la Cart. Geol. l’Algérie Paleontologie Mem.* 4, 5–159.
- Arambourg, C. (1979). *Vertébrés villafranchiens d’Afrique du Nord (Artiodactyles, Carnivores, Primates, Reptiles, Oiseaux)*. Paris: Fondation Singer-Polignac.
- Arambourg, C., and Coque, R. (1959). Le gisement villafranchien de l’Ain Brimba (Sud-Tunisien) et sa faune. *Bull. la Société Géologique Fr.* 8, 607–614.
- Barbour, M. M. (2007). Stable oxygen isotope composition of plant tissue: a review. *Funct. Plant Biol.* 34, 83–94. doi: 10.1071/FP06228
- Benefit, B. R. (2000). “Old World monkey origins and diversification: an evolutionary study of diet and dentition” in *Old World monkeys*. eds. P. F. Whitehead and C. J. Jolly (Cambridge: Cambridge University Press), 133–179.
- Bryant, J. D., and Froelich, P. N. (1995). A model of oxygen isotope fractionation in body water of large mammals. *Geochim. Cosmochim. Acta* 59, 4523–4537. doi: 10.1016/0016-7037(95)00250-4
- Calandra, I., Schulz, E., Pinnow, M., Krohn, S., and Kaiser, T. M. (2012). Teasing apart the contributions of hard dietary items on 3D dental microtextures in primates. *J. Hum. Evol.* 63, 85–98. doi: 10.1016/j.jhevol.2012.05.001
- Carter, M. L., and Bradbury, M. W. (2016). Oxygen isotope ratios in primate bone carbonate reflect amount of leaves and vertical stratification in the diet. *Am. J. Primatol.* 78, 1086–1097. doi: 10.1002/ajp.22432
- Cerling, T. E., Chritz, K. L., Jablonski, N. G., Leakey, M. G., and Manthi, F. K. (2013a). Diet of *Theropithecus* from 4 to 1 ma in Kenya. *Proc. Natl. Acad. Sci. U. S. A.* 110, 10507–10512. doi: 10.1073/pnas.1222571110
- Cerling, T. E., and Harris, J. M. (1999). Carbon isotope fractionation between diet and biopitite in ungulate mammals and implications for ecological and paleoecological studies. *Oecologia* 120, 347–363. doi: 10.1007/s004420050868
- Cerling, T. E., Manthi, F. K., Mbua, E. N., Leakey, L. N., Leakey, M. G., Leakey, R. E., et al. (2013b). Stable isotope-based diet reconstructions of Turkana Basin hominins. *Proc. Natl. Acad. Sci. U. S. A.* 110, 10501–10506. doi: 10.1073/pnas.1222568110
- Cerling, T. E., Mbua, E., Kirera, F. M., Manthi, F. K., Grine, F. E., Leakey, M. G., et al. (2011). Diet of *Paranthropus boisei* in the early Pleistocene of East Africa. *Proc. Natl. Acad. Sci. U. S. A.* 108, 9337–9341. doi: 10.1073/pnas.1104627108
- Chacón, M., Aouraghe, H., Agustí, J., Álvarez, C., Arnold, L., Benito-Calvo, A., et al. (2016). “Ten years of archaeological research in the Ain Béni-Mathar/Guefait region (eastern Morocco): results and perspectives,” in *58th Annual Meeting in Budapest. March 29th e April 2nd 2016. Hugo Obermaier-Gesellschaft für Erforschung des Eiszeitalers und der Steinzeit e.V., Erlangen*, 21–22.
- Codron, D., Luyt, J., Lee-Thorp, J. A., Sponheimer, M., De Ruiter, D., and Codron, J. (2005). Utilization of savanna-based resources by Plio-Pleistocene baboons. *S. Afr. J. Sci.* 101, 245–248. doi: 10.5167/uzh-25352

- Crowley, B. E. (2014). Oxygen isotope values in bone carbonate and collagen are consistently offset for New World monkeys. *Biol. Lett.* 10:20140759. doi: 10.1098/rsbl.2014.0759
- Crowley, B. E., Melin, A. D., Yeakel, J. D., and Dominy, N. J. (2015). Do oxygen isotope values in collagen reflect the ecology and physiology of neotropical mammals? *Front. Ecol. Evol.* 3, 1–12. doi: 10.3389/fevo.2015.00127
- Daegling, D. J., and Grine, F. E. (1999). Terrestrial foraging and dental microwear in *Papio ursinus*. *Primates* 40, 559–572. doi: 10.1007/BF02574831
- Daegling, D. J., McGraw, W. S., Ungar, P. S., Pampush, J. D., Vick, A. E., and Bitty, E. A. (2011). Hard-object feeding in sooty mangabeys (*Cercocebus atys*) and interpretation of early hominin feeding ecology. *PLoS One* 6:e23095. doi: 10.1371/journal.pone.0023095
- Deag, J. (1983). Feeding habits of *Macaca sylvanus* (primates: Cercopithecinae) in a commercial Moroccan cedar forest. *J. Zool.* 201, 570–575. doi: 10.1111/j.1469-7998.1983.tb05080.x
- Delson, E. (1974). Preliminary review of Cercopithecoid distribution in the Circum Mediterranean region. *Mem. du Bur. Rech. Geol. Minieres* 78, 131–135.
- Delson, E. (1980). “Fossil macaques, phyletic relationships and a scenario of deployment” in *The macaques. studies in ecology, behavior and evolution*. ed. D. E. Lindburg (New York: Van Nostrand), 10–30.
- Delson, E. (1993). “*Theropithecus* fossils from Africa and India and the taxonomy of the genus” in *Theropithecus: The rise and fall of a primate genus*. ed. N. G. Jablonski (Cambridge: Cambridge University Press), 157–189.
- DeMenocal, P. B. (1995). Plio-Pleistocene African climate. *Science* 270, 53–59. doi: 10.1126/science.270.5233.53
- Drucker, G. (1984). “The feeding ecology of the barbary macaque and cedar forest conservation in the Moroccan Moyen atlas” in *The barbary macaque: A case study in conservation*. ed. J. E. Fa (New York: Springer), 135–164.
- Dunbar, R. I. M., and Bose, U. (1991). Adaptation to grass-eating in gelada baboons. *Primates* 32, 1–7. doi: 10.1007/BF02381596
- Elton, S. (2007). Environmental correlates of the cercopithecoid radiations. *Folia Primatol.* 78, 344–364. doi: 10.1159/000105149
- Elton, S., and O'Regan, H. J. (2014). Macaques at the margins: the biogeography and extinction of *Macaca sylvanus* in Europe. *Quat. Sci. Rev.* 96, 117–130. doi: 10.1016/j.quascirev.2014.04.025
- El-Zaatari, S., Grine, F. E., Teaford, M. F., and Smith, H. F. (2005). Molar microwear and dietary reconstructions of fossil Cercopithecoidea from the Plio-Pleistocene deposits of South Africa. *J. Hum. Evol.* 49, 180–205. doi: 10.1016/j.jhevol.2005.03.005
- Fannin, L. D., and McGraw, W. S. (2020). Does oxygen stable isotope composition in primates vary as a function of vertical stratification or folivorous behaviour? *Folia Primatol.* 91, 219–227. doi: 10.1159/000502417
- Fannin, L. D., Yeakel, J. D., Venkataraman, V. V., Seyoum, C., Geraads, D., Fashing, P. J., et al. (2021). Carbon and strontium isotope ratios shed new light on the paleobiology and collapse of *Theropithecus*, a primate experiment in graminivory. *Palaeogeogr. Palaeoclimatol. Palaeoecol.* 572:110393. doi: 10.1016/j.palaeo.2021.110393
- Farquhar, G. D., Ehleringer, R., and Hubick, K. T. (1989). Carbon isotope discrimination and photosynthesis. *Annu. Rev. Plant Physiol. Plant Mol. Biol.* 40, 505–537.
- Fashing, P. J., Nguyen, N., Venkataraman, V. V., and Kerby, J. T. (2014). Gelada feeding ecology in an intact ecosystem at Guassa, Ethiopia: variability over time and implications for theropithecoid and hominin dietary evolution. *Am. J. Phys. Anthropol.* 155, 1–16. doi: 10.1002/ajpa.22559
- Fiedli, H., Löttscher, H., Oeschger, H., Siegenthaler, U., and Stauffer, B. (1986). Ice core record of the $^{13}\text{C}/^{12}\text{C}$ ratio of atmospheric CO_2 in the past two centuries. *Nature* 324, 237–238. doi: 10.1038/324237a0
- Fleagle, J. G. (2013). *Primate adaptation and evolution*. 3rd. San Diego: Academic Press.
- Fooden, J. (2007). Systematic review of the barbary macaque, *Macaca sylvanus* (Linnaeus, 1758). *FIELDIANA Zool.* 26, 1–60. doi: 10.5962/bhl.title.14256
- Fourie, N. H., Lee-Thorp, J. A., and Ackermann, R. R. (2008). Biogeochemical and craniometric investigation of dietary ecology, niche separation, and taxonomy of plio-pleistocene cercopithecoids from the Makapansgat limeworks. *Am. J. Phys. Anthropol.* 135, 121–135. doi: 10.1002/ajpa.20713
- Geraads, D. (1987). Dating the northern African cercopithecoid fossil record. *Hum. Evol.* 2, 19–27. doi: 10.1007/BF02436528
- Geraads, D. (2006). The late Pliocene locality of Ahl al Oughlam, Morocco: vertebrate fauna and interpretation. *Trans. R. Soc. South Africa* 61, 97–101. doi: 10.1080/00359190609519958
- Godfrey, L. R., Semperebon, G. M., Jungers, W. L., Sutherland, M. R., Simons, E. L., and Solounias, N. (2004). Dental use wear in extinct lemurs: evidence of diet and niche differentiation. *J. Hum. Evol.* 47, 145–169. doi: 10.1016/j.jhevol.2004.06.003
- Goldstein, S. J., and Richard, A. F. (1989). Ecology of rhesus macaques (*Macaca mulatta*) in Northwest Pakistan. *Int. J. Primatol.* 10, 531–567. doi: 10.1007/BF02739364
- Gonfiantini, R., Gratzu, S., and Tongiorgi, E. (1965). “Oxygen isotopic composition of water in leaves,” in *Isotopes and Radiation in Soil Plant Nutrition Studies* (Vienna: International atomic energy agency), 405–410.
- Grine, F. E., Lee-Thorp, J., Blumenthal, S., Sponheimer, M., Teaford, M. F., Ungar, P. S., et al. (2020). “Stable carbon isotope and molar microwear variability of south African australopithecids in relation to paleohabitats and taxonomy” in *Dental Wear in evolutionary and biocultural contexts* (New York: Elsevier Inc.), 187–223.
- Hammer, Ø., Harper, D. A., and Ryan, P. D. (2001). Past: paleontological statistics software package for education and data analysis. *Palaeontol. Electron.* 76, 543–551. doi: 10.1016/j.bcp.2008.05.025
- Hernando, R., Gamarra, B., McCall, A., and Cheronet, O. (2021). Integrating buccal and occlusal dental microwear with isotope analyses for a complete paleodietary reconstruction of Holocene populations from Hungary. *Sci. Rep.* 11:7034. doi: 10.1038/s41598-021-86369-x
- Hongo, S., Nakashima, Y., Akomo-Okoue, E. F., and Mindonga-Nguelet, F. L. (2017). Seasonal change in diet and habitat use in wild mandrills (*Mandrillus sphinx*). *Int. J. Primatol.* 39, 27–48. doi: 10.1007/s10764-017-0007-5
- Hoshino, J. (1985). Feeding ecology of mandrills (*Mandrillus sphinx*) in campo animal reserve, Cameroon. *Primates* 26, 248–273. doi: 10.1007/BF02382401
- Hughes, J. K., Elton, S., and O'Regan, H. J. (2008). *Theropithecus* and “out of Africa” dispersal in the Plio-Pleistocene. *J. Hum. Evol.* 54, 43–77. doi: 10.1016/j.jhevol.2007.06.004
- Ibáñez, J. J., Jiménez-Manchón, S., Blaise, É., Nieto-Espineta, A., and Valenzuela-Lamas, S. (2020). Discriminating management strategies in modern and archaeological domestic caprines using low-magnification and confocal dental microwear analyses. *Quat. Int.* 557, 23–38. doi: 10.1016/j.quaint.2020.03.006
- Jablonski, N. G. (2002). “Fossil Old World monkeys: the late Neogene radiation” in *The primate fossil record*. ed. W. Hartwig (Cambridge: Cambridge University Press), 225–300.
- Jablonski, N., and Frost, S. (2010). “Cercopithecoidea” in *Cenozoic mammals of Africa*. eds. L. Werdelin and W. J. Sanders (Berkeley: University of California Press), 393–428.
- Jablonski, N. G., Whitfort, M. J., Roberts-Smith, N., and Qinqi, X. (2000). The influence of life history and diet on the distribution of catarrhine primates during the Pleistocene in eastern Asia. *J. Hum. Evol.* 39, 131–157. doi: 10.1006/jhev.2000.0405
- Jarvey, J. C., Low, B. S., Pappano, D. J., Bergman, T. J., and Beehner, J. C. (2018). Graminivory and fallback foods: annual diet profile of geladas (*Theropithecus gelada*) living in the Simien Mountains National Park, Ethiopia. *Int. J. Primatol.* 39, 105–126. doi: 10.1007/s10764-018-0018-x
- Joleaud, L. (1926). “Les vestiges des anciennes associations biologiques de la Berbérie” in *Compte Rendu Publié par le Secrétaire Général du Congrès*. eds. A. Cattani and G. Douin (Cairo: Congrès International de Géographie), 128–134.
- Jolly, C. J. (1972). The classification and natural history of *Theropithecus* (*Simopithecus*) (Andrews, 1916), baboons of the African Plio-Pleistocene. *Bull. Br. Museum Geol.* 22, 1–124. doi: 10.5962/p.313829
- Kato, A., Tang, N., Borries, C., Papakyriakos, A. M., Hinde, K., Miller, E., et al. (2014). Intra- and interspecific variation in macaque molar enamel thickness. *Am. J. Phys. Anthropol.* 155, 447–459. doi: 10.1002/ajpa.22593
- Kay, R. F., and Hylander, W. L. (1978). “The dental structure of mammalian folivores with special reference to Primates and Phalangeroidea (Marsupialia),” in *The Ecology of arboreal folivores*. ed. G. Montgomery (Washington: Smithsonian Institution Press), 173–191.
- Keeling, R. F., Graven, H. D., Welp, L. R., Resplandy, L., Bi, J., Piper, S. C., et al. (2017). Atmospheric evidence for a global secular increase in carbon isotopic discrimination of land photosynthesis. *Proc. Natl. Acad. Sci. U. S. A.* 114, 10361–10366. doi: 10.1073/pnas.1619240114
- Koch, P. L., Tuross, N., and Fogel, M. L. (1997). The effects of sample treatment and diagenesis on the isotopic integrity of carbonate in biogenic hydroxylapatite. *J. Archaeol. Sci.* 24, 417–429. doi: 10.1006/jasc.1996.0126
- Kohn, M. J. (2010). Carbon isotope compositions of terrestrial C_3 plants as indicators of (paleo)ecology and (paleo)climate. *Proc. Natl. Acad. Sci. U. S. A.* 107, 19691–19695. doi: 10.1073/pnas.1004933107
- Kohn, M. J., and Cerling, T. E. (2002). Stable isotope compositions of biological apatite. Phosphates geochemical, Geobiol. *Mater. Importance* 48, 455–488. doi: 10.2138/rmg.2002.48.12
- Krigbaum, J., Berger, M. H., Daegling, D. J., and Scott McGraw, W. (2013). Stable isotope canopy effects for sympatric monkeys at Taï Forest, Côte d'Ivoire. *Biol. Lett.* 9, 20130466–20130410. doi: 10.1098/rsbl.2013.0466
- Lahm, S. A. (1986). Diet and habitat preference of *Mandrillus sphinx* in Gabon: implications of foraging strategy. *Am. J. Primatol.* 11, 9–26. doi: 10.1002/ajp.1350110103
- Lambert, J. E., Chapman, C. A., Wrangham, R. W., and Conklin-Brittain, N. L. (2004). Hardness of cercopithecine foods: implications for the critical function of enamel thickness in exploiting fallback foods. *Am. J. Phys. Anthropol.* 125, 363–368. doi: 10.1002/ajpa.10403
- Lee-Thorp, J. A., Sponheimer, M., Passey, B. H., De Ruiter, D. J., and Cerling, T. E. (2010). Stable isotopes in fossil hominin tooth enamel suggest a fundamental dietary shift in the Pliocene. *Philos. Trans. R. Soc. B Biol. Sci.* 365, 3389–3396. doi: 10.1098/rstb.2010.0059
- Lee-Thorp, J. A., van der Merwe, N. J., and Brain, C. K. (1989). Isotopic evidence for dietary differences between two extinct baboon species from Swartkrans. *J. Hum. Evol.* 18, 183–189. doi: 10.1016/0047-2484(89)90048-1
- Levin, N. E., Haile-Selassie, Y., Frost, S. R., and Saylor, B. Z. (2015). Dietary change among hominins and cercopithecids in Ethiopia during the early Pliocene. *Proc. Natl. Acad. Sci. U. S. A.* 112, 12304–12309. doi: 10.1073/pnas.1424982112

- Longinelli, A. (1984). Oxygen isotopes in mammal bone phosphate: a new tool for paleohydrological and paleoclimatological research? *Geochim. Cosmochim. Acta* 48, 385–390. doi: 10.1016/0016-7037(84)90259-X
- Luz, B., and Kolodny, Y. (1985). Oxygen isotope variations in phosphate of biogenic apatites. IV. Mammal teeth and bones. *Earth Planet. Sci. Lett.* 75, 29–36. doi: 10.1016/0012-821X(85)90047-0
- Madurell-Malapeira, J., Rodríguez-Hidalgo, A., Aouraghe, H., Haddoumi, H., Lucenti, S. B., Oujaa, A., et al. (2021). First small-sized *Dinofelis*: evidence from the Plio-Pleistocene of North Africa. *Quat. Sci. Rev.* 265:107028. doi: 10.1016/j.quascirev.2021.107028
- Malone, M. A., MacLatchy, L. M., Mitani, J. C., Kityo, R., and Kingston, J. D. (2021). A chimpanzee enamel-diet $\delta^{13}\text{C}$ enrichment factor and a refined enamel sampling strategy: implications for dietary reconstructions. *J. Hum. Evol.* 159:103062. doi: 10.1016/j.jhevol.2021.103062
- Manthi, F. K., Cerling, T. E., Chritz, K. L., and Blumenthal, S. A. (2020). Diets of mammalian fossil fauna from Kanapoi, northwestern Kenya. *J. Hum. Evol.* 140:102338. doi: 10.1016/j.jhevol.2017.05.005
- Martin, F., Plastiras, C. A., Merceron, G., Souron, A., and Boissier, J. R. (2018). Dietary niches of terrestrial cercopithecines from the Plio-Pleistocene Shungura formation, Ethiopia: evidence from dental microwear texture analysis. *Sci. Rep.* 8, 14052–14013. doi: 10.1038/s41598-018-32092-z
- Martínez, L. M., Estebanaranz-Sánchez, F., Romero, A., Ibáñez, J. J., Hidalgo-Trujillo, L., Avià, Y., et al. (2022). Effectiveness of buccal dental-microwear texture in African Cercopithecoidea dietary discrimination. *Am. J. Biol. Anthropol.* 179, 678–686. doi: 10.1002/ajpa.24635
- Mau, M., Südekum, K. H., Johann, A., Sliwa, A., and Kaiser, T. M. (2009). Saliva of the gaminivorous *Theropithecus gelada* lacks proline-rich proteins and tannin-binding capacity. *Am. J. Primatol.* 71, 663–669. doi: 10.1002/ajp.20701
- McCarroll, D., and Loader, N. J. (2004). Stable isotopes in tree rings. *Quat. Sci. Rev.* 23, 771–801. doi: 10.1016/j.quascirev.2003.06.017
- McGraw, W. S., Pampush, J. D., and Daegling, D. J. (2012). Brief communication: enamel thickness and durophagy in mangabeys revisited. *Am. J. Phys. Anthropol.* 147, 326–333. doi: 10.1002/ajpa.21634
- McGraw, W. S., Vick, A. E., and Daegling, D. J. (2011). Sex and age differences in the diet and ingestive behaviors of sooty mangabeys (*Cercocebus atys*) in the tai forest, Ivory Coast. *Am. J. Phys. Anthropol.* 144, 140–153. doi: 10.1002/ajpa.21402
- McGraw, W. S., Vick, A. E., and Daegling, D. J. (2014). Dietary variation and food hardness in sooty mangabeys (*Cercocebus atys*): implications for fallback foods and dental adaptation. *Am. J. Phys. Anthropol.* 154, 413–423. doi: 10.1002/ajpa.22525
- Mehlman, P. T. (1988). Food resources of the wild barbary macaque (*Macaca sylvanus*) in high-altitude fir forest, Ghomaran Rif. *Morocco. J. Zool.* 214, 469–490. doi: 10.1111/j.1469-7998.1988.tb03754.x
- Meloro, C., and Elton, S. (2012). The evolutionary history and palaeo-ecology of primate predation: *Macaca sylvanus* from Plio-Pleistocene Europe as a case study. *Folia Primatol.* 83, 216–235. doi: 10.1159/000343494
- Ménard, N. (1985). Le régime alimentaire de *Macaca sylvanus* dans différents habitats d'Algérie. I. Régime en chaîne décidue. *Rev. d'écologie* 40, 451–466. doi: 10.3406/rev.1985.5296
- Ménard, N., and Mohamed, Q. (1999). Bark stripping and water availability: a comparative study between Moroccan and Algerian barbary macaques (*Macaca sylvanus*). *Rev. Estomatol.* 54, 123–132. doi: 10.3406/rev.1999.2282
- Ménard, N., and Vallet, D. (1986). Le régime alimentaire de *Macaca sylvanus* dans différents habitats d'Algérie: II.—Régime en forêt sempervirente et sur les sommets rocheux. *Rev. d'écologie* 41, 173–192. doi: 10.3406/rev.1986.5381
- Ménard, N., and Vallet, D. (1996). “Demography and ecology of barbary macaques (*Macaca sylvanus*) in two different habitats” in *Evolution and ecology of macaque societies*. eds. J. E. Fa and D. G. Lindberg (Cambridge: Cambridge University Press), 106–131.
- Merceron, G., Kallend, A., Francisco, A., Louail, M., Martin, F., Plastiras, C.-A., et al. (2021). Further away with dental microwear analysis: food resource partitioning among Plio-Pleistocene monkeys from the Shungura formation, Ethiopia. *Palaeogeogr. Palaeoclimatol. Palaeoecol.* 572:110414. doi: 10.1016/j.palaeo.2021.110414
- Monson, T. A., and Hlusko, L. J. (2014). Identification of a derived dental trait in the Papionini relative to other old world monkeys. *Am. J. Phys. Anthropol.* 155, 422–429. doi: 10.1002/ajpa.22586
- Moritz, G. L., Fourie, N., Yeakel, J. D., Phillips-Conroy, J. E., Jolly, C. J., Koch, P. L., et al. (2012). Baboons, water, and the ecology of oxygen stable isotopes in an arid hybrid zone. *Physiol. Biochem. Zool.* 85, 421–430. doi: 10.1086/667533
- Oelze, V. M., Percher, A. M., Nsi Akoué, G., El Ksabi, N., Willaume, E., and Charpentier, M. J. E. (2020). Seasonality and interindividual variation in mandrill feeding ecology revealed by stable isotope analyses of hair and blood. *Am. J. Primatol.* 82, e23206–e23211. doi: 10.1002/ajp.23206
- Olupot, W. (1998). Long-term variation in mangabey (*Cercocebus albigena johnstoni* Lydekker) feeding in Kibale National Park, Uganda. *Afr. J. Ecol.* 8, 70–72. doi: 10.1016/S1468-1641(10)60457-4
- Ouahbi, Y., Aberkan, M., and Serre, F. (2001). Climatic effect on late Pleistocene mammals from the northern Rif Mountains, northern Morocco. *Paleontol. Zhurnal* 35, 641–646.
- Parés, J., Álvarez, C., Pla-Pueyo, S., Benito-Calvo, A., Duval, M., Aouraghe, H., et al. (2020). “Magnetostratigraphy of the sedimentary fill of the Ain Beni Mathar-Guefaït Basin (high plateau, E Morocco),” in *AGU fall meeting* (San Francisco).
- Passey, B. H., Cerling, T. E., Schuster, G. T., Robinson, T. F., Roeder, B. L., and Krueger, S. K. (2005). Inverse methods for estimating primary input signals from time-averaged isotope profiles. *Geochim. Cosmochim. Acta* 69, 4101–4116. doi: 10.1016/j.gca.2004.12.002
- Pederzani, S., and Britton, K. (2019). Oxygen isotopes in bioarchaeology: principles and applications, challenges and opportunities. *Earth Sci. Rev.* 188, 77–107. doi: 10.1515/9783110441154-001
- Perelman, P., Johnson, W. E., Roos, C., Seuánez, H. N., Horvath, J. E., Moreira, M. A. M., et al. (2011). A molecular phylogeny of living primates. *PLoS Genet.* 7, e1001342–e1001317. doi: 10.1371/journal.pgen.1001342
- Piñero, P., Agustí, J., Haddoumi, H., El Hammouti, K., Chacón, M. G., and Sala-Ramos, R. (2019). *Golunda aouraghei* sp. nov., the last representative of the genus *Golunda* in Africa. *J. Vertebr. Paleontol.* 39, 1–6. doi: 10.1080/02724634.2020.1742726
- Piñero, P., Agustí, J., Oms, O., Fierro, I., Montoya, P., Mansino, S., et al. (2017). Early Pliocene continental vertebrate fauna at Puerto de la Cadena (SE Spain) and its bearing on the marine-continental correlation of the late Neogene of eastern Betics. *Palaeogeogr. Palaeoclimatol. Palaeoecol.* 479, 102–114. doi: 10.1016/j.palaeo.2017.04.020
- Pomel, A. (1892). Sur un macaque fossile des phosphorites quaternaires de l'Algérie, *Macacus trarsensis*. *Comptes Rendus l'Académie des Sci. la vie* 115, 157–160.
- Poulsen, J. R., Clark, C. J., and Smith, T. B. (2001). Seasonal variation in the feeding ecology of the grey-cheeked mangabey (*Lophocebus albigena*) in Cameroon. *Am. J. Primatol.* 54, 91–105. doi: 10.1002/ajp.1015
- Powell, L. E., Isler, K., and Barton, R. A. (2017). Re-evaluating the link between brain size and behavioural ecology in primates. *Proc. R. Soc. B Biol. Sci.* 284, 20171765–20171768. doi: 10.1098/rspb.2017.1765
- Reitsema, L. J., Partrick, K. A., and Muir, A. B. (2015). Inter-individual variation in weaning among rhesus macaques (*Macaca mulatta*): serum stable isotope indicators of suckling duration and lactation. *Am. J. Primatol.* 78, 1113–1134. doi: 10.1002/ajp.22456
- Robinson, J. R., Rowan, J., Campisano, C. J., Wynn, J. G., and Reed, K. E. (2017). Late Pliocene environmental change during the transition from *Australopithecus* to *homo*. *Nat. Ecol. Evol.* 1, 1–7. doi: 10.1038/s41559-017-0159
- Rogers, E., Tutin, C., Parnell, R., Voysey, B., and Fernandez, M. (1994). “Seasonal feeding on bark by gorillas: an unexpected keystone food?,” in *Abstracts from the XIVTH Congress of the International Primatological Society* (Strasbourg), 154.
- Romero, A., Galbany, J., De Juan, J., and Pérez-Pérez, A. (2012). Brief communication: short- and long-term in vivo human buccal-dental microwear turnover. *Am. J. Phys. Anthropol.* 148, 467–472. doi: 10.1002/ajpa.22054
- Roos, C., Kothé, M., Alba, D. M., Delson, E., and Zinner, D. (2019). The radiation of macaques out of Africa: evidence from mitogenome divergence times and the fossil record. *J. Hum. Evol.* 133, 114–132. doi: 10.1016/j.jhevol.2019.05.017
- Sahnouni, M., Parés, J. M., Duval, M., Cáceres, I., Harichane, Z., van der Made, J., et al. (2018). 1.9-million- and 2.4-million-year-old artifacts and stone tool-cutmarked bones from Ain Boucherit, Algeria. *Science* 362, 1297–1301. doi: 10.1126/science.aau0008
- Sala-Ramos, R., Aouraghe, H., Haddoumi, H., Morales, J., Rodríguez-Hidalgo, A., Tornero, C., et al. (2022). Article Pleistocene and Holocene peopling of Jerada province, eastern Morocco: introducing a research project Le peuplement humain pendant le Pléistocène et l' Holocène dans la province de Jerada, Maroc oriental: introduction d' un projet de recherche. *Bull. d'Archéologie Marocaine* 27, 27–40.
- Schulz, E., Calandra, I., and Kaiser, T. M. (2013). Feeding ecology and chewing mechanics in hoofed mammals: 3D tribology of enamel wear. *Wear* 300, 169–179. doi: 10.1016/j.wear.2013.01.115
- Scott, R. S., Ungar, P. S., Bergstrom, T. S., Brown, C. A., Childs, B. E., Teaford, M. F., et al. (2006). Dental microwear texture analysis: technical considerations. *J. Hum. Evol.* 51, 339–349. doi: 10.1016/j.jhevol.2006.04.006
- Scott, R. S., Ungar, P. S., Bergstrom, T. S., Brown, C. A., Grine, F. E., Teaford, M. F., et al. (2005). Dental microwear texture analysis shows within-species diet variability in fossil hominins. *Nature* 436, 693–695. doi: 10.1038/nature03822
- Semprebon, G. M., Godfrey, L. R., Solounias, N., Sutherland, M. R., and Jungers, W. L. (2004). Can low-magnification stereomicroscopy reveal diet? *J. Hum. Evol.* 47, 115–144. doi: 10.1016/j.jhevol.2004.06.004
- Sengupta, A., Mcconkey, K. R., and Radhakrishna, S. (2014). Seed dispersal by rhesus macaques *Macaca mulatta* in northern India. *Am. J. Primatol.* 76, 1175–1184. doi: 10.1002/ajp.22302
- Sengupta, A., and Radhakrishna, S. (2016). Influence of fruit availability on fruit consumption in a generalist primate, the rhesus macaque *Macaca mulatta*. *Int. J. Primatol.* 37, 703–717. doi: 10.1007/s10764-016-9933-x
- Shah, N. (2003). *Foraging strategies in two sympatric mangabey species (Cercocebus agilis and Lophocebus albigena)*. PhD Dissertation, Stony Brook University.
- Shapiro, A. E., Venkataraman, V. V., Nguyen, N., and Fashing, P. J. (2016). Dietary ecology of fossil *Theropithecus*: inferences from dental microwear textures of extant geladas from ecologically diverse sites. *J. Hum. Evol.* 99, 1–9. doi: 10.1016/j.jhevol.2016.05.010
- Sirianni, J. E., and Swindler, D. R. (1985). *Growth and development of the pigtailed macaque*. Boca Raton: CRC Press.

- Solounias, N., and Semperebon, G. M. (2002). Advances in the reconstruction of ungulate ecomorphology with application to early fossil equids. *Am. Museum Novit.* 3366, 1–49. doi: 10.1206/0003-0082(2002)366<0001:AITROU>2.0.CO;2
- Souron, A. (2018). Morphology, diet, and stable carbon isotopes: on the diet of *Theropithecus* and some limits of uniformitarianism in paleoecology. *Am. J. Phys. Anthropol.* 166, 261–267. doi: 10.1002/ajpa.23414
- Sponheimer, M., Alemseged, Z., Cerling, T. E., Grine, F. E., Kimbel, W. H., Leakey, M. G., et al. (2013). Isotopic evidence of early hominin diets. *Proc. Natl. Acad. Sci. U. S. A.* 110, 10513–10518. doi: 10.1073/pnas.1222579110
- Stromer, E. (1913). Mitteilungen über Wirbeltierreste aus dem Mittelplicän des Natrontales (Ägypten). *Zeitschrift der Dtsch. Geol. Gesellschaft Band* 65, 350–372.
- Stromer, E. (1920). Mitteilungen über Wirbeltierreste aus dem Mittelplicän des Natrontales (Ägypten). 5. Nachtrag zu 1. Affen. *Sitz. Math.-Phys. Kl. Bay. Akad. Wiss. München: Verlag der Bayerischen Akademie der Wissenschaften*, 345–370.
- Szalay, F., and Delson, E. (1979). *Evolutionary history of the primates*. New York: Academic Press.
- Teaford, M. F. (1993). “Dental microwear and diet in extant and extinct *Theropithecus*: preliminary analyses” in *Theropithecus: The rise and fall of a primate genus*. ed. N. G. Jablonski (Cambridge: Cambridge University Press), 331–350.
- Teaford, M. F., and Oyen, O. J. (1989). Differences in the rate of molar Wear between monkeys raised on different diets. *J. Dent. Res.* 68, 1513–1518. doi: 10.1177/00220345890680110901
- Tipple, B. J., Meyers, S. R., and Pagani, M. (2010). Carbon isotope ratio of Cenozoic CO₂: a comparative evaluation of available geochemical proxies. *Paleoceanography* 25, 1–11. doi: 10.1029/2009pa001851
- Tornero, C., Bălăşescu, A., Ughetto-Monfrin, J., Voinea, V., and Balasse, M. (2013). Seasonality and season of birth in early Eneolithic sheep from Cheia (Romania): methodological advances and implications for animal economy. *J. Archaeol. Sci.* 40, 4039–4055. doi: 10.1016/j.jas.2013.05.013
- Tosi, A. J., Detwiler, K. M., and Disotell, T. R. (2005). X-chromosomal window into the evolutionary history of the guenons (primates: Cercopithecini). *Mol. Phylogenet. Evol.* 36, 58–66. doi: 10.1016/j.ympev.2005.01.009
- Tutin, C. E. G., Ham, R. M., White, L. J. T., and Harrison, M. J. S. (1997). The primate community of the lope reserve, Gabon: diets, responses to fruit scarcity, and effects on biomass. *Am. J. Primatol.* 42, 1–24. doi: 10.1002/(SICI)1098-2345(1997)42:1<1::AID-AJP1>3.0.CO;2-0
- Ungar, P. S. (1996). Dental microwear of European Miocene catarrhines: evidence for diets and tooth use. *J. Hum. Evol.* 31, 335–366. doi: 10.1006/jhev.1996.0065
- Ungar, P. S., Abella, E. F., Burgman, J. H. E., Lazagabaster, I. A., Scott, J. R., Delezene, L. K., et al. (2017). Dental microwear and Pliocene paleocommunity ecology of bovids, primates, rodents, and suids at Kanapoi. *J. Hum. Evol.* 140, 102315–102310. doi: 10.1016/j.jhev.2017.03.005
- Ungar, P. S., and Teaford, M. F. (1996). Preliminary examination of non-occlusal dental microwear in anthropoids: implications for the study of fossil primates. *Am. J. Phys. Anthropol.* 100, 101–113. doi: 10.1002/(SICI)1096-8644(199605)100:1<101::AID-AJPA10>3.0.CO;2-4
- Uno, K. T., Rivals, F., Bibi, F., Pante, M., Njau, J., and de la Torre, I. (2018). Large mammal diets and paleoecology across the Oldowan–Acheulean transition at Olduvai Gorge, Tanzania from stable isotope and tooth wear analyses. *J. Hum. Evol.* 120, 76–91. doi: 10.1016/j.jhev.2018.01.002
- Williams, F. L. E., and Geissler, E. (2014). Reconstructing the diet and paleoecology of Plio-Pleistocene *Cercopithecoides williamsi* from Sterkfontein, South Africa. *PALAIOS* 29, 483–494. doi: 10.2110/palo.2014.046
- Williams, F. L. E., and Holmes, N. A. (2011). Evidence of terrestrial diets in Pliocene Eurasian papionins (Mammalia: primates) inferred from low-magnification stereomicroscopy of molar enamel use-wear scars. *PALAIOS* 26, 720–729. doi: 10.2110/palo.2010.p10-139r
- Williams, F. L., and Patterson, J. W. (2010). Reconstructing the paleoecology of Taung, South Africa from low magnification of dental microwear features in fossil primates. *PALAIOS* 25, 439–448. doi: 10.2110/palo.2009.p09-116r
- Winkler, D. E., Clauss, M., Kubo, M. O., Schulz-Kornas, E., Kaiser, T. M., Tschudin, A., et al. (2022). Microwear textures associated with experimental near-natural diets suggest that seeds and hard insect body parts cause high enamel surface complexity in small mammals. *Front. Ecol. Evol.* 10, 1–16. doi: 10.3389/fevo.2022.957427
- Yakir, D. (1997). “Oxygen-18 of leaf water: a crossroad for plant associated isotopic signals” in *Stable isotopes: Integration of biological, ecological, and geochemical processes*. ed. H. Griffiths (London: BIOS, Oxford), 147–168.
- Zhang, Z., Ramstein, G., Schuster, M., Li, C., Contoux, C., and Yan, Q. (2014). Aridification of the Sahara desert caused by Tethys Sea shrinkage during the late Miocene. *Nature* 513, 401–404. doi: 10.1038/nature13705



OPEN ACCESS

EDITED BY

Carlo Meloro,
Liverpool John Moores University,
United Kingdom

REVIEWED BY

Marcus Clauss,
University of Zurich, Switzerland
Eline Naomi Van Asperen,
Durham University, United Kingdom

*CORRESPONDENCE

Christina I. Barrón-Ortiz
✉ christina.barron-ortiz@gov.ab.ca

[†]These authors have contributed equally to this work and share first authorship

RECEIVED 22 May 2022

ACCEPTED 03 April 2023

PUBLISHED 27 April 2023

CITATION

Mihlbachler MC, Barrón-Ortiz CI,
Rankin BD and Theodor JM (2023) Sharpening
the mesowear tool: geometric morphometric
analysis of cusp shape and diet in ruminants.
Front. Ecol. Evol. 11:950463.
doi: 10.3389/fevo.2023.950463

COPYRIGHT

© 2023 Mihlbachler, Barrón-Ortiz, Rankin and Theodor. This is an open-access article distributed under the terms of the [Creative Commons Attribution License \(CC BY\)](#). The use, distribution or reproduction in other forums is permitted, provided the original author(s) and the copyright owner(s) are credited and that the original publication in this journal is cited, in accordance with accepted academic practice. No use, distribution or reproduction is permitted which does not comply with these terms.

Sharpening the mesowear tool: geometric morphometric analysis of cusp shape and diet in ruminants

Matthew C. Mihlbachler^{1,2†}, Christina I. Barrón-Ortiz^{3*†},
Brian D. Rankin⁴ and Jessica M. Theodor⁵

¹Department of Anatomy, New York Institute of Technology College of Osteopathic Medicine, Old Westbury, NY, United States, ²Division of Paleontology, American Museum of Natural History, New York, NY, United States, ³Quaternary Palaeontology Program, Royal Alberta Museum, Edmonton, AB, Canada, ⁴Division of Dermatology, Department of Medicine, University of Calgary, Calgary, AB, Canada, ⁵Department of Biological Sciences, University of Calgary, Calgary, AB, Canada

Mesowear is a dietary proxy that relates attritive wear and abrasive wear to the shape of worn tooth cusps of ungulates. Traditional mesowear methods categorize cusps according to relief and sharpness. A geometric morphometric approach has the potential to measure shape with higher precision and to discover unrecognized aspects of cusp shape, possibly improving the efficacy of mesowear. We quantified mesowear in extant Ruminantia, using a 2-D semilandmark outline technique on upper second molar metacones generated from photographs. Among the 91 species sampled, 65 were preassigned to dietary categories, browser, grazer, mixed feeder, and frugivore based on substantiated documentation of diet in the wildlife literature. Metacone cusp shape and metacone mesowear score were found to be independent of size. Principal component and discriminant function analyses of Procrustes transformed semilandmark coordinates revealed two diet-related components of cusp shape. The primary component is related to the traditional mesowear variables of cusp height and side steepness. The secondary shape component reveals variation in the mesiodistal symmetry of the metacone and may relate to a proal vector during the power stroke phase or the relative orientation of the cusps with respect to the chewing stroke vector. Discriminant function analysis of semilandmark data accurately classified the diets of species more frequently (67.2%) than the traditional mesowear method (56.1%). The semilandmark data successfully recognized the diets of grazing and browsing species with correct classification rates ranging from 69% to 95%. The diets of frugivorous and mixed feeding species were less frequently correctly recognized (33%–53%). Mixed feeding diets may be more difficult to recognize due to more heterogeneous diets when compared to browsers and grazers. Frugivores are more difficult to recognize because their rounded cusp apices resemble those of mixed feeders and grazers. We conclude that quantitative shape analysis improves the potential of mesowear. When used as a dietary proxy, we anticipate that mesowear analysis will correctly categorize the diets of most species. When misclassifications are made, they may most often be misclassifications of generalist mixed feeders and frugivores as either browsers or grazers.

KEYWORDS

mesowear, tooth wear, paleodiet, Ruminantia, geometric morphometrics

Introduction

Mesowear analysis is a widely employed technique for testing hypotheses about the diets, feeding ecologies, and paleoenvironments of ungulates (Croft and Weinstein, 2008; Mihlbachler et al., 2011, 2017; Danowitz et al., 2016; Green and Croft, 2018; Jiménez-Hidalgo et al., 2019; Ackermans, 2020). Mesowear refers to the macroscopic morphologies of worn buccal cusp apices of the molar teeth of ungulates, which vary in ways that are correlated to the observed diets of extant species (e.g., Fortelius and Solounias, 2000; Franz-Odenaal and Kaiser, 2003; Fraser and Theodor, 2011; Louys et al., 2011, 2012; Fraser et al., 2014; Ackermans et al., 2020). Browsing species presumably have minimally abrasive diets and therefore experience predominantly attrition-dominated wear and maintain sharpened molar cusp apices with high amounts of occlusal relief as a consequence of their ability to maintain precise dental occlusion. Grazers, on the other hand, consume a greater abundance of highly-abrasive particles including opaline silicates, which are more abundant in grasses, and also higher amounts of geological particles (dust, silt, sand) as a consequence of feeding closer to the soil substrate (Sanson, 2006; Janis, 2008; Semprebon et al., 2019). The tendency for grazers to develop and maintain blunter and lower relief molar cusp apices has been explained as a result of more abrasion-dominated wear. Recent work has abundantly demonstrated tooth wear and occlusion to be a complex phenomenon whose causal factors are not easily unraveled (Sanson et al., 2018; Ackermans et al., 2020; Schulz-Kornas et al., 2020; Martin et al., 2021). While the general explanation of mesowear as a reflection of an attrition-abrasion gradient (Fortelius and Solounias, 2000) is, no doubt, an oversimplification (e.g., Erickson et al., 2016), there is, nonetheless, an abundantly demonstrated correlation between diet and apical cusp morphology among extant ungulates.

Fortelius and Solounias (2000) first evaluated molar cusp apical morphologies among ungulates and their relationship to diet using extant species. They found a strong association between diet (browsing, grazing, and mixed feeding) and the apical cusp morphology of worn buccal cusps of upper molars. They examined the buccal cusps of the second upper molars and categorized them based on relief and sharpness (Figure 1). Many mesowear studies have employed the original scoring technique or they have devised related scoring techniques that categorize cusps by some combination of relief and sharpness (Blondel et al., 2010; Semprebon and Rivals, 2010; Taylor et al., 2013; Ulbricht et al., 2015; Mihlbachler et al., 2017; Cohen et al., 2021). In its simplest representation (e.g., Mihlbachler et al., 2011), cusps are scored according to arbitrary stages along a shape continuum ranging from tall and sharp with steeply sloped sides, to low and dull with shallow sloping sides. Browsers and grazers occupy the extreme ends of this continuum and mixed feeders occupy the intermediate range. This conveniently tidy mesowear continuum is disrupted by frugivores which develop rounded cusp apices, presumably due to tip-crushing wear associated with mastication of hard objects (Janis, 1990; Fortelius and Solounias, 2000). The phenomenon of frugivore tooth wear has not been thoroughly studied in ruminants, nonetheless, small frugivorous ruminants maintain rounded cusp morphologies that resemble mixed feeders and grazers, thus rendering it difficult to differentiate the mesowear signatures of frugivorous diets from other diets in the fossil record (Mihlbachler and Solounias, 2006; Mihlbachler et al., 2011).

Prior attempts to develop quantitative measures of mesowear involve measures of cusp heights and angles (Widga, 2006; Valli and Palombo, 2008; Fraser and Theodor, 2010; Loffredo and DeSantis, 2014; Saarinen et al., 2014; Jiménez-Manchón et al., 2021). However, as we reveal below, cusp shape varies in other ways. Geometric morphometric methods have the potential to shed light on more nuanced aspects of tooth mesowear and its relation to diet. To our knowledge, geometric morphometric methods have not been widely applied to mesowear (see Rødven et al., 2006 for an example). One concern is expediency. Unlike more laborious and costly methods, such as stable isotope analysis and dental microwear texture analysis, mesowear is a simple technique that facilitates the expedient compilation of large datasets (Mihlbachler et al., 2011; Semprebon et al., 2019). More laborious approaches of mesowear quantification, such as 3-D quantification (Hernesniemi et al., 2011) may offer finer-grained insights into the shapes of the occlusal facets of teeth, but such approaches also limit the potential for building large data sets thus removing one of the primary advantages of the technique.

In this paper, we describe an expedient 2-D geometric morphometric mesowear analysis using photographs in lateral view of upper molars and apply it to 91 species of extant ruminants. We hypothesize that quantitative measurement of cusp shape will provide additional insights into how cusp shape varies with diet. Secondly, we hypothesize that a more nuanced view of mesowear provided by morphometrics will sharpen the mesowear tool for predicting the diets of extinct species and other ancient populations.

Materials and methods

This study consists of 834 skulls representing 91 extant species of Ruminantia, following the taxonomy of Groves and Grubb (2011), housed at the mammalogy collections of the American Museum of Natural History (New York, USA), the Royal Alberta Museum (Edmonton, Canada), and the National Museum of Natural History, Smithsonian Institution (Washington D.C., USA). We prioritized maximization of taxonomic and ecological diversity; therefore, we sampled specimens without regard for locality, as long as the specimen was collected from a non-feral wild population. Additional insights may be achieved from more focused population-level studies, but this approach also has limitations due to the finite coverage of natural history collections. The species are divided into two tables (Tables 1, 2) for reasons explained below. We attempted to sample a minimum number of 10 specimens when possible but the number of available specimens for many species was fewer than 10. Our sample size for each species ultimately ranged from 1 to 20 (Tables 1, 2).

This study focuses on the metacone of the upper second molar (M2). The cusps of the different tooth positions frequently have non-identical apical morphologies and there is most often a wear gradient among the molars. The M1 tends to be the most worn, while the M3 tends to be the least worn. M2 most often tends to be in an intermediate state of wear. This wear gradient is related to the different eruption times (Ungar, 2010) and possibly also to the variable spatial relationships that teeth have with the temporomandibular joint and muscles of mastication which may differentially influence occlusal dynamics at different positions along the tooth row. While it is likely that the general conclusions of this study about the relationship of tooth wear and diet can be generalized to other cusps along the molar

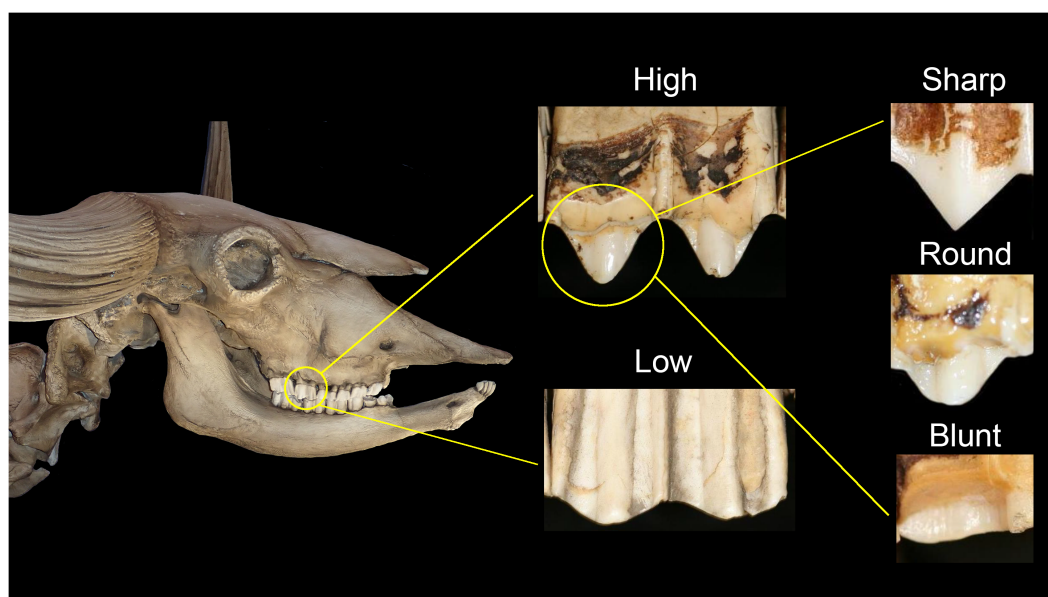


FIGURE 1

Traditional mesowear analysis uses a categorical approach to scoring cusp relief (high or low) and apical shape (sharp, round, or blunt). Browsing ungulates tend to have high and sharp cusp morphologies, whereas grazing ungulates tend to show low and blunt or rounded cusps, with mixed feeders showing intermediate morphologies.

row, we caution that any subsequent direct comparisons to our data would be most meaningful if based on the same M2 metacone.

The amount of tooth wear that an animal has accumulated during its lifetime is a consideration when selecting specimens for mesowear analysis. Experimental evidence suggests that mesowear is more of a general signal than a seasonal one (Ackermans et al., 2020). All but the most brachyodont ruminants tend to maintain their cusp morphologies in a state of relative stasis as the teeth wear, beginning with the initial development of wear facets and ending with the mechanical senescence of the tooth (Rivals et al., 2007). Bearing these basic findings in mind, we followed typical inclusion criteria for mesowear studies where young and old individuals were excluded. Inclusion criteria included a fully erupted adult dentition with visible wear on the third molar. Dentally senescent individuals, defined as having nearly all of the first molar crown worn away, were excluded.

Each species was assigned to one of four dietary categories based on the percentage of dicotyledons, monocotyledons, and fruits in their diet as follows: browsers (>70% leafy, woody components of dicotyledons), frugivores (>70% fruits), grazers (>70% monocotyledons), and mixed feeders (species external to the parameters of other categories). Evidence for diet in the literature for 65 out of the 91 species (Table 1), was considered by us to be sufficient and these were used extensively in the analyses described below. The remaining 26 species (Table 2) were used more sparingly as we were less confident about their dietary assignments. In these instances, the literature-based evidence for the diet was scant or of low quality, due to incomplete information or discrepancies in the percentages of food types reported between different studies. Other species relegated to Table 2, (e.g., *Rangifer tarandus*) have abundantly documented wild diets, but consume foods, such as moss and lichens, that fall outside of the scope of the four dietary categories. The species of Table 2 were used to gain a heuristic understanding of how insufficient evidence of

diet and peculiar diets not fitting typical criteria may complicate the use of mesowear as a dietary proxy.

Image acquisition

We photographed the upper left cheek tooth row with focus on the second molar (M2) using a Canon EOS5D or Nikon D200 digital camera. In instances when the left M2 was damaged or pathological, we photographed the right tooth row and horizontally inverted the image. The specimens were oriented so that the buccal wall of the M2 was perpendicular to the camera. If lingual parts of the molars were visible through the camera (Figure 2A), the specimen was rotated slightly so that these parts of the tooth were obscured (Figure 2B). The specimens were handheld by the photographer and aligned this way by eye. With this approach, we attempted to sufficiently standardize the orientation of the specimen without greatly compromising expediency. While more precise orientation of specimens would have been possible with anchoring devices, this would have further limited the potential to sample large numbers of specimens and would have constrained the sizes and shapes of skulls that could be photographed.

Landmark digitization and superimposition

Every image was renamed with a four-digit identifier generated at random, with the objective of mixing the sample of images and removing the identity of each image to minimize systematic biases during landmark digitization. We used tpsDig 2.32 (Rohlf, 2015) to digitize the outline of the occlusal edge of the metacone cusp, starting on the distal end of the metacone and finishing at the high point of the arch between the paracone and metacone. The resulting cusp outline

TABLE 1 Species with high-quality *a priori* dietary assignments derived from the literature.

Species	Abbr	Family	N	<i>a priori</i> diet	References
<i>Antilocapra americana</i>	ANT	Antilocapridae	11	B	5; 25
<i>Addax nasomaculatus</i>	an	Bovidae	1	G	12; 21; 28; 34
<i>Aepyceros melampus</i>	Am	Bovidae	12	M	12
<i>Alcelaphus buselaphus</i>	ab	Bovidae	11	G	12; 21
<i>Ammelaphus imberbis</i>	Ai	Bovidae	9	M	12
<i>Antidorcas marsupialis</i>	Ama	Bovidae	10	M	12
<i>Bos bison</i>	bb	Bovidae	18	G	25; 34
<i>Boselaphus tragocamelus</i>	Bt	Bovidae	2	M	19
<i>Bubalus depressicornis</i>	Bde	Bovidae	8	M	11; 34
<i>Cephalophus callipygus</i>	cC	Bovidae	9	F	12
<i>Cephalophus dorsalis</i>	cD	Bovidae	10	F	12
<i>Cephalophus leucogaster</i>	cL	Bovidae	16	F	12
<i>Cephalophus niger</i>	cNI	Bovidae	9	F	12; 16
<i>Cephalophus nigrifrons</i>	cNG	Bovidae	10	F	12
<i>Cephalophus rufilatus</i>	cR	Bovidae	11	F	12; 16
<i>Cephalophus silvicultor</i>	cS	Bovidae	12	F	12
<i>Connochaetes gnou</i>	cg	Bovidae	6	G	12; 21
<i>Connochaetes taurinus</i>	ct	Bovidae	10	G	12; 21
<i>Damaliscus lunatus</i>	dl	Bovidae	12	G	12
<i>Damaliscus pygargus</i>	dp	Bovidae	10	G	12; 21
<i>Eudorcas thomsonii</i>	et	Bovidae	11	G	12
<i>Hippotragus equinus</i>	he	Bovidae	10	G	12; 21
<i>Hippotragus niger</i>	hn	Bovidae	10	G	12; 21
<i>Kobus ellipsiprymnus</i>	ke	Bovidae	11	G	12; 21
<i>Kobus kob</i>	kk	Bovidae	10	G	10; 12; 21
<i>Kobus leche</i>	kl	Bovidae	7	G	12; 21; 22
<i>Litocranius walleri</i>	LW	Bovidae	20	B	12
<i>Madoqua kirkii</i>	MK	Bovidae	12	B	12
<i>Nanger granti</i>	Ng	Bovidae	16	M	12
<i>Neotragus moschatus</i>	NM	Bovidae	7	B	12
<i>Nyala angasii</i>	Na	Bovidae	4	M	12
<i>Oreotragus oreotragus</i>	Or	Bovidae	16	M	12
<i>Oryx gazella</i>	og	Bovidae	10	G	12
<i>Ourebia ourebi</i>	oo	Bovidae	10	G	12
<i>Pelea capreolus</i>	PC	Bovidae	2	B	12
<i>Philantomba maxwellii</i>	pM	Bovidae	10	F	12; 16
<i>Philantomba monticola</i>	pMO	Bovidae	19	F	12
<i>Procapra gutturosa</i>	Pg	Bovidae	13	M	4; 17
<i>Raphicerus campestris</i>	Rc	Bovidae	12	M	12
<i>Redunca arundinum</i>	ra	Bovidae	14	G	12
<i>Redunca fulvorufula</i>	rf	Bovidae	10	G	12; 21
<i>Redunca redunca</i>	rr	Bovidae	12	G	12
<i>Saiga tatarica</i>	St	Bovidae	2	M	1; 3; 29; 34
<i>Strepsiceros strepsiceros</i>	Ss	Bovidae	11	M	12

(Continued)

TABLE 1 (Continued)

Species	Abbr	Family	N	a priori diet	References
<i>Sylvicapra grimmia</i>	SG	Bovidae	11	B	6; 12
<i>Syncerus caffer</i>	sc	Bovidae	17	G	12; 21
<i>Taurotragus derbianus</i>	TD	Bovidae	6	B	12; 15
<i>Tragelaphus eurycerus</i>	TE	Bovidae	5	B	12
<i>Tragelaphus scriptus</i>	TSC	Bovidae	9	B	12
<i>Tragelaphus spekii</i>	Tsp	Bovidae	10	M	12
<i>Alces alces</i>	AA	Cervidae	15	B	3; 25
<i>Axis axis</i>	Ax	Cervidae	3	M	18; 26; 34; 35
<i>Axis porcinus</i>	Ap	Cervidae	4	M	9; 33; 34
<i>Blastocerus dichotomus</i>	BD	Cervidae	5	B	19; 23; 29
<i>Capreolus capreolus</i>	CA	Cervidae	9	B	3; 27; 34
<i>Cervus canadensis</i>	Cca	Cervidae	8	M	3; 7; 25
<i>Cervus elaphus</i>	Ce	Cervidae	5	M	3; 7; 25
<i>Hippocamelus antisensis</i>	Han	Cervidae	3	M	2; 34
<i>Odocoileus hemionus</i>	OH	Cervidae	20	B	14; 25; 34
<i>Odocoileus virginianus</i>	OV	Cervidae	16	B	25; 34
<i>Panolia eldii</i>	pe	Cervidae	5	G	31; 32
<i>Pudu mephistophiles</i>	PME	Cervidae	5	B	34
<i>Giraffa camelopardalis</i>	GC	Giraffidae	11	B	8; 23
<i>Okapia johnstoni</i>	OJ	Giraffidae	17	B	13; 34
<i>Hyemoschus aquaticus</i>	hA	Tragulidae	9	F	34

B = browser, G = grazer, M = mixed feeder, F = frugivore. References for *a priori* diet classifications: (1) Bannikov, 1976; (2) Barrio, 2013; (3) Baskin and Danell, 2003; (4) Campos-Arceiz et al., 2004; (5) Clemente et al., 2009; (6) Codron et al., 2007; (7) Cook, 2002; (8) Dagg, 2014; (9) Davis et al., 2008; (10) Djagoun et al., 2013; (11) Flores-Miyamoto et al., 2005; (12) Gagnon and Chew, 2000; (13) Hart and Hart, 1989; (14) Heffelfinger, 2018; (15) Hejmanová et al., 2010; (16) Hofmann and Roth, 2003; (17) Jiang et al., 2002; (18) Johnsingh and Sankar, 1991; (19) Leslie, 2008; (20) Marin et al., 2020; (21) Müller et al., 2011; (22) O'Shaughnessy et al., 2014; (23) Owen-Smith, 1997; (24) Pinder and Grosse, 1991; (25) Renecker and Schwartz, 1997; (26) Schaller, 1967; (27) Sempéré et al., 1996; (28) Seri et al., 2018; (29) Sokolov, 1974; (30) Tomas and Salis, 2000; (31) Tripathi et al., 2019; (32) Tuboi and Hussain, 2016; (33) Wegge et al., 2006; (34) Wilson and Mittermeier, 2011; (35) Watter et al., 2020.

was then resampled to obtain 24 evenly spaced points that were judged to adequately capture the metacone outline (Supplementary Table S1). Points 1 and 24 are regarded as landmarks and points 2–23 represent semilandmarks (Figure 2C). All of the specimens were digitized by the same researcher (CIB-O). Levels of photographing and digitization error were low (2.1%), as evidenced by Procrustes ANOVA performed on a subset of an earlier version of our dataset in which specimens were photographed and digitized twice (Barrón-Ortiz et al., 2013).

We superimposed the 834 landmark configurations in tpsRelw 1.75 (Rohlf, 2015) using a generalized least squares (GLS) Procrustes superimposition method in which semilandmarks were allowed to slide to minimize thin-plate spline bending energy. To accomplish this, we created a “sliders file” in tpsUtil 1.82 (Rohlf, 2015) to indicate that semilandmarks 2–23 were allowed to slide during GLS Procrustes superimposition. In standard GLS Procrustes superimposition, the configurations of landmarks are translated to the origin, scaled to unit centroid size (centroid size is the square root of the sum of squared distances of all the landmarks from their centroid), and rotated to minimize the summed square distances between homologous landmarks (Zelditch et al., 2004). A consensus (average) configuration is obtained and the deviation of each configuration of landmarks from the consensus yields the Procrustes residuals (Procrustes transformed coordinates). The standard GLS Procrustes superimposition is

extended in the sliding semilandmarks method. In addition to translating, scaling, and rotating the configurations of landmarks, the sliding semilandmarks method allows semilandmarks to slide along lines tangent to the outline curve to optimize their position with respect to the average shape of the entire sample (Zelditch et al., 2004; Perez et al., 2006; Gunz and Mitteroecker, 2013). Semilandmarks are allowed to slide to either minimize thin-plate spline bending energy or to minimize Procrustes distance (Perez et al., 2006; Gunz and Mitteroecker, 2013). The sliding semilandmarks method attempts to reduce the amount of shape variation that results solely from the arbitrary spacing of semilandmarks; thus, improving the geometric or biological correspondence of the semilandmarks across specimens (Zelditch et al., 2004; Perez et al., 2006; Gunz and Mitteroecker, 2013).

Scoring of traditional mesowear variables

In order to compare traditional mesowear analysis and 2-D geometric morphometric mesowear analysis, we also scored the metacones from the photographs for every specimen in our dataset (Supplementary Table S1) using the categorical methodology introduced by Fortelius and Solounias (2000). This methodology uses two categories: (1) cusp height (high or low) and (2) cusp shape (sharp, rounded, or blunt) (Fortelius and Solounias, 2000). Cusps

TABLE 2 Species with questionable *a priori* dietary assignments derived from the literature.

Species	Abbr	Family	N	<i>a priori</i> diet	References
<i>Ammodorcas clarkei</i>	AC*	Bovidae	1	B	5
<i>Bubalus mindorensis</i>	Bm*	Bovidae	4	M	4; 18
<i>Cephalophus natalensis</i>	cN*	Bovidae	5	F	5; 18
<i>Cephalophus weynsi</i>	cW*	Bovidae	9	F	5; 18
<i>Gazella dorcas</i>	GD*	Bovidae	8	B	2; 5
<i>Gazella subgutturosa</i>	GU*	Bovidae	10	B	3; 10; 19
<i>Madoqua guentheri</i>	MG*	Bovidae	11	B	5; 18
<i>Madoqua saltiana</i>	MS*	Bovidae	9	B	5; 18
<i>Nanger soemmerringii</i>	Ns*	Bovidae	12	M	2; 5
<i>Neotragus batesi</i>	NB*	Bovidae	10	B	5
<i>Taurotragus oryx</i>	TO*	Bovidae	2	B	5; 8
<i>Tetracerus quadricornis</i>	TQ*	Bovidae	3	B	13; 14; 18
<i>Tragelaphus buxtoni</i>	TB*	Bovidae	6	B	5
<i>Elaphodus cephalophus</i>	Ec*	Cervidae	6	M	13
<i>Mazama americana</i>	mA*	Cervidae	8	F	6; 15
<i>Mazama gouazoubira</i>	mGO*	Cervidae	8	F	6; 15
<i>Muntiacus muntjak</i>	mU*	Cervidae	7	F	9; 18
<i>Muntiacus putaoensis</i>	mP*	Cervidae	4	F	18
<i>Muntiacus reevesi</i>	mR*	Cervidae	8	F	18
<i>Rangifer tarandus</i>	Rt*	Cervidae	10	M	3; 16
<i>Rusa marianna</i>	Rm*	Cervidae	5	M	1; 17
<i>Rusa unicorn</i>	Ru*	Cervidae	7	M	13; 18; 20
<i>Moschus moschiferus</i>	Mm*	Moschidae	10	M	3; 7
<i>Moschiola meminna</i>	mME*	Tragulidae	5	F	18
<i>Tragulus javanicus</i>	tj*	Tragulidae	9	F	14; 18
<i>Tragulus napu</i>	tN*	Tragulidae	8	F	18

B = browser, G = grazer, M = mixed feeder, F = frugivore. References for dietary assignments: (1) Ali et al., 2021; (2) Baamrane et al., 2012; (3) Baskin and Danell, 2003; (4) Custodio et al., 1996; (5) Gagnon and Chew, 2000; (6) Gayot et al., 2004; (7) Green, 1987; (8) Hejmanová et al., 2020; (9) Ilyas and Khan, 2003; (10) Kingswood and Blank, 1996; (11) Leslie, 2011; (12) Leslie and Sharma, 2009; (13) Leslie et al., 2013; (14) Müller et al., 2011; (15) Prado, 2013; (16) Renecker and Schwartz, 1997; (17) Wiles et al., 1999; (18) Wilson and Mittermeier, 2011; (19) Xu et al., 2012; (20) Zhang et al., 2020.

judged to be at the border between high and low were measured using ImageJ 1.53 s (Rasband et al., 2022) to assign them to one of these two categories. Categorization of these borderline specimens was accomplished by measuring the maximum depth of the valley formed between the paracone and metacone (by measuring the vertical distance from a line connecting the paracone and metacone cusps) and dividing this value by the length of the molar, as indicated by Fortelius and Solounias (2000). Ratios ≥ 0.15 were assigned as high, conversely ratios < 0.15 were assigned to the low category. The same observer (CIB-O) evaluated all specimens in our dataset for traditional mesowear variables.

Following Fortelius and Solounias (2000), we calculated the percentage of individuals with high, low, sharp, rounded, and blunt cusps for every species. We confined analysis of traditional mesowear data to species with sample sizes of 5 or more individuals (Supplementary Table S2). We also calculated mesowear scores for individual specimens (Supplementary Table S1) by assigning a score of 0 to specimens with high and sharp cusps, a score of 1 to specimens with high and rounded cusps, a score of 2 to specimens

with low and rounded cusps, and a score of 3 to specimens with low and blunt cusps (Rivals and Semprebon, 2006; Rivals et al., 2007). Out of 834 specimens, 19 could not be scored because the paracone cusp was damaged preventing us from determining cusp height, and 26 specimens had peculiar metacone shapes that were difficult to score and were ignored; thus, we only report and analyze the mesowear score for the remaining 789 specimens (Supplementary Table S1).

Covariation between size and cusp shape/mesowear score

To test for allometry (covariation between size and shape), we performed multivariate regressions in MorphoJ 1.05f (Klingenberg, 2011), where size is the independent variable and the Procrustes transformed coordinates (Supplementary Table S1) are the dependent variables. Size was measured as either M2 ectoloph length (measured with a digital caliper accurate to 0.01),

metacone cusp length (obtained by calculating the Euclidean distance between the extreme points of the cusp), or metacone ln centroid size (Supplementary Table S1). We also evaluated covariation between size and metacone mesowear score by performing linear regressions in PAST 4.12b (Hammer et al., 2001), where size (as quantified above) is the independent variable and mesowear score (Supplementary Table S1) is the dependent variable. For each analysis, we report the amount of cusp shape variation predicted by size and *p*-values of permutation tests (10,000 replicates) used to evaluate the null hypothesis of independence.

In order to evaluate covariation between metacone mesowear score and metacone cusp shape, we performed a multivariate regression in MorphoJ 1.05f (Klingenberg, 2011). In this analysis, mesowear score (Supplementary Table S1) is treated as the independent variable and Procrustes transformed coordinates (Supplementary Table S1) are the dependent variables.

Principal component analysis

To identify directions of maximal shape variation in our dataset, we performed a principal component analysis (PCA) on the variance-covariance matrix of the Procrustes transformed coordinates

(Supplementary Table S1) using species in Tables 1, 2. PCA was performed in MorphoJ 1.05f (Klingenberg, 2011).

Discriminant function analysis

To test the efficacy of 2D cusp shape as a means of accurately classifying diets, stepwise discriminant function analyses (DFA) were run using SPSS v. 27 on the Procrustes transformed coordinates (Supplementary Table S1) using diet (browser, grazer, mixed feeder, frugivore) as the group variable (Table 1). In stepwise DFA, single variables are added to the discriminant model to optimize discrimination among groups according to predetermined inclusion criteria. We followed Meloro (2011) in using $p \leq 0.05$ and $p \geq 0.1$ for the probability of *F* for the entry and removal of variables, respectively (Supplementary Table S5). Attempts were made to match the dietary classifications of species made from the literature to dietary classifications generated from the DFAs. We refer to dietary classifications based on the literature as *a priori* and dietary classifications resulting from DFA of mesowear data as *a posteriori*.

DFAs were run including the individual specimens as observations. The analyses were done assuming equal prior classification probabilities for all dietary groups and using a within-groups covariance matrix. The modal (most common) *a posteriori* individual classification within each species was used to assign that species to an *a posteriori* dietary category. Modal classifications were not generated for species represented by fewer than three specimens.

The common method of DFA classification is resubstitution, where the DFA classifies the same specimens used to generate the discriminant model. A degree of circularity is inherent in this method because the resulting classifications are not independent of the observations (Lance et al., 2000) and the resulting apparent error rate of classification tends to be underestimated. To avoid this problem, we employed a leave-one-out jackknifing technique that maintains independence between the observations used to generate the discriminant function and the classifications (Lance et al., 2000; Louys et al., 2011). The leave-one-out method works by removing one observation from the data and then it classifies that observation based on the DFA of the remaining data. That observation is subsequently returned to the data set and the procedure is repeated for each observation. Because each classification is based on a model that excluded the observation, the resulting actual error rate is expected to be less biased than the apparent error rate generated from the resubstitution method. Species in Table 1 were used to generate the discriminant models. Species in Table 2 were entered into the analysis without *a priori* classifications and jackknifing was therefore not used for *a posteriori* classifications of these species' diets.

To visualize cusp shape features that covary with discriminant functions that maximize the separation between dietary groups, we performed multivariate regressions in MorphoJ 1.05f (Klingenberg, 2011). In these analyses, discriminant function scores were the independent variables and the Procrustes transformed coordinates (Supplementary Table S1) of species in Table 1 were the dependent variables.

Two additional series of DFAs were run using only the species in Table 1 to account for potential complications of our dataset:

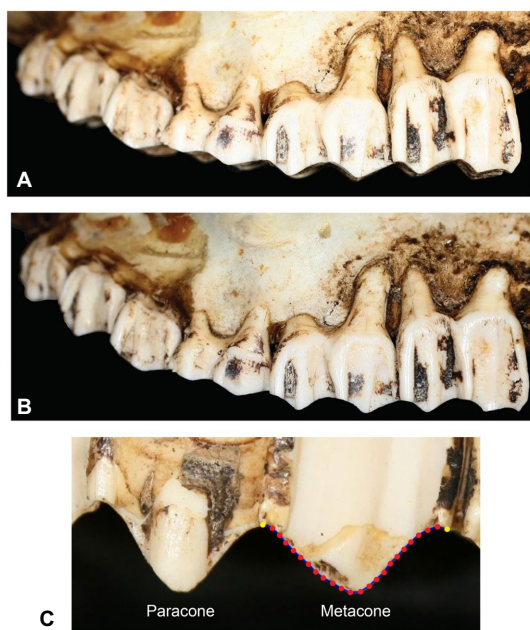


FIGURE 2

Left upper cheek tooth row of *Cervus canadensis* showing photographic angle. Specimens were oriented so the buccal wall of M2 was perpendicular to the camera lens. (A) When lingual sides of the cheek teeth were visible. (B) the specimen was rotated slightly until the lingual sides were obscured from view, and the photograph was taken. (C) Buccal view of the second upper molar (M2) of a specimen of *Syncerus caffer* (AMNH 53582) showing the landmarks (yellow) and semilandmarks (red) that were digitized on the occlusal outline of the metacone cusp. Digitization of the occlusal outline starts at the posterior end of the metacone (right side of the image) and ends at the metacone-paracone valley.

(1) Frugivores were excluded to examine the possibility that they interfere with discrimination of browsers, grazers, and mixed feeders, due to their potentially overlapping low-relief and rounded cusp morphologies.

(2) To compare the performance of 2D semilandmarks and the original categorical techniques, we ran standard DFAs (i.e., not stepwise DFAs) on the arcsine transformed traditional mesowear data we calculated (% high, % sharp, % round, and % blunt) (Supplementary Table S2).

Results

Covariation between size and cusp shape/mesowear score

Table 3 summarizes the results of the regression analyses. The amount of cusp shape variation predicted by size is minimal (values ranging from 0.13% to 0.34%) and none of the analyses produced a statistically significant result. Cusp shape does not appear to covary with either tooth size or cusp size. Similarly, the amount of mesowear score variation predicted by size is minimal (values ranging from 0.01% to 0.24%) and none of the analyses produced a statistically significant result.

TABLE 3 Results of regression analyses.

Independent / dependent variables	% predicted	p-value
Ln centroid size / metacone shape (91 species, $n = 834$)	0.13	0.33
Metacone length / metacone shape (91 species, $n = 834$)	0.34	0.06
M2 ectoloph length / metacone shape (91 species, $n = 834$)	0.28	0.09
Ln centroid size / mesowear score (90 species, $n = 789$)	0.01	0.83
Metacone length / mesowear score (90 species, $n = 789$)	0.24	0.17
M2 ectoloph length / mesowear score (90 species, $n = 789$)	0.23	0.18
Mesowear score / metacone shape (90 species, $n = 789$)	24.44	<0.0001

The table shows the amount of variation predicted by size or mesowear score and p-values of permutation tests (10,000 replicates) used to evaluate the null hypothesis of independence.

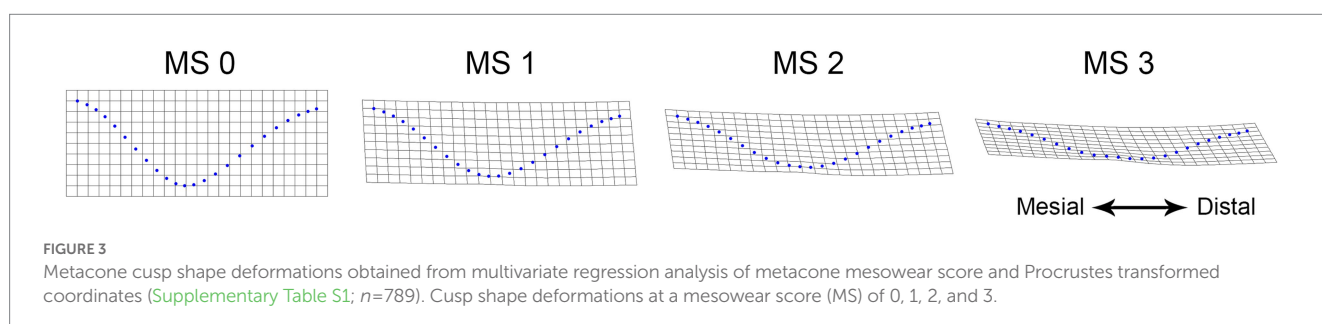
Cusp shape significantly covaries with mesowear score. The amount of cusp shape variation predicted by mesowear score is 24.4%. Features of cusp shape that covary with mesowear score are primarily related to the traditional mesowear variables of cusp height and side steepness. Low mesowear scores are associated with high cusps and steep sides, whereas high mesowear scores are associated with low cusps and shallow sides (Figure 3).

Principal component analysis

The first two principal components (PCs) account for over 90% of the variation (Supplementary Table S3). The resulting PC1 is related to variation in the height of the cusp and steepness of the sides, with positive scores corresponding to low relief and shallower sides, and negative scores corresponding to high relief and steeper sides (Figure 4). Dietary groups are distributed on PC1 as we might predict, with browsers tending to be positioned at one end of the axis (tall and steep) and grazers and frugivores tending to be positioned at the other (low and shallow), with mixed feeders tending to occupy the intermediate range. PC2 reveals a component of variation in the degree of mesiodistal cusp asymmetry (Figure 4). Browsers are more frequently distributed at one end of the component where the cusp apex is more mesially positioned with a longer and shallower distal slope. At the other extreme, grazers and frugivores tend to have a more distally positioned cusp apex with a longer and shallower mesial slope. There is considerable overlap between the dietary groups in the PCA results, however, the group centroids of browsers, mixed feeders and grazers form a trend that is negatively associated with both PC1 and PC2. The frugivore group centroid departs slightly from this overall trend, as they tend to possess lower cusp relief than expected with respect to cusp symmetry.

Discriminant function analysis

The DFAs produced significant results ($p < 0.001$ in all cases). The first two discriminant functions (DFs) account for 95% of the variation among groups (Supplementary Table S4). DF1 tends to separate browsers from grazers, with mixed feeders and frugivores occupying intermediate positions (Figure 5). DF1 is related to cusp height, side steepness, and mesiodistal asymmetry. The metacones of browsers tend to be taller, steeper, and with an apex that is more mesially positioned with a longer and shallower distal slope. The cusps of grazers are lower, shallower, and with a more distally positioned apex with a longer and shallower mesial slope. Along DF2, frugivores



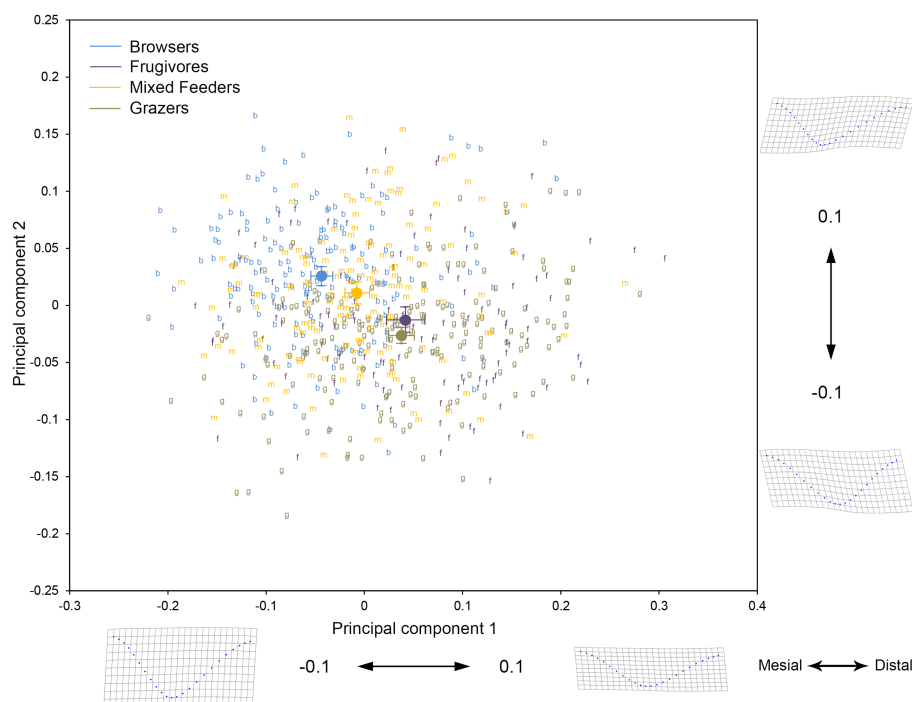


FIGURE 4

Scatter plot of the first two principal component scores derived from PCA of Procrustes transformed coordinates shown in [Supplementary Table S1](#). Indicated in the plot are the centroids for each dietary group with corresponding 95% confidence intervals. The shape models located along the margins of the plot demonstrate the change in cusp shape along each axis. Abbreviations are as follows: b=browser, f=frugivore, g=grazer, and m=mixed feeder. Procrustes transformed coordinates for all 834 specimens were used in this analysis, but only specimens of species with high-quality dietary information ([Table 1](#)) are shown in the plot.

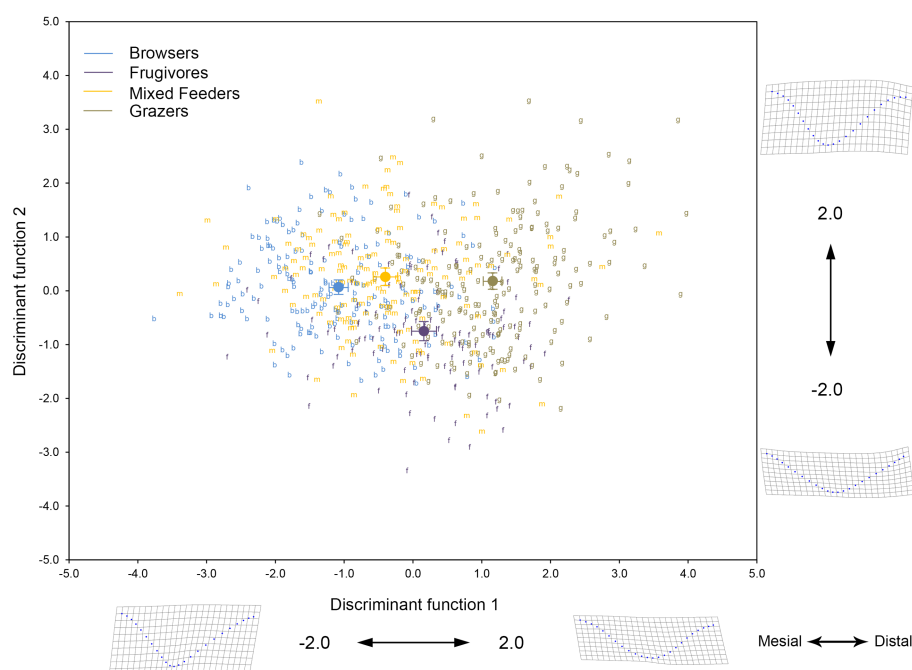
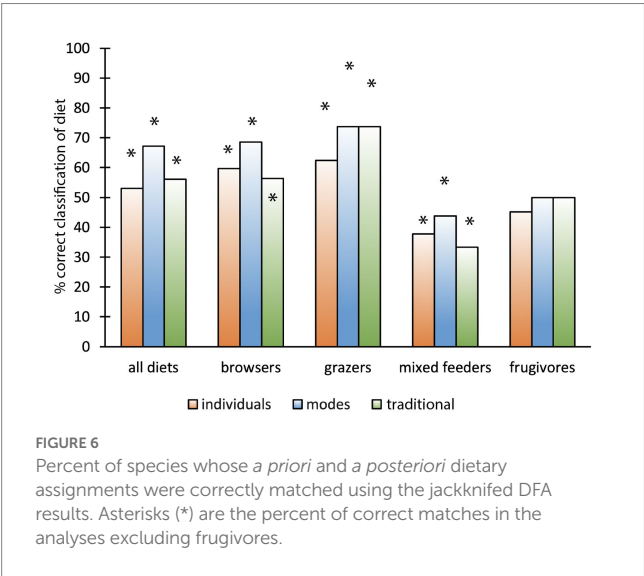


FIGURE 5

Scatter plot of the first two discriminant function scores derived from DFA of Procrustes transformed coordinates shown in [Supplementary Table S1](#). Indicated in the plot are the centroids for each dietary group with corresponding 95% confidence intervals. The shape models located along the margins of the plot demonstrate the change in cusp shape along each axis. Abbreviations are as follows: b=browser, f=frugivore, g=grazer, and m=mixed feeder. Only Procrustes transformed coordinates for specimens of species with high-quality dietary information ([Table 1](#)) were used in this analysis ($n=649$).

TABLE 4 Jackknifed percentages of correct *a priori* and *a posteriori* matches based on DFAs with high-quality data.

Individual specimens	All diets	Browsers	Grazers	Mixed feeders	Frugivores
All Diets	53	59.7	62.4	37.8	45.2
Frugivores excluded	65.5	66.9	81	42.6	NA
Modal classifications					
All diets	67.2	68.8	73.7	43.8	50
Frugivores excluded	76.5	75	94.7	56.3	NA
Traditional mesowear					
All diets	56.1	56.3	73.7	33.3	50
Frugivores excluded	63.7	50	89.5	41.7	NA



separate most strongly from the other dietary groups (Figure 5). The shape transformation in DF2 is strongly related to cusp height with aforementioned cusp asymmetry only transforming very subtly.

Supplementary Table S6 compares the *a priori* (literature) and *a posteriori* (DFA) dietary classifications of the species of Table 1, resulting in a match rate of 53% for individual cases (Table 4; Figure 6). The *a posteriori* classification of species correctly matched the mode based *a priori* classifications 67.2% of the time, and this rate is an improvement of 11 percentage points over match rates of species diets using traditional mesowear data (56.1%). Grazing diets were most frequently matched (73.7%) using the mode-based classifications, followed by browsers (68.8%), frugivores (50%) and mixed feeders (43.8%). Although the traditional data yielded lower frequency of correct match rates, the successful match rate for grazers was identical to that of the morphometric data (73.7%), but the traditional data yielded lower match rates for other diets in the same diminishing order: browsers (56.3%), frugivores (50%) and mixed feeders (33.3%). The order of the diminishing trend, common to both methods, seems to highlight a general problem with mesowear, and not a weakness of any particular method.

The exclusion of frugivores from the analysis had the tendency of improving correct match rates of individual specimens (65.5%) and species (based on modes: 76.5%) for the remaining dietary groups

(Table 4; Figure 6). The strongest improvement was among grazers (94.7%), with a diminishing magnitude of improvement in match rate among browsers (75%) and mixed feeders (56.3%). Exclusion of frugivores in the traditional mesowear data gave more mixed results with match rate improvements for grazers (89.5%) and mixed feeders (41.7%), but diminished match rates for browsers (50%). Mesowear most successfully identifies grazers and, to a lesser extent, browsers, but mesowear has more difficulty identifying mixed feeders and frugivores.

Small sample sizes were a concern for some species, however, the exclusion of the 17 species with fewer than 8 observations in Table 1 suggests that improved sampling may not substantially improve the apparent efficacy of mesowear analysis. Modal match rates of species from Table 1 with greater than 8 observations were 69.6%, only a 2.4 percentage-point increase over the modal match rate found in the entire sample in Table 1. Within the set of results from the traditional mesowear data, discarding species with fewer than 8 observations actually diminished the rate of correct classification by about 2 percentage points. Elimination of the most poorly sampled species did not have notable effects on the match rate, suggesting that improved sampling may not greatly improve the results.

Species in Table 2 are those species whose *a priori* dietary classifications were more uncertain or problematic. The individual classifications correctly matched 33.5% of the time and modal classifications correctly matched 37.5% of the time (Supplementary Table S7). Traditional mesowear data correctly matched only 14.3% (Supplementary Table S7). These match rates are considerably lower than species in Table 1 that were deemed to have more substantiated literature-based diets. These lower match rates are most easily explained by the more questionable *a priori* categorizations of the diets of these species.

Discussion

Cusp shape variation and distribution of dietary groups in morphospace

Neither tooth size nor cusp size was found to significantly influence metacone cusp shape or metacone mesowear score (Table 3). Previously, body mass and mesowear score were not found to be correlated in extant ungulates (Kaiser et al., 2013). The semilandmark data was found to significantly covary with mesowear score. However, the amount of cusp shape variation predicted by

mesowear score was less than 25% (Table 3), suggesting that there are aspects of cusp shape variation, discussed below that are not reflected by mesowear score.

The main shape transformations captured by the semilandmark data are related to the height of the cusp and steepness of the sides and the traditional mesowear variables cusp height and sharpness. These shape variables have been abundantly associated with relative amounts of abrasion and attrition and, thus far, this relationship has continued to serve as the theoretical basis for mesowear (Ackermans, 2020). A secondary shape component that has not yet been accounted for in mesowear analysis involves the relative position of the cusp apex along a mesiodistal axis and the differential slopes, lengths, and shapes of the mesial and distal sides of the cusp.

On average, the cusps of browsing species are taller, with steeper sides, and with cusp apices that are positioned more mesially. The distal slope of the cusp is longer than the mesial slope, has a shallower angle, and is more concave. Among grazers, the cusps are shorter, with shallower sides, with apices that are positioned slightly distally with the mesial slope of the cusp having a greater length, shallower slope, and more concave surface than the distal slope. Mixed feeders occupy an intermediate position and overlap all other dietary categories. Frugivores tend to resemble mixed feeders and grazers more frequently than browsers, but frugivores may have some subtle shape distinctions as suggested by DF2 (Figure 5).

In ungulates, the height of cusps and the complexity of the occlusal relief of the antagonistic dentition play an important role in guiding the movement of the jaw during food comminution (Fortelius, 1985; von Koenigswald et al., 2013). Attritional wear promotes precise occlusion and maintains the guiding effect of the cheek teeth during comminution thereby generating strongly defined attritional facets with high cusp relief and sharpened tips. Abrasion causes decreased tooth relief, thereby diminishing the guiding effect of the teeth, resulting in less precise chewing movements and less precise occlusion with rounded cusp apices. In browsers, attritional wear is the predominant mode of wear, while grazers experience high rates of abrasive wear.

Principal components are, by their very nature, uncorrelated. Because cusp relief is strongly reflected in PC1 (Figure 4) and has previously been associated with relative amounts of attrition and abrasion, it is difficult to explain the uncorrelated shape factor revealed by PC2, relating to cusp asymmetry, as also being a consequence of attrition and abrasion.

Cusp asymmetry may relate to differences in how ruminants chew or how their cusps are oriented with respect to the chewing direction that may have some correlation with diet. The power stroke of the ruminant chewing cycle occurs primarily in a transverse direction with a minor proal (from posterior to anterior) contribution (von Koenigswald et al., 2013). A proal vector during the power stroke may exert greater compressive loads and, consequently, more wear on the distal slopes of the upper cusps by the occluding lower teeth. This proal vector may play a role in creating asymmetrical cusp wear and could explain the condition observed more frequently among browsers (top of the PC2 axis in Figure 4; left of the DF1 axis in Figure 5) where the posterior slope of the metacone is more worn resulting in a mesial-ward shift in the position of the cusp apex.

Grazers tend to have more distally shifted cusp apices (bottom of the PC2 axis in Figure 4; right of the DF1 axis in Figure 5), suggesting the mesial and distal slopes of the cusp are subjected to

slightly more wear on the anterior cusp slope causing the cusp apex to shift slightly distally. For frugivores, a greater vertical inclination during phase I of the power stroke and a “tip crushing” type of wear associated with mastication of hard objects may explain the shape of frugivore cusps, but in this case, the similarity of frugivore cusp morphology with those of mixed feeders and grazers would be due to a different type of wear process compared to other dietary categories where the power stroke is mostly transverse and optimized for shearing.

On the efficacy of mesowear as a dietary proxy

Studies that attempt to match mesowear patterns with literature-based dietary classifications of extant species agree that while mesowear is strongly related to diet, it also yields some frequency of erroneous dietary classifications (Fortelius and Solounias, 2000; Fraser and Theodor, 2011; Louys et al., 2011; this study). Nonetheless, despite its shortcomings, mesowear seems to generate higher rates of correct diet classification than dental microwear and craniodental measurements (Fraser and Theodor, 2011), therefore it remains a promising means for predicting diet.

Fortelius and Solounias (2000) and Louys et al. (2011) reported accurate diet classification rates ranging from 49% to 58% using similar statistical methods (DFA jackknifing) to analyze traditional categorical mesowear data. Geometric morphometric data presented here produced higher correct classification rates ranging from 67.2–76.5%, depending on whether or not frugivores were considered. The semilandmark data improved the correct classification rates of species' diets by 12–13 percentage points in comparison to our results from traditional mesowear data. Geometric morphometric techniques seem capable of outperforming categorical techniques, but realistically, it seems that mesowear will inevitably lead to some proportion of erroneous dietary classifications.

The most widely recognized confounding variable when relating mesowear to diet is the relative impact of extrinsic geological material (e.g., dust, silt, sand) that is ingested along with food (Schulz et al., 2013; Wronski and Schulz-Kornas, 2015) and this additional source of abrasion may be responsible for some degree of dietary misclassification.

Intrinsic differences in the properties of the animals themselves may also obfuscate a simple relationship between mesowear and diet. Heritable (phylogenetic) differences in the dynamic aspects of mastication (bite force, occlusal vectors), functional morphology of the masticatory apparatus, and dental material properties cause teeth to wear differently regardless of diet. Phylogenetic methods are occasionally applied to mesowear analyses (Mihlbachler and Solounias, 2006; Mihlbachler et al., 2011; Kaiser et al., 2013; Fraser et al., 2014), although mesowear is most often assumed to be a taxon-free method (Fraser and Theodor, 2011; Ackermans, 2020). Nonetheless, phylogenetic influences on dental wear are demonstrable (Fraser et al., 2018). For example, dental microwear of ruminant artiodactyls differs from those of perissodactyls (Mihlbachler et al., 2016). Ruminants have highly specialized digestive adaptations allowing them to ingest, wash, and regurgitate their food before orally processing (ruminating) their food (Hatt et al., 2019, 2020, 2021). Ruminants adopt different chewing strategies than perissodactyls

(Zhou et al., 2019) who must process their food fully during initial ingestion, and this may contribute to differential tooth wear.

Despite the great diversity of Ruminantia, phylogenetic influence may not strongly obfuscate dietary classifications generated from mesowear within this group. Captive ruminants consistently show different mesowear patterns from their wild conspecifics due to artificial zoo diets (Clauss et al., 2007; Kaiser et al., 2009), and experimental approaches to mesowear in goats show that mesowear responds to feeding treatments with different abrasive properties (Ackermans et al., 2018). Such studies demonstrate that among ruminants mesowear is highly sensitive to proximate ecological variables and these, rather than phylogenetic influence, may be the primary drivers of the morphology of worn cusps. Although there are presently no clear signs that phylogeny complicates use of mesowear data within Ruminantia, phylogenetic methods are needed to ascertain the contribution of phylogenetic influence to mesowear (Barr and Scott, 2014). Ruminants are the dominant clade of herbivorous ungulates today, and all datasets of extant ungulate mesowear are overwhelmingly comprised of ruminants. Phylogeny may exert a stronger influence on more disparate assemblages of species that may include non-ruminant artiodactyls, perissodactyls, marsupials, and other extinct clades, such as South American notoungulates (Croft and Weinstein, 2008).

The heterogeneous quantity and quality of evidence for extant species' diets in the literature (Gagnon and Chew, 2000) is a third complication that may undermine the apparent efficacy of mesowear analysis. Incomplete, erroneous, or biased observations in the wildlife literature concerning species diets almost certainly explain, to some degree, the mismatches found in our DFA and other similar analyses (e.g., Fortelius and Solounias, 2000; Fraser and Theodor, 2011; Louys et al., 2011). Likewise, highly specialized diets that are not easily pigeonholed into basic dietary categories may have similar effects. Consequently, the match rates for species with uncertain dietary classifications (in Table 2) was far lower than species with more certain *a priori* dietary classifications (in Table 1).

Opportunities to examine independent evidence of diet (such as stable isotopes) and mesowear, where both proxies are measured in the same specimens, are rare (Louys et al., 2012). Within a species, diet may vary between populations and between individuals, and possibly within individuals' lifetimes. The literature and mesowear data may yield unmatched dietary classifications due to such ecological diversity. Mixed feeders are expected to have lower match rates than browsers and grazers as their diets are expected to be more heterogeneous in nature, possibly shifting seasonally or between populations in comparison to more specialized browsers and grazers. The mesowear data seem to reflect this expectation, as mixed feeders have lower match rates than browser and grazers.

We were able to correctly match literature-based and mesowear-based dietary classifications for species 67.2%–76.5% of the time, depending upon whether frugivores were excluded. However, these results underestimate, to some degree, the magnitude of error in species-level mesowear-based dietary classifications. Browsing, mixed feeding, and grazing are segments with arbitrary boundaries along a continuum of diets relating to the proportions of monocots and dicots consumed. It would be less erroneous to misclassify a browser as a mixed feeder than to misclassify a browser as a grazer. The former error still correctly acknowledges that the animal participates, to some

degree, in one aspect of its diet. Many of the mismatches in our results are of the lesser kind. Eleven of twenty mismatches of species in Table 1 are assignments to an adjacent category in the continuum. Four other misclassifications are more egregious errors involving failure to differentiate grazers and mixed feeders from frugivores and vice versa.

Removing frugivorous species from consideration is a reasonable strategy for improving dietary classification in some instances. Frugivorous diets only occur among small-bodied ruminants (<30 kg) from tropical and subtropical rainforests (Pineda-Munoz et al., 2016). Medium and large species and species from other environments that do not facilitate frugivory are unlikely to be specialized frugivores and, in these instances, frugivores can be removed from consideration. When frugivores are excluded, all 12 misclassifications in the species of Table 1 are classifications to the adjacent category in the browser-grazer continuum. In no instances were species at the opposite ends of the dietary continuum (browsers and grazers) confused with one another.

Conclusion

Laterally oriented photographs of upper molar cusps capture aspects of 2D cusp shape variation that, in ruminants, are correlated with diet and not with size. Geometric morphometric analysis of cusp shape can be used, with some expected degree of error, to classify species according to their type of diet (browser, grazer, mixed feeder, frugivore) that may improve upon traditional categorical approaches to mesowear analysis. Aspects of shape variation related to cusp relief and sharpness, the fundamental traditional mesowear variables, were found to be the primary elements of shape variation in the semilandmark data. The semilandmark data revealed a secondary shape aspect related to mesiodistal cusp asymmetry. Browsers more frequently have mesially positioned cusp apices with longer, shallower distal cusp slopes. Grazers more frequently have cusp apices that are slightly shifted distally. Mixed feeders and frugivores tend to have intermediate cusp morphologies. Mesiodistal cusp asymmetry in all but frugivores may be both influenced by the attritive and abrasive wear process and intrinsic differences in the relative strength of vertical and proal vectors in the power stroke phase of the chewing cycle, or the orientation of cusps with respect to that cycle. The cusp morphology of frugivores may relate to a greater vertical inclination during phase I of the power stroke and a "tip crushing" type of wear.

While geometric morphometric techniques show potential for providing a higher rate of correct dietary classification compared to categorical methods, researchers can expect a certain misclassification rate with either approach. The semilandmark data correctly classified diet ~67% of the time but when small frugivorous species are not considered mesowear was able to correctly classify browsers, grazers, and mixed feeders more than 75% of the time. With frugivores eliminated, mesowear correctly identifies browsing and grazing diets more frequently than it correctly identifies mixed feeding diets. Therefore, while mesowear remains a promising dietary proxy, we caution that its primary weakness may be its tendency to underestimate the proportion of generalized mixed feeders.

Data availability statement

The original contributions presented in the study are included in the article/[Supplementary material](#), further inquiries can be directed to the corresponding author.

Ethics statement

Ethical review and approval was not required for the animal study because we used museum specimens. No live animals were used in this study.

Author contributions

MM and CB-O conceived the study. MM, CB-O, and BR collected the data. MM and CB-O analyzed the data. JT provided supervision, materials and equipment. MM and CB-O prepared an earlier version of the manuscript. All authors contributed to the article and approved the submitted version.

Acknowledgments

We thank Eileen Westwig, Neil Duncan, Eleanor Hoeger (AMNH Mammalogy Dept.), John Ososky, Darrin Lunde (Smithsonian Institution), Mark A. Edwards, and Bill Weimann (Royal Alberta Museum) for providing access to specimens. Additional thanks go to

References

- Ackermans, N. L. (2020). The history of mesowear: a review. *PeerJ* 8:e8519. doi: 10.1016/j.palaeo.2021.110360
- Ackermans, N. L., Winkler, D. E., Martin, L. F., Kaiser, T. M., Clauss, M., and Hatt, J.-M. (2020). Dust and grit matter: abrasives of different size lead to opposing dental microwear textures in experimentally fed sheep (*Ovis aries*). *J. Exp. Biol.* 223:jeb220442. doi: 10.1242/jeb.220442
- Ackermans, N. L., Winkler, D. E., Schulz-Kornas, E., Kaiser, T. M., Müller, D. W., Kircher, P. R., et al. (2018). Controlled feeding experiments with diets of different abrasiveness reveal slow development of mesowear signal in goats (*Capra aegagrus hircus*). *J. Exp. Biol.* 221:jeb186411. doi: 10.1242/jeb.186411
- Ali, N. A. N. G., Abdullah, M. L., Nor, S. A. M., Pau, T. M., Kulaimi, N. A. M., and Naim, D. M. (2021). A review of the genus *Rusa* in the Indo-Malayan archipelago and conservation efforts. *Saudi J. Biol. Sci.* 28, 10–26. doi: 10.1016/j.sjbs.2020.08.024
- Baamrane, M. A. A., Shehzad, W., Ouhammou, A., Abbad, A., Naimi, M., Coissac, E., et al. (2012). Assessment of the food habits of the Moroccan dorcas gazelle in M'Sabih Talaa, west Central Morocco, using the trnL approach. *PLoS One* 7:e35643. doi: 10.1371/journal.pone.0035643
- Bannikov, A. G. (1976). Wild camels of the Gobi. *Wildlife* 18, 398–403.
- Barr, W. A., and Scott, R. S. (2014). Phylogenetic comparative methods compliment discriminant function analysis in ecomorphology. *Am. J. Phys. Anthropol.* 153, 663–674. doi: 10.1002/ajpa.22462
- Barrio, J. (2013). *Hippocamelus antisensis* (Artiodactyla: Cervidae). *Mamm. Species* 901, 49–59. doi: 10.1644/901.1
- Barrón-Ortiz, C., Mihlbachler, M., Rankin, B., and Theodor, J. (2013). Investigating the applicability of outline-based geometric morphometric techniques to the study of ungulate mesowear. *J. Vertebrate Paleontol.* 2013, 82A–83A.
- Baskin, L., and Danell, K. (2003). *Ecology of ungulates: a handbook of species in Eastern Europe and northern and Central Asia*. New York: Springer Science & Business Media.
- Blondel, C., Merceron, G., Androssa, L., Taisso, M. H., Vignaud, P., and Brunet, M. (2010). Dental mesowear analysis of late Miocene Bovidae from Toros-Menalla (Chad) and early hominid habitats in Central Africa. *Palaeogeogr. Palaeoclimatol. Palaeoecol.* 292, 184–191. doi: 10.1016/j.palaeo.2010.03.042
- Raúl Barrón-Corvera (Universidad Autónoma de Zacatecas) for assistance in data visualization and discussions on statistical analyses. We greatly appreciate the thorough and insightful comments we received from the Editor (Carlo Meloro) and the Reviewers (Marcus Clauss, Michael Berthaume, and Eline van Asperen); their comments significantly improved earlier versions of this manuscript.
- The authors declare that the research was conducted in the absence of any commercial or financial relationships that could be construed as a potential conflict of interest.
- All claims expressed in this article are solely those of the authors and do not necessarily represent those of their affiliated organizations, or those of the publisher, the editors and the reviewers. Any product that may be evaluated in this article, or claim that may be made by its manufacturer, is not guaranteed or endorsed by the publisher.
- The Supplementary material for this article can be found online at: <https://www.frontiersin.org/articles/10.3389/fevo.2023.950463/full#supplementary-material>
- Campos-Arceiz, A., Takatsuki, S., and Lhagvasuren, B. (2004). Food overlap between Mongolian gazelles and livestock in Omnogobi, southern Mongolia. *Ecol. Res.* 19, 455–460. doi: 10.1111/j.1440-1703.2004.00658.x
- Clauss, M., Franz-Odenaal, T. A., Brasch, J., Castell, J. C., and Kaiser, T. (2007). Tooth wear in captive giraffes (*Giraffa camelopardalis*): Mesowear analysis classifies free-ranging specimens as browsers but captive ones as grazers. *J. Zoo Wildl. Med.* 38, 433–445. doi: 10.1638/06-032.1
- Clemente, F., Holecchek, J. L., Valdez, R., and Mendoza, G. D. (2009). Influence of range condition on pronghorn (*Antilocapra americana*) and cattle diets in southern New Mexico. *J. Appl. Anim. Res.* 36, 13–16. doi: 10.1080/09712119.2009.9707021
- Codron, D., Codron, J., Lee-Thorp, J. A., Sponheimer, M., de Ruiter, D., Sealy, J., et al. (2007). Diets of savanna ungulates from stable carbon isotopes composition of faeces. *J. Zool.* 273, 21–29. doi: 10.1111/j.1469-7998.2007.00292.x
- Cohen, J. E., DeSantis, L. R., Lindsey, E. L., Meachen, J. A., O'Keefe, F. R., Southon, J. R., et al. (2021). Dietary stability inferred from dental mesowear analysis in large ungulates from rancho La Brea and opportunistic feeding during the late Pleistocene. *Palaeogeogr. Palaeoclimatol. Palaeoecol.* 570:110360. doi: 10.1016/j.palaeo.2021.110360
- Cook, J. G. (2002). *Nutrition and food. North American elk: ecology and management*. Smithsonian Institution Press, Washington, DC, 259–349.
- Croft, D. A., and Weinstein, D. (2008). The first application of the mesowear method to endemic south American ungulates (Notoungulata). *Palaeogeogr. Palaeoclimatol. Palaeoecol.* 269, 103–114. doi: 10.1016/j.palaeo.2008.08.007
- Custodio, C. C., Lepiten, M. V., and Heaney, L. R. (1996). *Bubalus mindorensis*. *Mamm. Species* 43, 1–5. doi: 10.2307/3504276
- Dagg, A. I. (2014). *Giraffe: biology, behaviour and conservation*. Cambridge: Cambridge University Press.
- Danowitz, M., Hou, S., Mihlbachler, M. C., Hastings, V., and Solounias, N. (2016). A combined-mesowear analysis of late Miocene giraffids from north Chinese and Greek localities of the Pliocene biome. *Palaeogeogr. Palaeoclimatol. Palaeoecol.* 449, 194–204. doi: 10.1016/j.palaeo.2016.02.026
- Davis, N. E., Coulson, G., and Forsyth, D. M. (2008). Diets of native and introduced mammalian herbivores in shrub-encroached grassy woodland, South-Eastern Australia. *Wildl. Res.* 35, 684–694. doi: 10.1071/WR08042

- Djagoun, C. A., Kassa, B., Mensah, G. A., and Sinsin, B. A. (2013). Seasonal habitat and diet partitioning between two sympatric bovid species in Pendjari biosphere reserve (northern Benin): waterbuck and western kob. *Afr. Zool.* 48, 279–289. doi: 10.1080/15627020.2013.11407594
- Erickson, G. M., Sidebottom, M. A., Curry, J. F., Kay, D. I., Kuhn-Hendricks, S., Norell, M. A., et al. (2016). Paleo-tribology: development of wear measurement techniques and a three-dimensional model revealing how grinding dentitions self-wear to enable functionality. *Surf. Topogr. Metrol. Properties* 4:024001. doi: 10.1088/2051-672X/4/2/024001
- Flores-Miyamoto, K., Clauss, M., Ortmann, S., and Sainsbury, A. W. (2005). Nutrition of captive lowland anoa (*Bubalus depressicornis*): a study on ingesta passage, intake, digestibility, and a diet survey. *Zoo Biol.* 24, 125–134. doi: 10.1002/zoo.20036
- Fortelius, M. (1985). Ungulate cheek teeth: developmental, functional, and evolutionary interrelations. *Acta Zool. Fenn.* 180, 1–76.
- Fortelius, M., and Solounias, N. (2000). Functional characterization of ungulate molars using the abrasion–attrition wear gradient: a new method for reconstructing paleodiets. *Am. Mus. Novit.* 3301, 1–36. doi: 10.1206/0003-0082(2000)301<0001:FCOUMU>2.0.CO;2
- Franz-Odenaal, T. A., and Kaiser, T. M. (2003). Differential mesowear in the maxillary and mandibular cheek dentition of some ruminants (Artiodactyla). *Am. Zool. Fenn.* 30, 395–410.
- Fraser, D., Haupt, R. J., and Barr, W. A. (2018). Phylogenetic signal in tooth wear dietary niche proxies. *Ecol. Evol.* 8, 5355–5368. doi: 10.1002/ece3.4052
- Fraser, D., and Theodor, J. M. (2010). The use of gross dental wear in dietary studies of extinct lagomorphs. *J. Paleontol.* 84, 720–729. doi: 10.1666/09-066.1
- Fraser, D., and Theodor, J. M. (2011). Comparing ungulate dietary proxies using discriminant function analysis. *J. Morphol.* 272, 1513–1526. doi: 10.1002/jmor.11001
- Fraser, D., Zybutz, T., Lightner, E., and Theodor, J. M. (2014). Ruminant mandibular tooth mesowear: a new scheme for increasing paleoecological sample sizes. *J. Zool.* 294, 41–48. doi: 10.1111/jzo.12149
- Gagnon, M., and Chew, A. E. (2000). Dietary preferences in extant African Bovidae. *J. Mammal.* 81, 490–511. doi: 10.1644/1545-1542(2000)081<0490:DPIEAB>2.0.CO;2
- Gayot, M., Henry, O., Dubost, G., and Sabatier, D. (2004). Comparative diet of the two forest cervids of the genus *Mazama* in French Guiana. *J. Trop. Ecol.* 20, 31–43. doi: 10.1017/S0266467404006157
- Green, M. J. (1987). Diet composition and quality in Himalayan musk deer based on fecal analysis. *J. Wildl. Manag.* 51, 880–892. doi: 10.2307/3801755
- Green, J. L., and Croft, D. A. (2018). “Using dental mesowear and microwear for dietary inference: a review of current techniques and applications” in *Methods in paleoecology: reconstructing Cenozoic terrestrial environments and ecological communities*. eds. D. A. Croft, D. F. Su and S. W. Simpson (Switzerland: Springer Nature), 53–73.
- Groves, C., and Grubb, P. (2011). *Ungulate taxonomy*. Baltimore, MA: Johns Hopkins University Press.
- Gunz, P., and Mitteroecker, P. (2013). Semilandmarks: a method for quantifying curves and surfaces. *Hystrix* 24, 103–109. doi: 10.4404/hystrix-24.1-6292
- Hammer, Ø., Harper, D. A. T., and Ryan, P. D. (2001). PAST: paleontological statistics software package for education and data analysis. *Palaeontol. Electron.* 4:4A.
- Hart, J. A., and Hart, T. B. (1989). Ranging and feeding behaviour of okapi (*Okapia johnstoni*) in the Ituri Forest of Zaire: food limitation in a rain-forest herbivore. in *Symposium of the Zoological Society of London*, 31–50.
- Hatt, J.-M., Codron, D., Ackermans, N. L., Martin, L. F., Richter, H., Kircher, P. R., et al. (2020). The effect of the rumen washing mechanism in sheep differs with concentration and size of abrasive particles. *Palaeogeogr. Palaeoclimatol. Palaeoecol.* 550:109728. doi: 10.1016/j.palaeo.2020.109728
- Hatt, J.-M., Codron, D., Müller, D. W., Ackermans, N. L., Martin, L. F., Kircher, P. R., et al. (2019). The rumen washes off abrasives before heavy-duty chewing in ruminants. *Mamm. Biol.* 97, 104–111. doi: 10.1016/j.palaeo.2020.109728
- Hatt, J.-M., Codron, D., Richter, H., Kircher, P. R., Hummel, J., and Clauss, M. (2021). Preliminary evidence for a forestomach washing mechanism in llamas (*Lama glama*). *Mamm. Biol.* 101, 941–948. doi: 10.1007/s42991-021-00142-1
- Heffelfinger, J. (2018). *Deer of the southwest: a complete guide to the natural history, biology, and management of southwestern mule deer and white*. College Station, TX: Texas A&M University Press.
- Hejmanová, P., Homolka, M., Antonínová, M., Hejman, M., and Podhájecká, V. (2010). Diet composition of western Derby eland (*Taurotragus derbianus* derbianus) in the dry season in a natural and a managed habitat in Senegal using faecal analyses. *Afr. J. Wildl. Res.* 40, 27–34. doi: 10.3957/056.040.0105
- Hejmanová, P., Ortmann, S., Stoklasová, L., and Clauss, M. (2020). Digesta passage in common eland (*Taurotragus oryx*) on a monocot or a dicot diet. *Comp. Biochem. Physiol. A Mol. Integr. Physiol.* 246:110720. doi: 10.1016/j.cbpa.2020.110720
- Hernesniemi, E., Blomstedt, K., and Fortelius, M. (2011). Multi-view stereo three-dimensional reconstruction of lower molars of recent and Pleistocene rhinoceroses for mesowear analysis. *Palaeontol. Electron.* 14, 1–15.
- Hofmann, T., and Roth, H. (2003). Feeding preferences of duiker (*Cephalophus maxwelli*, *C. rufilatus*, and *C. niger*) in Ivory Coast and Ghana. *Mamm. Biol.* 68, 65–77. doi: 10.1078/1616-5047-00065
- Ilyas, O., and Khan, J. A. (2003). Food habits of barking deer (*Muntiacus muntjak*) and goral (*Naemorhedus goral*) in Binsar wildlife sanctuary, India. *Mammalia* 67, 521–532. doi: 10.1515/mamm-2003-0406
- Janis, C. M. (1990). “The correlation between diet and dental wear in herbivorous mammals, and its dental relationship to the determination of diets in extinct species” in *Evolutionary Paleobiology of behavior and coevolution*. ed. J. Boucot (Amsterdam: Elsevier), 241–260.
- Janis, C. M. (2008). “An evolutionary history of browsing and grazing ungulates,” in *The ecology of browsing and grazing*, eds. Gordon, I. J., and Prins, H. H. T. (Berlin: Springer), 21–45.
- Jiang, Z., Takatsuki, S., Li, J., Wang, W., Gao, Z., and Ma, J. (2002). Seasonal variations in foods and digestion of Mongolian gazelles in China. *J. Wildl. Manag.* 66:40. doi: 10.2307/3802869
- Jiménez-Hidalgo, E., Carbot-Chanona, G., Guerrero-Arenas, R., Bravo-Cuevas, V. M., Holdridge, G. S., and Israde-Alcántara, I. (2019). Species diversity and paleoecology of late Pleistocene horses from southern México. *Front. Ecol. Evol.* 7:394. doi: 10.3389/fevo.2019.00394
- Jiménez-Manchón, S., Blaise, É., Albesso, M., Gardeisen, A., and Rivals, F. (2021). Quantitative dental mesowear analysis in domestic caprids: a new method to reconstruct management strategies. *J. Archaeol. Method Theory* 29, 540–560. doi: 10.1007/s10816-021-09530-w
- Johnsingh, A. J. T., and Sankar, K. (1991). Food plants of chital, sambar and cattle on Mundanthurai plateau, Tamil Nadu, South India. *Mammalia* 55, 57–66. doi: 10.1515/mamm.1991.55.1.57
- Kaiser, T., Brasch, J., Castell, J. C., Schulz, E., and Clauss, M. (2009). Tooth wear in captive ruminant species differs from that of free-ranging conspecifics. *Mamm. Biol.* 74, 425–437. doi: 10.1016/j.mambio.2008.09.003
- Kaiser, T., Müller, D. W. H., Fortelius, M., Schulz, E., Codron, D., and Clauss, M. (2013). Hypsodonty and tooth facet development in relation to diet and habitat in herbivorous ungulates: implications for understanding tooth wear. *Mammal Rev.* 43, 34–46. doi: 10.1111/j.1365-2907.2011.00203.x
- Kingswood, S. C., and Blank, D. A. (1996). Gazella subgutturosa. *Mammalian species* 518, 1–10. doi: 10.2307/3504241
- Klingenberg, C. P. (2011). MorphoJ: an integrated software package for geometric morphometrics. *Mol. Ecol. Resour.* 11, 353–357. doi: 10.1111/j.1755-0998.2010.02924.x
- Lance, R. F., Kennedy, M. L., and Leberg, P. L. (2000). Classification bias in discriminant function analyses used to evaluate putatively different taxa. *J. Mammal.* 81, 245–249. doi: 10.1644/1545-1542(2000)081<0245:CBIDFA>2.0.CO;2
- Leslie, D. M. (2008). Boselaphus tragocamelus (Artiodactyla: Bovidae). *Mamm. Species* 813, 1–16. doi: 10.1644/813.1
- Leslie, D. M. Jr. (2011). Rusa unicolor (Artiodactyla: Cervidae). *Mamm. Species* 43, 1–30. doi: 10.1644/871.1
- Leslie, D. M. Jr., Lee, D. N., and Dolman, R. W. (2013). Elaphodus cephalophus (Artiodactyla: Cervidae). *Mamm. Species* 904, 80–91. doi: 10.1644/904.1
- Leslie, D. M., and Sharma, K. (2009). Tetracerus quadricornis (Artiodactyla: Bovidae). *Mamm. Species* 843, 1–11. doi: 10.1644/843.1
- Loffredo, L. F., and DeSantis, L. R. G. (2014). Cautionary lessons from assessing dental mesowear observer variability and integrating paleoecological proxies of an extreme generalist Cormohippus emsliei. *Palaeogeogr. Palaeoclimatol. Palaeoecol.* 395, 42–52. doi: 10.1016/j.palaeo.2013.12.020
- Louys, J., Ditchfield, P., Meloro, C., Elton, S., and Bishop, L. (2012). Stable isotopes provide independent support for the use of mesowear variables for inferring diets in African antelopes. *Proc. R. Soc. B* 279, 4441–4446. doi: 10.1098/rspb.2012.1473
- Louys, J., Meloro, C., Elton, S., Ditchfield, P., and Bishop, L. (2011). Mesowear as a means of determining diets in African antelopes. *J. Archaeol. Sci.* 38, 1485–1495. doi: 10.1016/j.jas.2011.02.011
- Marin, V. C., Fernández, V. A., Dacar, M. A., Gutiérrez, D. G., Fergani, D., and Pereira, J. A. (2020). Diet of the marsh deer in the Paraná River Delta, Argentina—a vulnerable species in an intensive forestry landscape. *Eur. J. Wildl. Res.* 66, 1–9. doi: 10.1007/s10344-019-1358-3
- Martin, L. F., Ackermans, N. L., Richter, H., Kircher, P., Hummel, J., Codron, D., et al. (2021). Macrowear effects of external quartz abrasives of different size and concentration in rabbits (*Oryctolagus cuniculus*). *J. Exp. Zool. B Mol. Dev. Evol.* 338, 586–597. doi: 10.1002/jezb.23104
- Meloro, C. (2011). Feeding habits of Plio-Pleistocene large carnivores as revealed by the mandibular geometry. *J. Vertebr. Paleontol.* 31, 428–446. doi: 10.1080/02724634.2011.550357
- Mihlbachler, M. C., Campbell, D., Ayoub, M., Chen, C., and Ghani, I. (2016). Comparative dental microwear of ruminant and perissodactyl molars: implications for paleodietary analysis of rare and extinct ungulate clades. *Paleobiology* 42, 98–116. doi: 10.1017/pab.2015.33
- Mihlbachler, M. C., Campbell, D., Chen, C., Ayoub, M., and Kaur, P. (2017). Microwear-mesowear congruence and mortality bias in rhinoceros mass-death assemblages. *Paleobiology* 44, 131–154. doi: 10.1017/pab.2017.13
- Mihlbachler, M. C., Rivals, F., Solounias, N., and Semperebon, G. M. (2011). Dietary change and evolution of horses in North America. *Science* 331, 1178–1181. doi: 10.1126/science.1196166

- Mihlbachler, M. C., and Solounias, N. (2006). Coevolution of tooth crown height and diet in oreodonts (Merycoidodontidae, Artiodactyla) examined with phylogenetically independent contrasts. *J. Mamm. Evol.* 13, 11–36. doi: 10.1007/s10914-005-9001-3
- Müller, D. W., Lackey, L. B., Streich, W. J., Fickel, J., Hatt, J.-M., and Clauss, M. (2011). Mating system, feeding type and ex situ conservation effort determine life expectancy in captive ruminants. *Proc. R. Soc. B Biol. Sci.* 278, 2076–2080. doi: 10.1098/rspb.2010.2275
- O'Shaughnessy, R., Cain, J. W. III, and Owen-Smith, N. (2014). Comparative diet and habitat selection of puku and lech we in northern Botswana. *J. Mammal.* 95, 933–942. doi: 10.1644/13-MAMM-A-301
- Owen-Smith, N. (1997). Distinctive features of the nutritional ecology of browsing versus grazing ruminants. *Zeitschrift fuer Säugetierkunde (Germany)*. 62, 176–191.
- Perez, S. I., Bernal, V., and Gonzalez, P. (2006). Differences between sliding semi-landmark methods in geometric morphometrics, with an application to human craniofacial and dental variation. *J. Anat.* 208, 769–784. doi: 10.1111/j.1469-7580.2006.00576.x
- Pinder, L., and Grosse, A. P. (1991). *Blastocerus dichotomus*. *Mamm. Species* 1–4:1. doi: 10.2307/3504311
- Pineda-Munoz, S., Evans, A. R., and Alroy, J. (2016). The relationship between diet and body mass in terrestrial mammals. *Paleobiology* 42, 659–669. doi: 10.1017/pab.2016.6
- Prado, H. M. (2013). Feeding ecology of five Neotropical ungulates: a critical review. *Oecologia Australis* 17, 459–473. doi: 10.4257/oeco.2013.1704.02
- Rasband, W., et al. (2022). *ImageJ, image processing and analysis in Java, version 1.53s*. Bethesda, MD: National Institutes of Health.
- Renecker, L. A., and Schwartz, C. C. (1997). “Food habits and feeding behavior” in *Ecology and Management of the North American Moose*. eds. F. A. W. and C. C. Schwartz (Boulder, CO: University of Colorado Press), 403–440.
- Rivals, F., and Semperebon, G. M. (2006). A comparison of the dietary habits of a large sample of the Pleistocene pronghorn *Stockoceros onosurosagris* from the Papago Springs cave in Arizona to the modern *Antilocapra americana*. *J. Vertebr. Paleontol.* 26, 495–500. doi: 10.1671/0272-4634(2006)26[495:ACOTDH]2.0.CO;2
- Rivals, F., Solounias, N., and Mihlbachler, M. C. (2007). Evidence for geographic variation in the diets of late Pleistocene and early Holocene bison in North America, and differences from the diets of recent bison. *Quat. Res.* 68, 338–346. doi: 10.1016/j.yqres.2007.07.012
- Rødven, R., Yoccoz, N. G., Ims, R. A., and Wiig, Ø. (2006). Assessing dental wear in reindeer using geometric morphometrical methods. *Rangifer* 26, 29–34. doi: 10.7557/2.26.1.186
- Rohlf, F. J. (2015). The tps series of software. *Hystrix, the Italian Journal of Mammalogy* 26, 9–12. doi: 10.4404/hystrix-26.1-11264
- Saareinen, J., Karme, A., Cerling, T. E., Uno, K., Sällä, L., Kasiki, S., et al. (2014). A new tooth wear-based dietary analysis method for Proboscidea (Mammalia). *J. Vertebr. Paleontol.* 35:e918546. doi: 10.1080/02724634.2014.918546
- Sanson, G. D. (2006). The biomechanics of browsing and grazing. *Am. J. Bot.* 93, 1531–1545. doi: 10.3732/ajb.93.10.1531
- Sanson, G. D., Kerr, S., and Read, J. (2018). Dietary exogenous and endogenous abrasives and tooth wear in African buffalo. *Biosurf. Biotribol.* 3, 211–223. doi: 10.1016/j.bsbt.2017.12.006
- Schaller, G. B. (1967). *The deer and the Tiger: Study of wildlife in India*. Chicago IL, University of Chicago Press.
- Schulz, E., Fraas, S., Kaiser, T. M., Cunningham, P. L., Ismail, K., and Wronski, T. (2013). Food preferences and tooth wear in the sand gazelle (*Gazella marica*). *Mamm. Biol.* 78, 55–62. doi: 10.1016/j.mambio.2012.04.006
- Schulz-Kornas, E., Winkler, D. E., Clauss, M., Carlsson, J., Ackermans, N. L., Martin, L. F., et al. (2020). Everything matters: molar microwear texture in goats (*Capra aegagrus hircus*) fed diets of different abrasiveness. *Palaeogeogr. Palaeoclimatol. Palaeoecol.* 552:109783. doi: 10.1016/j.palaeo.2020.109783
- Semperebon, A. J., Sokolov, V. E., and Danilkin, A. A. (1996). *Capreolus capreolus*. *Mamm. Species* 1–9:1. doi: 10.2307/3504309
- Semperebon, G. M., and Rivals, F. (2010). Trends in the paleodietary habits of fossil camels from the tertiary and quaternary of North America. *Palaeogeogr. Palaeoclimatol. Palaeoecol.* 295, 131–145. doi: 10.1016/j.palaeo.2010.05.033
- Semperebon, G. M., Rivals, F., and Janis, C. M. (2019). The role of grass vs. exogenous abrasives in the paleodietary patterns of north American ungulates. *Front. Ecol. Evol.* 7:65. doi: 10.3389/fevo.2019.00065
- Seri, H., Chammem, M., Silva, S., Rodrigues, M., Khorchani, T., and Ferreira, L. (2018). Assessment of diet composition of free-ranging addax antelopes (*Addax nasomaculatus*) by the combination of microhistological procedures and n-alkanes and long-chain alcohols as fecal markers. *Can. J. Zool.* 96, 1284–1289. doi: 10.1139/cjz-2017-0320
- Sokolov, V. E. (1974). *Saiga tatarica*. *Mamm. Species* 1–4:1. doi: 10.2307/3503906
- Taylor, L. A., Kaiser, T. M., Schwitzer, C., Müller, D. W. H., Codron, D., Clauss, M., et al. (2013). Detecting inter-cusp and inter-tooth wear patterns in rhinocerotids. *PLoS One* 8, 1–12. doi: 10.1371/journal.pone.0080921
- Tomas, W. M., and Salis, S. M. (2000). Diet of the marsh deer (*Blastocerus dichotomus*) in the Pantanal wetland, Brazil. *Stud. Neotropical Fauna Environ.* 35, 165–172. doi: 10.1076/snfe.35.3.165.8861
- Tripathi, S., Basumatary, S. K., Singh, Y. R., McDonald, H. G., Tripathi, D., and Singh, L. J. (2019). Multiproxy studies on dung of endangered Sangai (*Rucervus eldii eldii*) and hog deer (*Axis porcinus*) from Manipur, India: implications for paleoherbivory and paleoecology. *Rev. Palaeobot. Palynol.* 263, 85–103. doi: 10.1016/j.revpalbo.2019.01.008
- Tuboi, C., and Hussain, S. A. (2016). Factors affecting forage selection by the endangered Eld's deer and hog deer in the floating meadows of Barak-Chindwin basin of north-East India. *Mamm. Biol.* 81, 53–60. doi: 10.1016/j.mambio.2014.10.006
- Ulbricht, A., Maul, L. C., and Schulz, E. (2015). Can mesowear analysis be applied to small mammals? A pilot-study on leporines and murines. *Mamm. Biol.* 80, 14–20. doi: 10.1016/j.mambio.2014.06.014
- Ungar, P. (2010). *Mammal teeth: origin, evolution, and diversity*. Johns Hopkins University Press, Baltimore, MD. 320.
- Valli, A. M., and Palombo, M. R. (2008). Feeding behaviour of middle-size deer from the upper Pliocene site of saint-Vallier (France) inferred by morphological and micro/mesowear analysis. *Palaeogeogr. Palaeoclimatol. Palaeoecol.* 257, 106–122. doi: 10.1016/j.palaeo.2007.09.006
- von Koenigswald, W., Anders, U., Engels, S., Schulz, J. A., and Kullmer, O. (2013). Jaw movement in fossil mammals: analysis, description and visualization. *Paläontol. Z.* 87, 141–159. doi: 10.1007/s12542-012-0142-4
- Watter, K., Baxter, G., Brennan, M., Pople, T., and Murray, P. (2020). Seasonal diet preferences of chital deer in the northern Queensland dry tropics, Australia. *Rangeland J.* 42, 211–220. doi: 10.1016/j.palaeo.2007.09.006
- Wegge, P., Shrestha, A. K., and Moe, S. R. (2006). Dry season diets of sympatric ungulates in lowland Nepal: competition and facilitation in alluvial tall grasslands. *Ecol. Res.* 21, 698–706. doi: 10.1007/s11284-006-0177-7
- Widga, C. (2006). Niche variability in late Holocene bison: a perspective from big bone lick, KY. *J. Archaeol. Sci.* 33, 1237–1255. doi: 10.1016/j.jas.2005.12.011
- Wiles, G. J., Buden, D. W., and Worthington, D. J. (1999). History of introduction, population status, and management of Philippine deer (*Cervus mariannus*) on Micronesian Islands. *Mammalia* 63, 193–216. doi: 10.1515/mamm.1999.63.2.193
- Wilson, D. E., and Mittermeier, R. A. (2011). *Handbook of the mammals of the world: Hoofed mammals 2*. Lynx Edicions, Barcelona.
- Wronski, T., and Schulz-Kornas, E. (2015). The Farasan gazelle—a frugivorous browser in an arid environment? *Mamm. Biol.* 80, 87–95. doi: 10.1016/j.mambio.2014.12.002
- Xu, F., Ma, M., Wu, Y., and Yang, W. (2012). Winter daytime activity budgets of Asiatic ibex *Capra sibirica* in Tomur National Nature Reserve of Xinjiang, China. *Pak. J. Zool.* 44, 389–392.
- Zelditch, M. L., Swiderski, D. L., Sheets, D., and Fink, W. L. (2004). *Geometric morphometrics for biologists: a primer*. San Diego, CA: Elsevier Academic Press.
- Zhang, Q., Yang, B., Fu, Q., Wang, L., Gong, X., and Zhang, Y. (2020). The winter diet of sambar (*Rusa unicorn*) in the Qionglai Mountains. *Biodivers. Sci.* 28, 1192–1201. doi: 10.17520/biods.2020063
- Zhou, Z., Winkler, D. E., Fortuny, J., Kaiser, T. M., and Marcé-Nogué, J. (2019). Why ruminating ungulates chew sloppily: biomechanics discern a phylogenetic pattern. *PLoS One* 14:e0214510. doi: 10.1371/journal.pone.0214510

Frontiers in Ecology and Evolution

Ecological and evolutionary research into our natural and anthropogenic world

This multidisciplinary journal covers the spectrum of ecological and evolutionary inquiry. It provides insights into our natural and anthropogenic world, and how it can best be managed.

Discover the latest Research Topics

[See more →](#)

Frontiers

Avenue du Tribunal-Fédéral 34
1005 Lausanne, Switzerland
frontiersin.org

Contact us

+41 (0)21 510 17 00
frontiersin.org/about/contact



Frontiers in Ecology and Evolution

